A STUDY OF POWER, KINETICS, AND MODELLING IN THE COMPOSTING PROCESS

A thesis

submitted in partial fulfilment

of the requirements for the Degree

of

Doctor of Philosophy

in the

University of Canterbury

by

Ian George Mason

University of Canterbury

2007

Copyright

TABLE OF CONTENTS

List of Figures

Photograph credits:

All photographs were taken by the author, except where otherwise indicated.

List of Tables

Abstract

This thesis explores the roles of physical and mathematical modelling in the prediction of temperature profiles in the composting process. A literature-based evaluation of the performance of laboratory- and pilot scale composting reactors, showed that physical models used in composting research frequently do not properly simulate the full-scale composting environment, and may therefore produce results which are not applicable at full scale. In particular, self-heating, laboratory-scale, reactors typically involve significant convective/conductive/radiative losses, even with insulation present. This problem can be overcome by using controlled temperature difference or controlled heat flux laboratory reactors, which allow convective/conductive/radiative heat fluxes to be controlled to levels close to those occurring in full-scale systems.

A new method of assessing the simulation performance of composting systems is presented. This utilises the areas bounded by the temperature-time profile and reference temperatures of 40 and 55 ^{o}C (A_{40} and A_{55}), the times for which these temperatures are exceeded (t_{40} and t_{55}), and times to peak temperature. An evaluation of published temperature profiles showed a marked difference in these parameters when comparing many laboratory- and full-scale reactors. The impact of aeration is illustrated, and laboratory- and pilot-scale reactors able to provide good temperature profile simulation, both qualitatively and quantitatively, are identified.

Mathematical models of the composting process are reviewed and their ability to predict temperature profiles assessed. The most successful models in predicting temperature profiles have incorporated either empirical kinetic expressions, or utilised a first-order model, with empirical corrections for temperature and moisture. However, no temperature models have been able to predict maximum, average and peak temperatures to within 5, 2 and 2 ^{o}C respectively, or to predict the times to reach peak temperatures to within 8 h, although many models were able to successfully predict temperature profile shape characteristics. An evaluation of published constant-temperature and varying-temperature substrate degradation profiles revealed very limited evidence to support the application of single exponential, double exponential or non-logarithmic Gompertz functions in modelling substrate degradation kinetics, and this was identified as a potential weakness in the temperature prediction model. A new procedure for correcting substrate degradation profiles generated at

varying temperature to a constant temperature of 40 ^{o}C was developed and applied in this analysis, and on experimental data generated in the present work.

A new approach to the estimation of substrate degradation profiles in the composting process, based on a re-arrangement of the heat balance around a reactor, was developed, and implemented with both a simulated data set, and data from composting experiments conducted in a laboratory-scale constant temperature difference (CTD) reactor. A new simulated composting feedstock for use in these experiments was prepared from ostrich feed pellets, office paper, finished compost and woodchips. The new modelling approach successfully predicted the generic shape of experimental substrate degradation profiles obtained from CO_2 measurements, but under the conditions and assumptions of the experiment, the profiles were quantitatively different. Both measured CO_2-carbon (CO_2-C) and predicted biodegradable volatile solids carbon (BVS-C) profiles were moderately to well fitted by single exponential functions with similar rate coefficients. When corrected to a constant temperature of 40 ^{o}C, these profiles gave either multi-phase or double exponential profiles, depending upon the cardinal temperatures used in the temperature correction procedure. If it is assumed that the double exponential model generated is correct, this work provides strong evidence that a substrate degradation curve generated under appropriate laboratory conditions at 40 ^{o}C would, given the correct cardinal temperatures, generate a correct substrate degradation profile under varying temperature conditions, and that this in turn would enable an accurate and precise prediction of the temperature profile using a heat and mass balance approach. This finding opens the door for the development of a simple laboratory test for composting raw material characterisation, but underlines the need for accurate estimates of the physical cardinal temperatures. Experimental factors appear to be the likely cause of the dysfunction between previously reported substrate degradation patterns and existing substrate degradation models, and suggestions for further research are provided in order to more precisely and accurately quantify these factors.

Acknowledgements

I would like to thank all the people who gave me support and encouragement over the duration of this research, especially:

Mark Milke, Roger Nokes, Peter Gostomski and Lawrence Boul. Many thanks to my great team of advisors for helpful comments and suggestions. Especial gratitude to *Mark Milke* whose warm and friendly style has contributed to making this journey a rewarding and enjoyable one.

Andy Buchanan – for making me so welcome in the department.

Bruce Steven – for finding "Engauge Digitiser" (not only incredibly useful, but even better - free!), and for providing pleasant company in E445.

Sandy Ferguson and Danny Leonard (Department of Chemistry) – for unfailingly friendly, expert and timely technical assistance. Thanks also to *Robert McGregor* (glassblowing) and *Bruce Whitfield* (stores) for willing and friendly help.

Ian Sheppard – special thanks for always being ready to help at a moments notice, and for sound and perceptive technical advice.

Peter Coursey, Lance Currie, Fliss Jackson, Peter McGuigan, Richard Newton, Stuart Toase, Michael Weavers and Kevin Wines - for technical contributions.

Darrel Amarasekara and Ken Morison – for Matlab programming advice and assistance.

Marney Brosan – for wonderful graphics and cartography.

Christine McKee, Ann Reddy, Dave Lane and Manja Pieters – for expert and friendly service in the engineering library.

Funding support for this research through the award of a University of Canterbury Doctoral Scholarship is gratefully acknowledged.

Of those nearest and dearest, I would especially like to thank:

Max, Sue, Alex, Sebastian, Georgia and Florence – for warm friendship and support.

Eric – for many enjoyable lunches and chats.

Tom and Tricia – for many good times, and for those to come.

Gail – for friendship, and always being there.

Thaniya - for inspiration.

Dedication

I dedicate this research to all who strive to preserve, nurture and sustain the environment we all share on this planet earth.

"…It's the way scientists write up a research report or paper: we follow different avenues of inquiry, going down blind alleys, hitting a fast lane or taking a short cut, zigzagging along as we probe an interesting observation or phenomenon. Then, when it's time to "write it up" we shuffle through the experiments, tossing some out and organising the remainder into an order that creates the illusion that a direct path was taken from the initial question to the final results"

David Suzuki, 2006.

"things should be made as simple as possible,
but not any simpler"

Attributed to Albert Einstein (Calaprice, 2000).

LIST OF PAPERS

This thesis includes the following papers:

I Mason, I.G. & Milke, M.W., 2005. Physical modelling of the composting environment: a review. Part 1: Reactor systems. Waste Management 25 (5), 481-500.

II Mason, I.G. & Milke, M.W., 2005. Physical modelling of the composting environment: a review. Part 2: Simulation performance. Waste Management 25 (5), 501-509.

III Mason, I.G., 2006. Mathematical modelling of the composting process: a review. Waste Management 26 (1), 3-21.

IV Mason, I.G., in press-a. An evaluation of substrate degradation patterns in the composting process. Part 1: Profiles at constant temperature. Waste Management. (Published on-line 17 September, 2007).

V Mason, I.G., in press-b. An evaluation of substrate degradation patterns in the composting process. Part 2: Temperature-corrected profiles. Waste Management. (Published on-line 12 September, 2007).

VI Mason, I.G., submitted. Design and performance of a simulated feedstock for composting experiments. Compost Science and Utilization.

VII Mason, I.G., submitted. A method for predicting biodegradable volatile solids degradation profiles in the composting process. Waste Management.

Material from the published papers has been reprinted here with the consent of the publisher.

Page intentionally left blank.

CHAPTER 1
INTRODUCTION

1.1 Foreword

The broad objective of this thesis is to examine, discuss, and make a contribution to, the use of modelling, both physical and mathematical, in relation to the composting process. The approach adopted was to examine how modelling has been, is being and might be, used in this application, and then to pursue one or more promising lines of enquiry thus revealed. One highly desirable outcome would be to make modelling a more useful predictive tool for engineers. The reader is kindly asked to note that in pursuing this research it was not the intention of the author to examine various component topics in isolation, and thus this thesis does not present a study of either the composting process, or modelling, per se.

Progress through this research may be likened to taking a journey and this analogy will be used to frame the research and to introduce each chapter. Figure 1.1 gives a conceptual view of the travels undertaken and this figure will re-appear throughout the thesis in order to inform and remind the reader of the stage being discussed.

As a prelude to our journey, we will first seek to understand the landscape from which we depart and the basic elements of the language we will speak along the way. In relation to figure 1.1, we are starting out from Composton-on-Wye, a town where large-scale composting is the main activity and everyone is a competent practitioner of their art. The aim of this first chapter therefore is to set the scene by providing an overview of composting in basic terms and to briefly discuss the role of this technology in organic resource residuals stabilisation and recycling. The chapter concludes with some comments on the role of modelling and an outline of the remaining thesis structure.

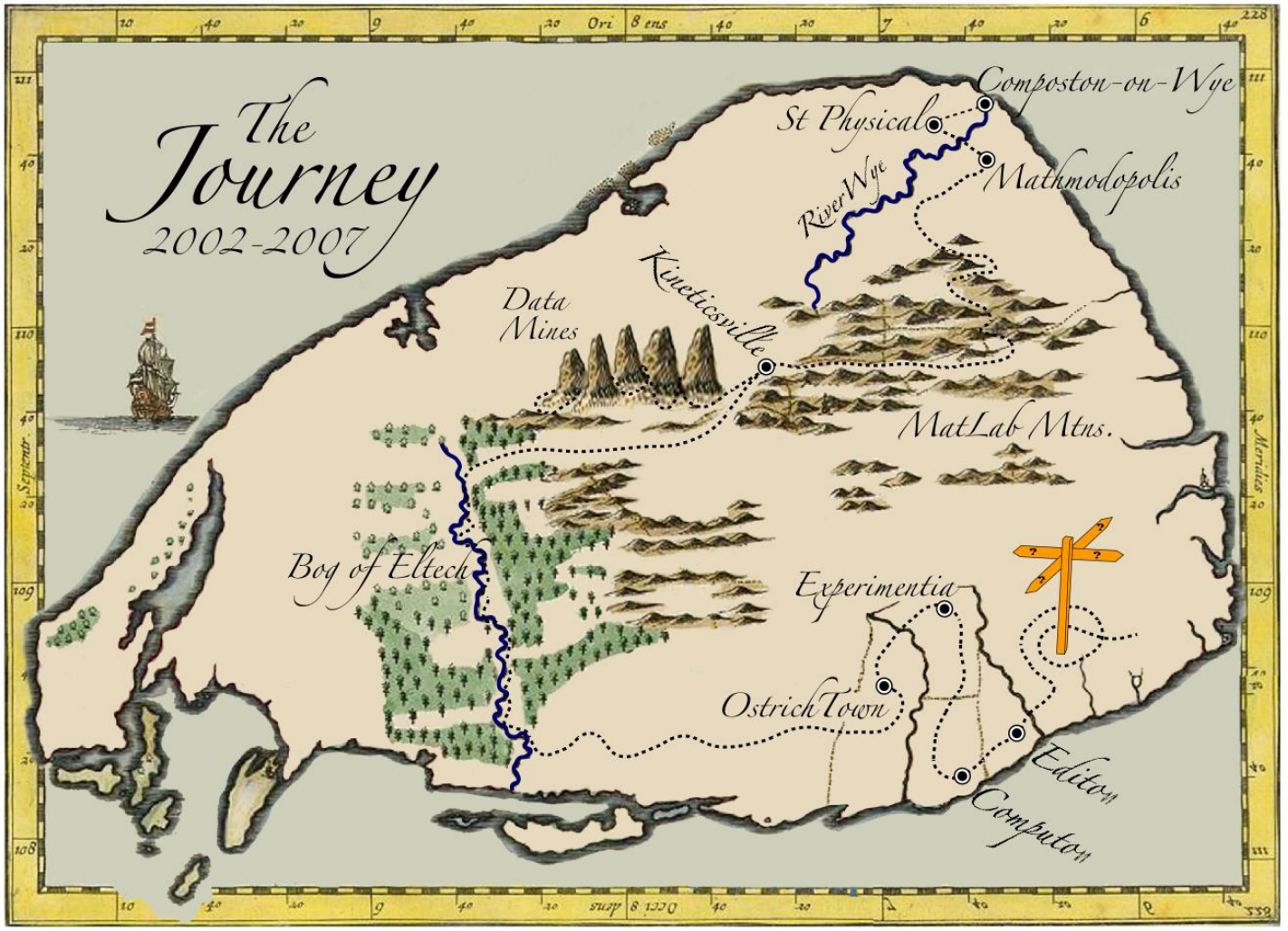

Figure 1.1: The conceptual map of the author's research travels. Our present location is - Composton-on-Wye.

1.2 Definitions of composting

Composting has been described as "an aerobic thermophilic degradation process" (Bell & Pos, 1971, as cited by Crawford, 1983), "the decomposition of heterogeneous organic matter by a mixed microbial population in a moist warm aerobic environment" (Biddlestone and Gray, 1973), "the biological reduction of organic wastes to humus" (Minnich and Hunt, 1979), "the *aerobic*, or oxygen requiring, decomposition of organic materials by *microorganisms* under controlled conditions" (Rynk, 1992) and, more recently, as "a high solids aerobic degradation process" (VanderGheynst et al., 1997).

These definitions, taken together, reflect several important points:

- composting is an aerobic microbial degradation process,
- composting operates in a high solids matrix
- conditions which allow the accumulation of sufficient heat to maintain temperatures in the thermophilic (> 40 ^{o}C) range for a certain period of time are required.

A broader and rather more useful definition, in which key process goals and end use criteria are incorporated, has been published by Haug (1993):

"Composting is the biological decomposition and stabilization of organic substrates, under conditions that allow development of thermophilic temperatures as a result of biologically produced heat, to produce a final product that is stable, free of pathogens and plant seeds, and can be beneficially applied to land."

This is a largely satisfactory definition, although omission of the high solids aspect of composting means that this description might apply equally to liquid phase aerobic digestion (for a description of aerobic digestion, the reader is referred to Metcalf & Eddy (1991)). However, the product stability criterion would not be met in the latter case, since the biological solids produced remain very wet, and thus prone to subsequent anaerobic biological activity. This leads to an important aspect of aerobic composting not incorporated in any of the previous definitions, namely the phenomenon of product drying, typically to < 40% (w/w) moisture content. Consequently, the definition of Haug might usefully be modified to read as follows:

"Composting is the biological decomposition and stabilization of solid organic substrates, under conditions that allow development of thermophilic temperatures as a result of biologically produced heat, to produce a final product that is stable, low in moisture, free of pathogens and plant seeds, and can be beneficially applied to land."

A related term, "anaerobic composting", has appeared relatively frequently in the literature over the past 20 or so years, e.g. (Debaere and Verstraete, 1984; Chynoweth et al., 1992; Haug, 1993; Kayhanian, 1993; Shin et al., 2001; Sadaka and Engler, 2003) and deserves comment. In relation to the above definitions the term is an oxymoron, and it is arguable that this usage is inappropriate, potentially confusing to readers and should be discouraged. It is suggested in this thesis that alternative terms with long histories of use in science and engineering, such as "anaerobic digestion" or "anaerobic fermentation", are more appropriate. When preceeded by terms like "high solids" (see Tchobanoglous et al., 1993), or "dry", such terminologies provide suitably accurate labels.

1.3 Process outline

1.3.1 Components of the composting mixture

A composting mixture typically comprises some or all of the following groups of materials:

- a substrate (i.e. the material to be stabilised),
- an amendment (i.e. a partially biodegradable material used to adjust the nutrient, moisture and/or energy balance, and/or physical structure),
- a bulking agent (i.e. a partially biodegradable or non-biodegradable material used primarily to adjust the physical structure in order to increase air-permeability).

Figure 1.2 provides a useful overview of substrate, amendment and bulking agent properties.

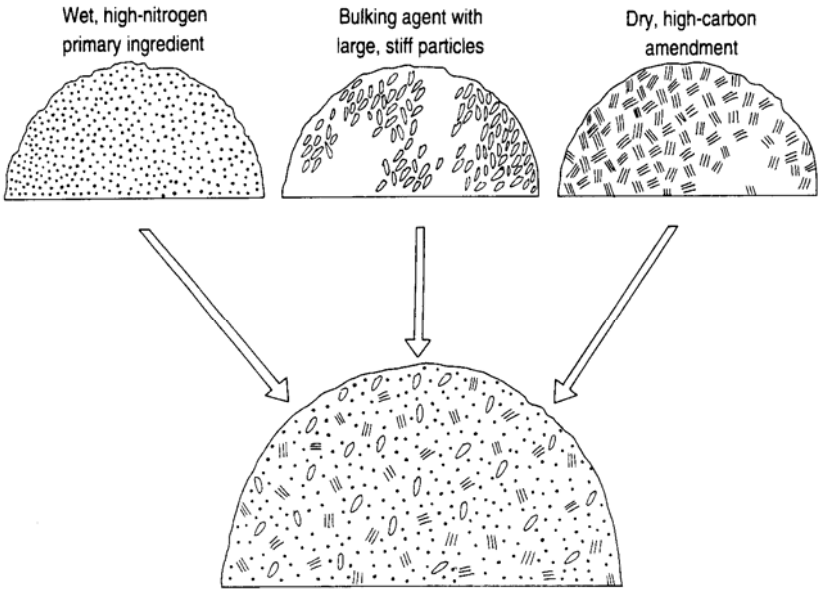

Figure 1.2: Raw materials typically used in composting recipes (from Rynk, 1992)

Common substrates include green waste (known as yard waste in North America), food residuals, domestic wastewater sludges, agricultural sludges and industrial organic residuals. Substrates are typically high in nitrogen and relatively high in moisture content. Amendment materials are normally dry (e.g. < 10% moisture) and high in carbon. Examples of amendment materials include sawdust, straw, peat, rice hulls, cotton gin trash (Haug, 1993) and paper. Woodchips are the most commonly used bulking agents, but the use of pelleted refuse, shredded tyres, peanut shells and tree trimmings has also been reported (Haug, 1993). In certain cases, for example mixtures of horse manure and stable bedding, the substrate may be adequately conditioned in terms of nutrient balance, energy and structure, as produced. However this tends to be the exception rather than the rule.

1.3.2 Basic process requirements

Successful composting requires attention to three key factors, which are essential to aerobic microbial growth:

- a balanced diet
- adequate moisture
- adequate oxygen supply

Figure 1.3 provides a useful schematic view of the composting process and table 1.1 shows the ranges of conditions recommended for rapid composting.

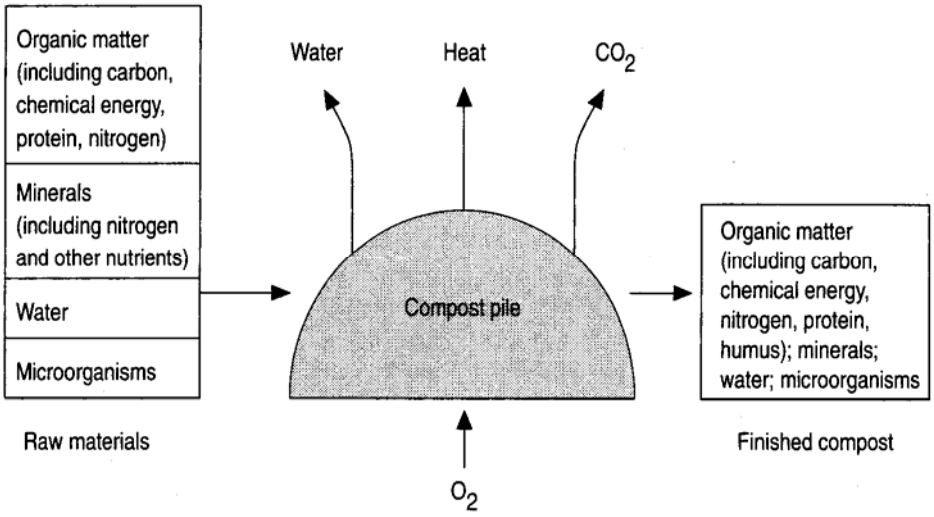

Figure 1.3: Composting process schematic (from Rynk, 1992)

Table 1.1: Recommended conditions for rapid composting (after Rynk, 1992)

Condition	Reasonable range[a]	Preferred range
Carbon to nitrogen (C:N) ratio	20:1-40:1	25:1-30:1
Moisture content (% w/w)	40-65	50-60
Oxygen concentration (% v/v)	> 5	>> 5
Particle size (mm)	3.2-12.7	varies[b]
pH	5.5-9.0	6.5-8.0
Temperature (^{o}C)	43-66	54-60

[a] These recommendations are for *rapid* composting. Conditions outside these ranges can also yield successful results.
[b] Depends on the specific materials, pile size and/or weather conditions

Dietary requirements are commonly expressed in terms of the total carbon:nitrogen (C:N) ratio of the mixture. Implicit in this approach is the assumption that if the C:N ratio is correct, then other macro and micro nutrients will also be present in adequate proportions

(Rynk, 1992) and this has been shown from experience to be satisfactory for many common organic substrates. However, caution is required in applying this rule, since some mixtures, particularly those with high cellulosic content (Haug, 1993), may be low in certain essential nutrients. Other substrates may require pH adjustment (Haug, 1993).

The use of ratios based on total C and N might also be taken to imply that similar proportions of the C and N present are bio-available under composting conditions. However, this is unlikely. The literature suggests that whilst most of the nitrogen in common organic substrates is likely to be bioavailable (Haug, 1993; Tchobanoglous et al., 1993), considerable quantities of the carbon present in the mixture will be unavailable, depending on the type of substrate, amendment or bulking agent present. Analysis by Haug (1993) of data reported by Kayhanian and Tchobanoglous (1992) shows a range of biodegradable organic carbon to total organic carbon ratios from 0.57:1-0.79:1, for food waste, paper, yard waste and mixed waste materials. Ideally C:N ratios should be based on biodegradable carbon and biodegradable nitrogen data, or if this is not possible, at least on the biodegradable carbon fraction. Where only total carbon and nitrogen figures are available, as is often the case, subjective knowledge of the nature and composting performance of the high carbon content materials can assist in the choice of suitable C:N ratios. Thus the total C:N ratio may be interpreted as a surrogate measure of compostability, rather than an accurate expression of available nutrients. In recognition of this, the terms total C:N and biodegradable C:N are used in chapters 7-8. Where C:N appears unmodified elsewhere, it should be taken to mean total C:N, as is commonly understood in the literature.

Recommended optimal initial moisture levels for composting range from 40-65% (w/w) with 50-60% (w/w) preferred (Rynk, 1992). Whilst successful composting has been reported for initial moisture levels well above this range (e.g. Mathur et al., 1990; Patni and Kinsman, 1997; Sartaj et al., 1997), final product moisture levels were also high in these cases (e.g. 70-75%).

The oxygen concentration criterion is typically addressed by ensuring that the structure of the composting mixture is sufficiently open to allow adequate airflow. The parameter “free air space” (FAS) provides an indication of air permeability with a value of approximately 30% recommended for most mixtures (Haug, 1993). In practice FAS is created using suitable amendments and/or bulking agents and maintained in windrows through periodic turning.

For a more detailed discussion and analysis of FAS the reader is referred to (Haug, 1993; Eftoda and McCartney, 2004).

1.3.3 Process formats

Composting process formats can be conveniently categorised according to whether the material is contained within a vessel (reactor system), or placed in open piles (non-reactor system) (Haug, 1993). Process formats may be chosen for a variety of engineering reasons including process control, site constraints, ease of odour management, leachate control and economics.

A wide range of full-scale reactor systems have been reported and many specific examples have been described by (Haug, 1993). Reactors vary substantially in size with volumes up to 2460 m^3 reported (after Haug, 1993). Non-reactor systems include windrows and aerated static piles. Typical cross sectional dimensions for windrows and piles range from 2.75-6.0 m base width and from 1.4-3.7 m in height (Rynk, 1992). Windrow lengths are restricted only by site constraints, whilst aerated static pile lengths will be limited by air supply considerations. For example, Rynk (1993) has recommended that aerated static pile lengths for on-farm systems should not exceed 70-90 ft (21-27 m). Reactor systems and aerated static piles utilise forced aeration, whilst windrows are aerated by natural convection mechanisms only. Figures 1.4a-c show examples of reactor, aerated static pile and windrow systems.

In order to allow the development of thermophilic temperatures appropriate management of both advective, and conductive/convective/radiative (CCR), heat losses is required. Both topics will be reviewed in detail later in this thesis. For a fuller description of reactor and non-reactor systems the reader is referred to Rynk (1992), Haug (1993) and Chiumenti et al. (2005).

a)

b)

c)

Figure 1.4: Composting process formats; a) horizontal agitated reactor system (Rolleston, New Zealand) (Photo: R. Rynk); b) aerated static pile (Lewiston, USA); c) windrows (Tauranga, New Zealand) (Photo: Anon)

1.4 The role of composting in resource residuals stabilisation

One useful starting point for the assessment of the role of various technologies in resource residuals stabilisation is to examine the extent to which the embodied solar energy in the organic material(s) is utilised. In composting systems, the majority of the energy released from organic substrates due to microbial activity exits the system as latent heat of evaporation of water (see chapter 2), resulting in "biodrying" and producing a product of relatively low moisture content (typically 35-40% w/w). In contrast, anaerobic digestion (AD) systems, which are presently enjoying a resurgence of interest (see for example Lens et al., 2004) generate biogas, which contains the majority of the input energy, plus wet sludge and a supernatant. Although the environmental performance of composting has been compared unfavourably to AD by some authors (e.g. Mata-Alvarez, 2002; Hamelers et al., 2003; Mata-Alvarez, 2003; Hogg, 2004) it is not clear that these comparisons are based on end-products with comparable moisture contents, or that they account for the beneficial effects of composts on plant health and soil properties. Further work is required in this area.

A second evaluation criterion is the extent and immediacy of materials return to productive use in the soil. In this respect composting may be expected to result in a higher return of carbon (due to a higher degree of organic matter retention within the system), a lower return of nitrogen (due to ammonia losses) and an equivalent return of phosphorus, when compared to AD.

On a practical level, composting systems are widely established, relatively well understood from an operational point of view, reasonably robust, and attractive in terms of their relatively simplicity and suitability to small, medium and large-scale operation. For example small-scale windrow systems for green waste composting can be started-up with low levels of capital investment and technical expertise, and can produce a satisfactory product whilst meeting environmental constraints. If necessary the system may then be grown to a more sophisticated level in terms of substrates stabilised, process modes, operation, monitoring, environmental control and product range. Thus aerobic composting can be attractive to small communities, due to simplicity of operation and low entry costs, through to large cities, where higher levels of capital and technical resources will typically be available. Advantages of compost products include their roles in carbon, nitrogen and phosphorus recycling, soil structural and textural improvement, improved soil moisture retention, and plant disease suppression. More recently, compost has begun to be employed in non-

traditional applications, including bank stabilisation and runoff minimisation e.g. (Goldstein et al., 2003).

Composting presently plays a major role in resource residuals stabilisation strategies in many parts of the world (e.g. de Bertoldi, 1998; Asdal and Breland, 2003; Diaz and Eggerth, 2003) and is predicted by some authors to have an important part in future waste management strategies (Supriyadi et al., 2000; Slater and Frederickson, 2001). Implementation varies on substantially a country by country basis, with a high rate of adoption in the Netherlands and Germany for example, whilst composting activity in the UK, although currently increasing, was reported in 1998 as being comparatively low (Holland and Proffitt, 1998). Kaufman et al. (2004) reported the existence, in 2000, of 3846 yard (green) waste processing facilities in the USA, a major increase over numbers a decade previously. Composting was reported as the most cost-effective way to reduce greenhouse gas emissions in Israel by Ayalon et al. (2000), although this conclusion is debatable. In New Zealand composting is presently widespread on a municipal and industrial scale, with a reported 27 sites operating in 2007 (UC Composting, 2007), plus an additional 2 sites not included in this reference. Of these, the majority process green waste, with smaller numbers processing industrial sludges, agricultural residuals and domestic wastewater biosolids.

With continuing trends, particularly in North America, Europe, Japan, Australia and New Zealand, toward increased source separation of organic residuals arising from municipal and industrial sources, the amounts of raw material potentially available for composting are predicted to increase substantially in the near future. Source separation has been implemented to a high degree in several European countries and in some Japanese municipalities, a phenomemon partly linked to failure of older unsegregated municipal solid waste (MSW) composting plants. Helsinki has been reported as having achieved 100% source separation, whilst Germany and the Netherlands are very active in this area (de Bertoldi, 1998). Whether these residuals will be stabilised by aerobic composting alone, or using other technologies, or combinations of technologies, is the subject of interesting current debate.

Composting and AD are not mutually exclusive technologies. In many cases where AD has been adopted as the primary stabilisation process, composting has been specified to follow as a means of producing an acceptable end solid product (e.g. La Brooy et al., 2003). This

scenario relies on sufficient energy remaining in the AD sludge to enable thermophilic temperatures to be reached in subsequent composting and thus demands an energy management approach. An interesting hybrid scheme using a composting-AD-composting sequence in which the temperature of the incoming substrate was raised aerobically, the mixture then fermented by AD, and then final product stabilisation achieved by post-AD composting, was described by (Mueller et al., 2003) and provides a useful example of an energy management approach. This idea is presently being implemented commercially in the Danish "Aikan" system (Solum, 2007).

At the present time it seems likely that composting will continue to play a significant role in resource residuals stabilisation worldwide for a variety of environmental, technical, economic and social reasons. Many composting plants are already in operation, the technology is largely proven and even with AD as a primary means of stabilisation, composting is likely to be utilised for post-anaerobic stabilisation and drying of the sludge product. In addition, composting is likely to remain the preferred technology for green waste stabilisation due to difficulties in anaerobic digestion of bulky, high cellulosic, substrates.

1.5 Roles of physical and mathematical modelling

Physical modelling enables laboratory and pilot-scale exploration of many aspects of the composting process (see chapter 2). If conditions are appropriately controlled, then such modelling, if successful, can simulate full-scale environments and process performance to an acceptable level. In contrast, mathematical modelling potentially allows process performance to be predicted from a knowledge of independently measured substrate properties and process conditions. A validated mathematical model will predict, within specified limits, process performance at laboratory, pilot and full-scale.

In this thesis it is implicit that physical and mathematical modelling are complementary and of greatest value when used together. Physical modelling, when relied upon alone, can result in useful, but time and resource consuming, experimentation, often with little or no exposition of general principles. On the other hand, mathematical modelling used alone merely results in simulations, whose relevance to the real world of engineering remains unknown until tested against empirical data. Such data may be obtained from full-scale operations, but this is often difficult (see chapter 2). Appropriate physical models however,

provide a convenient means of generating information against which mathematical models may be tested.

1.6 Thesis outline

This thesis is organised into 9 chapters, of which the majority are based on refereed journal papers by the author and others, that have either been published, or submitted for publication. Details of each paper are given in a foreword, and an update provided in an afterword to each chapter where appropriate. In chapter 2 reactor systems used in the physical modelling of the composting environment are reviewed and in chapter 3, their performance is assessed. Chapter 4 reviews mathematical models of the composting process and then assesses their performance. In chapters 5 and 6, models for substrate generation are examined in detail and a procedure for, and results of, de-coupling these from temperature effects is presented. In Chapter 7, the development of a simulated feedstock for composting experiments is described. Chapter 8 describes a procedure to derive substrate degradation profiles from temperature, airflow, humidity and mass loss data, and then compares the predictions to experimental data. Conclusions and recommendations for further work are presented in Chapter 9. Appendices conclude the thesis, and include a complete reference listing, a compilation of Matlab routines and detailed experimental results.

1.7 References

Asdal, A. and Breland, T.A., 2003. Compost quality related to product utilisation in Norway. In: Proceedings of the Fourth International Conference of ORBIT Association on Biological Processing of Organics: Advances for a Sustainable Society, 30th April-2 May, 2003, Perth, Australia, 230-240.

Ayalon, O., Avnimelech, Y. and Shechter, M., 2000. Alternative MSW treatment options to reduce global greenhouse gases emissions - the Israeli example. Waste Management & Research 18 (6), 538-544.

Biddlestone, A.J. and Gray, K.R., 1973. Composting - application to municipal and farm wastes. The Chemical Engineer(270), 76-79.

Chiumenti, A., Chiumenti, R., Diaz, L.F., Savage, G.M., Eggerth, L.L. and Goldstein, N., 2005. Modern Composting Technologies. JG Press, Emmaus, USA.

Chynoweth, D.P., Owens, J., Okeefe, D., Earle, J.F.K., Bosch, G. and Legrand, R., 1992. Sequential Batch Anaerobic Composting of the Organic Fraction of Municipal Solid-Waste. Water Science and Technology 25 (7), 327-339.

Crawford, J.H., 1983. Composting of Agricultural Wastes-A Review. Process Biochemistry 18, 14-18.

de Bertoldi, M., 1998. Composting in the European Union. Biocycle 39 (6), 74-75.

Debaere, L. and Verstraete, W., 1984. High-Rate Anaerobic Composting with Biogas Recovery. Biocycle 25 (2), 30-31.

Diaz, L.F. and Eggerth, L., 2003. Biological treatment of solid wastes in economically developing countries. In: Proceedings of the Fourth International Conference of ORBIT Association on Biological Processing of Organics: Advances for a Sustainable Society, 30th April-2 May, 2003, Perth, Australia, 14-23.

Eftoda, G. and McCartney, D., 2004. Determining the critical bulking agent requirement for municipal biosolids composting. Compost Science & Utilization 12 (3), 208-218.

Goldstein, J., Rynk, R. and Goldstein, N., 2003. 15 trends in composting and organics recycling. Biocycle 44 (4), 64-66.

Hamelers, H.V.M., Veeken, A.H.M. and Rulkens, W.H., 2003. Design methodology for sustainable organic waste treatment systems. In: Proceedings of the Fourth International Conference of ORBIT Association on Biological Processing of Organics: Advances for a Sustainable Society, 30th April-2 May, 2003, Perth, Australia, 34-.

Haug, R.T., 1993. The practical handbook of compost engineering. Lewis Publishers, Boca Raton, Florida, USA.

Hogg, D., 2004 Costs and benefits of bioprocesses in waste management. Resource recovery and reuse in organic solid waste management., P. Lens, Hamelers, B.V.F., Hoitink, H.A.J. and Bidlingmaier, W., 2004 , . ed., Integrated Environmental Technology Series, IWA, London, England, 95-121

Holland, F. and Proffitt, A., 1998. Overview of composting in the UK. Biocycle 39 (2), 69-71.

Kaufman, S.M., Goldstein, N., Millrath, K. and Themelis, N.J., 2004. The state of garbage in America. Biocycle 45 (1), 31-41.

Kayhanian, M. and Tchobanoglous, G., 1992. Computation of C/N ratios for various organic fractions. Biocycle 33 (5), 58-60.

Kayhanian, M., 1993. Anaerobic Composting for Msw. Biocycle 34 (5), 82-83.

La Brooy, S., Singh, D. and Lawson, J., 2003. The UR-3R facility: a fully integrated approach to municipal solid waste management. In: Proceedings of the Fourth International Conference of ORBIT Association on Biological Processing of Organics: Advances for a Sustainable Society, 30th April-2 May, 2003, Perth, Australia.

Lens, P., Hamelers, B.V.F., Hoitink, H.A.J. and Bidlingmaier, W., 2004 Resource recovery and reuse in organic solid waste management. Integrated Environmental Technology Series, IWA, London, England.

Mata-Alvarez, J., 2002. The biomethanisation of the organic fraction of municipal solid waste. Water 21(October 2002), 59-61.

Mata-Alvarez, J., 2003 Biomethanization of the organic fraction of municipal solid wastes. IWA, London, UK.

Mathur, S.P., N.K., P. and M.P., L., 1990. Static pile, passive aeration composting of manure slurries using peat as a bulking agent. Biological Wastes 34, 323-333.

Metcalf and Eddy, 1991. Wastewater Engineering: Treatment Disposal and Reuse. (3rd edition). McGraw-Hill Inc, New York, USA.

Minnich, J. and Hunt, M., 1979. The Rodale Guide to Composting. Rodale Press, Emmaus, USA.

Mueller, H., Schmidt, O., Daxl, A. and Bergmair, J., 2003. 3A-biogas; three step fermentation of solid state biowaste for biogas production and sanitation. In: Proceedings of the Fourth International Conference of ORBIT Association on Biological Processing of Organics: Advances for a Sustainable Society, 30th April-2 May, 2003, Perth, Australia, 327-332.

Patni, N.K. and Kinsman, R.G., 1997. Composting of dilute manure slurries to reduce bulk by water evaporation. In: ASAE Annual International Meeting, August 10-14, 1997, Minneapolis, Minnesota, USA.

Rynk, R., 1992 On-farm composting handbook. NRAES, Ithaca, New York USA.

Sadaka, S.S. and Engler, C.R., 2003. Effects of initial total solids on composting of raw manure with biogas recovery. Compost Science & Utilization 11 (4), 361-369.

Sartaj, M.L., Fernandes, L. and Patni, N.K., 1997. Performance of forced, passive, and natural aeration methods for composting manure slurries. Trans. ASAE 40 (2), 457-463.

Shin, H.S., Han, S.K., Song, Y.C. and Lee, C.Y., 2001. Multi-step sequential batch two-phase anaerobic composting of food waste. Environmental Technology 22 (3), 271-279.

Slater, R.A. and Frederickson, J., 2001. Composting municipal waste in the UK: some lessons from Europe. Resources Conservation and Recycling 32 (3-4), 359-374.

Solum, 2007. http://www.solum.com (accessed January, 2007)

Supriyadi, S., Kriwoken, L.K. and Birley, I., 2000. Solid waste management solutions for Semarang, Indonesia. Waste Management & Research 18 (6), 557-566.

Tchobanoglous, G., Theisen, H. and Vigil, S.A., 1993. Integrated solid waste management: engineering principles and management issues. McGraw-Hill, New York, USA.

VanderGheynst, J., Gossett, J. and Walker, L., 1997. High-solids aerobic decomposition: Pilot-scale reactor development and experimentation. Process Biochemistry 32 (5), 361-375.

CHAPTER 2
PHYSICAL MODELLING OF THE COMPOSTING ENVIRONMENT.
Part 1: Reactor systems

2.1 Foreword

We commence our journey proper with a thorough examination of the ways in which people have travelled across, and lingered within, the composting physical modelling world in the past, with a particular interest in their destinations. We will examine how composting experiments have been conducted historically, with the essential question asked being "how relevant are these physical models to the assessment and design of full-scale composting processes?" This will serve as a prelude to assessing reactor performance in simulating the composting environment (chapter 3). In the terms of our conceptual journey, we have left Composton-on-Wye behind, and are heading for the twin cities of St. Physical and Mathmodopolis (Fig. 2.1). In the former, the sole activity is the conduct of small and pilot-scale composting experiments, whilst across the river in the latter, people are concerned with building mathematical models of the composting process. The first stop will be in St. Physical.

This chapter primarily comprises the following journal paper:

> Mason, I.G. & Milke, M.W., 2005. Physical modelling of the composting environment: a review. Part 1: Reactor systems Waste Management 25 (5), 481-500.

The paper covers the literature up to early 2004. An update on significant literature and developments after this time, including some pre-2004 papers discovered subsequently, is given in the afterword (section 2.11). Readers are asked to note that the text may differ from that in the published paper in places and that corrections may have been incorporated.

The second author made editorial comments on various drafts of the journal paper, and in particular contributed valuable suggestions which resulted in the incorporation of discussion within the text as the review proceeded. Otherwise the paper is the sole work of the first author.

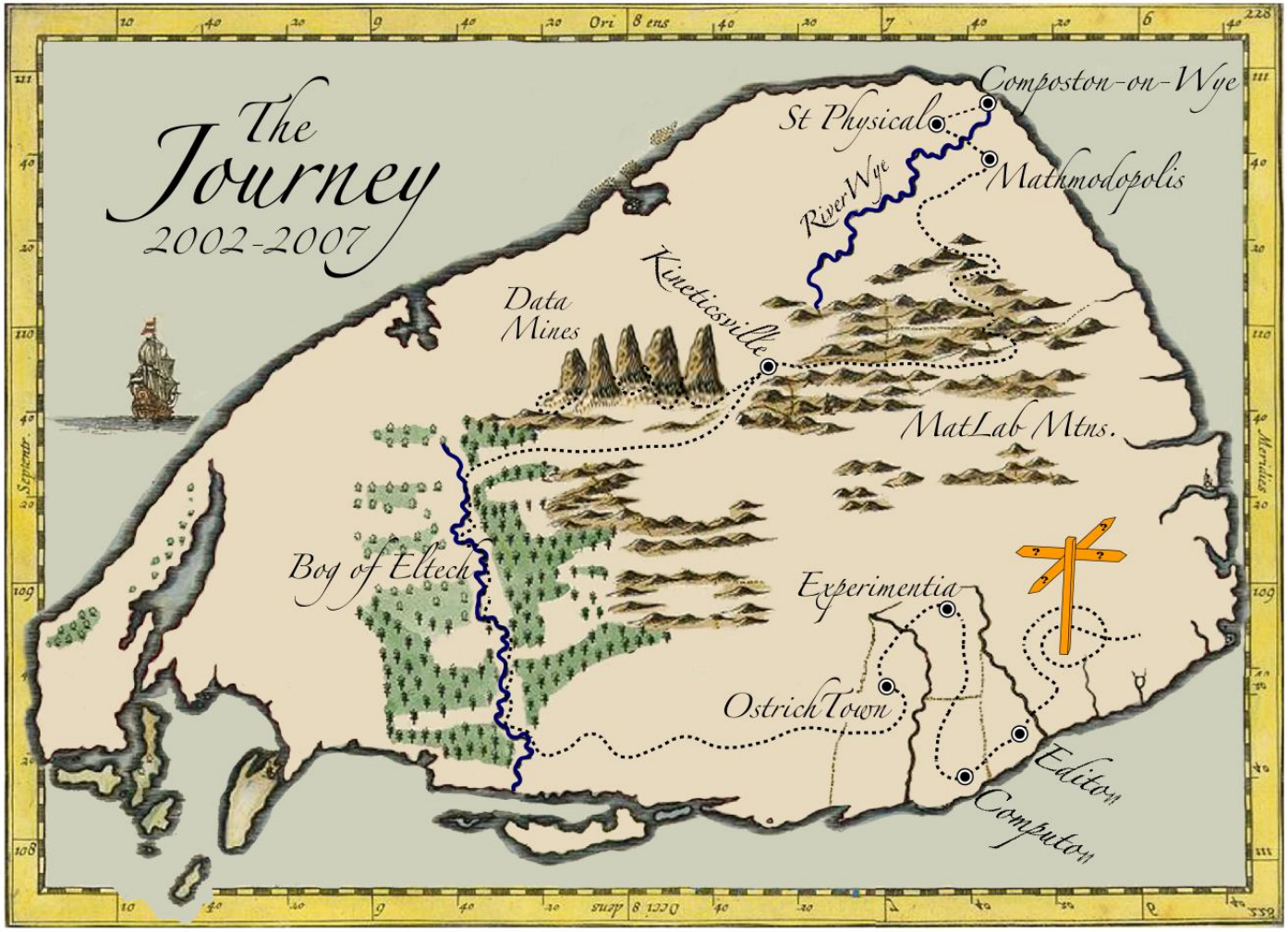

Figure 2.1: The conceptual map of the author's research travels. Our present location is - St. Physical.

2.2 Summary

In this paper, laboratory- and pilot-scale reactors used for investigation of the composting process are described and their characteristics and application reviewed. Reactor types were categorised by the present authors as fixed-temperature, self-heating, controlled temperature difference and controlled heat flux, depending upon the means of management of heat flux through vessel walls. The review indicated that fixed-temperature reactors have significant applications in studying reaction rates and other phenomena, but may self-heat to higher temperatures during the process. Self-heating laboratory-scale reactors, although inexpensive and uncomplicated, were shown to typically suffer from disproportionately large losses through the walls, even with substantial insulation present. At pilot scale however, even moderately insulated self-heating reactors, are able to reproduce wall losses similar to those reported for full-scale systems, and a simple technique for estimation of insulation requirements for self-heating reactors is presented. In contrast, controlled temperature difference and controlled heat flux laboratory reactors can provide spatial temperature differentials similar to those in full-scale systems, and can simulate full-scale wall losses. Surface area to volume ratios, a significant factor in terms of heat loss through vessel walls, were estimated by the present authors at 5.0-88.0 m^2/m^3 for experimental composting reactors and 0.4-3.8 m^2/m^3 for full-scale systems. Non-thermodynamic factors such as compression, sidewall airflow effects, channelling and mixing may affect simulation performance and are discussed. Further work to investigate wall effects in composting reactors, to obtain more data on horizontal temperature profiles and rates of biological heat production, to incorporate compressive effects into experimental reactors and to investigate experimental systems employing natural ventilation is suggested.

2.3 Introduction

Composting has been described as a high-solids aerobic degradation process (VanderGheynst et al., 1997a) and is typically characterised by attainment and extended maintenance of thermophilic temperatures and the production of a stabilised, agriculturally beneficial product (Haug, 1993). Many studies of the composting process have been reported in the literature and authors have frequently chosen to work at either laboratory or pilot scale when conducting their investigations. Experiments at less than full scale can allow a high degree of control and replication, whilst employing relatively small quantities of materials and other resources. However, laboratory and pilot-scale systems may not always represent full-scale

composting conditions, and in particular, the magnitude and duration of temperature and moisture profiles. Full-scale composting experimentation, on the other hand, can be both expensive and difficult to control (Hogan et al., 1989; Chalaux et al., 1991) and may limit replication and reproducibility. In fact a full-scale situation is frequently less than ideal, since operational practices may vary widely, both from site to site and within a site, and are rarely formalised or consistently applied (Hogan et al., 1989). Furthermore, costs and risks associated with process failures can be high (Elwell et al., 1996). Desired procedures and parameters may be modified to suit non-experimental, commercial criteria, whilst finished material may disappear to commercial outlets prior to the completion of the experiment. Quantification of important gas phase parameters, including oxygen, carbon dioxide, water vapour and ammonia concentrations is problematic, particularly in windrow and positive pressure aerated static pile formats. Control of boundary conditions is more difficult or impossible at full scale and raw material type and quality may vary seasonally, making repeatability difficult or impossible.

In laboratory or pilot-scale experimentation, an increase in control over process conditions is typically accompanied by a certain loss of the "reality" which is inherent at full scale. This is particularly relevant to the composting process, where heat transfer and fluid flow considerations are of critical importance. In order to adequately represent the full-scale composting process at laboratory and pilot level, appropriate "scale-down" techniques are therefore required. Thermodynamic factors affecting the generation and transfer of heat in the composting system, are of over-riding importance (Hogan et al., 1989), because of their effect on biological activity, moisture and water vapour transport, natural ventilation, volatilisation, oxygen status and temperature distribution patterns. Therefore, it may be expected that an experimental system capable of simulating the thermodynamic regime of a full-scale composting environment should enable reproduction of many other aspects of full-scale behaviour. Non-thermodynamic factors, such as mixture compression and spatial airflow patterns, can also be important, potentially influencing both the thermodynamic regime and other state variables. In order to simulate a particular type of full-scale system, variations in aeration methods, plus the presence or absence of ventilative heat management (VHM), mixing and in-process moisture addition need to be incorporated at the laboratory- or pilot-scale level.

In this review we propose that, because the terms laboratory-scale and pilot-scale are widely used in the literature, it would be useful to define them in relation to composting experimental practice. Whilst any such categorisation will be somewhat arbitrary, it is

proposed that laboratory-scale composting reactors may be generally identified as those with a volume < 100 l and a surface area to volume (SA:V) ratio > 10:1 , whilst pilot-scale reactors may be classified as those with a volume of 100-2000 l and a SA:V ratio in the range 4-10. In practical terms, reactor volume will have implications in terms of bench space, reactor cost and materials handling issues, whilst the SA:V ratio range will significantly influence the control of heat flux through the reactor walls.

The objective of this review is to examine the physical modelling approaches reported in the literature and to discuss their relevance to composting research, particularly in relation to simulation of the full-scale environment. This discussion has potential implications for planning and conducting composting experiments, for reporting experimental methods and for interpreting, and scaling-up from, laboratory- and pilot-scale information. The paper begins with an outline of the thermodynamic framework for analysis of a composting system, followed by a discussion of the various reactor formats, their applications and limitations. Aeration and physical factors are then addressed, followed by a discussion of how various full-scale composting environments may be simulated at laboratory and pilot scale.

2.4 Thermodynamic framework

The conceptual heat energy balance for a composting system can be written as follows:

$$accumulation = input - output \pm transformation \quad (1)$$

Here, the accumulation term refers to the sensible heating or cooling of the composting material during the process, the inputs are enthalpy in the incoming air and incoming radiation, the outputs are enthalpy in the exit gas, including latent heat of evaporation of water contained in exiting water vapour, and wall losses, and the transformation (reaction) term refers to biologically generated heat (Fig. 2.2). In mathematical terms the expression may be written as follows for a representative volume in which axial variation of conditions in the direction of airflow is minimal

$$\frac{d(mcT)}{dt} = GH_i - GH_o - UA(T - T_a) + \frac{dBVS}{dt} H_c \quad (2)$$

where:	m	mass of composting materials (kg)
	c	specific heat of compost mixture (kJ/kg. ^{o}C)
	T, T_a	temperature of compost mixture and ambient air (^{o}C)
	t	time (s)
	G	mass flux dry air (kg/s)
	$H_{i,o}$	enthalpy of inlet (i) and outlet (o) air(kJ/kg)
	U	overall heat transfer coefficient (kW/m^2. ^{o}C)
	A	heat transfer area (m^2)
	BVS	biodegradable volatile solids (kg)
	H_c	heat of combustion (kJ/kg-BVS removed)

Whilst the term "conduction" is commonly used in the composting literature when referring to wall losses, the heat transfer mechanisms of convection, conduction and radiation should be all considered when assessing heat transport at composting reactor system boundaries. In fact, mathematical models of the composting process typically include the overall heat-transfer coefficient (U), which enables conductive, convective, and radiative heat losses to be lumped together. This approach has the advantage of allowing bulk fluid, or solid, temperatures to be used in heat transfer calculations (see section 2.10). In this paper we have therefore adopted the term convective/conductive/radiative (CCR) when describing heat losses across reactor system boundaries (excluding those arising from advective heat transport), with system boundaries drawn around the outer walls of the composting reactor. The term "conductive" will only be used when quoting directly from published material.

The means of management of the CCR heat flux across reactor walls provides a basis for consideration of the types of reactor used in composting research, and this matter is addressed in the following section.

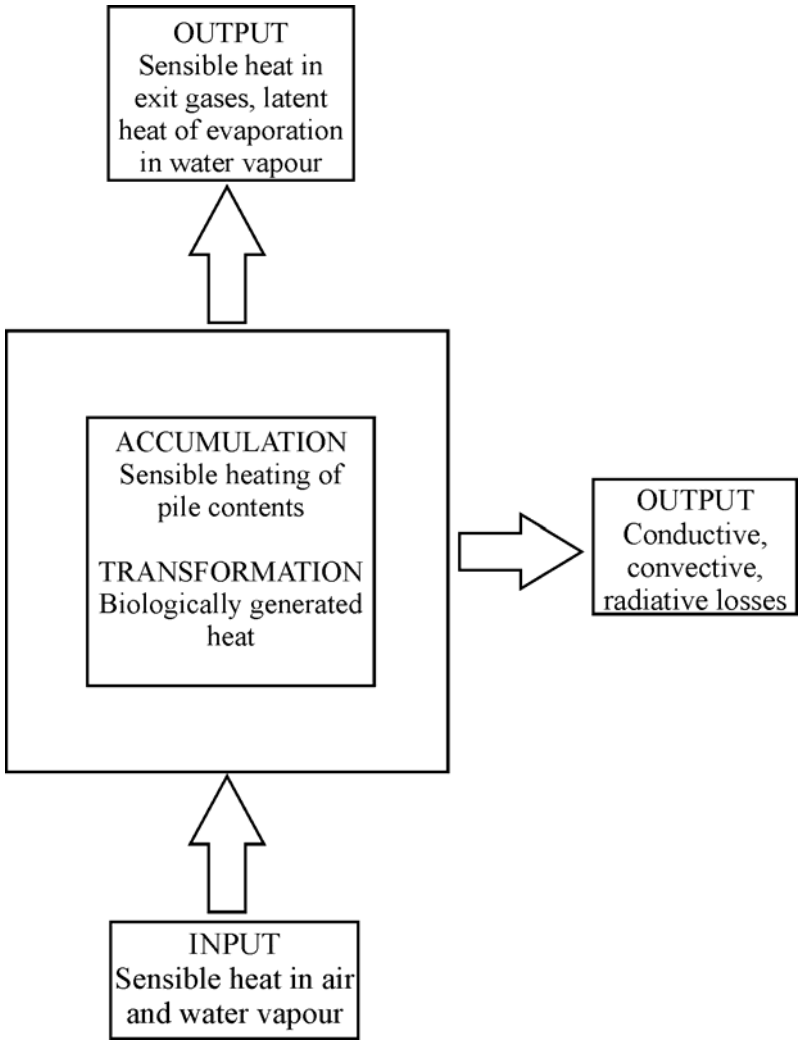

Fig. 2.2: Schematic representation of a composting heat balance.

2.5 Reactor formats

2.5.1 Introduction

A number of approaches to the design and operation of laboratory- and pilot-scale scale composting units may be observed in the literature. Finstein et al. (1983) classified reactors thermodynamically as fixed temperature, self-heating or adiabatic, whilst Ashbolt and Line (1982) further grouped reactors according to whether periodic mixing or agitation was used. In this review, we propose replacement of the category "adiabatic", with the category "controlled temperature differential (CTD)", and we propose the addition of a fourth category termed "controlled heat flux (CHF)". These reactors may be mixed or unmixed. Reactor categories and their formal definitions are presented in table 2.1. In the following sub-sections, reactor capacity and surface area to volume ratio information is given, then reactor formats are described and their applications and limitations discussed. Aeration and physical factors, including mixing, are discussed separately later in the paper.

2.5.2 Reactor capacity and surface area: volume ratios

Full-scale composting reactors and piles normally exceed 5 m^3 in volume, and have relatively low SA:V ratios. Values of SA:V for a range of full-scale systems were estimated by the present authors at between 0.4:1 to 3.8:1 m^2/m^3 (table 2.2). Base or ground contact area was included as part of the total surface area for these calculations, although this should be treated separately from the other surfaces in heat flux calculations.

Table 2.1 Reactor formats and definitions

Format	Definition	Reference
Fixed temperature (FT)	A reactor in which a desired composting temperature is imposed and maintained by means of external heating or cooling	After Campbell et al. (1990a)
Self heating (SH)	A reactor relying solely on microbial heat production to reach and maintain process temperatures and having no temperature control besides some external insulation	After Campbell et al. (1990a)
Controlled temperature difference (CTD)	A reactor relying solely on microbial heat production to reach and maintain process temperatures and where CCR heat losses are controlled by supplying heat to the outer surface of the vessel in order to maintain a pre-determined temperature difference across the composting material and/or the reactor wall(s).	–
Controlled heat flux (CHF)	A reactor relying solely on microbial heat production to reach and maintain process temperatures and where CCR heat losses are controlled by supplying heat to the outer surface of the vessel in order to maintain a pre-determined heat flux across the reactor walls(s)	–

Table 2.2 Surface area to volume ratios in full-scale composting systems

Type	Width or diameter (m)	Height or depth (m)	Length (m)	SA:V (m^2/m^3)
Agitated drum (horizontal flow)	1.8–3.5	–	11–18	2.0–3.8
Tower (vertical flow)	3	8	3	1.6
Bin (horizontal flow)[a]	3.7–6.1	3.0	13.4–122	0.67–1.24
Rotating drum[a]	3.7	–	55.0	1.13
Windrowb/ASP[b,c]	3.0–7.5	1.2–3.0	50.0	1.4–3.5
Siloa	14	16	–	0.4

[a] Dimensions from Haug (1993).

[b] For trapezoidal section piles with ends at 45° slopes.

[c] ASP = aerated static pile.

In contrast, laboratory- and pilot-scale reactors have ranged in volume from 0.4-2000 l (tables 2.3, 2.4). Laboratory-scale experimental units, with volumes typically between 0.4-50 l, were found by the present authors to have SA:V ratios ranging from 14.5:1 to 88.0:1 m^2/m^3 (table 2.3). Thus, laboratory reactor SA:V ratios can be one to two orders of magnitude greater than those for full-scale systems. In comparison, those reactors identified as pilot-scale generally had SA:V ratios ranging from 5.0-12.7 (tables 2.3, 2.4).

Table 2.3 Surface area to volume ratios for selected cylindrical laboratory-and pilot-scale reactors[a]

Surface area to volume ratios for selected cylindrical laboratory-and pilot-scale reactorsa

Diameter (mm)	Height (mm)	Volume (l)	SA:V (m^2/m^3)	Type	Reference
62–75	120	0.4	88.0[b]	CTD	Magalhaes et al. (1993)
100	250	2	48	CTD	After Sikora and Sowers (1985)
100	600	4.7	43.3	SH	After Day et al. (1998)
108	290	2.7	43.9	SH/CTD	After McCartney and Chen (2001)
140	240	3.7	36.9	FT	After Hamelers (1993)
140	500	7.7	32.6	SH	After Loser et al. (1999)
150	230	4.1	35.4	CTD	After Mote and Griffis (1979)
160	190	3.8	35.5	FT	After Ashbolt and Line (1982)
160	420	8.4	29.8	CTD	After Beaudin et al. (1996)
170	220	5	32.6	FT	After Bono et al. (1992)
180	240	6.1	30.6	SH	Namkoong and Hwang (1997)
200	250	7.9	28	CTD	After Sikora et al. (1983)
200	520	16.3	23.8	SH	After Palmisano et al. (1993)
200	600	18.8	23.3	SH	After Seki (2000)
203	310	10	26.2	CTD	Magalhaes et al. (1993)
210	305	10.6	25.6	CTD	After van Bochove et al. (1995)
210	450	15.6	23.5	CHF	After Hogan et al. (1989)
250	455	22.3	20.4	FT	After Komilis and Ham (2000)
250	483[e]	15.9	22.1	SH	After Schulze (1962)
260	300[e]	23.7	20.1	FT	After Bach et al. (1984)
300	400	28.3	18.3	SH	After Bach et al. (1987), and Nakasaki et al. (1987)
300	425[d]	30	18	SH	After VanderGheynst and Lei (2003)
300	470	33.3	17.6	SH	After Schloss et al. (2000)
300	1000	70.7	15.3	CTD	After Lehmann et al. (1999)
300	1200	84.8	15	SH	After Loser et al. (1999)
305	1110	81.1	14.9	SH	After Stombaugh and Nokes (1996)
340	2200	199.7	12.7	SH	After Bari et al. (2000a, 2000b)
381	495	56.4	14.5	SH	After Das et al. (2001)
400	850	119	12.1	SH	After Barrington et al. (2003)
400	1600	201	11.3	SH	After Choi et al. (2001)c
570	760	186	9.8	SH	After Elwell et al. (1994), Hansen et al. (1989), and Hong et al. (1998)
600	800	226	9.2	CTD	After Cronje et al. (2003)
600	2700	760	7.4	SH	After VanderGheynst et al. (1997a)
630	2000	620	7.3	SH	After Sundberg and Jonsson (2003)
660	585[d,e]	200	9.5	SH	After VanderGheynst and Lei (2003)
750	1000	442	7.3	SH	After Leth et al. (2001)
910	930	605	6.5	SH	After Papadimitriou and Balis (1996)
910	1830[e]	1190	5.5	SH	After Freeman and Cawthon (1999)
1800	700	1780	5.1	SH	After Schwab et al. (1994) (Schwab et al., 1994)

[a] Reactors were either described as, or assumed to be, cylindrical; (ii) SA includes all surfaces; (iii) plenum and headspace heights were subtracted where this was information included, otherwise volume and SA:V values were calculated from the overall dimensions.
[b] As reported by the authors.
[c] A horizontally mounted reactor, with an internal auger for materials mixing and transport.
[d] Calculated from diameter and volume data.
[e] Length of a horizontally mounted rotating drum.

Table 2.4 Surface area to volume ratios for selected rectangular section pilot-scale reactors

Width (mm)	Length (mm)	Height (mm)	Volume (l)	SA:V (m^2/m^3)	Type	Reference
950	950	1090	985	6.0	SH	After Pecchia et al. (2002)
1000	1000	1000	1000	6.0	SH	After Seymour et al. (2001)
1000	1000	2000	2000	5.0	SH	After Veeken et al. (2002)
1000	1200	700	840	6.5	SH	After Leth et al. (2001)
1030	1030	1820	1931	5.0	SH	After van Lier et al. (1994)

2.5.3 Fixed-temperature reactors

Fixed-temperature reactors, in which a desired temperature is imposed by means of external heating or cooling and the process is maintained and studied at or about that temperature, have been frequently employed in composting research (table 2.5). Figure 2.3 shows an example of a fixed temperature reactor system, in which the temperature of the reactor, plus parts of the air supply line, was controlled using an incubator. Although criticised for possibly creating artificial or unrealistic conditions (Sikora et al., 1983), these reactors have been used for a broad range of studies (table 2.5).

Table 2.5 Uses of fixed-temperature laboratory-scale reactors

Major focus of study	Reference
Apparatus development	Cappaert et al. (1976), Clark et al. (1977), Ashbolt and Line (1982)
Exit gas composition/odour studies	Michel and Reddy (1998), Kithome et al. (1999), He et al. (2000), Komilis and Ham (2000)
Fate of specific compounds including toxics	Kaplan and Kaplan (1982), Bono et al. (1992), Michel et al. (1995, 1997, 2001), Silviera and Ganho (1995), Itavaara and Vikman (1996), Joyce et al. (1998), Smith et al. (1998)
Microbial enumeration/survival	Strom (1985), Campbell et al. (1990b), Choi and Park (1998)
Mathematical model validation	Kishimoto et al. (1987), Hamelers (1993)
Optimum temperature determination	Clark et al. (1978), Finstein et al. (1983) as cited by Campbell et al. (1990b), Chalaux et al. (1991)
Preparation of compost for further evaluation	Suler and Finstein (1977), Namkoong et al. (1999)
Process evaluation[a]	Suler and Finstein (1977), Clark et al. (1978), Bach et al. (1984), Chalaux et al. (1991), Hamelers (1993), Jackson and Line (1997), Noble et al. (1997), Michel and Reddy (1998), Richard and Walker (1998), Huang et al. (2000)
Substrate compostability[b]	Clark et al. (1978), Ashbolt and Line (1982), Bono et al. (1992), Libmond and Savoie (1993), Michel et al. (1993), Rajbanshi and Inubushi (1997), Razvi and Kramer (1996), Kithome et al. (1999)

[a] Process evaluation is defined as: ''the measurement of reaction rates, kinetic parameters, and mathematical modelling related data''.
[b] Substrate compostability studies are defined as: ''the assessment, by using composting process, of the suitability of raw material mixtures for conversion to compost, including investigation of the effects of feed conditioning and additives''.

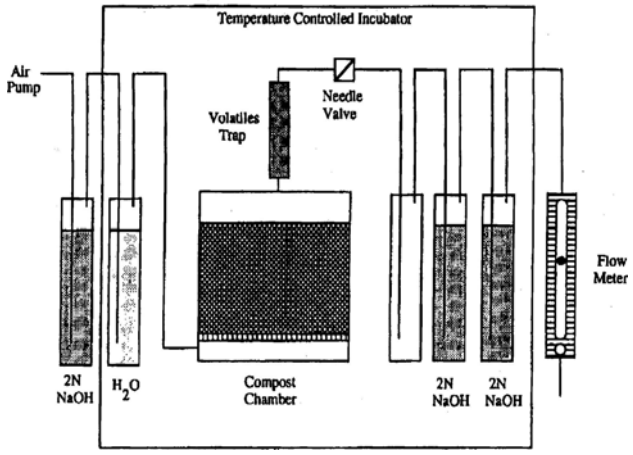

Figure 2.3: Fixed temperature reactor (from Michel et al., 1993)

More recently, several investigators have developed systems in which the imposed temperature may be varied with time according to pre-determined profiles (Michel et al., 1993; Michel et al., 1995; Negro and Solano, 1996; Tseng et al., 1995; Roy et al., 1997; Joyce at al., 1998; Kithome et al., 1999). Such profiles may deliberately mimic the temperature profile of a full-scale system (e.g. Michel et al., 1993; Michel et al., 1995; Kithome et al., 1999). A significant modification to fixed temperature systems was reported by Tseng et al. (1995) who used a series of trays on which thin (ca. 1 cm) layers of composting material, while maintaining relatively fixed temperature, moisture and bulk air oxygen concentrations. This modification permits the determination of the relationships of these variables with other aspects of composting behaviour. In a different approach, Smårs et al., (2001) utilised heating and cooling of separate streams of exit gas from a reactor to maintain temperatures at a fixed level, following a period of initial self-heating. The heated stream, and a proportion of the cooled stream, were reintroduced into the composting reactor in order to control the temperature.

Where the research objective is to take "snapshots" of the composting process at a particular temperature, rather than following the dynamics of the process, then a fixed temperature system is appropriate and offers a relatively cheap option. Relevant applications include the study of reaction rates, temperature optima, microbiological activity, the degradation of specific compounds and the study of exit gas composition. Fixed-temperature reactors may, however, self-heat and cause process temperatures to exceed the imposed temperature. Thus, monitoring of internal temperatures will be important in order to allow any departures to be

taken into account. The apparatus described by Tseng et al. (1995) incorporates such compost temperature monitoring.

2.5.4 Self-heating reactors

A self-heating reactor may be defined as a reactor relying solely on microbial heat production to obtain process temperatures, and having no temperature control besides some external insulation (Campbell et al., 1990a). An example of an insulated pilot-scale self-heating reactor, with a dual flowrate forced aeration system, is shown in figure 2.4. Self-heating reactors have been extensively employed in composting research, especially for process evaluation and substrate compostability applications (table 2.6).

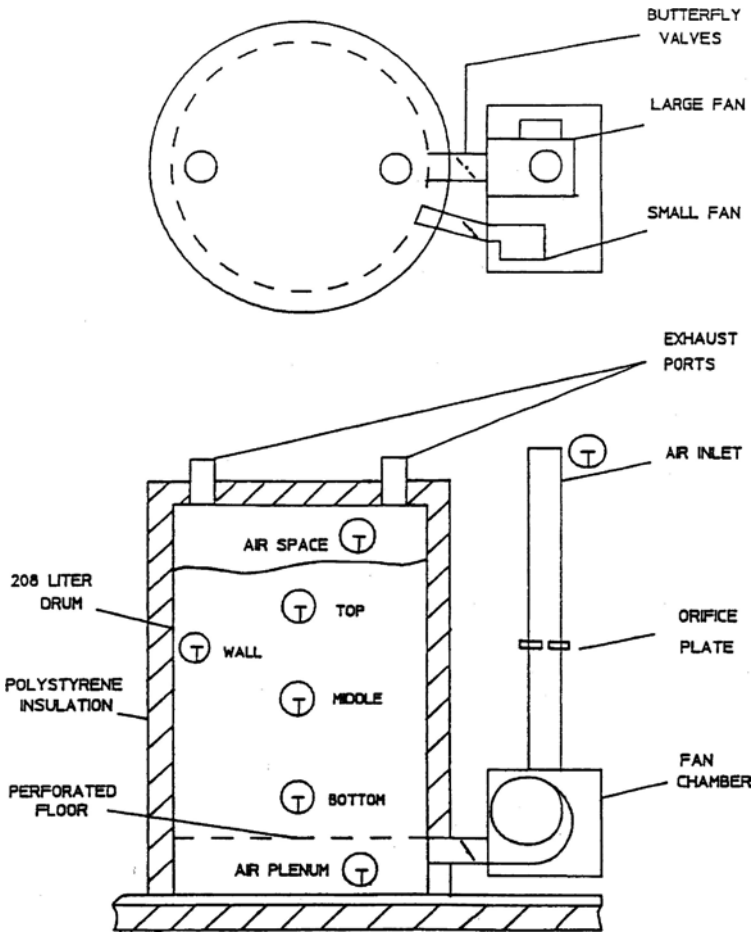

Figure 2.4: Self-heating reactor (from Hansen et al., 1989).

Table 2.6 Uses of self-heating laboratory-and pilot-scale reactors.

Major focus of study	Reference
Apparatus development	Schulze (1962), Hogan et al. (1989)
Exit gas composition/odour studies	Witter and Lopez-Real (1988), Day et al. (1998), Hong et al. (1998), VanderGheynst et al. (1998), Ekinci et al. (1999), Krzymien et al. (1999), Smet et al. (1999), Elwell et al. (2001), Wiles et al. (2001), Elwell et al. (2002), Park et al. (2002), Pecchia et al. (2002)
Fate of specific compounds including toxics	Itavaara and Vikman (1996), Brown et al. (1997), Day et al. (1997),Loser et al. (1999), Korolewicz et al. (2001)
Mathematical model validation	Nakasaki et al. (1987), van Lier et al. (1994), Kaiser (1996), Stombaugh and Nokes (1996), VanderGheynst et al. (1997b), Mohee et al. (1998), Seki (2000)
Microbial enumeration/survival	Herrmann and Shann (1997), Horiuchi et al. (2003), VanderGheynst and Lei (2003)
Preparation of compost for further evaluation	Adani et al. (2001), Dinel et al. (1996), Helfrich et al. (1998), Freeman and Cawthon (1999), Ouatmane et al. (2000)
Process evaluation[a]	Bach et al. (1985, 1987), Lau et al. (1992), Marugg et al. (1993), Elwell et al. (1996), Papadimitriou and Balis (1996), Namkoong and Hwang (1997), VanderGheynst et al. (1997a), Hong et al. (1998), Bari et al. (2000a), Huang et al. (2000), Larsen and McCartney (2000), Schloss et al. (2000), Choi et al. (2001), Seymour et al. (2001), Ekinci et al. (2002), Elwell et al. (2002), Veeken et al. (2002), Sundberg and Jonsson (2003)
Substrate compostability[b]	Deschamps et al. (1979), Campbell et al. (1990a), Lau et al. (1992), Palmisano et al. (1993), Elwell et al. (1994), Schwab et al. (1994), Boelens et al. (1996), Elwell et al. (1996), Brown et al. (1998), Day et al. (1998), Elwell et al. (1998); Laos et al. (1998), Minkara et al. (1998), Sharma et al. (1999), Shaw et al. (1999), Larsen and McCartney (2000), Das et al. (2001), Eiland et al. (2001), Keener et al. (2001), Leth et al. (2001), Barrington et al. (2002), Ekinci et al. (2002), Garcia-Gomez et al. (2002), Keener et al. (2002)

[a] Process evaluation is defined as: ''the measurement of reaction rates, kinetic parameters, and mathematical modelling related data''.

[b] Substrate compostability studies are defined as: ''the assessment, by using a composting process, of the suitability of raw material mixtures for conversion to compost, including investigation of the effects of feed conditioning and additives''.

Both reactor size (tables 2.3, 2.4) and insulation specifications have varied widely. Insulation materials have included glass wool, mineral wool, polystyrene, polyurethane and proprietary materials, with thicknesses ranging from 12.7-120 mm (table 2.7). Additionally, Choi et al. (2001) used sawdust, and subsequently 50 mm urethane sheeting, placed between their reactor and an outer sheet steel cover. Polyurethane panels (thickness not specified) were used to insulate the reactor system described by van Lier et al. (1994). Several other authors have indicated the presence of insulation, but supplied no details of the type or thickness used (Papadimitriou and Balas, 1996; Brown et al, 1998; Freeman and Cawthon, 1999; Smet et al., 1999). The CTD reactor described by Magalhaes et al. (1993) had walls insulated with 2.54 cm fibreglass, plus insulation caps covered with three layers of 1.78 cm foil-faced polystyrene,

whilst the reactor described by Bach et al. (1985), although not insulated directly, was operated inside a box constructed from 400 mm thick "Styrofoam" material.

Table 2.7 Reported insulation data for self-heating reactors

Material	Thickness (mm)	Thermal properties	Reference
Polystyrene	10	—	Park et al. (2002)
—	12.7	10.5 K/W	VanderGheynst et al. (1997a)
			VanderGheynst and Lei (2003)
''Styrofoam''	25.4[a]	—	Schulze (1962)
''Kaiflex''	50	—	Loser et al. (1998)
Polystyrene	50	—	Hansen et al. (1989), Seki (2000)
''Rockwool'' mats	50	—	Leth et al. (2001)
Glass wool	50	—	Deschamps et al. (1979)
	50	0.036 W/m. ^{o}C	Sundberg and Jonsson (2003)
Polystyrene	57	—	Adani et al. (2001)
Polyurethane foam	73	$9.3 \cdot 10^{5}$ cal/s.cm.^{o}C	Hogan et al. (1989)
Expanded polystyrene	75	—	Campbell et al. (1990a)
''Foam insulation''	76	—	Das et al. (2001)
Mineral wool	100	2.5 m^{2} ^{o}C/W	Barrington et al. (2002)
Polyurethane	100	—	Bari et al. (2000a, 2000b)
			Day et al. (1997)
Glass wool	120	0.036 W/m ^{o}C	Sundberg and Jonsson (2003)

[a] reported as 1 in.

In addition to the use of insulation to minimise CCR losses, VHM has been employed to control peak temperatures in self-heating reactors by a number of authors (Nakasaki et al., 1985; Hansen et al., 1989; Herrmann and Shann, 1997; Namkoong and Hwang, 1997; Qiao and Ho, 1997; Smet et al., 1999; Fraser and Lau, 2000; Das et al., 2001; Elwell et al., 2001; Seymour et al., 2001; Das and Tollner., 2003), whilst heat removal from a self-heating composting system, using a water jacket heat exchanger, has also been documented (Viel et al., 1987). Veeken et al. (2001) described an interesting but more complex variation on VHM, in which exit gas was passed over a waterbath, and then reintroduced into the reactor. In several cases authors have controlled the ambient temperature of the reactor environment at 30-40 ^{o}C (Palmisano et al., 1993; Namkoong and Hwang, 1997; Day et al., 1998; Schloss et al., 2000). In contrast to the fixed-temperature mode of operation, self-heating in these reactors raised process temperatures well above these controlled ambient values.

Precise prediction of the temperature/time profile for a given self-heating composting reactor, and therefore CCR losses, requires a dynamic mathematical modelling approach, the

discussion of which is outside the scope of this review. However, an estimate of the requirements for reactor insulation may be made by assuming steady-state conditions, with a peak, or plateau, design temperature; a selected rate of biological heat output; and a specified ratio of CCR losses to biological heat output. The peak or plateau region of the temperature/time curve is important in terms of assessing ability to meet regulatory disinfection related criteria, for example ensuring that temperatures exceed 55 ^{o}C for either 3 or 15 days (USEPA, 1995). Relevant equations for steady-state heat transfer across and from cylinder surfaces are given in the appendix to this chapter (section 2.10). An example of the application of these models to the estimation of CCR losses and insulation requirements is now given. For a 5 mm PVC walled laboratory reactor measuring 210 mm in internal diameter and 450mm in height, and insulated with 73 mm polyurethane, we estimate, assuming the data listed in table 2.8, a ratio of instantaneous CCR losses to peak biological heat production of 18.0%. It can also be shown that in order to limit CCR heat losses to 10% and 5% of the peak biological heat production rate, approximately 180 mm and 620 mm thicknesses of this insulation would be required. In order to assess the validity of this approach over an extended period, the instantaneous calculations were then compared with the ratio of integrated CCR losses to total biological heat production for the same system over 7.8 days using a finite-difference steady-state approach and data of van Lier et al. (1994). The estimated overall ratio in this case was 19.7%, suggesting that the simple instantaneous peak temperature approach will in fact provide a realistic guide to overall CCR loss:biological heat ratios and associated insulation requirements. Peak biological heat values may vary considerably, however, as indicated by a range of 20-28 W/kg-DM reported by Mote and Griffis (1982), and a maximum value of 38 W/kg-VS reported by Harper et al. (1992). Thermal conductivity values for commonly used insulation and reactor construction materials are readily available in the literature (e.g., Mills, 1995). Values of UA and U may also be determined experimentally (e.g., Bach et al., 1987).

Thus, at high SA:V ratios, severe practical limitations are indicated when relying upon insulation alone in order to simulate full-scale heat loss conditions in a self heating reactor. The inability of insulation to practically permit simulation of core conditions at laboratory scale was discussed by Hogan et al. (1989) who estimated that even with 3000 mm of insulation around their 15 l reactor, and with a temperature differential between the vessel surfaces and the surrounding air of 14 ^{o}C, the instantaneous conductive flux would still be 50 times that occurring in a CHF system. At pilot scale however the problem is greatly

diminished and whilst design insulation requirements may sometimes be greater than historically used, they remain practically feasible. The impact of SA:V on insulation design is illustrated in figure 2.5, which shows the estimated range of polyurethane insulation thicknesses required to maintain a steady state CCR loss:biological heat ratio of 5% for cylindrical reactors with SA:V ratios varying between 3-50 under specified conditions. Similar curves may be established for other reactor insulation materials and alternative steady-state conditions.

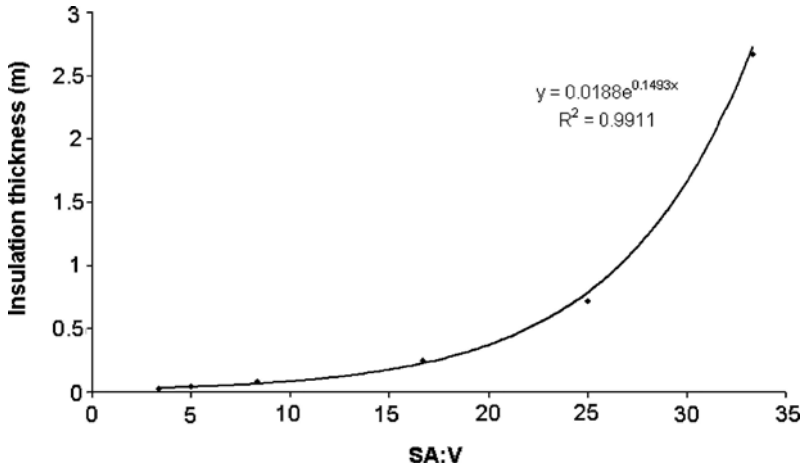

Figure 2.5: Calculated insulation thickness at varying SA:V for self-heating reactors, along with a best fit power law

As a further improvement to the experimental process, we propose that when using pilot-scale, unmixed self-heating reactors, a core volume (figure 2.6) be identified on the basis of horizontal and vertical temperature profiles, plus other parameters such as moisture distribution if possible, indicating similarity of process conditions and degree of stabilisation within that region. This would provide a suitable inner region for sampling and the interpretation of results, and would indicate clearly that material subjected to non-representative conditions outside the core was not included. Whilst the boundaries of the core should be based on experimental data, an indication of the minimum thickness of the insulating layer may be obtained by noting the specification of a 150 mm (6 in.) insulating layer of material such as peat or finished compost for full-scale aerated static piles (Rynk et al., 1992). In terms of horizontal temperature gradients, a difference of about 4 ^{o}C, over an approximately 450 mm radius in an insulated pilot-scale self-heating reactor, was reported by Papadimitriou and Balis (1996), whilst differences closer to 2 ^{o}C were found by both

VanderGheynst et al. (1997a), in the absence of excessive drying and Sundberg and Jonsson (2003), for 300 mm and 315 mm radius pilot-scale reactors respectively. These values are similar to the full-scale reactor differences reported by Finger et al. (1976) and Harper et al. (1992). Schloss et al. (2000) reported a 2 ^{o}C radial temperature difference for an insulated, 150 mm radius, laboratory scale reactor.

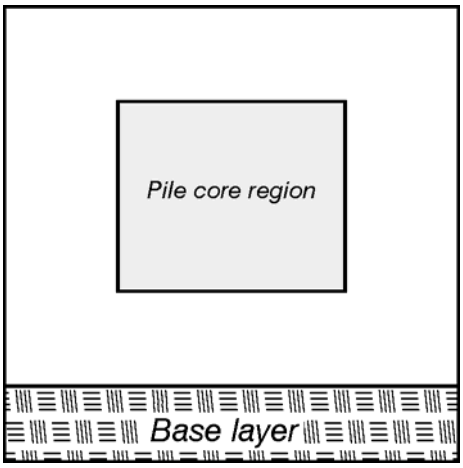

Figure 2.6: Pile core volume schematic

In summary, self-heating reactors at laboratory-scale appear to have limited application, since they have relatively large SA:V ratios, and may therefore suffer from high radial temperature gradients and excessively high CCR losses via reactor walls, even when apparently substantial quantities of insulation are employed. In such cases it may be anticipated that both heat accumulation and the length of the thermophilic phase will be shortened, and also that drying from metabolic heat may be less than would occur at larger scale (Hogan et al., 1989). Self-heating reactors at pilot-scale have SA:V ratios closer to those in full-scale systems and may, with appropriate insulation, be able to provide a suitable thermodynamic environment.

2.5.5 CTD and CHF reactors

The term ‘adiabatic reactor’ has been used to describe a reactor using an external heat source to conserve heat generated by the composting process (Campbell et al., 1990b). The external temperature of the reactor is typically maintained slightly below that of the composting material using a temperature feedback control system, with the objective of maintaining a minimal net outflow of heat. These reactors are not strictly adiabatic, since CCR heat flux is minimised,

rather than prevented, and heat exchange will also occur advectively via the air stream. Control in these systems may be based either on temperature differentials only, or on calculated heat fluxes. Therefore we have proposed the use of two new terms, "controlled temperature differential (CTD)" and "controlled heat flux (CHF)". These reactors have been less widely employed in than either the fixed temperature or self-heating formats, although the reports detailing application of the CTD concept date back to at least 1941 (Walker and Harrison, 1960). Systems described by Walker and Harrison (1960), Mote and Griffis (1979), Sikora et al., (1983), Witter and Lopez-Real (1988), Campbell et al. (1990b), Bernal et al. (1993), Magalhaes et al. (1993), Cook et al. (1994); van Bochove et al. (1995), Cook et al., (1997); Beaudin et al. (1996), Lehmann et al. (1999), Dao et al. (2001), McCartney and Chen (2001), Stocks et al. (2002), Cronje et al. (2003) and Scholwin and Bidlingmaier (2003) fall into the CTD category, whilst the systems of Hogan et al. (1989) and Atkinson et al. (1996a) fall into the CHF classification, (although the latter provided few details of the control procedure used). Although Magalhaes et al. (1993) have used the term "controlled heat flux" in their paper, system control was apparently based on temperature difference only, whilst the system reported by McCartney and Chen (2001) was operated in both self-heating and semi-continuous CTD modes. Apparatus described by Fraser and Lau (2000) and Korner et al. (2003) also appear to be CTD reactors. The system described by Cook et al. (1997), in which the temperature difference was controlled using a waterbath, is shown in figure 2.7.

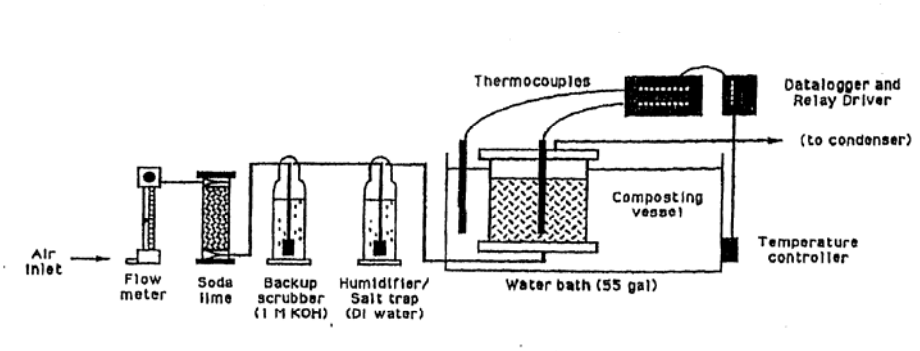

Figure 2.7: CTD reactor using a heated water bath (from Cook et al., 1997)

Reported temperature differentials between the composting material and wall, or insulating medium, for temperature-differential controlled systems have ranged from 0, 0.5 and 0.8 ^{o}C

(Sikora et al., 1983), to 0.25 ± 0.08 ^{o}C (Walker and Harrison, 1960), to 0.5 ^{o}C (Witter and Lopez-Real, 1988; Bernal et al., 1993; McCartney and Chen, 2001), to 1 ^{o}C (Cook et al., 1994; Cronje et al., 2003), to 1- 5 ^{o}C (van Bochove et al., 1995), to 5 ^{o}C (Campbell et al., 1990b), whilst Magalhaes et al. (1993) reported a control temperature differential of 0.001 ^{o}C. Campbell et al. (1990b) cited errors in temperature measurements and the observed gradients within the reactor as dictating the magnitude of the differential. Heat input to the system may arise where the temperature differential is close to zero (Hogan et al. 1989), or lies within the error range of the sensing devices (Currie and Festenstein, 1971; Magalhaes et al., 1993). This phenomenon has been demonstrated for a 0.4 l reactor, and to a lesser extent for a 10 l reactor (figure 2.8).

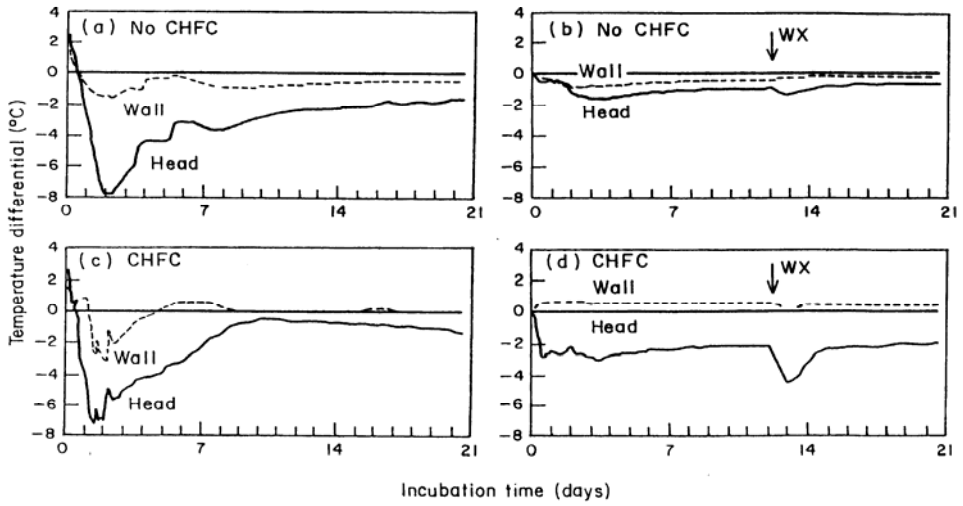

Figure 2.8: Temperature differentials between the compost centre and reactor wall in SH (a, b) and CTD (CHFC) (c, d) modes (from Magalhaes et al., 1993). Positive differentials, indicating wall temperatures exceeding those in the compost centre can be seen in figures c and d. Key: CHFC: controlled temperature differential; WX: water addition

Hogan et al. (1989) and Magalhaes et al. (1993) also demonstrated differences in compost centre temperature profiles between reactors operated in CTD and self-heating modes. For both the 0.4 1 and 10 l capacity vessels used by Magalhaes et al (1993), temperatures reached higher peaks, and remained higher for longer periods with CTD operation. A distinctive high temperature plateau was maintained, for approximately 6 days, in the 10 l reactor (figure 2.9). Additionally, differences in CO_2 production and dry matter loss between the two vessels were less pronounced with CTD operation. Ventilative heat management has been used as an additional temperature control mechanism in CTD systems (Sikora and Sowers, 1985; Beaudin et al., 1996; Fraser and Lau, 2000; Stocks et al., 2002; Cronje et al., 2003). Uses of CTD reactors (table 2.8) have included many of the applications cited for self-heating reactors.

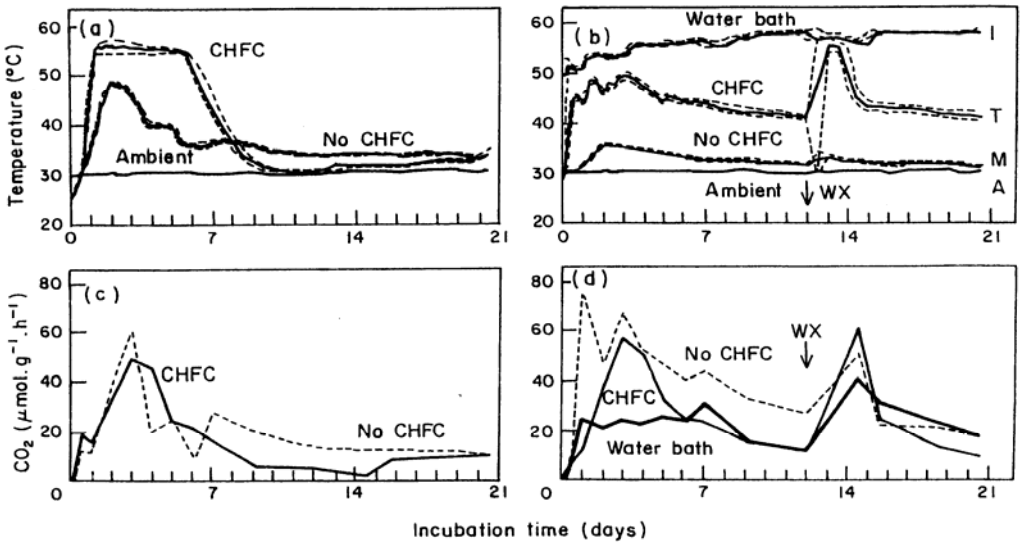

Figure 2.9: CTD (CHFC) vs self heating mode temperature and CO_2 profiles (from Magalhaes et al., 1993). Key: a) and c), 10 l reactor; b) and d), 0.4 l reactor; solid lines: mean values; dotted lines: maximum or minimum values.

In a controlled heat flux system, heat transport rates, rather than temperature differences, provide the basis for system design and operation. Only two CHF systems (Hogan et al., 1989; Atkinson et al., 1996a) appear to have been reported in the literature. The laboratory-scale composting system developed by Hogan et al (1989), was designed to dynamically control CCR losses in combination with deliberate ventilative heat control referenced to a

temperature ceiling. The objective was to mimic the structure of a full-scale system heat balance, as opposed to minimising CCR losses only, with emphasis on an appropriate level of heat removal via the appropriate mechanism. The authors described this system, comprising an insulated 15 l vessel was operated within a laboratory oven maintained at suitable temperatures, as a "composting physical model". Heat fluxes were calculated separately for the cylinder wall and two end plates and then totalled. CCR heat flux was purposely maintained at an essentially constant level, and accounted for 2.4% of the heat evolved over a 10 day period. The horizontal spatial temperature gradient was slight and temperatures in a vertical plane had values similar to those expected at full scale, although the gradient was much steeper. The authors suggested that, given highly humid inlet air, inlet and outlet conditions over a full 2 to 3 m airflow pathway in the field would thus be simulated in the 0.4 m high laboratory core. In preliminary experiments, control based on temperature differentials only was reported to be less than ideal for managing CCR losses, since the fluxes through each of the three segments of the cylinder (side wall and two end plates) were different, depending upon changes in the vertical temperature gradient in the system. In terms of qualitative behaviour, including oxygen and CO_2 concentration profiles, water removal patterns and aeration system operation in response to temperature feedback control, the laboratory CHF and full-scale composting systems showed similar responses. The CHF concept was subsequently employed by Atkinson et al. (1996a) who used a 28 l reactor comprising an inner vessel containing the compost mixture, surrounded by an air-filled outer chamber wrapped with a heating tape. The authors stated that "the outer chamber surface was warmed at a rate comparable to the rate of metabolic heat generation in order to minimise energy loss through the reactor walls (less than 10% of the heat generated)". Ventilative heat management was also used in this system in order to limit temperatures to < 55 ^{o}C, although the data presented indicated some degree of overshoot above this limit. Uses of CHF reactors to date have been focused on apparatus development and substrate degradability studies (table 2.8).

The introduction of reactors incorporating control of either temperature differentials or CCR heat flux via the maintenance of small, outward, negative temperature gradients across the reactor walls has provided the opportunity to more closely simulate the dynamics of the full-scale composting process at laboratory scale. One of the issues surrounding the design and operation of both CTD and CHF reactors is the maintenance of appropriate boundary condition values for temperature and we suggest that defining appropriate temperature

differentials and horizontal gradients more extensively is an area worthy of further research. Evenness of external heating is also an important consideration in CTD and CHF systems. The earlier CTD reactors were completely immersed in water (Walker and Harrison, 1960; Mote and Griffis, 1979; Sikora et al., 1983; Cook et al., 1994), whilst those of van Bochove et al. (1995), Lehmann et al. (1999) and Scholwin and Bidlingmaier (2003) were reported to be surrounded by a heating jacket. Reactors described by McCartney and Chen (2001) were placed in an insulated container, within a temperature-controlled chamber. In both reported CHF reactor systems, the air temperature surrounding the reactor vessel was controlled, in which case a single "ambient" temperature at all surfaces may be anticipated. In other CTD systems either heating tape (Campbell et al., 1990b; Magalhaes et al., 1993; Stocks et al., 2002; Cronje et al., 2003), or a coil through which heated water was circulated (Beaudin et al., 1996), were wrapped around all or part of the vessel. Where heating tapes or coils are used even distribution of external heating may be an issue. Both Stocks et al. (2002) and Cronje et al. (2003) wrapped aluminium foil around the reactor surfaces in order to address this issue. However, vertical temperature gradients can still occur in either type of reactor and these should be noted. Cronje et al. (2003) also provided controlled heating for the base and head-space surfaces in order to prevent internal condensation, and consequent mass balance inaccuracies, in their reactor.

Table 2.8 Uses of CTD and CHF laboratory-scale reactors

Type	Major focus of study	Reference
CTD	Apparatus development	Mote and Griffis (1979), Sikora et al. (1983), Magalhaes et al. (1993), Cook et al. (1994), McCartney and Chen (2001)
	Compression effects	McCartney and Chen (2001)
	Exit gas composition/odour studies	Fraser and Lau (2000), Cronje et al. (2003), Korner et al. (2003)
	Fate of specific compounds including toxics	Beaudin et al. (1996), Lehmann et al. (1999)
	Mathematical model validation	Cronje et al. (2003), Scholwin and Bidlingmaier (2003)
	Preparation of compost for further evaluation	Campbell et al. (1990b), Dao et al. (2001)
	Process evaluation[a]	Walker and Harrison (1960), Sikora and Sowers (1985), van Bochove et al. (1995), McCartney and Chen (2001), Korner et al. (2003)
	Substrate compostability[b]	Campbell et al. (1990b), Stocks et al. (2002), Cronje et al. (2003)
CHF	Apparatus development	Hogan et al. (1989)
	Substrate degradability[c]	Atkinson et al. (1996a, 1996b, 1996c)

[a] Process evaluation is defined as: ''the measurement of reaction rates, kinetic parameters, and mathematical modelling related data''.

[b] Substrate compostability studies are defined as: ''the assessment, by using a composting process, of the suitability of raw material mixtures for conversion to compost, including investigation of the effects of feed conditioning and additives''.

[c] Substrate degradability assessment is defined as: ''the measurement of the fraction of VS degraded during a composting process''.

The difference between CTD and CHF reactors is simply a matter of the way control is implemented, with the former using temperature differentials and the latter calculated heat fluxes. Hogan et al. (1989) indicated that reactor operation in the CTD mode was less than ideal for controlling CCR losses and that this was better achieved when the calculated fluxes, rather than temperature differentials only, were used as the basis for controlling the external temperature. Given that computer-based control systems are now widely available and are relatively inexpensive, the use of CHF laboratory systems should become increasingly feasible.

2.6 Reactor aeration

The majority of laboratory-scale reactors have utilised forced aeration. Fixed aeration rates have been most frequently reported, although dual aeration systems, to facilitate VHM, have also been used. Aeration has typically been continuous and in an upflow direction. Intermittent aeration strategies for pilot-scale reactors were reported by Keener et al. (2001), whilst downflow and alternating flow direction experiments were described by Bari et al. (2000a). These strategies will therefore potentially simulate a range of full-scale forced-aeration regimes. At appropriate rates, natural ventilation might also be approximated. In view of the relatively small number of published laboratory- and pilot-scale studies involving aeration by natural ventilation (Barrington et al., 2002; Veeken et al., 2002; Barrington et al., 2003), further work in this area would be valuable. A more detailed discussion of aeration rates and their significance is presented in part 2 of this paper (chapter 3).

Many laboratory-scale composting systems operating with forced aeration have utilised pre-conditioned inlet air. Investigators have commonly humidified the airstream in order to prevent excessive drying of the composting mass (Sikora et al., 1983; Bach et al., 1984; Strom, 1985; Hogan et al., 1989; Campbell et al., 1990a; Chalaux et al., 1991; Bono et al., 1992; Magalhaes et al. 1993; Michel et al., 1993; Palmisano et al., 1993; Stegemann et al., 1993; Cook et al., 1994; Michel et al., 1995; van Bochove et al. 1995; Qiao and Ho, 1997; Cook et al., 1997; VanderGheynst et al., 1997a; Day et al 1998; Michel and Reddy, 1998; van der Zee et al., 1998; Loser et al., 1999; Lehmann et al., 1999; Komilis and Ham, 2000; Larsen and McCartney, 2000; Schloss et al., 2000; Hwang et al., 2001; Michel et al., 2001; Garcia-Gomez et al., 2002; Cronje et al., 2003; Scholwin and Bidlingmaier, 2003; VanderGheynst and Lei, 2003). Humidified inlet air may not be fully saturated however, as shown by Cronje

et al. (2003) who reported approximately 50% relative humidity in an airstream which had been bubbled through a water cylinder at 40 ^{o}C. In addition, authors have removed incoming carbon dioxide in order to facilitate carbon dioxide generation measurements (Mote and Griffis, 1979; Sikora et al., 1983; Sikora and Sowers, 1985; Campbell et al., 1990a; Chalaux et al., 1991; Bono et al., 1992; Magalhaes et al., 1993; Michel et al., 1993; van Bochove et al. 1995; Cook et al., 1997; Komilis and Ham, 2000), removed inlet ammonia (Mote and Griffis, 1979; Sikora et al., 1983; van Bochove et al. 1995)(van Bochove et al., 1995), stripped out volatile organic compounds (Magalhaes et al. 1993; Komilis and Ham 2000) and controlled the air temperature to that of the system (Sikora et al., 1983; Chalaux et al., 1991; van Bochove et al. 1995; Larsen and McCartney, 2000; Garcia-Gomez et al., 2002). In one case oxygen was replenished using a closed-circuit respirometer-like arrangement (Mote and Griffis, 1979), whilst Michel and Reddy (1998) used a synthetic inlet gas comprising O_2 plus N_2. Hogan et al. (1989) adjusted incoming air to 18 ^{o}C and 100% RH, whilst in a laboratory system used to investigate spontaneous ignition of hay, inlet air humidity was adjusted to a range of values using appropriate electrolyte solutions (Currie and Festenstein, 1971). Pilot-scale, self-heating, systems have typically not utilised pre-conditioned inlet air, although VanderGheynst et al. (1997a) both humidified and heated the airstream used in their experiments.

The widespread use of inlet air conditioning for laboratory-scale reactors has an important function in eliminating excessive drying effects as well as facilitating the monitoring of various gas phase constituents. Whilst this strategy is appropriate for scientific investigation purposes, interpretation of results must consider the varying temperature and humidity of inlet air when assessing likely effects at full scale.

2.7 Physical considerations

Laboratory- and pilot-scale reactors typically reproduce neither the vertical height nor the horizontal dimensions found in full-scale composting systems. In this regard, materials compression, airflow wall effects and airflow channelling through the matrix, analogous to macropore flow in soils, merit consideration.

As pointed out by McCartney and Chen (2001), even the more advanced laboratory-scale reactors have not simulated the compressive loads experienced in full-scale composting piles. In general terms, inter-particle bridging effects between granular materials within a column can result in incomplete transmission of the static load to material at the base of the column (Shamlou, 1988). For a packed material height to column diameter ratio of 1:1 for example, approximately 75% of the load due to the height of material can be expected, with only relatively minor increases in the absolute load "seen" at the base occurring once the height:diameter ratio exceeds 4:1. This phenomenon may be expected to apply to columns of composting materials, and would indicate that laboratory- or pilot-scale simulation of compressive loads is unlikely to be achieved simply by reproducing the full-scale height. In order to address the issue of compressive loading, Larsen and McCartney (2000) applied a 12 kg weight to composting material contained within a laboratory-scale reactor in order to simulate a load of 12.8 kPa, which they reported would be experienced at the bottom of a 3.7 m high windrow. Subsequently, McCartney and Chen (2001) reported the construction of a biological load cell, which they termed a "biocell", enabling a range of compressive loads to be applied. In a different approach, Veeken et al. (2002) conducted pilot-scale experiments using a range of initial mixture bulk densities.

Attention to compression and airflow issues in laboratory-scale reactors will further enhance the ability to simulate full-scale composting behaviour. Variations in bulk density have been incorporated into several mathematical models of the composting process (Keener et al., 1993; van Lier et al., 1994; Das and Keener, 1997) and into process design methods (Veeken et al., 2003). In addition, the relationship between height and substrate degradation rates has been investigated experimentally by Bari et al. (2000b). We suggest that this is an important area for future laboratory research, given the range of reactor and pile heights that can occur in practice.

Preferential sidewall airflow may occur in small-scale reactor systems, due to variations in behaviour at the mixture/wall interface. The effects depend on the ratio of container diameter (D) to particle diameter (d_p) and the Reynolds number (Re). Cohen and Metzner (1981) suggested that to minimise wall effects D/d_p should exceed 30 for Newtonian fluids, whilst Dullien (1992) reported that the wall effect is generally concluded to be negligible if $D/d_p > 10$. The latter ratio has been confirmed in a more recent review by Eisfeld and Schnitzlein (2001), who also showed that for spherical and cylindrical packings where $D/d_p < 10$, an

increase in pressure drop has been reported at low values of Re, whilst for higher Re values, a decrease has been shown. However a report by Gostomski and Liaw (2001) questioned this ratio for a compost-packed biofilter and indicated that pressure drops can be affected at much higher D/d_p values. Additionally, they demonstrated a non-linear relationship between compost permeability and velocity, and showed that pressure drop readings can be distorted by water holdup at the bottom of the reactor.

An examination of the relevant particle sizes for composting can help in understanding the reactor diameter needed to minimise sidewall airflow effects. Reported particle size data for conventionally shredded green (yard) waste has indicated the presence of material with dimensions ranging from < 2.5-100 mm, with a dominance in the 10-25 mm range (Hannon and Mason, 2003), whilst an analysis of food residuals/yard trimmings and chicken manure showed a majority of material < 9.5 mm in size, with substantial quantities in the 9.5-19.5 mm range and typically < 9% in the > 19.5 mm range (Elwell et al., 1996). Given pre-sorting, or additional shredding, of green waste, particle dimensions of up to 25-50 mm may be anticipated in practice. With significant quantities of particles of 20 mm in size, specification of minimum reactor diameters of 200 mm would be prudent in order to reduce sidewall air effects, given a critical D/d_p ratio of 10:1. As shown in table 2.3, this diameter has been equalled, or exceeded, in a majority of experimental reactors to date. However, further research in this area is suggested.

The possibility of side-wall effects in a laboratory-scale composting column was addressed by Scholwin and Bidlingmaier (2003), who placed four PVC rings, with the same external diameter as the internal diameter of the column, at equally spaced intervals inside their reactor. However, gas tracer studies on a 300 l pilot-scale column (diameter not given), containing a mixture of wastewater treatment sludge and pine bark chips, showed no evidence of short circuiting, and furthermore, that airflow could be satisfactorily described using a plug flow model with dispersion (Tremier and de Guardia, 2003). Further investigation is required on this topic, in particular to understand the effects of non-homogenous irregularly shaped particles typically present in initial compost mixtures. In addition, channelling of airflow through larger fissures in the composting matrix is a phenomenon sometimes observed in full-scale systems. This could be difficult to account for at smaller scales but may be important when translating results to full scale.

Laboratory- and pilot-scale reactor procedures typically do not include mixing and in this case simulate the operation of static bed reactors, such as aerated static piles, passively aerated piles or non-agitated tower reactors. Where periodic turning of the composting mixture has been used, operation of turned windrows and agitated in-vessel systems is simulated. Turning methods at laboratory- and pilot-scale have included the use of horizontally mounted rotating drum reactors (Schulze, 1962; Palmisano et al., 1993; Schwab et al., 1994; Crohn and Bishop, 1999; VanderGheynst and Lei, 2003); internally mounted stirrer blades (Mote and Griffis, 1979; Ashbolt and Line, 1982; He et al., 2000), manual mixing (Bach et al., 1985; Papadimitriou and Balis, 1996; Herrmann and Shann, 1997; Lehmann et al., 1999; Smars et al., 2001); or contents removal, external mixing and re-loading (Hansen et al., 1989; Elwell et al., 1994; Smet et al., 1999; Schloss et al., 2000; Das and Tollner, 2003). The pilot-scale reactor described by Choi et al. (2001) employed an internal auger for both mixing and material transport, whilst the contents of the 2 l reactors described by Namkoong et al. (1999) were mixed using a glass rod. As well as increasing mixture free air space and providing an opportunity for re-wetting, turning will, as has been pointed out by the latter authors, assist in the prevention of channelling. For further discussion of mixing in composting reactors the reader is referred to Petiot and de Guardia (2004).

2.8 Reactor selection for composting environment simulation

The choice of which laboratory- or pilot-scale system to use will vary according to the aims of each investigation. In some cases, specific aspects of the composting process, such as the potential compostability of new raw material/amendment/bulking agent combinations, the reaction kinetics of a substrate, or the growth rate of a particular micro-organism, will require elucidation under closely controlled conditions. Here, fixed-temperature systems are appropriate. In other cases, researchers will wish to conduct investigations with a view to relating the results to full-scale operations. For example, the ability of the overall process sequence to stabilise the substrate, or the length of time over which temperatures exceeding a specified limit are maintained, may need to be established.

When investigating the composting process in relation to dynamic full-scale performance, self-heating (pilot-scale), CTD and CHF reactors may be considered. In general terms, the level of CCR losses allowed, the aeration method selected, the presence or absence of VHM

and mixing and the use of in-process moisture addition, will then determine the type of full-scale environment most closely simulated, and the degree to which full-scale process behaviour is likely to be reproduced. In order to simulate conditions within an aerated static pile, forced aeration with VHM and appropriate control of CCR losses would be required, however mixing would not be needed. Aeration may also be intermittent and it should be noted that natural aeration may occur during the fan-off periods. Alternatively, dynamic conditions within a windrow may be partially simulated using natural aeration, controlled CCR losses and by incorporating mixing. Compression, particle size and side-wall issues also merit consideration. Selected full-scale reactor characteristics relevant to laboratory and pilot-scale design are listed in table 2.9 and these may also be used to ascertain which full-scale system characteristics are most closely reproduced in existing experimental reactors.

Table 2.9 Composting system attributes for consideration in scaled-down reactors

System to be simulated	Aeration	VHM[b]	Mixing[b]	Moisture addition[b]	Comments
Agitated bin/tunnel	Forced	O	Y	O	–
Tower	Natural or forced	O	O	O	–
Drum	Forced	O	Y	O	Rotating or internally mixed
Passive pile	Natural	N	N	O	–
Windrow	Natural	N	Y	O	–
ASP[a]	Forced	Y	N	O	–

[a] ASP = aerated static pile.
[b] Y=Yes; N= no; O = optional.

The pilot-scale reactor of VanderGhenyst et al. (1997a) was designed to simulate conditions within an aerated static bed system. However in most cases, the type of composting environment simulated must be inferred from the information reported by researchers. It is suggested that greater attention to the reporting of reactor characteristics, and associated operational details, would thus be most helpful in aiding the interpretation of experimental findings in the future.

2.9 Conclusions

1. Laboratory- and pilot-scale reactors may be categorised as fixed temperature, self-heating, controlled temperature difference and controlled heat flux, depending upon the means of management of heat flux through vessel walls.

2. Surface area:volume ratios for experimental composting reactors range from 5.0 to 88.0 m^2/m^3 whilst the range for full scale systems is 0.4 to 3.8 m^2/m^3.

3. Fixed temperature reactors have useful applications in studying reaction rates, temperature optima, microbial diversity and the effect of process additives; however they may self-heat to higher temperatures during the process and may not simulate dynamic process conditions.

4. Self-heating, laboratory-scale, reactors may involve significant convective/conductive/radiative losses, even with insulation present. However, at pilot-scale, convective/conductive/radiative losses may be limited to full-scale levels using moderate quantities of insulation.

5. Controlled temperature difference and controlled heat flux laboratory reactors allow temperature differences and convective/conductive/radiative heat fluxes to be controlled to levels close to those occurring in full-scale systems.

6. Compression effects in laboratory- and pilot-scale composting reactors may not be simulated by height alone, due to inter-particle bridging effects. Preferential airflow at reactor walls may be significant where reactor to particle diameter ratios are less than 10:1.

7. Future work is suggested to investigate wall effects in composting reactors, to obtain more data on horizontal temperature profiles and rates of biological heat production, to incorporate compressive effects into experimental reactors and to investigate experimental systems employing natural ventilation.

2.10 Appendix. (adapted from Mills, 1995):

Steady state heat transfer across a wall may be modelled by:

$$Q = UA(T_o - T_i) \tag{1}$$

For a two-component wall, the UA product may be determined from:

$$\frac{1}{UA} = \frac{1}{h_{c,i}A} + \frac{X_A}{k_A A} + \frac{X_B}{k_B A} + \frac{1}{(h_{c,o} + h_r)A} \tag{2}$$

For a cylinder with a two-component wall, it can be shown that:

$$\frac{1}{UA} = \frac{1}{2\pi r_i L h_{c,i}} + \frac{\ln(r_2 / r_1)}{2\pi k_A L} + \frac{\ln(r_3 / r_2)}{2\pi k_B L} + \frac{1}{2\pi r_o L(h_{c,o} + h_r)} \tag{3}$$

where: Q heat flux (watts)

U overall heat transfer coefficient (watts/m^2.C)

A surface area (m^2)

T temperature (^{o}C)

h_c convective heat transfer co-efficient (watts/m^2. ^{o}C)

X thickness (m)

k thermal conductivity (watts/m. ^{o}C)

h_r radiative heat transfer co-efficient (watts/m^2. ^{o}C)

r_i radius (m)

L length (or height) of cylinder (m)

i,o inside and outside (NB: inner and outer locations are those in the bulk fluid immediately adjacent to, but not within, the wall boundary layers)

A,B types of materials

1,2,3 inner to outer radii respectively.

2.11 Afterword

This section presents several pre-2004 papers missed during the first round of research, and then selected papers of interest published up until 2006. No attempt has been made to comprehensively update the literature for the 2004-2006 period, on account of the very large number of papers published.

Two additional laboratory-scale fixed temperature systems were found in the pre-2004 literature. Hamoda et al. (1998) used 2 l Erlenmeyer flasks immersed in a water bath, and supplied with moist air. This system was used for kinetics studies at 20, 40 and 60 ^{o}C. A very small fixed temperature reactor, used for plastics degradation studies, was reported by Ohtaki and Nakasaki (2000). Glass tubes, 45 mm in diameter and 100 mm (SA:V 109 m^{-1}) containing a sample weight of 10-14 g were placed in incubator at 50 ^{o}C. Moisture saturated air, stripped of CO_2, was supplied at aeration rate estimated by the present author at 0.40-0.56 l/min.kg-TS. Fixed temperature experiments continued to be reported in the 2004-2006 period. Cronje et al. (2004) employed a 3 l reactor for kinetics investigations over 30 h on a pig manure/straw mixture. Another very small fixed temperature reactor system, this time with tubes of 118 ml capacity, was used by Sundberg et al. (2004) for kinetics studies, over 24 h. This system was operated in batch mode with no through airflow, air being replaced manually when the CO_2 concentration in the headspace exceeded 15%. Useful information concerning in-compost temperatures in a fixed temperature system operated at 55 ^{o}C was reported by Zavala et al. (2004). At maximum oxygen consumption, temperatures within the 330-390 g samples rose above 55 ^{o}C by 1.3 and 5.5 ^{o}C, but for relatively short periods of time. Tremier et al., (2005a) utilised a 10 l glass cell, supplied with humidified air for a study of composting kinetics, using wastewater treatment plant sludge and pine bark. Yamada and Kawase (2006) used 4 l and 20 l equal diameter reactors for kinetics studies on waste activated sludge and sawdust. Heating was achieved using a ribbon heater, giving a wall temperature of 50 ^{o}C and airflows of 0, 0.4, 1.0, 2.0, 3.0, and 4.0 l/kg.min were utilised. Komilis (2006) and Komilis and Ham (2006) reported fixed temperature experiments in a 25 l stainless steel reactor located in incubator at 52 ^{o}C.

Several additional self-heating reactors of both laboratory- and pilot-scale were found in the pre-2004 literature and a number of interesting systems were reported in the 2004-2006 period. At laboratory scale, Bengtsson et al. (1998) utilised vertical cylindrical reactors made from galvanised sheet iron 400 mm in diameter and 880 mm in height, with a working

volume of 75 l (SA:V 12.3), for compostability studies on oily sludge. Mixing was achieved by rolling the barrels weekly. Nakasaki et al. (1998) and Nakasaki and Ohtaki (2002) used a 3.6 l stainless steel apparatus enclosed in a Styrofoam box for kinetic studies, using dog food and sawdust as the initial mixture. Their low and high aeration rates, as estimated by the present author, were 0.22 and 2.2 l/min.kg-TS respectively. Several other authors reported systems in the 1.5-25 l range. Leiva et al. (2003) used 1.5 and 4.5 Dewar flasks, and a 25 l reactor, for municipal sludge compostability studies, whilst Lhadi et al. (2004) used a 12.6 l (SA:V 25) PVC reactor "covered with insulating material" for compostability studies on separated MSW mixed with poultry manure. At larger scale, a 300 l stainless steel self-heating reactor (SA:V 8.2) insulated with 100 mm polyurethane was reported by Tremier et al. (2005b) and de Guardia et al. (2006). An interesting reactor, relevant to the increasing number of horizontal, mixed, full-scale reactors was described Alkoaik and Ghaly (2005). These authors used a 16.8 l laboratory-scale horizontal reactor (SA:V 23.6) for compostability studies on greenhouse tomato residues and dairy manure. Mixing was achieved using a rotating horizontal shaft fitted with bolts, and airflow introduced from beneath. Insulation comprised 38.1 mm of fibreglass around the tubular section and 38.1 mm Styrofoam at the two ends.

The largest of the pilot-scale reactors was a horizontal cylindrical unit of 1935 l calculated total volume (SA:V 4.5), used by de Bertoldi et al. (1988) for process control studies. The raw material was the "biodegradable organic fraction of municipal solid waste". The mixture was placed on a perforated grid above the cylinder wall and no mixing took place during the composting process. A 1340 l stainless steel reactor with a diameter of 960 mm and a height of 1850 mm (SA:V 5.2) was used for process optimisation studies by Hogland et al. (2003) and reactor evaluation (Lyberg and Hogland, 2004). The reactor was insulated with polyethylene foam. The study reported heat production of 0.35-0.67 kW, inlet air heating of 0.02-0.06 kW, "cooling effect by the composting mass" of 0.14-0.37 kW and wall losses of 0.15-0.27 kW. The ratio wall losses to biological power (heat production) is large in comparison to that expected for full-scale systems and indicates insufficient insulation. Another large pilot-scale reactor was reported by Suzuki et al. (2004). The 6080 l (SA:V 3.1) column was used for compostability studies on wood chips. Hong and Park (2004) used a 605 l pilot-scale reactor (SA:V 6.5) insulated with 50 mm polystyrene as part of a system for the study of ammonia removal from the exit gas using biofilters.

In summary, investigators have continued to use a variety of reactors for a range of purposes. For self-heating reactors, insulation thicknesses remained in the 25-50 mm range, regardless of SA:V ratio and, apart from Lyberg and Hogland (2004), without discussion of the heat flux through the walls in relation to other fluxes. An encouraging trend towards the reporting of more dimensional and airflow details was discernable. In view of the increasing use of horizontal mixed in-vessel systems at full scale, the horizontal mixed reactor of Alkoaik and Ghaly (2005) looks particularly useful for future studies.

2.12 References

Adani, F., Lozzi, P. and Genevini, P., 2001. Determination of biological stability by oxygen uptake on municipal solid waste and derived products. Compost Science & Utilisation 9 (2), 163-178.

Alkoaik, F. and Ghaly, A.E., 2005. Effect of innoculum size on the composting of greenhouse tomato plant trimmings. Compost Science and Utilisation 13 (4), 262-273.

Ashbolt, N.J. and Line, M.A., 1982. A bench-scale system to study the composting of organic wastes. Journal of Environmental Quality 11 (3), 405-408.

Atkinson C.F., Jones, D.D. and Gauthier, J.J., 1996a. Biodegradabilities and microbial activities during composting of poultry litter. Poultry Science 75 (5), 608-617.

Atkinson, C.F., Jones, D.D. and Gauthier, J.J., 1996b. Biodegradabilities and microbial activities during composting of oxidation ditch sludge. Compost Science & Utilisation 4 (1), 84-96.

Atkinson, C.F., Jones, D.D. and Gauthier, J.J., 1996c. Biodegradabilities and microbial activities during composting of municipal solid waste in bench scale reactors. Compost Science & Utilisation 4 (4), 14-23.

Bach Phan Dinh, Shoda,M. and Kubota,H., 1984. Rate of composting of dewatered sewage sludge on continuously mixed isothermal reactor. Journal of Fermentation Technology 62 (3), 285-292.

Bach Phan Dinh, Shoda,M. and Kubota,H., 1985. Composting reaction rate of sewage sludge in an autothermal packed bed reactor. Journal of Fermentation Technology 63 (3), 271-278.

Bach Phan Dinh, Nakasaki,K., Shoda,M. and Kubota,H., 1987. Thermal balance in composting operations. Journal of Fermentation Technology 65 (2), 199-209.

Bari, Q.H., Koenig, A. and Guihe, T., 2000a. Kinetic analysis of forced aeration composting – I. Reaction rates and temperature. Waste Management & Research 18 (4), 303-312.

Bari, Q.H., Koenig, A. and Guihe, T., 2000b. Kinetic analysis of forced aeration composting – II. Application of multilayer analysis for the prediction of biological degradation. Waste Management & Research 18 (4), 313-319.

Barrington, S., Choiniere, D., Trigui, M. and Knight, W., 2002. Effect of carbon source on compost nitrogen and carbon losses. Bioresource Technology 83 (3), 189-194.

Beaudin, N., Caron, R.F., Legros, R., Ramsay, J., Lawlor, L. and Ramsay, B., 1996. Cocomposting of weathered hyrocarbon contaminated soil. Compost Science & Utilisation 4 (2), 37-45.

Bengtsson, A., Quednau, M., Haska, G., Nilzen, P. and Persson, A., 1998. Composting of oily sludges - degradation, stabilized residues, volatiles and microbial activity. Waste Management & Research 16 (3), 273-284.

Bernal, M.P., Lopez-Real, J.M. and Scott, K.M., 1993. Application of natural zeolites for reduction of ammonia emissions during the composting of organic wastes in a laboratory composting simulator. Bioresource Technology 43, 35-39.

Boelens, J., De Wilde, B. and Baere, L., 1996. Comparative study on biowaste definition: effects on biowaste collection, composting process and compost quality. Compost Science & Utilisation 4 (1), 60-72.

Bono, J.J., Chalaux, N. and Chabbert, B., 1992. Bench-scale composting of two agricultural wastes. Bioresource Technology 40, 119-124.

Brown, K.W., Thomas, J.C. and Whitney, F., 1997. Fate of volatile organic compounds in composted municipal solid waste. Compost Science & Utilisation 5 (4), 6-14.

Brown, K.H., Bouwkamp, J.C. and Gouin, F.R., 1998. The influence of C:P ratio on the biological degradation of municipal solid waste. Compost Science & Utilisation 6 (1), 53-58.

Campbell, C.D. and Darbyshire, J.F., and Anderson, J.G., 1990a. The composting of tree bark in small reactors: self-heating experiments. Biological Wastes 31, 145-161.

Campbell, C.D., Darbyshire, J.F. and Anderson, J.G., 1990b. The composting of tree bark in small reactors: adiabatic and fixed-temperature experiments. Biological Wastes 31, 175-185.

Cappaert, I., Verdonck, O. and de Boodt, M., 1976. A respiratory apparatus for studying the behaviour of organic materials. Soil Organic Matter Studies. Proceedings of a Symposium. IAEA-SM-211/62, Braunschweig, Germany. pp131-136.

Chalaux, N., Olivier, J.M. and Minvielle, N., 1991. Bench scale composting and wheat straw biodegradability. in: Maher, Ed. Science and Cultivation of Edible Fungi. Rotterdam: Balkema; pp 207-214.

Choi, M.H. and Park, Y.H., 1998. The influence of yeast on thermophilic composting of food waste. Letters in Applied Microbiology 26 (3), 175-178.

Choi, H.L., Richard, T.L. and Ahn, H.K., 2001. Composting high moisture materials: biodrying poultry manure in a sequentially fed reactor. *Compost Science and Utilization* 9 (4), 303-311.

Clark, C.S., Buckingham, C.O., Charbonneau, R. and Clark, R.H., 1977. Laboratory scale composting: techniques. Journal of the Environmental Engineering Division, ASCE. 103 (EE5), 893-906.

Clark, C.S., Buckingham, CO., Charbonneau, R. and Clark, RH., 1978. Laboratory scale composting: studies. Journal of the Environmental Engineering Division, ASCE. 104 (EE1), 47-59.

Cohen, Y. and Metzner, A.B., 1981. Wall effects in laminar flow of fluids through packed beds. AICHE Journal 27, 705-715.

Cook, B.D., Bloom, P.R. and Halbach, T.R., 1994. A method for determining the ultimate fate of synthetic chemicals during composting. Compost Science & Utilisation 2 (1), 42-50.
Cook, BD., Bloom, PR. and Halbach, TR., 1997. Fate of a polyacrylate polymer during composting of simulated municipal solid waste. Journal of Environmental Quality 26 (3), 618-625.

Crohn, D.M. and Bishop, M.L., 1999. Proximate carbon analysis for compost production and mulch use. Trans. ASAE 42 (3), 791-797.

Cronje, A., Turner, C., Williams, A., Barker, A. and Guy, S., 2003. Composting under controlled conditions. Environmental Technology 24 (10), 1221-1234.

Cronje, A.L., Turner, C., Williams, A.G., Barker, A.J. and Guy, S., 2004. The respiration rate of composting pig manure. Compost Science & Utilization 12 (2), 119-129.

Currie, J.A. and Festenstein, G.N., 1971. Factors defining spontaneous heating and ignition of hay. J.Sci.Fd.Agric. 22, 223-230.

Dao, T., Sikora, L., Hamasaki, A. and Chaney, R., 2001. Manure phosphorus extractability as affected by aluminum and iron by-products and aerobic composting. Journal of Environmental Quality 30 (5), 1693-1698.

Das, K. and Keener, H.M., 1997. Numerical model for the dynamic simulation of a large scale composting system. Trans. ASAE 40 (4), 1179-1189.

Das, K.C., Tollner, EW. and Tornabene, TG., 2001. Composting by-products from a bleached kraft pulping process: effect of type and amount of nitrogen amendment. Compost Science & Utilisation 9 (3), 256-265.

Das, K. C. and Tollner, E., 2003. Comparison between composting of untreated and anaerobically treated paper mill sludges. Trans. ASAE 46 (2), 475-481.

Day, M., Shaw, K., Cooney, D., Watts, J. and Harrigan, B., 1997. Degradable polymers: The role of the degradation environment. Journal of Environmental Polymer Degradation 5 (3), 137-151.

Day, M., Krzymien, M., Shaw, K. Zaremba, L., Wilson, W.R., Botden, C. and Thomas, B., 1998. An investigation of the chemical and physical changes occuring during commercial composting. Compost Science & Utilisation 6 (2), 44-66.

de Bertoldi, M., Rutili, A., Citterio, B. and M, C., 1988. Composting management: a new process control through O2 feedback. Waste Management & Research 6 (3), 239-259.

de Guardia, A., Petiot, C. and Rogeau, D., 2006. Influence of aeration rate and biodegradability fraction on composting kinetics. Waste Management in press.

Dinel, H., Schnitzer, M. and Dumontet, S., 1996. Compost maturity: extractable lipids as indicators of organic matter stability. Compost Science & Utilisation 4 (2), 6-20.

Dullien, F.A.L., 1992. Porous media: fluid transport and pore structure. Academic Press, New York, USA. p 78.

Eiland, F., Leth, M., Klamer, M., Lind, A.-M., Jensen, H.E.K. and Iversen, J.J.L., 2001. C and N turnover and lignocellulose degradation during composting of Miscanthus straw and liquid pig manure. Compost Science & Utilisation 9 (3), 186-196.

Eisfeld, B. and Schnitzlein, K., 2001. The influence of confining walls on the pressure drop in packed beds. Chemical Engineering Science 56, 4321-4329.

Ekinci, K., Keener, H.M., and Elwell, D.J., 1999. Composting short paper fibre with broiler litter and additives part I: Effects of initial pH and carbon/nitrogen ratio on ammonia emission. Compost Science & Utilisation 8 (2), 160-171.

Elwell, D.J., Keener, H.M., Hoitinck, H.A.J., Hansen, R.C. and Hoff, J., 1994. Pilot and full scale evaluations of leaves as an amendment in sewage sludge composting. Compost Science & Utilisation 2 (2), 55-74.

Elwell, D.J., Keener H.M., Hansen R.C., 1996. Controlled, high rate, composting of mixtures of food residuals, yard trimmings and chicken manure. Compost Science & Utilisation 4 (1), 6-15.

Elwell, D.J., Keener, H.M., Carey, D.S. and Schlak, P.P., 1998. Composting unamended chicken manure. Compost Science & Utilisation 6 (2), 22-35.

Elwell, D.J., Keener, H.M., Wiles, M.C., Borger, D.C. and Willett, L.B., 2001. Odorous emissions and odor control on composting swine manure/sawdust mixtures using continuous and intermittent aeration. Trans. ASAE 44 (5), 1307-1316.

Elwell, D.J., Hong, J.H. and Keener, H.M., 2002. Composting hog manure/sawdust mixtures using intermittent and continuous aeration: ammonia emissions. Compost Science & Utilisation 10 (2), 142-149.

Finger, S.M., Hatch, R.T. and Regan, T.M., 1976. Aerobic microbial growth in semi-solid matrices: heat and mass transfer limitations. Biotechnol. Bioeng. 18, 1193-1218.

Finstein, M.S., Miller, F.C., Strom, P.F., MacGregor, S.T. and Psarianos, K.M., 1983. Composting ecosystem management for waste treatment. Biotechnology June 1983, pp 347-353.

Fraser, B.S. and Lau, A.K., 2000. The effects of process control strategies on composting rate and odour emissions. Compost Science & Utilisation 8 (4), 274-292.

Freeman, T.M. and Cawthon, D.L., 1999. Use of composted dairy cattle solid biomass, poultry litter and municipal biosolids as greenhouse growth media. Compost Science & Utilisation 7 (3), 66-71.

Garcia-Gomez, A., Szmidt, R.A.K. and Roig, A., 2002. Enhancing the composting rate of spent mushroom substrate by rock dust. Compost Science & Utilisation 10 (2), 99-104.

Gostomski, P.A. and Liaw, L.P., 2001. Air permeability of biofilter media. Proceedings of the Air and Waste Management 94th Annual Meeting and Exhibition, Orlando, USA. 18-24 June, 2001. Published on CD-ROM. Air and Waste Management Association, Pittsburgh, USA.

Hamelers, B.V.F., 1993. A theoretical model of composting kinetics. In: Science and Engineering of Composting: Design, Environmental and Microbial and Utilisation aspects. Pp 59-94. Hoitink, H.A.J. and Keener, H.M. (Eds), Renaissance Publications, Worthington, USA.

Hamoda, M.F., Abu Qdais, H.A. and Newham, J., 1998. Evaluation of municipal solid waste composting kinetics. Resources Conservation and Recycling 23 (4), 209-223.

Hansen, R., Keener, H. and Hoitinck, H., 1989). Poultry manure composting: an exploratory study. Trans. ASAE 32 (6), 2151-2158.

Harper, E., Miller, F.C. and Macauley, B.J., 1992. Physical management and interpretation of an environmentally controlled composting ecosystem. Australian Journal of Experimental Agriculture 32 (5), 657-667.

Haug, R.T., 1993. The practical handbook of compost engineering. Lewis Publishers, Boca Raton, Florida, USA.

Helfrich, P., Chefetz, B., Hadar, Y. Chen, Y. and Schnabl, H., 1998. A novel method for determining phytotoxicity in composts. Compost Science & Utilisation 6 (3), 6-13.

Herrmann, R.F. and Shann, J.F., 1997. Microbial community changes during the composting of municipal solid waste. Microbial Ecology 33 (1), 78-85.

Hogan, J.A., Miller, F.C. and Finstein, M.S., 1989. Physical modeling of the composting ecosystem. Applied and Environmental Microbiology 55 (5), 1082-1092.

Hogland, W., Bramryd, T., Marques, M. and Nimmermark, S., 2003. Physical, chemical and biological processes for optimizing decentralized composting. Compost Science & Utilization 11 (4), 330-336.

Hong, J.H., Keener, H.M. and Elwell, D.J., 1998. Preliminary study on the effect of continuous and intermittent aeration on composting of hog manure ammended with sawdust. Compost Science & Utilisation 6 (3), 74-88.

Hong, J.H. and Park, K.J., 2004. Wood chip biofilter performance of ammonia gas from composting manure. Compost Science & Utilisation 12 (1), 25-30.

Horiuchi, J.I., Ebie, K., Tada, K., Kobayashi, M. and Kanno, T., 2003. Simplified method for estimation of microbial activity in compost by ATP analysis. Bioresource Technology 86 (1), 95-98.

Hwang, E.-Y., Namkoong, W. and Park, J.-S., 2001. Recycling of remediated soil for effective composting of diesel contaminated soil. Compost Science & Utilisation 9 (2), 143-148.

Huang, J.S., Wang, C.H. and Jih, C.G., 2000. Empirical model and kinetic behavior of thermophilic composting of vegetable waste. Journal of Environmental Engineering-ASCE 126 (11), 1019-1025.

Itavaara, M. and Vikman, M., 1996. An overview of methods for biodegradability testing of biopolymers and packaging materials. Journal of Environmental Polymer Degradation 4 (1), 29-36.

Jackson, M.J. and Line, M.A., 1997. Composting pulp and paper mill sludge – effect of temperature and nutrient addition method. Compost Science & Utilisation 5 (1), 74-81.

Joyce, J.F., Sato, C., Cardenas, R. and Surampalli, RY., 1998. Composting of polycyclic aromatic hydrocarbons in simulated municipal solid waste. Water Environment Research 70 (3), 356-361.

Kaiser, J., 1996. Modelling composting as a microbial ecosystem: A simulation approach. Ecological Modelling 91 (1-3), 25-37.

Kaplan, D.L. and Kaplan, A.M., 1982. Thermophilic transformations of 2,4,6-trinitrotoluene under simulated composting conditions. Applied and Environmental Microbiology 44, 757-760.

Keener, H.M., Elwell, D.J., Ekinci, K. Hoitink, H.A.J., 2001. Composting and value added utilisation of manure from a swine finishing facility. Compost Science & Utilisation 9 (4), 312-321.

Keener, H. M., Elwell, D. J. and Grande, D., 2002. NH_3 emissions and N-balances for a 1.6 million caged layer facility: manure belt composting vs deep pit operation. Trans. ASAE 45 (6), 1977-1984.

Kishimoto, M., Preechaphan, C., Yoshida, T. and Taguchi, H., 1987. Simulation of an aerobic composting of activated sludge using a statistical procedure. MIRCEN J. 3, 113-124.

Kithome, M., Paul, J.W. and Bomke, A.A., 1999. Reducing nitrogen losses during simulated composting of poultry manure using adsorbents or chemical amendments. Journal of Environmental Quality 28 (1), 194-201.

Koenig, A. and Tao, G.H., 1996. Accelerated forced aeration composting of solid waste. Proceedings of the Asia-Pacific Conference on Sustainable Energy and Environmental Technology, Singapore, 450-457.

Komilis, D.P. and Ham, R.H., 2000. A comparison of static pile and turned windrow methods for poultry litter compost production. Compost Science & Utilisation 8 (3), 254-265.

Komilis, D., 2006. A kinetic analysis of solid waste composting at optimal conditions. Waste Management 26 (1), 82-91.

Komilis, D.P. and Ham, R.H., 2006. Carbon dioxide and ammonia emissions during composting of mixed paper, yard waste and food waste. Waste Management 26, 62-70.

Korolewicz, T., Turek, M., Ciba, J. and Cebula, J., 2001. Speciation and removal of zinc from composted municipal solid wastes. Environmental Science and Technology, 35 (4), 810-814.

Krzymien, M., Day, M., Shaw, K., Mohmad, R. and Sheehan, S., 1999. The role of feed composition on the composting process. II. Effect on the release of volatile organic compounds and odours. Journal of Environmental Science and Health Part A-Toxic/Hazardous Substances and Environmental Engineering 34 (6), 1369-1396.

Laos, F., Mazzarino, MJ., Walter, L. and Roselli, L., 1998. Composting of fish wastes with wood by-products and testing compost quality as a soil amendment: experiences in the Patagonia region of Argentina. Compost Science & Utilisation 6 (1), 59-66.

Larsen, K.L. and McCartney, D.M., 2000. Effect of C:N ratio on microbial activity and N retention: bench scale study using pulp and paper biosolids. Compost Science & Utilisation 8 (2), 147-159.

Lau, A.K., Lo, K.V., Liao, P.H. and Yu, J.C., 1992. Aeration experiments for swine waste composting. Bioresource Technology 41 145-152.

Liao, P.H., May, A.C. and Chieng, S.T., 1995. Monitoring process efficiency of a full-scale in-vessel system for composting fisheries wastes. Bioresource Technology 54 (2), 159-163.

Leiva, M.T.G., Casacuberta, A.A. and Ferrer, A.S., 2003. Application of experimental design technique to the optimization of bench-scale composting conditions of municipal raw sludge. Compost Science & Utilization 11 (4), 321-329.

Lehmann, R.G., Smith, D.M., Narayan, R., Kozerski, G.E. and Miller, J.R., 1999. Life cycle of silicone polymer, from pilot scale composting to soil amendment. Compost Science & Utilisation 7 (3), 72-82.

Leth, M., Jensen, H.E.K. and Iversen, J.J.L., 2001. Influence of different nitrogen sources on composting of Miscanthus in open and closed systems. Compost Science & Utilisation 9 (3), 197-205.

Lhadi, E.K., Tazi, H., Aylaj, M., Tambone, F. and Adani, F., 2004. Cocomposting separated MSW and poultry manure in Morocco. Compost Science & Utilization 12 (2), 137-144.

Libmond, S. and Savoie, J-M., 1993. Degradation of wheat straw by a microbial community-stimulation by a polysaccharidase complex. Appl.Microbiol.Biotechnol. 40 567-574.

Loser, C., Ulbricht, H., Hoffman, P. and Seidel, H., 1999. Composting of wood containing polycyclic aromatic hydrocarbons (PAHs). Compost Science & Utilisation 7 (3), 16-32.

Lyberg, M.D. and Hogland, W., 2004. Performance of a vertically fed compost reactor. Compost Science & Utilization 12 (2), 169-174.

Magalhaes, A.M.T., Shea, P.J., Jawson, M.D., Wicklund, E.A. and Nelson, D.W., 1993. Practical simulation of composting in the laboratory. Waste Management & Research 11, 143-154.

Marrug, A.C., Maruscik, D.A., Ritchie, C.J., Schwab, B.S., Harper, S.R. and Rapaport, S.A., 1993. A novel bioreactor simulating composting of municipal solid waste J. Microbiol. Methods 18, 99-112.

McCartney, D. and Hongtu Chen., 2001. Using a biocell to measure effect of compressive settlement on free air space and microbial activity in windrow composting. Compost Science & Utilisation 9 (4), 285-302.

Michel, F.C., Reddy, C.A. and Forney, L.J., 1993. Yard waste composting: studies using different mixes of leaves and grass in a laboratory scale system. Compost Science & Utilisation 1, 85-96.

Michel, F.C. Reddy, C.A. and Forney, L.J., 1995. Microbial-degradation and humification of the lawn care pesticide 2,4-dichlorophenoxyacetic acid during the composting of yard trimmings. Applied and Environmental Microbiology 61 (7), 2566-2571.

Michel, F.C. and Reddy, C.A., 1998. Effect of oxygenation level on yard trimmings composting rate, odor production and compost quality in bench-scale reactors. Compost Science & Utilisation 6 (4), 6-14.

Michel, F.C., Quensen, J. and Reddy, C.A., 2001. Bioremediation of a PCB-contaminated soil via composting. Compost Science & Utilisation 9 (4), 274-284.

Mills, A.F., 1995. Basic heat and mass transfer. Richard D. Irwin Inc., Chicago, USA.

Minkara, M.Y., Lawson, T.B., Breitenbeck, G.A. and Cochran, B.J., 1998. Cocomposting of crawfish and agricultural processing by-products. Compost Science & Utilisation 6 (1), 67-74.

Mohee, R., White, R.K. and Das, K.C., 1998. Simulation model for composting cellulosic (bagasse) substrates. Compost Science & Utilisation 6 (2), 82-92.

Mote, C.R. and Griffis, C.L., 1979. A system for studying the composting process. Agricultural Wastes 1 (3), 191-203.

Mote, C.R. and Griffis, C.L., 1982. Heat production by composting organic matter Agricultural Wastes 4 65-73.

Nakasaki, K., Sasaki, Y., Shoda, M. and Kubota, H., 1985. Change in microbial numbers during thermophilic composting of sewage sludge with reference to CO_2 evolution rate. Applied and Environmental Microbiology 49 37-41.

Nakasaki, K., Kato, J., Akiyama, T. and Kubota, H., 1987. A new composting model and assessment of optimum operation for effective drying of composting material. Journal of Fermentation Technology 65 (4), 441-447.

Nakasaki, K., Akakura, N., Atsumi, K. and Takemoto, M., 1998. Degradation patterns of organic material in batch and fed-batch composting operations. Waste Management & Research 16 (5), 484-489.

Nakasaki, K. and Ohtaki, A., 2002. A simple numerical model for predicting organic matter decomposition in a fed-batch composting operation. Journal of Environmental Quality 31 (3), 997-1005.

Namkoong, W. and Hwang, E-Y., 1997. Operational parameters for composting night soil in Korea. Compost Science & Utilisation 5 (4), 46-51.

Namkoong, W., Hwang, E-Y., Cheong, J-G. and Choi, J-Y., 1999. A comparative evaluation of maturity parameters for food waste composting. Compost Science & Utilisation 7 (2), 55-62.

Negro, NJ. and Solano, ML., 1996. Laboratory composting assays of the solid residue resulting from the flocculation of olive mill wastewater with different lignocellulosic residues. Compost Science & Utilisation 4 (4), 62-71.

Noble, R., Fermor, T.R., Evered, C.E and Atkey, P.T., 1997. Bench scale preparation of mushroom substrates in controlled environments. Compost Science & Utilisation **5** (3), 6-14.

Ohtaki, A. and Nakasaki, K., 2000. Report: Ultimate degradability of various kinds of biodegradable plastics under controlled composting conditions. Waste Management & Research 18 (2), 184-189.

Ouatmane, A., Provenzano, M.R., Hafidi, M. and Senesi, N., 2000. Compost maturity assessment using calorimetry, spectroscopy and chemical analysis. Compost Science & Utilisation 8 (2), 124-134.

Pagga, U., Beimborn, D.B., Boelens, J. and DeWilde, B., 1995. Determination of the aerobic biodegradability of polymeric material in a laboratory controlled composting test. Chemosphere 31 (11-12), 4475-4487.

Palmisano, A.C., Maruscik, D.A., Ritchie, C.J., Schwab, B.S., Harper, S.R. and Rapaport, S.A., 1993. A novel bioreactor simulating composting of municipal solid waste. J. Microbiol. Methods 18 99-112.

Papadimitriou, E.K. and Balis, C., 1996. Comparative study of parameters to evaluate and monitor a composting process. Compost Science & Utilisation 4 (4), 52-61.

Park, K.J., Choi, M.H. and Hong, J.H., 2002. Control of composting odour using biofiltration. Compost Science & Utilisation 10 (4), 356-362.

Pecchia, J.A., Beyer, D.M. and Wuest, P.J., 2002. The effects of poultry manure based formulations on odour generation during phase 1 mushroom composting. Compost Science & Utilisation 10 (3), 188-196.

Petiot, C. and de Guardia, A., 2004. Composting in a laboratory reactor: a review. Compost Science & Utilisation 12 (1), 69-79.

Qiao, L. and Ho, G., 1997. The effects of clay amendment on composting of digested sludge. Water Research 31 (5), 1056-1064.

Rajbanshi, S.S. and Inubushi, K., 1997. Chemical and biochemical changes during laboratory scale composting of allelopathic plant leaves (Eupatorium adenophorum and Lantana camara). Biology and Fertility of Soils 26 (1), 66-71.

Razvi, A.S. and Kramer, D.W., 1996. Evaluation of compost activators for composting grass clippings. Compost Science & Utilisation 4 (4), 72-80.

Robinzon, R., Kimmel, E., Avnimelech, Y., 2000. Energy and mass balances of windrow composting system. Trans. ASAE 43 (5), 1253-1259.

Roy, S., Leclerc, P., Auger, F., Soucy, G., Moresoli, C., Cote, L., Potvin, D., Beaulieu, C and Brzezinski, R., 1997. A novel two-phase composting process using shrimp shells as an amendment to partly composted biomass. Compost Science & Utilisation 5 (4), 52-64.

Rynk, R. (Ed), 1992. On-farm composting handbook. NRAES, Ithaca, New York, USA.

Scholwin, F. and Bidlingmaier, W., 2003. Fuzzifying the composting process: a new model based control strategy as a device for achieving a high grade and consistent product quality. Proceedings of the Fourth International Conference of ORBIT Association on Biological Processing of Organics: Advances for a Sustainable Society, 30th April-2 May, 2003, Perth, Australia, 739-751. ORBIT Association, Weimar, Germany.

Schwab, B.S., Ritchie, C.J., Kain, D.J., Dobrin, G.C., King, L.W. and Palmisano, A.C., 1994. Characterization of compost from a pilot plant-scale composter utilizing simulated solid waste. Waste Management & Research 12, 289-303.

Schulze, K.L., 1962. Continuous thermophilic composting. Applied Microbiology 10 108-122.

Seki, H, 2000. Stochastic modeling of composting processes with batch operation by the Fokker-Planck equation. Trans. ASAE 43 (11), 169-179.

Seymour, R.M, Donahue, D., Bourdon, M., Evans, J.R. and Wentworth, D., 2001. Intermittent aeration for in-vessel composting of crab processing waste. Compost Science & Utilisation 9 (2), 98-106.

Shamlou, P.A., 1988. Handling of bulk solids: theory and practice. London, UK. Butterworths.

Sharma, S., Mathur, R.C. and Vasudevan, P., 1999. Composting silkworm culture waste. Compost Science & Utilisation 7 (2), 74-81.

Shaw, K., Day, M., Krzymien, M., Mohmad, R. and Sheehan, S., 1999. The role of feed composition on the composting process. I. Effect on composting activity. Journal of Environmental Science and Health Part A-Toxic/Hazardous Substances and Environmental Engineering 34 (6) 1341-1367.

Sikora, L.J., Ramirez, M.A. and Troeschel, T.A., 1983. Laboratory composter for simulation studies. Journal of Environmental Quality 12 219-224.

Sikora, L.J. and Sowers, M.A., 1985. Effect of temperature control on the composting process. Journal of Environmental Quality 14 434-439.

Silviera, A.E. and Ganho R.B., 1995. Composting wastes contaminated with naphthalene. Compost Science & Utilisation 3 (4), 78-81.

Smårs, S., Beck-Friis, B., Jönsson, H. and Kirchmann, H., 2001. An advanced experimental composting reactor for schematic simulation studies. Journal of Agricultural Engineering Research 78 (4), 415-422.

Smet, E., van Langenhove, H., and De Bo, I., 1999. The emission of volatile compounds during the aerobic and the combined anaerobic/aerobic composting of biowaste. Atmospheric Environment 33 (8), 1295-1303.

Smith, D.M, Lehmann, R.G, Narayan, R. and Kozerski, G.E. and Miller, J.R., 1998. Fate and effects of silicone polymer during the composting process. Compost Science & Utilisation 6 (2), 6-12.

Stombaugh, D.P. and Nokes, S.E., 1996. Development of a biologically based aerobic composting simulation model. Trans. ASAE 39 (1), 239-250.

Strom, P.F., 1985. Effect of temperature on bacterial species diversity in thermophilc solid-waste composting. Applied and Environmental Microbiology 50 (4), 899-905.

Suler, D.J. and Finstein, M.S., 1977. Effect of temperature, aeration and moisture on CO_2 formation in bench-scale, continuously thermophilic composting of solid waste. Applied and Environmental Microbiology 33 (2), 345-350.

Sundberg, C. and Jonsson, H., 2003. Down-scaling a large composting plant to pilot-scale for systematic research. Proceedings of the Fourth International Conference of ORBIT Association on Biological Processing of Organics: Advances for a Sustainable Society, 30th April-2 May, 2003, Perth, Australia, pp 388-397. ORBIT Association, Weimar, Germany.

Sundberg, C., Smars, S. and Jonsson, H., 2004. Low pH as an inhibiting factor in the transition from mesophilic to thermophilic phase in composting. Bioresource Technology 95 (2), 145-150.

Suzuki, T., Ikumi, Y., Okamoto, S., Watanabe, I., Fujitake, N. and Otsuka, H., 2004. Aerobic composting of chips from clear-cut trees with various co-materials. Bioresource Technology 95 (2), 121-128.

Tremier, A. and de Guardia, A., 2003. Heat and mass transfers prediction thanks to gas flow RTD characterisation during sewage sludge and bulking agent composting in a 300 liter pilot reactor. Proceedings of the Fourth International Conference of ORBIT Association on Biological Processing of Organics: Advances for a Sustainable Society, 30th April-2 May, 2003, Perth, Australia, pp 721-731. ORBIT Association, Weimar, Germany.

Tremier, A., de Guardia, A., Massiani, C., Paul, E. and Martel, J.L., 2005a. A respirometric method for characterising the organic composition and biodegradation kinetics and the tmeperature influence on the biodegradation kinetics, for a mixture of sludge and bulking agent to be composted. Bioresource Technology 96 (2), 169-180.

Tremier, A., De Guardia, A., Massiani, C. and Martel, J.L., 2005b. Influence of the airflow rate on heat and mass transfers during sewage sludge and bulking agent composting. Environmental Technology 26 (10), 1137-1149.

Tseng D.Y., Chalmers, J.J., Tuovinen, O.H. and Hoitink, H.A.J., 1995. Characterisation of a bench scale system for studying the biodegradation of organic solid wastes. Biotechnol. Progr. 11, 443-451.

USEPA, 1995. Land application of sewage sludge and domestic septage. Process design manual. EPA/625/K-95/001, pp 15-19. US Environmental Protection Agency, Washington DC, USA.

van Bochove, E., Couillard, D. and Nolin, M.C., 1995. Characterization of the Composting Stages By a Multivariate- Analysis - Application to the Nitrogen-Cycle. Environmental Technology 16 (10), 929-941.

VanderGheynst, JS., Gossett, JM., Walker, LP., 1997a. High-solids aerobic decomposition: Pilot-scale reactor development and experimentation. Process Biochemistry 32 (5), 361-375.

VanderGheynst, J.S., Walker, L.P., Parlange, J.Y., 1997b. Energy transport in a high-solids aerobic degradation process: Mathematical modeling and analysis. Biotechnology Progress 13 (3), 238-248.

VanderGheynst, J., Cogan, D., Defelice, P., Gossett, J. and Walker, L., 1998. Effect of process management on the emission of organosulfur compounds and gaseous antecedents from composting processes. Environmental Science & Technology 32 (23), 3713-3718.

VanderGheynst, J.S. and Lei, F., 2003. Microbial community structure dynamics during aerated and mixed composting. Trans. ASAE 46 (2), 577-584.

Van der Zee, M., Stoutjesdijk, J.H., Feil, H. and Feijen, J., 1998. Relevance of aquatic biodegradation tests for predicting degradation of polymeric materials during biological solid waste treatment. Chemosphere 36 (3), 461-473.

VanLier, J.J.C., VanGinkel, J.T., Straatsma, G., Gerrits, J.P.G. and VanGriensven, L.J.L.D., 1994. Composting of mushroom substrate in a fermentation tunnel – compost parameters and a mathematical model. Netherlands Journal of Agricultural Science 42 (4), 271-292.

Veeken, A., de Wilde, V. and Hamelers, B., 2002. Passively aerated composting of straw-rich pig manure: effect of compost bed porosity. Compost Science & Utilisation 10 (2), 114-128.

Veeken, A., Timmermans, J., Szanto, G. and Hamelers, B.V.F., 2003. Design of passively aerated compost systems on basis of compaction-porosity-permeability data. Proceeding of the Fourth International Conference of ORBIT Association on Biological Processing of Organics: Advances for a Sustainable Society, 30th April-2 May, 2003, Perth, Australia, pp 85-96. ORBIT Association, Weimar, Germany.

Viel, M., Sayang, D., Peyre, A. and Andre, L., 1987. Optimisation of in-vessel co-composting through heat recovery. Biological Wastes 20, 167-185.

Walker, I.K. and Harrison, W.J., 1960. The self-heating of wet wool. *NZ Journal of* Agricultural Research 3, (6), 861-895.

Weppen, P., 2001. Process calorimetry on composting of municipal organic wastes. Biomass and Bioenergy 21, 289-299.

Witter, E. and Lopez-Real, J., 1988. Nitrogen losses during the composting of sewage sludge and the effectiveness of clay soil, zeolite and compost in adsorbing volatilised ammonia. Biological Wastes 23, 279-294.

Yamada, Y. and Kawase, Y., 2006. Aerobic composting of waste activated sludge: Kinetic analysis for microbiological reaction and oxygen consumption. Waste Management 26, 49-61.

Zavala, M.A.L., Funamizu, N. and Takakuwa, T., 2004. Modeling of aerobic biodegradation of feces using sawdust as a matrix. Water Research 38 (5), 1327-1339.

CHAPTER 3
PHYSICAL MODELLING OF THE COMPOSTING ENVIRONMENT.
Part 2: Simulation Performance

3.1 Foreword

A number of options for further investigation presented themselves at the end of chapter 2. The one chosen here was to attempt a qualitative and quantitative assessment of the performance of various physical models, in terms of their ability to simulate aspects the full-scale composting environment. In other words the question of interest was "how good are these physical models in replicating conditions in full-scale systems"? In order to address this, several new techniques had to be developed. With reference to the conceptual journey, we remain in St. Physical.

This chapter consists primarily of the following journal paper:

> Mason, I.G. & Milke, M.W., 2005. Physical modelling of the composting environment: a review. Part 2: Simulation performance Waste Management 25 (5), 501-509.

The paper covers the literature up to early 2004. An update on significant literature and developments after this time is given in the afterword (section 3.9). Readers are asked to note that the text may differ from that in the published paper in places and that corrections may have been incorporated. In particular, a corrected Fig. 3.2 appears in this chapter. The second author made editorial comments on various drafts of the journal paper, and in particular contributed valuable suggestions resulting in the inclusion of discussion within the text as the review proceeded. Otherwise the paper is the sole work of the first author.

3.2 Summary

This paper reviews previously published heat balance data for experimental and full-scale composting reactors, and then presents an evaluation of the simulation performance of laboratory and pilot-scale reactors, using both quantitative and qualitative temperature profile characteristics. The review indicates that laboratory-scale reactors have typically demonstrated markedly different heat balance behaviour in comparison to full-scale systems,

with ventilative heat losses of 36-67%, and 70-95% of the total flux, respectively. Similarly, conductive/convective/radiative (CCR) heat losses from laboratory reactors have been reported at 33-62% of the total flux, whereas CCR losses from full-scale composting systems have ranged from 3-15% of the total. Full-scale windrow temperature-time profiles from the literature were characterised by the present authors. Areas bounded by the curve and a 40 ^{o}C baseline (A_{40}) exceeded 624 ^{o}C.days, areas bounded by the curve and a 55 ^{o}C baseline (A_{55}) exceeded 60 ^{o}C.days, and times at 40 ^{o}C and 55 ^{o}C were > 46 days and > 24 days respectively, over periods of 50-74 days. For forced aeration systems at full scale, values of A_{40} exceeded 224 ^{o}C.days, values of A_{55} exceeded 26 ^{o}C.days, and times at 40 ^{o}C and 55 ^{o}C were > 14 days and > 10 days respectively, over periods of 15-35 days. Values of these four parameters for laboratory-scale reactors were typically considerably lower than for the full-scale systems, although temperature shape characteristics were often similar to those in full-scale profiles. Evaluation of laboratory-, pilot- and full-scale profiles from systems treating the same substrate showed that a laboratory-scale reactor, and two pilot-scale reactors operated at comparatively high aeration rates, poorly simulated the full-scale temperature profiles. However, the curves from two moderately insulated, self-heating, pilot-scale reactors operated at relatively low aeration rates appeared to closely replicate full-scale temperature profiles. The importance of controlling aeration rates and CCR losses is discussed and further work suggested in order to investigate the links between simulation of the composting environment and process performance.

3.3 Introduction

The pattern of heat accumulation within a composting system (Mason and Milke, 2005; Chapter 2) will be reflected in the temperature-time profile. For a given substrate, the profile will be determined by the magnitude of: a) the ventilative losses, and b) the conductive/convective/radiative (CCR) losses (Mason and Milke, 2005; Chapter 2) through the reactor walls, or at the system boundaries. Control of both factors is important in laboratory- and pilot-scale tests where the aim is to simulate full-scale temperature-time profiles. In typical full-scale systems, temperature profile shape characteristics include a short lag phase, a period of rapid temperature increase into the thermophilic range (> 40 ^{o}C), a plateau (or near plateau) region, and a gradual return toward ambient temperatures (figure 3.1). Peak temperatures in excess of 55 ^{o}C are normally reached in full-scale systems, and temperatures may remain in the thermophilic region for extended periods.

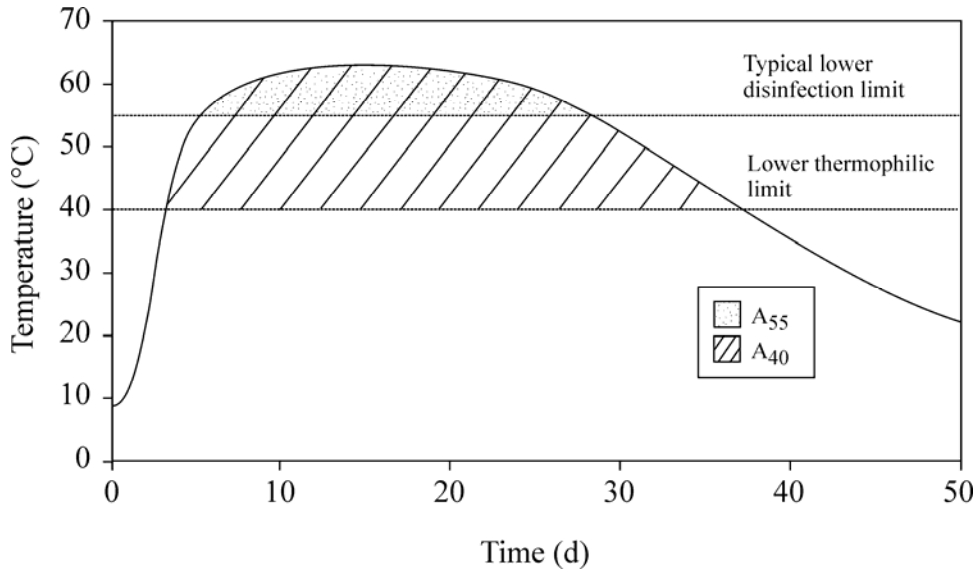

Figure 3.1: Generic composting process temperature profile (adapted from Rynk, 1992)

For the evaluation of reactor simulation performance, we propose that a quantitative assessment of a temperature-time profile may be made using i) the area bounded by the temperature curve and selected baselines, ii) the time for which baseline temperatures are equalled or exceeded and iii) the times taken to reach peak temperatures. Both 40 ^{o}C and 55 ^{o}C are useful reference temperatures, indicating the extent of thermophilic activity, and exposure of material to recommended disinfection conditions, respectively. Given identical raw material and operating conditions (e.g., moisture addition, mixing), these parameters may be used, in combination with the general shape characteristics, to evaluate the extent to which laboratory- and pilot-scale temperature data provide a good simulation of full-scale profiles.

The objectives of this paper are to review heat balance data for laboratory-, pilot- and full-scale composting reactors, and to evaluate the ability of laboratory- and pilot-scale composting reactors to simulate full-scale composting temperature profile characteristics.

3.4 Methods

For temperature-time profile assessment, published graphs were scanned using CanonScan (Canon Inc, Tokyo, Japan), amended with additional gridlines using Corel Draw (Corel Corporation, Ottawa, Canada) and the curves then digitised using Engauge (VA Software,

Fremont, USA). Areas bounded by the profile and a 40 ^{o}C baseline (A_{40}), and the profile and a 55 ^{o}C baseline (A_{55}) (figure 3.1), were calculated using Engauge, the times for which both temperatures were equalled or exceeded (t_{40}, t_{55}) measured, times to peak temperature noted and the general shape characteristics compared to those of the generic profile shown in figure 3.1.

3.5 Heat balance simulation

3.5.1 Ventilative losses

The most significant terms in the heat balance for a composting system at full scale have been identified as biologically generated heat, and the latent heat of vaporisation of water (Bach et al., 1987; Haug, 1993; Robinzon et al., 2000). In contrast, sensible heating of solids, water, dry gas and water vapour have been reported as making relatively small contributions (Bach et al., 1987; Haug, 1993), whilst the effect of heat transport through vessel walls, and subsequent loss from the system, has been found to be relatively minor at full scale (Bach et al., 1987; Weppen, 2001). For a commercial open-bin type reactor and a commercial multi-stage tower, Bach et al. (1987) reported approximately 76% and 86% loss by latent heat of evaporation of water (table 3.1). Ventilative (latent and sensible heat) losses in the airstream were approximately 88% and 95%, respectively. Similar values were reported for a 26.4 m^3 tunnel type reactor, with latent heat counting for > 70% to approximately 90% of total losses and exit gas sensible heat losses for approximately 10 to < 20% of total losses (Harper et al., 1992). For a full-scale in-vessel system assessed by Weppen (2001), evaporation accounted for approximately 85%, and sensible heat in the exit gases 11%, of losses after 12 days. Sensible heat losses in exiting water vapour were omitted from the heat balance of Bach et al. (1987), although this loss was estimated at 8.4% of total outgoing energy in another analysis (Haug, 1993). Energy balance results for a full-scale windrow system (a non-reactor system) indicated that, of the total heat output, evaporation accounted for about 70%, nett radiation about 20% and boundary convection about 10% (Robinzon et al., 2000), showing broad agreement with the findings of Bach et al. (1987).

Table 3.1 Relative heat output from full-scale and laboratory-scale composting systems (%)[a]

Heat term	Full scale		Laboratory scale
	Open-bin reactor	Multi-stage tower reactor	Cylindrical reactor
Sensible heat dry air (q_a)	12.4	8.5	3.3
Heat loss from walls (q_l)	10.9	3.9	61.6
Latent heat water (q_w)	75.8	86.2	34.3
Sensible heat solids and reactor (q_s)	0.9	1.4	0.8
Total	100.0	100.0	100.0

[a] Data of Bach et al. (1987)

At laboratory-scale, proportional ventilative heat losses are typically considerably lower than those expected for full-scale systems. Data for the 28 l cylindrical self-heating reactor (300 mm diameter x 400 mm height) of Bach et al. (1987) show a markedly different heat removal distribution pattern to that reported for full-scale systems. For this reactor, ventilative heat losses were reported as only 37.6% of the heat budget (table 3.1). Similar results were reported for a 30 l reactor, where approximately 36% of the heat loss was attributed to ventilative losses (Weppen, 2001), whilst Koenig and Tao (1996) showed that about one third of losses from a pilot-scale reactor were attributable to evaporation of water and heating of the airstream. Conversely, data provided for an insulated 15 l vessel by Hogan et al. (1989), showed that ventilative losses comprised about 66.5 % of the total heat evolved.

Aeration rates are a key factor in the control of ventilative heat losses, and are commonly expressed on an initial total solids (TS) basis. Natural aeration rates of 0.34-3.2 l/min.kg-TS, may be estimated from superficial velocities of 0.002-0.018 m/s reported for passively aerated piles by Veeken et al. (2002). In contrast, a lower range of 0.035-0.075 l/min.kg-TS at 25 ^{o}C, can be estimated from rates of 0.7-1.5 mg-dry air/s.kg-TS reported for a laboratory-scale passively aerated reactor by Barrington et al. (2003). Design forced aeration rates quoted by Rynk (1992) for full-scale aerated static piles range from 0.3-2.8 l/min.kg-TS, depending on whether the air supply is continuous or intermittent. Similar aeration rates may be calculated from stoichiometric, drying and heat removal considerations, as described by Haug (1993). Excessive aeration, or turning in the case of windrow systems, will result in overcooling of the composting mass, with consequent impacts on the temperature/time profile.

3.5.2 CCR losses and effects of scale

At full-scale, CCR losses have typically comprised a minor proportion of the total heat flux. Losses by conduction of 10.9% and 3.9% were reported for commercial scale plants by Bach et al. (1987), whilst Harper et al. (1992) reported 3-15% conduction losses as a proportion of total losses for a tunnel system. For the full-scale in-vessel system assessed by Weppen (2001), conduction losses after 12 days comprised 4% of cumulative losses.

On reduction of scale, vessel surface area to volume (SA:V) ratios increase to the extent that experimental reactors may display disproportionately large CCR losses (Mason and Milke, 2005; Chapter 2). For the 28 l cylindrical self-heating reactor of Bach et al. (1987), CCR losses were reported to comprise 61.6% of the heat budget (table 3.1). Similar results were reported for the 30 l reactor of Weppen (2001), where 61% of the heat loss was attributed to "conductive" losses, even though the vessel was described as "well insulated", whilst with the 15 l vessel of Hogan et al. (1989), wrapped with 73 mm of polyurethane foam, CCR losses were 33.5% of the total heat evolved. Koenig and Tao (1996) reported that about two thirds of the biologically generated heat was lost through the walls of their pilot-scale reactor. These patterns contrast sharply with the data on commercial-scale systems and highlight the significance, as scale decreases, of heat loss by CCR mechanisms.

Horizontal temperature gradients will reflect the degree of CCR losses. In full-scale composting systems such gradients are reported as typically slight, a phenomenon likely due to the continuing production of heat across the profile, with conductive and convective losses occurring principally at the periphery (Hogan et al., 1989). Data for a 7 ft (2100 mm) wide windrow showed a relatively flat profile with a maximum difference of 2.1 ^{o}C, over a distance of 1.5 ft (460 mm) from the pile centre, but with a rapid decline from 78.9 ^{o}C to 52.9 ^{o}C over the next 1.5 ft (Finger et al., 1976). In a full-scale tunnel reactor, cross-container differences < 2 ^{o}C were typically found, except near the walls where differences of up 3 ^{o}C were occasionally measured (Harper et al., 1992). In pilot-scale reactors, the attainment of radial temperature differences of approximately 1-4 ^{o}C has been demonstrated by Papadimitriou and Balis (1996), VanderGheynst et al. (1997), Cronje et al. (2003) and Sundberg and Jonsson (2003).

3.6 Temperature profile simulation

3.6.1 Profile locations

Temperatures in the full-scale windrow of Keener et al. (2001) were measured at points located one-third and two-thirds along the length of the windrow and 0.5 m below the windrow surface. Sunderg and Jonsson (2003) stated that full-scale reactor temperatures were measured "in a central position". For the other full-scale systems, temperature measurement details were not reported. In the laboratory- and pilot-scale trials assessed, temperature profile data were typically measured at several locations along the central vertical axis of the reactor (Hogan et al., 1989; Day et al., 1997; VanderGheynst et al., 1997; Bari et al., 2000; Seki, 2000; Schloss et al., 2000; Keener et al., 2001; Sundberg and Jonsson, 2003). The profiles of Seki (2000) and Bari et al. (2000) represented the average of 12 and 6 data points respectively. In the present assessment, where temperature profiles at more than one height were reported (Hogan et al., 1989; Day et al., 1997; Keener et al., 2001; Sundberg and Jonsson, 2003), the profile showing the highest values was analysed. Magalhaes et al. (1993) reported that temperatures were measured at the "compost matrix centre", and similarly, Scholwin and Bidlingmaier (2003) used the term "central temperature in the reactor". The profiles reported by Mohee et al. (1998) were described as "top" and "bottom", whilst temperature measurement details for the profile of Atkinson et al. (1996) were not reported.

3.6.2 Comparison of full-, pilot- and laboratory-scale profiles

Full-scale windrow profiles examined showed similar shape characteristics to those in the generic temperature-time profile shown in figure 3.1. However, in all cases (apart from the generic curve of Rynk (1992)), temperatures remained above 40 ^{o}C at the end of the reported data periods (50-74 days). The resultant A_{40} values exceeded 640 ^{o}C.days, whilst A_{55} values ranged from 60 to > 644 ^{o}C.days (table 3.2). Thermophilic temperatures were maintained for > 46 to > 73 days, and t_{55} values ranged from approximately 24 to > 71 days.

Full-scale aerated static pile profiles either showed similar shape characteristics to those in figure 3.1 (Pereira-Neto et al., 1987; Rynk, 1992), or where the trial was curtailed early, of the ascending part of the profile (Liao et al., 1995), over periods of 15-35 days. In contrast to the windrow profiles, the curves presented by Rynk (1992) and Pereira-Neto et al. (1987) returned to below 40 ^{o}C within 32 days, showing lower A_{40} and A_{55} values and also shorter times at the two reference temperatures (table 3.2). In contrast, the profile of Liao et al. (1995), where temperatures remained above 55 ^{o}C after 18 days, showed 18 day A_{40} and A_{55}

values near the top of the range obtained in the windrow systems after 15 days (table 3.2, figure 3.2).

The in-vessel system profiles showed either generally similar shape characteristics to those in figure 3.1 (Sundberg and Jonsson, 2003), or where the trial was curtailed early, to the ascending part of the profile (Plana et al., 2001). Analysis of the curve presented by Sundberg and Jonsson (2003) showed an A_{40} value after 35 days within the windrow range, whilst the A_{55} value was comparable to those found for the aerated static pile systems. In contrast, the in-vessel profile of Plana et al. (2001) had an A_{40} value similar to that for the aerated static pile data of Liao et al. (1995), but had lower A_{55} and t_{55} values after 15 days. To facilitate comparison between these systems, full-scale A_{40}, A_{55}, t_{40} and t_{55} parameters after a common time of 15 days, are shown in figure 3.2.

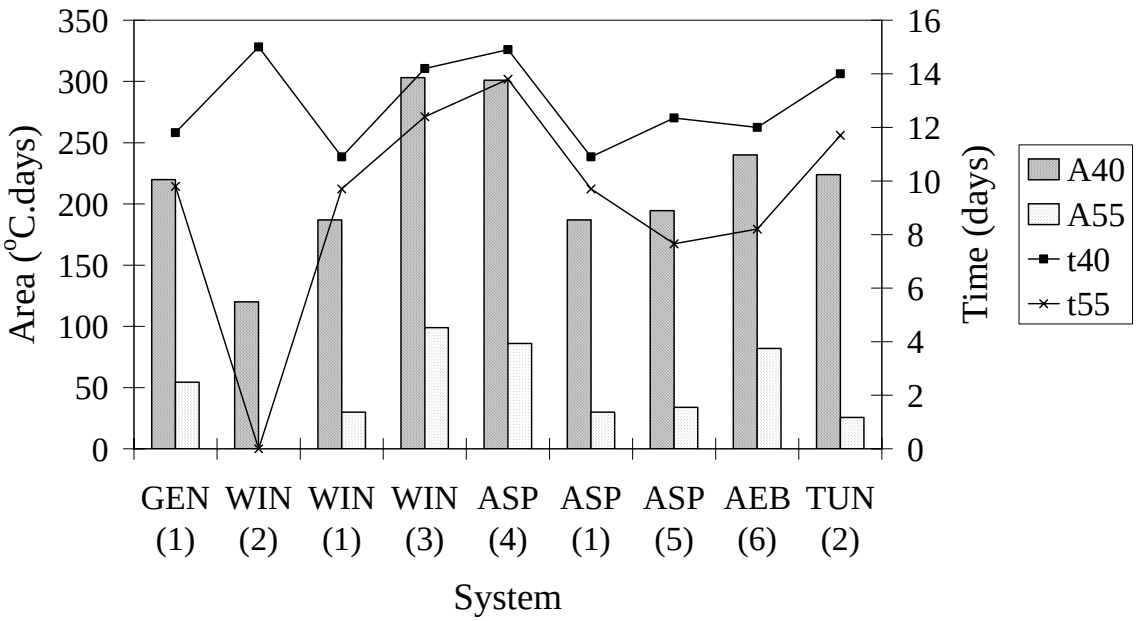

Figure 3.2: Area and time parameters for full-scale composting systems at 15 days. Key: GEN – generic profile; WIN - windrow; ASP – aerated static pile; AEB – aerated bin; TUN – tunnel reactor; 1 – Rynk (1992); 2 – Plana et al. (2001); 3 – Keener et al. (2001); 4 – Liao et al. (1995); 5 – Sundberg and Jonsson (2003)

Table 3.2 Temperature–time data for selected full-scale composting systems

Type	Area > 40 °C (°C days)	Area >55 °C (°C days)	Time >40 °C (days)	Time >55 °C (days)	Length of data set (days)	Substrate	Source of temperature data
Generic	560	120	34.0	22.6	50	Not reported	Rynk (1992)
Windrow	>642[b]	60	>45.9[b]	23.8	50	Not reported	Rynk (1992)
Windrow	>1729[b]	>644[c]	>72.6[b]	>70.8[c]	73.4	Swine manure	Keener et al. (2001)
Windrow	>994[b]	>201[c]	>60[b]	>45.4[c]	60	Food residuals, green waste	Plana et al. (2001)
ASP[a]	426	97	25.0	18.3	32	Refuse, sewage sludge	Pereira-Neto et al. (1987)
ASP[a]	449	114	29.4	16.4	32	Not reported	Rynk (1992)
ASP[a,d]	>276[b]	>71[c]	>15.3[b]	>10.0[c]	18	Fish waste, sawdust	Liao et al. (1995)
Aerated bin	>894[b]	>436[c]	>32.0[b]	>28.2[c]	35	Food residuals, paper	Sundberg and Jonsson (2003)
Tunnel reactor	>224[b]	>25.7[c]	14	11.7	15	Food residuals, green waste	Plana et al. (2001)

[a] ASP = aerated static pile.
[b] Temperatures remained >40 at end of data set.
[c] Temperatures remained >55 at end of data set.
[d] Average of data from two trials using substrate:amendment ratios of 1:and 1.3:1.

Table 3.3 Temperature–time data for selected laboratory-and pilot-scale self-heating column style composting systems

Scale	Area >40 °C (°C days)	Area >55 °C (°C days)	Time >40 °C (days)	Time >55 °C (days)	Aeration rate (l/min kg-TS)	Substrate/comments	Source of temperature data
Lab	313	20	5.7	3.0	0.47[a]	Rabbit chow, corn cobs, paper, compost, sand.	Day et al. (1997)
Lab	150	36	9.8	4.9	0.6	Dog food, wood chips/ static reactor	Schloss et al. (2000)
Lab	83	17	5.6	3.3	0.21[a]	Chicken manure, rice bran, sawdust.	Seki (2000)
Pilot[b,c]	>318[d]/>328[d]	>86[e]/>100[e]	>15.6[d]/15.4[d]	>15.2[e]/>14.5[e]	0.06	Dog food, wood chips	VanderGheynst et al. (1997)
Pilot[d]	>374[d]	>106[e]	>18.1[d]	>16.6[e]	0.07	’’	VanderGheynst et al. (1998)
Pilot[d]	>318[d]	50.4	>18.1[d]	15.4	0.16	’’	’’
Pilot[f]	>452[d]	>206[e]	>17.6[d]	>15.4[e]	0.07	’’	’’
Pilot[f]	>391[d]	>136[e]	>17.8[d]	>16.2[e]	0.16	’’	’’
Pilot[f,g]	85.5	2.2	8.1	1.6	0.6	’’	VanderGheynst et al. (1997)
Pilot	52.5/3.3[h]	0/0[h]	4.7/1.5[h]	0/0[h]	—	Bagasse	Mohee et al. (1998)
Pilot	180	18	19.1	4.4	—	Food residuals, paper,	Bari et al. (2000)

a Calculated by the present authors.
b Trial 1/trial 2; 150 cm measuring point
c Initial moisture 45% .
d Temperatures remained >40 _at end of data set.
e Temperatures remained >55 _at end of data set.
f Initial moisture 55%.
g 90 cm measuring point.
h Upper temperature monitoring point/bottom temperature monitoring point.

Analysis of profiles from laboratory- and pilot-scale reactors, although highly variable, showed several common features. Profile shapes were mainly similar (Hogan et al., 1989; Magalhaes et al., 1993; Atkinson et al., 1996; Mohee et al., 1998; VanderGheynst et al., 1997a; VanderGheynst et al., 1998; Bari et al., 2000; Fraser and Lau, 2000; Schloss et al., 2000; Keener et al., 2001; Scholwin and Bidlingmaier, 2003) to that shown in figure 3.1, along with several notably dissimilar curves (Day et al., 1997; Keener et al., 2001; Sundberg and Jonsson, 2003). However, laboratory- scale self-heating reactors generally had rather low A_{40} and A_{55} values, with relatively short times at both 40 and 55 ^{o}C (table 3.3). Low values for A_{40}, A_{55}, t_{40} and t_{55} were also found for some of the CTD and CHF reactor generated data (table 3.4). In most cases temperatures returned to less than 40 ^{o}C within short time periods, with area and time parameters either within, or below, the range shown for full-scale systems at 15 days (figure 3.2).

It was not possible to conclude definitively whether these experimental results reflected the reactor performance, the available substrate energy, other limitations, or a combination of these factors. However, one CTD profile, where temperatures remained above 40 ^{o}C at the end of the reported data period (Scholwin and Bidlingmaier, 2003), had values of A_{40} comparable to those for full-scale systems (table 3.4, figure 3.2), indicating the possibility of good full-scale simulation at longer times in this reactor, with the food residuals and paper substrate used. For pilot-scale self-heating reactors, both low and similar A_{40}, A_{55}, t_{40} and t_{55} values in comparison to full-scale profiles were found (tables 3.3, 3.5, 3.6). Analysis of data presented by VanderGheynst et al. (1997), for aeration of the same substrate at rates of 0.06 and 0.60 l/min.kg-TS, and initial moisture levels of 45% and 55% respectively, showed a good simulation of full-scale parameter values at the lower aeration rate and moisture level, but substantially decreased parameter values under the other set of operating conditions (table 3.3).

Further profiles from the same reactor at aeration rates of 0.07 and 0.16 l/min.kg-TS (VanderGheynst et al., 1998), yielded similar results to those obtained at 0.06 l/min.kg-TS (table 3.3). Aeration rates estimated from reported data by the present authors for the experiments of Seki (2000), Day et al. (1997) and Hogan et al. (1989) (baseline rate) tended toward the higher end of the design range, at 0.21, 0.47 and 0.55 l/min.kg-TS respectively.

Table 3.4 Temperature–time data for selected laboratory-scale CTD and CHF composting systems

Classification	Scale	Area >40 °C (°C days)	Area >55 °C (°C days)	Time >40 °C (days)	Time >55 °C (days)	Aeration rate (l/min kg-TS)	Substrate/comments	Source of temperature data
CTD	Lab	85	3.2	6.6	3.7	—	Horse manure, alfalfa, paper, soil	Magalhaes et al. (1993)
CTD	Lab	>133[a]	>60[b]	>4.9[a]	>4.8[b]	—	House organic waste, green waste; data to 5 days	Scholwin and Bidlingmaier (2003)
CTD	Pilot	218	101	8.9	6.9	0.17	Vegetables, fish, yard waste, wood chips	Fraser and Lau (2000)
CHF	Lab	68	0	6.5	0	0.55[c,d]/2.3[c,d]	Rice flour, rice hulls	Hogan et al. (1989)
CHF	Lab	182	0.7	16.0	0.5	—	Poultry litter	Atkinson et al. (1996)

[a] Temperatures remained > 40C at end of data set.
[b] Temperatures remained > 55C at end of data set.
[c] Baseline rate/VHM rate.
[d] Calculated by the present author.

Similarly, the estimated aeration rate of 2.3 l/min.kg-TS used by Hogan et al. (1989) for VHM is also toward the upper end of the design range given by Rynk (1992). In order to compare full-, pilot- and laboratory-scale temperature-time performance directly, studies in which a) a swine manure substrate was composted at full-scale and pilot-scale (Keener et al., 2001), and b) a food residuals substrate was composted at full-scale, pilot-scale and laboratory-scale (Sundberg and Jonsson, 2003), were evaluated. For the swine manure substrate, the full-scale and intermittently aerated pilot-scale temperature profile shape characteristics were as expected for full-scale systems (figures 3.3, 3.4).

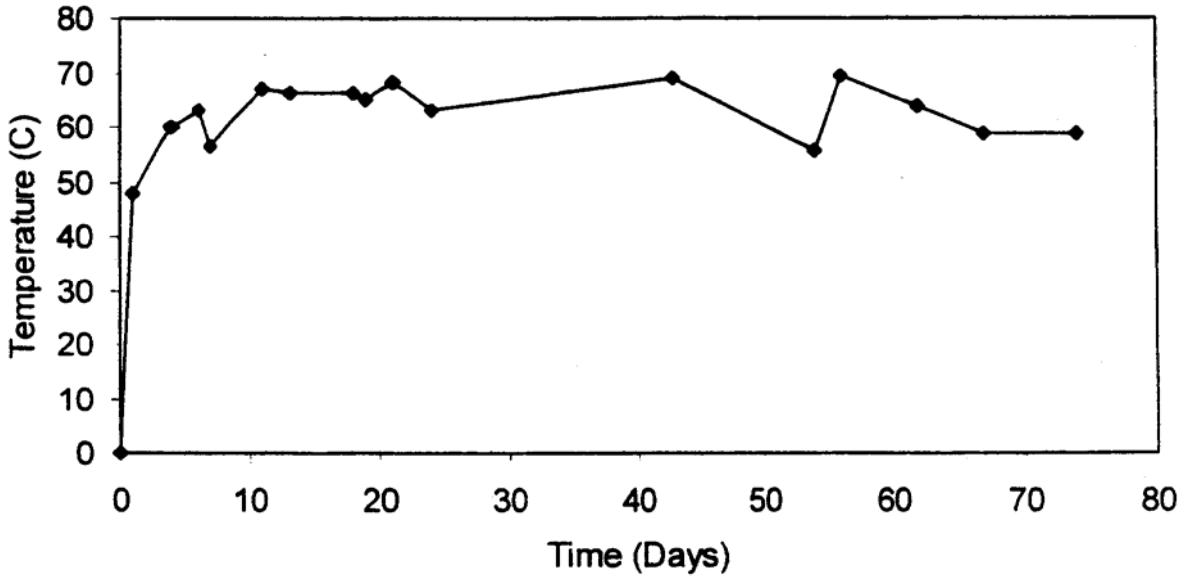

Figure 3.3: Temperature-time profile for full-scale composting of a swine manure substrate (Keener et al., 2001).

Area and time parameters showed close agreement, and were within the expected full-scale system range (table 3.5). However, when continuous aeration was used at pilot scale, the shape characteristics were atypical of full-scale systems, and the both area and time parameter values were considerably diminished. Peak temperatures were reached at markedly different times in all cases, although for the intermittently aerated, pilot-scale, reactor, the peak time was similar to that at which near maximum temperatures (i.e., within 3 ^{o}C) were reached in the windrow system.

Table 3.5: Temperature –time curve parameters for full-scale and experimental composting systems treating a swine manure substrate [a,b]

Type (classification)	Scale	Area >40 °C (°C days)	Area >55 °C (°C days)	Time >40 °C (days)	Time >55 °C (days)	Time to peak temperature (days)	Comments
Windrow	Full	613	226	26.2	24.4	55.4	Temperature within 3 °C of peak reached at 10.9 days
Column (SH)	Pilot	592	217	26.9	22.4	7.4	Run A; intermittent aeration[c]
Column (SH)	Pilot	207	15	21.9	3.6	0.5	Run B; continuous aeration[d,e]

[a] Based on temperature data of Keener et al. (2001); data to day 27 only.
[b] Swine manure/sawdust/shavings mixture.
[c] Approximately 0.83 l/min kg-TS (36 l/min), for min per hour (after Hong et al., 1998); (mass based rate calculated by the present authors).
[d] Approximately 0.25 l/min kg-TS (11 l/min), increasing to approximately 0.86 l/min kg-TS (37.5 l/min) for cooling (after Hong et al., 1998); (mass based rate calculated by the present authors).
[e] Water addition required at day 21 in order to return moisture level to above 45% (wet basis).

Table 3.6 Temperature–time curve parameters for full-scale and experimental composting systems treating a food residuals substrate [a,b]

Type (classification)	Scale	Area >40 °C (°C days)	Area >55 °C (°C days)	Time >40 °C (days)	Time >55 °C (days)	Time to peak temperature (days)	Comments
Aerated bin	Full	889	438	32.0	28.2	27.4	Curve A; linear interpolation across data gap.
Column (SH)	Pilot	136	30	13.7	4.4	15.8	Reactor A; 50 mm insulation; intermittent aeration[c]
Column (SH)	Pilot	885	378	34.9	31.0	15.0	Reactor B; 120 mm insulation; continuous aeration[d]
Dewar flask (SH)	Lab	162	44	10.4	6.5	4.9	–

[a] Based on temperature data of Sundberg and Jonsson (2003); data to day 35 only.
[b] Food waste/paper mixture.
[c] Aeration controlled manually; rates not monitored but thought to be higher than for reactor
[d].Approximately 0.04 l/min kg-TS (0.3 m3/h); (mass based rate calculated by the present authors).

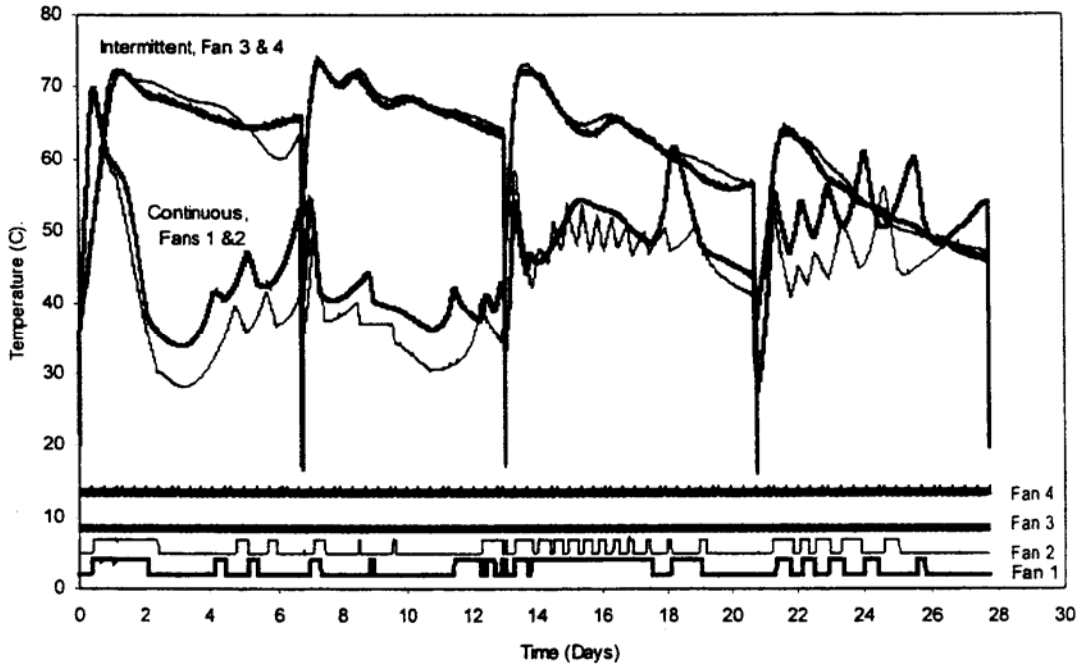

Figure 3.4: Temperature-time profile for pilot-scale composting of a swine manure substrate (Keener et al., 2001).

For the food residuals substrate, temperature profile shape characteristics for a full-scale bin and a continuously aerated pilot-scale reactor were broadly similar, but those for an intermittently aerated pilot-scale reactor, and a laboratory Dewar flask were atypical of full-scale profiles (figure 3.5).

Agreement between A_{40}, A_{55}, t_{40} and t_{55} parameters for the full-scale bin and a continuously aerated pilot-scale reactor was relatively close; however for both the intermittently aerated pilot scale reactor and the laboratory flask it was poor (table 3.6). Peak temperatures were reached at increasing, and substantially different, times for the laboratory-, pilot- and full-scale systems, respectively.

Examination of the pilot-scale reactor aeration rates and expected CCR losses in both studies, indicated that the poor simulation performance of the continuously aerated pilot-scale reactor treating swine waste and the intermittently aerated pilot-scale reactor treating food residuals may be associated with the aeration rates used, rather than excessive CCR losses. Aeration rates of 5 and 11 l/min were used for continuous aeration of the food residuals and swine

waste respectively, with peak rates of 36 and 37.5 l/min used for intermittent aeration (5 min/hour) and cooling, respectively, for the swine waste.

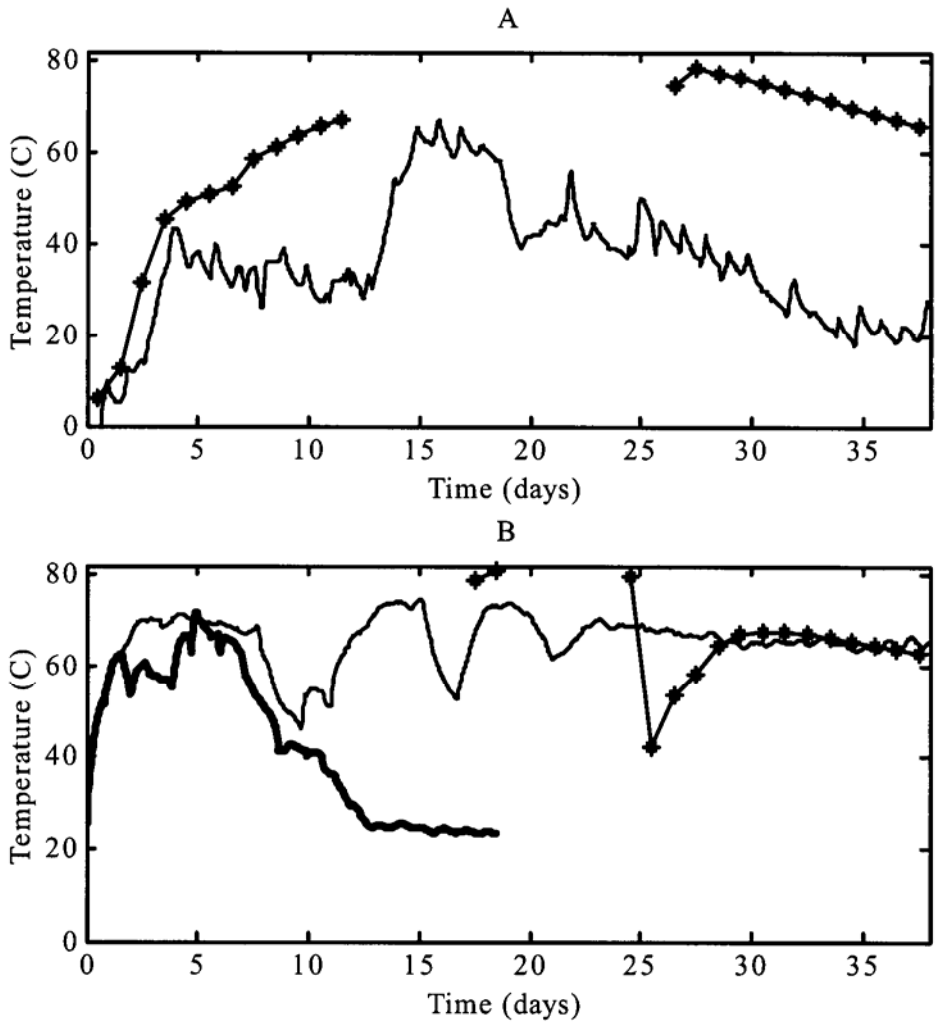

Figure 3.5: Temperature-time profiles for full, pilot and laboratory-scale composting of a food residuals substrate (Sundberg & Jonsson, 2003). Key: * full-scale reactor; thin lines, pilot-scale reactors, thick line, laboratory-scale reactor (Dewar flask).

Using reported moisture content and wet bulk density data for the respective substrates, these airflow rates were calculated to be equivalent to mass-based airflows of 0.04, 0.25, 0.83 and 0.86 l/min.kg-TS respectively, with the intermittent rate of 0.83 l/min.kg-TS equivalent to approximately 0.07 l/min.kg-TS on a continuous basis. In comparison to the values listed earlier, the airflow rates used in the two reactors which simulated full-scale operation most closely, were close to both the natural ventilation rates reported by Barrington et al. (2003) and the lowest forced aeration rate reported by VanderGheynst et al. (1997). Predicted ratios of CCR losses to biological heat production, based on a hypothetical peak heat production rate of 11 W/kg-TS were 8.4%, 7.9% and 3.9% for the pilot scale columns of Keener et al. (2001), Sundberg and Jonsson (2003) with 50 mm insulation and Sundberg and Jonsson (2003) with 120 mm insulation, respectively. Thus, although all the reported aeration rates were within normal design ranges, it appears that higher aeration rates may have been linked to the poor simulation performances at pilot-scale in these two cases. These examples emphasise the importance of controlling both aeration rates and CCR losses to appropriate levels in laboratory- and pilot-scale physical modelling of the composting environment.

3.7 Future issues

Analyses of composting temperature profiles would be facilitated by the establishment of more standardised procedures for temperature measurement, particularly regarding location and frequency. For example, locations along the vertical axis in reactor systems might be expressed in dimensionless form, as a ratio of location height to the total height of the composting material and standard positions selected. In relation to data logging frequency, since modern equipment enables temperatures to be recorded at intervals of seconds or minutes, appropriate intervals and associated data smoothing techniques are suggested as topics worthy of future discussion.

Similarly, the consistent reporting of aeration rates would be highly beneficial when assessing composting experiments. The adoption of l/min.kg-TS as a standard unit of expression is proposed.

Links between composting environments and process performance are not well established. Keener et al. (2001) reported 30.5% and 33.5% removals of TS, after 27 days, for continuously and intermittently aerated pilot scale reactors respectively, and the composts from both reactors

were stable, as assessed by CO_2 evolution rate. In comparison, it was reported that "dry matter loss was less" (data not given) for the full-scale windrow after 106 days. In the other laboratory and pilot-scale reactors analysed in the present review, TS removals ranged from 7.8% over 20 days (Magalhaes et al., 1993) to 25-43%, over periods ranging from 5 days (Scholwin and Bidlingmaier, 2003) to 65 days (Sundberg and Jonsson, 2003). Further work is required to more closely investigate the relationships between temperature profile characteristics and process performance indicators in laboratory-, pilot- and full-scale composting systems.

3.8 Conclusions

1. Reported ventilative heat losses from full-scale composting systems have ranged from 70 to 95% of the total flux, whilst losses from laboratory reactors were in the range 36 to 67%. In comparison, conductive/radiative/convective (CCR) heat losses from full-scale composting systems have ranged from 3 to 15% of the total flux, whereas CCR losses from laboratory reactors have been estimated at approximately 33 to 62% of the total.

2. Full-scale windrow temperatures remained above 40 ^{o}C, and in some cases 55 ^{o}C, after periods of 50-74 days, with areas bounded by the curve and a 40 ^{o}C baseline (A_{40}) exceeding 624 ^{o}C.days, areas bounded by the curve and a 55 ^{o}C baseline (A_{55}) exceeding 60 ^{o}C.days, and times at 40 ^{o}C and 55 ^{o}C > 46 days, and > 24 days respectively.

3. Full-scale forced aeration system temperatures remained above 40 ^{o}C, and in some cases 55 ^{o}C, after periods of 15-35 days. Values of A_{40} exceeded 224 ^{o}C.days, values of A_{55} exceeded 26 ^{o}C.days, and times at 40 ^{o}C and 55 ^{o}C were > 14 days, and > 10 days respectively.

4. Laboratory-scale reactor temperatures typically returned to under 40 ^{o}C within relatively short time periods, with lower temperature-time profile parameters than those measured after 15 days for full-scale systems. Where temperatures returned to under 40 ^{o}C within the data period, A_{40} values ranged between 68-313 ^{o}C.days, A_{55} values between 0-44 ^{o}C.days, and times at 40 ^{o}C and 55 ^{o}C were approximately 6-16 days, and 0-7 days, respectively. Temperature shape characteristics were generally

similar to full-scale profiles. At pilot-scale, temperature-time parameters were shown to be comparable to full-scale values in three cases, and lower than full-scale values in other cases.

5. A laboratory-scale reactor and two pilot-scale reactors operated at comparatively high aeration rates were shown to poorly simulate full-scale temperature profiles. However, moderately insulated self-heating, pilot-scale, reactors operated at relatively low aeration rates were shown, with the exception of times to peak temperature, to be able to provide good temperature profile simulation, both quantitatively and qualitatively.

3.9 Afterword

Two new temperature data sets were found to supplement those reported above. In both cases, parameters were estimated from a simple graphical and visual assessment, rather than the digitisation technique used above, and thus are indicative only. Full-scale windrow temperature data over a 21 week period from the composting of pulp and paper mill sludge was published by Jackson and Line (1997). Values for A_{40} and A_{55} values were estimated by the present author at > 2800 and 1274 ^{o}C.d, whilst t_{40} and t_{55} values were >140 and 98 d respectively. In contrast the temperature-time history from laboratory-scale experiments of Leiva et al. (2003) showed A_{40} and A_{55} values of 37 and 12 ^{o}C.d, with t_{40} and t_{55} values of 2.5 and 1.7 d respectively. These authors utilised the area between the compost temperature and ambient temperature profiles as a measure of heat retention, as previously done by Larsen and McCartney (2000) and Leth et al. (2001). Temperature profiles from the full-scale composting of yard trimmings were reported by Brewer and Sullivan (2003). These results confirm the findings reported in this chapter. Otherwise, no significant new developments in the area of simulation performance assessment have been reported.

3.10 References

Atkinson C.F., Jones, D.D. and Gauthier, J.J., 1996. Biodegradabilities and microbial activities during composting of poultry litter. Poultry Science 75 (5), 608-617.

Bach Phan Dinh, Nakasaki,K., Shoda,M. and Kubota,H., 1987. Thermal balance in composting operations. Journal of Fermentation Technology 65 (2), 199-209.

Bari, Q.H., Koenig, A. and Guihe, T., 2000a. Kinetic analysis of forced aeration composting – I. Reaction rates and temperature. Waste Management & Research 18 (4), 303-312.

Brewer, L.J. and Sullivan, D.M., 2003. Maturity and stability evaluation of composted yard trimmings. Compost Science and Utilisation 11 (2), 96-112.

Day, M., Shaw, K., Cooney, D., Watts, J. and Harrigan, B., 1997. Degradable polymers: The role of the degradation environment. Journal of Environmental Polymer Degradation 5 (3), 137-151.

Finger, S.M., Hatch, R.T. and Regan, T.M., 1976. Aerobic microbial growth in semi-solid matrices: heat and mass transfer limitations. Biotechnol. Bioeng. 18, 1193-1218.

Harper, E., Miller, F.C. and Macauley, B.J., 1992. Physical management and interpretation of an environmentally controlled composting ecosystem. Australian Journal of Experimental Agriculture 32 (5), 657-667.

Haug, R.T., 1993. The practical handbook of compost engineering. Lewis Publishers, Boca Raton, Florida, USA.

Hogan, J.A., Miller, F.C. and Finstein, M.S., 1989. Physical modeling of the composting ecosystem. Applied and Environmental Microbiology 55 (5), 1082-1092.

Hong, J.H., Keener, H.M. and Elwell, D.J., 1998. Preliminary study on the effect of continuous and intermittent aeration on composting of hog manure ammended with sawdust. Compost Science & Utilisation 6 (3), 74-88.

Jackson, M.J. and Line, M.A., 1997. Windrow composting of a pulp and paper mill sludge: Process performance and assessment of product quality. Compost Science & Utilization 5 (3), 6-14.

Keener, H.M., Elwell, D.J., Ekinci, K. Hoitink, H.A.J., 2001. Composting and value added utilisation of manure from a swine finishing facility. Compost Science & Utilisation 9 (4), 312-321.

Koenig, A. and Tao, G.H., 1996. Accelerated forced aeration composting of solid waste. Proceedings of the Asia-Pacific Conference on Sustainable Energy and Environmental Technology, Singapore, 450-457.

Larsen, K. and McCartney, D., 2000. Effect of C:N ratio on microbial activity and N retention: bench scale study using pulp and paper biosolids. Compost Science & Utilisation 8 (2), 147-159.

Leiva, M.T.G., Casacuberta, A.A. and Ferrer, A.S., 2003. Application of experimental design technique to the optimization of bench-scale composting conditions of municipal raw sludge. Compost Science & Utilization 11 (4), 321-329.

Leth, M., Jensen, H. and Iversen, J., 2001. Influence of different nitrogen sources on composting of Miscanthus in open & closed systems. Compost Science & Utilisation 9 (3), 197-205.

Liao, P.H., May, A.C. and Chieng, S.T., 1995. Monitoring process efficiency of a full-scale in-vessel system for composting fisheries wastes. Bioresource Technology 54 (2), 159-163.

Magalhaes, A.M.T., Shea, P.J., Jawson, M.D., Wicklund, E.A. and Nelson, D.W., 1993. Practical simulation of composting in the laboratory. Waste Management Research 11 143-154.

Mason, I.G. & Milke, M.W., 2005. Physical modelling of the composting environment: a review. Part 1: Reactor systems Waste Management 25 (5) 481-500.

Mohee, R., White, R.K. and Das, K.C., 1998. Simulation model for composting cellulosic (bagasse) substrates. Compost Science & Utilisation 6 (2), 82-92.

Papadimitriou, E.K. and Balis, C., 1996. Comparative study of parameters to evaluate and monitor a composting process. Compost Science & Utilisation 4 (4), 52-61.

Plana, R., Mato, S., Aguilera, F., Artola, A., Perez, C., and Sanchez, A., 2001. Comparison between in-vessel and turned pile composting systems. Biocycle 42 (10), 63-65.

Robinzon, R., Kimmel, E., Avnimelech, Y., 2000. Energy and mass balances of windrow composting system. Trans. ASAE 43 (5), 1253-1259.

Rynk, R. (Ed), 1992. On-farm composting handbook. NRAES, Ithaca, New York, USA.

Scholwin, F. and Bidlingmaier, W., 2003. Fuzzifying the composting process: a new model based control strategy as a device for achieving a high grade and consistent product quality. Proceedings of the Fourth International Conference of ORBIT Association on Biological Processing of Organics: Advances for a Sustainable Society, 30th April-2 May, 2003, Perth, Australia, 739-751. ORBIT Association, Weimar, Germany.

Seki, H., 2000. Stochastic modeling of composting processes with batch operation by the Fokker-Planck equation. Trans. ASAE 43 (11), 169-179.

Sundberg, C. and Jonsson, H., 2003. Down-scaling a large composting plant to pilot-scale for systematic research. Proceedings of the Fourth International Conference of ORBIT Association on Biological Processing of Organics: Advances for a Sustainable Society, 30th April-2 May, 2003, Perth, Australia, pp 388-397. ORBIT Association, Weimar, Germany.

VanderGheynst, J.S., Gossett, J.M., Walker, L.P., 1997. High-solids aerobic decomposition: Pilot-scale reactor development and experimentation. Process Biochemistry 32 (5), 361-375.

Veeken, A., de Wilde, V. and Hamelers, B., 2002. Passively aerated composting of straw-rich pig manure: effect of compost bed porosity. Compost Science & Utilisation 10 (2), 114-128.

Weppen, P., 2001. Process calorimetry on composting of municipal organic wastes. Biomass and Bioenergy 21, 289-299.

CHAPTER 4
MATHEMATICAL MODELLING OF THE COMPOSTING PROCESS

4.1 Foreword

We saw in chapters 2 and 3 how physical models have been used, and then examined ways to improve their utility. Now the question is "where to next"? One obvious route forward leads to a more detailed examination of physical modelling, whilst another charts a path on which the ways mathematical modelling has been applied to the composting process may be explored. The second option seemed more interesting and relevant. However, as indicated in chapter 1, it is expected that these two paths do not lead to separate destinations, but will converge later on in the journey. For the moment however the journey leads conceptually across the River Wye to the twin city of Mathmodopolis (figure 4.1) to explore what the folks there are doing. The intention is also to identify whether there are any aspects of compost modelling which require further work - in other words "are there any holes in the knowledge and if so, what are they".

This chapter primarily consists of the following journal paper:

> Mason, I.G., 2006. Mathematical modelling of the composting process: a review. Waste Management 26 (1), 3-21.

The paper covers the literature up to December 2003. An update on significant literature and developments after this time is given in the afterword (section 4.10). Readers are asked to note that the text may differ from that in the published paper in places and that corrections may have been incorporated.

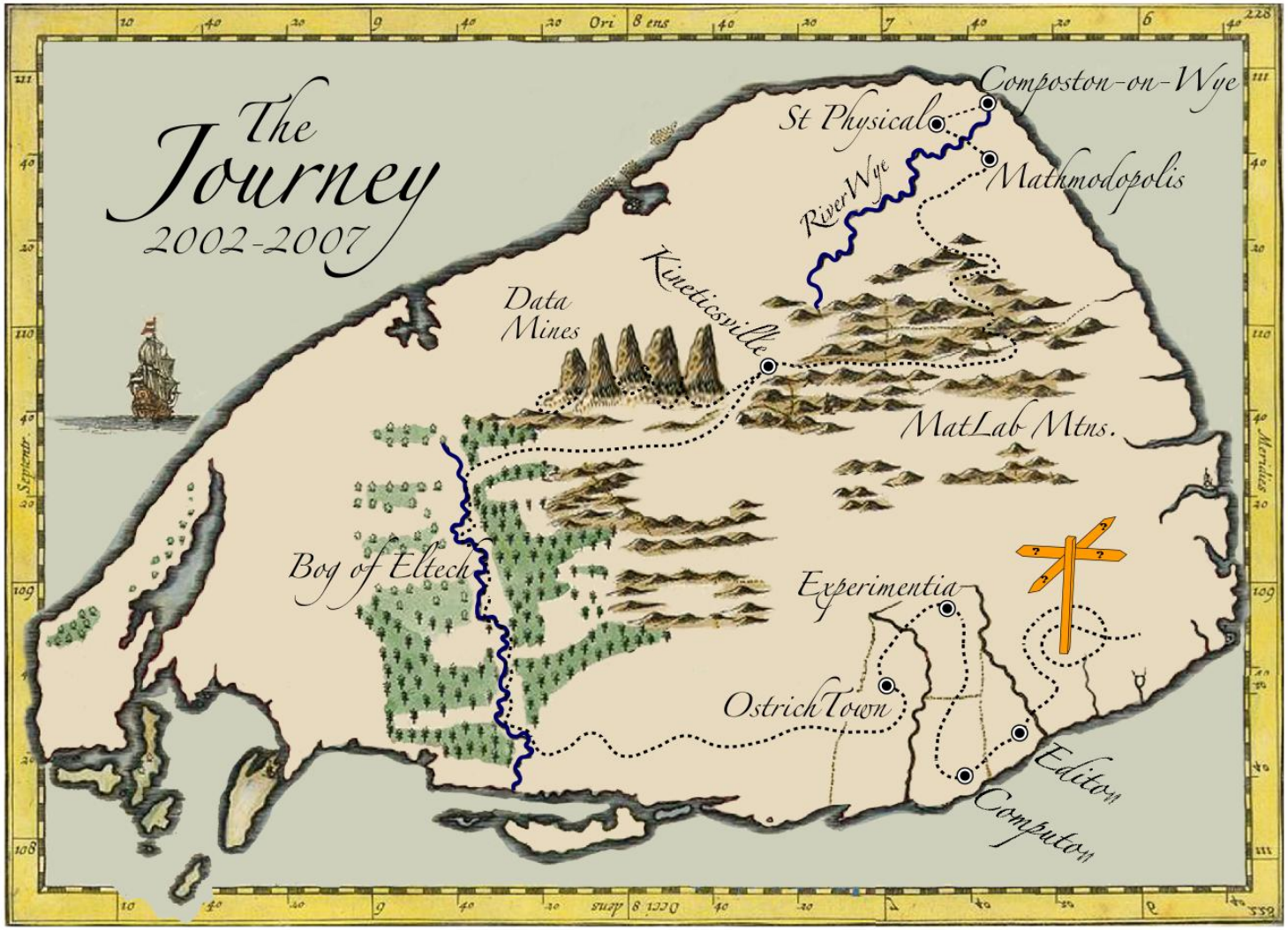

Figure 4.1: The conceptual map of the author's research travels. Our present location is - Mathmodopolis.

4.2 Summary

In this paper mathematical models of the composting process are examined and their performance evaluated. Mathematical models of the composting process have been derived from both energy and mass balance considerations, with solutions typically derived in time, and in some cases, spatially. Both lumped and distributed parameter models have been reported, with lumped parameter models presently predominating in the literature. Biological energy production functions present within the models included first-order, Monod-type or empirical expressions, and these have predicted volatile solids degradation, oxygen consumption or carbon dioxide production, with heat generation derived using heat quotient factors. Rate coefficient correction functions for temperature, moisture, oxygen and/or free air space have been incorporated in a number of the first-order and Monod-type expressions. The most successful models in predicting temperature profiles were those which incorporated either empirical kinetic expressions for volatile solids degradation or CO_2 production, or which utilised a first-order model for volatile solids degradation, with empirical corrections for temperature and moisture variations. Models incorporating Monod-type kinetic expressions were less successful. No models were able to predict maximum, average and peak temperatures to within criteria of 5, 2 and 2 ^{o}C respectively, or to predict the times to reach peak temperatures to within 8 h. Limitations included the modelling of forced aeration systems only and the generation of temperature validation data for relatively short time periods in relation to those used in full-scale composting practice. Moisture and solids profiles were well predicted by two models, but oxygen and carbon dioxide profiles were generally poorly modelled. Further research to obtain more extensive substrate degradation data, develop improved first-order biological heat production models, investigate mechanistically-based moisture correction factors, explore the role of moisture tension, investigate model performance over thermophilic composting time periods, provide more information on model sensitivity and incorporate natural ventilation aeration expressions into composting process models is suggested.

4.3 Nomenclature

A	heat transfer area (m^2); OM loss model saturation constant (%) (Bernal et al., 1996; Paredes et al., 2000; Paredes et al., 2001; Paredes et al., 2002)
A,B	BOD model saturation constants (kg or g/m^3) (Haug, 1993)
Á	Arrhenius constant (cm/hr) (Finger et al., 1976)
B	respiratory quotient (kg-O_2/kg-CO_2) (Kaiser, 1996); maintenance coefficient (kg-substrate/kg-cell mass.hr) (Stombaugh and Nokes, 1996)
B, β_r	respiratory quotient (kg-O_2/kg-CO_2) (Kaiser, 1996; Higgins and Walker, 2001)
BOD	biochemical oxygen demand (kg or g/m^3)
BVS	biodegradable volatile solids (kg)
c	specific heat of compost mixture (kJ/kg. ^oC)
c*, c	oxygen concentration (g/m^3) (Finger et al., 1976)
c_c	mass fraction of carbon (dimensionless) (Kaiser, 1996)
DM	dry matter (kg)
ε	porosity (dimensionless)
E_a	activation energy (cal/mole)
E_b	biological heat (kJ or cal)
F	aeration rate (kg-dry air/hr) (Kishimoto et al., 1987)
FAS	free air space (dimensionless) (Haug, 1993)
FS	solids fraction (dimensionless) (Smith and Eilers, 1980)
G	mass flow dry air (kg/s)
G_o	molar flow rate dry air (mole/hr or mole/d) (Bach et al., 1987)
h_c	heat of combustion (MJ/kg) (Keener et al., 1993)
H, H_c	heat of combustion (kJ/kg-BVS removed)
ΔH^o	heat of combustion for cellulose (17,498 kJ/kg) (van Lier et al., 1994)
$H_{i,o}$	enthalpy of inlet (i) and outlet (o) air (kJ/kg)
H_R, H_{rx}	heat of reaction (kJ/g-TS or kJ/g-VS)
H_s	saturated humidity (kg-H_2O/kg-dry air)
HCOMB	heat of combustion (cal/g-VS) (Smith and Eilers, 1980)
k	first-order rate coefficient (d^{-1})
m	mass (kg); moisture (kg/kg wet basis) (Stombaugh and Nokes, 1996)
$m_{DS,R}$	mass of composting materials (kg) (Scholwin and Bidlingmaier, 2003)
M	moisture (kg), or mass of composting material (kg) (Kaiser, 1996)

M_b	moisture content (kg-H_2O/kg-dry solids) (Higgins and Walker, 2001)
M_c	moisture content (kg/kg; wet basis)
M_c(opt)	optimum moisture content (kg/kg; wet basis)
MM	molecular mass (Kaiser, 1996)
$[O_2]$	oxygen concentration in the exit gas (% v/v)
OM loss	organic matter loss (%) (Bernal et al., 1996; Paredes et al., 2000; Paredes et al., 2001; Paredes et al., 2002)
q_r	rate of heat generation (kcal/hr) (Kishimoto et al., 1987)
Q	heat generation factor (kJ/kg-O_2) (VanderGheynst et al., 1997)
Q_o	heat generated per mole of oxygen consumed (kcal/mole-O_2) (Bach et al., 1987; Nakasaki et al., 1987)
ρ_{db}	dry bulk density (kg/m^3)
R	universal gas constant (cal/^{o}K.mole)
rO_2, RO_2	oxygen consumption rate (mole-O_2/h.g-VS) (Nakasaki et al., 1987) or (kg-O_2/m^3.h) (VanderGheynst et al., 1997)
RCO_2	carbon dioxide evolution rate (g-CO_2/kg-VS.d) (Higgins and Walker, 2001)
s	substrate concentration (g/m^3)
SMOUT	solids content of the mixture output (Haug, 1993)
t	time (s, h or d)
T	temperature (^{o}C)
T_{max}	maximum temperature for microbial growth (^{o}C)
T_{min}	minimum temperature for microbial growth (^{o}C)
T_{opt}	optimum temperature for microbial growth (^{o}C)
TS	total solids (kg)
U	overall heat transfer coefficient (kW/m^2. ^{o}C)
V	volume (m^3)
VOLPO2	volume percentage oxygen in exhaust gas (Haug, 1993)
VS	volatile solids (kg)
w_c	water content (%) (Kishimoto et al., 1987)
W	density (g/cm^3) (Smith and Eilers, 1980)
W_s	weight dry solids (g) (Nakasaki et al., 1987)
X	cell mass (kg/m^3)
X_{O2}	concentration of oxygen (kg-O_2/kg-dry air) (Higgins and Walker, 2001)

$y_{O2,DS,R}$	specific oxygen consumption (kg-O_2/kg-DS time) (Scholwin and Bidlingmaier, 2003)
y, Y	yield (kg/kg)
$Y_{H2O/BVS}$	stoichiometric yield of moisture (kg-H_2O/kg-BVS); 0.6 for glucose
$Y_{O2/BVS}$	stoichiometric consumption of oxygen (kg-O_2/kg-BVS); 1.07 for glucose; mean 1.27 for food waste/office paper/sawdust mixture (Bari et al., 2000a)
Z_o	molar fraction oxygen in inlet and exit air (dimensionless) (Bach et al., 1987)

4.4 Introduction

Mathematical modelling has been widely utilised in science and engineering in order to improve understanding of the behaviour of systems, explore new theoretical concepts, predict system performance and in an increasing number of cases, to aid in the solution of practical design problems. In the latter context, mathematical models offer the potential to reduce, or even replace, the need for physical experimentation when exploring new material and/or process options. Given the challenges and costs involved in conducting appropriate laboratory and pilot scale investigations, increased ability to assess new process options through such modelling is to be welcomed.

Mathematical models of the composting process have appeared in the literature since 1976, with more than 30 papers addressing this topic published through to December 2003. In addition, contributions from studies on liquid-phase aerobic digestion, and the broader field of high solids aerobic degradation, have provided some models with potential relevance to the understanding and prediction of composting system behaviour.

This review will examine compost process models, their structure, kinetic foundations, simulation abilities and validation performance. The discussion will provide a basis for an assessment of the present status of compost process modelling, and has potential implications for developing new and improved models for the future.

4.5 Conceptual frameworks

4.5.1 Overview

The solution of coupled heat and mass balance equations in time, and in some cases, spatially has provided the basis for most compost process models. The general form adopted for heat and mass balance analysis has been as follows:

$$accumulation = input - output \pm transformation. \quad (1)$$

A deterministic approach has been adopted for all published models (table 4.1). However, stochastic elements have been incorporated into two of these models which have appeared within the past few years (Seki, 2000; Scholwin and Bidlingmaier, 2003). Modellers have typically looked at the composting system on a macro-scale, in which the focus of analytical attention has been on the reactor as a whole, however several authors have approached the problem by starting from a microbiological point of view (Kaiser, 1996; Stombaugh and Nokes, 1996; Seki, 2000). Adopting a different perspective, Hamelers (1993) used the composting particle as the basis for analysis.

Model parameters have either been lumped over the complete reactor (Kishimoto et al., 1987; Nakasaki et al., 1987; Haug, 1993; Kaiser, 1996; VanderGheynst et al., 1997; Mohee et al., 1998; Ndegwa et al., 2000; Seki, 2000; Higgins and Walker, 2001), or distributed, over horizontal layers (Finger et al., 1976; Keener et al., 1993; van Lier et al., 1994; Stombaugh and Nokes, 1996; Das and Keener, 1997), rectangular and triangular shaped elements (Smith and Eilers, 1980), or regions based on temperature homogeneity (Scholwin and Bidlingmaier, 2003). The finite element approach has allowed mixture compressibility and other spatially distributed factors to be taken into account (Das and Keener, 1997). Finite elements were also used by Bari et al. (2000b) in a layer-wise analysis of BVS degradation.

A number of these models have been further investigated, typically by different groups of authors. The model of Haug (1993) was used as the basis for subsequent studies reported by Bertoni et al. (1997), Kim et al. (2000) and Ndegwa et al. (2000), whilst Das and Keener (1997) and Mohee et al. (1998) utilised elements of the model originally proposed by Keener et al. (1993). The model of VanderGheynst et al. (1997) was further developed by Higgins and Walker (2001).

Table 4.1: General overview of composting models

References	Deterministic	Stochastic	Parameters		Terms in energy balance (see Table 4.2 for key)	Comments
			Lumped	Distributed		
Finger et al. (1976)	Y	–	–	Y	1, 8[a],11	[a]Thermal diffusion only
Smith and Eilers (1980)	Y	–	–	Y	1, 2, 3, 5, 6, 7, 8, 10, 11	Radiation input only
Bach et al. (1987)	Y	–	na	na	1, 2, 3, 6, 7, 8, 10, 11	Heat balance only
Kishimoto et al. (1987)	Y	–	Y	–	1, 2, 3, 6, 7, 8, 10, 11	–
Nakasaki et al. (1987)	Y	–	Y	–	1, 2, 3, 6, 7, 8, 10, 11	–
Hamelers (1993)	Y	–	Y	–	none	–
Haug (1993)	Y	–	Y	–	1, 2, 3, 6, 7, 8, 10, 11	–
Keener et al. (1993)	Y	–	–	Y	1, 2, 3, 6, 7, 10, 11	No conduction or radiation losses
van Lier et al. (1994)	Y	–	–	Y	1, 2, 3, 6, 7, 8, 10, 11	–
Kaiser (1996)	Y	–			1, 2, 3, 6, 7, 8, 10, 11	–
Stombaugh and Nokes (1996)	Y	–	–	Y	1, 2, 3, 6, 7, 8, 10, 11	Conduction constant
Das and Keener (1997)	Y	–	–	Y	1, 2, 3, 6, 7, 8, 10, 11	–
VanderGheynst et al. (1997)	Y	–	Y	–	1, 2, 3, 6, 7, 10, 11	No radial conduction
Mohee et al. (1998)	Y	–	Y	–	1, 2, 3, 6, 7, 8, 10, 11	–
Seki (2000)	Y	Y	Y	–	1, 2, 3, 6, 7, 8, 10, 11	–
Higgins and Walker (2001)	Y	–	Y	–	1, 2, 3, 6, 7, 10, 11	No radial conduction
Robinzon et al. (2000)	Y	–	na	na	1, 2, 3, 5, 6, 7, 8, 9, 10, 11	Radiation included; heat balance only
Scholwin and Bidlingmaier (2003)	Y	Y	–	Y	1, 2, 3, 6, 7, 8, 10, 11	–

4.5.2 Heat balance considerations

Heat balance components in composting models have included sensible heating of the system contents, sensible heat of input and output streams (input air, water vapour and any supplementary water, exit gases and vapours), conductive/convective losses, radiative inputs and losses, latent heat of evaporation of water and biological heat production (table 4.2). Biological heat production and latent heat of evaporation of water have been shown to be the most significant terms in the heat balance for full-scale systems (Bach et al., 1987; Harper et al., 1992; Weppen, 2001) and these have been incorporated in nearly all reported models (table 4.1). In the majority of cases, latent heat of evaporation of water has been accounted for by the enthalpy term for exit gas water vapour, appearing within an advective gas transport expression. Heat loss through reactor walls has generally been incorporated (Bach et al., 1987; Kishimoto et al., 1987; Nakasaki et al., 1987; Haug, 1993; van Lier et al., 1994; Kaiser, 1996; Stombaugh and Nokes, 1996; Das and Keener, 1997; Mohee et al., 1998; Seki, 2000; Scholwin and Bidlingmaier, 2003), whilst convective boundary losses were included in the models of Smith and Eilers (1980) and Ndegwa et al. (2000). The overall heat transfer

coefficient (U), which incorporates the combined roles of convection, conduction and radiation at system boundaries, has typically been employed, although the term conduction is frequently used in this context. Radiation as a separate term has typically been ignored, although it was explicitly included as an input in the aerated static pile focused model of Smith and Eilers, (1980), and was found to be important for open windrows in the heat balance of Robinzon et al. (2000), with a nett radiation gain indicated.

Table 4.2 Energy balance in composting models

Accumulation terms	Input terms	Output terms	Transformation terms
Sensible heating of reactor contents (1)	Sensible heat of inlet dry air (2) Sensible and latent heat of inlet water vapour (3) Sensible heat of supplementary water (4) Radiation (5)	Sensible heat of dry exit gas (6) Sensible heat of exit water vapour (7) Conductive/convective losses (8) Radiation losses (9) Latent heat of evaporation (10)	Biologically generated heat (11)

However, in the model of Hamelers (1993), which predicted oxygen concentration, oxygen uptake rate, substrate utilisation and biomass growth patterns, temperature gradients at the particle level were considered negligible and were neglected. Wall losses were ignored by VanderGheynst et al. (1997) who modelled heat transport as a 1-dimensional problem along a vertical axis, and were likewise not incorporated in the models of Keener et al. (1993) and Higgins and Walker (2001). Where wall losses comprise only a small proportion of the overall heat budget, it may be argued that this simplification is acceptable. However wall losses can be significant in small-scale systems, even with substantial insulation present (Mason and Milke, 2005a; Chapter 2). Finger et al. (1976) modelled heat transport by thermal diffusion only, with no explicit reference to advective, or other, transport mechanisms. However, advective heat transport is known to play a major role in most composting systems, particularly where forced aeration is used. Heat balance analyses, without predictive equations, were presented by Bach et al. (1987), Harper et al. (1992), Koenig and Tao (1996) and Bari et al. (2000a) and, along with a mass balance evaluation, by Robinzon et al. (2000). Useful mass balance analyses have also been reported by Batista et al. (1995) and Straatsma et al. (2000).

A generalised heat balance model for a representative volume of material in which axial heat and moisture variations in the direction of airflow are small, and configured for sensible heat accumulation as the dependent variable, is presented below:

$$\frac{d(mcT)}{dt} = GH_i - GH_o - UA(T - T_a) + \frac{dBVS}{dt} H_c \quad (2)$$

Here m is the mass of the composting material (kg), c is the specific heat of the composting material (kJ/kg.^{o}C), T is the temperature of the composting material (^{o}C), t is the time (s), G is the mass flow rate of air (kg/s), H_i and H_o are the inlet and exit gas enthalpies (kJ/kg), BVS is the mass of biodegradable volatile solids (kg), H_c is the heat of combustion of the substrate (kJ/kg), U is the overall heat transfer coefficient (kW/m^2. ^{o}C), A is the reactor surface area (m^2), and T_a is the ambient temperature (^{o}C). Eq. (2) has units of kJ/s (kW).

In order to solve this expression without simplification, advective, conductive/convective/radiative (CCR) and biological heat energy terms, plus associated rates of moisture and solids change must be known. Solutions to the enthalpy containing terms have typically been obtained in conjunction with psychometric models, commonly assuming 100% relatively humidity in the exit gas (e.g. Haug, 1993; VanderGheynst et al., 1997), plus representative values for relative humidity and temperature of the inlet air. Haug (1993) predicted saturation exit gas water vapour levels as a function of temperature, and applied an adjustment at low mixture moisture levels, when saturated conditions could not reasonably be assumed. This model also allowed for supplementary water addition and prediction of ammonia levels. To date all models have simulated forced aeration systems, using fixed aeration rates. Given the widespread use of naturally ventilated systems, future research aimed at the incorporation of natural ventilation sub-models into composting process models would be valuable. Diffusive transport of moisture and gases was incorporated into the distributed parameter models of Finger et al. (1976), Smith and Eilers (1980) and van Lier et al. (1994) and was also modelled by VanderGheynst et al. (1997). Oxygen limitation was assumed as the rate controlling factor by Finger et al. (1976). However as pointed out by Agnew and Leonard (2003) in their review paper, oxygen diffusion is unlikely to be significant in the composting process, except at the particle level (Hamelers, 1993). The CCR heat loss term may be readily solved using either commonly available heat transfer information (e.g. Mills, 1995) or experimental heat transfer data (e.g. Bach et al., 1987).

A number of authors have treated ‘mc’ in Eq. (2) as a constant term (van Lier et al., 1994; Stombaugh and Nokes, 1996; Das and Keener, 1997; VanderGheynst et al., 1997; Mohee et al., 1998; Higgins and Walker, 2001) resulting in expressions of the following form:

$$mc\frac{dT}{dt} = GH_i + \frac{d(BVS)}{dt}H_c - GH_o - UA(T - T_a) \tag{3}$$

from which the expression for the rate of temperature change is:

$$\frac{dT}{dt} = \frac{GH_i + \frac{d(BVS)}{dt}H_c - GH_o - UA(T - T_a)}{mc} \tag{4}$$

Nakasaki et al. (1987) assumed constant specific heat only. Since the accumulation term will likely account for a relatively small proportion of the heat balance (see Weppen, 2001), this simplification may introduce relatively little error into model performance.

VanderGheynst et al. (1997) assumed a constant moisture content in the composting material over the period of their study, and validated this supposition experimentally. Additional assumptions discussed and implemented by VanderGheynst et al. (1997) included those of constant mass air flux, minimal diffusion of mass and energy (since forced aeration was used), and equilibrium between solid and gas phases (homogenous assumption). These authors also used simplified equations for calculating the enthalpy of dry air and assumed that both influent and effluent air were saturated and at constant total pressure. Both air mass and water vapour mass were assumed constant by Keener et al. (1993).

Models for the degradation of BVS, from which the generation of biological heat, release of biological water and oxygen consumption are predicted, are of key importance in the heat balance expression and will be examined in detail later.

4.5.3 Mass balance considerations

Approaches to moisture prediction based on an analysis of inlet air content, exit gas content and biologically produced water, have typically been used, with the latter term estimated from yield factors (*y* or Y) based on BVS degradation (Keener et al., 1993; Kaiser, 1996; Stombaugh and Nokes, 1996; Das and Keener, 1997; Mohee et al., 1998; Higgins and Walker, 2001). A similar approach has been used to estimate oxygen consumption or carbon dioxide evolution. The following expressions from Higgins and Walker (2001) typify these models:

$$\frac{dM_b}{dt} = \frac{G_a(H_s(T_a) - H_s(T)) - y_{H_2O/BVS}\dfrac{d(BVS)}{dt}}{\rho_{db}V_r} \tag{5}$$

$$\frac{dX_{O_2}}{dt} = \frac{G_a(X_{O_2.a} - X_{O_2.exit}) - y_{O_2/BVS}\dfrac{d(BVS)}{dt}}{V_r\varepsilon\rho_a(T)} \tag{6}$$

where M_b is the moisture content (kg-H_2O/kg-dry solids), t is the time (d), G_a is the mass flowrate of dry air (kg-dry air/d), H_s is the saturated humidity (kg-H_2O/kg-dry air), T is the temperature of the composting material (^oC), T_a is the ambient temperature (^oC), y is the metabolic yield of water (kg-H_2O/kg-BVS removed) (equation 5), or metabolic consumption of oxygen (kg-O_2/kg-BVS removed) (equation 6), BVS is the mass of biodegradable volatile solids (kg), V_r is the working volume of the reactor (l), ρ_{db} is the dry bulk density of the composting material (kg/m^3), X_{O2} is the concentration of oxygen (kg-O_2/kg-dry air), ε is the porosity of the composting material (dimensionless), and ρ_a is the density of dry air (kg/l). In these equations the volume of the composting material and the descriptive parameters were held constant.

4.5.4 Prediction of state variables

The state variables of primary interest in composting are temperature, moisture content and oxygen concentration. Temperature has been predicted by all models, excepting that of Hamelers (1993). In the model of Haug (1993), temperatures were determined iteratively for a series of discrete steady state heat and mass balances, rather than predicted for non-steady state conditions. Moisture content has been predicted by several authors (Kishimoto et al.,

1987; Nakasaki et al., 1987; Ndegwa et al., 2000), and oxygen concentration by Finger et al. (1976), van Lier et al. (1994) and Mohee et al. (1998). Other variables predicted have included oxygen uptake rate (Hamelers, 1993; Stombaugh and Nokes, 1996; Higgins and Walker, 2001), carbon dioxide evolution rate (Kishimoto et al., 1987; Nakasaki et al., 1987; van Lier et al., 1994), dry exit gas mass and exit gas water vapour (Haug, 1993), bulk weight (van Lier et al., 1994; Ndegwa et al., 2000), biomass (Hamelers, 1993; Kaiser, 1996; Stombaugh and Nokes, 1996), total solids (Kishimoto et al., 1987; Hamelers, 1993; Stombaugh and Nokes, 1996; Mohee et al., 1998; Ndegwa et al., 2000) and product solids composition (Haug, 1993; Kaiser, 1996). Given the importance of moisture tension in soil processes, the absence of this term as a state variable is worthy of consideration and may be an important factor at low moisture levels. Miller (1989) has discussed the application of matric potential to composting systems, and has reported an empirical relationship between matric potential and gravimetric water content.

4.5.5 Related models

Related models include those describing the thermophilic aerobic digestion of waste activated sludge and ground garbage (Andrews and Kambhu, 1973), and cassava fermentation by *Aspergillus spp* (Saucedo-Castaneda et al., 1990; Rodriguez Leon et al., 1991). In common with the composting models, analytical approaches were based around the solution of heat and mass balance expressions, with biological heat and latent heat of evaporation of water identified by Andrews and Kambhu (1973) as the most important items in the heat balance. Temperature was predicted in all cases, although the solution presented by Andrews and Kambhu (1973) was for steady state conditions only. The Saucedo-Castaneda et al. (1990) model also predicted substrate, biomass and carbon dioxide production. One of the features of the latter model was the use of the Peclet (Pe), Biot (Bi) and Damkohler (Da_m) dimensionless numbers, plus dimensionless geometric reactor ratios, in modelling heat transport. The Peclet number also was employed by van Lier et al. (1994), as a guide to which finite difference method to utilise in their model discretisation procedure. The use of dimensionless numbers in future composting process models would be beneficial for scale-up purposes and may offer advantages in helping to explain variations in reactor performance.

4.6 Substrate degradation and biological energy expressions

4.6.1 Introduction

The general approach to modelling biological energy production in composting energy balances has been to describe solids degradation, either explicitly using BVS, or implicitly using oxygen consumption or carbon dioxide generation, and then to apply appropriate heat yield factors in order to obtain an energy expression.

4.6.2 Kinetic foundations

Modellers have used first-order substrate degradation kinetics, Monod-type expressions or empirical substrate degradation equations in modelling biological energy production (Tables 4.3, 4.5, 4.6). Alternatively, Kishimoto et al. (1987) used an empirical expression (without a substrate term), whilst Rodriguez Leon et al. (1991) employed an electron balance technique, in conjunction with an exponential growth function, for biological heat estimation.

The first-order kinetic relationships have been based on either oxygen utilisation (Finger et al., 1976) or volatile solids degradation (Smith and Eilers, 1980; Haug, 1993; Keener et al., 1993; Das and Keener, 1997; Mohee et al., 1998; Higgins and Walker, 2001) (table 4.3). It should be noted that the expression used by Haug (1993), although written in terms of biodegradable volatile solids (BVS), was based on BOD data. First-order rate coefficient values ranging between 0.002-0.15 d^{-1}, depending on substrate type and temperature, have been reported (table 4). Additionally, high temperature values, ranging from 0.025-0.190 d^{-1} at 50-60 ^{o}C, were tabulated by (Keener et al., 1993). Corrections to first-order rate coefficients have been made for temperature, moisture content, oxygen concentration and free air space. The models used for these correction factors are discussed later.

The Monod-type expressions have proceeded from cell growth (first-order) and/or substrate utilisation considerations, and have been used to predict either oxygen uptake rates (Kaiser, 1996) or solids production rates (Stombaugh and Nokes, 1996; Seki, 2000) (table 4.5). Kaiser (1996) separately modelled the degradation of four different substrates (sugars and starches, hemicellulose, cellulose and lignin) by four microbial groups (bacteria, actinomycetes, brown-rot fungi, white rot fungi). In two models, temperature corrections to the rate coefficients were made using empirical expressions related to microbial growth (Kaiser, 1996; Stombaugh and Nokes, 1996). Substrate limitation was accounted for in all

Table 4.3: First-order biological energy (E_b) rate expressions used in composting models

Biological energy rate equation	Rate coefficient corrections used	References
$\frac{dE_b}{dt} = A' e^{-\frac{E_a}{RT}} a(c^* - c_l) H_R$	Temperature	(Finger et al., 1976)
$\frac{dE_b}{dt} = \left[RO_2(\max) * e^{-\frac{(T-57)^2}{254}} * e^{-10.973(FS-0.3)^2} \right] \frac{[HCOMB * W * BVS]}{1200}$	Temperature, moisture	after (Smith and Eilers, 1980) (p 24)
$\frac{dE_b}{dt} = -[k_{T(fast)}.BVS_{(fast)} + k_{T(slow)}BVS_{(slow)}].H$	Temperature, oxygen, moisture, FAS	(Haug, 1993)
$\frac{dE_b}{dt} = -k(m_t - m_e).\Delta h_c$	Temperature	(Keener et al., 1993) (Das and Keener, 1997)
$\frac{dE_b}{dt} = -k(m_t - m_e).h_c$	Temperature, moisture	(Mohee et al., 1998)
$\frac{dE_b}{dt} = -[k_{BVS}.BVS].H_{rx}$	Temperature, oxygen	(Higgins and Walker, 2001)
$\frac{dE_b}{dt} = -9760.y_{O_2,DS,R}.m_{DS,R}$	-	(Scholwin and Bidlingmaier, 2003)

Table 4.4: Rate coefficients and goodness of fit for first-order models of substrate degradation

Model	Rate coefficient	Goodness of fit[a]	Time	Substrate	Reference
	(d^{-1})		(d)		
$BOD_t = A[1-e^{-k_1.t}]+B[1-e^{-k_2 t}]$	0.15/0.05[b]	-	60	raw sludge	(Haug, 1993)
	0.015/0.004[b]	-	242	raw sludge	
	-/0.0095[b]	-	200	pulp mill sludge	
	0.15/0.02[b]	-	90	softwood sawdust	
	-/0.0081[b]	-	368	hardwood sawdust	
$\frac{m(\theta)-m_e}{m_o-m_e}=e^{-k.t}$	0.048	-	3	poultry manure, corn cobs	(Keener et al., 1993)
	0.0665	RMS = 67.94	> 70	sorghum bagasse, pig manure, poultry manure	(Bernal et al., 1996)
$OM\,loss = A[1-e^{-k.t}]$				sorghum bagasse, sewage sludge	
	0.0279	RMS = 29.76	> 70		"
				Food waste, paper, sawdust	
	0.002-0.013[c]	R^2 = 0.450-0.844	28		(Bari et al., 2000)
	0.018-0.051[d]				
$\frac{\Delta BVS}{BVS_0}=1-(1-k_1'\Delta t)...x(1-k_n'\Delta t)$				Poultry manure, cotton waste, olive mill ww[e]	
	0.0598	RMS = 4.03	> 84	Sewage sludge, cotton waste, olive mill ww	(Paredes et al., 2000)
	0.0226	RMS = 32.34	> 84	Sewage sludge, cotton waste[e]	"
				Sewage sludge, cotton waste	
				Orange waste, cotton waste[e]	
$OM\,loss = A[1-e^{-k.t}]$	0.0594	RMS = 13.48	> 84	Orange waste, cotton waste	(Paredes et al., 2001)
	0.0749	RMS = 12.20	> 84		"
	0.0377	RMS = 12.72	> 84	Olive mill sludge, cotton gin waste	"
	0.0203	RMS = 33.50	> 84		"
$OM\,loss = A[1-e^{-k.t}]$	0.0181	RMS = 23.55	> 168		(Paredes et al., 2002)
$OM\,loss = A[1-e^{-k.t}]$					

a. R^2 = correlation coefficient; RMS = residual mean square
b. Data obtained from constant temperature and pressure respirometry, with substrates present in solution. The data is tabulated as fast coefficient (k_1)/slow coefficient (k_2).
c. At 25 °C; d. At 50 °C; e. Watered with olive mill wastewater (ww);

models and adjustments for moisture level and oxygen concentration made by Stombaugh and Nokes (1996).

Table 4.5: Monod-type biological energy (E_b) rate expressions used in composting models

Biological energy rate equation	Rate coefficient corrections	References
$\frac{dE_b}{dt} = c_c \frac{MM_{CO_2}}{MM_c}(Y-1).$ $\left(\frac{ds_1}{dt}+\frac{ds_2}{dt}+\frac{ds_3}{dt}+\frac{ds_4}{dt}\right)$ $.M.\beta.14000$	Temperature, substrate type	Kaiser (1996) (NB: β and 14000 (kJ/kg O_2) terms added)
$\frac{dE_b}{dt} = \left[\frac{1}{Y_{X/S}}\frac{dX}{dt} + \beta X\right] Y_{H/S}$	Temperature, substrate type, moisture, oxygen	Stombaugh and Nokes (1996)
$\frac{dE_b}{dt} = V\left\{\frac{dS}{dt}+\frac{dX}{dt}\right\}\Delta h_s$	Temperature, substrate type	Seki (2000)

Monod-type kinetics, with temperature correction using an Arrhenius type expression, were also used by Saucedo-Castaneda et al. (1990). In a related approach, a Michaelis-Menten type kinetic expression for carbon disappearance in a composting system, based on the formation of an intermediate enzyme/substrate complex, was derived by Whang and Meenaghan (1980) and rate constants were evaluated using a Lineweaver-Burke analysis. However, the kinetic model was not utilised for the prediction of biological heat production. An exponential microbial growth expression was used to model biological heat production by Rodriguez Leon et al. (1991).

Empirical kinetic relationships have utilised either oxygen consumption data (Bach et al., 1987; VanderGheynst et al., 1997), carbon dioxide generation data (Nakasaki et al., 1987) or total solids degradation data (van Lier et al., 1994) (table 4.6). The data used by Nakasaki et al. (1987) were obtained from the work of Bach et al. (1984). A polynomial relationship describing total solids degradation over a 7 day period in a forced aeration system composting a horse manure and straw mixture, was fitted to experimental results by van Lier et al. (1994). The model used by VanderGheynst et al. (1997) incorporated a power law relationship, and was fitted to O_2 consumption rates from the composting of a dog food substrate over a period of 35 hr. As previously mentioned, Kishimoto et al. (1987) used an

empirical relationship in which biological heat generation was expressed in terms of temperature, moisture content, cumulative energy and airflow rate. The relationship described data from seven previous runs in the same apparatus and using the same substrate.

4.6.3 Temperature correction functions

Models of the effect of temperature on composting reaction rates have been developed from Arrhenius functions (Finger et al., 1976; Haug, 1993; Bari et al., 2000a; Neilsen and Berthelsen, 2002), empirically from composting data (Schulze, 1962; Smith and Eilers, 1980; VanderGheynst et al., 1997; Mohee et al., 1998), empirically from microbial growth data (Kaiser, 1996; Stombaugh and Nokes, 1996) or based on cardinal (minimum, maximum and optimum) temperatures for microbial growth (Rosso et al., 1993) (tables 4.7 and 4.8).

Experimental composting data has shown that as temperature is increased from about 20 ^{o}C, biological activity tends to first increase slowly, then rise moderately to a peak value, following which a rapid decline in activity occurs, typically over a small temperature range. Thus a right-hand skewed curve results, with the optimum and maximum temperatures generally very close together. Similar behaviour has been described for other microbial growth studies. A number of models have generated profiles which reflect this phenomenon well (Haug, 1993; Rosso et al., 1993) or are relatively close to it (Smith and Eilers, 1980). However, in other cases this pattern has been less well represented. For example, the temperature correction functions used by Kaiser (1996) showed parabolically shaped curves, with a high degree of activity indicated at 20 ^{o}C, peak temperatures of 40 ^{o}C for all substrates and organisms, and a relatively slow decline above the optimum temperature. A simpler approach was used by Stombaugh and Nokes (1996), who adopted three linear temperature correction functions over the ranges 0-30 ^{o}C, 30-55 ^{o}C and > 55 ^{o}C, with a constant value for peak activity from 30-55 ^{o}C.

Table 4.6: Empirical biological energy (E_b) rate expressions used in composting models

Basis	Biological energy rate equation	Rate coefficient corrections used	References
-	$\frac{dE_b}{dt} = G_o(Z_0 - Z_e^{'}).Q_0$	none	(Bach et al., 1987)
Regression	$\frac{dE}{dt} = e_o + e_1 T + e_2 w_c + e_3 \int q_r dt + e_4 F$	na.	(Kishimoto et al., 1987)
Linear	$\frac{dE_b}{dt} = -r_{O_2}.W_s.Q_0$	none	(Nakasaki et al., 1987)
Polynomial model of substrate degradation data	$\frac{dE_b}{dt} = f(\Delta DM).\Delta H^0$	none	(van Lier et al., 1994) NB: f(ΔDM) is a fitted polynomial)
Exponential model of oxygen consumption data	$\frac{dE_b}{dt} = [RO_{2,0} + a(1 - e^{-C(T-T_0)})].Q$	Temperature: $(a[1 - e^{-C(T-T_0)}])$	(VanderGheynst et al., 1997)

Table 4.7: Temperature correction functions used in conjunction with first-order biological energy rate expressions

Temperature correction function	Reference
$k_g = A^{'}.e^{-\frac{E_q}{R.T}}$	(Finger et al., 1976)
$e^{-\frac{(T-57)^2}{254}}$	(Smith and Eilers, 1980)
$k_T = k_{20}.[1.066^{(T-20)} - 1.21^{(T-60)}]$	(Haug, 1993) Haug (1993)
$k = \{-8e^{-6} * T^3 + 0.008 * T^2 - 0.0238 * T + 0.2643\}$	(Mohee et al., 1998)
$k_{BVS(T)} = k_{BVS}(f_T)$	(Higgins and Walker, 2001)
$k_{BVS} = \frac{\beta_r R_{CO_2 opt}}{10^3 \gamma_{O_2}(BVS)}(f_T)(f_{O_2})$	
$f_T = \frac{(T - T_{\max})(T - T_{\min})^2}{(T_{opt} - T_{\min})\{(T_{opt} - T_{\min})(T - T_{opt}) - (T_{opt} - T_{\max})(T_{opt} + T_{\min} - 2T)\}}$	(Rosso et al., 1993)

The temperature correction model of Neilsen and Berthelsen (2002) was based on an enzyme/substrate mechanism in combination with an Arrhenius type expression. It was developed to overcome problems with negative values at high temperature (i.e., above 80 ^{o}C) occurring with the Haug (1993) model. Whilst it is unlikely that many composting systems would operate at, or above 80 ^{o}C, the model may be useful for related solid-state processes. No validation data was presented.

In contrast to the models showing a peak, followed by a decrease, in activity, the Arrhenius model utilised by Finger et al. (1976) increased exponentially. The empirical model developed by VanderGheynst et al. (1997) tended to a plateau at a temperature differential of about 30 ^{o}C, which is equivalent to 50 ^{o}C given a starting temperature of 20 ^{o}C. However, given the high degree of scatter in the experimental data and evidence of a declining trend in the rate at higher temperatures, a model of the skewed form described above might also be fitted in this case. A polynomial expression for the rate coefficient k, with a form similar to the skewed models in their sub-optimal temperature range, was used for temperature correction by Mohee et al. (1998). However a peak and subsequent decrease within the biologically active range was not indicated and the function continued to increase beyond 80 ^{o}C.

Three models used to correct for the effect of temperature on the microbial growth rate (Andrews and Kambhu, 1973; Ratkowsky et al., 1983; Rosso et al., 1993) were evaluated in detail by Richard and Walker (1998), using new experimental data. Whilst all models showed an acceptable fit, it was concluded that the model of Rosso et al. (1993) provided the best description of the rate coefficient temperature dependence, since it involved the fewest parameters, all of which were easily measurable and each of which had a physical meaning in terms of the composting process.

4.6.4 Moisture, oxygen and FAS correction functions

Published moisture correction functions (table 4.9) have all been derived empirically. An exponential expression indicating maximum activity at 70% moisture content was used by Smith and Eilers (1980). A similar model, reportedly based on data of Smith and Eilers (1980), was employed by Mohee et al. (1998), although in the form presented in the literature, this produces an unrealistic curve.

Table 4.8: Temperature correction functions used with Monod-type biological energy (E_b) rate expressions

Temperature correction	References
$f_1^{temp} = \frac{T(80-T)}{1600} \text{K}\ 0 < 80^0 C$	(Kaiser, 1996)
$f_{2...4}^{temp} = \frac{T(60-T)}{20(80-T)} \text{K}\ 0 < 60^0 C$	
$ktemp = \frac{T}{T_2 - T_1} \text{K K K K}\ T_1 < T < T_2$	(Stombaugh and Nokes, 1996)
$ktemp = 1.0 \text{K K K K K K}\ T_2 < T \le T_3$	
$ktemp = 3.75 - \left[\frac{T}{T_2 - 10}\right] \text{K}\ T_3 < T$	
$T_1 = 0 \text{K}\ C$	
$T_2 = 30 \text{K}\ C$	
$T_3 = 55 \text{K}\ C$	

However, following adjustment to ensure that a negative exponent is always present and the moisture content is expressed as a fraction, a curve with a peak at 0.56 moisture content may be produced. However, the modified function is negative at fractional moisture levels of < 0.17 and > 0.97 and has a different profile to the model of Smith and Eilers (1980). In contrast, a function with a plateau above 70%, was proposed by Haug (1993). As noted by Haug, a decreasing trend in data at higher moisture levels, which was not described by the model, was probably attributable to diminishing free air space. In order to correct for this, Haug (1993) also presented a free air space correction function of similar mathematical form to that used for moisture dependence. When the moisture and free air space correction functions are combined, a model of similar form to that of Smith and Eilers (1980) is produced, illustrating the interdependence of these two factors in terms of their influence on reaction rates. As noted by Haug (1993), it can be difficult to separate out the effects of moisture, free air space and also bulk weight. More recently, a mechanistic model relating moisture content and respiration rate has been proposed by Hamelers and Richard (2001). This model predicts a relationship of similar form to that generated by the temperature correction model of Rosso et al. (1993) and has shown a promising fit to experimental data as reported by Richard et al. (2002).

The effect of oxygen concentration has been modelled using Monod-type and exponential, expressions (Haug, 1993; Richard et al., 1999). A simple one-parameter model was used by Haug (1993), with a half saturation constant value of 2%. More recently, Richard et al. (1999) compared the performance of one-parameter, modified one-parameter and two-parameter Monod-type models, plus an exponential model, using an extensive data set. It was concluded that the Monod-type models gave the best performance over the complete temperature range, and suggested that the simple one parameter model was best suited to windrow composting applications where low oxygen levels may be encountered, whilst the modified one parameter model may be preferable for forced aeration systems operating at relatively high oxygen concentrations. The simple one parameter model, with the half saturation constant expressed as an empirical function of temperature and moisture concentration, was subsequently used in the composting model validation study of Higgins and Walker (2001).

Table 4.9: Moisture, oxygen and free air space rate constant adjustment expressions used in composting models

Moisture correction	Oxygen correction	FAS correction	References
$F1(I) = \frac{1}{e^{[-17.684(1-SMOUT)+7.0622]}+1}$	$FO2(I) = \frac{VOLPO2(I)}{VOLPO2(I)+2}$	$F1(I) = \frac{1}{e^{[-23.675FAS(I)+3.4945}+1}$	Haug (1993)
$e^{-10.973(FS-0.3)^2}$	none	none	Smith and Eilers (1980)
$f(m_c) = -56.97 + 57.98e^{((-0.5(m_c-0.56)/1.52)^2)}$	none	none	Mohee et al. (1998)
none	$f_{O_2} = \frac{O_2}{k_{O_2}(T, X_{H_2O}) + O_2}$ $k_{O_2} = 0.79 - 0.041T + 0.040X_{H_2O}$	none	(Higgins and Walker, 2001)
$kH_2O = 0.0\text{K K K K } m_1 < m < m_2$ $kH_2O = \frac{m}{m_2} - 1.0\text{K } ...m_2 < m \le m_3$ $kH_2O = 1.0\text{K } .....m_3 < m$ $m_1 = 0\text{K } kg/kg(wb)$ $m_2 = 0.2\text{K } kg/kg(wb)$ $m_3 = 0.4\text{K } kg/kg(wb)$	Monod	None (Note: moisture factor = 1, when m > 0.4)	{Stombaugh and Nokes (1996)

4.6.5 Heat conversion factors

Most modellers have utilised simple heat conversion factors, based on volatile solids degradation or oxygen consumption, to obtain energy, or power, values from substrate degradation models. Values have been obtained from calorimetric measurements, calculated from COD data (Haug, 1993), or determined using an electron balance method (Rodriguez Leon et al., 1991). The reported available energy from organic substrates has ranged from 17.8-24.7 kJ/g-TS removed (sometimes expressed as kJ/g-volatile solids (VS) removed) (Haug, 1993; Keener et al., 1993; van Ginkel, 1996), or, on an oxygen basis, been reported as 9,760 kJ/kg-O_2 consumed (Harper et al., 1992) and 14,000 kJ/kg-O_2 consumed (Kaiser, 1996). Given the range of values reported and the importance of biologically generated heat in composting process models, it is suggested that the sensitivity of models to variations in this parameter would be worthy of further investigation.

4.6.6 Model parameters

The number of model parameters required, and the ease by which their values may be obtained, will influence the utility of mathematical models, and to some extent determine whether they are employed as operational or research tools. Furthermore, whether the parameters are obtained independently, or fitted by the model, will impact on the usefulness of the model. Whilst fitted parameters may facilitate the demonstration of general trends, they do not enable the model to be properly validated.

Parameters may be considered under three major categories: a) those describing fundamental properties of air, water and insulating materials (e.g., specific heat of water, density of air, thermal conductivity), b) those describing the raw composting material characteristics (e.g., bulk density, porosity), and c) those relating to substrate degradation rates and microbial growth. Total numbers of parameters (not including reactor dimensions or fitted mathematical constants) specified in composting process models have ranged from approximately 6, for a model comprised largely of empirical expressions (Nakasaki et al., 1987), to 20-30 for models where extensive heat and mass related calculations, or Monod-type expressions, are incorporated (Kaiser, 1996; Stombaugh and Nokes, 1996; Scholwin and Bidlingmaier, 2003). Fundamental parameter values for air, water and insulation materials used in composting process models have generally been independently measured and/or previously reported elsewhere in the literature, and may comprise a large proportion of the

total number of parameters utilised (e.g., Scholwin and Bidlingmaier, 2003). Likewise, compost material, reaction rate and microbial growth parameters have typically been measured independently. First-order rate models require a single rate coefficient, plus parameters for temperature, moisture and oxygen correction factors, whereas the Monod-type models require four, or more, reaction rate related parameters, including maximum specific growth rate (μ_{max}), decay coefficient (λ), half-saturation coefficient (k_s) and maintenance coefficient (β). In the model of Seki (2000) initial values for μ_{max} and λ were adjusted in order to obtain a good simulation. Monod-type models also require an estimate of initial microbial mass (X_i) (Kaiser, 1996; Stombaugh and Nokes, 1996; Seki, 2000). Up to five yield factors, based on BVS removal (moisture, O_2, CO_2, heat, cell mass), may be employed. In several models mathematical constants have been fitted from experimental data (e.g. VanderGheynst et al., 1997; Seki, 2000).

Other fitted parameters have included a thermal diffusion coefficient value of 6.86 $x10^{-12}$ ft^2/hr (1.77 $x10^{-16}$ m^2/s) (Finger et al., 1976) and a heat coefficient of 9500 kJ/kg-O_2 obtained by VanderGheynst et al. (1997). Whilst the heat coefficient compared closely to the value reported by Harper et al. (1992), the thermal diffusivity coefficient value of was low compared to expected values (e.g., Iwabuchi et al., 1999).

4.7 Simulation performance

4.7.1 Temperature

Temperature profile simulations have been reported by Kishimoto et al. (1987), Kaiser (1996), Stombaugh and Nokes (1996), Bertoni et al. (1997), Das and Keener (1997) and Mohee et al. (1998). The profiles presented by Stombaugh and Nokes (1996) showed patterns similar to those reported for full-scale systems, whilst those of Das and Keener (1997) showed general similarities over 7 d. In contrast, the profile predicted by the model of Kaiser (1996) showed a typical lag phase and rapid rise at early time, but subsequently showed a low slope, apparently linear, relationship. The latter was similar to data and predictions reported by van Lier et al. (1994). The model simulations of Mohee et al. (1998) suggested a relatively flat temperature rise compared to typical rapid temperature increases at early time in response to variations in airflow rate. A simulation to determine the optimum aeration regime for composting waste activated sludge was reported by Kishimoto et al.

(1987). This produced a schedule of gradually decreasing aeration rates, with the objective of reaching a temperature of 65 ^{o}C in 16.7 hr, rather than the 40 hr achieved experimentally. A temperature versus time simulation for a biosolids/woodchips mixture at constant airflow (Haug, 1993), showed a realistic profile over a 10 d period. Additional simulations, in which temperature set points were used, and airflow rates varied, showed an eventual decline in temperature, following the initially flat profiles.

4.7.2 Moisture, oxygen & solids

Other simulations have included moisture profiles (Kishimoto et al., 1987; Kaiser, 1996; Stombaugh and Nokes, 1996; Bertoni et al., 1997; Das and Keener, 1997; Ndegwa et al., 2000), oxygen concentrations (Hamelers, 1993; van Lier et al., 1994; Bertoni et al., 1997; Mohee et al., 1998) and solids levels (Hamelers, 1993; Kaiser, 1996; Stombaugh and Nokes, 1996; Das and Keener, 1997; Mohee et al., 1998; Ndegwa et al., 2000; Seki, 2000). Profiles of oxygen, substrate and biomass concentration with time, plus oxygen uptake rates for four different substrates were reported by Hamelers (1993), whilst effects of pad insulation, pile height, mixture density, external temperature and external oxygen, on compost uniformity, were explored by Finger et al. (1976). Haug (1993) presented a range of simulations as a function of time, airflow rate and other variables.

The simulations described have provided valuable insights into the response and sensitivity of models to a range of operating parameter variations. However, their value is limited when validation against experimental data is not included.

4.7.3 Model sensitivity

The sensitivity of a Monod-type model to variations in key microbial parameters was investigated by Stombaugh and Nokes (1996). It was reported that variations in μ_{max} and λ had the greatest effect on biomass, substrate and maximum temperature values, whilst the model was relatively insensitive to changes in k_s, X_i, the decay coefficient (k_d), the cell yield ($Y_{X/S}$) and the oxygen half saturation coefficient (k_{O2}). VanderGheynst et al. (1997) explored the effect of assumptions of saturation, constant dry mass air flux and constant moisture on their model, and concluded that these were not significant enough to account for the observed discrepancies between the model and the data. They noted however that their rate equation

was expressed as a function of temperature only, and not of time, and suggested that the differences were most likely due to an error in the heat generation equation.

4.8 Validation

4.8.1 Temperature

In comparing model performance to experimental data, quantitative measures of performance may be provided by differences in maximum, average and peak temperatures, relative times to reach peak temperatures, the relative areas beneath the curves and a specified baseline, and times for which specified temperatures are maintained. Profile shape characteristics may also be compared to typical curves for a qualitative assessment. In the following analysis, parameters used were areas bounded by the profiles and a 40 ^{o}C baseline (A_{40}), the times for which thermophilic temperatures were equalled or exceeded (t_{40}), the times to reach peak temperatures and the general shape characteristics compared to those of a generic profile. Details of the methods used to determine A_{40} and t_{40}, plus a description of the generic profile characteristics, are given in (Mason and Milke, 2005b; Chapter 3). Summaries of model performance on the above bases are presented in tables 4.10-4.11 and example temperature profiles presented in figures 4.2-4.5.

Maximum differences between modelled and experimental temperature-time profiles have varied widely, ranging from 1.2 to 30.4 ^{o}C, but with discrepancies > 10 ^{o}C predominating (table 4.10). In several profiles (van Lier et al., 1994; Bertoni et al., 1997; Kim et al., 2000; Scholwin and Bidlingmaier, 2003) these differences occurred during the initial period of rapid temperature rise, however in most cases they occurred at later time. Average temperature discrepancies also varied considerably, ranging from < 0.5 to 17.5 ^{o}C, but with most values < 10 ^{o}C. Peak temperatures tended to be more precisely predicted, with many values within 3 ^{o}C of the experimental data. In a majority of cases, times at which peak temperatures occurred were predicted to within 0.5 d of the data, however differences ranged from 0.1 to 4.5 d. In contrast, predicted and experimental A_{40} values were in relatively close agreement. The duration of studies varied from about 1.7 d to 29 d, but most were conducted over 10 days or less.

Table 4.10 Temperature-time profile validation performance of composting models

System description			Performance							
Authors	Reactor type	Scale	Temperature difference between model and data (°C)			Times to peak		A_{40} ratio[a]	Duration of study	Comments
			Maximum	Mean	Peak[b]	Model	Data			
Kishimoto et al. (1987)	ASP	Full	27.5	17.5	6.6	7.6 d	3.1 d	2.49	29 d	Data for piles A, B, C and D respectively. Model simulated shape characteristic well, but fit to experimental data was generally poor.
			26.5	16.3	6.6	7.6 d	3.5 d	2.30		
			22.4	8.8	1.8	8.4 d	6.1 d	1.07		
			15.3	7.7	1.8	8.4 d	8.1 d	0.82		
Nakasaki et al. (1987)	Column	Lab	4.0	1.7	< 0.5	32.8 hr	35.9 hr	1.09	40 hr	Generally close fit between model and data.
van Lier et al. (1994)	Column	Lab	6.9	1.6	2.8	26.2 hr	30.4 hr	1.03	90 hr	Model over-predicted at later time. Model over-predicted at early and later time.
			10.6	1.9	< 0.5	71.1 hr	78.3 hr	1.06	130 hr	
	Bin	Pilot	1.2	< 0.5	1.2	0.4 d	0.5 d	1.04	7 d	Data for top and bottom measuring locations respectively. Generally close fit between model and data.
			4.2	1.0	2.5	0.6 d	0.5 d	1.03		

Kaiser (1996)	Column	Pilot	13.3	4.1	3.3	3.9 d	1.7 d	0.83	10 d	Model under-predicted to about 2 days and from 7.5 days; shape well simulated from 2-7.5 days.
Bertoni et al. (1997)	Trench	Full	30.4	8.1	1.5	4.2 d	5.0 d	0.93	33 d	-
Das and Keener (1997)	Bin	Full	17.3-29.9	8.4-13.3	1.7-8.0	0.8 d	0.8-1.0 d	0.87-1.40	7 d	Data range for 5 'slices' in the top layer of the reactor; atypical shape characteristics.
Mohee et al. (1998)	Column	Lab	16.5[c]	4.2[c]	0.5[c]	9.4 d	8.9 d	1.66[c]	15 d	Model predicted to within 4.3 °C (average 1.8 °C) to day 11 then over-predicted at later time; atypical shape characteristics.
Kim et al. (2000)										Model over-predicted peak and at later time.
Ndegwa et al. (2000)	Bin	Pilot	9.7	6.1	5.4	2.7 d	5.2 d	0.95	45 d	Deep bed system " Shallow bed system "
	Tray	Full	16.5 24.1 26.5 20.4	4.1 7.5 4.5 4.3	14.0 17.7 23.6 16.8	- - - -	- - - -	- - - -	60-120 d 120-180 d 60-120 d 120-180 d	
Seki (2000)	Column	Lab	16.5/17.1[d]	5.4/6.5[d]	9.0/10.9[d]	66.1/ 65.2 hr	75.5 hr	0.97/1.10[d]	190 hr	Both models under-predicted from about 9-59 hr and 149-190 hr; shape poorly simulated at early time.
Higgins and Walker (2001)	Column	Pilot	-	-	1.5-11.8	-	-	-	-	Prediction temperatures varied with initial moisture, airflow and respiration quotient.
Scholwin and Bidlingmaier (2003)	Column	Lab	11.4	3.0	1.8	34.7 hr	20.8 hr	1.00	120 hr	Model under-predicted to 35.5 hr, then under-predicted by an average 1.9 °C to 120 hr; good shape characteristics.

a. A_{40} is the area bounded by the curve and a baseline of 40 °C; ratio is A_{40} (model)/A_{40} (data)
b. Peak temperatures regardless of time of occurrence.
c. Top layer data only.; d. Deterministic model/stochastic model.

Table 4.11: Temperature-distance profile validation performance of composting models

System description			Performance			
Authors	Reactor type	Scale	Temperature difference between model and data (°C)		Distance	Comments
			Maximum	Mean		
Finger et al. (1976)	Windrow	Full	2.8	1.0	3.0 ft	Model over-predicted at centre (2.8 °C), otherwise a close fit was shown
VanderGheynst et al. (1997)	Column	Pilot	3.4	1.6	1.8 m	Data at 24 hr and 29 hr respectively
			12.1	3.2		
			10.3	5.2	0.6 m	Data at 29 hr.

In terms of shape characteristics, several models simulated the typical profile closely, although this was not always well correlated with experimental data (e.g. Smith and Eilers, 1980). In several studies (e.g., Kishimoto et al., 1987; Nakasaki et al., 1987) the short time frame precluded presentation of the overall shape of the profile. The model developed by Ndegwa et al. (2000) tracked the overall temperature-time patterns in a semi-continuous system, with bed depths of 0.41 and 0.61 m, relatively well over selected time periods, but was unable to reliably predict peak temperatures arising after mixing.

The ability of models to predict process temperatures to within a specified margin through to the end of the thermophilic phase, to closely simulate the magnitude and timing of peak temperatures, is important if models are to be used to indicate process performance. Whilst acceptable margins are open to debate, it is suggested that maximum, average and peak temperature discrepancies of 5, 2 and 2 ^{o}C respectively, with peak times predicted to within about 8 h, would be appropriate for the purposes of discussion. Based on these criteria, no models have shown an acceptable predictive ability, although many have met one or more of the goals. In particular, the models of Kishimoto et al. (1987), Nakasaki et al. (1987) and van Lier et al. (1994) met the average temperature difference goal of < 2 ^{o}C and predicted the timing of peak temperatures to within 8 h, although some peak temperature differences were slightly > 2 ^{o}C. The profile presented by van Lier et al. (1994) is shown in figure 4.2. Whilst values of A_{40} agreed to within 3-9%, the studies of Kishimoto et al. (1987), Nakasaki et al. (1987) and van Lier et al. (1994) were all relatively short term, and none was run through to the end of the naturally occurring thermophilic phase. Other models showing good individual predictions included those of Mohee et al. (1998) and Scholwin and Bidlingmaier (2003) (figures 4.3 and 4.4), where peak temperatures were predicted to within < 2 ^{o}C, and the model of Das and Keener (1997) which also predicted temperatures to within < 2 ^{o}C in some cases. It should be noted that whilst the model of Scholwin and Bidlingmaier (2003) showed a large discrepancy during the initial rapid temperature rise phase, it agreed with the experimental data to within 2 ^{o}C, from about 36 hr onwards.

Steady state spatial temperature predictions in a horizontal plane by Finger et al. (1976) agreed closely with experimental data over most of the profile (table 4.11), but, as noted above, this model used several fitted parameters. Non-steady state spatial predictions in a vertical plane by VanderGheynst et al. (1997) showed varying performance with time. The

model predicted temperatures to within < 2 ^{o}C on average over a depth of 1.8 m after 24 hr, with a peak discrepancy of 3.4 ^{o}C, but predictions at 29 hr were considerably less precise (table 4.11).

Temperature predictions by the cassava fermentation model of Saucedo-Castaneda et al. (1990) showed good agreement with experimental data between 15 to 30 hr, with maximum and average discrepancies at the centre of the column of 2.4 and 1.0 ^{o}C respectively. Modelled and experimental temperatures reported by Rodriguez Leon et al. (1991) between 0-20 hr were particularly close. However, it should be noted that the overall experimental temperature range in this study was very small (< 2 ^{o}C).

The most successful models in temperature profile prediction have incorporated empirical data into the biological energy rate model (Nakasaki et al., 1987; van Lier et al., 1994; Scholwin and Bidlingmaier, 2003), used a first-order model with empirical correction factors (Mohee et al., 1998), or alternatively, utilised a regression analysis (Kishimoto et al., 1987). Whilst the performance of these models indicated that the basic structure of the heat balance was sound, the use of empirical biological energy expressions limits their application. As already noted, VanderGheynst et al. (1997) considered that the biological heat generation component of their model may have been responsible for the discrepancies between model predictions and experimental data in their work, as the influence of errors in air saturation, dry air mass flux and moisture were found to be insufficient to explain the discrepancies observed. Additionally, CCR losses were omitted from this model, and it would be useful to establish whether this mechanism was significant for the type of experimental system used by these authors. The results presented by Mohee et al. (1998) indicated that a first-order kinetic expression, corrected for temperature and moisture variations, was reasonably appropriate for a bagasse substrate over a period of 0 to 9 days, even though the temperature profiles showed a large difference between modelled and experimental A_{40} values. The subsequent discrepancy between the model and data is reflected in the solids removal model (figures 4.3 and 4.8). Given that the typical time frame for thermophilic composting is 20-30 days (Rynk, 1992) any further work should involve the prediction of temperature and other profiles over similar time periods.

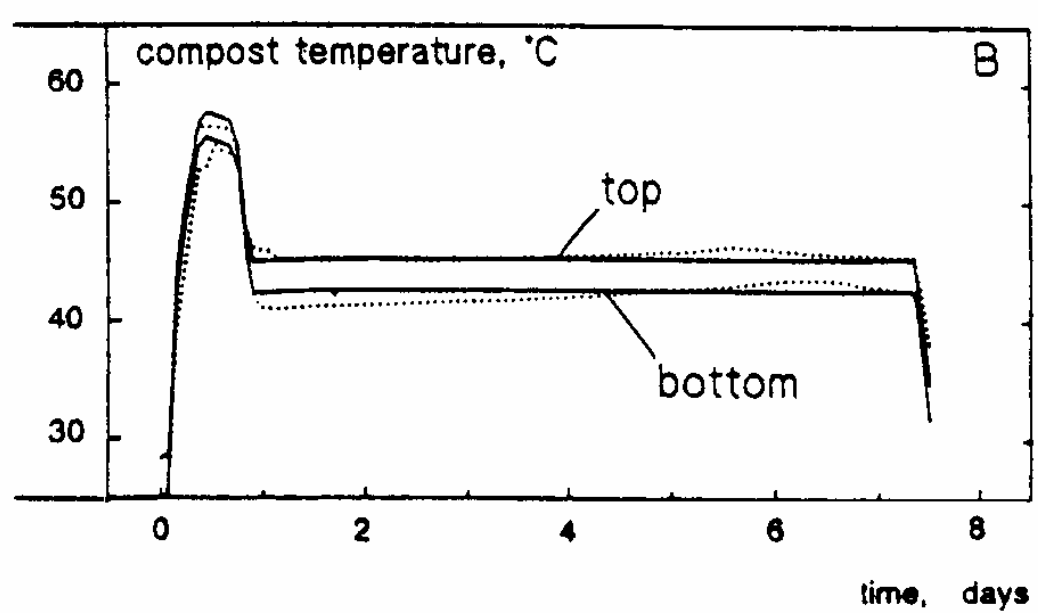

Figure 4.2: Temperature-time profile of van Lier et al. (1994) (adapted) (reproduced with permission)

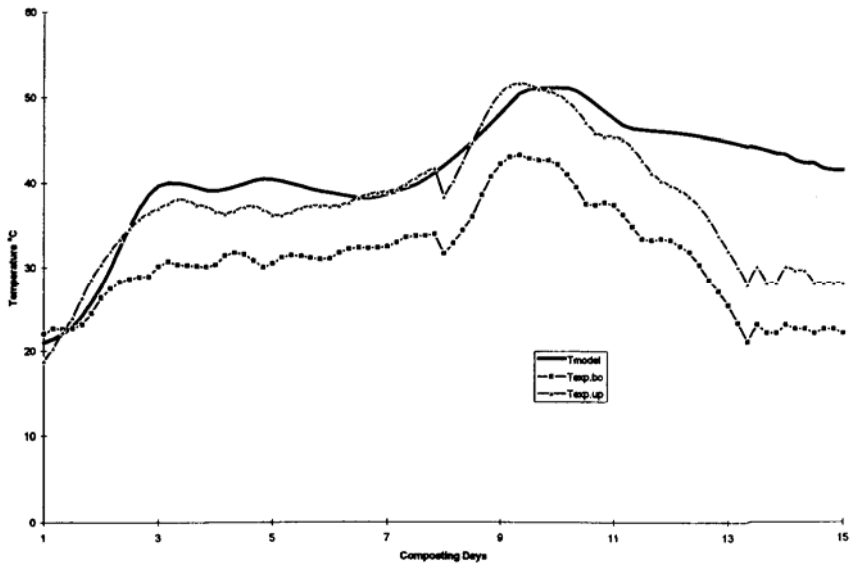

Figure 4.3: Temperature-time profile of Mohee et al. (1998) (reproduced with permission)

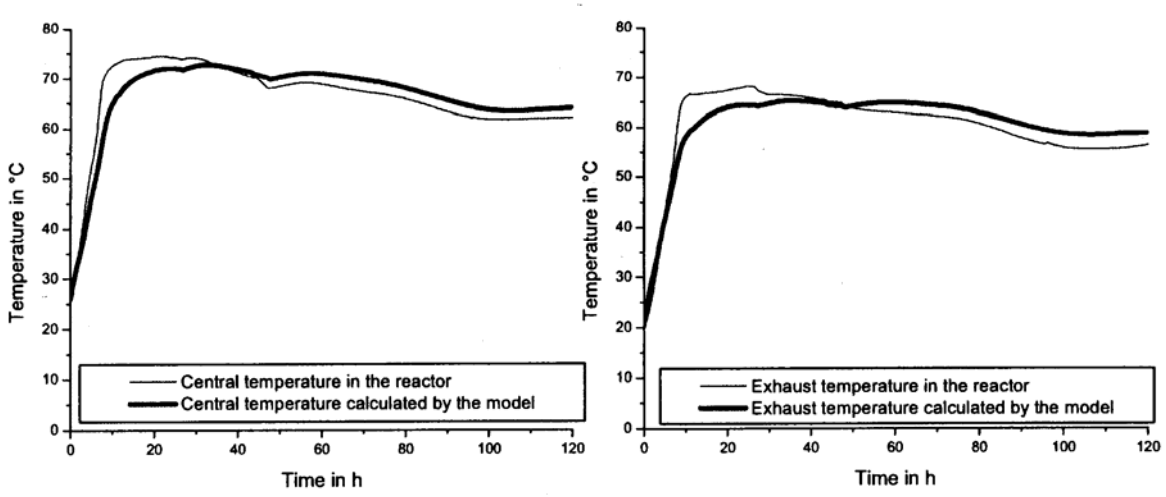

Figure 4.4: Temperature-time profile of Scholwin and Bidlingmaier (2003) (reproduced with permission

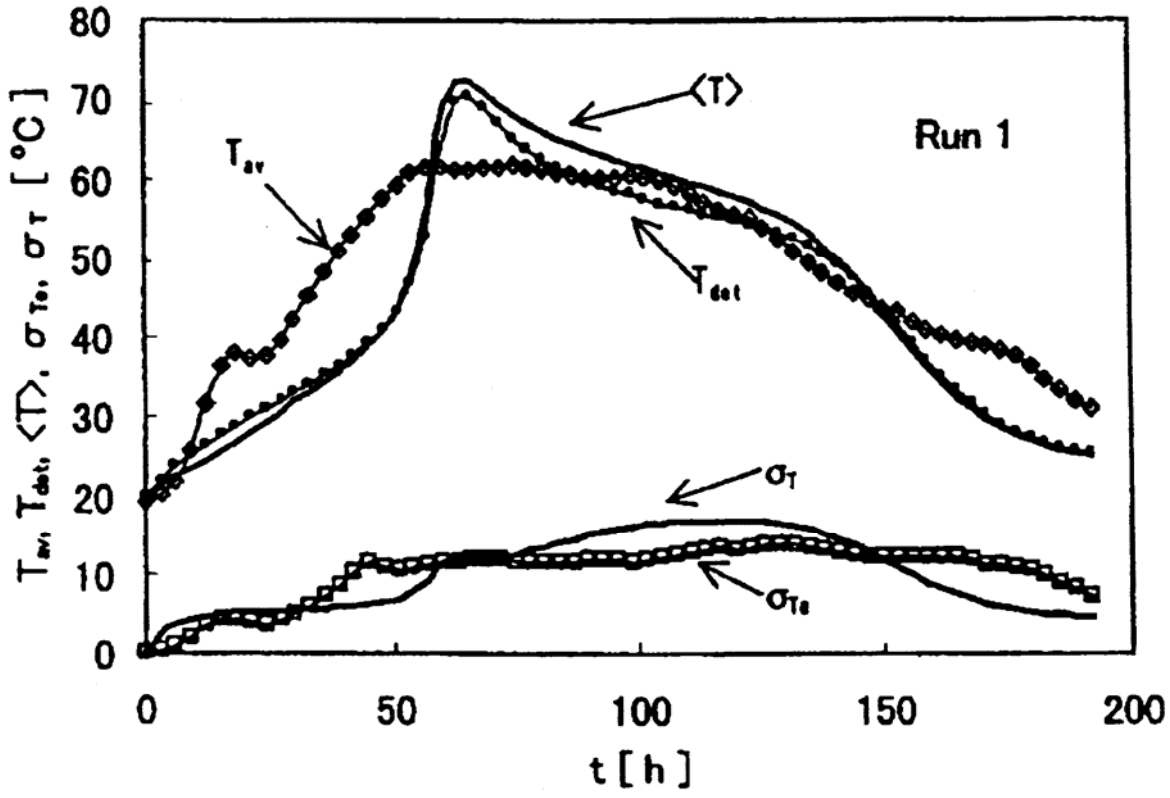

Figure 4.5: Temperature-time profile of Seki (2000)

In terms of adjustment of first-order rate coefficients, the temperature correction model of Rosso et al. (1993) (figure 4.6) has been shown to work well, whilst saturation-type expressions evaluated by Richard et al. (1999) have given good results for oxygen concentration. However, the moisture correction functions are all empirical and although some may be realistic (e.g., Smith and Eilers, 1980) (figure 4.7), further research in this area, in conjunction with free air space considerations, is suggested.

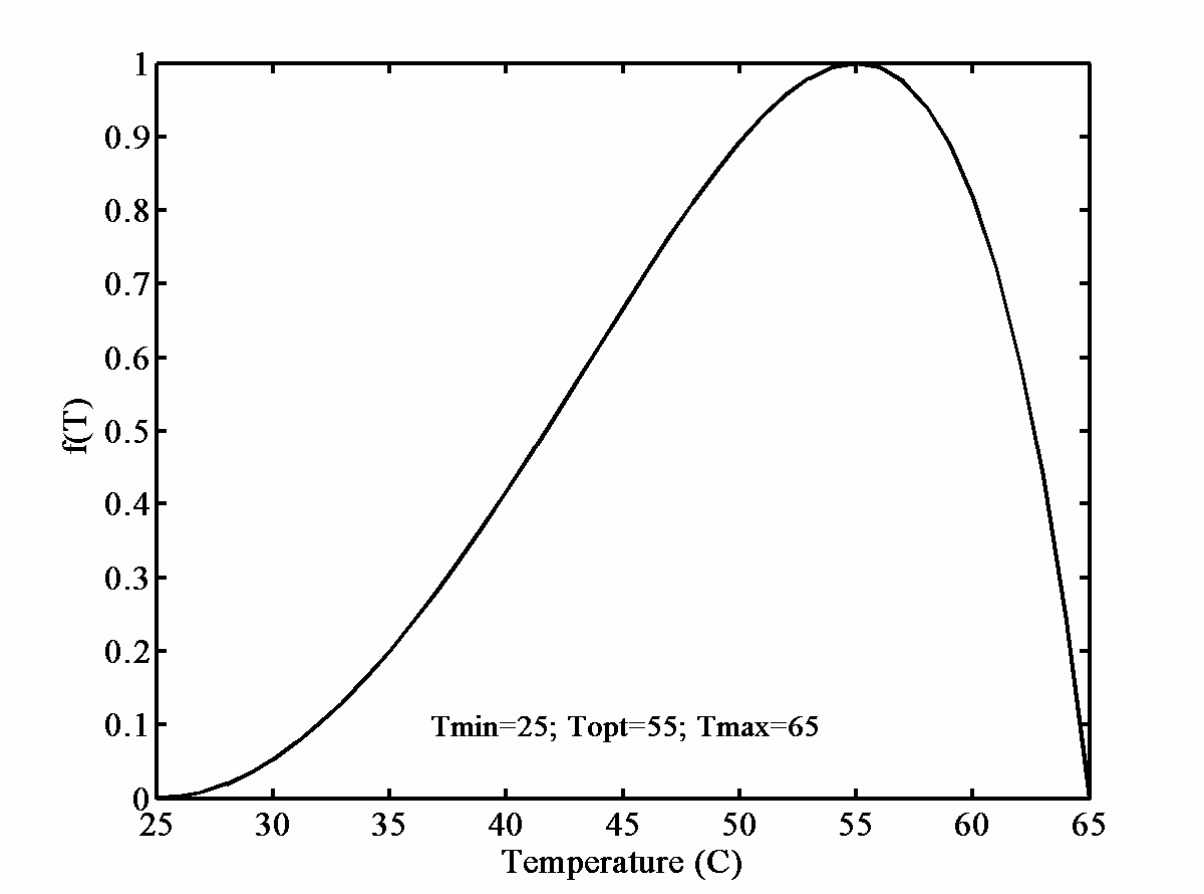

Figure 4.6: Temperature correction function of Rosso et al. (1993)

The models incorporating Monod-type biological energy rate expressions were generally less successful in temperature-time profile prediction. In two cases (Kaiser, 1996; Seki, 2000) the models under-predicted temperature at both early and later time. Whilst soundly based on microbial growth mechanisms, the Monod approach may be difficult to adopt on a broader basis for mixed and variable microbial composting populations, due to difficulties in parameter estimation.

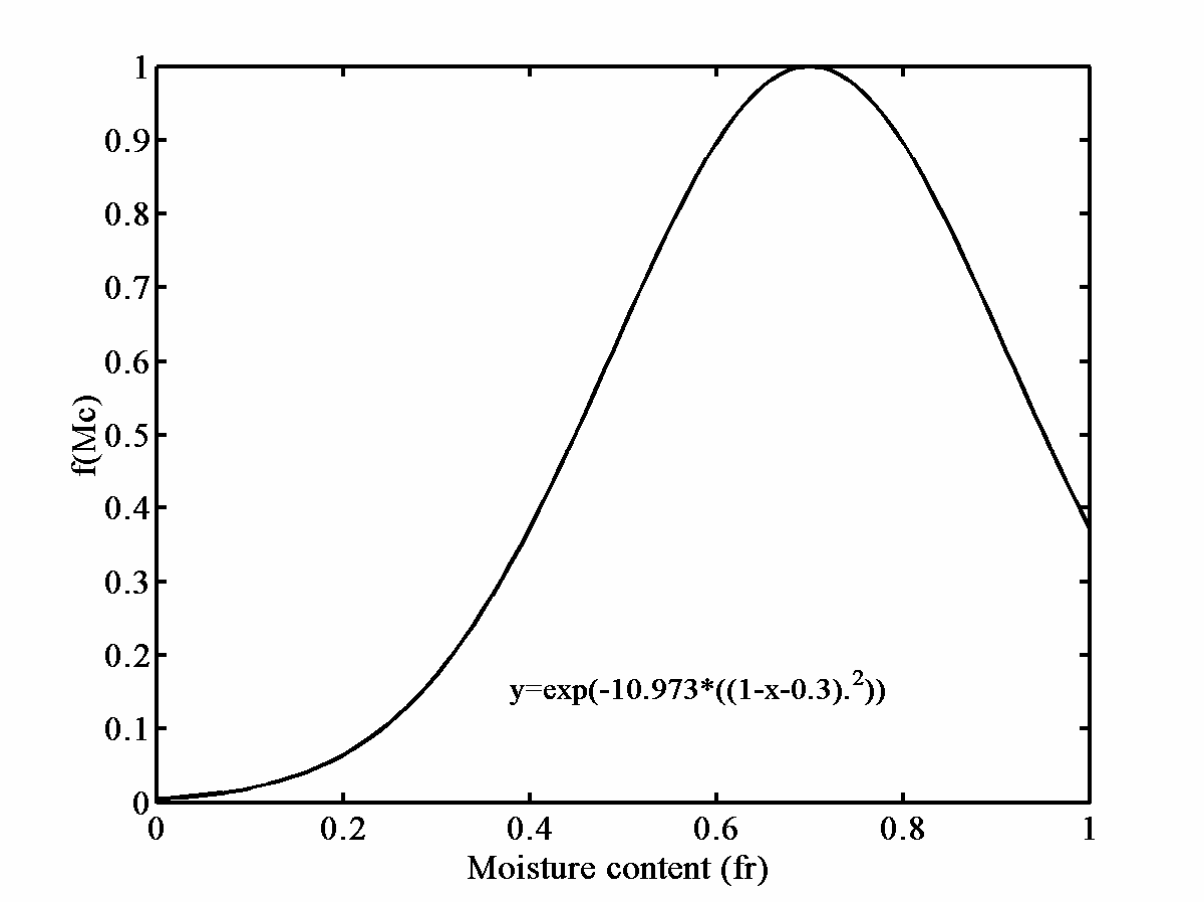

Figure 4.7: Moisture correction function of Smith and Eilers (1980)

4.8.2 Solids

Considerable variation in the performance of the first-order models with respect to substrate degradation is evident. Both the single and double exponential BOD expressions used by Haug (1993) as the basis for the BVS model showed reasonably good fit to selected BOD data at constant temperature, over 60-348 days. However, these data were generated from respirometry with the substrate in solution, rather than in a composting environment, and the fit to BVS data under composting conditions was not shown. Solids data from a composting trial presented by Keener et al. (1993) showed that an uncorrected first-order model described substrate removal adequately for two experimental data sets over the first 3 days of composting only. In contrast, when this model was corrected for temperature and moisture Mohee et al. (1998), it showed relatively close agreement with experimental data over a period 0-8 days, with a subsequent maximum deviation of 2.6% between days 9-15 (figure 4.8). More recently, Bari et al. (2000a) have shown evidence of a relatively good fit (R^2 =

0.844), using a temperature-corrected first-order model (figure 4.9), but have also presented data sets with poorer correlations. It should be noted that volatile solids data in the latter work were calculated from CO_2 data, rather than measured directly. A first-order model without temperature correction has shown evidence of a fairly good fit at later time over periods exceeding 70, 84 and 168 days (Bernal et al., 1993; Paredes et al., 2001; Paredes et al., 2002) (table 4.4). However the number of data points at early time was low, and the fit in this region generally poor.

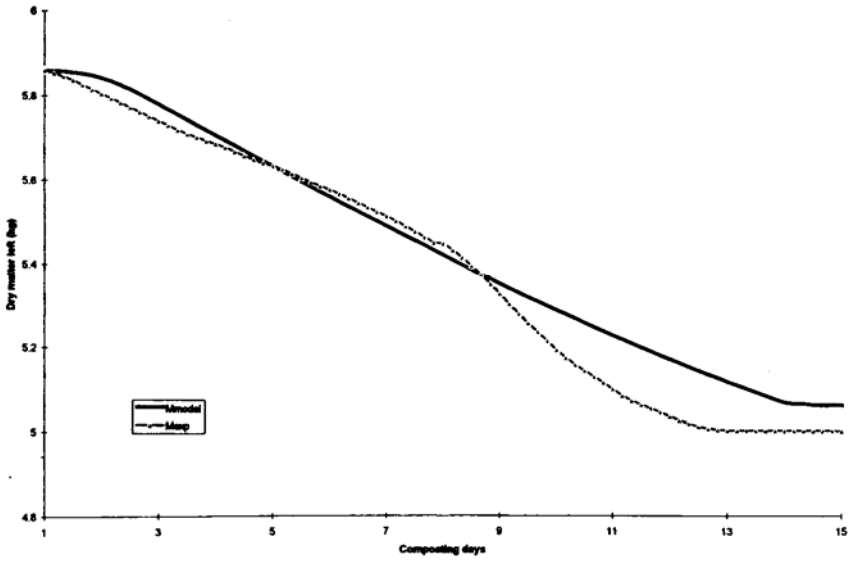

Figure 4.8: Dry mass vs time profile of Mohee et al. (1998)

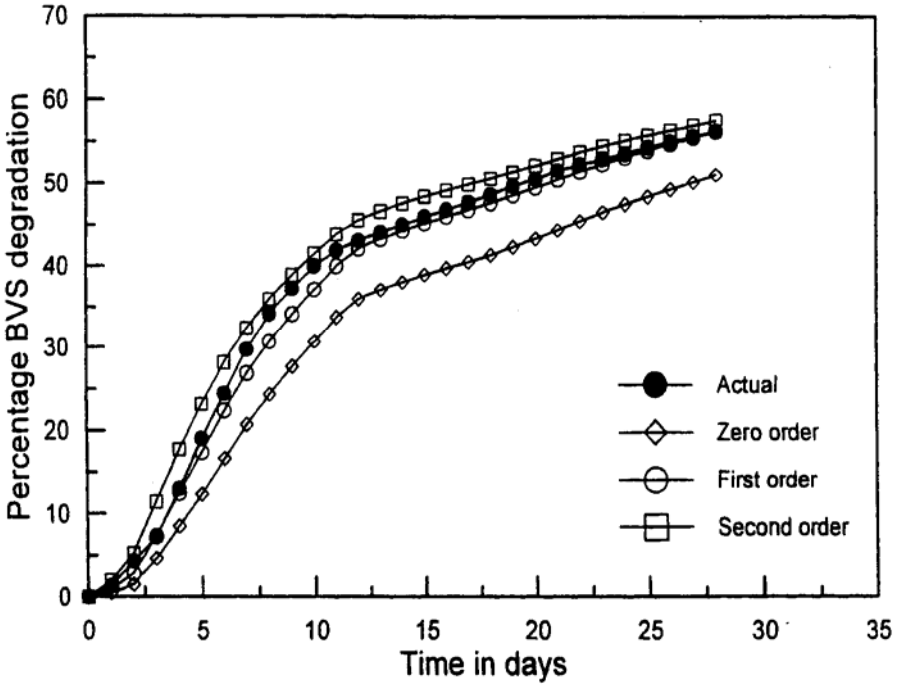

Figure 4.9: BVS vs time profile of Bari et al. (2000a)

In the case of Seki (2000) the model predictions for substrate degradation and biomass production fitted experimental data closely (figure 4.10), but the goodness of fit of the other Monod-type models to experimental substrate degradation data was not shown. The success in solids modelling was not always reflected in the temperature profile predictions however (e.g., Seki, 2000) (figures 4.5 and 4.10), and further investigation of the reasons for this discrepancy is indicated. Predictions of compost mass (Kishimoto et al., 1987; Mohee et al., 1998), volatile solids conversion (Nakasaki et al., 1987) and dry bulk density (Seki, 2000) all showed close agreement with experimental data (table 4.12).

Given the relatively successful fit of a first-order model with temperature correction to BVS degradation data over a 28 day period (Bari et al., 2000a), more research aimed at exploring the development of improved first-order biological heat production models would seem worthwhile. A similar approach, in which the first-order rate coefficient was adjusted using stochastic techniques, has been successfully applied to the modelling of BOD data (Borsuk and Stow, 2000). Alternatively, a double exponential approach, incorporating separate terms for rapidly and slowly degradable substrates (Haug, 1993) along with temperature and moisture correction functions, is suggested for further investigation. Bari et al. (2000a) also

showed that BVS degradation could be adequately predicted using exit gas temperatures to adjust the value of the first-order rate coefficient.

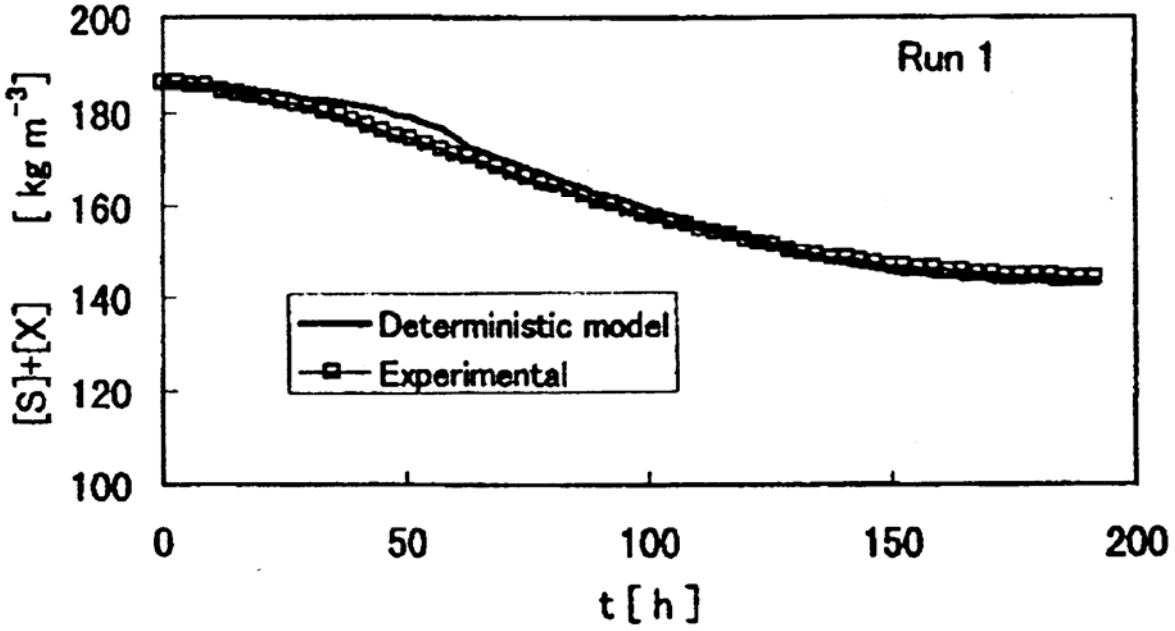

Figure 4.10: Dry matter vs time profile of Seki (2000)

4.8.3 Moisture

Two models appear to have successfully predicted moisture levels over time. Moisture data presented by Kishimoto et al. (1987) showed good agreement with experimental results between 0 and 20 hr, after which the model slightly under-predicted the data, whilst mixture moisture content predictions by Nakasaki et al. (1987) showed very close agreement with the experimental data (table 4.12). In both cases the discrepancies were small in relation to the moisture levels reported. In contrast, the model of Ndegwa et al. (2000) indicated fair to good agreement only.

4.8.4 Oxygen and carbon dioxide

Predictions of CO_2 concentration by Kaiser (1996) followed the data reasonably closely at low concentrations, when aeration was off, but showed large differences immediately following the onset of each aeration cycle (table 4.12). Modelled oxygen concentrations reported by Mohee et al. (1998) generally tracked the overall pattern of the data (table 12), except for a single major downward excursion between days 3 and 5. In both studies, the

differences were relatively large in relation to the values reported. Spatial oxygen concentrations predicted by Finger et al. (1976) showed only fair agreement with experimental measurements.

Predicted carbon dioxide production rates reported by Nakasaki et al. (1987) showed moderate agreement with the data, and the differences in proportion to the range of values reported were relatively high. Whilst oxygen uptake rates predicted by the model of Hamelers (1993) were of a similar profile to experimental data curves, these data were not presented on the same plot for closer assessment of validation. Modelled maximum oxygen uptake rates reported by Higgins and Walker (2001), showed average discrepancies ranging from 42 to 98% of the data, with an overall range of 2 to 285%. Differences varied according to airflow rate, initial moisture content and the adopted values of the respirometric quotient.

Overall, modelled gas consumption or evolution rates showed relatively large errors in relation to the data presented. Further research on the modelling of oxygen consumption and carbon dioxide evolution is indicated.

Table 4.12: Moisture, oxygen, carbon dioxide and solids vs time validation performance of composting models

System description			Performance assessment							
			Differences between model and data							
Authors	Reactor type	Scale	Moisture		O_2 or CO_2 concentration		O_2 or CO_2 rate		Solids	
			Maximum	Mean	Maximum	Mean	Maximum	Mean	Maximum	mean
Kishimoto et al. (1987)	Column	Lab	0.54%	0.23%	-	-	-	-	0.12 kg	0.04 kg
Nakasaki et al. (1987)	Column	Lab	-[a]	-[a]	-	-	4.46[b]	1.33[b]	1.94%[c]	0.75%[c]
Hamelers (1993)	Column	Lab	-[a]	-[a]	-	-	2.81[b]	0.81[b]	1.08%[c]	0.31%[c]
Keener et al. (1993)	-	-	-	-	-	-	-	-	-[d]	-[d]
Kaiser (1996)	Column	Pilot	-	-	-	-	-	-	0.16[e]	0.07-0.09[e]
Mohee et al. (1998)	Column	Lab	-	-	8.86%[f]	1.77%[f]	-	-	-	-
Seki (2000)	Column	Lab	-	-	0.11%[g]	0.02%[g]	-	-	0.14 kg	0.05 kg
Higgins and Walker (2001)	Column	Pilot	-	-	-	-	-	-	4.19 kg/m^3	1.49 kg/m^3
			-	-	-	-	2.23-5.14[h]	0.96-1.95[h]	-	-

a. Very close fit between model and data.
b. mol-CO_2 x 10^5/kg-DS.hr.
c. % conversion.
d. Experimental and modelled data were presented separately.
e. Dry matter ratio (range 0-1)
f. CO_2
g. O_2
h. g-O_2/kg-VS.hr; differences varied with initial moisture, airflow and respiration quotient.

4.9 Conclusions

1. Mathematical models of the composting process have been based on the solution of heat and mass balances in time, and in a limited number of cases, spatially. A deterministic approach has been adopted in all cases, with stochastic elements incorporated into two models, and parameters either lumped over the complete reactor, or distributed over finite reactor elements.

2. Biological energy production has been predicted using either first-order, Monod-type, or empirical expressions, in conjunction with heat conversion factors. Temperature correction functions have been incorporated into most biological energy models, with corrections for moisture, oxygen and free air space also incorporated in some cases.

3. The most successful models in predicting temperature profiles have incorporated either empirical kinetic expressions, or utilised a first-order model, with empirical corrections for temperature and moisture. Models incorporating Monod-type kinetic expressions were less successful. However, no models were able to predict maximum, average and peak temperatures to within 5, 2 and 2 ^{o}C respectively, or to predict the times to reach peak temperatures to within 8 h. Many models were able to successfully model temperature profile shape characteristics.

4. A number of successful non-empirical rate coefficient temperature and oxygen correction functions suitable for use in composting models are available. Existing functions for moisture correction are all empirically based.

5. Moisture and solids profiles were well predicted by two models, whereas oxygen and carbon dioxide profiles were generally poorly modelled. Limited evidence exists for the applicability of a first-order model to substrate degradation.

6. Further work is suggested to obtain additional substrate degradation data, explore the development of improved first-order biological heat production models, develop mechanistically-based moisture correction factors, explore the role of

moisture tension, investigate model performance over thermophilic composting time periods, provide further model sensitivity information and incorporate natural ventilation aeration expressions into composting process models.

4.10 Afterword

A number of papers relevant to mathematical modelling of the composting process have appeared during the period 2004-2006. In addition, several pre-2004 papers previously missed are included here. Many of the publications concern substrate degradation modelling, and these are discussed below, followed by the papers on other aspects of process modelling.

The first-order, single exponential model of Keener et al. (1993) was used in 4 papers. Firstly, Keener et al. (1997) provided a summary of first-order rate coefficient values on a range of substrates. Goodness of fit was not indicated, but the four graphs presented illustrated a generally poor fit of the model to experimental data. A lag period was built into the model by Nakasaki and Ohtaki (2002), who then fitted the model to carbon loss data at varying temperature. In this case, the visual fit showed that the model provided an incomplete description of the data, particularly at early time. However, a similar data set from Nakasaki et al. (1998) was well modelled by the present author using a double exponential function, once the lag phase had been removed (see chapter 5). Cekmecelioglu et al. (2005) employed the single exponential model, along with the temperature correction function of Haug (1993), in a compost process model, which is discussed below. A single exponential model was also incorporated into a process optimisation model, for prediction of airflow and fan on/off times, by Keener et al. (2005).

Multi stage kinetics, involving rapidly and slowly biodegradable substrate fractions, received increased attention during the 2004-2006 period. Cronje et al. (2004) analysed data from the composting of a pig manure and straw mixture at 30 and 50 ^{o}C over a 30 hour period using two first order expressions, for fast and slow fractions, respectively. However, an analysis by the present author showed that a very good fit to these data was in fact provided by a single exponential model, and that a double exponential model provided only a slight improvement (Mason, I.G., unpublished results). Cronje et al. (2004) also presented rate coefficient vs temperature data, which was reasonably well modelled by the correction function of Haug

(1993), although very few data points were present around the peak of the curve. Two-stage kinetics were also employed by de Guardia et al. (2006) to analyse data from the composting of a pig processing wastewater sludge and woodchips. Rate coefficients for fast and slow biodegradable fractions were presented as a function of temperature, but no goodness of fit for the substrate degradation vs time data was reported. Komilis (2006) proposed a three stage kinetic model for readily, moderately and slowly hydrolysable material, although by setting the slowly hydrolysable rate coefficient to zero, this became a de facto two-stage model. The visual fits showed variable degrees of correlation, with none describing the complete data sets well. These data sets were also analysed by the present author and the results are presented in chapter 5.

A new development since 2003 was the application of the activated sludge model (Henze et al, 2000) to the composting process. Zavala et al. (2004a) utilised a simplified version of this model to describe oxygen uptake rate (OUR) data from the composting of raw faeces and sawdust at 55 ^{o}C over 16 days. Both batch and fed-batch operation experiments were conducted, using 330-390 g samples (these weights estimated by the present author). The visual fit appears good on the OUR curves shown, but no measurement of goodness of fit was reported, and cumulative oxygen uptake data was not presented, so it was not possible to make comparisons with the bulk of the information in the composting literature. When experiments were conducted at temperatures ranging from 20 to 60 ^{o}C, particularly poor fits were obtained at 20, 30 and 40 ^{o}C. These were improved by fractioning the substrate into easily and slowly hydrolysable material (Zavala et al., 2004b). A similar model was adopted by Tremier et al. (2005a), for the analysis of data from the composting of sewage sludge and pine bark at various fixed temperatures. The substrate was classified into readily biodegradable, hydrolysable, and inert material. A good agreement between model and OUR data at 39.6 C over 490 hours (approximately 20 d) was reported, but only the one result presented.

A model developed from bacterial growth kinetics, and incorporating Monod kinetics, was reported by Yamada and Kawase (2006). When applied to substrate decomposition data from the composting of waste activated sludge and sawdust, the visual fit showed considerable discrepancies between the model and the data over airflow rates ranging from 0-4 l/min.kg-TS. Uncertainties in the parameters used in this type of model were investigated using fuzzy

set theory by Qin et al. (2004). Also new is the application of the sigmoidal model of Gompertz (1825) to composting data by Chang et al. (2005) and Chang et al. (2006). This model is discussed in more detail in Chapter 5.

Gas flow patterns through composting media were modelled by Tremier et al. (2005b). Retention time distribution curves, obtained using methane as a tracer gas, were well described by a plug flow with dispersion model. The authors have proposed to incorporate this model into future compost process models. Since gas flow pattern modelling is a largely ignored aspect of composting process studies (although not for other solid-state biological processes), this is a welcome addition to the literature.

A temperature prediction model, incorporating the first order kinetic model of Keener et al. (1993) along with the temperature correction function of Haug (1993), was presented by Cekmecelioglu et al. (2005). The visual fit of the model was poor when compared to experimental data from the composting of a food waste, manure, hay, wood shavings and wood chips mixture in full-scale windrows.

A review of approaches to the modelling of composting kinetics was provided by Hamelers, (2004). Inductive (black box) and deductive (white box) approaches were outlined and the limitations of both discussed. A modified deductive approach in which basic parameters are lumped into a smaller number of identifiable parameters was proposed and illustrated for composting at the particle level. This paper provides a good analysis of the state of the art in composting kinetics modelling and highlights the need to develop models based on sound process understanding, but which are sufficiently simple to be usable in practical applications.

In summary, there remains no consensus in the literature concerning which kinetic model, or models, should be used in describing the kinetics of the composting process. Whilst there is some new evidence in support of the first order single exponential model (see chapter 5), there are also new cases where this model does not provide a good fit. Increasing interest in fractionating substrates into two or three fractions has been demonstrated in the literature, but apart from the analysis of the data of Nakasaki et al. (1998) by the present author, good fits are rare. The application of the activated sludge model is an interesting development, but

again this does not describe the data well in all circumstances. Examples to date have been limited to wastewater sludges. The discussion by Hamelers (2004) is useful, but more work is needed in this area in order to progress toward some wider agreement on the topic of kinetics modelling. The work of Tremier et al. (2005b) on gas flow modelling is a welcome innovation, but otherwise there have been no significant developments in compost process modelling during the 2004-2006 period.

In this chapter the term 'Monod-type kinetics' is used to describe models based on bacterial growth, which incorporate Monod kinetics. From this perspective the models are deductive, although the Monod component itself is empirical. A more precise term would be 'expressions derived from bacterial growth modeling and incorporating Monod kinetics'. Readers are kindly asked to interpret the term "Monod-type kinetics" in this way.

Particle size is recognized as affecting composting kinetics (Gray and Sherman, 1991; as cited by Hamlers, 2004) and Hamlers (1993). Hamoda et al. (1998) reported k values of 0.26, 0.26, and 0.33 d-1 for particle sizes of 20, 30 and 40 mm respectively, although these results may not be statistically different due to experimental error. This area deserves further study in the composting context.

4.11 References

Agnew, J.M. and Leonard, J.J., 2003. The physical properties of compost. Compost Science & Utilisation 11 (3), 238-264.

Andrews, J.F. and Kambhu, K., 1973. Thermophilic aerobic digestion of organic solid wastes. *EPA-670/2-73-061, PB-222 396*, USEPA, Springfield, Il, USA

Bach, P.D., Shoda, M. and Kubota, H., 1984. Rate of composting of dewatered sewage sludge on continuously mixed isothermal reactor. Journal of Fermentation Technology 62 (3), 285-292.

Bach, P.D., Nakasaki, K., Shoda, M. and Kubota, H., 1987. Thermal balance in composting operations. Journal of Fermentation Technology 65 (2), 199-209.

Bari, Q.H, Koenig, A. and Guihe, T., 2000a. Kinetic analysis of forced aeration composting - I. Reaction rates and temperature. Waste Management & Research 18 (4), 303-312.

Bari, Q. H., Koenig, A. and Guihe, T., 2000b. Kinetic analysis of forced aeration composting - II. Application of multilayer analysis for the prediction of biological degradation. Waste Management & Research 18 (4), 313-319.

Batista, J.G.F., van Lier, J.J.C., Gerrits, J.P.G., Straatsma, G. and Griensven, L.J.L.D., 1995. Spreadsheet calculations of physical parameters of phase II composting in a tunnel. Mushroom Science 14, 189-194.

Bernal, M.P., Lopez-Real, J.M. and Scott, K.M., 1993. Application of natural zeolites for reduction of ammonia emissions during the composting of organic wastes in a laboratory composting simulator. Bioresource Technology 43, 35-39.

Bernal, M.P., Navarro, A.F., Roig, A., Cegarra, J. and Garcia, D., 1996. Carbon and nitrogen transformation during composting of sweet sorghum bagasse. Biology and Fertility of Soils 22 (1-2), 141-148.

Bertoni, I.A., Papi, T. and Zanzi, A., 1997. Utilisation of a computer simulation model to improve composting process management. In: Proceedings of the ORBIT '97 conference "Into the next millenium", Harrogate, UK., 175-182. ORBIT Association, Weimar, Germany.

Borsuk, M.E. and Stow, C.A., 2000. Bayesian parameter estimation in a mixed-order model of BOD decay. Water Research 34 (6), 1830-1836.

Cekmecelioglu, D., Heinemann, P.H., Demirci, A. and Graves, R.E., 2005. Modeling of compost temperature and inactivation of Salmonella and E-coli O157 : H7 during windrow food waste composting. Transactions of the Asae 48 (2), 849-858.

Chang, J.I., Tsai, J.J. and Wu, K.H., 2005. Mathematical model for carbon dioxide evolution from the thermophilic composting of synthetic food wastes made of dog food. Waste Management 25 (10), 1037-1045.

Chang, J.I., Tsai, J.J. and Wu, K.H., 2006. Thermophilic composting of food waste. Bioresource Technology 96, 116-122.

Cronje, A.L., Turner, C., Williams, A.G., Barker, A.J. and Guy, S., 2004. The respiration rate of composting pig manure. Compost Science & Utilization 12 (2), 119-129.

Das, K. and Keener, H.M., 1997. Numerical model for the dynamic simulation of a large scale composting system. Trans. ASAE 40 (4), 1179-1189.

de Guardia, A., Petiot, C. and Rogeau, D., 2006. Influence of aeration rate and biodegradability fraction on composting kinetics. Waste Management in press.

Finger, S.M., Hatch, R.T. and Regan, T.M., 1976. Aerobic microbial growth in semi-solid matrices: heat and mass transfer limitations. Biotechnol. Bioeng 18, 1193-1218.

Gompertz, B., 1825. On the nature of the function expressive of the law of human mortality, and on a new mode of determining the value of life contingencies. Philos. Trans R. Soc. London 115, 513-585.

Gray, K.R. and Sherman, K., 1971. Review of composting part 1. Process Biochemistry 6 (6), 32-36.

Hamelers, H.V.M., 1993. A theoretical model of composting kinetics. Science & Engineering of Composting: Design, Environmental & Microbial & Utilisation aspects, H.A.J. Hoitink and H.M. Keener, eds., Renaissance Publications, Worthington, USA., 36-58.

Hamelers, B.V.F. and Richard, T.L., 2001. The effect of dry matter on the composting rate: theoretical analysis and practical implications. In: ASAE paper 017004, ASAE, St Joseph, MI, USA.

Hamelers, H.V.M., 2004. Modeling composting kinetics: A review of approaches. Reviews in Environmental Science and Biotechnology 3, 331-342.

Harper, E., Miller, F.C. and Macauley, B.J., 1992. Physical management and interpretation of an environmentally controlled composting ecosystem. Australian Journal of Experimental Agriculture 32 (5), 657-667.

Haug, R.T., 1993. The practical handbook of compost engineering. Lewis Publishers, Boca Raton, Florida, USA.

Higgins, C. and Walker, L., 2001. Validation of a new model for aerobic organic solids decomposition: simulations with substrate specific kinetics. Process Biochemistry 36 (8-9), 875-884.

Iwabuchi, K., Kimura, T. and Otten, L., 1999. Effect of volumetric water content on thermal properties of dairy cattle feces mixed with sawdust. Bioresource Technology 70 (3), 293-297.

Kaiser, J., 1996. Modelling composting as a microbial ecosystem: A simulation approach. Ecological Modelling 91 (1-3), 25-37.

Keener, H.M., Marugg, C., Hansen, R.C. and Hoitink, H.A.J., 1993 Optimising the efficiency of the composting process. Science & Engineering of Composting: Design, Environmental & Microbial & Utilisation aspects, H.A.J. Hoitink and H.M. Keener, eds., Renaissance Publications, Worthington, USA., 59-94

Keener, H.M., Elwell, D.L., Das, K.C. and Hansen, R.C., 1997. Specifying design/operation of composting systems using pilot scale data. Applied Engineering in Agriculture 13 (6), 767-772.

Keener, H.M., Ekinci, K. and Michel, F.C., 2005. Composting process optimisation - using on/off controls. Compost Science and Utilisation 13 (4), 288-299.

Kim, D. S., Kim, J.O. and Lee, J.J., 2000. Aerobic composting performance and simulation of mixed sludges. Bioprocess Engineering 22 (6), 533-537.

Kishimoto, M., Preechaphan, C., Yoshida, T. and Taguchi, H., 1987. Simulation of an aerobic composting of activated sludge using a statistical procedure. MIRCEN J. 3, 113-124.

Koenig, A. and Tao, G.H., 1996. Accelerated forced aeration composting of solid waste. In: Proceedings of the Asia-Pacific Conference on Sustainable Energy and Environmental Technology, Singapore, 450-457.

Komilis, D., 2006. A kinetic analysis of solid waste composting at optimal conditions. Waste Management 26 (1), 82-91.

Mason, I.G. and Milke, M.W., 2005a. Physical modelling of the composting environment: a review. Part 1: Reactor systems. Waste Management 25 (5), 481-500.

Mason, I.G. and Milke, M.W., 2005b. Physical modelling of the composting environment: a review. Part 2: Simulation performance. Waste Management 25 (5), 501-509.

Miller, F.C., 1989. Matric potential as an ecological determinant in compost, a substrate dense system. Microbial Ecology 18, 59-71.

Mills, A.F., 1995. Basic heat and mass transfer. Richard D. Irwin Inc, Chicago, USA.

Mohee, R., White, R. and Das, K., 1998. Simulation model for composting cellulosic (bagasse) substrates. Compost Science & Utilisation 6 (2), 82-92.

Nakasaki, K., Kato, J., Akiyama, T. and Kubota, H., 1987. A new composting model and assessment of optimum operation for effective drying of composting material. Journal of Fermentation Technology 65 (4), 441-447.

Nakasaki, K., Akakura, N., Atsumi, K. and Takemoto, M., 1998. Degradation patterns of organic material in batch and fed-batch composting operations. Waste Management & Research 16 (5), 484-489.

Nakasaki, K., Akakura, N. and Takemoto, M., 2000. A prediction for the degradation pattern of organic materials in the composting of a fed-batch operation as inferred from the results of batch operation. Journal of Material Cycles Waste Management 2 (31-37).

Nakasaki, K. and Ohtaki, A., 2002. A simple numerical model for predicting organic matter decomposition in a fed-batch composting operation. Journal of Environmental Quality 31 (3), 997-1005.

Navaee-Ardeh, S., Bertrand, F. and Stuart, P.R., 2006. Emerging biodrying technology for the drying of pulp and paper mixed sludges. Drying Technology 24 (7), 863-878.

Ndegwa, P.M., Thompson, S.A. and Merka, W.C., 2000. A dynamic simulation model of in-situ composting of caged layer manure. Compost Science & Utilisation 8 (3), 190-202.

Neilsen, H. and Berthelsen, L., 2002. A model for the temperature dependency of thermophilic composting rate. Compost Science & Utilisation 10 (3), 249-257.

Paredes, C., Roig, A., Bernal, M.P., Sanchez-Monedero, M.A. and Cegarra, J., 2000. Evolution of organic matter and nitrogen during co-composting of olive mil wastewater with solid organic wastes. Biology & Fertility of Soils 32, 222-227.

Paredes, C., Bernal, M.P., Roig, A. and Cegarra, J., 2001. Effects of olive mill wastewater addition in composting of agroindustrial and urban wastes. Biodegradation 12 (4), 225-234.

Paredes, C., Bernal, M., Cegarra, J. and Roig, A., 2002. Bio-degradation of olive mill wastewater sludge by its co-composting with agricultural wastes. Bioresource Technology 85 (1), 1-8.

Qin, X.S., Huang, G.H., Jiang, X.Y., Xi, B.D., Liang, Z.W., Christine, W.C. and Liu, H.L., 2004. Fuzzy approach for dynamic simulation of composting process under uncertainty. Transactions of Nonferrous Metals Society of China 14, 18-24.

Ratkowsky, D.A., Lowry, R.K., McMeekin, T.A., Stokes, A.N. and Chandler, R.E., 1983. Model for bacterial culture and growth rate throughout the entire biokinetic temperature range. J. Bacteriol. 154, 1222-1226.

Richard, T.L. and Walker, L.P., 1998. Temperature kinetics of aerobic solid state biodegradation. Proceedings of the Institute of Biological Engineering 1, A22-A39.

Richard, T.L., Walker, L.P. and Gossett, J.M., 1999. The effects of oxygen on solid-state biodegredation kinetics. Proceedings of the Institute of Biological Engineering 2, A10-A30.

Richard, T.L., Hamelers, H.V.M., Veeken, A. and Silva, T., 2002. Moisture relationships in composting processes. Compost Science & Utilization 10 (4), 286-302.

Robinzon, R., Kimmel, E. and Avnimelech, Y., 2000. Energy and mass balances of windrow composting system. Trans. ASAE 43 (5), 1253-1259.

Rodriguez Leon, J.A., Torres, A., Echevarria, J. and Saura, G., 1991. Energy balance in solid state fermentation processes. Acta Biotechnol. 11, 9-14.

Rosso, L., Lobry, J.R. and Flandrois, J.P., 1993. An unexpected correlation between cardinal temperatures of microbial growth highlighted by a new model. J. Theor. Biol. 162, 447-463.

Rynk, R., 1992 On-farm composting handbook. NRAES, Ithaca, New York USA.

Saucedo-Castaneda, G., Gutierrez-Rojas, M., Baquet, G., Raimbault, M. and Viniegra-Gonzalez, G., 1990. Heat transfer simulation in solid substrate fermentation. Biotechnol. Bioeng. 35, 802-808.

Scholwin, F. and Bidlingmaier, W., 2003. Fuzzifying the composting process: a new model based control strategy as a device for achieving a high grade and consistent product quality. In: Proceedings of the Fourth International Conference of ORBIT Association on Biological Processing of Organics: Advances for a Sustainable Society, 30th April-2 May, 2003, Perth, Australia, 739-751. ORBIT Association, Weimar, Germany.

Schulze, K.L., 1962. Continuous thermophilic composting. Applied Microbiology 10, 108-122.

Seki, H., 2000. Stochastic modeling of composting processes with batch operation by the Fokker-Planck equation. Trans. ASAE 43 (11), 169-179.

Smith, R. and Eilers, R.G., 1980. Numerical simulation of activated sludge composting. *EPA-600/2-8C-191*, USEPA, Cincinnati, Ohio, USA

Stombaugh, D.P. and Nokes, S.E., 1996. Development of a biologically based aerobic composting simulation model. Trans. ASAE 39 (1), 239-250.

Straatsma, G., Gerrits, J.P.G., Thissen, J.T.N.M., Amsing, J.G.M., Loffen, H. and van Griensven, L.J.L.D., 2000. Adjustment of the composting process for mushroom cultivation based on initial substrate composition. Bioresource Technology 72 (1), 67-74.

Tremier, A., de Guardia, A., Massiani, C., Paul, E. and Martel, J.L., 2005a. A respirometric method for characterising the organic composition and biodegradation kinetics and the temperature influence on the biodegradation kinetics, for a mixture of sludge and bulking agent to be composted. Bioresource Technology 96 (2), 169-180.

Tremier, A., De Guardia, A., Massiani, C. and Martel, J.L., 2005b. Influence of the airflow rate on heat and mass transfers during sewage sludge and bulking agent composting. Environmental Technology 26 (10), 1137-1149.

van Ginkel, J.T., 1996. Physical and biochemical processes in composting material. PhD thesis, Wageningen Agricultural University (Landbouwuniversiteit te Wageningen), The Netherlands.

van Lier, J.J. C., van Ginkel, J.T., Straatsma, G., Gerrits, J.P.G. and van Griensven, L.J.L.D., 1994. Composting of mushroom substrate in a fermentation tunnel - compost parameters and a mathematical model. Netherlands Journal of Agricultural Science 42 (4), 271-292.

VanderGheynst, J., Walker, L. and Parlange, J., 1997. Energy transport in a high-solids aerobic degradation process: Mathematical modeling and analysis. Biotechnology Progress 13 (3), 238-248.

Weppen, P., 2001. Process calorimetry on composting of municipal organic wastes. Biomass & Bioenergy 21, 289-299.

Whang, D.S. and Meenaghan, G.F., 1980. Kinetic model of the composting process. Compost Science/Land Utilisation 21 (3), 44-46.

Yamada, Y. and Kawase, Y., 2006. Aerobic composting of waste activated sludge: Kinetic analysis for microbiological reaction and oxygen consumption. Waste Management 26, 49-61.

Zavala, M.A.L., Funamizu, N. and Takakuwa, T., 2004a. Modeling of aerobic biodegradation of feces using sawdust as a matrix. Water Research 38 (5), 1327-1339.

Zavala, M.A.L., Funamizu, N. and Takakuwa, T., 2004b. Temperature effect on aerobic biodegradation of feces using sawdust as a matrix. Water Research 38 (9), 2406-2416.

CHAPTER 5
AN EVALUATION OF SUBSTRATE DEGRADATION IN THE COMPOSTING PROCESS.
Part 1: Profiles at Constant Temperature

5.1 Foreword

In chapter 4 we saw how substrate degradation sub-models appeared to be a weak link in mathematical modelling of the composting process. Thus the next stage of the journey seemed clear – to take a path to places which would reveal more information about this highly significant part of the larger model. A novel proposition was decided upon, namely to re-arrange the energy balance in order to produce a solution for the substrate degradation term, and then to attempt to validate this prediction experimentally. In conceptual terms, the author planned to depart promptly for the Matlab Mountains to work on the software and data manipulation tools which would be needed, and then take the long hike through to Experimentia, where laboratory work would be conducted (figure 5.1). It was known that the route would pass though Kineticsville, where useful chats concerning substrate degradation modelling might be had, and then through the Bog of Eltech, the passage of which, based on previous experience, was expected to be relatively straightforward. Therefore Mathmodopolis was farewelled, and after a pleasant and productive few summer months in the Matlab Mountains, the author eventually set off for Experimentia. As it turned out however, the Bog of Eltech proved impassable, despite several attempts to cross it, and so the author returned to Kineticsville to await more favourable circumstances. In the event, this stop proved to be very worthwhile, in particular because of the presence of the nearby Data Mines. It was decided to use this unexpected opportunity to search the data mines for evidence in support of those substrate degradation models previously adopted by modellers. Since it was known that many substrate degradation profiles had been generated under varying temperature, moisture and oxygen conditions, it was decided to develop a procedure to de-couple them from these effects, in order to reveal profiles at constant temperature, optimal moisture and non-limiting oxygen levels. The results are reported in chapter 6. The advantages of profiles at constant conditions are a) that they potentially allow a more fundamental model to be applied and b) that they can be readily generated at laboratory scale (chapters 2 and 3) in more controlled environments.

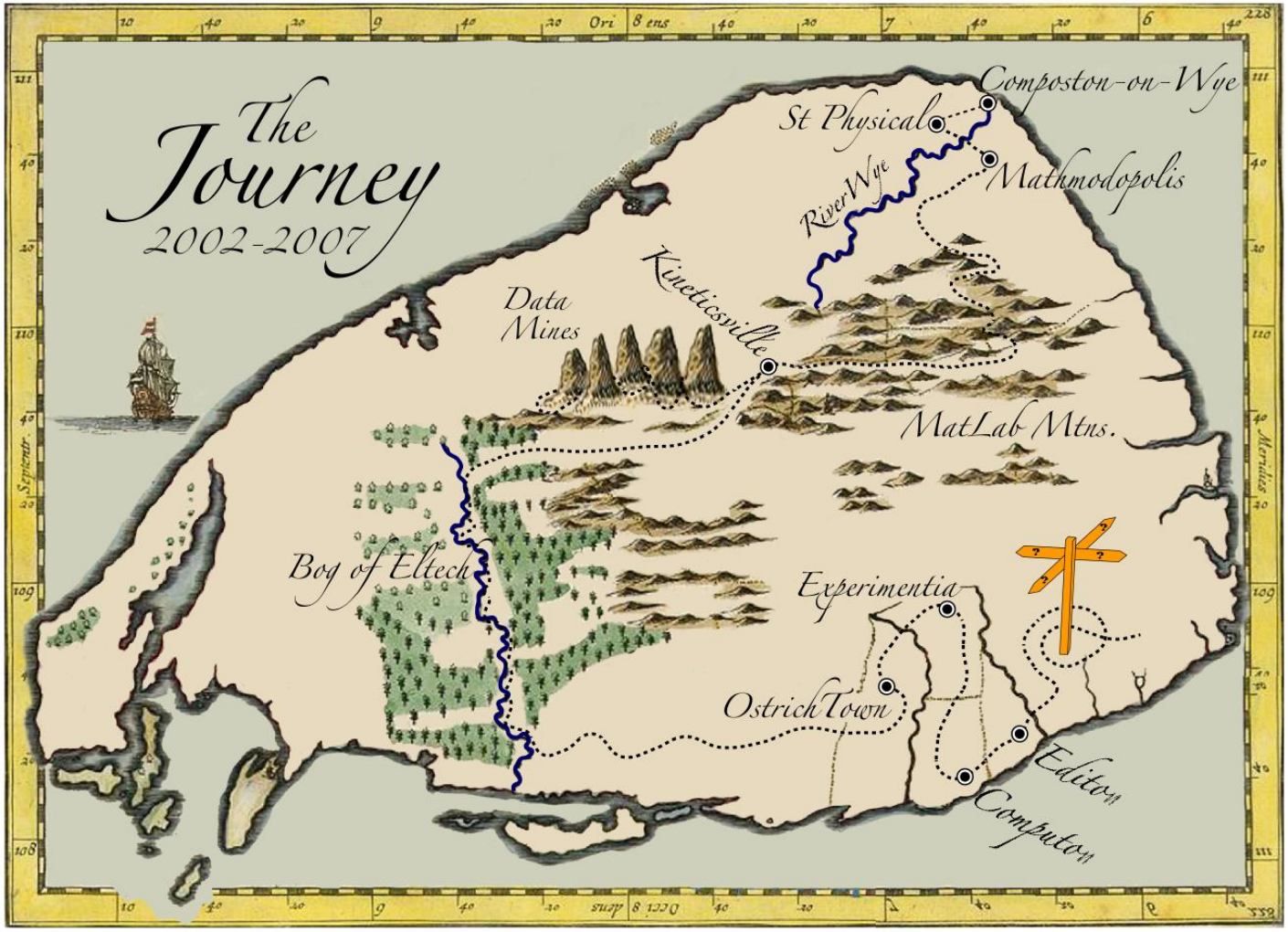

Figure 5.1: The conceptual map of the author's research travels. Our present locations are – Kineticsville and the Data Mines.

This chapter consists of the following journal paper:

Mason, I.G., in press. An evaluation of substrate degradation patterns in the composting process. Part 1: Profiles at constant temperature. Waste Management. (Published on-line 17 September, 2007).

Readers are asked to note that the text may differ from that in the published paper in places and that corrections may have been incorporated.

5.2 Summary

This paper examines the patterns of 32 constant-temperature substrate degradation profiles obtained from the composting literature, and evaluates the use of a single exponential model, a double exponential model and a non-logarithmic Gompertz model, in describing their behaviour. Profiles were found to be predominantly either sigmoidal in shape, or to exhibit multi-phase behaviour, with a relatively small proportion of convex curves. Of the constant-temperature profiles, 26 were either not well modelled by any of the above functions, or of such differing profiles, that none of the above functions was applicable. Goodness of fit was measured using a normalised error function, and rated using a 5-category descriptive scale, ranging from excellent to poor. No fits rated as excellent were observed. Fits rated as good were obtained for 3 data sets when using a single exponential function, for 2 data sets when using a double exponential function, and for 1 data set when using the non-logarithmic Gompertz function. The remainder of the fits were rated as moderate to poor. It is concluded that the evidence supporting the use of either the single exponential model, the double exponential model or the non-logarithmic Gompertz model to describe substrate degradation profiles generated at constant temperature is limited. Further work is suggested in order to establish standard procedures and a standard simulated composting mixture for substrate degradation studies and to build a more comprehensive set of long-term substrate degradation profile data at constant temperature, and under non-limiting moisture and oxygen concentration conditions.

5.3 Nomenclature

β	bacterial maintenance coefficient (kg-BVS/kg-X.h)
BVS	biodegradable volatile solids present (kg or g/m^3)
BVS_{rem}	biodegradable volatile solids removed (kg or g/m^3)
BVS'	apparent maximum BVS (Eq. 13) (kg or g/m^3)
DM	dry matter
e	2.178282
H(t)	cumulative quantity of CO_2 evolved
k	first-order rate coefficient (d^{-1})
k_d	microbial decay coefficient
λ	lag time (d)
μ	specific bacterial growth rate (d^{-1})
μ_{max}	maximum bacterial specific growth rate (d^{-1})
M	cumulative quantity of CH_4 evolved
N	number of bacterial cells at time *t*
N_o	number of bacterial cells at time zero
NRMSE	normalised root mean square error
OM	organic matter
P	CH_4 evolution potential (Lay et al., 1998) or CO_2 evolution potential (Chang et al., 2005; Chang et al., 2006)
R_m	maximum CH_4 evolution rate (Lay et al., 1998) or maximum CO_2 evolution rate (Chang et al., 2005; Chang et al., 2006)
t	time
T	temperature (^oC)
VS	volatile solids present (kg or g/m^3)
VS_{rem}	volatile solids removed (kg or g/m^3)
X	biomass (kg or g/m^3)
$Y_{X/BVS}$	maximum cell yield per unit substrate consumed
a, b, c	empirical constants (Gompertz model)
1, 2	rapidly and slowly degradable substrates respectively (Eq. 13)

5.4 Introduction

Correct modelling of the progress of substrate degradation is of vital importance in the prediction of temperature, moisture and other state variable profiles of interest in the composting process. The most commonly employed approach has been to use substrate degradation models derived from first-order rate assumptions, where the independent variable is either a) the quantity, or concentration, of substrate remaining (Smith and Eilers, 1980; Haug, 1993; Keener et al., 1993; Das and Keener, 1997; Mohee et al., 1998; Higgins and Walker, 2001; Scholwin and Bidlingmaier, 2003) or b) the quantity, or concentration, of biomass present (Kaiser, 1996; Stombaugh and Nokes, 1996; Seki, 2000). When substrate is expressed as biodegradable volatile solids (BVS), and biomass as bacterial cell mass (X), the corresponding fundamental rate expressions are as follows:

$$\frac{dBVS}{dt} = -kBVS \tag{1}$$

$$\frac{dX}{dt} = \mu X - k_d X \tag{2}$$

Application of a cell biomass yield coefficient to Eq.2 leads to the following expression for substrate utilisation (Metcalf and Eddy, 1991; Stombaugh and Nokes, 1996):

$$\frac{dBVS}{dt} = -\frac{\mu}{Y_{X/BVS}} X - \beta X \tag{3}$$

In an alternative approach, the sigmoidal shaped model of Gompertz (1825) has been applied to composting data at varying temperature by Chang et al. (2005) and Chang et al. (2006). The Gompertz model was first applied to microbial growth data by Gibson et al. (1987) and is widely used for describing microbial growth of pure cultures at constant temperature (Zwietering et al., 1990; Whiting, 1995). The basic form of the Gompertz expression, as commonly used in bacterial growth modelling, is as follows:

$$y = \ln\frac{N}{N_o} = a.\exp(-\exp(b - ct) \tag{4}$$

where: N is the number of bacterial cells at time t

N_o is the number of bacterial cells at time zero

a is a constant, representing the maximum value of *y*

b is a constant, representing the slope of the tangent at the point of inflexion

c is a constant, representing the intercept of the tangent on the *x* axis

Zwietering et al. (1990) reparameterised the Gompertz model, showing that the three mathematical parameters a, b and c, could be replaced by biological parameters representing i) the maximum value (A) of the function, ii) the maximum microbial specific growth rate (μ_{max}) and iii) a lag time (λ). In this case:

$$y = \ln\frac{N}{N_o} = A.\exp\left\{-\exp\left[\frac{\mu_{\max}.e}{A}(\lambda - t) + 1\right]\right\} \quad (5)$$

A non-logarithmic form of the Gompertz model has also been employed (Mackey and Kerridge, 1988). Here:

$$y = \frac{N}{N_o} = A.\exp\left\{-\exp\left[\frac{\mu_{\max}.e}{A}(\lambda - t) + 1\right]\right\} \quad (6)$$

Adaptations of the non-logarithmic form of the Zweitering modification have been used to model methane production from landfills (Lay et al., 1998):

$$M = P.\exp\left\{-\exp\left[\frac{R_m.e}{P}(\lambda - t) + 1\right]\right\} \quad (7)$$

where: M is the cumulative quantity of CH_4 evolved

P is the CH_4 evolution potential

R_m is the maximum CH_4 evolution rate

and more recently carbon dioxide evolution in composting systems (Chang et al., 2005; Chang et al., 2006):

$$H(t) = P.\exp\left\{-\exp\left[\frac{R_m.e}{P}(\lambda - t) + 1\right]\right\} \quad (8)$$

where: H(t) is the cumulative quantity of CO_2 evolved

P is the CO_2 evolution potential

R_m is the maximum CO_2 evolution rate

The exponential and Gompertz expressions are applicable to modelling substrate degradation at constant temperature without rate co-efficient correction, provided that non-limiting moisture and oxygen conditions are maintained. A further grouping of substrate degradation models may be classed as empirical (Chapter 4; Mason, 2006) and will not be considered here.

Hamoda et al. (1998) reported that a linearised first-order model gave a good fit to total organic carbon (TOC) data from the composting of municipal solid waste (MSW) over 15 days, at temperatures of 20, 40 and 60 ^oC (R^2 = 0.987, 0.933, 0.855 respectively). However, when the substrate profiles are assessed visually against the model, the fit is poor. Activated sludge models incorporating Monod-type kinetics were fitted to oxygen uptake rate data from the composting of raw faeces and sawdust over 16 days at 55 ^oC by Zavala et al. (2004a), and sewage sludge and pine bark over 20 days at 39.6 ^oC by Tremier et al. (2005). In both cases a good visual fit was shown, but cumulative substrate degradation patterns were not reported or modelled. Agreement between the model and experimental data for raw faeces and sawdust composting at 20, 30 and 40 ^oC was improved after fractionation of the modelled substrate into easily and slowly hydrolysable material (Zavala et al., 2004b). Komilis (2006) fitted a model incorporating three first-order functions, describing the degradation of readily, moderately and slowly hydrolysable feedstock fractions respectively, to CO_2 data arising from the separate composting of food waste, yard waste, mixed paper, leaves, branches and grass clippings at 52 ^oC over 26-198 d. The slowly hydrolysable rate coefficient was set to zero, and readily and moderately rate coefficients ranging between 0.06-0.1 d^{-1} and 0.002-0.06 d^{-1} respectively reported. Goodness of fit was described using R^2, with values ranging from 86-100%. Otherwise the literature appears to contain no modelled substrate degradation data generated under composting conditions at constant temperature, and no strong evidence in support of those expressions above which are proposed to describe substrate degradation rates in the composting process.

The objectives of this paper are to examine published substrate degradation data at constanttemperature to see a) what generic degradation patterns are present, and b) which existing model(s) are appropriate to fit the data.

5.5 Methods

Published graphs of substrate degradation vs time were scanned using CanonScan (Canon Inc, Tokyo, Japan) and the curves then digitised using Engauge (VA Software, Fremont, USA). Profiles were initially classified into one of six generic shape categories as follows:

Convex curve	a curve of rising exponential or similar profile
Convex curve +	a convex curve followed by non-convex profile
Lag + convex curve	a concave lag phase followed by a convex curve
Sigmoidal	an "S" shaped profile
Multi-phase	more than two curves in series
Other	patterns not included above

Profiles were fitted with single and double exponential and Gompertz expressions by a least squares technique using "Matlab" (The Mathworks Inc, Natick, Mass., USA). The single (Eq. 9) and double (Eq. 10) exponential expressions were of the following forms:

$$BVS_{rem} = BVS_{\max}(1 - e^{-kt}) \tag{9}$$

$$BVS_{rem} = BVS'_{\max 1}(1 - e^{-k_1 t}) + BVS'_{\max 2}(1 - e^{-k_2 t}) \tag{10}$$

Further details on the double exponential model are given in Mason et al. (2006). The non-logarithmic variant of the Gompertz model (Eq. 8) was used. Due to the unavailability of biomass data, modelling based on cell growth (Eq. 3) was not considered.

Accuracy of fit was determined from the root mean square error (RMSE) of the differences between the modelled and experimental values of the dependent variable. These values were normalised by expressing them as a percentage of the maximum value of the function concerned i.e.

$$Error(\%) = \frac{RMSE}{BVS_{\max}} 100 \tag{11}$$

A qualitative assessment of the goodness of fit was made using a five-category scale, ranging from excellent to poor. The descriptive criteria for each category were as follows:

Excellent	close visual fit; good shape relationship; early time well modelled; projected direction of model at later time in line with the data trend
Good	occasional discrepancies in fit; good shape relationship; projected direction of model at later time close to the data trend
Moderate	discrepancies in fit; recognisable shape relationship; projected direction of model at later time typically different to the data trend
Fair	major discrepancies in fit; recognisable shape relationship; projected direction of model at later time typically different to the data trend
Poor	major discrepancies in fit; less recognisable shape relationship; projected direction of model at later time different to the data trend

Particular note was taken of the closeness of fit at early time, and in the projected direction of the modelled curve at the end of the data set. The latter was considered especially important since modellers commonly use such models to extrapolate substrate degradation beyond experimental time frames. Data patterns and data scatter were considered separately. Summary details of the rating scheme are given in the footnotes to the relevant tables and examples of excellent through poor fits are provided in Figs. 5.1-5.5. A total of 32 fixed temperature data sets was examined.

Curves were selected for fitting by each model by visual observation, and included rather than excluded if there was any doubt. Where the visual assessment indicated a post-lag phase profile of exponential shape, the lag phase was removed and the remaining data modelled. Similarly, where post-exponential phase data appeared to deviate markedly from prior patterns, these were removed. Where data were removed, the profiles were referred to as modified. Details of the experimental conditions under which these data sets were generated are given in table 5.1. With one exception (Hamoda et al., 1998) errors in these data sets was not reported, and the results in this chapter should be interpreted accordingly. Further discussion on this matter in given in the afterword to this chapter (Section 5.9).

Table 5.1: Details of the 32 constant temperature substrate degradation profiles

Mixture	Scale	Temperature	Measured parameter		Airflow	Time	Comments	Reference
		°C	Par	Units	l/min.kg	d		
Sewage sludge/rice husks	Lab	56	CO_2	mol/g- DM.hr	1.86	3.3	Cumulative CO_2 data derived from a rate curve starting at 0.08 d; initial moisture 58%	Bach et al. (1984)
Corn stalk	Lab	35	CO_2	mg/g-DM	1.00	20	Corn stalks amended with $FeSO_4$	Bono et al. (1992)
		45	CO_2	mg/g-DM	1.00	20		
Wheat straw		35	CO_2	mg/g-DM	0.47	20	Wheat straw amended with $CaCO_3$	
/$(NH_4)_2SO_4$		45	CO_2	mg/g-DM	0.47	20		
Simulated feedstock	Lab	40	CO_2	mol	ns	9.8	-	Tseng et al. (1995)
		50						
MSW	Lab	20	TOC	% of initial TOC	ns	15	Airflow 0.1 l/kg.min (wet basis); moisture not stated	Hamoda et al. (1998)
		40						
		60						
Yard trimmings	Lab	55	CO_2	% (of initial C)	3[a]	40	[a] oxygen flowrates (g-O_2/kg-OM.hr)	Michel and Reddy (1998)
		55			0.3[a]			
		55			0.03[a]			
		55			0[a]			
Dog food/ sawdust	Lab	45	CO_2	% C (of dog food)	0.73	8	Airflow increased to 9.7 l/min.kg for cooling	Nakasaki et al. (1998)
Yard waste	Lab	32	CO_2	% (of initial	ns	52	[b] no seed;	Komilis and Ham (2000)
Yard waste		55		organic -C)		74[c]	[c] for comparative purposes initial evaluations reported in tables 2-5 were restricted to a time of 52 days for each of the substrates.	
Yard waste[b]		55				70[c]		
Food waste		55				57[c]		
Food waste[b]		55				92[c]		
Mixed paper		55				198[c]		
Seed		55				66[c]		
PAHs/ woodchips	Lab	20	CO_2	% (C of initial C)	8.33	28	-	Loser et al. (2004)
		30						
		40						
		50						
Food waste	Lab	52	CO_2	g-C/kg-TS	ns	91	-	Komilis (2006)
Yard waste		52				69	-	
Mixed paper		52				198	Mixed paper amended with NH_4NO_3	
Leaves		52				71	-	
Branches		52				56	Branches amended with NH_4NO_3	
Grass		52				26	-	

Abbreviations: DM: dry matter; Lab: laboratory; ns: not stated; MSW: municipal solid waste; OM: organic matter; PAH: polyaromatic hydrocarbon; TOC: total organic carbon

Table 5.2: Profile shape summary: constant-temperature BVS/CO_2 profiles

Profile shape characteristic	Number	Comments
Convex curve	6	Beginning of a 2nd phase suggested in 2 cases
Concave lag phase + convex curve	3	-
Convex curve + second phase	7	-
Sigmoidal curve	8	
Multi-phase	6	3 of these were for PAH/woodchips composting
Other	2	
TOTAL	32	

Table 5.3: Modelling summary: unmodified constant-temperature BVS/CO_2 profiles

Model	Excellent	Good	Moderate	Fair	Poor	Data sets modelled	Profile rejected
	no.	no.	no.	no.	no.	no.	no.
Single exponential	0	3	5	2	1	11	21
Double exponential	0	2	3	-	-	5	27[a]
Modified Gompertz	0	1	4	3	-	8	24

[a] including "no improvement shown over the single exponential model"

5.6 Results

5.6.1 Shape profiles

The majority of constant-temperature profiles incorporated convex shapes (50%), which formed either the entire profile, or the main part, after a concave lag phase, or prior to a subsequent period of divergence from the convex form at later time. Smaller numbers of sigmoidal (25%) and multi-phase (19%) patterns were found (table 5.2). These observations suggested exponential and Gompertz functions as promising mathematical models for a substantial number of the profiles. In addition it seemed likely that the convex portions of selected profiles could be modelled using exponential functions. No attempt was made in the present work to model the multi-phase profiles.

5.6.2 Modelling

When data were modelled using a single exponential first-order function, no fits rated as excellent were observed, and fits rated as good were obtained for only 3 of the 16 data sets showing convex or convex plus second-phase profiles, plus 2 data sets initially classified as sigmoidal on visual appearance only (tables 5.2, 5.3, 5.4). Of these three, the profile derived from Bach et al. (1984), which described the composting of a sewage sludge/woodchips mixture, was generally well modelled over a time period of 3.1 days at 56 ^{o}C (figure 5.2), but showed a lag phase of approximately 0.2 days from the beginning of CO_2 monitoring, or approximately 0.4 d from the beginning of the experiment, which was not modelled, as expected, by the single exponential function. The single exponential model also gave a fit rated as good to yard trimmings data of Michel and Reddy (1998) at 55 ^{o}C, over a period of 40 days, with no forced aeration. As previously, the lag phase was not modelled, but the fit to the remaining data was excellent. A good fit was found for data of Komilis (2006), from the composting of grass clippings at 52 ^{o}C, over 26 days.

Table 5.4: Single exponential model parameters: constant-temperature BVS/CO_2 profiles (including modified profiles)

Mixture	Temperature	BVS_{max}		k	NRMSE	Visual fit*	t(95%)	Comments	Data source
	°C	Value	Units	d^{-1}	%		d		
Sewage sludge/rice husks	56	484	mol/g-DM x 10^5	0.41	0.93	good	7.3	Lag phase (0.4 d) not modelled	Bach et al. (1984)
Corn stalk	35	236	mg/g-DM	0.17	2.16	moderate**	17.5	Lag phase (6.1 d) eliminated	Bono et al. (1992)
	45	196	mg/g-DM	0.08	1.43	moderate**	36.9	Lag phase (5.0 d) eliminated	
Wheat straw	35	389	mg/g-DM	0.07	1.88	moderate	45.7	-	
	45	348	mg/g-DM	0.09	1.40	moderate	33.7	-	
MSW	40	14.3	%	0.10	5.73	poor	nd	-	Hamoda et al. (1998)
Yard trimmings	55	45.8	%	0.10	3.03	moderate	29.5	3 g-O_2/kg-OM.h	Michel and Reddy (1998)
	55	13.2	%	0.02	1.06	good	132.5	0 g-O_2/kg-OM.h	
Yard waste	55	47.0	%	0.14	4.23	fair**	22.1	First 38.6 d only	Komilis and Ham (2000)
Yard waste[a]	55	45.0	%	0.11	1.55	moderate**	26.8	[a] no seed; first 29.9 d only	
Food waste	55	76.1	%	0.10	1.83	moderate	31.4	-	
Food waste[a]	55	60.9	%	0.11	3.80	fair**	26.9	[a] no seed; first 36.6 d only	
Mixed paper[b]	55	14.1	%	0.08	3.12	fair**	36.7	[b] lag phase (6.5 d) eliminated	
Seed	55	22.8	%	0.08	2.66	fair	39.9	-	
Seed[c]	55	19.4	%	0.10	1.54	moderate**	28.9	[c] First 18.4 d only	
PAHs/ woodchips	50	1.36	%	0.07	1.47	moderate	43.0	-	Loser et al. (2004)
Leaves	52	84	g-C/kg-TS	0.04	3.24	fair	74.3	-	Komilis (2006)
Grass	52	291	g-C/kg-TS	0.05	0.90	good	63.5	-	

Abbreviations: BVS: biodegradable volatile solids; DM: dry matter; MSW: municipal solid waste; nd: not determined; OM: organic matter; PAH: polyaromatic hydrocarbon
* Scale based on discrepancies between data and fitted curve: Excellent = close fit; Good = occasional discrepancies, good shape relationship; Moderate = some discrepancies, recognisable shape relationship; Fair = many discrepancies, recognisable shape relationship; Poor = major discrepancies, less recognisable shape relationship
** modified data sets (not included in Tab. 5.3)

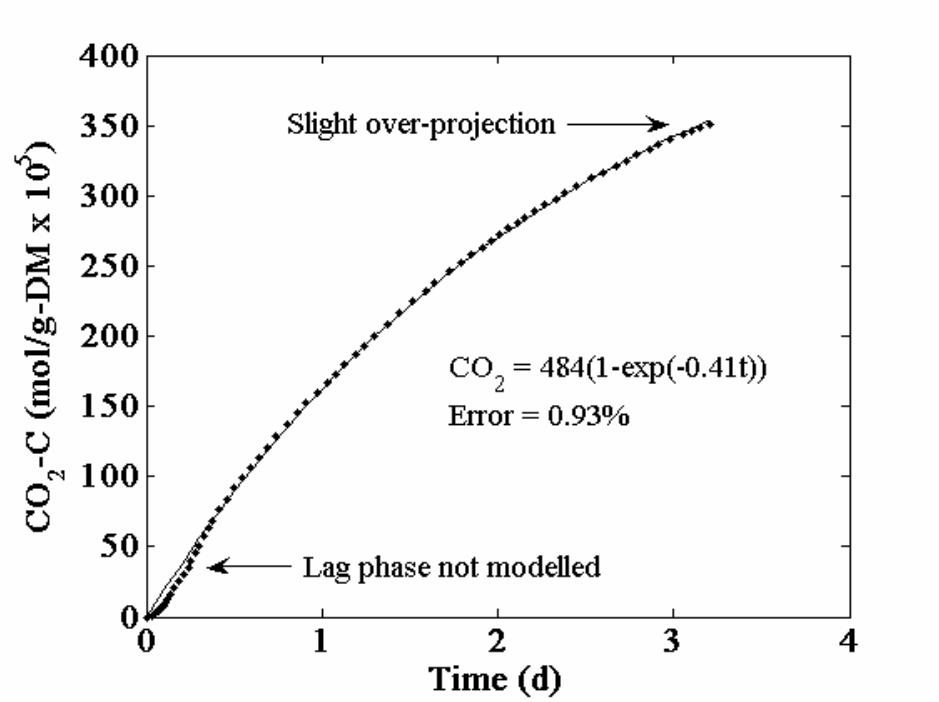

Figure 5.2: CO_2 evolution data for sewage sludge/woodchips composting at 56 ^oC, fitted with a single exponential model. Fit rated as good. After Bach et al. (1984).

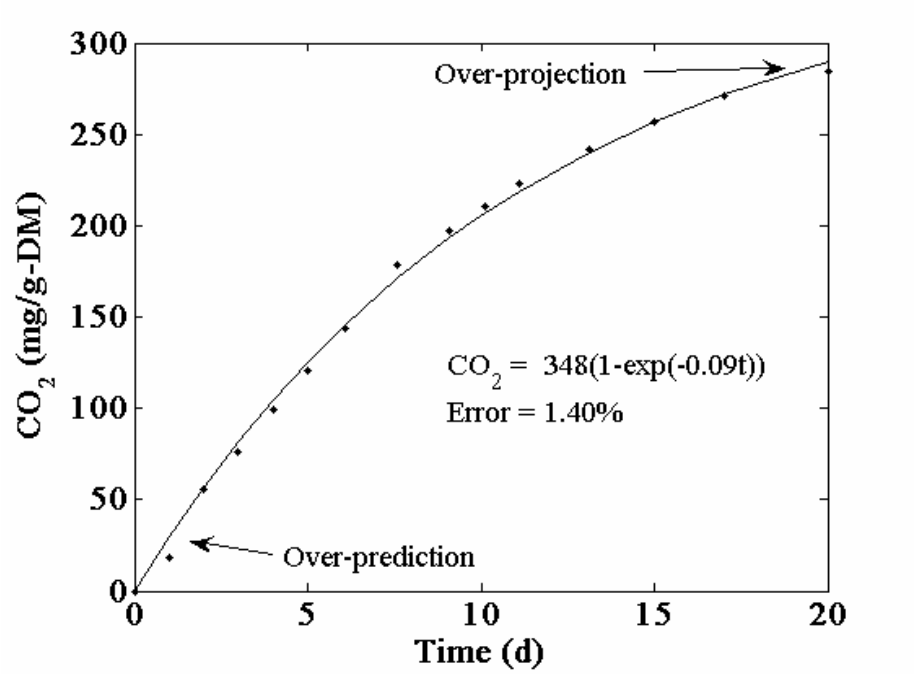

Figure 5.3: CO_2 evolution data for wheat straw composting at 45 ^oC, fitted with a single exponential model. Fit rated as moderate. After Bono et al. (1993)

The performance of the single exponential model was rated as moderate for a further 5 data sets (tables 5.3, 5.4). Generally, data in the middle time period were reasonably well modelled, with discrepancies at both early and later time. Data of Bono et al. (1992), from the composting of wheat straw over a period of 20 days at 45 ^{o}C, showed evidence of a lag phase, which was not modelled, and a visual indication that the fitted saturation function was likely an overestimate (figure 5.3). Similarly, when data of Loser et al. (2004) from the composting of a polyaromatic hydrocarbon (PAH)/woodchips mixture over 28 days at 50 ^{o}C, was modelled using a single exponential function, the lag phase not modelled, and a likely underestimation of the saturation function observed. For data generated when yard trimmings were composted with forced aeration at 3 g-O_2/kg-OM.h (Michel and Reddy, 1998), there was no experimental evidence of a lag phase, but again a visual indication that the saturation function was likely underestimated (figure 5.4a). In this case, an improved fit was obtained with a double exponential model, with a better estimate of the saturation function indicated (figure 5.4b, table 5.5). Double exponential models also gave fits rated as good in a further two cases (tables, 5.3, 5.5). The performance of the single exponential model with 3 data sets was rated as fair to poor, whilst the model was not considered applicable to the remaining 16 data sets. Examples of fair and poor fits are shown in figures 5.5-5.6.

Elimination of a lag phase, or removal of multi-phase patterns at later time, resulted in moderate and fair fits on the remaining data, in 7 cases (table 5.3). The data of Bono et al. (1998) for the composting of corn stalks at 45 ^{o}C for example, was moderately well fitted by a single exponential model following removal of a 5.0 d lag phase (figure 5.7). In a number of other instances, the duration of the modified plots remained within the typical "hot composting" timeframe, suggesting that this approach may be useful for predictions over selected composting periods. A double exponential model gave a fit rated as good when a 1.3 d lag phase was eliminated from data of Nakasaki et al. (1998) for the composting of dog food and sawdust at 45 ^{o}C (table 5.5).

Table 5.5: Double exponential model parameters: constant-temperature BVS/CO_2 profiles (including modified profiles)

Mixture	BVS_{max}	k_1	k_2	NRMSE	Visual fit*	Comments	Data source
		d^{-1}	d^{-1}	%			
Yard trimmings	48.3	0.46	0.07	1.70	good	3 O_2/kg-OM.h	Michel and Reddy (1998)
Dog food/sawdust	152	1.90	0.11	0.48	good**	Lag phase (1.3 d) eliminated	Nakasaki et al. (1998)
Food waste[a]	68.9	0.56	0.06	0.79	good**	First 36.6 d only; [a] no seed	Komilis and Ham (2000)
Yard waste[a]	58.6	0.22	0.04	2.70	moderate	[a] no seed	Komilis and Ham (2000)
Food waste	352	0.57	0.06	3.0	moderate	-	Komilis (2006)
Yard waste	440	0.18	0.008	1.07	good	-	
Branches	110	0.50	0.02	1.95	moderate	Starts from 2.5 d	

* Scale based on discrepancies between data and fitted curve: Excellent = close fit; Good = occasional discrepancies, good shape relationship; Moderate = some discrepancies, recognisable shape relationship; Fair = many discrepancies, recognisable shape relationship; Poor = major discrepancies, less recognisable shape relationship
** modified data sets (not included in Tab. 5.3)

Table 5.6: Gompertz model parameters for constant-temperature BVS/CO_2 profiles (including modified profiles)

Mixture	Temperature	BVS_{max}		μ	λ	NRMSE	f(0)	Visual fit*	Comments	Data source
	°C	Value	Units	BVS/d	d	%	BVS			
Corn stalk	35	330	mg/g-DM	25.7	3.5	2.63	1.2	fair	-	Bono et al. (1992)
	45	172	mg/g-DM	13.6	3.3	1.16	0.7	good	-	
Simulated feedstock	40	1.9	mol	0.5	3.1	4.21	0	fair	Undershoots at early time	Tseng et al. (1995)
	50	3.5	mol	1.5	5.9	4.57	0	fair	Undershoots at early time	
Yard	55	34.8	%	0.88	4.53	1.24	0.85	moderate	0.3 O_2/kg-OM.h	Michel and Reddy (1998)
trimmings	55	14.3	%	0.97	12.29	2.66	0	moderate	0.03 O_2/kg-OM.h	
Yard waste	32	35.9	%	1.05	6.32	2.45	0.40	moderate	-	Komilis and Ham (2000)
Mixed paper	55	19.8	%	0.90	1.91	1.36	0.63	moderate	-	
Mixed paper	52	86	g-C/kg-TS	4.0	2.6	1.36	1.92	good**	First 41.2 d only	Komilis (2006)

Abbreviations: BVS: biodegradable volatile solids
* Scale based on discrepancies between data and fitted curve: Excellent = close fit; Good = occasional discrepancies, good shape relationship; Moderate = some discrepancies, recognisable shape relationship; Fair = many discrepancies, recognisable shape relationship; Poor = major discrepancies, less recognisable shape relationship
** modified data set (not included in Tab. 5.3)

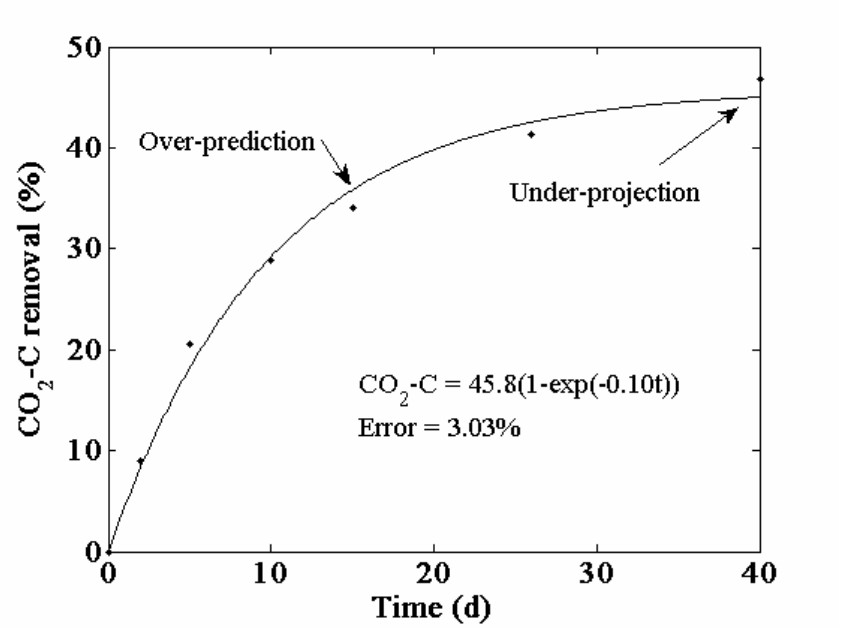

Figure 5.4a: CO_2 evolution data for yard waste composting at 55 ^oC, with forced aeration at 3 g-O_2/kg-OM.h, fitted with a single exponential model. Fit rated as moderate. After Michel and Reddy (1998).

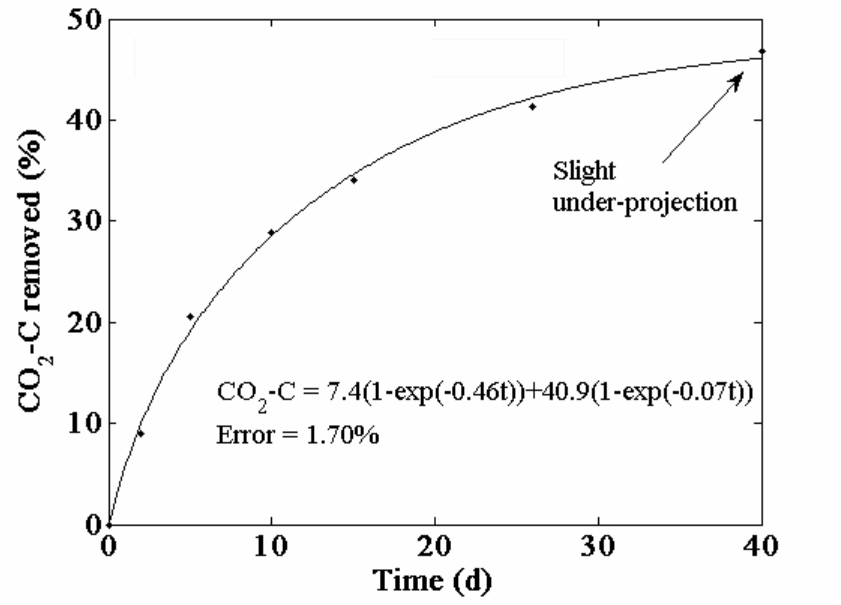

Figure 5.4b: CO_2 evolution data for yard waste composting at 55 ^oC, with forced aeration at 3 g-O_2/kg-OM.h, fitted with a double exponential model. Fit rated as good. After Michel and Reddy (1998).

Single exponential model rate coefficients for the fits rated as good and moderate ranged from 0.02 d^{-1}, for yard waste to 0.41 d^{-1}, for sewage sludge, at temperatures of 45-56 ^{o}C respectively (table 5.2). Apart from the value of 0.41 d^{-1}, indicating a relatively rapid reaction, these coefficients are in line with those previously reported by Hamoda et al. (1998). Along with the rate coefficient values, predicted times to 95% exertion of the BVS present (t(95%)) indicated the relative ease of substrate degradability. With two exceptions, predicted t(95%) values for moderate and good fits ranged from approximately 30-63 days. The values of 7.6 and 132.5 days for sewage sludge and naturally aerated yard waste respectively, indicated very rapid and very slow degradation times respectively, in comparison to normal composting time frames.

The modified non-logarithmic Gompertz model was fitted to 9 data sets, chosen on the basis of visual evidence of a sigmoidal pattern. No fits rated as excellent were observed. Two fits were rated as good, 4 as moderate and 3 as fair (tables 5.3, 5.6). The Gompertz model provided a good fit to the full data set of Bono et al. (1992) for corn stalks composted 45 ^{o}C over 20 days, with realistic estimates of the saturation function and lag time (figure 5.8). A moderate fit was obtained at 35 ^{o}C, due to an almost linear lag phase. Moderate fits were also found when data of Michel and Reddy (1998) for yard waste composted with forced aeration at 0.03 g-O_2/kg-OM.h (figure 5.9) and 0.3 g-O_2/kg-OM.h, over 40 days, were modelled. In both cases the lag phase was not well fitted however. A good fit was obtained to data from the first 41 days of mixed paper composting at 52 ^{o}C (Komilis, 2006). However data for mixed paper composting at 55 ^{o}C over 52 days (Komilis and Ham, 2000) was modelled only moderately well (table 5.4), with discrepancies mainly around the lag phase. One problem observed with the Gompertz function when fitting in a least squares sense is the frequent occurrence of non-zero values for y at time zero. These are noted in the table as f(0). An example of a fair fit is shown in figure 5.10.

Descriptive classifications and normalised error were reasonably well correlated, as shown in figure 5.11. Variations within a descriptive category occurred due to non-numerical assessments of fit, such as the degree to which the lag phase was modelled, and the projection of the curve beyond the modelled time period.

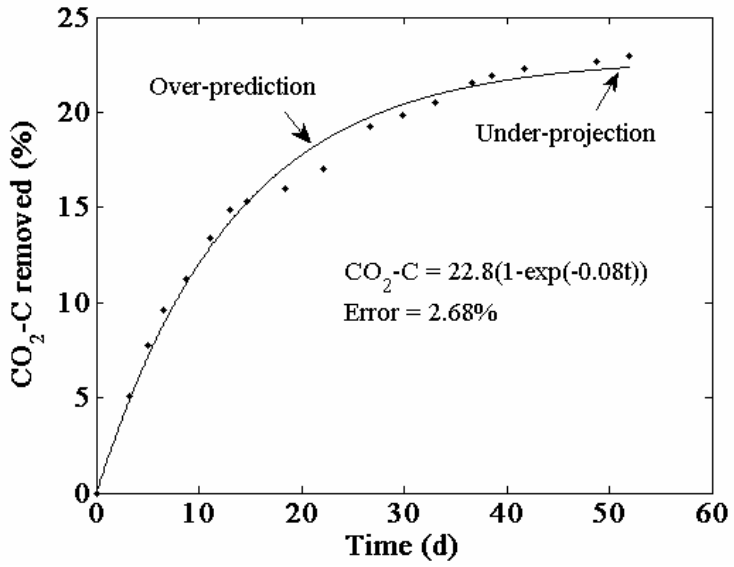

Figure 5.5: CO_2 evolution data for seed material composting at 55 ^oC, fitted with a single exponential model. Fit rated as fair. Komilis and Ham (2000).

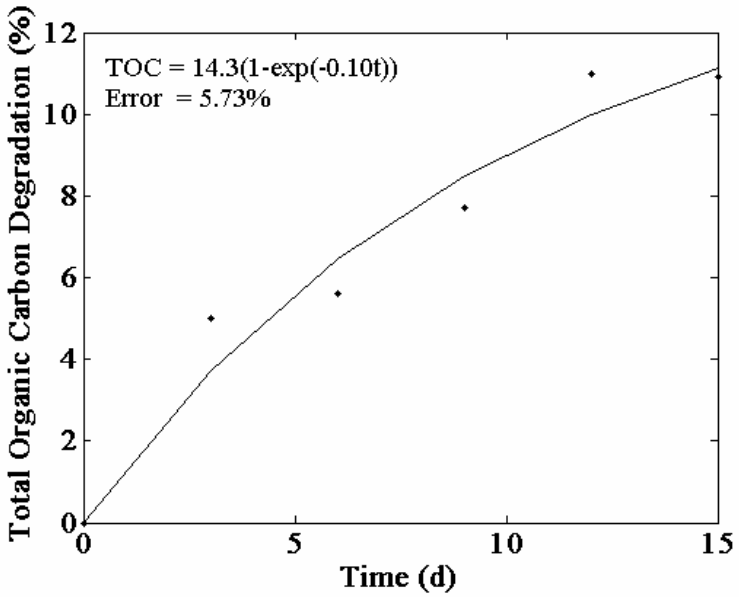

Figure 5.6: CO_2 evolution data for MSW composting at 40 ^oC, fitted with a single exponential model. Fit rated as poor. After Hamoda et al. (1998). (See note in afterword).

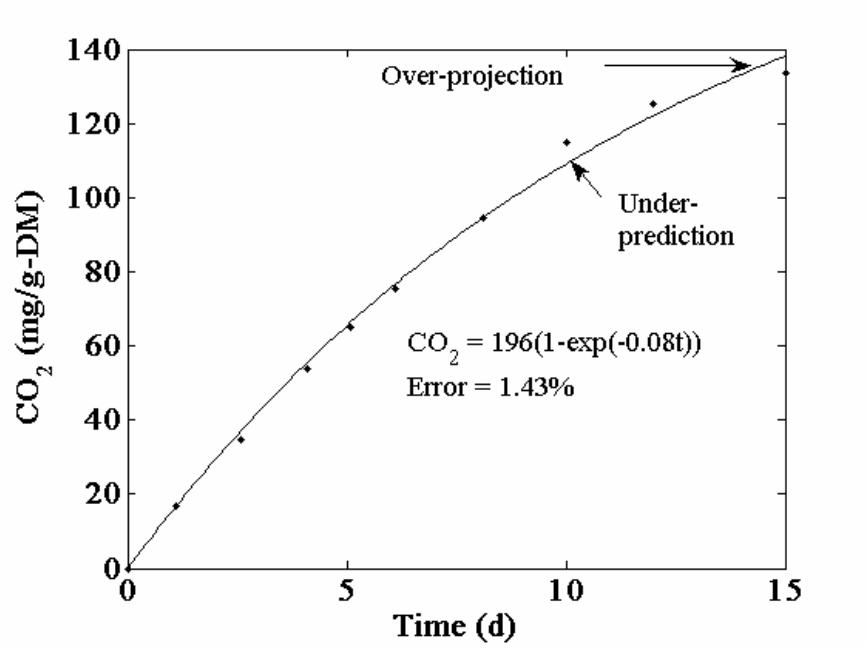

Figure 5.7: CO_2 evolution data for composting of corn stalks at 45 ^oC, following removal of a 5.0 d lag phase, fitted with a single exponential model. Fit rated as moderate. After Bono et al. (1998).

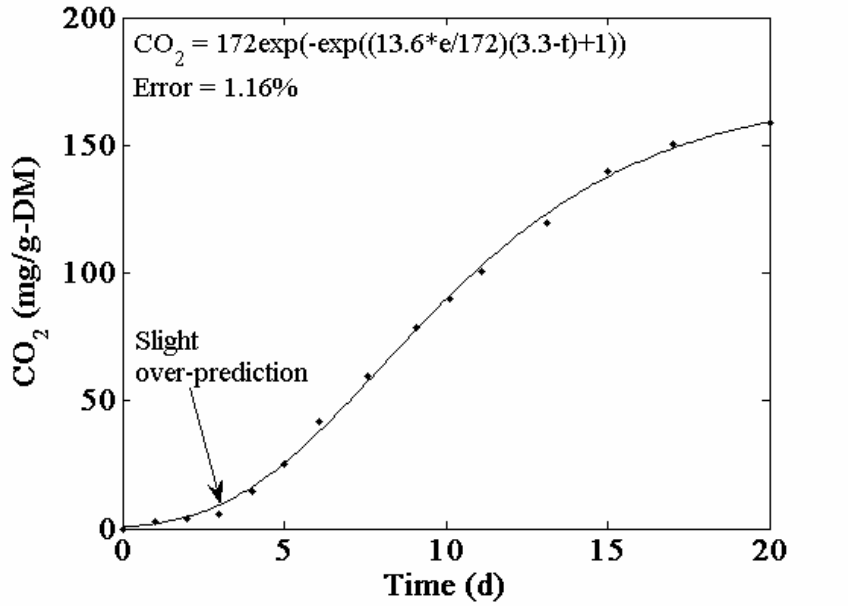

Figure 5.8: CO_2 evolution data for corn stalks composting at 45 ^oC, fitted with the non-logarithmic Gompertz model. Fit rated as good. After Bono et al. (1992).

5.7 Discussion

5.7.1 Model applicability

From this analysis, good evidence for the first order assumption for substrate degradation, and consequent single or double exponential model, is supplied by five full data sets, one for sewage sludge, three for yard waste and one for grass clippings. The time periods for yard waste composting encompassed the thermophilic time period expected for full-scale composting processes, but the sewage sludge data, monitored over 3.3 days (Bach et al., 1984), did not. Predicted times to 95% saturation also generally indicated that the substrate would be largely consumed within realistic time frames, provided the model continued to be valid at later time.

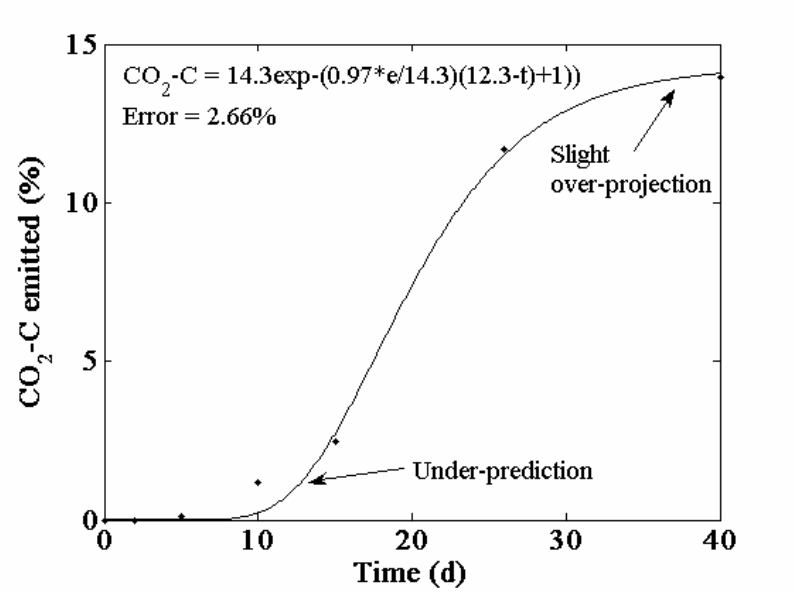

Figure 5.9: CO_2 evolution data for yard waste composting at 55 ^oC, with forced aeration at 0.03 g O_2/kg-OM.h, fitted the non-logarithmic Gompertz model. Fit rated as moderate. After Michel and Reddy (1998).

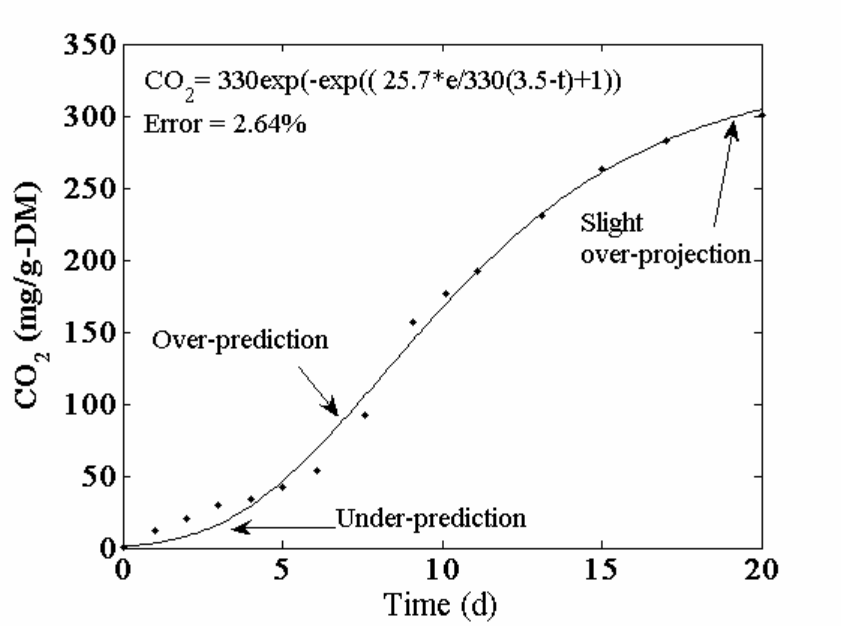

Figure 5.10: CO_2 evolution data for composting of corn stalks at 35 ^oC, fitted with the non-logarithmic Gompertz model. Fit rated as fair. After Bono et al. (1998).

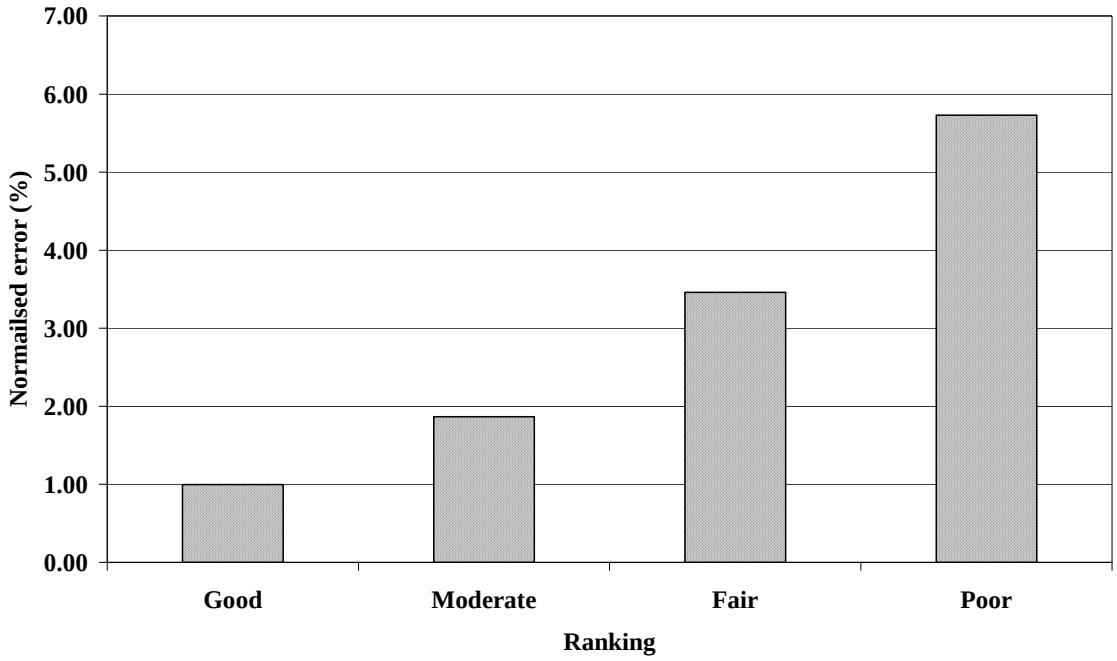

Figure 5.11: The relationship between descriptive classifications and average values of normalised error, for substrate degradation profiles at constant temperature.

The single and double exponential functions do not model the inherent lag phase (noting that this may not always be visible due to the data collection frequency adopted). Failure to correctly model the lag phase will result in over-estimation of temperature at early time, when substrate models are inserted into temperature prediction models, but whether this is of practical significance remains to be determined. The validity of the Gompertz model is similarly supported by limited experimental data, with only one fit rated as good obtained. The Gompertz model has been shown to suffer from frequent overestimation of substrate degradation at zero time, which would again result in overestimation of temperature at early time.

Use of the double exponential model with four fitted parameters, rather than the single exponential model with two fitted parameters can be justified in this work by considering the mechanistic derivation of the model, in which two simultaneously utilised substrate groups, readily degradable material and slowly degradable material, are modelled. The existence of rapidly and slowly degradable substrates is widely accepted (e.g. Haug, 1993) and thus the applicability of this model derives from more than simply adding two more parameters in order to obtain a better mathematical fit, which would normally occur. It is noteworthy that, in situations where a single exponential model is adequate, the double exponential model will satisfactorily model the data, showing identical rate coefficients in each of the two terms. From a mathematical point of view however a single exponential model, with only two parameters, is preferred. For further details on the development of the double exponential model the reader is referred to Mason et al. (2006).

5.7.2 Normalised substrate degradation models

Single exponential, double exponential and Gompertz models with fits rated as good are presented in dimensionless form in figure 5.12. For the single exponential model the form of the function is:

$$\frac{BVS_{rem}}{BVS_{\max}} = (1 - e^{-kt}) \tag{12}$$

For the double exponential model the form of the function is:

$$\frac{BVS_{rem}}{BVS_{\max}} = \frac{(1-e^{-k_1 t})}{\left(1+\frac{BVS_2'}{BVS_1'}\right)} + \frac{(1-e^{-k_2 t})}{\left(1+\frac{BVS_1'}{BVS_2'}\right)} \tag{13}$$

For the non-logarithmic Gompertz model the form of the function is:

$$\frac{BVS_{rem}}{BVS_{\max}} = \exp\left\{-\exp\left[\frac{\mu_{\max}.e}{A}(\lambda - t)+1\right]\right\} \tag{14}$$

The term BVS is used for convenience in these comparisons and should be understood to represent data measured as either volatile solids (VS) or carbon dioxide (CO_2), noting that, in the latter case, data may sometimes be expressed as CO_2-C.

Comparison of the six unmodified constant-temperature modelling results rated as good clearly shows the effects of substrate type and composting conditions. As expected, the degradation of sewage sludge is rapid, which may be attributed to a high proportion of readily degradable substrate, a high initial micro-organism population, and a relatively high aeration rate (table 5.1). The breakdown of corn stalks, at a temperature 11 ^{o}C lower than that for the sewage sludge, and at a lower aeration rate, proceeds only slightly more slowly, once the clearly visible lag phase is over. In contrast, the degradation of yard waste, with a more complex substrate composition, and expected lower initial inoculum, proceeds at a considerably slower overall rate. Degradation under forced aeration conditions proceeds relatively rapidly however, in comparison to that relying on natural aeration alone. In the case of grass, degradation proceeded at a rate intermediate between that found for yard wastes with and without forced aeration. Apart from the sewage sludge plot, these curves cover time frames corresponding to typical "hot composting" periods, suggesting that they would be appropriate for use in composting process models.

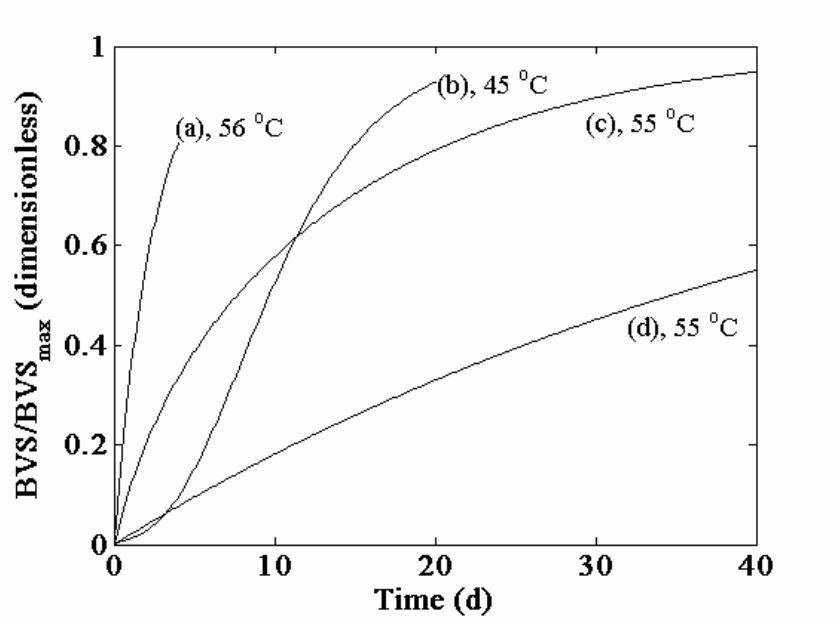

Figure 5.12: Normalised BVS removal models for which the fit to data obtained at constant temperature was rated as good: a) a single exponential model fitted to sewage sludge composting data (after Bach et al. (1984)); b) a non-logarithmic Gompertz model fitted to corn stalk composting data (after Bono et al. (1998)); c) a double exponential model fitted to yard trimmings composting data (after Michel and Reddy (1998); d) a single exponential model fitted to yard trimmings composting data (after Michel and Reddy (1998)).

5.7.3 Future work

The results of this study indicate that the evidence supporting the use of either single exponential, double exponential or Gompertz substrate degradation models to describe data generated at constant temperature is rather limited. Good fits were found for only 20% of the unmodified data sets examined, leaving the remaining 80% of profiles either moderately to poorly fitted, or not suitable at all for the models tested. Reasons for this might include a) that experimental factors resulted in a poor data set, and/or, b) that new mathematical models are required. From an experimental point of view, there is a case for a more rigorous examination of the progress of substrate degradation in the composting process at laboratory scale. In particular, the question of whether experimental factors are an issue, or whether the previously observed patterns properly reflect the nature of the process, is worthy of attention. A deliberate attempt to recreate those multi-phase profiles which were not modelled by any of the three functions utilised in the present work may assist in understanding

how these may be successfully modelled, or avoided, in the future. It may be of most immediate value to modellers if sound substrate degradation profile data sets were to be generated at constant temperature, using agreed experimental procedures and a standard substrate/amendment/bulking agent mixture. Experimental conditions should ensure that neither moisture nor oxygen are limiting, include mixing as appropriate, and control the heat fluxes to suitable levels. It would be particularly useful for modellers to have access to a greater number of data sets covering composting periods relevant to full-scale "hot composting" periods, i.e. 20-40 days. Details of a number of simulated composting mixtures have been published e.g. (Palmisano et al., 1993; Cook et al., 1994; VanderGheynst et al., 1997), and work presently in progress suggests that a convenient mixture, potentially suitable for international comparisons could be readily established (Mason, I.G.; unpublished data). Such information would enable the applicability of the single exponential, double exponential and Gompertz models to be either established or questioned with greater certainty, and for alternative models to be proposed as necessary. It would also help build a more comprehensive bank of kinetic parameters. The models described by Zavala et al. (2004a,b), Tremier et al. (2005), and Komilis (2006) have provided promising results and merit inclusion in future work.

5.8 Conclusions

1. When 31 constant-temperature substrate degradation profiles from the literature were assessed for profile shape, the majority (48%) were found to incorporate convex shapes, which formed either the entire profile, or the main part, after a concave lag phase, or prior to a subsequent period of divergence from the convex form at later time. Smaller numbers of sigmoidal (26%) and multi-phase (19%) patterns were found.

2. When the profiles were modelled, 3 fits rated as good were obtained when using a single exponential function, 2 fits rated as good were obtained when using a double exponential function and 1 fit rated as good was obtained when using a non-logarithmic Gompertz function. Remaining fits were either rated as moderate to poor, or the models were not applicable.

3. The lag phase observed in many data sets was successfully modelled using the non-logarithmic Gompertz function where a good fit was obtained, but not otherwise. The lag phase was, as expected, not modelled by either the single or double exponential functions.

4. Removal of the lag phase from 3 data sets resulted in improvements in fit to convex curve data when using the single exponential function on the post-lag phase data. Similar improvements were obtained following removal of post-convex curve data from an additional 4 data sets. A double exponential model provided a good fit to post-lag phase convex curve data in one case.

5 The results obtained indicate that rather limited evidence exists supporting the use of either the single exponential model, the double exponential model or the non-logarithmic Gompertz model, in describing substrate degradation profiles generated at constant temperature.

5.9 Afterword

Two additional papers relevant to the present work provide useful data in relation to constant-temperature profiles. Martinez-Inigo and Almendros (1994) reported CO_2 evolution data from 10 g samples of forestry waste, amended with NH_4NO_3 to adjust C:N ratio from 159 to 30, and incubated in Erlenmeyer flasks at 27 ^oC. There was no airflow, but the flask atmosphere was periodically replaced with CO_2-free air. A further set of CO_2 evolution data from the composting of a range of raw materials was reported by Komilis and Ham (2006).

Error bars on the graphs reported by Hamoda et al. (1998), showed an uncertainty of up to ± 1% TOC, or up to approximately ± 10% error. In this case the difference between the curve fitting error and the experimental error may not be statistically significant. Otherwise no error data were available, and the remaining fits reported in this chapter were consequently carried out in the absence of this information. Were such information available, a more accurate assessment of fit incorporating a statistical metric would be possible, and an improved number of fits in the excellent

and good categories might be obtained. For further discussion of error in this context, and for example rejected data sets, the reader is referred to Appendix 10.

Potential also exists to explore more mechanistic approaches to substrate degradation modelling and in particular to learn from the experience of biochemical engineering models of the fermentation of solid materials (see Chapter 4, section 4.8.1, p 126).

5.10 References

Bach, P.D., Shoda, M. and Kubota, H., 1984. Rate of composting of dewatered sewage sludge in continuously mixed isothermal reactor. Journal of Fermentation Technology 62 (3), 285-292.

Bono, J.J., Chalaux, N. and Chabbert, B., 1992. Bench-scale composting of two agricultural wastes. Bioresource Technology 40, 119-124.

Chang, J.I., Tsai, J.J. and Wu, K.H., 2005. Mathematical model for carbon dioxide evolution from the thermophilic composting of synthetic food wastes made of dog food. Waste Management 25 (10), 1037-1045.

Chang, J.I., Tsai, J.J. and Wu, K.H., 2006. Thermophilic composting of food waste. Bioresource Technology 96, 116-122.

Cook, B.D., Bloom, P.R. and Halbach, T.R., 1994. A method for determining the ultimate fate of synthetic chemicals during composting. Compost Science and Utilisation 2 (1), 42-50.

Das, K. and Keener, H.M., 1997. Numerical model for the dynamic simulation of a large-scale composting system. Trans. ASAE 40 (4), 1179-1189.

Gibson, A.M., Bratchell, N. and Roberts, T.A., 1987. The effect of sodium chloride and temperature on the rate and extent of growth of clostridium boulinum type A in pasteurised pork slurry. Journal of Applied Bacteriology 62, 479-490.

Gompertz, B., 1825. On the nature of the function expressive of the law of human mortality, and on a new mode of determining the value of life contingencies. Philos. Trans R. Soc. London 115, 513-585.

Hamoda, M.F., Abu Qdais, H.A. and Newham, J., 1998. Evaluation of municipal solid waste composting kinetics. Resources Conservation and Recycling 23 (4), 209-223.

Haug, R.T., 1993. The practical handbook of compost engineering. Lewis Publishers, Boca Raton, Florida, USA.

Higgins, C. and Walker, L., 2001. Validation of a new model for aerobic organic solids decomposition: simulations with substrate specific kinetics. Process Biochemistry 36 (8-9), 875-884.

Kaiser, J., 1996. Modelling composting as a microbial ecosystem: A simulation approach. Ecological Modelling 91 (1-3), 25-37.

Keener, H.M., Marugg, C., Hansen, R.C. and Hoitink, H.A.J., 1993 Optimising the efficiency of the composting process. Science & Engineering of Composting: Design, Environmental, Microbial and Utilisation Aspects, H. A. J. Hoitink and H. M. Keener, eds., Renaissance Publications, Worthington, USA., 59-94

Komilis, D. and Ham, R., 2000. A comparison of static pile & turned windrow methods for poultry litter compost production. Compost Science and Utilisation 8 (3), 254-265.

Komilis, D., 2006. A kinetic analysis of solid waste composting at optimal conditions. Waste Management 26 (1), 82-91.

Lay, J.J., Li, Y.Y. and Noike, T., 1998. A mathematical model for methane production from a landfill. Journal of Environmental Engineering ASCE 124 (8), 730-736.

Loser, C., Ulbrict, H. and Seidel, H., 2004. Degradation of polycyclic aromatic hydrocarbons in waste wood. Compost Science and Utilisation 12 (4), 335-341.

Mackey, B.M. and Kerridge, A.L., 1988. The Effect of Incubation-Temperature and Inoculum Size on Growth of Salmonellae in Minced Beef. International Journal of Food Microbiology 6 (1), 57-65.

Mason, I.G., 2006. Mathematical modelling of the composting process: a review. Waste Management 26 (1), 3-21.

Mason, I.G., McLachlan, R.I. and Gerard, D.T., 2006. A double exponential model for biochemical oxygen demand. Bioresource Technology 97 (2), 273-282.

Michel, F.C. and Reddy, C.A., 1998. Effect of oxygenation level on yard trimmings composting rate, odor production and compost quality in bench-scale reactors. Compost Science and Utilisation 6 (4), 6-14.

Mohee, R., White, R. and Das, K., 1998. Simulation model for composting cellulosic (bagasse) substrates. Compost Science and Utilisation 6 (2), 82-92.

Nakasaki, K., Akakura, N., Atsumi, K. and Takemoto, M., 1998. Degradation patterns of organic material in batch and fed-batch composting operations. Waste Management & Research 16 (5), 484-489.

Palmisano, A.C., Maruscik, D.A., Ritchie, C.J., Schwab, B.S., Harper, S.R. and Rapaport, S.A., 1993. A novel bioreactor simulating composting of municipal solid waste. J. Microbiol. Methods 18, 99-112.

Scholwin, F. and Bidlingmaier, W., 2003. Fuzzifying the composting process: a new model based control strategy as a device for achieving a high grade and consistent product quality. In: Proceedings of the Fourth International Conference of ORBIT Association on Biological Processing of Organics: Advances for a Sustainable Society, 30th April-2 May, 2003, Perth, Australia, 739-751.

Seki, H., 2000. Stochastic modeling of composting processes with batch operation by the Fokker-Planck equation. Trans. ASAE 43 (11), 169-179.

Smith, R. and Eilers, R.G., 1980. Numerical simulation of activated sludge composting. *EPA-600/2-8C-191*, USEPA, Cincinnati, Ohio, USA

Stombaugh, D.P. and Nokes, S.E., 1996. Development of a biologically based aerobic composting simulation model. Trans. ASAE 39 (1), 239-250.

Tseng, D.Y., Chalmers, J.J., Tuovinen, O.H. and Hoitink, H.A.J., 1995. Characterisation of a bench scale system for studying the biodegradation of organic solid wastes. Biotechnol. Progr 11, 443-451.

Tremier, A., de Guardia, A., Massiani, C., Paul, E. and Martel, J.L., 2005. A respirometric method for characterising the organic composition and biodegradation kinetics and the temperature influence on the biodegradation kinetics, for a mixture of sludge and bulking agent to be composted. Bioresource Technology 96 (2), 169-180.

VanderGheynst, J., Gossett, J. and Walker, L., 1997. High-solids aerobic decomposition: Pilot-scale reactor development and experimentation. Process Biochemistry 32 (5), 361-375.

Whiting, R.C., 1995. Microbial Modeling in Foods. Critical Reviews in Food Science and Nutrition 35 (6), 467-494.

Zavala, M.A.L., Funamizu, N. and Takakuwa, T., 2004a. Modeling of aerobic biodegradation of feces using sawdust as a matrix. Water Research 38 (5), 1327-1339.

Zavala, M.A.L., Funamizu, N. and Takakuwa, T., 2004b. Temperature effect on aerobic biodegradation of feces using sawdust as a matrix. Water Research 38 (9), 2406-2416.

Zwietering, M.H., Jongenburger, I., Rombouts, F.M. and Vantriet, K., 1990. Modeling of the Bacterial-Growth Curve. Applied and Environmental Microbiology 56 (6), 1875-1881.

CHAPTER 6
AN EVALUATION OF SUBSTRATE DEGRADATION PATTERNS IN THE COMPOSTING PROCESS.
Part 2: Temperature-corrected Profiles

6.1 Foreword

In the language of our journey, we remain in Kineticsville for the second part of this work in which existing substrate degradation profiles are evaluated. Here, a temperature correction procedure is implemented on profiles generated under dynamic temperature conditions, so as to see what they might look like if generated at a constant temperature of 40 ^{o}C. The idea behind this is to attempt to reveal the fundamental shape of the relationship at a single temperature, and ideally, non-limiting moisture and oxygen conditions. However, since dynamic moisture and oxygen data are rarely reported in the literature, corrections for these variables are not attempted on these particular data sets.

This chapter consists of the following journal paper**:**

Mason, I.G., in press. An evaluation of substrate degradation patterns in the composting process. Part 2: Corrected-temperature profiles. Waste Management. (Published on-line 12 September, 2007).

Readers are asked to note that the text may differ from that in the published paper in places and that corrections may have been incorporated.

6.2 Summary

In this paper, the patterns of 44 substrate degradation profiles obtained from the composting literature are examined following their correction to a constant temperature of 40 ^{o}C, using a new procedure presented in this work. The applicability of a single exponential model, a double exponential model and a non-logarithmic Gompertz model in describing their behaviour is then evaluated. Multi-phase profiles were most commonly seen, with convex shapes observed in only a relatively small proportion of the profiles. Convex shapes were embedded within other profiles however, either preceeded by a lag phase, or followed by non-convex behaviour. Sigmoidal patterns were relatively rare. Of the temperature-corrected data sets examined, 33 were found to be either not well modelled by, or inappropriate for, any of the above models. Two fits rated as good were obtained when using the single exponential model, and 1 fit rated as excellent, plus 1 fit rated as good, were obtained when using the double exponential model. A single fit rated as excellent was found when using the non-logarithmic Gompertz model. The lag phase, which was observed in many data sets, was successfully modelled using the non-logarithmic Gompertz function where excellent and good fits were obtained, but as expected this phase of the profile could not be modelled by either the single or double exponential functions. When the lag phase or post-convex curve data was removed from 20 data sets, use of the single exponential function resulted in 3 fits rated as excellent and 2 rated as good. When a double exponential model was applied to these data sets, 3 fits rated as good were obtained, whilst application of the modified Gompertz model gave one fit rated as good. The remainder of the fits were rated as moderate to fair. It is concluded that the evidence supporting the use of the single exponential model, the double exponential model or the non-logarithmic Gompertz model to describe full substrate degradation profiles in composting following their adjustment for temperature effects, is limited. Further work is suggested in order to investigate the nature of those profiles which were not well modelled, to more precisely ascertain the cardinal temperatures for composting used in the function of Rosso et al. (1993), which was employed in the present temperature correction procedure, and to incorporate correction for varying moisture and oxygen concentrations.

6.3 Nomenclature

β	microbial maintenance coefficient (kg-BVS/kg-X.h)
β_{max}	maximum microbial maintenance coefficient (kg-BVS/kg-X.h)
BVS	biodegradable volatile solids present (kg or g/m^3)
BVS_{rem}	biodegradable volatile solids removed (kg or g/m^3)
e	2.178282
ε_s	volumetric solids content (m^3/m^3)
k	first-order rate coefficient (d^{-1})
k_d	microbial decay coefficient
k_s	substrate half-velocity constant (kg or g/m^3)
k_{O_2}	half-velocity constant (Eq.
λ	lag time (d)
NRMSE	normalised root mean square error
μ	specific bacterial growth rate (d^{-1})
μ_{max}	maximum bacterial specific growth rate (d^{-1})
OM	organic matter
t	time
T	temperature (^{o}C)
Θ_w	volumetric water content (m^3/m^3)
VS	volatile solids present (kg or g/m^3)
VS_{rem}	volatile solids removed (kg or g/m^3)
X	biomass (kg or g/m^3)
ξ	value of the function as O_2 tends to infinity (Eq. 10)
$Y_{X/BVS}$	maximum cell yield per unit substrate consumed
m, n	exponents related to moisture effects and pore dimensions
max	maximum value of the parameter

6.4 Introduction

A limited number of composting substrate degradation profiles generated at constant temperature have been reported in the literature, and analysis of these provides only a small body of evidence to support the use of either exponential or non-logarithmic Gompertz

models in describing their behaviour (Mason, in press). One path forward is to build a more extensive body of substrate degradation profiles at constant temperature, under non-limiting moisture and oxygen conditions. However, substrate degradation profiles are frequently generated under varying environmental conditions, e.g. in self-heating, or constant temperature difference (CTD), reactors, and this is likely to continue to be the case in the future, given the range of objectives pursued by researchers in composting experimentation (Mason and Milke, 2005). This body of information is potentially of value to modellers if it could be "deconstructed" to represent behaviour under constant environmental conditions. In this paper, the potential for substrate degradation profiles generated at varying temperature to yield useful kinetic information for incorporation into subsequent composting process models is explored.

The first-order rate co-efficient (k), the maximum specific growth rate (μ_{max}) and the maximum microbial maintenance coefficient (β_{max}) in the rate expressions introduced in part 1 of this paper (Mason, in press) are known to be variables and may, in principle, be influenced by a large number of environmental factors (Hamelers, 2004). Most frequently, however, rate coefficients in the composting context are adjusted for changes in temperature, moisture level and oxygen concentration only, using correction functions (Mason, 2006). It has generally been assumed that correction function effects are multiplicative, and operate independently of each other, although the independence of correction functions has been questioned (Hamelers, 2004). The following general expression summarises the conventional approach for substrate-based, first-order models:

$$\frac{dBVS}{dt} = -k(T, H_2O, O_2)BVS \tag{1}$$

where: $k(T,H_2O,O_2)$ is the value of the first-order rate coefficient under actual temperature, moisture and oxygen conditions.

The assumption of independent multiplicative adjustment for the three state variables leads to:

$$k(T, H_2O, O_2) = f_{c1}(T)\, f_{c2}(H_2O)\, f_{c3}(O_2)k \tag{2}$$

where: $f_{c,\,c2,c3}(\,)$ are various correction functions the nature of which will be discussed later in this paper and k is the value of the first-order rate coefficient at a chosen reference temperature, and at non-limiting values of moisture level, and oxygen concentration.

For models derived from cell growth expressions, and incorporating Monod kinetics to describe substrate limitation, the corresponding expressions to Eqs. 1 and 2 are:

$$\frac{dBVS}{dt} = -\left[\left(\frac{BVS}{k_s + BVS}\right)\frac{\mu(T,H_2O,O_2)}{Y_{X/BVS}}X + \left(\frac{BVS}{k_s + BVS}\right)\beta(T,H_2O,O_2)X\right] \tag{3}$$

where:

$$\mu(T,H_2O,O_2) = f_{c1}(T)\,f_{c2}(H_2O)\,f_{c3}(O_2)\,\mu_{\max} \tag{4}$$

and:

$$\beta(T,H_2O,O_2) = f_{c1}(T)\,f_{c2}(H_2O)\,f_{c3}(O_2)\,\beta_{\max} \tag{5}$$

The half velocity function in Eq. 3 is dimensionless, with a value of 0.5 when BVS = k_s, and tending to a value of 1, when BVS >> k_s. Where growth is not substrate limited, the expression reverts to a first-order model in X.

Functions for the correction of first-order substrate degradation rates for the effects of temperature, moisture and oxygen in the composting context have been investigated by Richard and Walker (1998), Richard et al. (1999) and Richard et al. (2002). Temperature correction factors were examined by Richard and Walker (1998) who concluded that the Cardinal Temperature Model with Inflexion (CTMI) model of Rosso et al. (1993) not only provided a good fit, but contained easily measurable parameters with biological meaning. The model is:

$$f_{c1}(T) = \frac{(T - T_{\max})(T - T_{\min})^2}{(T_{opt} - T_{\min})\{(T_{opt} - T_{\min})(T - T_{opt}) - (T_{opt} - T_{\max})(T_{opt} + T_{\min} - 2T)\}} \tag{6}$$

where T_{min}, T_{opt} and T_{max} are the cardinal temperatures, representing the temperature at which growth is optimal, plus the lower and upper temperature bounds of microbial activity.

This function produces a dimensionless ratio which has a value of one when $T = T_{opt}$. Alternative functions e.g. Haug (1993), Richard and Walker (1998), Cronje et al. (2004), will not be considered here.

A mechanistic model relating oxygen uptake rate to moisture content and porosity was developed by Richard et al. (2002). The function is:

$$f_{c4}(\Theta_w, \varepsilon_s) = \left\{ \frac{1 - \varepsilon_s.(1 + \Theta_w)}{\Theta_w.(1 - \varepsilon_s)} \right\}^n . \left\{ \frac{\Theta_w}{1 + \Theta_w} \right\}^m \tag{7}$$

where: Θ_w is the volumetric water content (m^3/m^3)

ε_s is the volumetric solids content (m^3/m^3)

m, n are exponents related to moisture effects and pore dimensions

It modifies the normalised oxygen uptake rate (*OUR*) as follows:

$$\frac{OUR_m(\Theta_w, \varepsilon_s)}{OUR_{\max}} = \frac{f_{c4}(\Theta_w, \varepsilon_s)}{f_{c4}(\Theta_{w,\max}, \varepsilon_{s,\max})} \tag{8}$$

where: *max* is the maximum value of the parameter

This dimensionless expression also has a value of one when conditions are optimal.

Richard et al. (1999) investigated a number of models relating the effects of oxygen concentration to reaction rate. They concluded that for windrows a simple half-velocity expression was most suitable, whilst a slightly modified version would better model the effects for forced aeration systems. The models are:

$$f_c(O_2) = \frac{O_2}{k_{O_2} + O_2} \tag{9}$$

$$f_c(O_2) = \frac{\xi O_2}{k_{O_2} + O_2} \tag{10}$$

where: k_{O_2} is the half-velocity constant

ξ is the value of the function as O_2 tends to infinity

Both expressions are dimensionless and Eq. 9 tends to a value of one when oxygen is non-limiting.

Evidence from temperature-adjusted profiles in the peer-reviewed literature in support of those expressions proposed to describe substrate degradation rates in the composting process is limited. A first-order model, empirically corrected for temperature effects, was applied to the modelling of solids degradation in yard waste composting by Marugg et al. (1993). Rate constants of 0.165-0.190 d^{-1} (sd 0.005-0.007) at 60 ^oC, were reported. The goodness of fit for the model was not indicated, but considerable deviation is evident within the data plots presented. The same first-order model, when empirically corrected for both temperature and moisture effects, showed relatively close agreement with experimental bagasse composting data over the first 8 days of a run, but gave a visibly poorer fit over the subsequent 7 days (Mohee et al., 1998). Stronger support for a first-order approach was provided by Bari et al. (2000) who showed that a first-order model gave a relatively good fit (reported $R^2 = 0.844$) to volatile solids versus time data from the composting of food waste, paper and sawdust, when corrected for temperature using an Arrhenius-type expression. Visually the fit appears very good. However, it should be noted that these authors also presented data sets with poorer correlations. Other authors who have used first-order models to describe substrate degradation e.g. Bernal et al. (1993), Keener et al. (1993), Keener et al. (1997), Namkoong and Hwang (1997), Paredes et al. (2001), Paredes et al. (2002), Keener et al. (2005), have not de-coupled them from temperature, moisture or oxygen effects. Keener et al. (1997) reported a data set of first-order model parameters derived from pilot-scale studies on poultry manure, separated dairy solids, biosolids, MSW, food waste and yard waste mixes, using a self-heating reactor with upper temperature set points ranging from 57-72 ^oC. The goodness of fit was not reported numerically, but the four graphs presented by these authors showed a generally poor visual fit of the model over periods ranging from 22-54 days. A close fit with experimental solids degradation data by a cell growth derived Monod-type model was shown by Seki (2000), but again, this was not de-coupled from changes in the state variables. Chang

et al. (2005) demonstrated a good visual fit to experimental results at varying temperature by applying a modified Gompertz function separately to each of two stages observed in the cumulative generation of CO_2. Co-efficients of determination (r^2) for the fitted parameters were reported as "generally above 0.950." Effects of changes in the state variables previously listed were not explicitly accounted for in the model.

In this paper, a new approach is proposed, which seeks to extract useful kinetic information from such data sets. The proposition is that the underlying nature of *dBVS/dt* can be revealed by removing one or more of the temperature, moisture and oxygen effects from substrate vs time profiles generated under varying environmental conditions. The assumptions inherent in this proposal are that the effects of temperature, moisture and oxygen act on the derivative and that these effects are independent and multiplicative. That is:

$$\frac{dBVS}{dt} = -f_{c(1)}(T)\, f_{c(2)}(H_2O)\, f_{c(3)}(O_2)\, f(BVS) \tag{11}$$

so that:

$$f(BVS) = \frac{\dfrac{dBVS}{dt}}{-f_{c(1)}(T)\, f_{c(2)}(H_2O)\, f_{c(3)}(O_2)} \tag{12}$$

In this case, an uncorrected substrate vs time profile may be modelled using any mathematical function which fits the data to an acceptable level. So given that:

$$f(t) = \int_0^t f_c(T)\, f_c(H_2O)\, f_c(O_2)\, f(BVS).dt \tag{13}$$

where: *f(t)* is a function relating BVS and time,

then:

$$\frac{df(t)}{dt} = f(BVS)\, f_{c(1)}(T)\, f_{c(2)}(H_2O)\, f_{c(3)}(O_2) \tag{14}$$

and:

$$\frac{\frac{df(t)}{dt}}{f_{c(1)}(T)\,f_{c(2)}(H_2O)\,f_{c(3)}(O_2)} = \frac{df(t)}{dt}(corrected) = f(BVS) \tag{15}$$

Integrating the new function:

$$f(t)corrected = \int_0^t \frac{df(t)}{dt}(corrected).dt = \int_0^t f(BVS) \tag{16}$$

Given that polynomial functions are able to fit a wide variety of data sets and are readily implemented, they are specified here. As their purpose is to model the given temperature-time profile accurately, a visual inspection of the fit is required in order to detect any inappropriate polynomial behaviour, and enable corrective action to be taken. The new profile may then be modelled by any appropriate mathematical expression having a biological basis (e.g. first-order, cell growth based with Monod kinetics, Gompertz). The temperature-correction procedure may be summarised as follows:

1. A polynomial function is fitted to the original substrate vs time data.
2. The first derivative of the function is obtained.
3. The first derivative is adjusted to 40 ^{o}C, using the Rosso function.
4. The adjusted derivative is integrated to give a new polynomial function which describes substrate degradation vs time at 40 ^{o}C.
5. Substrate vs time data points are derived from the new polynomial function.
6. The new substrate vs time data is modelled using the single exponential, double exponential and/or Gompertz functions.

The objectives of this paper are to a) decouple "raw" substrate vs time patterns from temperature effects and b) to model the revealed profiles using existing functions. Decoupling from moisture and oxygen effects is not considered due to inadequate data.

6.5 Methods

Published graphs of substrate degradation vs time were scanned and digitised, corrected profiles categorised, and corrected profiles modelled, as described in part 1 of this paper (Chapter 5; Mason; in press).

The CTMI model of Rosso et al. (1993) (Eq. 6) was used for temperature correction, using values of 5, 59 and 71 ^{o}C for T_{min}, T_{opt}, T_{max} respectively, chosen on the basis of work by Richard and Walker (1998). Profiles were corrected to a constant temperature of 40 ^{o}C. This temperature was selected since it is relevant to composting process design, being located on the cusp of the mesophilic and thermophilic regions, and is also convenient for practical laboratory purposes. Since moisture data were sporadically reported, and porosity and oxygen concentration data were not reported, for the data sets analysed, the profiles have not been corrected for the effects of these variables. The temperature correction procedure was implemented using "Matlab" (The Mathworks Inc, Natick, Mass., USA).

The sensitivity of temperature-corrected profiles to the order of the polynomial used to fit the original substrate degradation data was examined for two data sets, one from Bach et al. (1985) and one from Michel et al. (1993). The fits obtained with polynomials from 4th to 10th order were assessed visually and by noting the normalised error (Mason; in press). The sensitivity of the temperature correction methodology to changes in cardinal temperatures was examined for the same data sets, after using a 6th order polynomial used to fit the original data. Minimum, optimum and maximum temperatures were increased by 5 ^{o}C, to 10, 64 and 76 ^{o}C respectively, and then decreased by 5 ^{o}C, giving 0, 54 and 66 ^{o}C, respectively.

Temperature-corrected profiles were generated and assessed for a total of 44 data sets. Details of the experimental conditions under which the original data sets were generated are given in table 6.1. Errors in these data sets were not reported, and as for chapter 5, the results in this chapter should be interpreted accordingly. Further discussion on this matter in given in the afterword to this chapter (Section 6.9). As in chapter 5, curves were selected for fitting by each model by visual observation, and included rather than excluded if there was any doubt. Where the visual assessment indicated a post-lag phase profile of exponential shape, the lag phase was removed and the remaining data modelled. Similarly, where post-exponential phase data appeared to deviate markedly from prior patterns, these were removed. Where data were removed, the profiles were referred to as modified.

Table 6.1: Details of varying temperature substrate degradation profile sources from the literature

Mixture	Scale	Type	Temperature range	Measured parameter (par)		Airflow	Time	Comments	Reference
			°C	Par	Units	l/min.kg	(d)		
Dairy manure/rice hulls	Lab	CTD	25-60	O_2	g	ns	6	Run 112; graphed data starts at day 1	Mote and Griffis (1979)
Dairy manure/rice hulls/corn starch			22-58	O_2	g	ns	17	Run 114; graphed data starts at day 1	
Cabbage/dairy manure/rice hulls	Lab	CTD	22-62	CO_2	g	ns	10	Supplemented with NH_4NO_3	Mote and Griffis (1980)
Dairy manure/rice hulls			26-65	CO_2	g	ns	5	-	
Cotton/dairy manure/rice hulls			22-50	CO_2	g	ns	11.7	Supplemented with NH_4NO_3	
Sewage sludge/ wood chips	Lab	SH	20-60	VS	% of total VS	0.17[a] 1.00[b]	5-10	Dewatered lime or polymer conditioned sewage sludges	Bach et al. (1985)
Sewage sludge (no bulking agent)	Lab	SH	20-60	VS	% of total VS	0.3[c] 3.0[c, d]	5-5.8	Dewatered limed and $FeCl_3$ conditioned sewage sludges	Nakasaki et al. (1985)
Sewage sludge/wood chips	Lab	CTD	22-65	CO_2	mg-C	15, 30	10-13	Dewatered limed raw sewage sludge; airflows 900 and 1800 l/kg-TS.h	Sikora and Sowers (1985)
Sewage sludge/rice hulls	Lab	SH	25-75	VS	% of total VS	0.08	4.2-6.2	Dewatered limed and $FeCl_3$ conditioned sewage sludges.	Nakasaki et al. (1987)
Sitka spruce	Lab	SH	16-40 16-50	CO_2 CO_2	g-C/kg g-C/kg	0.05-0.06	10 10	Temperature held at 40 or 50 °C after 5 days.	Campbell et al. (1990)
Yard waste	Lab	FT	22-60	CO_2	% (C of initial C)	0.08[f] 0.04[f]	40	Temperature increased stepwise over 0-7 days; then held at 60 °C until day 40	Michel et al. (1993)
Poultry manure/straw/gypsum	Pilot	SH	25-55	DM	% DM	3.3[g]	7	Straw compost	van Lier et al. (1994)
Poultry litter /sawdust	Lab	CHF	20-57	CO_2	g	ns	29	-	Atkinson et al. (1996c)
Municipal solid waste	Lab	CHF	20-60	CO_2	g	ns	43	-	Atkinson et al. (1996a)

Oxidation ditch sludge	Lab	CHF	24-55	CO_2	g	ns	28	-	Atkinson et al. (1996b)
Bagasse	Lab	SH	19-52	DM	g	ns	15	-	Mohee et al. (1998)
Pine chips with various N sources	Lab	SH	22-41	CO_2	g	0.67	21.7	-	Loser et al. (1999)
Food residuals/ paper/sawdust	Pilot	SH	24-60	BVS [h]	% degraded	0.67[i] 0.33[j]	27.5	-	Bari et al. (2000)
Broiler litter /paper mill sludge	Lab	FT	approx. 55[k] approx. 60[k]	CO_2	g/g-DM	ns	14 7	-	Ekinci et al. (2004)
Kitchen waste/dog food/rice husks	Lab	SH	30-62	CO_2	g	0.8 1.2 1.6 2.0	3.7	-	Chang et al. (2005) Chang et al. (2006)

[a] air converted from 10 and 60 Nl/hr.kg-TS
[b] "boost" airflow
[c] estimated
[d] temperature control airflow
[f] aeration at 0.08 for first 15 days, then 0.04
[g] maximum
[h] calculated from CO_2 data; i: for first 2 days;
[j] 5 min on with either 5 min off or 10 min off
[k] nominal set points; temperatures varied around these values
ns: not stated

Table 6.2: Profile shape summary: temperature-corrected BVS/CO_2 profiles

Profile shape characteristic	Number	Comments
Convex curve	8	-
Lag + convex curve	10	Includes 6 profiles with a post-convex curve phase
Convex curve + second phase	6	-
Sigmoidal curve	2	-
Multi-phase	14	-
Other	4	
TOTAL	44	

Table 6.3: Modelling summary: unmodified temperature-corrected BVS/CO_2 profiles

Model	Excellent	Good	Moderate	Fair	Poor	Model not applicable
	no.	no.	no.	no.	no.	no.
Single exponential	0	2	5	1	0	36
Double exponential	0	1	0	0	0	43
Modified Gompertz	1	1	1	0	0	41

6.6 Results

6.6.1 Shape profiles

The most commonly observed pattern was multi-phase, which occurred in 32% of cases (table 6.2). Convex shapes appeared throughout the entire time periods of experiments in 18% of the profiles, but were also present in a further 37%, either preceeded by a lag phase, or followed by non-convex behaviour. Sigmoidal patterns were relatively rare, appearing in only 2 cases (5%). These observations suggested that single exponential, double exponential and modified Gompertz models would be suitable on unmodified curves in a minority of cases only, but that selected sections of other profiles might be satisfactorily modelled using one of the exponential functions.

6.6.2 Modelled profiles corrected for varying temperature

Results reported in this section were obtained using a 6^{th} order polynomial to fit the original substrate-time data, and cardinal temperatures of 5, 59 and 71 ^{o}C in the Rosso temperature correction function. The sensitivity of the methodology to changes in polynomial order and in cardinal temperatures is reported in the next section.

The effect of the temperature correction procedure on a "raw" substrate profile is illustrated in figure 6.1, which shows an increase in CO_2-C values at early time, and a reduction at later time, in accordance with changes in the temperature profile. In this example, temperatures increased stepwise from 30, to 50, to 60 ^{o}C. Occasionally, incorrect polynomial fitting to original data profiles was observed, and the impacts of this phenomenon are demonstrated in figures 6.2 and 6.3. In figure 6.2, the corrected profile is seen to rise above the original data as expected, since temperatures remained above t_{opt} (59 ^{o}C), for the majority of the time, but shows an unexpected increase from day 6 onwards. This increase is directly attributable to a small section of incorrect polynomial fitting of the original data set at later time (figure 6.3), and required elimination of the equivalent temperature corrected data from subsequent analysis.

Of the varying temperature data sets corrected to 40 ^{o}C, no fits rated as excellent were observed when using a single exponential function on unmodified data sets, and only 2 analyses gave fits rated as good (table 6.4). The good fits were obtained on profiles derived from the composting of a cotton/dairy manure/rice hulls mixture over a period of 11.7 days (Mote and Griffis, 1980), and from yard waste composting data (mix 3) of Michel et al.

(1993), which was generally well modelled over a period of 40 days, although less so at later time (figure 6.4). Moderate fits were observed in a further 5 cases (tables 6.3, 6.4). Discrepancies observed in this group included poor fits at early time and under- or over-projection beyond the modelled time period. One fit, on data derived from the composting of a dairy manure/rice hulls mixture, was rated as fair (tables, 6.3, 6.4). Remaining profiles (36) were considered unsuitable for modelling using a single exponential expression. However, one fit rated as good was obtained for the temperature-corrected dairy manure/rice hulls profile, when the double exponential model was applied to this data set (table 6.5).

When lag phase and/or post-convex curve data were omitted from a further 20 data sets, 3 fits rated as excellent, and 2 rated as good, were observed when using the single exponential function (table 6.4). One of the excellent fits was obtained for a dairy manure substrate (figure 6.5) (Mote and Griffis, 1980) and the remaining excellent and good fits were for sewage sludge (Bach et al., 1985; Nakasaki et al., 1987). An example good fit is presented in figure 6.1.

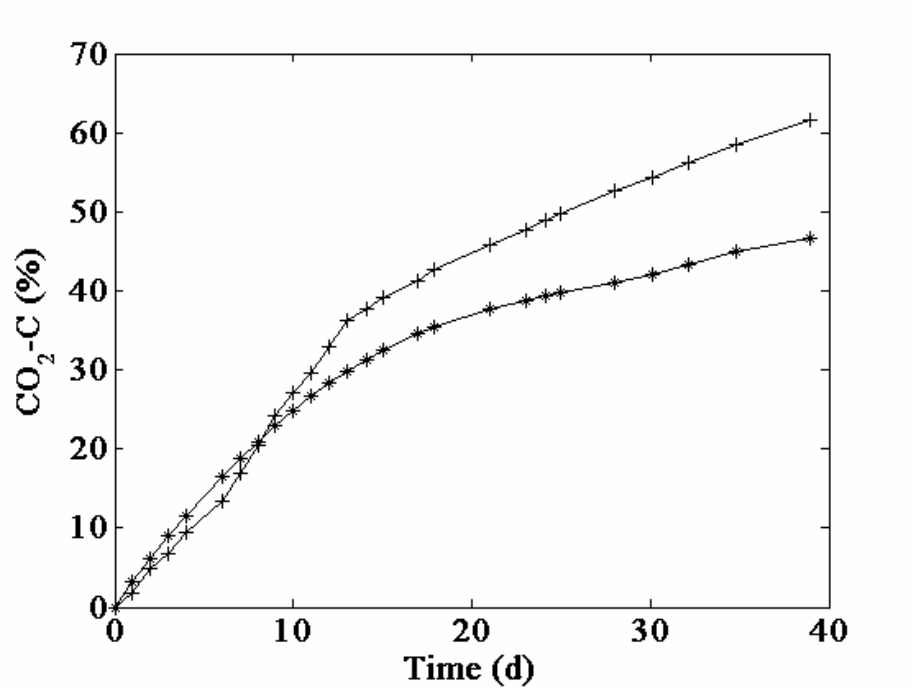

Figure 6.1: CO_2 evolution data for yard waste composting at varying temperature (+) and following correction to 40 ^oC (*). After Michel et al. (1993).

Rate coefficients ranged from 0.40-0.44 d^{-1} in 4 cases, comparing closely with a constant temperature value of 0.41 d^{-1} previously reported (Mason; in press), with 0.19 d^{-1} in 1 case (table 6.4). Corresponding predicted t(95%) values ranged from 7.0-7.5 days in the first group and 15.7 days for the second case, confirming the rapid degradation rates which would be expected. A further 11 fits were classified as moderate and 4 as fair (table 6.4). These were generally characterised by under-prediction or over-prediction by the model, either at early or at later time. A double exponential function provided substantial improvements in 3 cases, resulting in one excellent and two good fits, plus one moderate fit (table 6.5). An example good fit is shown in figure 6.7. In this case, over-projection of the model beyond the experimental time period can be observed, otherwise the fit is excellent.

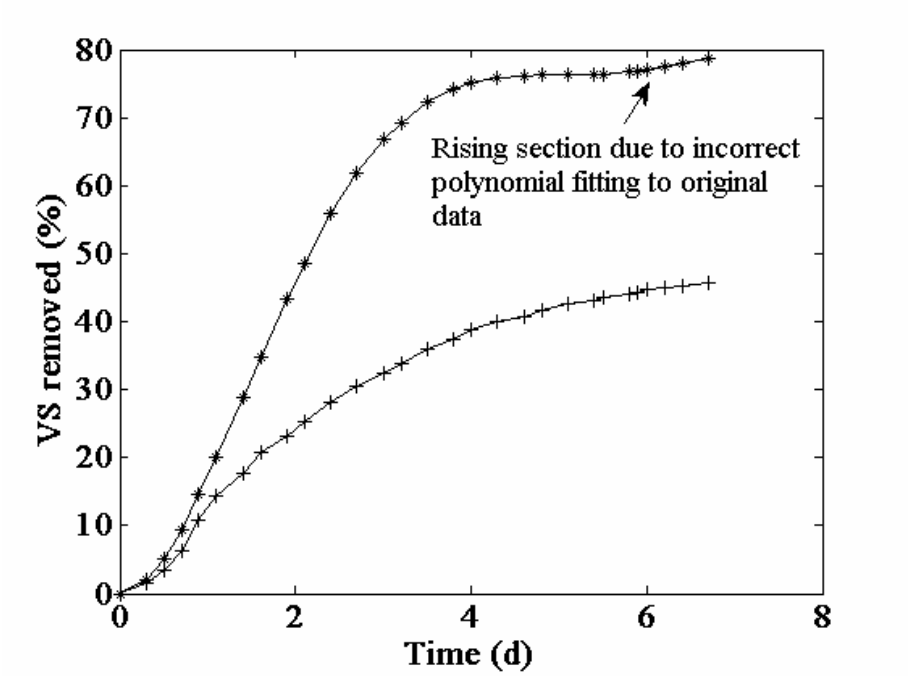

Figure 6.2: VS removal data for sewage sludge composting at varying temperature, with a set point of 70 ^{o}C, (+) and following correction to 40 ^{o}C (*). After Bach et al. (1985).

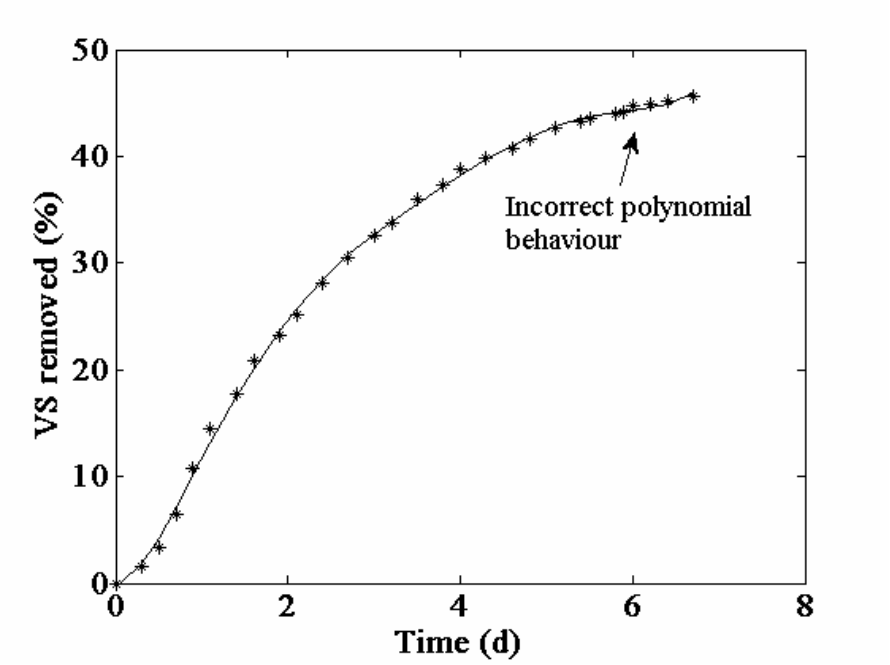

Figure 6.3: Fitted polynomial to VS removal data for sewage sludge composting at varying temperature, with a set point of 70 °C, showing incorrect polynomial behaviour at later time (approximately 6 d onwards). After Bach et al. (1985).

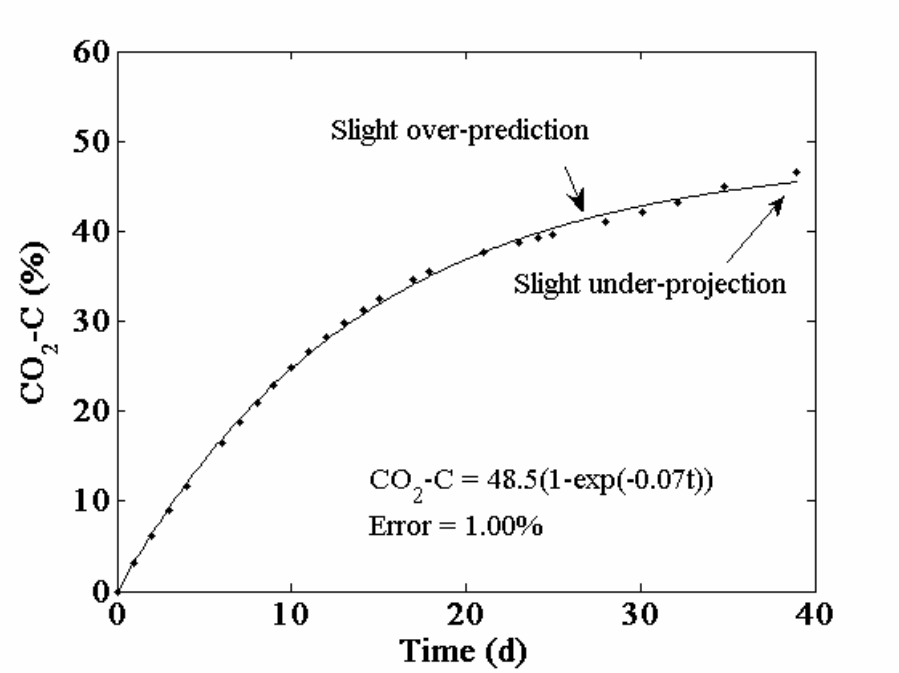

Figure 6.4: CO_2 evolution data for yard waste composting corrected to 40 °C, fitted with a single exponential model. Fit rated as good. After Michel et al. (1993).

Table 6.4: Single exponential model parameters for temperature-corrected BVS/CO_2 profiles (including modified profiles)

Mixture	BVS_{max}		k	Error	Visual fit*	t(95%)	Comments	Data source
	Value	Units	d^{-1}	%		d		
Dairy manure/rice hulls	56.1	g	0.44	4.43	fair	6.7	Run 112	Mote and Griffis (1979)
Cabbage/dairy manure/rice hulls	86.9	g	0.07	1.20	moderate	45.5	-	Mote and Griffis (1980)
Dairy manure/rice hulls	19.1	g	0.40	0.53	excellent**	7.4	Lag phase (0.83 d) eliminated; NB: 6 data points over 4 days	Mote and Griffis (1980)
Cotton/dairy manure/rice hulls	42.8	g	0.08	0.98	good	37.1	-	Mote and Griffis (1980)
Sewage sludge/ wood chips	31.4	%	0.43	0.54	excellent[a] **	7.0	Lime sludge; [a] lag phase (0.57 d) and last 4 data points eliminated	Bach et al. (1985) (figure 2a)
	53.1	%	0.20	1.36	moderate[b] **	15.3	Polymer sludge; [b] lag phase (0.55 d) and last 8 data points eliminated	Bach et al. (1985) (figure 2b)
	27.6	%	0.44	0.54	excellent[c] **	6.9	Lime sludge, 60 ^{o}C set point; [c] lag phase (0.7 d) eliminated	Bach et al. (1985) (figure 5a)
	74.5	%	0.63	2.24	fair[d] **	4.8	Lime sludge, 70 ^{o}C set point; [d] lag phase (0.7 d) eliminated	Bach et al. (1985) (figure 5a)
	45.6	%	0.19	1.16	moderate[e] **	16.1	Polymer sludge, 60 ^{o}C set point; [e] lag phase (1.3 d) eliminated	Bach et al. (1985) (figure 5b)
	56.6	%	0.25	1.50	moderate[f] **	11.9	Polymer sludge, 60 ^{o}C set point; [f] lag phase (1.3 d) and last 4 data points eliminated	Bach et al. (1985) (figure 5b)
	19.9	%	0.43	0.80	good[g] **	7.0	Airflow 60 Nl/kg.hr; [g] lag phase (0.8 d) eliminated	Bach et al. (1985) (figure 6)
	43.9	%	0.19	1.14	good[h] **	15.7	Airflow variable; [h] lag phase (1.3 d) eliminated	Bach et al. (1985) (figure 6)

Sewage sludge	19.5	%	0.59	0.96	moderate[i] **	5.1	[i] lag phase (0.8 d) and last 4 data points eliminated	Nakasaki et al. (1985)
	36.4	%	0.47	2.57	fair[j] **	6.4	[j] lag phase (0.7 d) and last 2 data points eliminated	Nakasaki et al. (1985)
Sewage sludge/wood chips	10.1	g	0.31	2.08	moderate[k] **	9.6	Airflow 15 l/kg-TS.min; [k] lag phase (2 d) and last data point eliminated	Sikora & Sowers (1985)
	8.1	g	0.27	2.85	fair[l] **	11.0	Airflow 30 l/kg-TS.min; [l] lag phase (2 d) and last 3 data points eliminated	Sikora & Sowers (1985)
Sewage sludge	31.6	%	0.33	1.38	moderate[m] **	8.6	[m] lag phase (0.2 d) and last 4 data points eliminated	Nakasaki et al. (1987)
	34.6	%	0.07	1.44	moderate[n] **	40.6	[n] lag phase (1.0 d) eliminated; 5 data points; full scale	Nakasaki et al. (1987)
Sitka spruce	41.6	g/kg	0.19	2.48	moderate**	15.4	40 ^{o}C set point; lag phase (2.0 d) eliminated	Campbell et al. (1990)
	26.7	g/kg	0.24	3.87	fair**	12.7	50 ^{o}C set point; lag phase (2.0 d) eliminated	
Yard waste	32.7	%	0.03	1.48	moderate	90.3	mix 1	Michel et al. (1993)
	31.6	%	0.06	1.92	moderate**	48.9	mix 2; last data point eliminated	Michel et al. (1993)
	48.5	%	0.07	1.00	good	41.9	mix 3	Michel et al. (1993)
Pine chips with various N sources	153	g	0.05	1.49	moderate**	55.0	Mineral medium 1; eliminated last 2 data points	Loser et al. (1999)
Food residuals/ paper/sawdust	72.9	%	0.05	0.86	moderate**	61.0	Test 3; last 3 data points eliminated	Bari and Koenig (2000)
	55.6	%	0.09	0.98	moderate	33.8	Test 4	Bari and Koenig (2000)
	64.1	%	0.11	1.97	moderate	27.0	Test 5	Bari and Koenig (2000)
Broiler litter /paper mill sludge	146	g/g	0.14	1.91	moderate	21.5	Temperature set point 55 ^{o}C	Ekinci et al. (2004)

Abbreviations: BVS: biodegradable volatile solids; MSW: municipal solid waste; nsd: no seed; RMSE: root mean square error

* Scale based on discrepancies between data and fitted curve: Excellent = close fit; Good = occasional discrepancies, good shape relationship; ; Moderate = some discrepancies, recognisable shape relationship;. Fair = many discrepancies, recognisable shape relationship; Poor = major discrepancies, less recognisable shape relationship;

** modified data sets (not included in Tab. 6.3)

Table 6.5: Double exponential model parameters for temperature-corrected BVS/CO_2 profiles (including modified profiles)

Mixture	BVS_{max} [a]	k_1	k_2	Error	Visual fit*	t(95%)	Comments	Data source
		d^{-1}	d^{-1}	%		d		
Dairy manure/rice hulls	73.6	3.40	0.20	1.35	good	15.5	Run 112	Mote and Griffis (1979)
Sewage sludge/ wood chips	55.3	0.59	0.09	0.57	excellent[b] **	37.8	Polymer sludge; temperature set point 60 °C; [b] lag phase (1.3 d) eliminated	Bach et al. (1985)
	73.6	0.57	0.10	0.56	good[c] **	35.7	Polymer sludge; temperature set point 60 °C; [c] lag phase (1.3 d) and last 4 data points eliminated	Bach et al. (1985)
Sewage sludge/ wood chips	66.6	0.32	0.05	0.74	moderate[d] **	68.0	Airflow variable; [d] lag phase (1.3 d) eliminated	Bach et al. (1985)
Sewage sludge/ wood chips	55.3	4.53	0.24	0.38	good[e] **	13.0	[e] lag phase (0.7 d) and last 2 data points eliminated	Nakasaki et al. (1985)

[a] units as table 5

Abbreviations: BVS: biodegradable volatile solids; MSW: municipal solid waste; nsd: no seed; RMSE: root mean square error

* Scale based on discrepancies between data and fitted curve: Excellent = close fit; Good = occasional discrepancies, good shape relationship; ; Moderate = some discrepancies, recognisable shape relationship;. Fair = many discrepancies, recognisable shape relationship; Poor = major discrepancies, less recognisable shape relationship; ** modified data sets (not included in Tab. 6.3)

Table 6.6: Gompertz model parameters for temperature-corrected BVS/CO_2 profiles (including modified profiles)

Mixture	BVS_{max} [a]	μ	λ	Error	f(0)	Visual fit*	Comments	Data source
		BVS/d	d	%	BVS			
Sewage sludge/ wood chips	78.1	32.24	0.50	0.92	0.65	good	Lime sludge; temperature set point 70 °C;	Bach et al. (1985)
	19.4	7.49	0.27	1.75	0.52	moderate	Airflow 60 Nl/kg.hr;	Bach et al. (1985)
Sewage sludge/ wood chips	9.3	2.21	1.85	0.86	.001	excellent	Airflow 15 l/kg-TS.min	Sikora & Sowers (1985)
Sitka spruce	34.2	6.66	0.9	0.66	0.40	good**	Temperature set point 40 °C; last 3 data points eliminated	Campbell et al. (1990)

[a] units as table 5

Abbreviations: BVS: biodegradable volatile solids; MSW: municipal solid waste; nsd: no seed; RMSE: root mean square error

* Scale based on discrepancies between data and fitted curve: Excellent = close fit; Good = occasional discrepancies, good shape relationship; ; Moderate = some discrepancies, recognisable shape relationship;. Fair = many discrepancies, recognisable shape relationship; Poor = major discrepancies, less recognisable shape relationship; ** modified data sets (not included in Tab. 6.3)

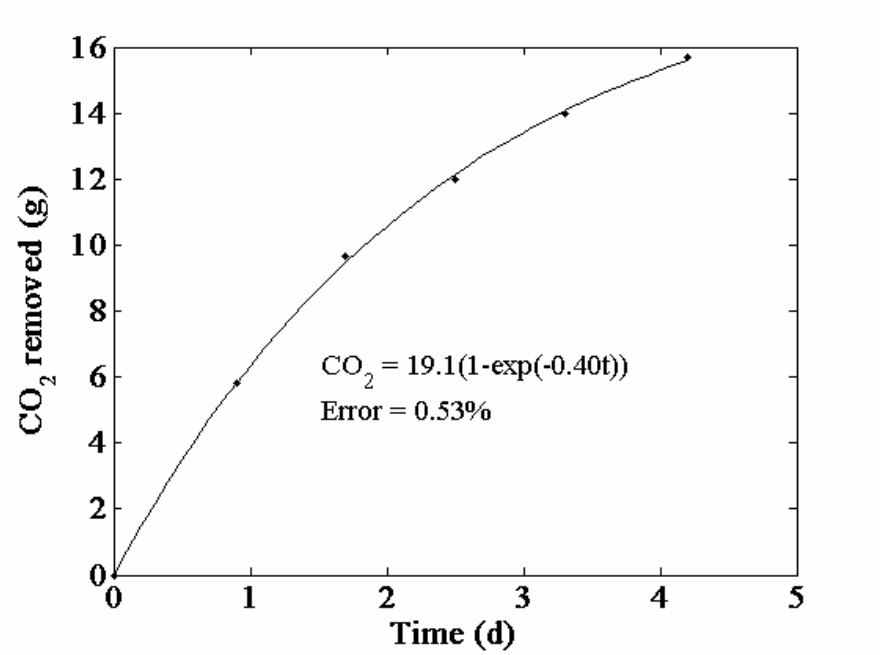

Figure 6.5: CO_2 evolution data for dairy manure composting, corrected to 40 ^oC, with the lag phase removed, and fitted with a single exponential model. Fit rated as excellent. After Mote and Griffis (1980).

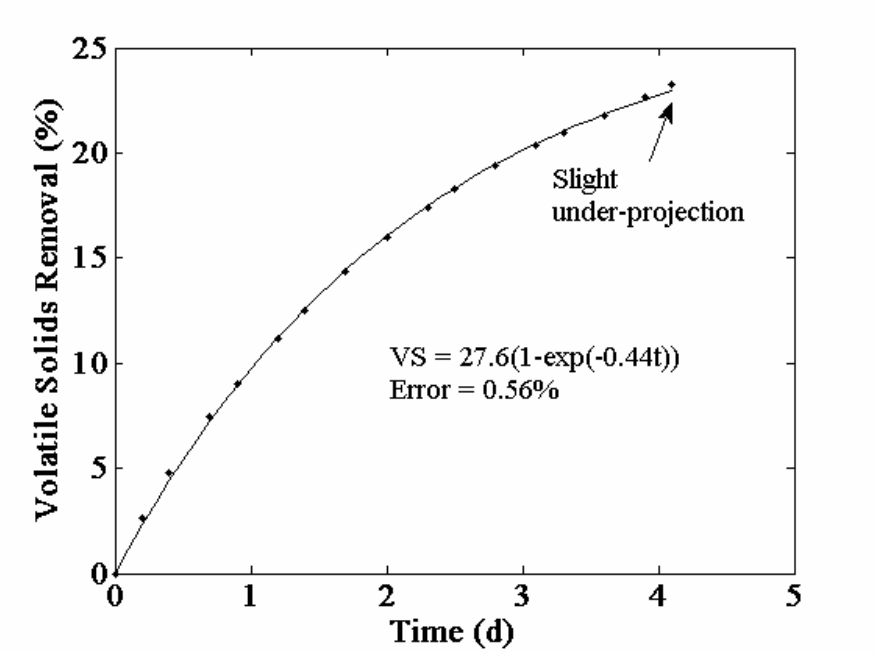

Figure 6.6: Volatile solids removal data for lime conditioned sewage sludge composting, with a temperature set point of 60 ^oC, corrected to 40 ^oC, with the lag phase (0.7 d) removed and fitted with a single exponential model. Fit rated as good. After Bach et al. (1985).

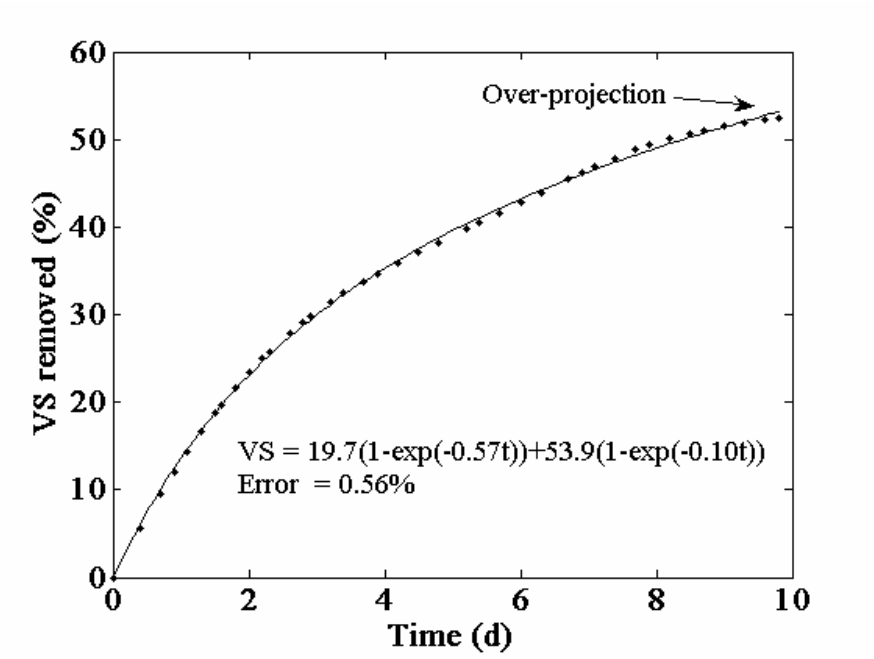

Figure 6.7: Volatile solids removal data for polymer conditioned sewage sludge composting, with a temperature set point of 60 ^{o}C, corrected to 40 ^{o}C, with the lag phase (1.3 d) removed and fitted with a double exponential model. Fit rated as good. After Bach et al. (1985).

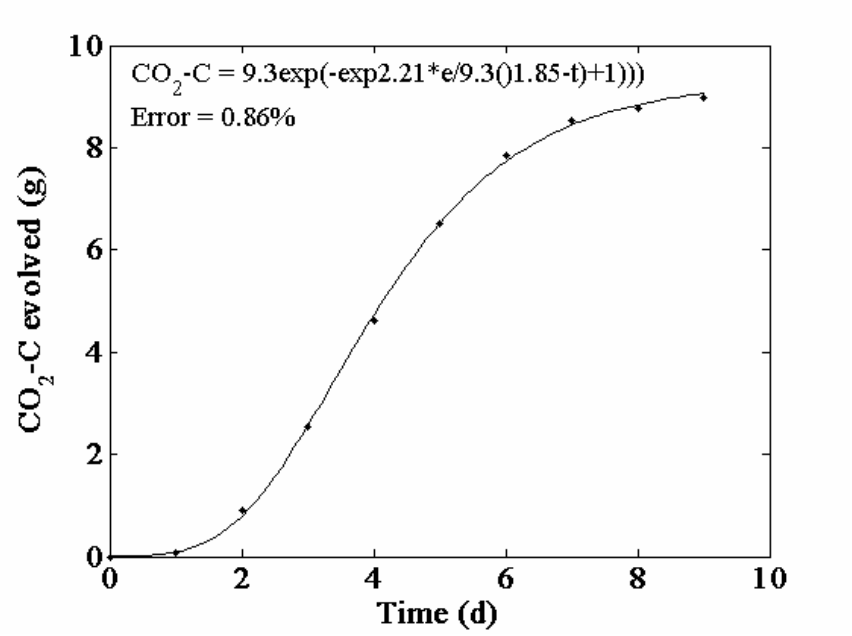

Figure 6.8: CO_2 evolution data for limed sewage sludge composting, with forced aeration at 15 l/kg-TS.min, corrected to 40 ^{o}C, fitted with the non-logarithmic Gompertz model. Fit rated as excellent. After Sikora and Sowers (1985).

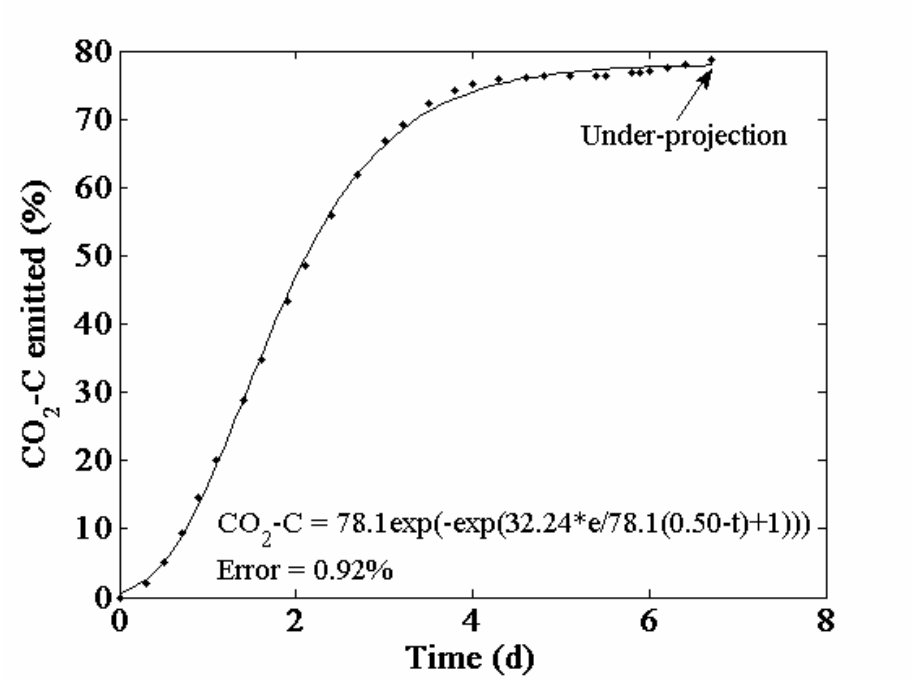

Figure 6.9: Volatile solids removal data for lime conditioned sewage sludge composting (with a temperature set point of 70 ^{o}C), corrected to 40 ^{o}C, fitted with the non-logarithmic Gompertz model. Fit rated as good. After Bach et al. (1985).

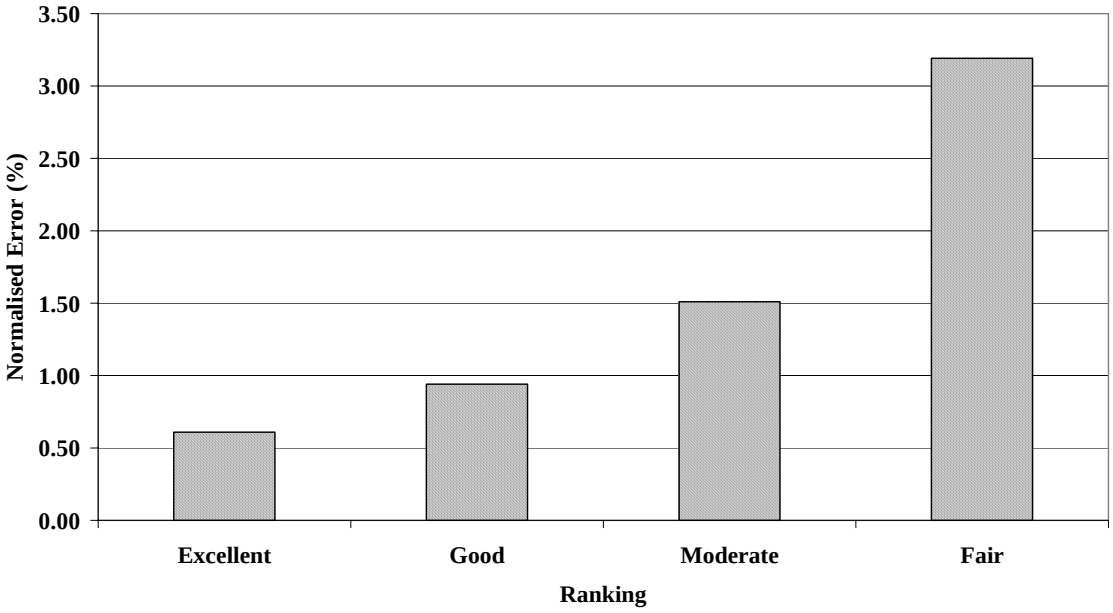

Figure 6.10: The relationship between descriptive classifications and average values of normalised error for temperature-corrected substrate degradation profiles.

When the non-logarithmic Gompertz function was used to model temperature-corrected profiles, 1 fit rated as excellent, two fits rated as good, and 1 fit rated as moderate were obtained on full data sets (table 6.3). All these were for sewage sludge/woodchips composting using forced aeration, over periods of approximately 4-9 days. The fits rated as excellent and good are shown in (figures 6.8-6.9). The Gompertz function was not applicable to the remaining 41 data sets. However, following removal of a small amount of multi-phase data at later time, a further good fit was obtained for a profile derived from the composting of Sitka spruce (table 6.6).

As in part 1, descriptive classifications and normalised error were reasonably well correlated, as shown in figure 6.10. Variations within a descriptive category occurred due to non-numerical assessments of fit, such as the degree to which the lag phase was modelled, and the projection of the curve beyond the modelled time period.

6.6.3 Temperature correction procedure sensitivity to polynomial order and cardinal temperatures

The first step in the temperature correction methodology involves fitting a suitably ordered polynomial function to the original substrate-time data. As the order of the polynomial used to fit the original substrate data of Bach et al. (1985) and Michel et al. (1993) was increased from 4 to 10, the visual fit generally improved and normalised error values decreased, as expected (table 6.7). For both data sets, a 4^{th} order polynomial gave a visually poor fit with a relatively high error. In comparing 5^{th} and 6^{th} order polynomials, a 6^{th} order polynomial gave an improved fit at early time, but deviated noticeably from the data at later time, for the Bach et al. (1985) data. Identical fits were obtained for both 5^{th} and 6^{th} order polynomials in the case of the Michel et al. (1993) data set. Improvements beyond 7^{th} order were slight for the data set of Bach et al. (1985), whilst minimal improvement occurred when using 8^{th} and higher order polynomials for the data set of Michel et al. (1993). In the latter case, polynomials of 7^{th} order and higher were badly conditioned and thus error prone. Thus either a 5^{th} or 6^{th} order polynomial was indicated, with the lower order, and consequent fewer parameters, preferred. However, given the importance of good agreement between the polynomial and the original data at early time, a 6^{th} order polynomial seemed more appropriate for the temperature correction analyses reported below. It was noted however that when the resultant temperature corrected data were fitted using a single exponential

Table 6.7: Effect of polynomial order on the temperature correction procedure: Corrected data modelled using a single exponential function

Polynomial				Single exponential					Data source
Order	RMSE[a]	Visual fit*	BVS_{max}[a]	k	Error	Visual fit*	t(95%)	Profile shape	
n				d^{-1}	%		d		
4	0.51	moderate	31.3	0.48	0.99	good	6.2	Convex except later time	Bach et al. (1985)
5	0.49	moderate	31.4	0.46	0.41	excellent	6.5	Convex	
6	0.38	moderate	31.7	0.42	0.63	excellent	7.1	Convex	
7	0.25	good	32.1	0.39	1.18	moderate	7.7	Convex except early time	
8	0.23	excellent	32.0	0.39	1.19	moderate	7.7	Convex except early time	
9	0.22	excellent	32.1	0.39	1.25	moderate	7.8	Convex except early time	
10	0.19	excellent	32.0	0.39	1.16	moderate	7.6	Convex except early time	
4	1.17	fair	52.1	0.12	4.03	fair	25.6	Convex.early time only	Michel et al.
5	0.69	moderate	48.5	0.07	0.76	good	41.4	Convex	(1993)
6	0.69	moderate	48.5	0.07	1.01	good	41.9	Convex	
7**	0.51	moderate	-	-	-	poor	-	Model not applicable	
8**	0.38	moderate	-	-	-	poor	-	Model not applicable	
9**	0.36	good	-	-	-	poor	-	Model not applicable	
10**	0.30	excellent	49.2	0.09	2.22	moderate	34.9	Model not applicable	

a units as table 5

Abbreviations: BVS: biodegradable volatile solids; RMSE: root mean square error

* Scale based on discrepancies between data and fitted curve: Excellent = close fit; Good = occasional discrepancies, good shape relationship; ; Moderate = some discrepancies, recognisable shape relationship;. Fair = many discrepancies, recognisable shape relationship; Poor = major discrepancies, less recognisable shape relationship

** polynomial badly conditioned

Table 6.8: Effect of cardinal temperatures on the temperature correction procedure. Data modelled using a single exponential function

Cardinal temperatures (T_{min}, T_{opt}, T_{max})	BVS_{max} [a]	k	Error	Visual fit*	t(95%)	Profile shape	Data source
		d^{-1}	%		d		
0, 54, 66	44.8	0.41	1.16	fair	7.3	Lag phase at early time; then convex	Bach et al. (1985)
5, 59, 71	31.7	0.42	0.63	excellent	7.1	Convex	
10, 64, 76	25.3	0.44	0.71	excellent	6.9	Convex (except later time)	
0, 54, 66	57.5	0.06	1.30	moderate	53.3	Convex	Michel et al.
5, 59, 71	48.5	0.07	1.01	good	41.9	Convex	(1993)
10, 64, 76	44.5	0.09	1.15	good	34.6	Convex (except later time)	

a units as table 5

Abbreviations: BVS: biodegradable volatile solids; RMSE: root mean square error

* Scale based on discrepancies between data and fitted curve: Excellent = close fit; Good = occasional discrepancies, good shape relationship; ; Moderate = some discrepancies, recognisable shape relationship;. Fair = many discrepancies, recognisable shape relationship; Poor = major discrepancies, less recognisable shape relationship

model, those data arising from the prior use of a 5th order polynomial gave the best fits in both cases (table 6.7).

The third step in the temperature correction methodology involves adjusting the first derivative of the polynomial used to model the original substrate-time data, using the temperature correction function of Rosso et al. (1993). Varying the cardinal temperatures used in the Rosso function by ±5 ^{o}C was found to result in some minor alterations to the corrected profile, at either early or later time, but not to alter the essential form (table 6.8). The single exponential function parameter values were also affected. In the case of the Bach et al. (1985) data, the rate coefficient and t(95%) values changed only slightly, but the saturation constant (BVS_{max}) increased or decreased markedly (table 6.8). For the Michel et al. (1993) data, substantial changes in all 3 parameters were seen (table 6.8). These results emphasise the need for accurate estimates of the cardinal temperatures, if accurate fitted parameter values are required.

6.7 Discussion

6.7.1 Normalised substrate degradation models

Single exponential, double exponential and Gompertz models with fits rated as either excellent or good are presented in dimensionless form in figures 6.11 and 6.12. The dimensionless functions used are given in part 1 of this paper (Mason; in press).

The relatively rapid degradation of sewage sludge is illustrated in figure 6.11, with double exponential and non-logarithmic Gompertz models shown to be applicable in four cases. All data sets covered less than 10 days, although near attainment of saturation was indicated, within that time frame, for the two non-logarithmic Gompertz models. The cotton/dairy manure mixture and a yard waste mixture were both well modelled by the single exponential function, showing slower degradation rates, over a 40 day data period in the latter case. The success in modelling post-lag-phase, and pre-multi-phase, temperature corrected data is clearly illustrated in figure 6.12, with the single exponential model shown to be applicable in the modelling of both sewage sludge in 3 cases, and dairy manure in 1 case. The double exponential model was applicable in the modelling of sewage sludge in 4 cases and the non-logarithmic Gompertz model in one case. As previously, the relatively rapid degradation of these substrates under a variety of composting conditions is evident.

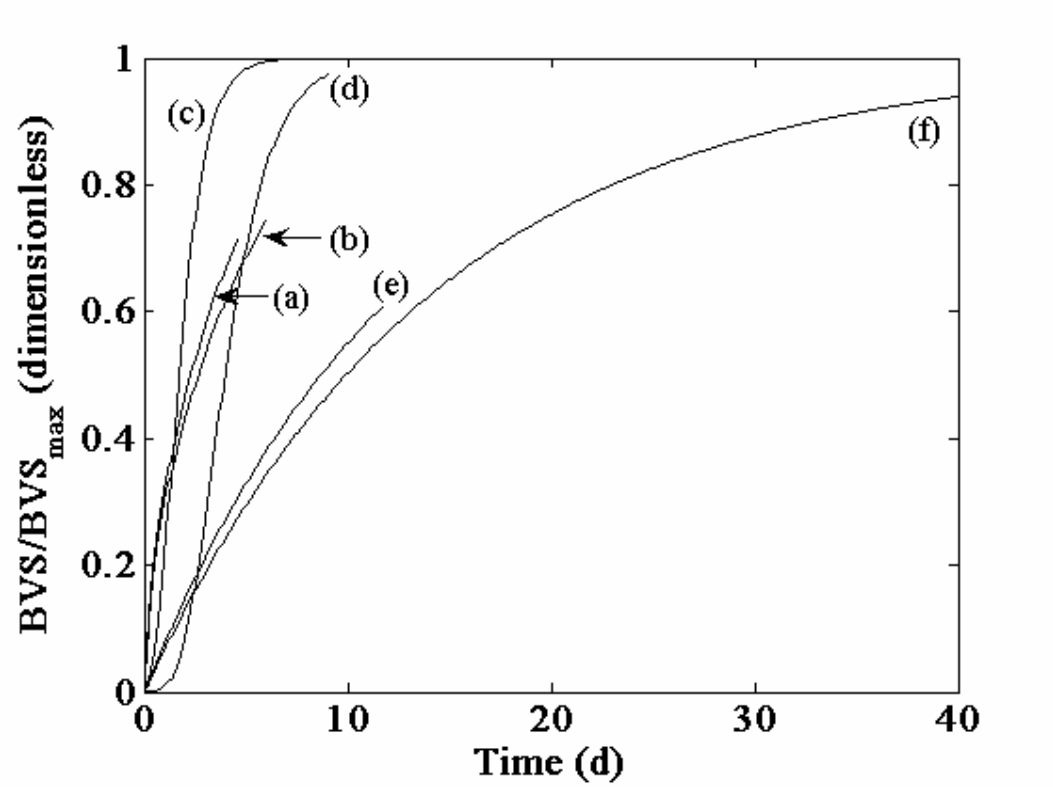

Figure 6.11: Normalised BVS removal models rated as excellent and good in the analysis of data sets corrected to 40 ^{o}C. a) a double exponential model fitted to sewage sludge composting data (after Nakasaki et al., 1985); b) a double exponential model fitted to dairy manure composting data (after Mote and Griffis, 1979); c) a non-logarithmic Gompertz model fitted to limed sewage sludge composting data obtained with a temperature set point of 70 ^{o}C (after Bach et al., 1985); d) a non-logarithmic Gompertz model fitted to limed sewage sludge composting data obtained with forced aeration at 15 l/kg-TS.h (after Sikora and Sowers, 1985); e) a single exponential model fitted to cotton/dairy manure composting data (after Mote and Griffis, 1980); f) a single exponential model fitted to yard trimmings composting data (after Michel et al., 1993).

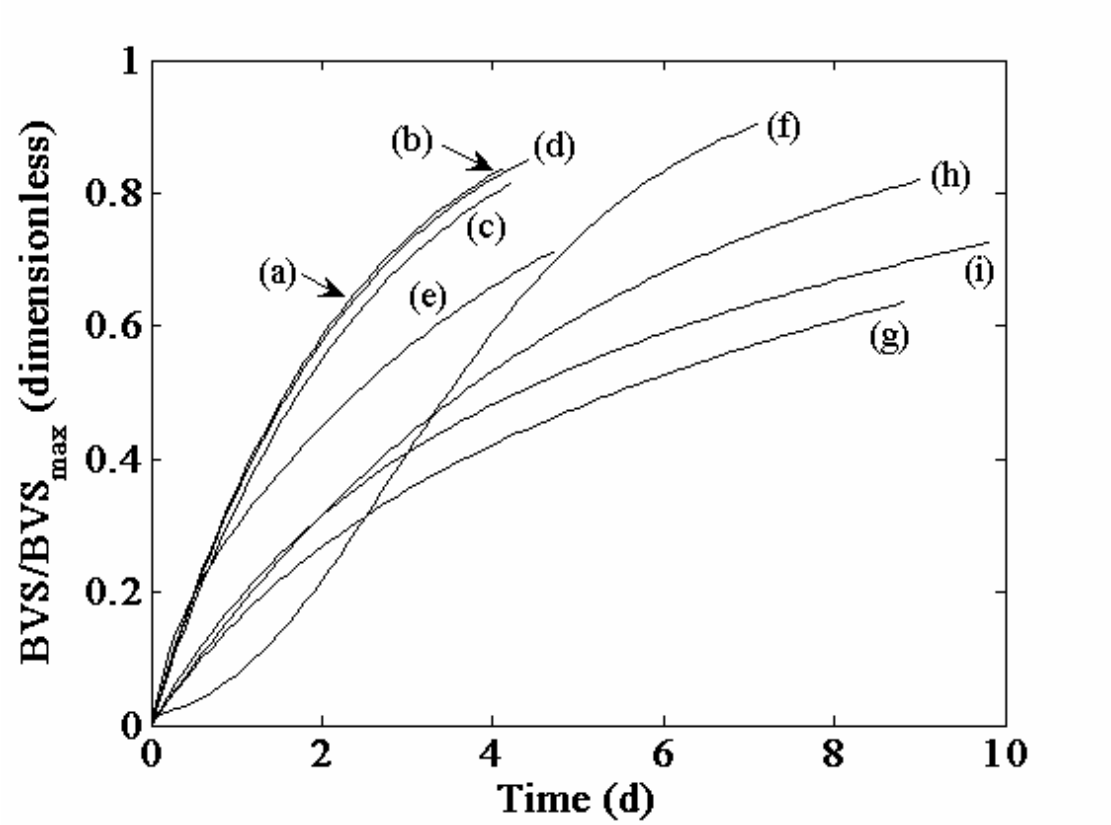

Figure 6.12: Normalised single exponential BVS removal models rated as excellent and good following the removal of lag periods and multi-phase data in the analysis of data sets corrected to 40 ^{o}C. a) a single exponential model fitted to data from lime conditioned sewage sludge composting with forced aeration at 60 Nl/ hr. kg-TS (after Bach et al., 1985); b) a single exponential model fitted to data from lime conditioned sewage sludge composting with a temperature set point of 60 ^{o}C (after Bach et al., 1985); c) a single exponential model fitted to data from dairy manure composting (after Mote and Griffis 1985); d) a single exponential model fitted to data from lime conditioned sewage sludge composting (after Bach et al., 1985); e) a double exponential model fitted to data from sewage sludge composting (after Nakasaki et al., 1985); f) a non-logarithmic Gompertz model fitted to Sitka spruce composting data (after Campbell et al., 1990); g) a double exponential model fitted to data from polymer conditioned sewage sludge composting with a temperature set point of 60 ^{o}C (after Bach et al., 1985); h) a double exponential model fitted to data from lime conditioned sewage sludge composting with variable forced aeration (after Bach et al., 1985); i) a double exponential model fitted to data from lime conditioned sewage sludge composting with a temperature set point of 60 ^{o}C (after Bach et al., 1985).

6.7.2 Temperature correction procedure

In certain situations, the best fit of the polynomial function to original substrate degradation data may generate negative function values, and/or slopes, which do not correctly model the data during this period. This phenomenon was observed in a small number of cases, at early time, where the lag phase was relatively flat. In order to prevent unrealistic values of the derivative propagating through the temperature correction procedure, negative values arising in the fitted polynomial were set to zero. In a limited number of cases where the polynomial fit was poor at later time, the corresponding data were removed prior to final curve fitting. The occurrence of poorly conditioned higher order polynomials illustrates the need to ensure that the lowest order function consistent with a reasonable fit to the data is used in the temperature correction procedure. On three occasions, temperatures exceeded the chosen value for T_{max} of 71 ^{o}C, with consequent failure of the temperature correction procedure. In the present work these data sets were not re-analysed, due to the absence of reliable alternative values for T_{max}, and their details are not included here.

Moisture profiles reported by Bach et al. (1985) showed a decrease from 58 to 50% over 5 days for lime conditioned sewage sludge composting, and from 60 to 40% over 10.1 days for polymer sewage sludge composting. There was no visually discernable effect on the VS profiles at later time in either case, suggesting that the absence of correction for moisture may not have been important in these examples. In both experiments moisture contents remained within the reasonable range suggested by Rynk (1993).

6.7.3 Future work

The results of this study indicate that the evidence supporting the use of either single exponential or Gompertz substrate degradation models on temperature-corrected substrate degradation data remains relatively limited. Excellent and good fits were found for only 14% of the data sets examined, leaving the remaining 86% of profiles either moderately to poorly fitted, or not suitable at all for the models tested. Reasons for this might include a) the need for profile correction for variations in moisture and/or oxygen levels, b) that experimental factors resulted in a poor data set, and/or, c) that new mathematical models are required. As discussed in part 1 of this paper, there is a case for more a rigorous examination of the progress of substrate degradation in the composting process at laboratory scale, and in particular the question of whether experimental factors are an issue, or whether the previously observed patterns which could not be modelled using existing functions, properly reflect the

nature of the process. If sound substrate degradation profile data sets were to be generated under varying-temperature conditions, using agreed experimental procedures and a standard substrate/amendment/bulking agent mixture, then this would be of considerable value.

As with the constant temperature profiles shown in part 1 of this paper, elimination of lag phase and multi-phase sections of temperature-corrected substrate degradation profiles for sewage sludge composting, allowed application of a single exponential function to model to convex portions of these profiles, with relative success. This provides further evidence of the scope for modellers to consider modelling substrate degradation over selected time periods when using this function.

A more substantial set of cardinal temperatures for composting is needed to support the Rosso correction function. If the temperature correction procedure is to be extended to correct for moisture and oxygen variations, then values for the appropriate parameters in the correction functions of Richard et al. (1999) and Richard et al. (2002) also need to be established and appropriate experimental data collected.

As proposed by Hamelers (2004), a deductive approach to future modelling, tempered with limited and readily identifiable parameters, seems most appropriate in order to provide relevant, but practical, models. It is clear however that a more reliable body of data and improved model validation are required before modellers can confidently use substrate degradation models in the prediction of state variables in the composting process.

6.8 Conclusions

1. A new procedure for correcting substrate degradation profiles generated at varying temperature to 40 ^{o}C was developed, and applied to 44 varying-temperature data sets.

2. Multi-phase patterns were most commonly observed for the temperature-corrected profiles, with convex shapes appearing relatively infrequently. Convex shapes were found to be embedded within other profiles, either preceeded by a lag phase, or followed by non-convex behaviour. Sigmoidal patterns were relatively rare.

3. In modelling the temperature-corrected profiles, 2 fits rated as good were obtained when using the single exponential model, 1 fit rated as excellent and 1 fit rated as good were obtained when using a double exponential model and 1 fit rated as excellent, plus 1 fit rated as good, were obtained when using the non-logarithmic Gompertz model. Use of the double exponential model resulted in minor improvements over the single exponential model in 2 cases. Remaining fits were either rated as moderate to poor, or the models were not applicable.

4. The lag phase observed in many data sets was successfully modelled using the non-logarithmic Gompertz function in cases where excellent and good fits were obtained, but not otherwise. The lag phase was not modelled by either the single or double exponential functions.

5. Removal of the lag phase or multi-phase data from 20 data sets, resulted in 3 fits rated as excellent and 2 rated as good, when using the single exponential function. Use of a double exponential model gave 3 fits rated as good, and the modified Gompertz model gave one fit rated as good.

6. Strong evidence supporting the use of a single exponential function, a double exponential function or a non-logarithmic Gompertz for substrate degradation modelling was limited to approximately 16% of the data sets examined. For the remaining 84% of data sets these models gave either moderate to poor fits, or were not applicable.

7. Further work is suggested in order to investigate the nature of those profiles which were not well modelled, to more precisely ascertain cardinal temperatures for composting for use in the Rosso et al (1993) temperature correction function, and to incorporate correction for varying moisture and oxygen concentration conditions into the present temperature correction procedure.

6.9 Afterword

Temperature profiles have continued to appear in the literature since this paper was completed. Correction of these profiles for temperature, and if possible moisture, variations would be a worthwhile exercise in order to add to the database reported here. In relation to moisture data, it is worth noting the temperature and moisture profiles reported for a pilot-scale in-vessel reactor by Bertoldi et al. (1988). Meanwhile "deconstruction" of experimental data generated in the present work will be reported in chapter 8.

The absence of error estimates for CO_2 measurements reported in the composting literature is noteworthy. The analysis of goodness fit in this chapter was carried out in the absence of information on the degree of error present in the original data. Were such information available, a more accurate assessment of fit incorporating a statistical metric would be possible, and an increased number fits in the excellent and good categories might reasonably be expected. For further discussion of error in this context, and for example rejected data sets, the reader is referred to Appendix 10.

6.10 References

Atkinson, C.F., Jones, D.D. and Gauthier, J.J., 1996a. Biodegradabilities and microbial activities during composting of municipal solid waste in bench scale reactors. Compost Science and Utilisation 4 (4), 14-23.

Atkinson, C.F., Jones, D.D. and Gauthier, J.J., 1996b. Biodegradabilities and microbial activities during composting of oxidation ditch sludge. Compost Science and Utilisation 4 (1), 84-96.

Atkinson, C.F., Jones, D.D. and Gauthier, J.J., 1996c. Biodegradabilities and microbial activities during composting of poultry litter. Poultry Science 75 (5), 608-617.

Bach, P.D., Shoda, M. and Kubota, H., 1985. Composting reaction rate of sewage sludge in an autothermal packed bed reactor. Journal of Fermentation Technology 63 (3), 271-278.

Bari, Q.H., Koenig, A. and Guihe, T., 2000. Kinetic analysis of forced aeration composting - I. Reaction rates and temperature. Waste Management & Research 18 (4), 303-312.

Bernal, M.P., Lopez-Real, J.M. and Scott, K.M., 1993. Application of natural zeolites for reduction of ammonia emissions during the composting of organic wastes in a laboratory composting simulator. Bioresource Technology 43, 35-39.

de Bertoldi, M., Rutili, A., Citterio, B. and M, C., 1988. Composting management: a new process control through O2 feedback. Waste Management & Research 6 (3), 239-259.

Campbell, C.D., Darbyshire, J.F. and Anderson, J.G., 1990. The composting of tree bark in small reactors: self-heating experiments. Biological Wastes 31, 145-161.

Chang, J.I., Tsai, J.J. and Wu, K.H., 2005. Mathematical model for carbon dioxide evolution from the thermophilic composting of synthetic food wastes made of dog food. Waste Management 25 (10), 1037-1045.

Chang, J.I., Tsai, J.J. and Wu, K.H., 2006. Thermophilic composting of food waste. Bioresource Technology 96, 116-122.

Cronje, A.L., Turner, C., Williams, A.G., Barker, A.J. and Guy, S., 2004. The respiration rate of composting pig manure. Compost Science & Utilization 12 (2), 119-129.

Ekinci, K., Keener, H.M., Michel, F.C. and Elwell, D.L., 2004. Modeling composting rate as a function of temperature and initial moisture content. Compost Science & Utilization 12 (4), 356-364.

Hamelers, H.V.M., 2004. Modeling composting kinetics: A review of approaches. Reviews in Environmental Science and Biotechnology 3, 331-342.

Haug, R.T., 1993. The practical handbook of compost engineering. Lewis Publishers, Boca Raton, Florida, USA.

Keener, H.M., Marugg, C., Hansen, R.C. and Hoitink, H.A.J., 1993 Optimising the efficiency of the composting process. Science & Engineering of Composting: Design, Environmental, Microbial and Utilisation Aspects, H. A. J. Hoitink and H. M. Keener, eds., Renaissance Publications, Worthington, USA., 59-94

Keener, H.M., Elwell, D.L., Das, K.C. and Hansen, R.C., 1997. Specifying design/operation of composting systems using pilot scale data. Applied Engineering in Agriculture 13 (6), 767-772.

Keener, H.M., Ekinci, K. and Michel, F.C., 2005. Composting process optimisation - using on/off controls. Compost Science and Utilisation 13 (4), 288-299.

Loser, C., Ulbricht, H., Hoffman, P. and Seidel, H., 1999. Composting of wood containing polycyclic aromatic hydrocarbons (PAHs). Compost Science and Utilisation 7 (3), 16-32.

Marugg, C., Grebus, M., Hansen, R., Keener, H.M. and Hoitink, H.A.J., 1993. A kinetic model of the yard waste composting process. Compost Science and Utilisation 1 (1), 8-51.

Mason, I.G. and Milke, M.W., 2005. Physical modelling of the composting environment: a review. Part 1: Reactor systems. Waste Management 25 (5), 481-500.

Mason, I.G., 2006. Mathematical modelling of the composting process: a review. Waste Management 26 (1), 3-21.

Mason, I.G., (in press). Modelling substrate degradation in the composting process. Part 1: Profiles at constant temperature. Waste Management. (Published on-line 17 September, 2007).

Michel, F.C., Reddy, C.A. and Forney, L.J., 1993. Yard waste composting: studies using different mixes of leaves and grass in a laboratory scale system. Compost Science and Utilisation 1 (3), 85-96.

Mohee, R., White, R. and Das, K., 1998. Simulation model for composting cellulosic (bagasse) substrates. Compost Science and Utilisation 6 (2), 82-92.

Mote, C.R. and Griffis, C.L., 1979. A system for studying the composting process. Agricultural Wastes 1 (3), 191-203.

Mote, C.R. and Griffis, C.L., 1980. Variations in the composting process for different organic carbon sources. Agricultural Wastes 2, 215-223.

Nakasaki, K., Sasaki, Y., Shoda, M. and Kubota, H., 1985. Change in microbial numbers during thermophilic composting of sewage sludge with reference to CO2 evolution rate. Applied & Environmental Microbiology 49, 37-41.

Nakasaki, K., Kato, J., Akiyama, T. and Kubota, H., 1987. A new composting model and assessment of optimum operation for effective drying of composting material. Journal of Fermentation Technology 65 (4), 441-447.

Namkoong, W. and Hwang, E.Y., 1997. Operational parameters for composting night soil in Korea. Compost Science and Utilisation 5 (4), 46-51.

Paredes, C., Bernal, M.P., Roig, A. and Cegarra, J., 2001. Effects of olive mill wastewater addition in composting of agroindustrial and urban wastes. Biodegradation 12 (4), 225-234.

Paredes, C., Bernal, M., Cegarra, J. and Roig, A., 2002. Bio-degradation of olive mill wastewater sludge by its co-composting with agricultural wastes. Bioresource Technology 85 (1), 1-8.

Richard, T.L. and Walker, L.P., 1998. Temperature kinetics of aerobic solid state biodegradation. Proceedings of the Institute of Biological Engineering 1, A22-A39.

Richard, T.L., Walker, L.P. and Gossett, J.M., 1999. The effects of oxygen on solid-state biodegradation kinetics. Proceedings of the Institute of Biological Engineering 2, A10-A30.

Richard, T.L., Hamelers, H.V.M., Veeken, A. and Silva, T., 2002. Moisture relationships in composting processes. Compost Science and Utilization 10 (4), 286-302.

Rosso, L., Lobry, J.R. and Flandrois, J.P., 1993. An unexpected correlation between cardinal temperatures of microbial growth highlighted by a new model. J. Theor. Biol 162, 447-463.

Seki, H., 2000. Stochastic modeling of composting processes with batch operation by the Fokker-Planck equation. Trans. ASAE 43 (11), 169-179.

Sikora, L.J. and Sowers, M.A., 1985. Effect of temperature control on the composting process. Journal of Environmental Quality 14, 434-439.

van Lier, J.J.C., van Ginkel, J.T., Straatsma, G., Gerrits, J.P.G. and van Griensven, L.J.L.D., 1994. Composting of mushroom substrate in a fermentation tunnel - compost parameters and a mathematical model. Netherlands Journal of Agricultural Science 42 (4), 271-292.

CHAPTER 7
DESIGN AND PERFORMANCE OF A SIMULATED FEEDSTOCK.

7.1 Foreword

In Chapters 3-6 it was revealed that the evidence for substrate degradation sub-models was somewhat limited, and by chapter 5, that an experimental path forward was favoured. It had been noted however that what validation data does exist has been generated using a wide range of feedstocks, and in a variety of reactor types. Since the purpose of our proposed research was to investigate only the kinetics of the composting process per se, there was no need to choose any particular "real world" substrate. Thus, it seemed worthwhile to investigate the use of a standard, reproducible, feedstock, prepared from dry ingredients, in addition to appropriate reactor design. This would also engender benefits in terms of reliability of supply, ease of storage and ease of handling.

In the language of the journey, the author has now been delivered from the Bog of Eltech, and is proceeding rapidly in the direction of Experimentia. En route however he has stopped over at Ostrich Town (figure 7.1). The significance of the name of this small town is revealed within this chapter. Reactor selection and the rationale for the experimental programme will be discussed in chapter 8.

This chapter comprises the following draft article:

Mason, I.G., submitted. Design and performance of a simulated feedstock for composting experiments. Compost Science and Utilization.

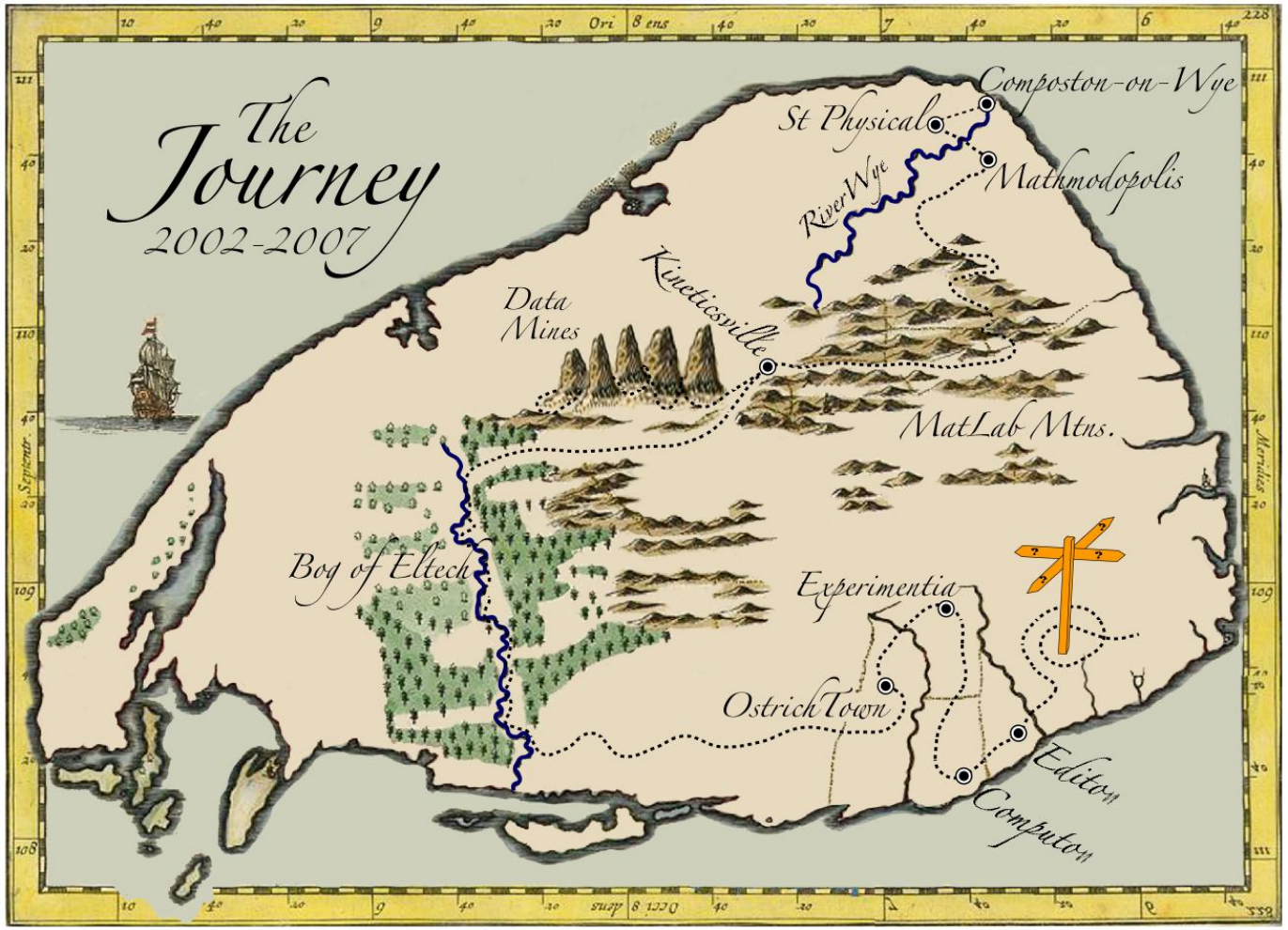

Figure 7.1: The conceptual map of the author's research travels. Our present location is – Ostrich Town

7.2 Summary

This paper reviews the composition and performance of simulated feedstock mixtures previously employed in composting research, and presents a new simulated feedstock, the composition of which was derived from a rational design procedure. The new simulated feedstock was prepared using readily available dry ingredients - ostrich feed pellets, office paper, finished compost and woodchips – representing the substrate, amendment, seed, bulking agent components of a composting mixture respectively. The design criteria chosen were a) an amendment:paper total C:N ratio of 30, b) an energy ratio of > 800 cal/g-H_2O, c) a water ratio of < 8 g-H_2O/g-BVS, d) a wet bulk density of < 600 kg/m^3 and e) a moisture content of 60% (w/w). Resultant final proportions of the substrate:amendment:seed:bulking-agent:added-water mix were 0.071:0.098:0.009:0.267:0.555 (w/w). When composted in a controlled temperature difference (CTD), forced-aeration, reactor operated with condensate return, the mixture was shown to self-heat rapidly and remain at realistic temperatures for extended periods. Thermophilic temperatures were reached within 22-33 h of start-up, following lag periods of 13-22 h, and maintained for up to 34 d. Finished compost characteristics were consistent with a normal composting process. It is suggested that future variations in the simulated feedstock composition could be made, and proposed that use of this type of feedstock would facilitate future experimental work associated with composting kinetics and temperature profile modelling.

7.3 Introduction

Composting experiments are typically carried out using “real world” feedstocks such as green (yard) waste, food residuals, biosolids, animal manures and organic residuals of industrial origin. In such investigations, the compostability of the substrate and the ability of the amendment and/or bulking agent to facilitate adequate substrate stabilisation, are typically the issues of primary interest (Mason and Milke, 2005). However, when the composting process itself is the major focus of an investigation, the use of “real world” mixtures can be of secondary importance. The main requirement in this case becomes that the substrate/amendment/bulking agent mix should possess physical, biochemical and micro-biological characteristics which will allow aeration, self-heating, and moisture transport to occur in an manner representative of “real world” composting processes. To this end, the use of simulated composting mixtures is potentially both practical and attractive from an

experimental point of view. If prepared from dry, readily available and reproducible materials, which are easy to handle and store, such mixtures are convenient. Provided that nutrient, moisture and energy conditions are satisfied, and a sufficient initial population of micro-organisms is present, compostable mixtures may be produced, and from a variety of ingredients. Advantages include removal of the spatial and temporal variability inherent in many "real world" materials, and the avoidance of the odour and public health problems associated with their collection, storage and handling.

Of the simulated feedstock "recipes" reported in the literature, the majority have been based on a formulation intended to simulate municipal solid waste (Palmisano et al., 1993). The mixture reported by Palmisano et al. (1993) comprised rabbit chow (food), newspaper, soil, leaf compost and cow manure (table 7.1). A similar mixture comprising rabbit chow, shredded newspaper, manure and sand was reported by Schwab et al. (1994). Subsequent modifications (table 7.1) included the addition of corn cob piths and sand, plus variations in the relative proportions of each ingredient. Cook et al. (1994) varied the original composition, in order to lengthen the thermophilic period, whilst Tseng et al. (1995) made alterations in order to reduce nitrogen availability. Sand was added as an abrasive material for use in large-scale composting systems by Cook et al. (1994), however these authors counselled against the use of sand in small-scale systems, due to problems of non-uniform distribution. In the above recipes, rabbit chow and corn piths may be identified as substrates, newspaper as an amendment and the compost, manure and/or soil generally as seed materials.

All mixtures were adjusted to desired initial moisture levels prior to composting. An alternative approach, in which dry dog food and maple chips were used as the components of the feedstock, was reported by VanderGheynst et al. (1997) and more recently in admixture with chicken litter as a seed material, by Lemus et al. (2004). Dry dog food has also been used in combination with sawdust and rice hull amendments, plus seed materials, by Nakasaki and Ohtaki (2002), Nakasaki et al. (2004), Chang et al. (2005) and Chang et al. (2006). Cotton linters pulp and soil were used by Clark et al. (1977).

Table 7.1: Simulated feedstock composition – literature data

Substrate	Amendment	Bulking agent	Seed	Other	Composition (fraction; w/w)[a]	Reference
Casein; soluble starch; corn oil	Cotton linters pulp	-	Soil	-	0.10 seed	(Clark et al., 1977)
Rabbit chow (alfalfa and non-alfalfa)	Shredded newspaper;	-	Soil; leaf compost; cow manure	-	0.28;0.28;0.28;0.06;0.06;0.06[b]	(Palmisano et al., 1993)
Rabbit chow	Shredded newspaper	-	Manure	Sand	0.30;0.23;0.01;0.46	(Schwab et al., 1994)
Rabbit food	Shredded newspaper	-	Composted cow manure	-	0.40;0.30;0.30	(Cook et al., 1994; Cook et al., 1997; Herrmann and Shann, 1997)
Rabbit food; corn cob piths	Shredded newspaper	-	Composted cow manure	-	0.52;0.44;0.03;0.01	(Cook et al., 1994; Herrmann and Shann, 1997)
Rabbit chow; corn cob piths	Shredded newspaper	-	Composted cow manure	Sand	0.42:0.36:0.01:0.01:0.20	(Day et al., 1997)
Rabbit chow; corn cob piths	Shredded newspaper	-	Seed compost; manure	Sand	0.41;0.35;0.01;0.03;0.01;0.20[b]	(Tseng et al., 1995)
Dry dog food	-	Maple chips	-	-	0.41;0.59	(VanderGheynst et al., 1997)
Dry dog food	Sawdust	-	Commercial seed material	-	0.52:0.47:0.01	(Nakasaki and Ohtaki, 2002; Nakasaki et al., 2004)
Dry dog food	-	Hemlock shavings and chips		-	0.03 (chicken litter)	(Lemus et al., 2004)
Dry dog food	Rice husks	-	Chicken litter; compost products	-	e.g. 0.24:0.60:0.16	(Chang et al., 2005; Chang et al., 2006)

Note: a. Ingredient fractions listed vertically within columns for each mixture and then across columns (left to right).
b. Total differs from 1.00 due to rounding.

Performance of the Palmisano (1993) feedstock, and derivatives thereof, has typically been non-representative of full-scale behaviour, when assessed in terms of the shape of the temperature profiles generated and the length of the thermophilic period (see Mason and Milke, 2005 for details). Similar comments apply to the temperature profile reported by Chang et al. (2005). It is not clear however whether these behaviours were due to the formulation, the reactor type, the aeration regime, or a combination of these factors. When assessed on shape and time criteria, the feedstock developed by VanderGheynst et al. (1997) performed well in large pilot-scale experiments, and also in the laboratory-scale experiments (6 l reactor volume) of Lemus et al. (2004). No data is available for the mixtures reported by Nakasaki and Ohtaki (2002) and Nakasaki et al. (2004).

The objectives of this paper are to report on the design, characteristics and performance of a new simulated feedstock comprising readily available substrate, amendment, seed and bulking agent materials. The intention was to create a simple, convenient, reproducible and reliable mixture, capable of generating full-scale temperature profiles at laboratory and pilot scale, and potentially able to be used and/or adapted by composting process researchers in a range of laboratory situations.

7.4 Design

7.4.1 Component materials

The substrate was selected from a range of dried animal feeds available in New Zealand. These included rabbit, horse, pig, poultry, ostrich, ruminant, deer and rabbit feeds, in either pelletised or ground form (McMillan Stock Foods Ltd., Christchurch, New Zealand). The rationale for selecting dried animal feeds was that these have a high degree of biodegradability, tend to be relatively high in nitrogen and energy content, and are easy to store, handle and re-hydrate. Of the available range, the "Ostrich Breeders" feed (figure 7.2), offered relatively high protein and fat levels (20.2% and 5.0% (w/w) respectively), providing a relatively high nitrogen and energy content. Ingredients for this preparation were listed as being selected from lucerne, maize, fish meal, meat meal, seed fibre, soya bean meal, soya oil and copra, plus minerals and amino acids. According to the supplier however all were typically present. The pelletised form of the feed (13-23 mm long and approximately 10.5 mm in diameter) was used in the present experiments, and selected characteristics are listed

in table 7.2. Office paper was chosen as the amendment since it is dry, highly biodegradable, relatively high in carbon, widely available, and known to degrade well in the composting process (Stocks et al., 2002; Mason et al., 2004). For the present experiments, post-consumer white office paper, printed with black toner only, was collected within the Department of Civil Engineering, University of Canterbury, Christchurch, New Zealand and shredded into approximately 21 mm by 3.4 mm strips using a paper shredder located in the university printery. Office paper was preferred to newspaper, since the latter is less biodegradable, being manufactured using mechanical, rather than chemical, pulping. Black toners are typically non-toxic to humans and non-hazardous in the environment (Lin and Mermelstein, 1994), and were expected to be non-toxic to micro-organisms in the composting process. Characteristics of the office paper used are listed in table 7.2 and a sample illustrated in figure 7.2. Finished compost from a local green (yard) waste composting facility of the Christchurch City Council, Christchurch, New Zealand, was selected as the seed, primarily because it was readily available. The compost was screened through a 2 mm sieve prior to use in order to eliminate large woody particles. Screened compost characteristics are listed in table 7.2 and a sample shown in figure 7.2. Wood chips were selected as the bulking agent. Although woodchips are frequently only available seasonally, and are of varying moisture content, they can be readily dried, and stored until needed. The nitrogen content of woodchips can be minimised by utilising material obtained from deciduous trees when not in leaf and minimising bark content. For the present experiments chipped English oak (*Quercus robur*) was obtained during the New Zealand winter season of 2004, spread out on a mezzanine floor in a heated building and allowed to air-dry for approximately 5 months. The woodchips were hand-sieved (approximately 15 seconds) through 26 mm and 3/16 inch (approximately 4.76 mm) sieves prior to use, discarding the over- and under-size fractions respectively.

Table 7.2: Feedstock ingredient characteristics

Parameter	Units	Ostrich breeder feed	Office paper	Finished compost	Woodchips
Total solids	% w/w	89.9 (0.0)	94.8 (0.0)	64.5 (0.0)	90.1 (0.0)
Moisture	% w/w	10.1 (0.0)	5.2 (0.0)	35.5 (0.0)	9.9 (0.0)
Volatile solids	g-/kg-TS	900 (0.5)	810 (6)	415 (0.2)	965 (0.3)
Carbon	g-C/kg-TS	441 (9)	411 (8)	223 (4)	493 (10)
Nitrogen	g-N/kg-TS	34 (2)	0.65 (0.05)	23.8 (1.7)	3.3 (0.2)
C:N	-	13 (1)	633 (46)	9.4 (1)	151 (11)
Energy	kJ/g-TS	18.2 (0.3)	14.0 (0.2)	8.5 (0.1)	19.5 (0.3)
Bulk density	kg/m^3	-	-	-	213 (nd)

Note: Errors in brackets; nd: not determined

Table 7.3: Mixture design criteria

Parameter	Units	Value	Comments	Reference
C:N ratio	-	25-30	Feed + paper only	Rynk (1992)
Moisture	% w/w	60	-	Rynk (1992)
Energy ratio	cal/g-H_2O	>700	-	Haug (1993)
Water ratio	g-H_2O/g-BVS	< 8	-	Haug (1993)
Wet bulk density	kg/m^3	600	-	-

a) Ostrich feed pellets

b) shredded paper

c) finished compost, ex 2 mm sieve

d) woodchips

Figure 7.2: Feedstock materials

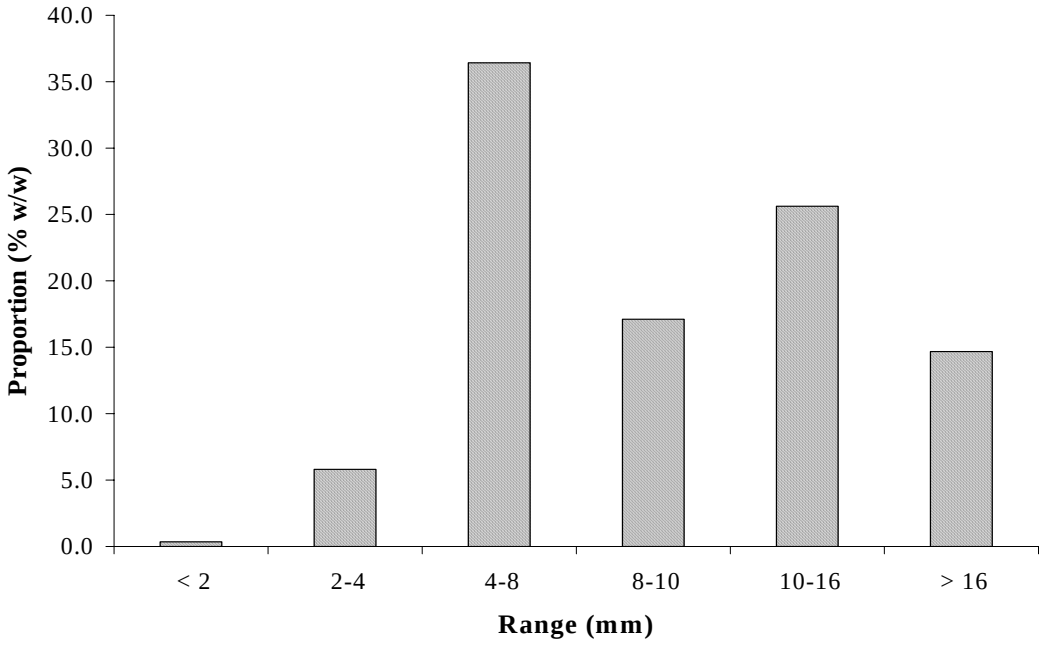

Figure 7.3 Woodchips particle size distribution

Characteristics of the woodchips used are listed in table 7.2, the appearance shown in figure 7.2 and the particle size distribution given in figure 7.3. The woodchip particle shapes were predominantly rectangular, mainly in the form of thin slivers. Smaller quantities of bark strips, bark fibre and twigs were also present.

7.4.2 Mixture parameters and proportions

Adopted design parameters were total C:N ratio, initial moisture level, energy ratio (E), water ratio (W) and wet bulk density (table 7.3). For simplicity, initial calculations were based achieving a total C:N ratio of approximately 30:1 on the substrate/amendment combination only. The calculated weight ratio of feed to paper required for this target was approximately 0.73:1. A seed fraction of 0.05, on a total substrate/amendment/seed weight basis, was selected from values reported in the literature (table 7.1). The design substrate/amendment/seed proportions were thus 0.40:0.55:0.050 (w/w).

Bulking agent quantity was arrived at experimentally, beginning with a weight ratio of bulking agent to substrate/amendment/seed of 0.5:1, and proceeding through 1:1 and 1.5:1. The initial choice of 0.5:1 was based on previous work reported by Mason et al. (2004). A final ratio of 1.5:1 was selected following observations on structure and initial compaction

occurring after approximately l l of various preliminary wet mixtures had stood in a 110 mm diameter mm clear plastic column for 12-24 hr. Following woodchips incorporation, the moisture content of the solid ingredients was calculated at 10%. Required added water to reach a total mixture target of 60%, was approximately 125% of the total weight of dry ingredients, resulting in final substrate/amendment/seed/bulking agent/added water proportions of 0.071:0.098:0.009:0.267:0.555 (w/w).

Energy (E) and water (W) ratios were estimated using assumed biodegradability fractions for volatile solids (VS), in order to estimate biodegradable volatile solids (BVS). The biodegradable faction of the ostrich feed VS was assumed by the present author to be 0.80, the value for paper was taken as 0.82 (Haug, 1993) and the value for woodchips was taken as 0.45, which is the average for four types of oak in data reported by Haug (1993). The latter assumption implies that woodchips would be degraded in the composting process, a factor not incorporated in the original feed design. Calculated values for E and W were 1225 cal/g-H_2O and 3.4 g-H_2O/g-BVS, both more than adequate compared to their respective recommended values (table 7.3). In the absence of any contribution from the woodchips, E and W values of 675 cal/g-H_2O and 5.6 g-H_2O/g-BVS were estimated, suggesting that performance should be satisfactory under this scenario, even though the values are close to the suggested limits. Previous experience however, suggested that the woodchips would participate in the process (Mason et al., 2004).

The original feedstock design was then re-assessed on the basis of the estimated component biodegradabilities. This analysis assumed that both C and N were available in proportion to the availability of VS. Values for biodegradable and total C:N were 24.2 and 30.0 for the substrate/amendment only, and 33.0 and 55.3 for the total mixture (ignoring the seed). These values reflect the experience that whilst composting design based on total C:N targets of 25-30:1 are reasonably accurate for many feedstocks, success is also possible at much higher ratios when composting materials such as green (yard) wastes with a high woody biomass content.

7.4.3 *Preparation*

Feedstock quantities were determined in order to prepare approximately 75 l of mixture. Ostrich feed pellets were weighed out, approximately 65% of the total quantity of water

required added, and the material left to hydrate at room temperature with occasional manual stirring. After 2-3 hours the material had disintegrated into slurry form (total solids content approximately 18% w/w). The slurry was then transferred to a large mixing bowl using the remaining water, and the seed sprinkled onto the surface and dispersed by stirring. Shredded paper was then added in approximately 1 kg lots, and mixed in each time with a garden fork. Finally the woodchips were added in two 6 kg lots, again with thorough mixing at each addition. The preparation was then further mixed for approximately 5 minutes. At the end of this time the shredded paper had broken down into short (approximately 10 mm) lengths and was well dispersed. The feedstock preparation process is illustrated in figure 7.4.

7.5 Experimental

7.5.1 Composting trials

Composting was carried out in a 65 l working capacity, 0.3 m diameter, controlled temperature difference (CTD) reactor, supplied with moisture-conditioned air. This reactor is described in detail in chapter 8. A preliminary trial was conducted using the design feedstock as specified, except that the initial moisture content was increased to 62% in order to partially compensate for exit gas moisture losses. Airflow rates varied between 0.08 and 0.39 l/min.kg-TS in this trial, with rates at the higher end of the range used for ventilative heat management, in order to control the peak temperature. Exit gas condensate was returned to the reactor at intervals during the trial. Two subsequent runs were conducted using a feedstock of 60% initial moisture content, with airflows varying between 0.15 to 0.23 l/min.kg-TS, and continuous exit gas moisture return via a reflux condenser.

7.5.2 Analyses

Total solids and moisture were determined gravimetrically after drying at 105°C for 16 hours in a Contherm Digital Series Oven (Contherm Scientific Ltd, Lower Hutt, New Zealand). Volatile solids were determined after incineration at 550°C for 3 hours, in a Lab III Muffle Furnace (W.D.McGregor Ltd., Auckland, New Zealand). Total carbon and total nitrogen were measured using a LECO CNS 2000 automated analyser, with infrared and thermal conductivity detection (LECO Corporation, Michigan, USA). Calorific values were measured using a Gallenkamp Autobomb model CBA 305 010M bomb calorimeter (Sanyo

a) ostrich feed slurry

d) paper mixed (all)

b) seed added

e) woodchips mixed

c) paper added (1 kg)

f) mixture close-up

Figure 7.4 Feedstock preparation

Gallenkamp PLC, Loughborough, UK). Bulk density measurements were carried out using a 110 mm internal diameter, 1045 ml capacity, clear plastic cylinder. The woodchips particle size distribution was determined using set of British Standard sieves placed on a mechanical shaker (Endecotts Ltd, London, UK). Mesh sizes were 16 mm, 10 mm, 8 mm, 4 mm and 2 mm, and the sieve stack was agitated for 10 minutes.

7.6 Results and discussion

7.6.1 Mixture properties

The fresh mixture showed no signs of free moisture immediately after preparation, either in the mixing bowl, or after gentle squeezing by hand. Initial mixture wet and dry bulk densities for the mixture used in run A were 419 and 167 kg/m^3 respectively. Following loading into the column the overall wet bulk density was approximately 510 kg/m^3. These values compare with wet and dry bulk density values of 710 and 240 kg/m^3 respectively, obtained for a bovine manure/sawdust woodchips mixture, and with 920 and 320 kg/m^3, for a bovine manure/sawdust woodchips mixture, both of which composted satisfactorily in a passive pile (Mason et al., 2004). These results were taken as an indication that sufficient free air space would likely be present in the mixture, a supposition confirmed by the type of self-heating behaviour subsequently observed (section 7.6.2). The mixture was easy to handle, and virtually odourless.

Odours occurred during the early stages of each run, however these were of an “earthy” compost character, and representative of those emitted from normal green waste composting operations. The presence of ammonia could be detected organoleptically at early time. Leachate production commenced between day 5.5 and 6.5, in runs A and B, showing a decreasing production rate with time in run B. Leachates were mid-brown in colour, and had a light musty odour, with no indication of anaerobic conditions, and in run B amounted to about 10% of the initial added water over the 34 d composting period.

At the conclusion of each run, a decrease in the mixture height was observed, indicating volume losses varying between 6.2% of the initial volume in the preliminary run, 6.7% in run B and 7.1% in run A. Final compost properties were measured following run B and these are compared to initial mixture values in table 7.4. Changes in the total carbon to nitrogen ratio (C:N) and wet bulk values are commensurate with significant composting activity. The

relatively high total C:N values occurred because of the inclusion of woodchips in these analyses, and it can be seen that when substrate, amendment and seed only are considered in the initial mixture, the total C:N value is within the normal design range. The final composts in each run had a light musty odour representative of finished green waste compost. Visual appearance was characterised by a mid-brown colouration, with the woodchips primarily intact but some non-degraded paper evident throughout. Moisture distribution was relatively even in the top half of the column, but in runs A and B, preferential moisture flow resulted in over-drying in some portions of the lower half of the column. This resulted in some segments where paper decomposition was prematurely halted. Further details are presented in chapter 8.

Table 7.4: Properties of initial and final mixtures

Parameter	Units	Value		
		Initial mixture [a]	Initial mixture [b]	Finished compost [c]
Total solids	% w/w	40	40	37.7
Moisture	% w/w	60	60	62.3
Volatile solids	g/kg-TS	910	830	-
Carbon	g/kg-TS	444	426	462
Nitrogen	g/kg-TS	7.0	14	10.5
C:N	-	63.2	29.6	44.2
Gross energy	kJ/g-TS	17.9	15.5	16.7
Wet bulk density	kg/m^3	515	-	430
Dry bulk density	kg/m^3	210	-	-

Notes: [a] Calculated from table 7.3 for runs A and B; [b] Calculated from table 7.3 for runs A and B - substrate, amendment and seed only; [c] Average results, Run B.

7.6.2 Self-heating performance

The feedstock temperature increased rapidly following a short lag phase, and temperatures were subsequently maintained in the thermophilic region for periods typical of those occurring in full-scale composting operations. This behaviour is illustrated in Fig. 7.5, which shows the temperature profiles measured at the mid-point of the reactor (i.e. 450 mm above the baseplate, on the central vertical axis), in the preliminary run (Fig. 7.5a) and in runs A and B (Fig. 7.5b-c). The duration of lag phases varied between 13 – 22 h, and the peak rates of temperature rise thereafter were 4.1 $^oC/h$ for the preliminary run, and 5.3 $^oC/h$ for runs A and B. Thermophilic temperatures were reached within 33 h of start-up in the preliminary run, and 22-23 h of start-up in runs A and B. The extent to which temperatures were maintained in the thermophilic range is quantified using the parameter A_{40} (Mason and

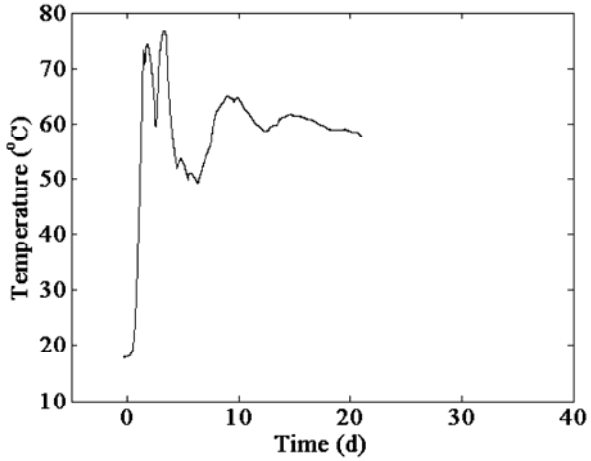

a) preliminary run

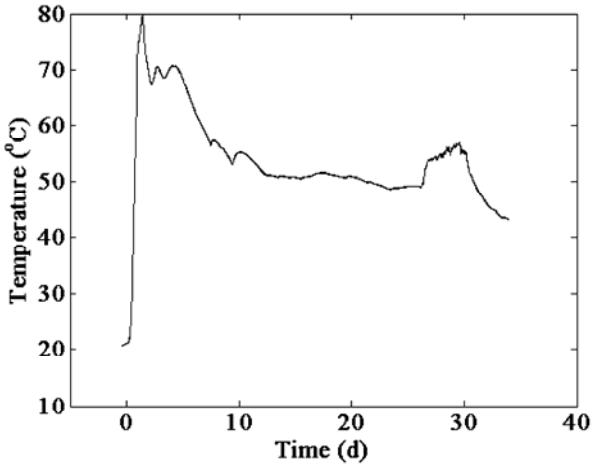

b) run A

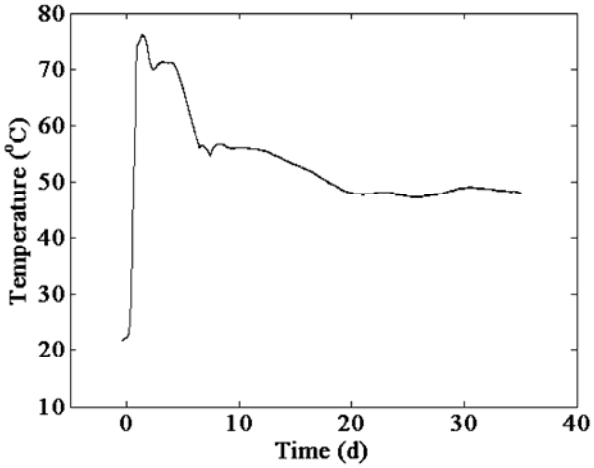

c) run B

Figure 7.5: Temperature profiles at the mid-point of the reactor.

Milke, 2005) which gives the areas bounded by the curve above 40 ^{o}C, and the 40 ^{o}C line. Values of A_{40} were 416, 491, and 484 ^{o}C.days for the preliminary run, run A and run B respectively, all of which are representative of full-scale behaviour (Chapter 3; Mason and Milke, 2005) and indicative that the self-heating capacity of the feedstock was satisfactory. A more detailed account of the temperature performance of the feedstock in runs A and B is given in chapter 8.

7.6.3 Discussion

The designed feedstock proved easy and convenient to prepare and handle. One improvement to the procedure which became evident relates to the form of the shredded paper, which would more readily hydrate and mix if supplied in chopped, rather than shredded, form. In addition, mechanical, rather than manual, mixing of the dried feed pellets during the hydration step could shorten the dissolution time for this material.

Future feedstock design based on biodegradable C:N ratios should give an improved likelihood of successful self-heating, as opposed to the present widespread practice of using total C:N values. In the present work, the total C:N ratio was rather high, but the biodegradable C:N value for the mixture was within the guidelines for optimal composting given by Rynk (1992), and as seen this mixture composted satisfactorily. A similar situation was noted by Clark et al. (1977) who wrote "The C:N ratio of the total feed was 108:1. The C:N ratio for the readily degradable materials, however, was 24:1". Further biodegradability data obtained under composting conditions is needed to progress this aspect of feedstock design, since much of the present data has been generated under anaerobic conditions. Free airspace measurements should be made on this and similar mixtures in order to more fully characterise them physically, and to understand their performance and applicability in composting experiments. In relation to the present simulated feedstock the CO_2 evolution data presented in Chapter 8 provides respirometric information which is useful in further characterising this mixture (see Figs. 8.22 and 8.32, and section 8.6.4).

The more widespread adoption of a standardised feedstock for composting process investigations would enable researchers to assemble a substantial body of necessary kinetic and mass transport data, without the complications arising from different and variable "real world" feedstocks. Useful variations on the present simulated feedstock in this context might

include low and high lipid content dried feed substrates, a range of bulking agent particle sizes, and inert bulking agents. If combined with appropriate reactor types, aeration rates and moisture control regimes, this could greatly facilitate the validation and verification of composting process kinetics and temperature prediction models.

7.7 Conclusions

1. A simulated composting feedstock was successfully prepared from a substrate, amendment, seed, bulking agent combination comprising ostrich feed pellets, office paper, finished compost and woodchips, respectively. Selected design criteria for the mixture were an amendment:paper total C:N ratio of 30, an energy ratio of > 800 cal/g-H_2O, a water ratio of < 8 g-H_2O/g-BVS, a wet bulk density of < 600 kg/m^3 and a moisture content of 60% (w/w). Application of these criteria resulted in final proportions of substrate:amendment:seed:bulking-agent:added-water of 0.071:0.098:0.009:0.267:0.555 (w/w).

2. The mixture self-heated rapidly in a CTD reactor environment with condensate return, following lag periods of 13-22 h. Thermophilic temperatures were reached within 22-33 h of start-up at the mid-point of the reactor, and temperatures were subsequently maintained in the thermophilic range for periods representative of full-scale composting behaviour, demonstrating that the self-heating performance of the feedstock in this context was satisfactory. Finished compost characteristics were consistent with a normal composting process.

3. The simulated feedstock proved easy to prepare, using readily available dry ingredients and tap water. It is suggested that variations in composition could be made to assess the impact of lipids and the contribution of bulking agents and that this type of feedstock would facilitate experimental work associated with composting kinetics and temperature profile modelling.

7.8 References

Chang, J.I., Tsai, J.J. and Wu, K.H., 2005. Mathematical model for carbon dioxide evolution from the thermophilic composting of synthetic food wastes made of dog food. Waste Management 25 (10), 1037-1045.

Chang, J.I., Tsai, J.J. and Wu, K.H., 2006. Thermophilic composting of food waste. Bioresource Technology 96, 116-122.

Clark, C.S., Buckingham, C., Charbonneau, R. and Clark, R., 1977. Laboratory scale composting: techniques. Journal of the Environmental Engineering Division, ASCE 103 (EE5), 893-906.

Cook, B.D., Bloom, P.R. and Halbach, T.R., 1994. A method for determining the ultimate fate of synthetic chemicals during composting. Compost Science & Utilisation 2 (1), 42-50.

Cook, B.D., Bloom, P.R. and Halbach, T.R., 1997. Fate of a polyacrylate polymer during composting of simulated municipal solid waste. Journal of Environmental Quality 26 (3), 618-625.

Day, M., Shaw, K., Cooney, D., Watts, J. and Harrigan, B., 1997. Degradable polymers: The role of the degradation environment. Journal of Environmental Polymer Degradation 5 (3), 137-151.

Herrmann, R. and Shann, J., 1997. Microbial community changes during the composting of municipal solid waste. Microbial Ecology 33 (1), 78-85.

Lemus, G.R., Lau, A.K., Branion, R.M.R. and Lo, K.V., 2004. Bench-scale study of the biodegradation of grease trap sludge with yard trimmings or synthetic food waste via composting. Journal of Environmental Engineering and Science 3 (6), 485-495.

Lin, G.H.Y. and Mermelstein, R., 1994. Acute Toxicity Studies of Xerox Reprographic Toners. Journal of the American College of Toxicology 13 (1), 2-20.

Mason, I.G., Mollah, M.S., Zhong, M.F. and Manderson, G.J., 2004. Composting of high moisture content bovine manure using passive aeration. Compost Science & Utilisation 12 (3), 249-267.

Nakasaki, K. and Ohtaki, A., 2002. A simple numerical model for predicting organic matter decomposition in a fed-batch composting operation. Journal of Environmental Quality 31 (3), 997-1005.

Nakasaki, K., Nagasaki, K. and Ariga, O., 2004. Degradation of fats during thermophilic composting of organic waste. Waste Management & Research 22 (4), 276-282.

Palmisano, A.C., Maruscik, D.A., Ritchie, C.J., Schwab, B.S., Harper, S.R. and Rapaport, S.A., 1993. A novel bioreactor simulating composting of municipal solid waste. J. Microbiol. Methods 18, 99-112.

Schwab, B.S., Ritchie, C.J., Kain, D.J., Dobrin, G.C., King, L.W. and Palmisano, A.C., 1994. Characterization of compost from a pilot plant-scale composter utilizing simulated solid waste. Waste Management & Research 12, 289-303.

Stocks, C., Barker, A.J. and Guy, S., 2002. The composting of brewery sludge. Journal of the Institute of Brewing 108 (4), 452-458.

Tseng, D.Y., Chalmers, J.J., Tuovinen, O.H. and Hoitink, H.A.J., 1995. Characterisation of a bench scale system for studying the biodegradation of organic solid wastes. Biotechnol. Progr 11, 443-451.

VanderGheynst, J., Gossett, J. and Walker, L., 1997. High-solids aerobic decomposition: Pilot-scale reactor development and experimentation. Process Biochemistry 32 (5), 361-375.

CHAPTER 8
PREDICTING BIODEGRADABLE VOLATILE SOLIDS DEGRADATION IN THE COMPOSTING PROCESS.

8.1 Foreword

It was clear from chapters 5 and 6 that over 80% of previously reported substrate degradation profiles were not well modelled by either single exponential, double exponential or Gompertz functions. Two important questions can be posed from this finding, a) "what profile shape would one expect from a composting process?" and, b) "is it the quality of the data which causes the dysfunction, or is it the aforementioned models?". This chapter reports research intended to address both of these questions.

Experimentally, two options were considered, either, i) fixed-temperature experiments at laboratory scale, or, ii) dynamic, varying-temperature, experiments at either laboratory or pilot scale. In the present work, option ii) was chosen, primarily because it seemed more interesting to explore and develop the methodologies and techniques required, and secondly, because the work would be relevant to the analysis of varying temperature composting experiments, which, as discussed in chapter 6, are expected to predominate in the composting research field in the future. The practical challenges involved in developing a suitable reactor, and the probability of unexpected information being revealed, were additional attractions.

In chapter 2 we saw that reactor choice is an important consideration in composting experimentation. For the present work the need for an accurate estimation of the heat flux and a desire to dynamically simulate the environmental conditions within a full-scale composting system as closely as possible, led to the consideration of either a controlled temperature difference (CTD) or a controlled heat flux (CHF) reactor. Since the reactor was to be constructed from scratch, and with no prior experience with this type of system, a CTD reactor was considered a preferable choice to a CHF system, although the latter would be better from a thermodynamic point of view. One major compromise in the design was the choice to simulate an aerated static pile, rather than an intermittently mixed system. The implications of this choice are discussed later in this chapter. Chapter 7 reported on the development of a suitable feedstock for these experiments.

In the language of the journey, the author has now arrived in Experimentia (figure 8.1). Having developed the feedstock in Ostrich Town, the task is now to construct the reactor and conduct the experiments. The results will be analysed in neighbouring Computon, and finally the work written up in Editon (figure 8.1).

This chapter comprises an expanded version of the following paper:

> Mason, I.G., submitted. Predicting biodegradable volatile solids degradation profiles in the composting process. Waste Management.

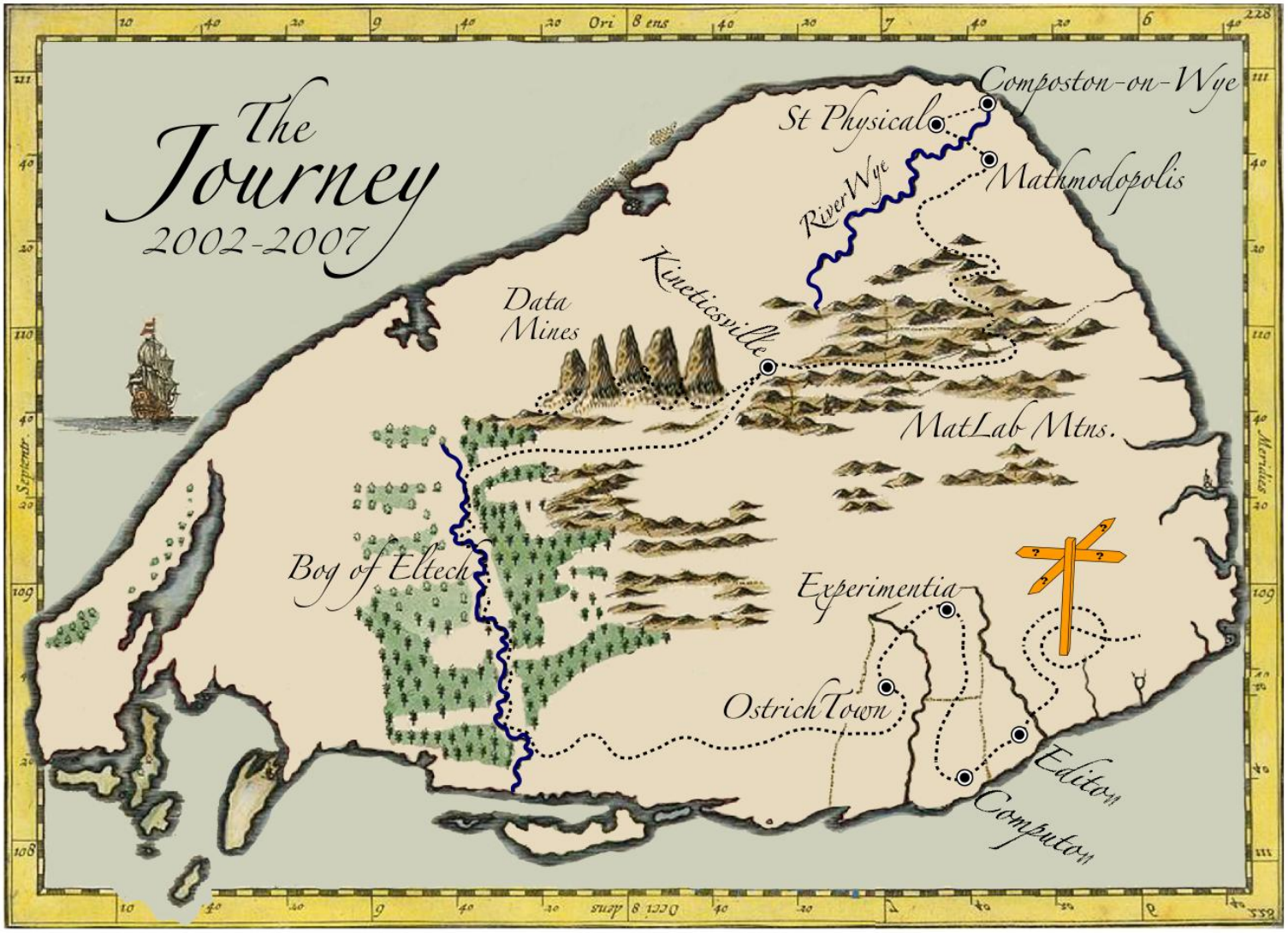

Figure 8.1: The conceptual map of the author's research travels. Our present locations are - Experimentia, Computon and Editon.

8.2 Summary

This paper presents a new method for the prediction of the pattern of biodegradable volatile solids (BVS) degradation in the composting process. The procedure is based on a re-arrangement of the heat balance (Mason, 2006), which is normally set up to predict composting temperatures, to numerically solve for the rate of BVS disappearance. Input data for the model was obtained from composting experiments conducted in a laboratory-scale, constant temperature difference (CTD) reactor simulating a section of an aerated static pile, and using a simulated feedstock comprising ostrich feed, shredded paper, finished compost and woodchips. These experiments also provided validation data in the form of exit gas CO_2-C profiles. The model successfully predicted the generic shape of experimental substrate degradation profiles obtained from CO_2 measurements, but under the conditions and assumptions of the experiment, the profiles were quantitatively different, giving an over-estimate of BVS-C. Both measured CO_2-C and predicted BVS-C profiles were moderately to well fitted by a single exponential function, with replicated rate coefficient values of 0.08 and 0.09 d^{-1}, and 0.06 and 0.07 d^{-1} respectively. In order to explore the underlying shape of the profiles, measured and predicted data at varying temperature were corrected to a constant temperature of 40 ^{o}C, using the temperature-correction function of Rosso et al. (1993), and cardinal temperatures of 5, 59 and 85 ^{o}C. Multi-phase profiles were generated for both the measured CO_2-C and the predicted BVS-C data in this case. However, when alternative cardinal temperatures of 5, 55 and 80 ^{o}C, or 5, 50 and 80 ^{o}C, were used, the predicted profiles assumed an exponential shape, and excellent fits were obtained using a double exponential function. These findings support the argument that a substrate degradation curve generated under laboratory conditions at 40 ^{o}C, would, given correct cardinal temperatures, generate a correct substrate degradation profile under varying temperature conditions and that this in turn would enable an accurate and precise prediction of the temperature profile, using a heat and mass balance approach. In order to realise this prospect, it is proposed that further work to obtain experimental data under completely mixed conditions, more accurately estimate the overall heat transfer coefficient and obtain physically correct values for the cardinal temperature used in the temperature correction function, is required.

8.3 Nomenclature:

a, b c	empirical constants in the Antoine expression (Eq. 5), with values of -2238, 8.896 and 273 respectively
A	surface area for heat transfer (m^2)
BVS	biodegradable volatile solids (kg)
c	specific heat of the composting materials (kJ/kg.^oC)
c_{drygas}	specific heat of dry air (kJ/kg.^oC)
c_{watvap}	specific heat of water vapour (kJ/kg.^oC)
E_{bio}	biologically produced energy (kJ)
G	mass flow rate of dry air (kg/s)
H_c	heat of combustion (kJ/kg-VS)
H_i	enthalpy of inlet air (kJ/kg-dry air)
H_o	enthalpy of exit gas (kJ/kg-dry gas)
L_e, latwat	latent heat of evaporation of water (kJ/kg)
m	mass of composting material (kg)
NRMSE	normalised root mean square error
p	pressure (mm Hg)
pv	vapour pressure (mm Hg)
pvs	saturation vapour pressure (mm Hg)
RH	relative humidity (fr)
t	time (s)
T	temperature (^oC)
TS	total solids (kg)
U	overall heat transfer co-efficient (kW/m^2. ^oC)
VS	volatile solids (kg)
w	weight of water vapour on a dry air basis (kg-H_2O/kg-dry-air)
Subscripts:	
a	ambient; air (table 8.1)
av	average
i	inlet
o	exit
1	inside wall
2	outside wall

8.4 Introduction

Substrate degradation models play a key role in the mathematical modelling of temperature, moisture and oxygen profiles in the composting process. In relation to temperature prediction, mathematical models have been shown to be largely successful in simulating the generic shape of composting temperature profiles, but they are less accurate in predicting key parameters of engineering importance, such as peak temperature, and the time required to reach it (Mason, 2006). It has also been shown that the majority of published substrate degradation data patterns are not well modelled by the single exponential, double exponential and Gompertz functions commonly applied in this area (Mason, in press-a; Mason, in press-b). Given that models for the estimation of the ventilative heat transport and wall loss components of temperature prediction models are well established, some further investigation of substrate degradation models, and their validation, therefore seemed useful. Possible explanations for the present situation include the use of inappropriate experimental systems, inadequate kinetic models, inaccuracies in the correction factors used to adjust reaction rates for changes in temperature, moisture level and oxygen concentration, and/or problems with the heat balance approach per se.

As previously discussed (Chapter 4; Mason, 2006), a differential expression with the rate of heat accumulation as the dependent variable may be derived from a heat balance around a volume of material in a composting system and has the following form:

$$\frac{d(mcT)}{dt} = G(H_i - H_o) - UA(T - T_a) + \frac{dBVS}{dt} H_c \qquad (1)$$

When the units used in this expression are as per the nomenclature listing for the present paper, then the accumulation, ventilative transport, CCR loss and substrate degradation groupings in Eq.1 all have units of power in kW. It should be noted that where the differential expression for BVS degradation is written with a negative sign, to denote BVS disappearance, then H_c will require a negative sign, in order to indicate that biological energy is being produced whilst substrate is being degraded. When Eq. 1 is solved in conjunction with the associated mass balances for biodegradable volatile solids (BVS), and moisture, a temperature profile is generated from independently measured and/or pre-set data e.g. Higgins and Walker (2001).

Alternatively, Eq.1 may be rearranged in order to predict the rate of substrate degradation. To obtain a solution, it is necessary that the temperature profile and aeration conditions are known, and that the sensible heating rate and CCR losses can be predicted. Koenig and Bari (2000) have previously utilised this approach to estimate heat generation and respiration rates in a composting system. In their case, an energy balance derived temperature rate expression was written as follows:

$$\frac{dT}{dt} = \frac{dVS}{dt}\left(\frac{H_c}{mc}\right) - \left(\frac{UA}{mc}\right)(T - T_a) - \frac{dH_2O}{dt}\left(\frac{L_e}{mc}\right) \tag{2}$$

By discretising the expression, making simplifying assumptions, integrating between time zero and the time at which the temperature returned back to the starting value, and using experimental data, values for the maximum heat production rate were found, and then multiplied by an oxygen consumption factor to give a maximum respiration rate.

In this paper it is proposed that this approach may be adapted and extended to enable the prediction of the dynamic pattern of BVS degradation from temperature, airflow, enthalpy, heat loss and composting materials mass loss data. Rearranging Eq. 1 for the solution of the rate of BVS degradation gives:

$$\frac{dBVS}{dt} = \frac{\frac{d(mcT)}{dt} - G(H_i - H_o) + UA(T - T_a)}{H_c} \tag{3}$$

Since analytical solutions for mass, specific heat and temperature rate changes in composting systems are unknown, a discrete numerical approach is necessary in order to obtain a solution. If rates of change are approximated over finite time elements (Δt) of the temperature/time profile, a model for BVS degradation in discrete form may be written as follows:

$$\frac{\Delta BVS}{\Delta t} = \frac{m_{av}c\frac{\Delta T}{\Delta t} - G(H_i - H_o) + UA(T_{av} - T_a)}{H_c} \tag{4}$$

Here m_{av} represents the average mass of composting material present during the chosen time interval. Specific heat is assumed constant in this analysis and steady state heat transfer at each interval is assumed. If changes in total composting mass are measured experimentally, then Eq. 4 is sufficient. The cumulative pattern of BVS degradation is then determined by integration. Should the revealed profile mimic that for bacterial growth patterns in batch culture, then sigmoidal profile shapes would be expected and be amenable to modelling by Gompertz, or similar, functions. If not, then exponential, or other, functions will be required.

BVS degradation profiles in composting systems have most commonly been quantified from carbon dioxide (CO_2) evolution measurements. Whilst supported by stoichiometry, practical evidence to support a strong correlation between these two parameters is limited. Namkoong and Hwang (1997) presented a linear relationship between log VS reduction and cumulative CO_2-C evolution data from nightsoil composting experiments. However the data showed a high degree of scatter, with a correlation coefficient (r) of approximately 0.65. Elwell et al. (1996) compared dry matter losses, determined by weighing, with estimates based on CO_2 and energy production, and found a substantial discrepancy between the two, with lower estimated losses at early time, and higher losses at later time. These authors postulated that losses of volatile carbonaceous material in the gas phase may have been responsible for the differences at early time. Techniques for the measurement of carbon dioxide in the exit gas stream of composting systems, have typically involved either carbon dioxide absorption into an alkaline liquid, or electro-chemical sensors. Both approaches are non-intrusive in the composting mass, but are subject to experimental limitations. Absorption systems are labour intensive, limited in practice to minimum data collection intervals of 8-24 hr, and the data cannot be automatically logged. Whilst the use of CO_2 sensors overcomes these limitations, they may have upper temperature limits lower than peak composting temperatures, and typically require non-condensing environments.

The objectives of this work were, a) to simulate BVS degradation profiles from a synthetic data set, b) to validate the simulation procedure using experimentally generated CO_2 evolution data, c) to assess the fit of single and double exponential models, and the modified Gompertz model, to the substrate degradation profiles generated and d) to deconstruct the profiles generated at varying temperature to a constant temperature and assess the fit of single and double exponential models, and the modified Gompertz model to these profiles.

8.5 Materials and Methods

8.5.1 Experimental reactor

A laboratory-scale controlled temperature difference (CTD) composting reactor (SA:V approximately 13.2:1) was constructed from a 1100 mm long section of nominal 315 mm outside diameter, 5.5 mm wall thickness polyvinylchloride (PVC) "Farmtuff" culvert pipe (Iplex Pipelines NZ Ltd, Auckland, New Zealand). The nominal inside diameter of the column was 304.5 mm. Removable flat end caps manufactured from 6 mm PVC, were fitted to the top and base of the column respectively. A reduction fitting on the top cap was added to reduce the exit gas section diameter to 100 mm in order to facilitate exit gas treatment, and CO_2 measurement. An enamel-painted perforated steel plate (8 mm holes, 60% open area) was placed 100 mm above the base of the column to support the composting material. To minimise airflow wall effects, strips of 12 mm width x 9 mm depth self-adhesive rubber material ("Sponge Seal", Batavian Rubber Company, Featherston, New Zealand) were fixed around the inside circumference of the column immediately beneath, and 900 mm above, the baseplate. The nominal working volume of the column between the baseplate and the 900 mm level was 65.5 l. Side wall effects are discussed in more depth Chapter 2, section 2.7.

Three separate sections of the column, between 0-300, 300-600 and 600-900 mm above the base plate, were separately wrapped with 56 micron thickness aluminium foil (Argus Heating Ltd, Christchurch, New Zealand) and then a 6 m length of 40 W/m parallel Raychem heating cable (Tyco Thermal Controls, Menlo Park, California, USA) arranged in a helical pattern at 50 mm spacings. The top end cap was covered with aluminium foil and then a 300 mm diameter silicone rubber heating mat (Holroyd Components Ltd, Saffron Walden, England) placed on it. The aluminium foil was used in order to more evenly distribute the applied heat. A 50 mm thick layer of expanded polyurethane foam (Dunlop Flexible Foams, Christchurch, New Zealand) was then wrapped around the heated sections, and placed over the top cap. Three proportional-integral (PI) temperature controllers, able to individually control the temperature drop across the PVC wall of each section within a range of 0 - 2.5 ^{o}C, with a precision of ± 0.1 ^{o}C, were constructed in-house. A fourth PI controller was used to control the end cap temperature in order to minimise internal condensation. The reader is referred to appendix 12 for a schematic diagram of the control system.

Temperature was measured using LM35DZ temperature sensors (National Semiconductor Corporation, Santa Clara, California, USA) located centrally along the vertical axis of the

column at heights of 0, 150, 300, 450, 600, 750 and 900 mm above the base plate, at heights of 150, 450 and 750 mm on the inside wall, at the same heights on the outside wall between the aluminium foil and the insulation layer, in the inlet air plenum, in the exit gas plenum, on the inside surface of the lid and in the exit gas line following the CO_2 probe. Sensor assemblies were encapsulated in stainless steel rods with the sensor element seated in a close fitting copper end cap sealed using an adhesive compound (Loctite, USA), except for those used at the inlet plenum, baseplate and exit gas outlet, which were encapsulated in an underwater cable-sealing compound (Endurapak 7025, Polymer Developments Group Ltd, Auckland, New Zealand), and those on the outside wall, which were covered with a "heat-shrink" material only. Copper end caps were chosen due to their superior thermal conductivity of 386 W/m.^{o}K, as compared to 15 W/m.^{o}K for stainless steel (Mills, 1995). Reactor weight was measured by mounting the column on a steel framework containing a LC4103-K100 load cell (A&D Co. Ltd, Milpitas, California, USA). Relative humidity in the inlet air was measured using Honeywell HIH-3602-C humidity sensor (Honeywell Inc, Freeport, Illinois, USA). Inlet air was supplied from an oil free compressor, and then humidified by passing it over water in a 500 ml Erlenmeyer flask at ambient temperature. Inlet airflow was measured using a Honeywell AWM5101VN mass flow meter with a range of 0-5 l/min (Honeywell Inc, Freeport, Illinois, USA). The exit gas was cooled using two laboratory-scale, water-cooled, Quickfit glass condensers connected in series and the condensate either collected, or allowed to return to the column directly by gravity flow. The exit gas was then slightly warmed above dew point in an electrically heated section of stainless steel piping to create non-condensing conditions for carbon dioxide measurement. Carbon dioxide in the exit gas stream was then measured using a Vaisala GMT 220 detector, with a range of 0-20% (v/v), and an upper temperature limit of 60 ^{o}C (Vaisala, Helsinki, Finland). Temperature, weight, RH, airflow and CO_2 data were logged at 1 minute intervals using "Serial Box Logger" software (in-house) running on a desktop personal computer. The experimental reactor system is shown schematically in figure 8.2, the heating cable installation illustrated in figure 8.3 and the selected photographs of the experimental system shown in figure 8.4.

Manufacturers accuracy specifications were as follows: for the temperature sensors ± 0.6-0.9 ^{o}C; for the load cell ± 0.0015% of rated output; for the RH sensors ± 2% RH; for the airflow meter ± 0.5% of the reading; and for the CO_2 sensor, ± 0.02+2% of the reading. Factory calibration of the CO_2 sensor gave 0.000%+0.001% CO_2 and 20.000+ 0.142 % CO_2.

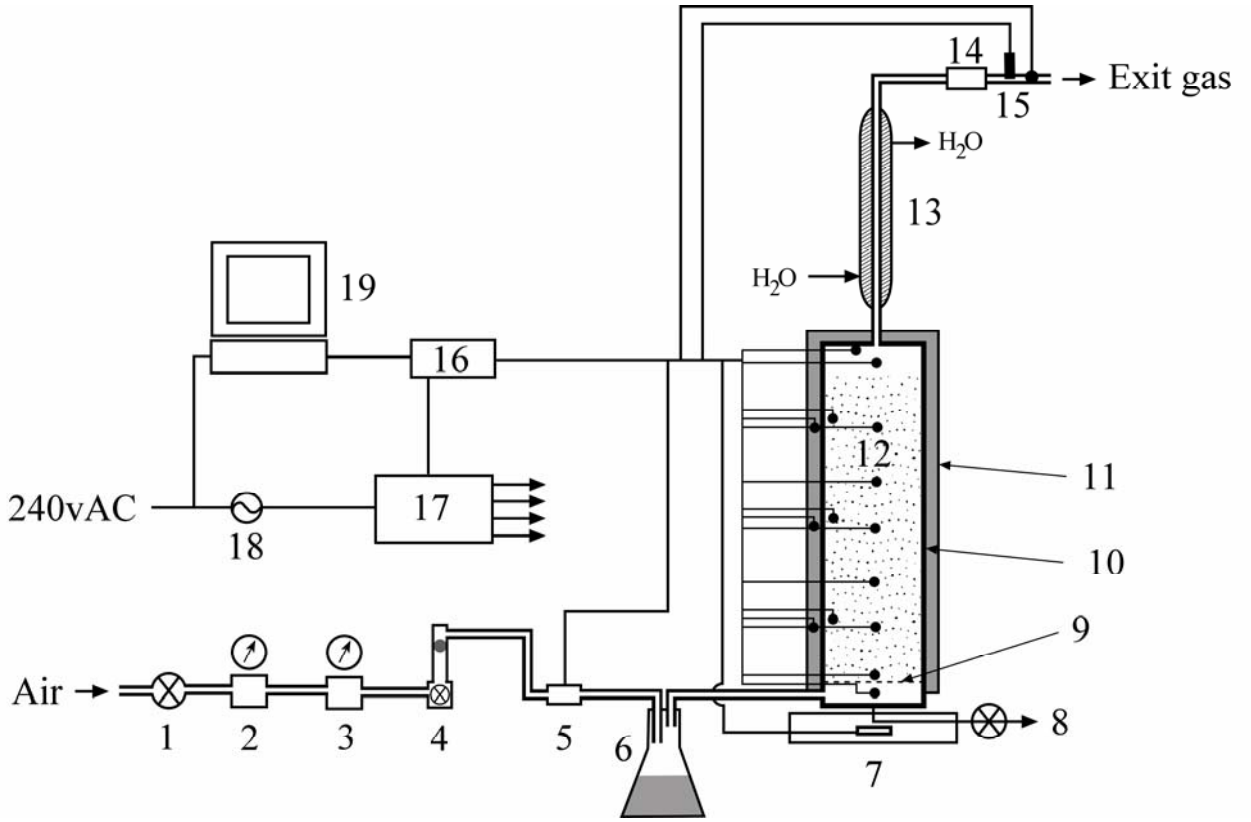

Figure 8.2: Schematic of the experimental system.

Key: 1. on/off valve; 2. pressure regulator (coarse); 3. pressure regulator (fine); 4. flowmeter; 5. electronic flowmeter; 6. humidifier flask; 7. load cell; 8. leachate drain valve; 9. perforated baseplate; 10. column wall; 11. insulation layer; 12. composting material; 13. condensers; 14. heater; 15. CO_2 probe; 16. data reception box; 17. heater controllers; 18. voltage adjustment device; 19. computer; ○ temperature sensors.

Note: Relative humidity sensor in inlet plenum wall omitted for clarity of presentation.

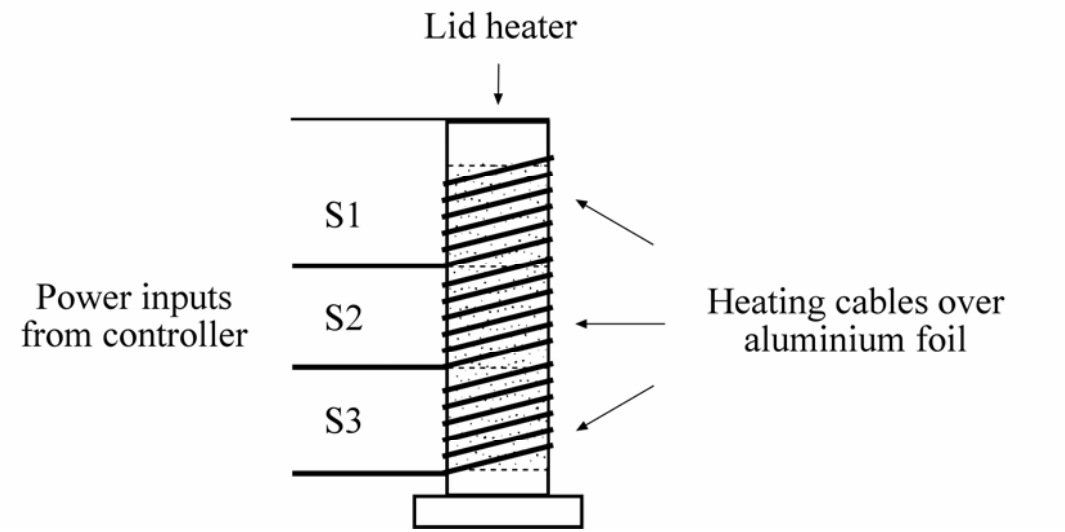

Figure 8.3: Schematic of the CTD apparatus showing the column and lid heating arrangements.

Key: S1 = section 1; S2 = section 2; S3 = section 3.

a) system over-view

d) outside wall temperature sensor

b)

heating cable in 3 sections

e) lid temperature sensor and heating pad

c) core and inside wall temperature sensors

f) baseplate and inlet plenum temperature sensor

Figure 8.4 Photographs of the system.

8.5.2 Simulated feedstock

A simulated raw composting mixture was prepared using approximately 7.1% (w/w) ostrich breeder feedstuff (McMillan Stockfoods Ltd, Christchurch, New Zealand), 9.8% (w/w) shredded post-consumer white office paper (printed with black toner only), 0.9% (w/w) finished green waste compost, and 26.7% (w/w) woodchips (*Quercus robur* - English oak). Addition of 55.5% (w/w) tap water resulted in an initial moisture content for the mixture of 60% (w/w). A more detailed account of the development and performance of this mixture was given in chapter 7.

8.5.3 Composting runs

Two composting runs, A and B, were conducted over periods of 34 and 35 days respectively. In each case, the temperature difference across the side walls was set at 1 ^{o}C, and across the lid at 0 ^{o}C. In order to help limit core temperature rises, without risking over-drying from excessive airflow rates, power input to the heaters was curtailed when inside wall temperatures exceeded approximately 65 ^{o}C. This enabled across wall differentials greater than 1 ^{o}C, and a higher rate of CCR losses, to occur. Airflows were varied between 0.15, 0.19 and 0.23 l/min.kg-TS (2.0, 2.5 and 3.0 l/min), with the higher values chosen in order to limit the magnitude and duration of peak temperatures. The highest value was, at the same time, restricted in order to minimise drying of the compost mixture at the bottom of the column. The duration of the peak airflow was varied slightly between runs. In order to retain a moisture concentration of approximately 60%, and avoid moisture limitation, exit gas condensate was returned automatically to the column, via a condenser system (see figure 8.2). Leachate was drained periodically from the base, and returned immediately to the top of the column during run A, in order to explore the impact on drying in the lower part of the column. In run B, the leachate was drained, but not returned, in order to avoid the temporary temperature depressions at the 750 mm probe, observed in run A. Initial mixture wet weights added to the column were 33.025 kg for Run A and 32.280 kg for run B.

8.5.4 Sampling and analysis

Samples of finished compost were taken from layers located at 0-150, 150-300, 300-450, 450-600, 600-750 and 750-900 mm above the baseplate, at the conclusion of each run, and either stored at 4 ^{o}C, or frozen, prior to analysis. Total solids and moisture were determined gravimetrically after drying at 105°C for 16 hours in a Contherm Digital Series Oven (Contherm Scientific Ltd, Lower Hutt, New Zealand). Volatile solids were determined after

incineration at 550°C for 3 hours, in a Lab III Muffle Furnace (W.D. McGregor Ltd., Auckland, New Zealand). Total carbon and total nitrogen were measured using a LECO CNS 2000 automated analyser, with infrared and thermal conductivity detection (LECO Corporation, Michigan, USA). Calorific values were measured using a Gallenkamp Autobomb model CBA 305 010M bomb calorimeter (Sanyo Gallenkamp PLC, Loughborough, UK). Bulk density measurements were carried out using a 110 mm internal diameter, 1045 ml capacity, clear plastic cylinder. Reported errors for the energy, carbon and nitrogen analyses were 1.44%, 1.5-2.0% and 6-7% respectively. Root square errors were calculated.

8.5.5 Mathematical modelling

Enthalpy values (H_i and H_o) were calculated using the procedure given in Haug (1993). The relevant expressions, which were computed in descending sequence, are:

$$pvs = 10^{\left((\frac{a}{T+c})+b\right)} \tag{5}$$

$$pv = pvs * RH \tag{6}$$

$$w = \left(\frac{MW_{H_2O}}{MW_{air}}\right)\left(\frac{pv}{p_a - pv}\right) \tag{7}$$

$$H = ((c_{drygas} + (w * c_{watvap})) * T_a) + (w * latwat) \tag{8}$$

BVS profiles were calculated using Eq. 4 implemented in "Matlab" (The Mathworks Inc, Natick, Mass., USA). Power values for each of the components of the energy balance were calculated by omitting the heat of combustion (H_c) from Eq. 4, and cumulative energy profiles were then derived from these results. Curve fitting and profile correction to constant temperature were carried out as previously described by Mason (in press-a). Matlab routines are presented in Appendix 2. Additional optimisation studies utilised Microsoft "Solver" (Microsoft Corporation, Seattle, USA)

8.5.6 Simulation

Prior to analysing the experimental data, a simulation was carried out using a temperature profile from Bari et al. (2000), in combination with estimated airflow, humidity, mass loss and wall heat loss data (table 8.1). This was done in order to see what profile shape would be predicted, and to examine the sensitivity of the model to realistic variations in the input

parameters. A mixture wet weight of 50 kg, with an initial moisture content of 60%, was assumed. Mass airflow was derived from a specific airflow of 0.5 l/min.kg-TS, UA (the product of the overall heat transfer coefficient and the column surface area) set at 0.004 kW/^{o}C, the temperature difference across the reactor walls set at 2 ^{o}C, atmospheric pressure (p_a) set at 760 mm and the integration interval set at 1 day. The weight loss pattern was derived from preliminary experimental results. Variations in each parameter were based on the degree of error considered likely in practice and ranged from 1-10% (see table 8.3). A constant value of 2367 kJ/kg for latent heat of vaporisation of water was assumed in the simulation.

Table 8.1: Simulation data set (compost temperatures after Bari et al. (2000))

Time	m_{av}	$\Delta T/\Delta t$	T_{w1}	T_{w2}	T_{ai}	T_{ao}	T_{amb}	G	RH_i	RH_o
d	kg	^{o}C/s	^{o}C	^{o}C	^{o}C	^{o}C	^{o}C	kg/s	fr	fr
0.5	50.0	1.16E-05	20.5	18.5	18.5	21.5	20	0.0002	0.5	0.75
1.5	49.9	3.47E-05	22.5	20.5	19.5	23.5	20	0.0002	0.5	1
2.5	49.1	1.04E-04	28.5	26.5	19.5	29.5	20	0.0002	0.5	1
3.5	47.8	1.04E-04	37.5	35.5	18	38.5	20	0.0002	0.5	1
4.5	46.7	6.94E-05	45	43	17.5	46	20	0.0002	0.5	1
5.5	45.8	2.31E-05	49	47	19	50	20	0.0002	0.5	1
6.5	44.8	-1.16E-05	49.5	47.5	20.5	50.5	20	0.0002	0.5	1
7.5	44.0	2.31E-05	50	48	22.5	51	20	0.0002	0.5	1
8.5	43.3	0	51	49	23.5	52	20	0.0002	0.5	1
9.5	42.6	2.31E-05	52	50	21.5	53	20	0.0002	0.5	1
10.5	42.0	-1.16E-05	52.5	50.5	20	53.5	20	0.0002	0.5	1
11.5	41.5	-1.16E-05	51.5	49.5	20	52.5	20	0.0002	0.5	1
12.5	41.0	-1.16E-05	50.5	48.5	20	51.5	20	0.0002	0.5	1
13.5	40.5	-1.16E-05	49.5	47.5	20	50.5	20	0.0002	0.5	0.95
14.5	40.1	-1.16E-05	48.5	46.5	20	49.5	20	0.0002	0.5	0.90
15.5	39.7	0	48	46	20	49	20	0.0002	0.5	0.85
16.5	39.3	-1.16E-05	47.5	45.5	20	48.5	20	0.0002	0.5	0.80
17.5	38.9	-1.16E-05	46.5	44.5	20	47.5	20	0.0002	0.5	0.75
18.5	38.6	-1.16E-05	45.5	43.5	20	46.5	20	0.0002	0.5	0.70
19.5	38.3	-4.63E-05	43	41	20	44	20	0.0002	0.5	0.65
20.5	38.0	-3.47E-05	39.5	37.5	20	40.5	20	0.0002	0.5	0.60
21.5	37.7	-3.47E-05	36.5	34.5	20	37.5	20	0.0002	0.5	0.55
22.5	37.4	-2.31E-05	34	32	20	35	20	0.0002	0.5	0.50

Assumptions: UA = 0.004 kW/^{o}C; P_a = 760 mm

8.5.7 Data spikes, noise and error

Data spikes in temperature, weight loss, airflow rate and CO_2 concentration resulting from manual interventions on the system such as leachate removal (both runs), and leachate return (run A), were removed prior to analysis of the data sets. Such spikes typically occurred over

5-15 min periods on sampling days, at intervals typically varying from 24- 72 h, depending on the leachate removal and return regime.

Signal noise, or random error, arising from temperature sensors, the load cell, the airflow meter, and the CO_2 probe was evaluated by examining fluctuations occurring over arbitrarily selected 1 hour periods during, before and after the experimental runs (Appendix 11). The potential impact of these fluctuations, and the way in which they were handled, are discussed in the next section.

Systematic error arising from sensor calibration uncertainties, and thus affecting accuracy rather than precision, was evaluated by calculating cumulative CO_2-C and BVS profiles for input values ± either the maximum deviation, or a deviation considered realistic. Details are given later in this chapter where such errors are reported.

8.5.8 Model parameters

Selected values for fixed parameters required to solve Eqs.4 and 8 for the experimental data sets are listed in table 8.2.

Table 8.2: Set values used in the solution of Eq. 4

Parameter	Units	Value	Source
Density of dry air	g/l	1.20	Calculated from ideal gas law; 20 ^oC, 1 atm
Specific heat of water	kJ/kg.^oC	4.184	- ; 20 ^oC
Specific heat of dry air	kJ/kg.^oC	1.004	Haug (1993)
Specific heat of water vapour	kJ/kg.^oC	1.841	Haug (1993)
Heat of combustion	kJ/g-VS	19.6	Calculated from data in Table 7.3
Thermal conductivity of PVC	W/m. ^oC	0.092	Mills (1995)
Convective heat transfer coefficient	W/m^2. ^oC	3	Mills (1995); free convection
BVS carbon fraction	-	0.507	Calculated from data in Table 7.3

The latent heat of vaporisation of water for the BVS-C predictions from experimental data was computed from the following expression, adapted from Haug (1993):

$$latwat = ((1093.7 - (0.5683 * ((T + 32) * 9/5))) * 1055/454) \quad (9)$$

where: *latwat* latent heat of vaporisation of water (kJ/kg)

T temperature (^oC).

8.6 Results

8.6.1 Simulation and model sensitivity analysis

A sigmoidal BVS versus time profile was generated from the synthetic data set (figure 8.5). This pattern was well modelled by the modified Gompertz function (figure 8.5), with just a slight deviation at early time, and a relatively low normalised root mean square error (NRMSE) of 0.77%. Removal of the lag phase data revealed a convex curve, but this was not well fitted by either a single or double exponential model (curve not shown). An analysis of the sensitivity of the simulation to changes in the input parameters (Eq. 4, table 8.3), showed that the basic shape of the profile remained unaltered, but that it was shifted spatially according to the direction of each variation, with cumulative impacts. An example is shown in figure 8.6, where the effect of a ± 2% variation in exit gas temperature (± 1.0 ^{o}C at 50 ^{o}C) is shown. As anticipated, changes in airflow, inlet gas relative humidity, exit gas relative humidity and exit gas temperature resulted in the greatest impact on the maximum cumulative value for BVS degraded (table 8.3). The full set of sensitivity plots are presented in Appendix 3. Cumulative energy profiles for ventilative transport, wall losses and accumulation within the reactor were also calculated (figure 8.7), and these were consistent with patterns previously reported (see Weppen, 2001). It is worthwhile to note here that the shapes of the BVS and bioenergy profiles (figures 8.5, 8.7) are the same, since the conversion involves only a scalar quantity, the heat of combustion (H_c).

Table 8.3: Sensitivity analysis

Parameter	Symbol	Variation (±%)	Error in BVS_{max} (±%)[a]
Specific heat (compost)	c	10.0	0.4
Temperature difference	$\Delta T/\Delta t$	10.0	0.4
Airflow	G	5.0	3.8
Heat of combustion	H_c	0.5	0.5
Average mass	m_{av}	0.2	0.008
Atmospheric pressure	p_a	1.0	0.73-0.75
Relative humidity-inlet	RH_i	5.0	3.5-3.9
Relative humidity-exit	RH_o	5.0	4.1-4.2
Temperature – inlet air	T_{ai}	2.0	0.4
Temperature – exit gas	T_{ao}	2.0	4.4-4.6
Temperature – inner wall	T_1	2.0	8.3
Temperature – outer wall	T_2	2.0	8.0
Heat transfer coefficient*area	UA	10.0	1.9

[a] % of maximum cumulative BVS degraded.

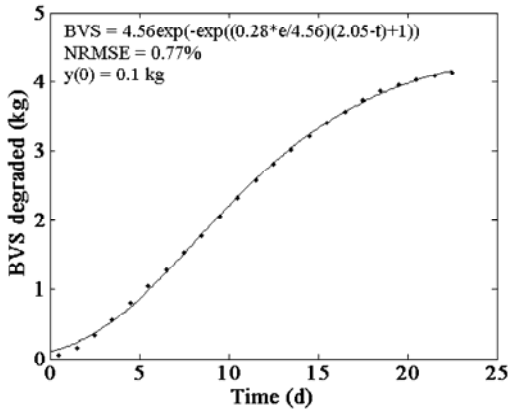

Figure 8.5: Simulated BVS profile modelled using the modified Gompertz function.

Key: ─ model; ··· data

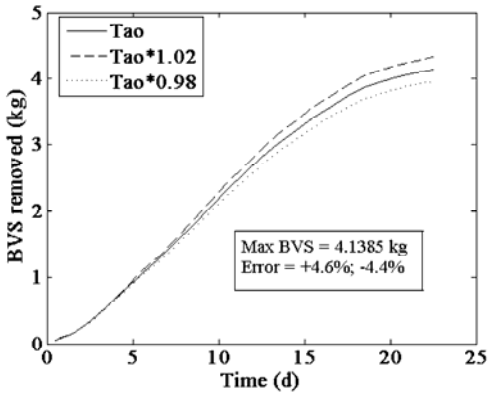

Figure 8.6: Sensitivity of the simulated BVS profile to changes in exit gas temperature.

Key: Tao = exit gas temperature; Max BVS = maximum BVS.

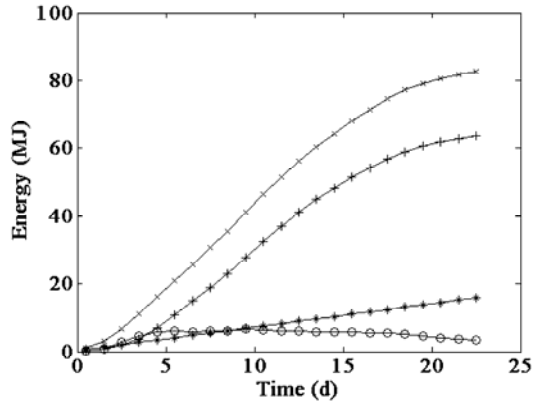

Figure 8.7: Simulated energy profiles. Key: x = bioenergy; + = ventilative transport; * = CCR losses; o = accumulation.

8.6.2 Sensor noise

Variations in sensor outputs over selected 1 h periods are summarised in table 8.4. The fluctuations in mass readings were consistently small, both with and without the applied load of the full column. Airflow meter variations were similarly minor. Both these were treated as insignificant noise, and not smoothed in subsequent calculations. Whilst the CO_2 probe readings showed minor fluctuations at ambient conditions (figure 8.8), the variations increased at higher exit gas concentrations (figure 8.9, table 8.4). Examination of both profiles did not reveal any conclusive evidence as to whether these variations reflected real concentration changes, or random noise. However, given the much lower "at rest" fluctuations in ambient air, it was decided to treat the operational readings as real data.

Table 8.4: Sensor noise

Sensor	Units	Typical excursion (± unit)	Typical error (±%)	Comments
Load cell	kg	0.005-0.009	0.1-0.2	Mass loss
Airflow meter	l/min	0.0004-0.0008	0.02	Operating airflows
CO_2 probe	%	0.006	-	Ambient air
		0.02-0.03	1.6-1.8	Exit gas
Temperature probe 1	^oC	0.1	0.2	Compost temperatures
Temperature probe 2	^oC	0.1	0.4-0.6	Ambient temperatures

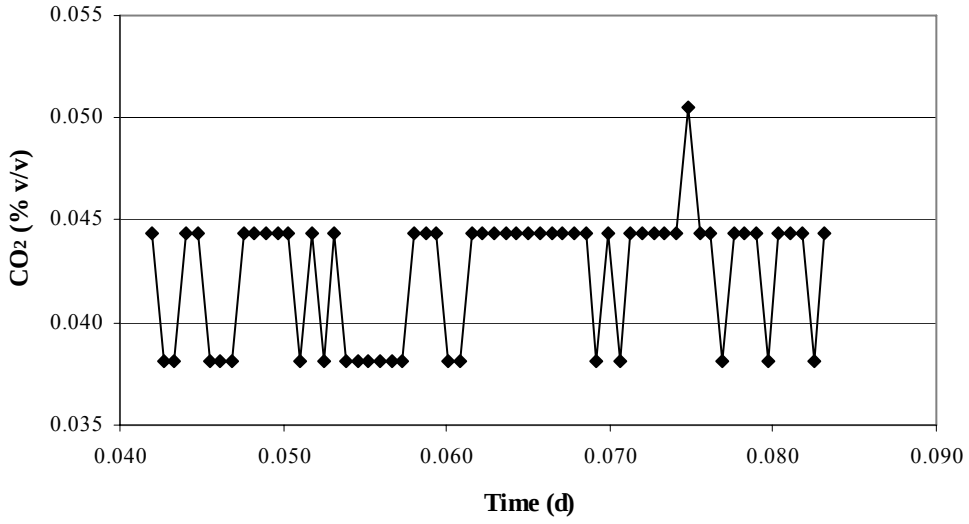

Figure 8.8 CO_2 concentrations in ambient air over a 1 h period.

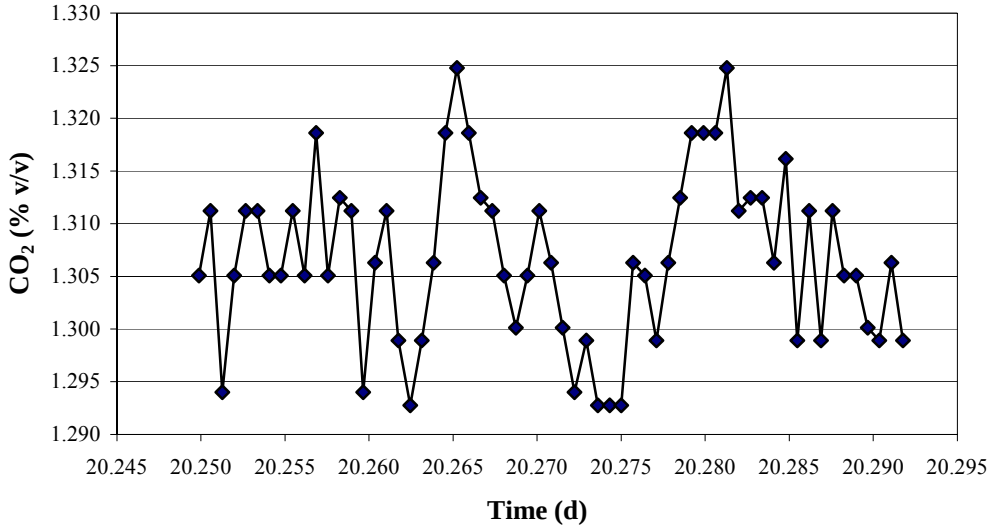

Figure 8.9 CO_2 concentrations in the exit gas over a 1 h period.

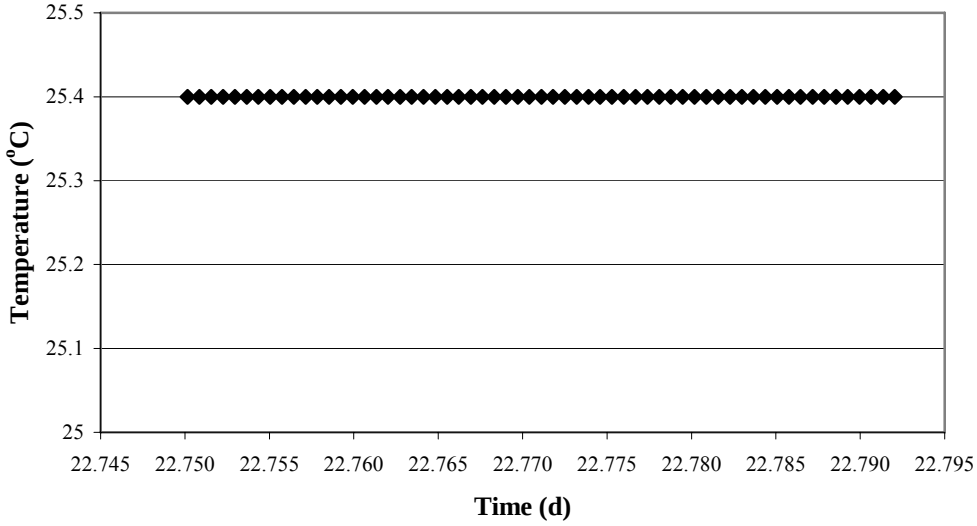

Figure 8.10 Ambient air temperature readings over a 1 h period.

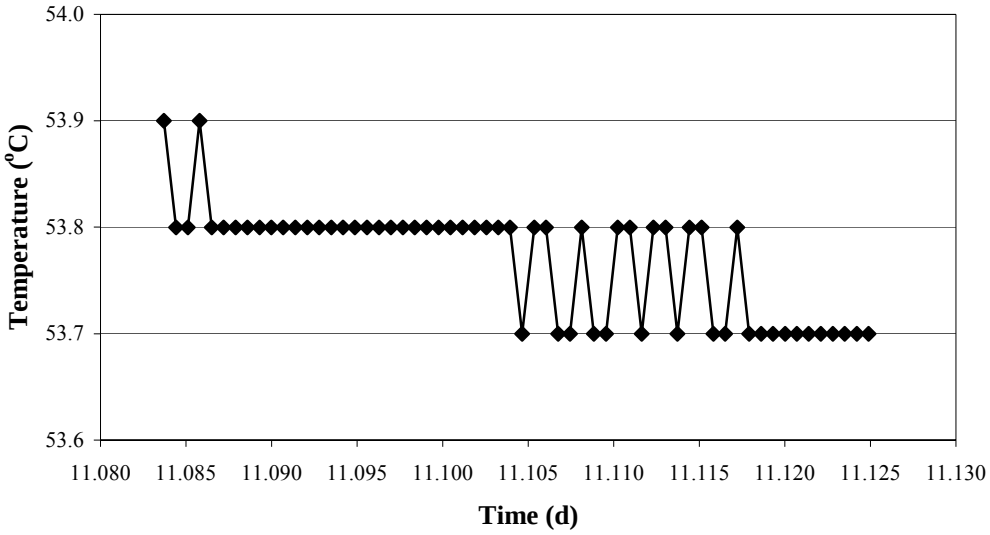

Figure 8.11 Compost temperature readings over a 1 h period.

Temperature sensor readings showed both no change at all (figure 8.10), and fluctuations of 0.1 °C, over the selected hourly periods (figure 8.11). The patterns suggested that these fluctuations were most likely due to the sensor moving between two real readings, rather than indicating random noise. However, in order to avoid the possibility of computing false rates of temperature change in subsequent calculation routines (i.e. 0.1 °C/min = 6 °C/hr), a minimum calculation interval of 60 minutes was specified (see Appendix 2). A complete set of example graphs for each sensor is given in appendix 11.

8.6.3 Composting system performance

The experimental column and simulated feedstock reproduced conditions similar to those reported at full-scale. Temperatures within the column increased rapidly following the commencement of aeration, with thermophilic temperatures attained within 22-23 hr of start-up, and the lower disinfection limit of 55 °C reached within 26-35 h (figures 8.12, 8.13). Maximum rates of increase were 5.4 and 5.7 °C/h, for runs A and B respectively (table 8.5). These rates are similar to those around 4 °C/h reported by Alkoaik and Ghaly (2006) for the composting of dairy manure, tomato plant residues, wood shavings and urea, in a laboratory-scale completely-mixed horizontal reactor, but greater than rates for tomato plant residues and woodchips, seeded with municipal solid waste compost, reported by Alkoaik and Ghaly (2005).

Table 8.5: Temperature profile parameters

Parameter	Units	Location (mm above baseplate)	Run A	Run B	Comments
Peak temperature	^{o}C	[a,b]750; [b]600	82.3	78.7	[a]: Run A; [b]: Run B
Time to peak	h	-	43	42	-
Maximum rate of temperature increase	^{o}C/h	750	5.3	4.7	-
		600	5.2	5.7	-
		450	5.1	5.3	-
		300	5.4	5.6	-
		150	4.4	3.8	-
A_{40}	^{o}C.d	750	787	868	Full-scale aerated static pile: >276-449 ^{o}C.d (Mason and Milke, 2005)
		600	707	691	
		450	491	484	
		300	412	391	
		150	207	189	
A_{55}	^{o}C.d	750	278	330	Full-scale aerated static pile: >71-114 ^{o}C.d (Mason and Milke, 2005)
		600	204	178	
		450	85	84	
		300	64	59	
		150	25	25	

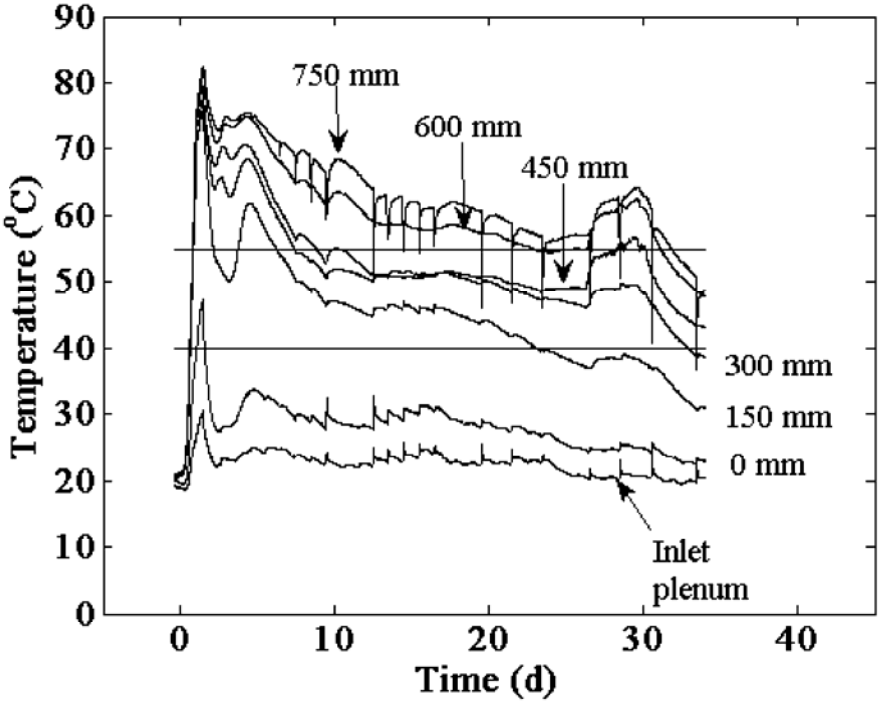

Figure 8.12: Temperature profiles for run A. Numbers in mm are distances above the baseplate.

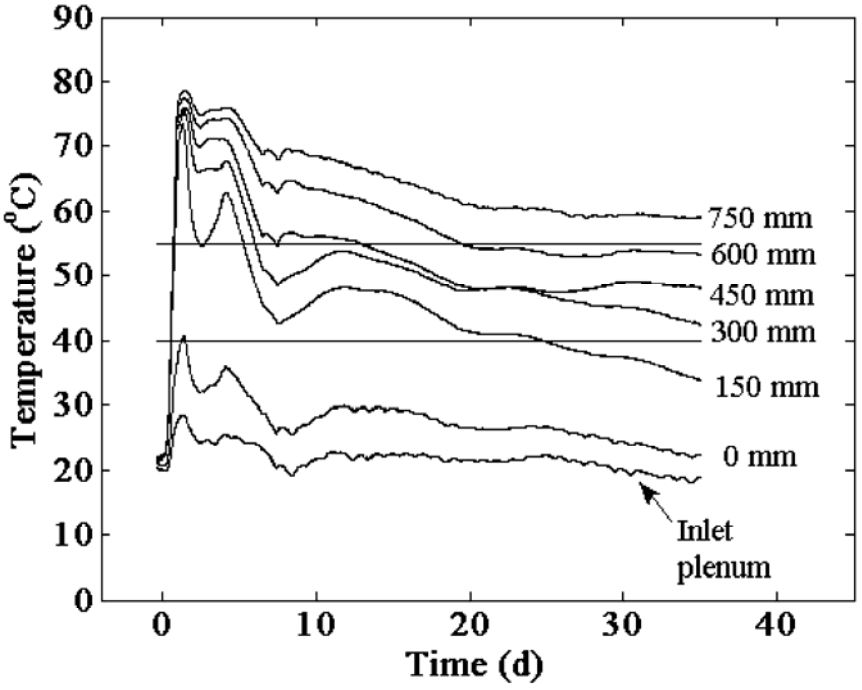

Figure 8.13: Temperature profiles for run B. Numbers in mm are distances above the baseplate.

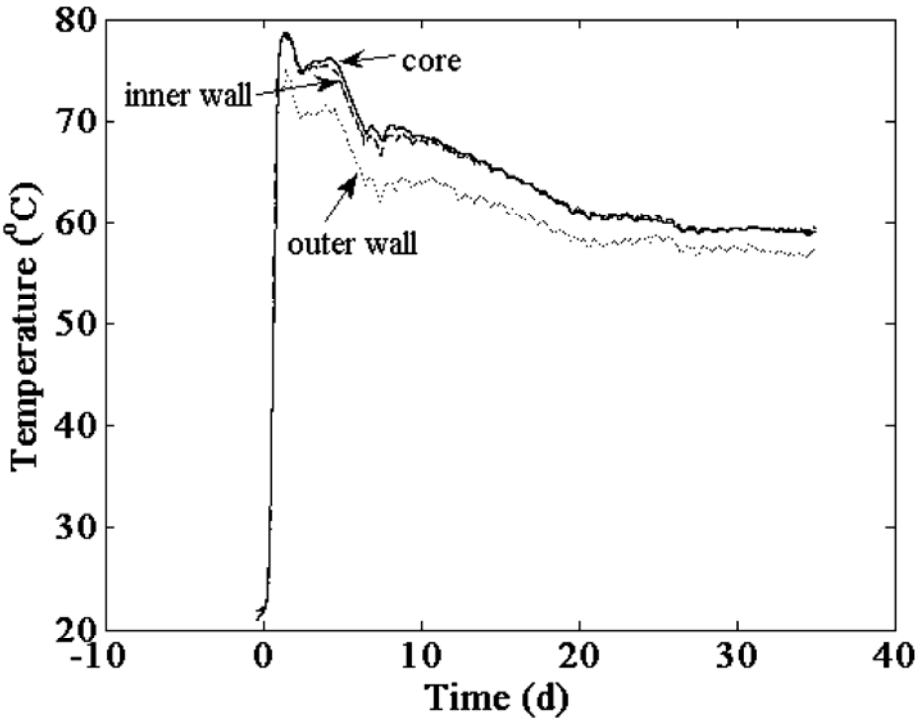

Figure 8.14 Temperature profiles in the upper section of the column (600-900 mm above the baseplate) for run B. Across-wall temperature differences are detailed in Appendix 4.

Peak temperatures of 82.3 °C (run A) and 78.7 °C (run B) were attained 42-44 h after start-up, however the magnitude and duration of these peaks was determined by the manual ventilative heat management (VHM) strategies employed. In order to keep temperatures within the optimal range for composting in future runs, earlier increases in airflow rate are indicated. The time-temperature performance indicators A_{40} and A_{55} (Mason and Milke, 2005) showed that conditions were on average representative of a full-scale aerated static pile environment (table 8.5). However, considerable variation occurred along the column vertical axis, indicating that related variations in the degree of substrate degradation could be expected. Temperatures across the walls and lid were generally controlled to within design specifications, noting that differentials > 1 °C were allowed at temperatures over 60-65 °C to augment the VHM strategies. An example graph of core and wall temperature profiles in the upper section of the column is shown in figure 8.14. Here radial temperature differences can be seen, with a very flat radial profile at later time. It is also clear that in this section across wall differences frequently exceeded 1 °C. In the middle section, a declining temperature gradient across the wall, from inside to outside, was measured, but inner wall temperatures in excess of those at the core were recorded in both runs. An example graph from run B is

shown in figure 8.15. This was unexpected and did not occur in either the upper or lower sections. Possible explanations include a faulty core temperature sensor in which case the core temperature readings may be incorrect, downward movement of the core sensor, or a faulty controller circuit, in which case the middle section heating cable could have been actively heating the compost, rather than simply controlling the heat loss as intended.

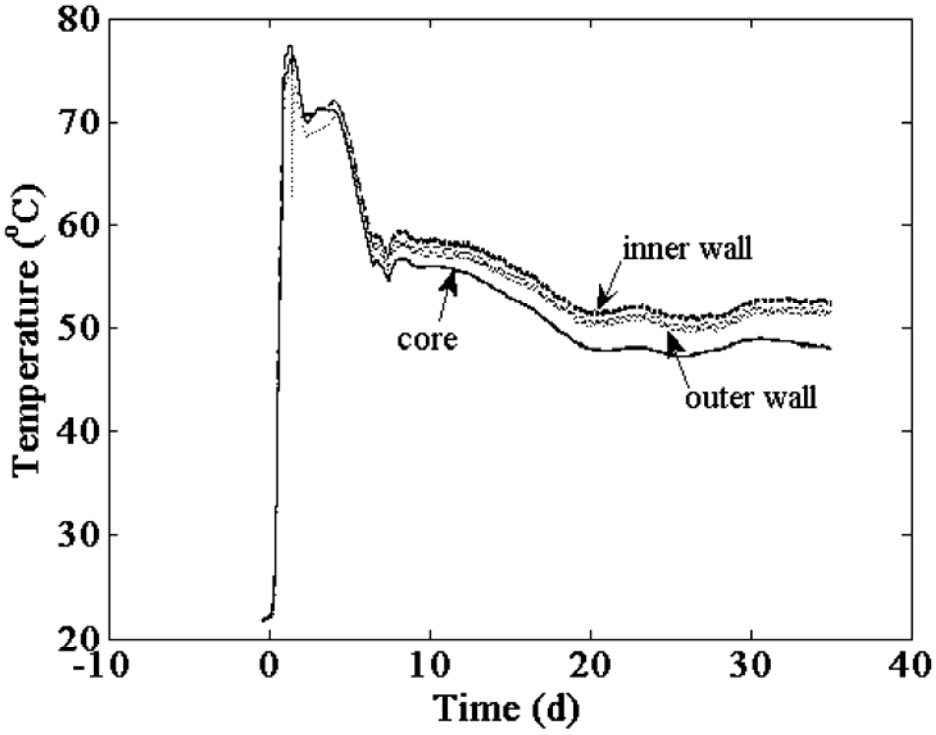

Figure 8.15 Temperature profiles in the middle section of the column (450 mm above the baseplate) for run B. Across-wall temperature differences are detailed in Appendix 4.

Temperature differences between the core and inner wall sensors in the same ambient air after the experimental period ranged between 0 to +0.4 ^{o}C (figure 8.16), which suggests that the first proposition was incorrect. In figure 8.15 it can also be seen that the inner wall temperature remained greater than the outer wall temperature, which would not be expected if heat was flowing into the column. When inspected at the end of each run core temperature sensors were found to have moved from their original positions, and the movement for run B is shown in table 8.6. Given the relatively steep temperature gradient existing along the vertical axis (figure 8.13), it is feasible that the lower core temperature could have been due to the lower position of the sensor.

Table 8.6: Core temperature sensor movement in Run B

Initial height (mm)	Final height (mm)	Movement (mm)	Comments
750	745	-5	Mid-point section 1
600	560	-40	-
450	430	-20	Mid-point section 2
300	295	-5	-
150	155	+5	Mid-point section 3

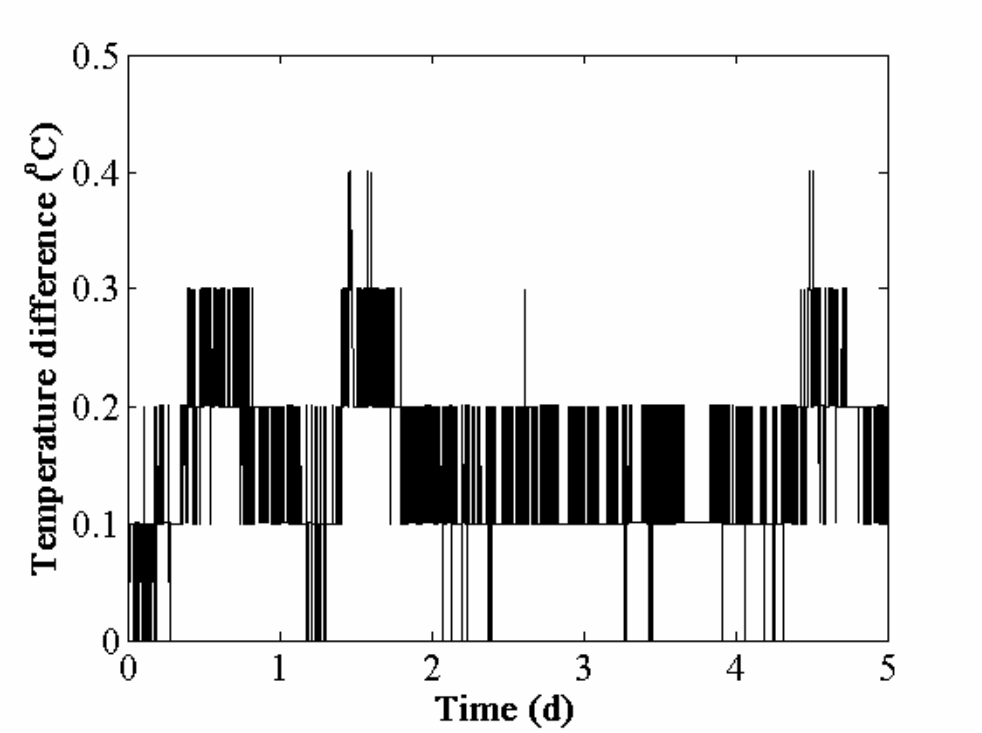

Figure 8.16 The temperature differential between the 450 mm core and inner wall temperature sensors, in ambient air, following the experimental period.

Unwanted heating due to false differential signals arriving at the controller on account of inherent differences in sensor output was prevented by the matching inner and outer wall temperature sensors prior to the experimental period, and placing them so that any sensor which read slightly higher on calibration was located on the inside wall. However from casual observations during both runs it appeared that the middle section heater was on full power more often than were the other two wall section heaters. Additionally, an unexpected rise in the core temperature at 450 mm from day 25 is mirrored in a temperature rise at the inner wall (figures 8.14 and 8.15), which could be attributed either to heat inflow or to moisture fluctuations. Thus it seems possible that this particular heating control system may

have been faulty, but the evidence remains inconclusive at this point. For a complete set of temperature results the reader is referred to Appendix 4.

Peak biological power output ("biopower") values for runs A and B were approximately 14.0 and 14.3 W/kg-TS, respectively (table 8.7). The latter values compare to 20-28 W/kg-DM reported by Mote and Griffis (1982), and a maximum value of 38 W/kg-VS reported by Harper et al. (1992). If the present results are expressed on a substrate plus amendment TS basis only, i.e. woodchips are ignored, the peak specific power values become 35 and 37 W/kg-TS, which are very close to the Harper et al. result.

Table 8.7: Calculated "biopower" values

Power	Units	Run A	Run B	Comments
Peak	W	186.7	184.5	-
	W/kg-TS	14.0	14.3	-
Average	W	23.9	31.5	Run A,33.2 d; Run B 34.2 d
	W/kg-TS	1.8	2.4	

Cumulative energy profiles showed the expected distribution between the components of the energy balance for a CTD reactor, with nett ventilative transport accounting for about 90 and 88% of the "bioenergy" generated for runs A and B respectively (table 8.7). This confirms the ability of this experimental system, given the stated assumptions, to simulate a full-scale composting temperature environment (see chapter 3). Cumulative energy and energy ratio curves for run B are shown in figures 8.17 and 8.18, and a full set of power and energy profiles for both runs is presented in Appendix 5.

Table 8.8: Final cumulative energy distribution (% of "bioenergy")

Energy	Run A	Run B	Comments
Nett ventilative	90.4	87.6	-
CCR	5.6	8.8	-
Accumulation	4.0	3.6	-

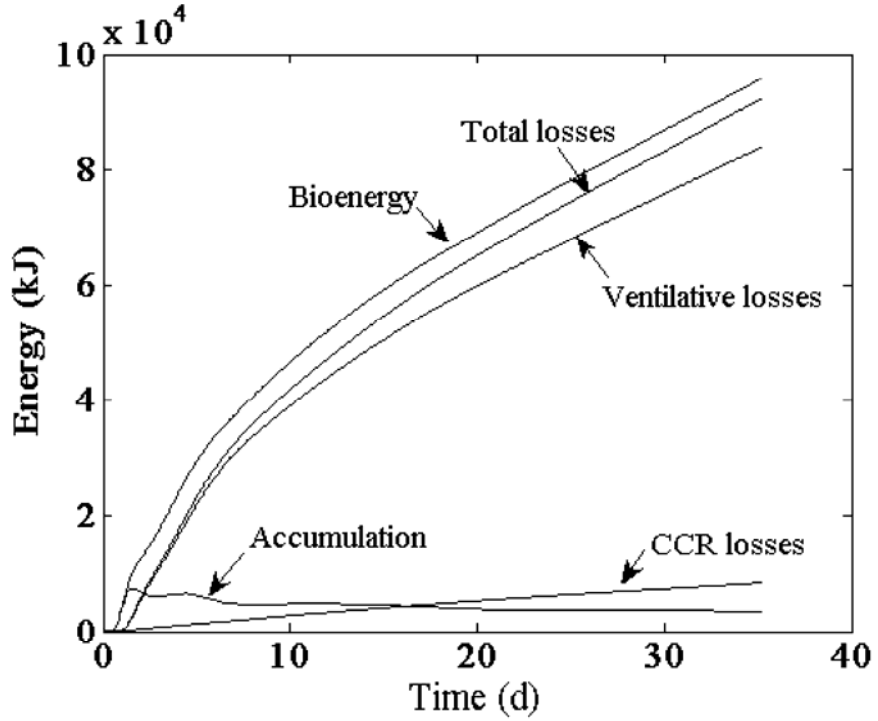

Figure 8.17 Energy profiles for run B.

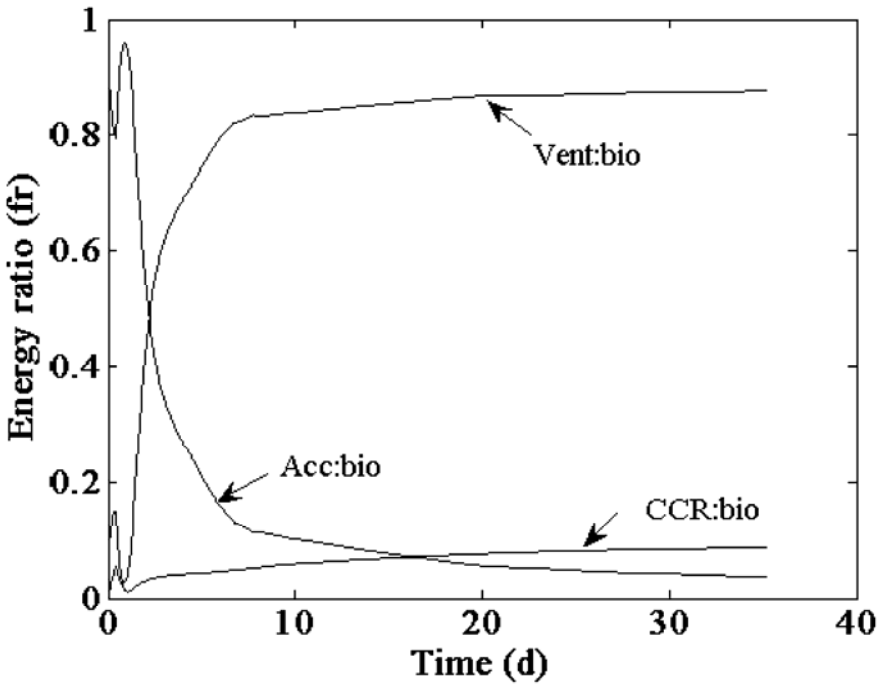

Figure 8.18 Energy ratios for run B.

Abbreviations: Vent = ventilative; Acc = accumulation; bio = biological

Energy and power calculations reported by Hogland et al. (2003) and Lyberg and Hogland (2004), show energy distributions obtained when wall losses are relatively high, but otherwise cannot be directly compared with the present results, due to lack of mixture solids information in these papers. The important calorimetric work of Weppen (2001) on a 30 l laboratory-scale composting reactor has been already been referred to earlier (see also chapter 4), and is cited again later in this chapter.

The present system was shown to maintain moisture levels within the optimum range reported by Rynk (1993). Average moisture levels in the composting material at the end of both runs ranged between 54 and 71% (figure 8.19).

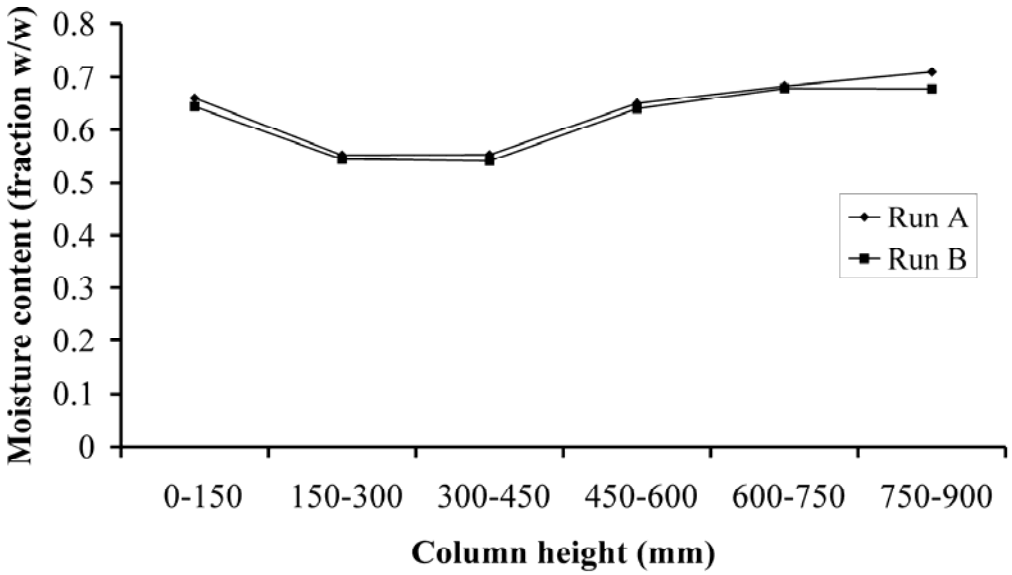

Figure 8.19: Moisture profiles at the conclusion of runs A and B.

However, the radial distribution of moisture in the lower half of the column was found to be uneven at the end of both runs, with some segments showing evidence of preferential moisture flow, whilst other segments in the same plane showed overdrying. Typical dry areas located between 0 to 450 mm above the baseplate had moisture levels of 10.2-12.6%, whilst neighbouring wet areas had moisture levels between 70.7-79.5%. Thus some proportion of the mixture would be expected to have degraded to a lesser degree than if moisture had been distributed evenly. A qualitative layerwise depiction of the moisture distribution at each layer is shown in figure 8.20.

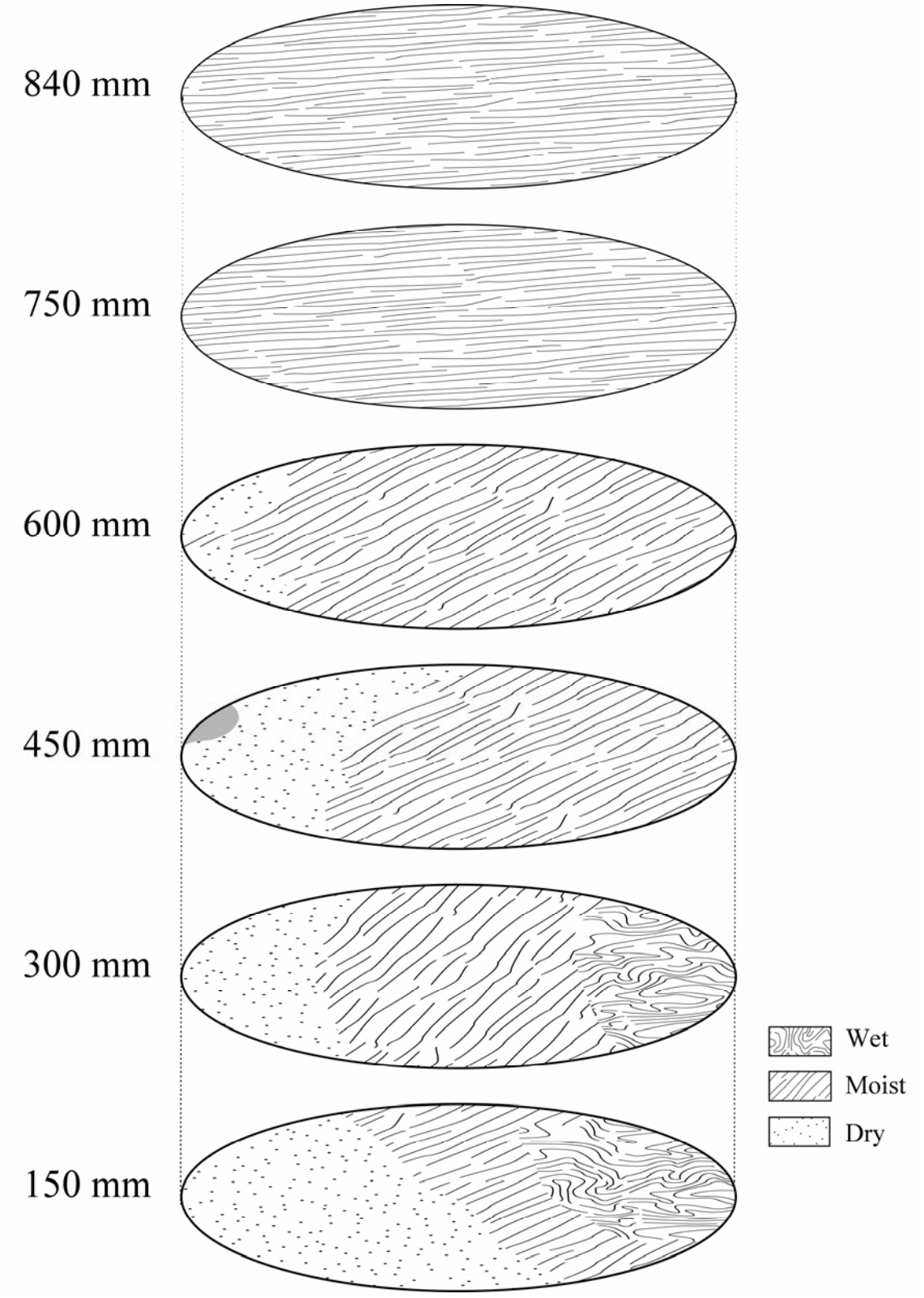

Figure 8.20 Moisture distribution in horizontal cross sections of the composting material at the conclusion of run B, at marked distances above the baseplate. NB: i) 840 mm was the top surface of the compost; ii) the light grey shaded area at 450 mm represents a hollow space.

Leachate was produced in both runs, commencing between day 5.5 and 6.5, in both cases, and showing a decreasing production rate with time in run B (figure 8.21). Leachates were mid-brown in colour, and had a light musty odour, with no indication of anaerobic conditions. The final quantity produced in run B (including residual leachate in the inlet plenum) amounted to 10% of the initial water added with the mixture (Appendix 6).

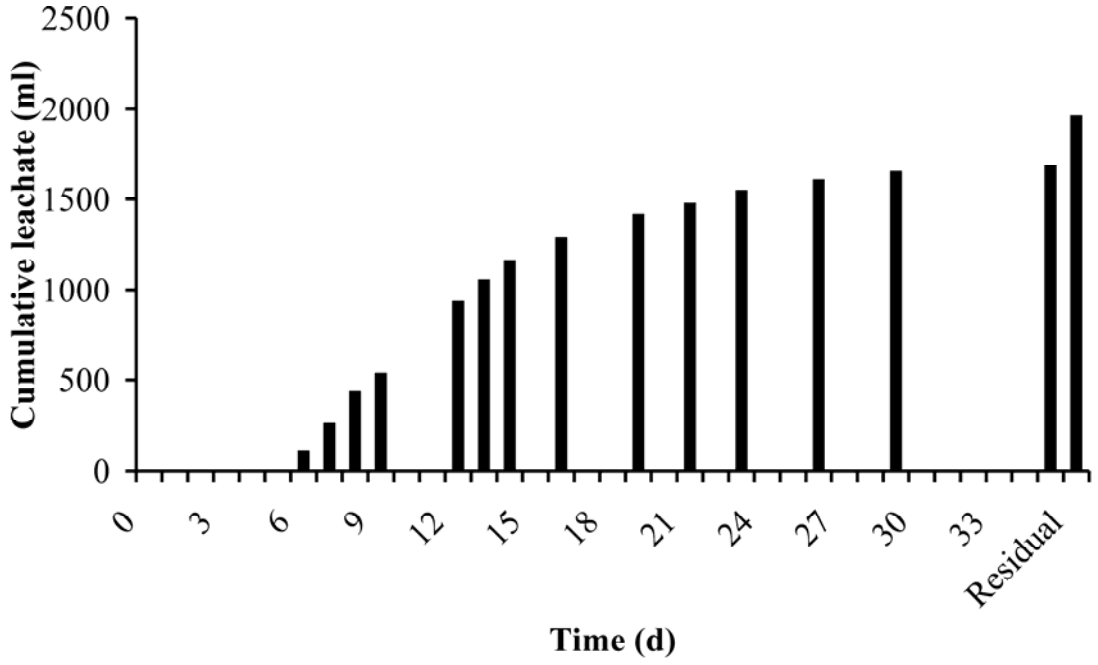

Figure 8.21: Leachate production during run B.

Total carbon levels in the leachate from run B ranged from 1540 to 6250 g-C/m^3, and the quantity of carbon removed amounted to approximately 8 g-C (Appendix 6).

The patterns of total mass loss followed a curvilinear profile, which was more pronounced in run A where leachate was returned, than in run B, in which leachate was removed. The step changes resulting from the latter may be observed in the profile (Appendix 7). Total mass losses (including residual leachate) amounted to 14.6 and 17.2% of the initial wet weight of material in runs A and B respectively. This is low in comparison to expectations for normal composting, due to the return of condensate to the present system.

8.6.4 Measured substrate degradation profiles

Measured cumulative CO_2 carbon (CO_2-C) evolution patterns for both runs were derived from CO_2 concentration profiles (Appendix 8), using the ideal gas law (see "plotdata"; Appendix 2). The cumulative patterns were characterised by a short lag phase followed a convex curve, with close replication obtained between runs (figure 8.22). Some irregularities occurred in both curves, coincident with changes in airflow rates, and at later time. When modelled using a single exponential expression, the fit was moderate to good, but with clear under-prediction at later time (figure 8.23). As expected the lag phase was not modelled. The total amount of CO_2-C removed was approximately 1.2 kg, which compares with 1.1 (±0.1) kg carbon removal obtained from raw mixture and finished compost analyses in Run B (table 8.9) and represents about 20% biodegradable carbon (total mixture basis) or approximately 50% biodegradable carbon (substrate plus amendment only).

Table 8.9: Energy, carbon and nitrogen in compost materials (Run B)

Parameter	Units	Initial mix	Final compost	Removal	Removal (%)
Gross energy	MJ	231.2 (2)	164.1 (3)	67.1 (4)	29.0 (1.8)
Carbon	kg-C	5.7 (0.1)	4.6 (0.1)	1.1 (0.1)	19.9 (2.1)
Nitrogen	g-N	102 (5)	103 (4)	-1 (5)	-1.5 (4.9)

Note: errors in brackets

Errors in the values of cumulative CO_2-C emitted were estimated using the mid-point of the observed error range in exit gas CO_2 concentrations of ± 0.025% (Figure 8.22). Since the error in airflow readings was an order of magnitude less, this was ignored. The discrepancy between the loss of carbon from the solid phase and in CO_2-C emitted is within experimental error. However, as previously noted, non-CO_2 volatile organic compounds (VOCs) will be lost in the exit gas (Elwell et al., 1996), and losses can also occur in leachate. Carbon losses in the leachate removed from run B were approximately 0.5% of CO_2-C losses in the exit gas and can be ignored. No information on VOC levels in the exit gas was available, but these can be expected to be similarly insignificant. The energy loss shown in table 8.9 is broadly consistent with the change in solid phase carbon, whilst the nitrogen results are within experimental error. The duration of the lag phase was less than 1 d in both runs (figure 8.24). Modelling from 0.5 d onwards would eliminate that part of the data, which cannot be modelled by a single or double exponential function, and thus provide a better fit for these functions. This idea was first mooted in chapter 5 and will be further discussed later.

a) Run A

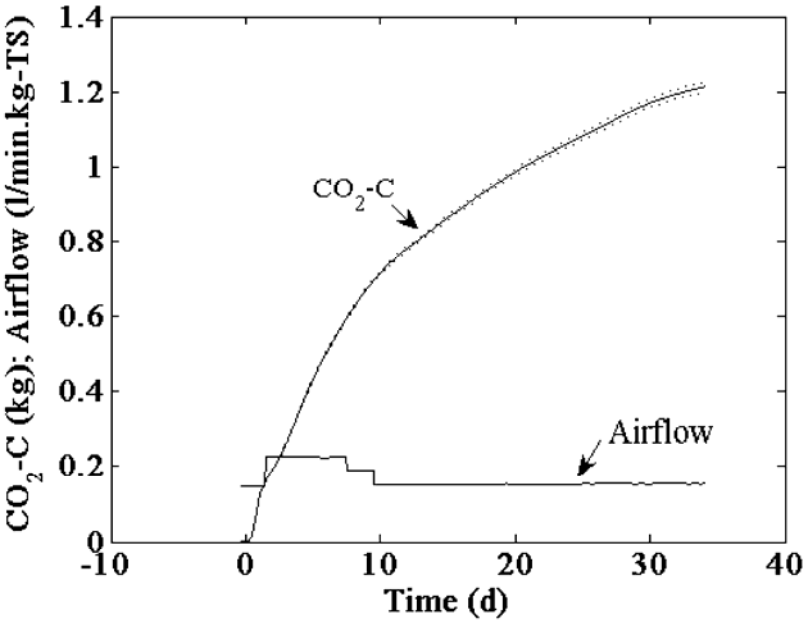

b) Run B

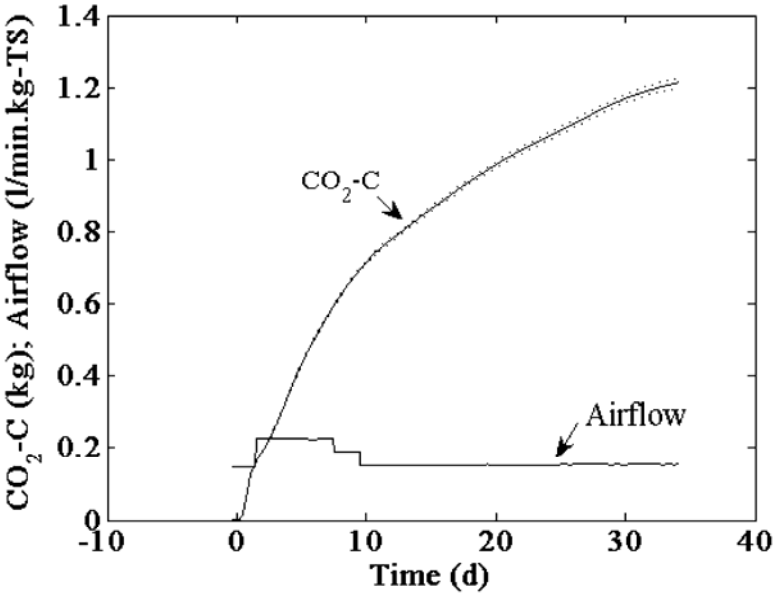

Figure 8.22: CO_2 and airflow profiles. Key: ___ data; … data ± observed error. Uncertainty in the final mass of CO_2-C emitted due to the observed error was ± 0.014 kg, or ± 1.1% of the maximum calculated value of CO_2-C.

a) Run A

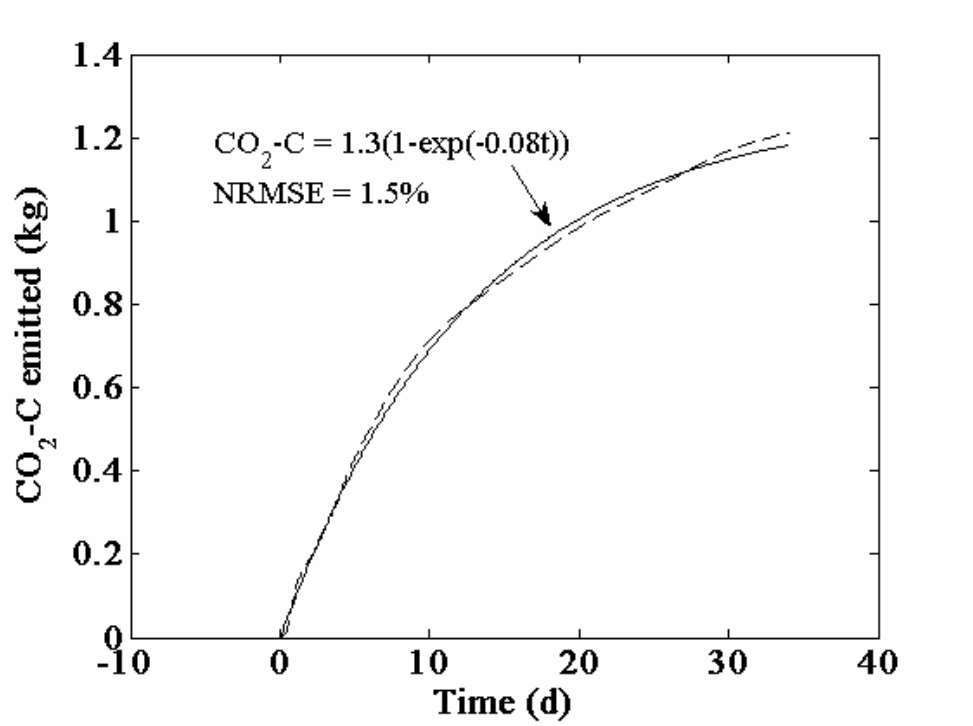

b) Run B.

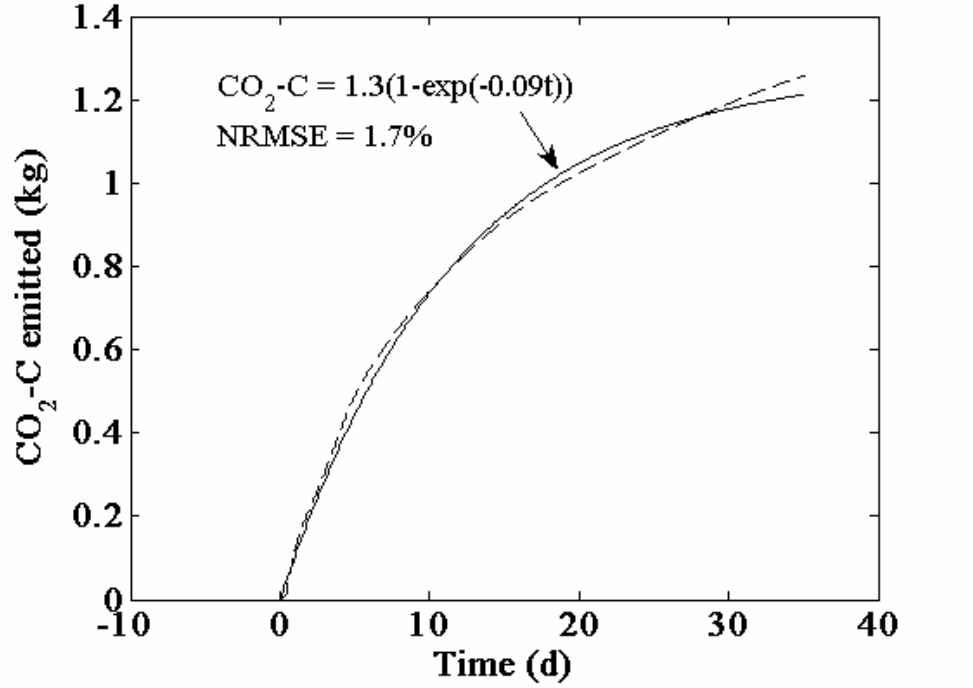

Figure 8.23: CO_2-C profiles fitted with a single exponential model.

Key: ___ model; --- data

Uncertainty in the final data value of CO_2-C is 1.1% of the modelled CO_2-C max.

a) run A

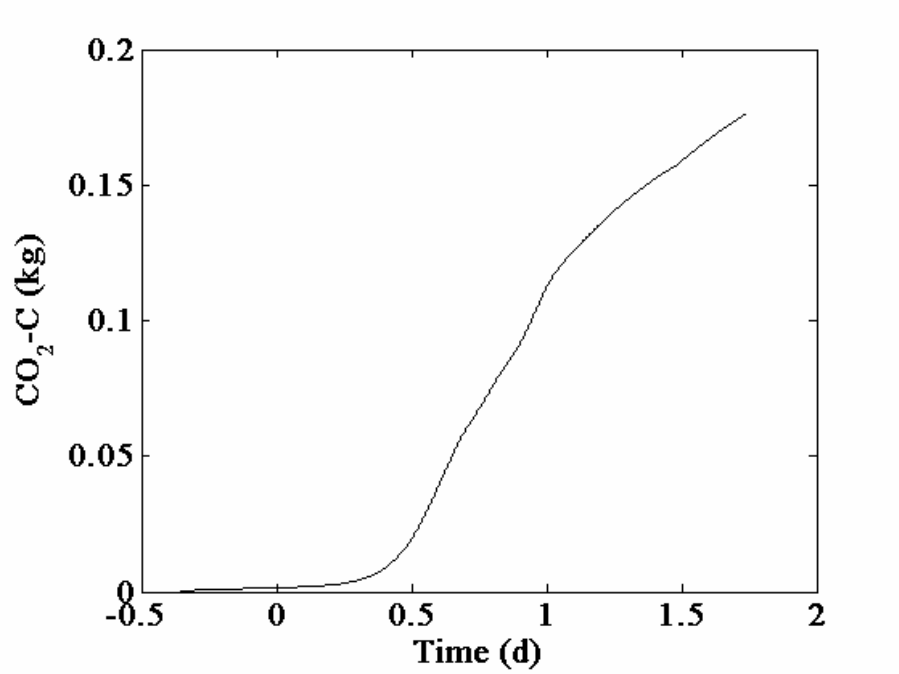

b) run B

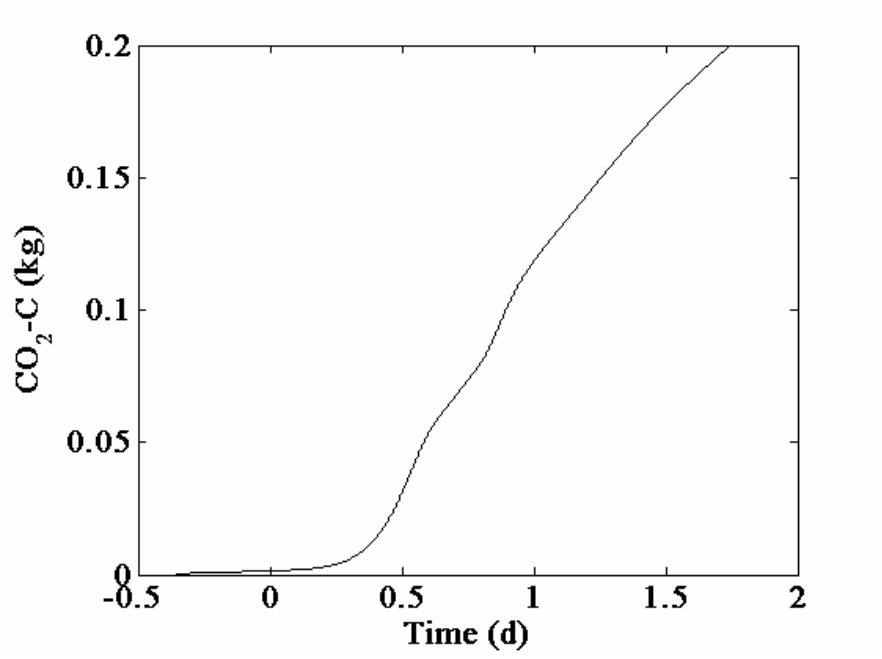

Figure 8.24 CO_2-C profiles at early time.

8.6.5 Predicted substrate degradation profiles

Predicted BVS carbon (BVS-C) profiles were calculated from Eqs. 4 through 8, using the input values reported in table 8.2 and Eq. 9. Profile shapes were generically similar to those for CO_2-C, but different in detail, particularly at later time, when the two profiles diverged markedly (figure 8.25). It appeared that the BVS-C data would also be amenable to fitting by a single exponential model, and results are illustrated in figure 8.26. The fit was rated as moderate in both cases, but replication between the two runs was good, with the model under- and over-predicting at the same times. The quantitative difference between the predicted BVS-C and measured CO_2-C profiles is more readily seen in figure 8.27, and this may be attributed to a number of experimental and modelling factors, which will be discussed in section 8.7.

Random errors were estimated using the observed fluctuation in temperature readings of ± 0.1 ^{o}C (Tab. 8.4). Airflow and mass errors were significantly less on a proportional basis and were therefore ignored.

Run A

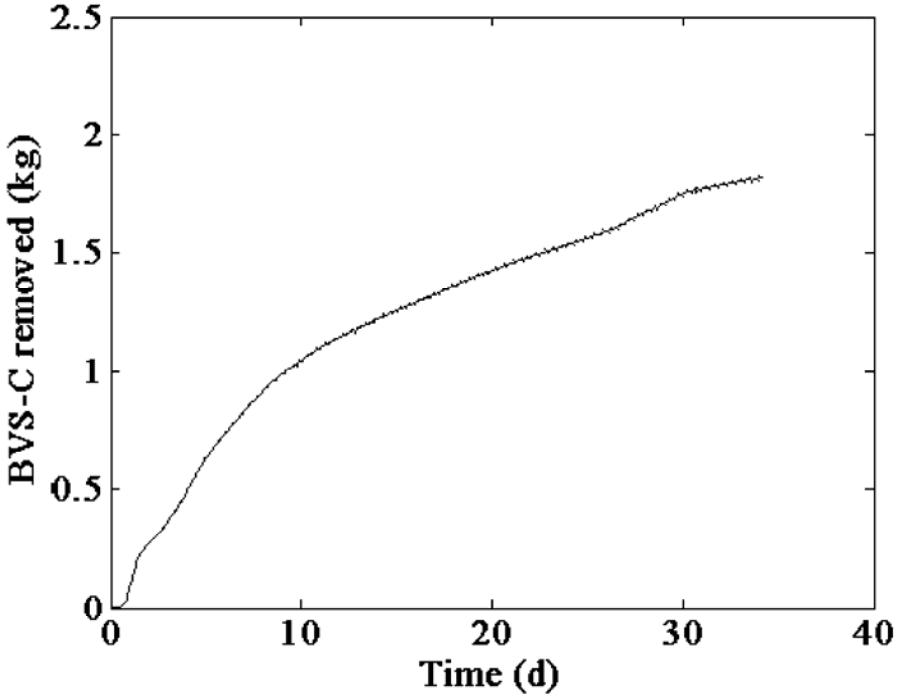

Run B

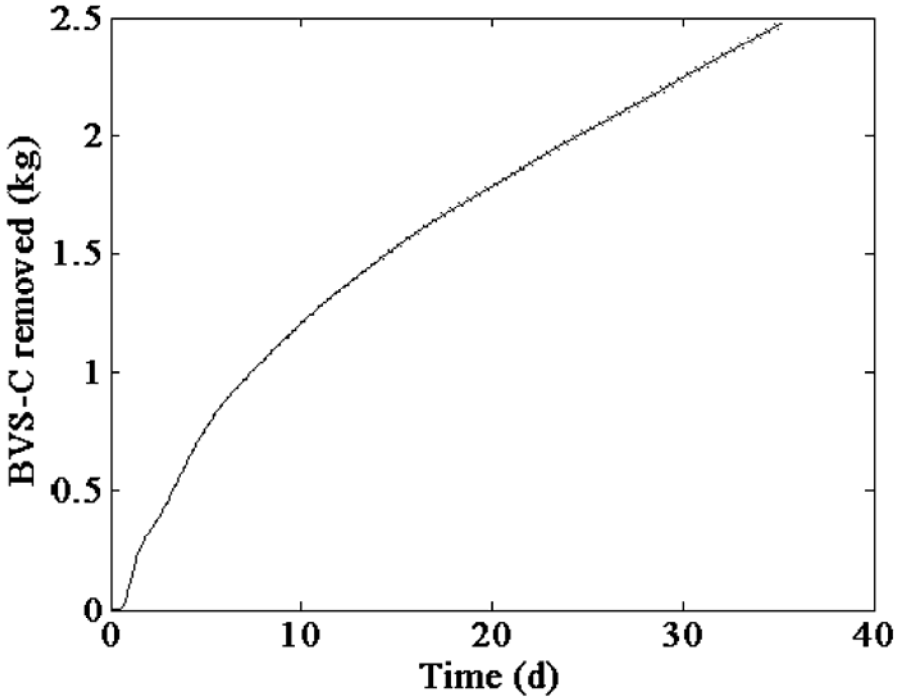

Figure 8.25. Predicted BVS-C profiles. Key: ___ data; … data ± observed error. Uncertainty in the final mass of BVS-C emitted due to the observed error was ± 0.010 (run A) and 0.014 kg (run B), or ± 0.6% of the maximum calculated value of BVS-C.

Run A

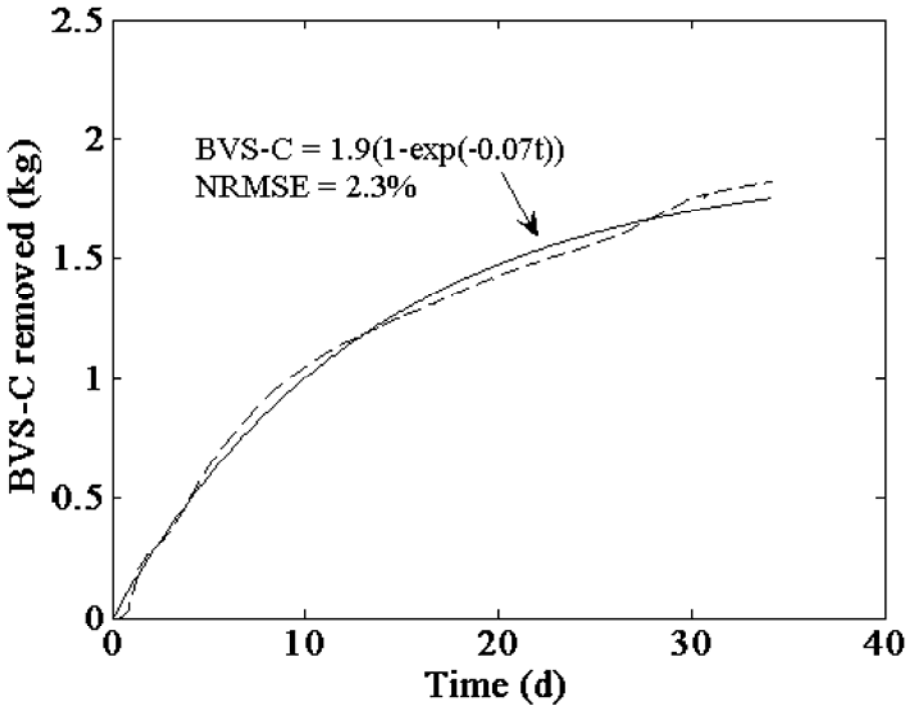

Run B

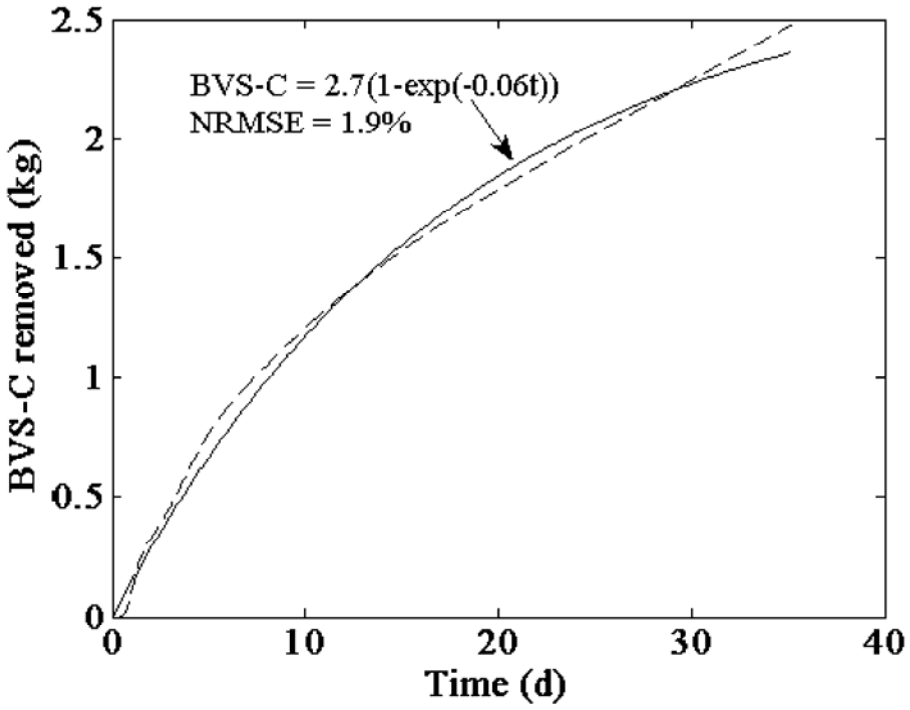

Figure 8.26. Single exponential model fitted to BVS-C data.

Uncertainty in the final data value of BVS-C was 0.5% of the modelled BVS-C max for both run A and run B.

Run A

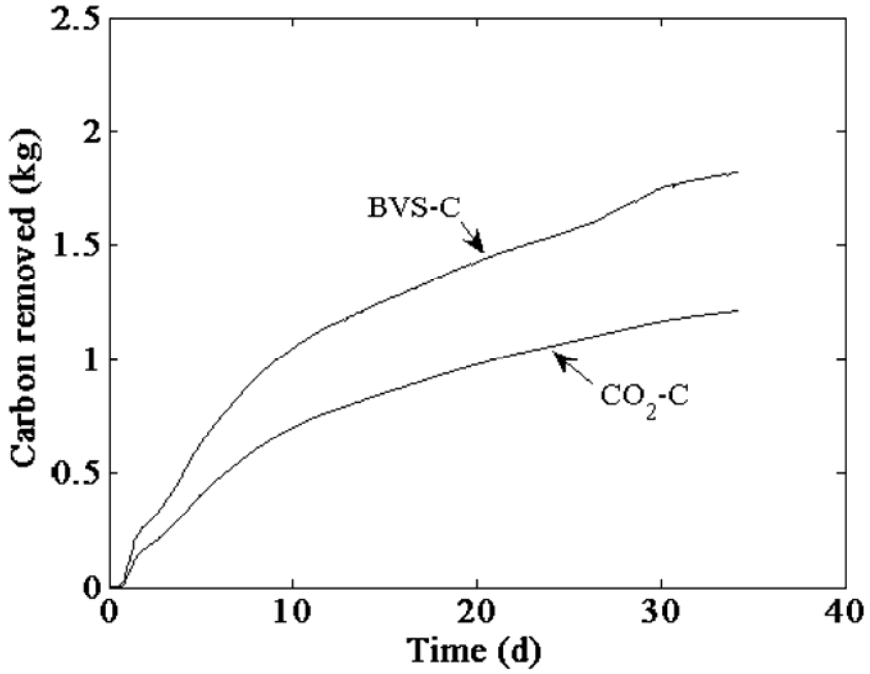

Run B

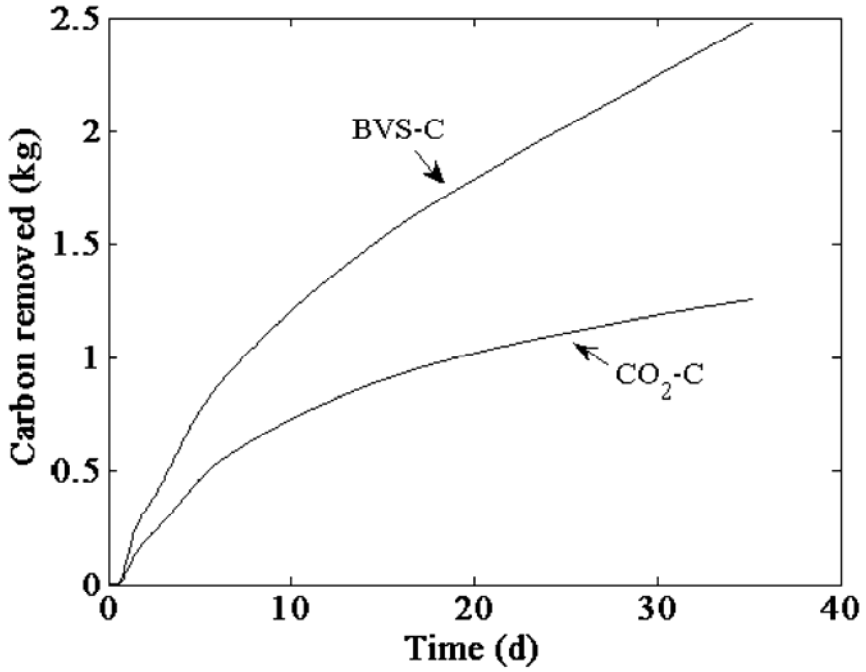

Figure 8.27. Measured and predicted carbon removal

8.6.6 Temperature-corrected profiles

The temperature correction procedure to adjust the CO_2-C and BVS-C profiles to 40 ^oC, requires a single temperature profile (see chapter 6, and "VSplot_p6_exp" in appendix 2). This was selected by taking the average A_{40} value for each run, noting the height at which this was most closely matched, and then using the temperature profile measured at that level. In both runs the temperature profile at 450 mm above the baseplate i.e. the mid-point of the column, was selected. Cardinal temperatures used in this case were 5, 59 and 85 ^oC. The minimum and optimum values were as used previously (Chapter 6; Mason, in press-b;) and the maximum value was chosen in response to the fact that although peak temperatures of approximately 76 ^oC were recorded at this level, there was not a major decline in CO_2 output, and therefore a 9 ^oC margin between this and a maximum temperature for microbial growth seemed reasonable.

Temperature-corrected profiles for both CO_2-C and BVS-C were multi-phase in shape (figures 8.28 and 8.29). Similar results were obtained when applying the temperature correction procedure to varying temperature profiles from the literature (see chapter 6) and these findings together with the present experimental results suggest that a re-examination of the way in which temperature-correction factors are applied and/or the cardinal temperatures chosen, may be in order. These matters are explored further in section 8.7.

Random error in both the CO_2-C and BVS-C profiles shown in figures 8.22 and 8.25 is applied to the temperature corrected profiles in the same proportion. Thus the 1.1% uncertainty in the final data value of CO_2-C, and 0.5% uncertainty in the final data value of BVS-C, are taken into account when assessing the goodness of fit of the double exponential model later in this chapter. In qualitative terms, this means that a conservative approach is required in which it is conceded that a curve showing a moderate degree of fit based on appearance and NRMSE alone, may in fact be providing a good fit, when the random error band around each data point is considered.

Run A

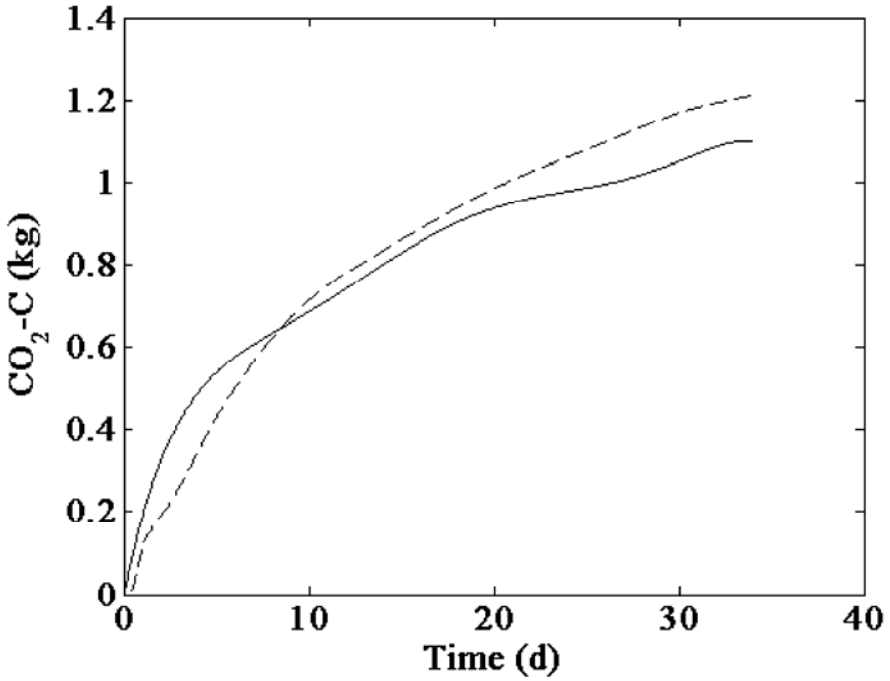

Run B

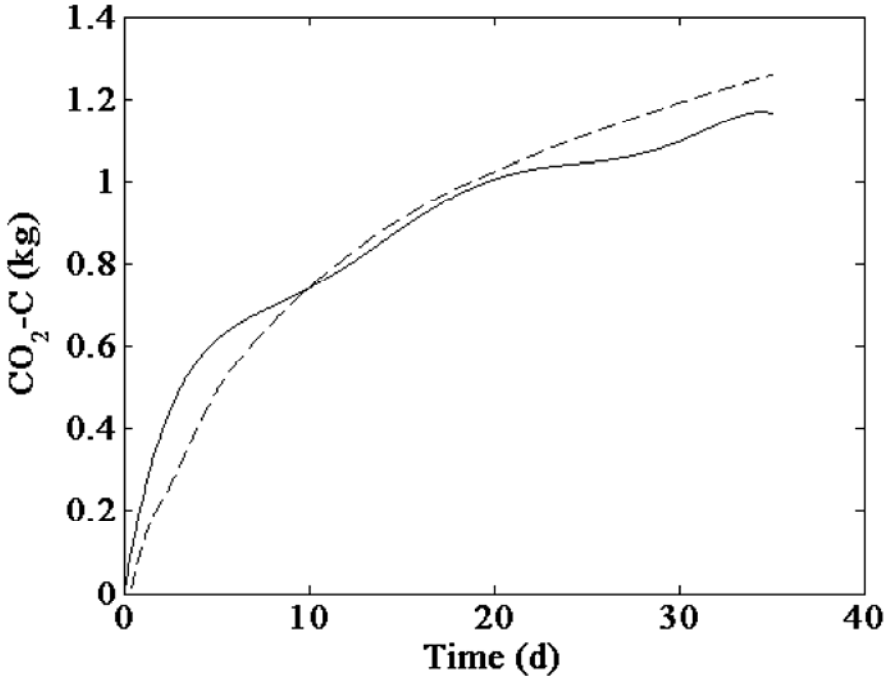

Figure 8.28 Temperature-corrected CO_2-C profiles. Cardinal temperatures: 5, 59 and 85 ^{o}C.

Key: ___ 40 ^{o}C; --- varying temperature

Run A

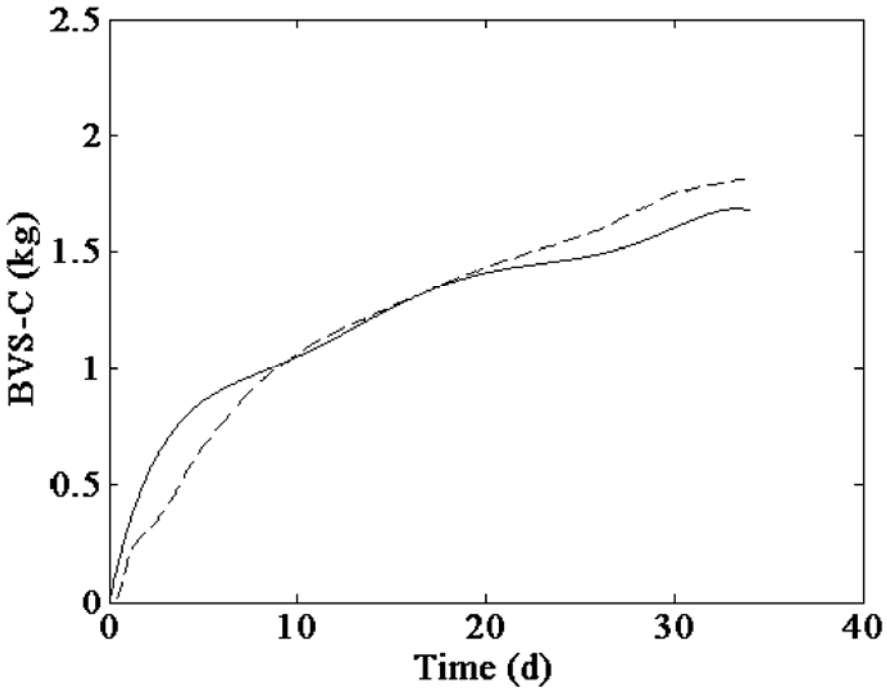

Run B

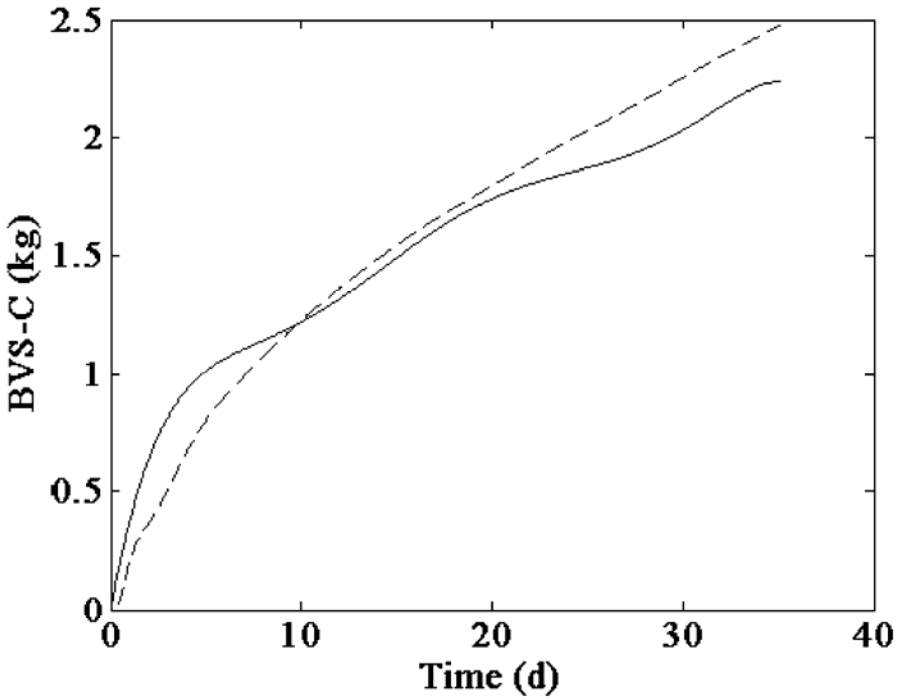

Figure 8.29 Temperature-corrected BVS-C profiles. Cardinal temperatures: 5, 59 and 85 ^{o}C

Key: ___ 40 ^{o}C; --- varying temperature

8.7 Discussion

8.7.1 Simplifications and assumptions

Experimental simplifications included setting the bottom system boundary at the baseplate of the column rather than at the bottom of the plenum chamber, ignoring the enthalpies associated with leachate removal, leachate return and condensate return, and assuming a standard atmospheric pressure of 760 mm Hg in the enthalpy calculations. The enthalpy associated with leachate removal in run B was estimated at 250 kJ over the entire run, whilst the sensible load for reheating returned leachate in run A was estimated at 1300 kJ over the entire run (see Appendix 5, figure A5.15). Both are negligible in relation to the enthalpies generated by microbiological activity, transported ventilatively and lost through the column walls. It was not possible to measure the enthalpy associated with condensate return, due to a shortage of temperature sensors and data logging channels. However, since cooled condensate travelled along the same tube as hot exit gas, some heat exchange would be expected before the condensate re-entered the system, leading to a decreased load on the top compost layer. As there was no discernable drop in compost temperatures at the 750 mm level, in contrast to the severe depressions recorded following leachate return in run A (figure 8.12), this assumption was considered reasonable. Fluctuations in atmospheric pressure were not recorded due to a shortage of equipment, but as shown in the sensitivity analysis (Appendix 3, figure A3.6) the likely impact was negligible.

Similarly the density of inlet air was not corrected for temperature and pressure fluctuations, nor for moisture content, but these were considered to be of negligible importance. However, it would be a useful improvement to future experiments to place a silica gel filter upstream of the air flowmeter to address the latter issue, and also upstream of the CO_2 probe, in order to minimise unwanted condensation on the sensor surface. As mentioned in section 8.6.4, non-CO_2 volatile carbon losses in the exit gas were not measured. These losses would be expected to be highest at early time and, whilst it would be valuable to know their magnitude, it would be surprising if they amounted to a significant quantity of carbon. The convective heat transfer coefficients used represented the low end the range for free convection quoted by Mills (1995), but may not accurately describe the across-wall resistance to heat transfer in this reactor. This comment applies particularly to the outside wall, where the temperature sensor was fixed in position using a PVC block (figure 8.4d) with a small airspace surrounding the sensor, and the wall and heating cables were wrapped with insulation. In this respect the use of a convective heat transfer coefficient on the outside wall is simply a

surrogate for the actual heat transfer characteristics of this environment. The assumption of a constant overall heat transfer coefficient should be examined prior to future work. Weppen (2001) presented data for a 30 l laboratory-scale reactor showing that experimentally measured heat conductivity increased by a factor of approximately 1.5, as the temperature increased from around 30 to 80 ^{o}C, admittedly with a wide spread in the data. However, it was shown in the present sensitivity analysis that the shape of the predicted BVS curve is not altered by variations in set values of U. Exit gas relative humidity was not measured in the present work, due to lack of a sensor resistant to the condensing conditions in the headspace, and was assumed to be 100% throughout each run. This seemed to be a reasonable assumption, given the constant return of condensate, but should be addressed in future work, as any errors will significantly impact on the magnitude of the bioenergy, and thus, BVS predictions. It was noted that the same sensor performed well in the inlet plenum, under near saturation, but low temperature, conditions. The saturated exit gas assumption is widely held amongst composting researchers (see chapter 4). Lyberg and Hogland (2004) reported that outlet air humidity from a vertically-fed pilot-scale reactor varied between 90 and 100%. The heat of combustion (Hc) was assumed to be constant and to represent microbial heat output under composting conditions. Weppen (2001) reported that the specific heat of degradation ranged from 15-19 kJ/g for municipal organic wastes, rising to 22-25 kJ/g when pig fat was added, and these values compare with the mixture value in the present work of 19.6 kJ/kg.

8.7.2 Non-homogeneity

The physical simulation of an aerated static pile, with upflow aeration, led to the development of non-homogenous conditions within the reactor. In particular, vertical temperature gradients occurred (figures 8.12 and 8.13) and moisture distribution was uneven in both the vertical and horizontal planes (figure 8.20). In respect of the latter, there is evidence of a drying front moving up the column, despite the condensate return strategy, and of preferential downwards moisture flow favouring one side of the column, particularly in run A where leachate was returned. It is reasonable therefore to believe that some portions of the mixture, for example dry areas, were not fully contributing to the composting process throughout the duration of each run, as could be said for very wet areas, particularly those towards the bottom of the column. Weppen (2001) suggested that axial temperature and "humidity" gradients resulted in "a deactivation of about 50% of the solid matrix". Thus a compromise situation occurred in the present work in the monitoring of composting performance, where

bulk measures of activity, namely exit gas temperature, relative humidity and CO_2 concentration, were taken to represent the activity of the entire composting mass. The unmixed column format was chosen for experimental convenience, and periodic removal of the contents for mixing and moisture adjustment rejected because of the heat losses which would occur, and for other practical reasons. Thus the results from, and performance of, the system should be interpreted with the non-homogeneity of the contents in mind.

8.7.3 Comparison of measured and predicted profiles

The thermodynamic model (Eq. 4) successfully predicted the generic shape of the measured substrate degradation profile, but under the experimental and modelling conditions adopted, it was found that the values differed in magnitude, and at certain points, the curve shapes differed in detail. As seen previously, the measured CO_2-C data from both runs was moderately to well fitted by a single exponential function, with close replication shown both visually, and in the values of the fitted rate coefficients. The latter are within the range previously reported (see Table 4.4, chapter 4; also chapters 5 and 6). This indicates a robustness in the experimental procedures in spite of the internal variations in moisture distribution and different leachate management strategies (see section 8.7.2). The final amount of CO_2-C removed, at approximately 1.2 kg in both runs, compares to a value of 1.1 kg determined from analysis of the initial and final composts in run B. These values are considered sufficiently close, given experimental error, to give confidence in the use of CO_2 measurements as a true indication of carbon removal. In comparison, the predicted BVS-C profiles had a similar curvilinear shape and were moderately well modelled by a single exponential function, with similar values for the fitted rate coefficients. Some portions of these profiles can be seen to mirror changes in the CO_2-C curves, especially at early time, but in other areas clearly different behaviour is apparent. In particular, the trend of each BVS-C curve toward linear behaviour at later time, in comparison to the tendency of the CO_2-C curves to decay towards an asymptote is noteworthy. The final values of BVS-C removed, at approximately 1.8 and 2.5 kg in runs A and B respectively, are clearly well in excess of those measured, and also different from each other, and this finding requires discussion.

In exploring possible reasons for the discrepancies between the measured CO_2-C and BVS-C several key factors will be invoked. As already discussed, the predictive model is particularly sensitive to inlet and exit relative humidity, exit gas temperature, and wall temperatures. Additional factors include the overall heat transfer coefficient U, the fraction of carbon

present within the BVS, the assumption that the entire mass of composting material was contributing to the measured parameters, and the possibility that the mid-section of the column was inadvertently over-heated due to control system malfunction. Should any of these factors (apart from the carbon fraction) cause an over-estimation of the enthalpies associated with either ventilative transport or CCR losses, then biological heat production and consequently BVS-C values will be over-predicted. Should the carbon fraction be too high, then BVS-C will be too high. Considering run B, a reduction of exit gas relative humidity from 100 to 60% would be necessary in order to close the gap between the BVS-C and CO_2-C curves (figure 8.30). Clearly this is an unrealistic proposition, but one which indicates that errors in exit gas relative humidity alone cannot account for the discrepancy. A reduction in the inner and outer convective heat transfer coefficients from 3 to 1 $W/m^2.^oC$ reduces the final value of BVS-C to 2.3 kg, which is also insufficient. A value of 1 $W/m^2.^oC$ is unlikely however. The assumption that the measured wall temperatures represented conditions around the entire circumference of each section can be questioned, particularly given the uneven distribution of moisture shown in figure 8.20. Different temperature gradients would lead to under- or over-estimation of actual CCR losses. The value for the carbon fraction of BVS in the complete composting mixture was calculated from total carbon values for each of the components (see chapter 7). Given that the more biodegradable components have lower carbon fractions, the BVS-C may be over-estimated by the model. At a lower overall fraction of 0.45 for example, predicted BVS-C is reduced to approximately 2.2 kg, which is insufficient to explain the discrepancy. The likely magnitude of any suspected heat input from the heating cable in section 2 of the reactor is unknown, but in order to account for the discrepancy in BVS-C would need to be approximately 17 W over the entire run (1.3 kg-C, 19.6 kJ/g-BVS, 35 d). This is technically possible given the presence of 240 W heating capacity in each section. Since the heater cables were operated at 95 V as opposed to 240 V, a maximum power output of 95 W was available, so it is not unrealistic to suppose a transfer of 17 W into the column. However as discussed earlier, the evidence for heat input is inconclusive. As indicated in section 8.7.2, the model assumes that the entire composting mass was contributing to the calculated enthalpy profiles used to calculate BVS-C, but the moisture distribution shown in figure 8.20 indicates that this was unlikely throughout the entire composting period. Therefore it is probable that some proportion of the discrepancy between the predicted and measured substrate degradation profiles, in particular the divergence at later time, is attributable to non-participation of some of the composting

material. Combinations of the above factors may explain the difference between BVS-C profiles in runs A and B.

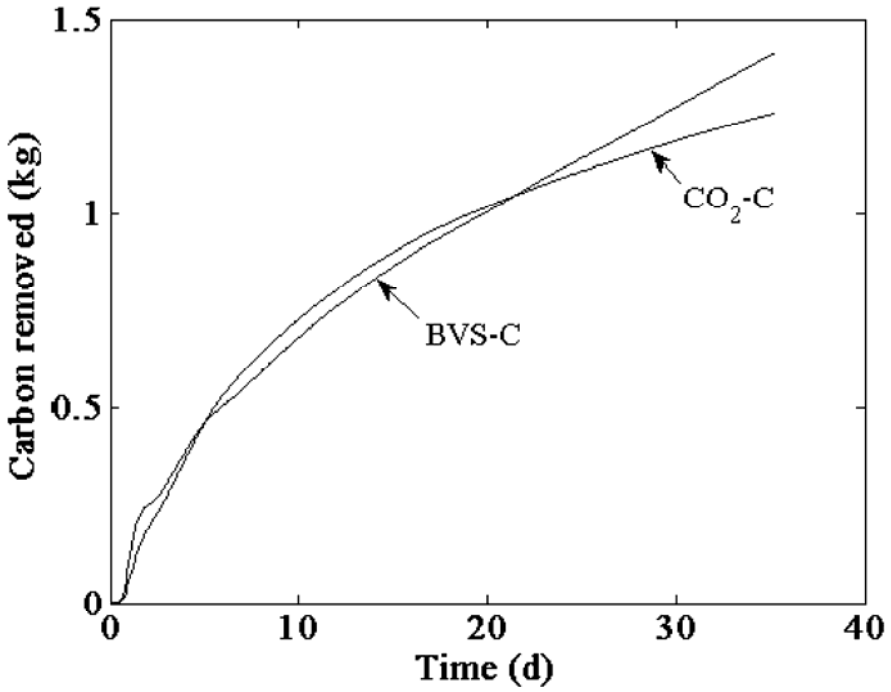

Figure 8.30 Measured carbon removal compared to predicted carbon removal for run B with an exit gas relative humidity of 60%.

This observation raises the interesting possibility of using the difference between measured and modelled profiles as a diagnostic tool for composting systems If all other experimental factors used in the heat balance model are correct, then the observed discrepancy will indicate the amount of non-participating material, in the same way that tracer studies indicate "dead" hydraulic volume in stirred tank reactors. This may then be used to prompt investigation into poor moisture distribution, inadequate mixing and/or uneven aeration.

Both the BVS-C and CO_2-C curves included a small initial lag phase of less than 1 d, which was not modelled by either the single or double exponential functions. Given that the post-lag phase data was well modelled by these functions, and given similar findings reported in chapters 5 and 6, it is suggested that modellers consider commencing temperature profile modelling once the lag phase is over, in which case single or double exponential functions can often be used. In practice the point of commencement might be taken as the time at which the compost temperature has reached 30 or 40 ^{o}C.

The considerable non-homogeneity observed along the vertical axis emphasises it would be prudent in future to

In terms of the goals of this work (see section 8.3, page 241) we can now say that three objectives have been either fulfilled, or partially fulfilled: a) BVS degradation profiles from a synthetic data set have been simulated, b) the simulation procedure has been validated in qualitative, but not quantitative, terms against experimentally generated CO_2-C evolution data, and c) a single exponential model has been found to give moderate to good fits to the measured and predicted substrate degradation profiles generated.

8.7.4 Temperature-corrected curves

The multi-phase temperature-corrected profiles produced in the present work were unexpected and raise several interesting issues. From the work presented in chapter 5 it is clear that no experimental evidence for a constant-temperature substrate degradation profile of this type exists. Neither has any conceptual model which would support such a pattern been published, and it is most unlikely that these curves represent any real pattern of microbial behaviour. Therefore either the assumptions underlying the temperature correction procedure, or the cardinal temperatures chosen, or both, need to be questioned. It should be noted at this point that multi-phase patterns were produced from some, but not all, literature data sets at varying temperature, which were evaluated using the temperature correction procedure (see chapter 6). One useful line of inquiry would be to investigate the assumption that, as temperature changes, there will be an instantaneous response of microbial activity. In other words, in deconstructing the present exponential profiles to a constant temperature of 40 ^{o}C, it is supposed that the rate of substrate degradation will reduce or increase at once, in response to each temperature fluctuation. A second useful line of inquiry, as mentioned, would be to question the values of the cardinal temperatures. The shape and location of the temperature-corrected profiles are sensitive to the cardinal temperatures chosen as can be seen in figure 8.31, where the effect of using 5, 65 and 90 ^{o}C, and 5, 50 and 80 ^{o}C, for T_{min}, T_{opt} and T_{max} respectively, is shown for run B. By increasing the optimal and maximum temperatures from 59 and 85 ^{o}C respectively, the multi-phase pattern is maintained and the corrected profile shifted downwards. In contrast, choosing lower values for T_{opt} and T_{max} resulted in an exponential curve, which was translocated upwards. This makes sense in terms of shape and location, the latter since most of the run operated at temperatures above the optimum. When this profile was modelled using a double exponential function, an excellent

a)

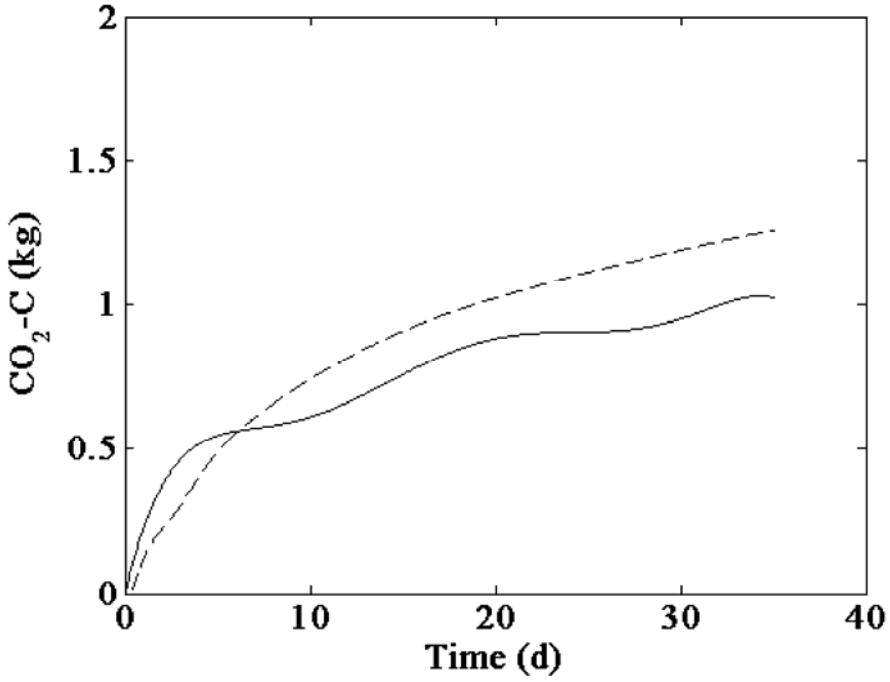

b)

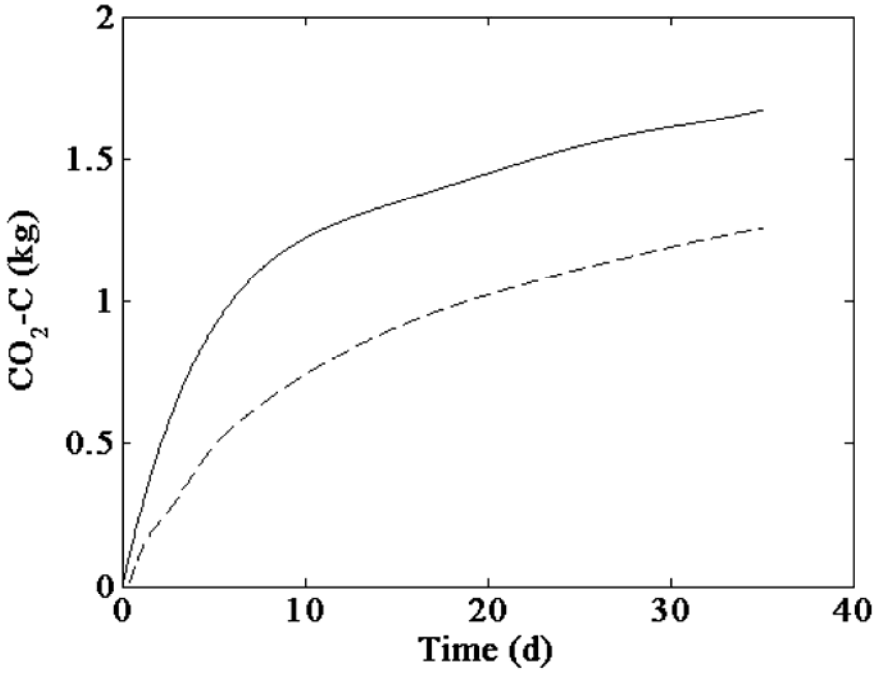

Figure 8.31 Temperature-corrected CO_2-C profiles for run B, at alternative cardinal temperatures. a) cardinal temperatures: 5, 65 and 90 ^{o}C; b) cardinal temperatures: 5, 50 and 80 ^{o}C. Key: ___ 40 ^{o}C; --- varying temperature.

a)

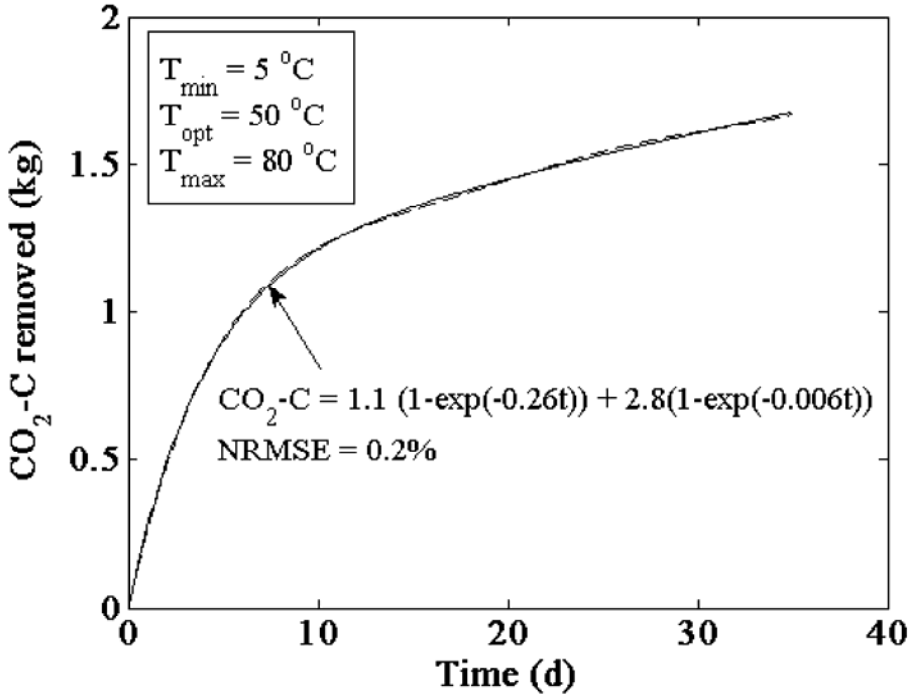

b)

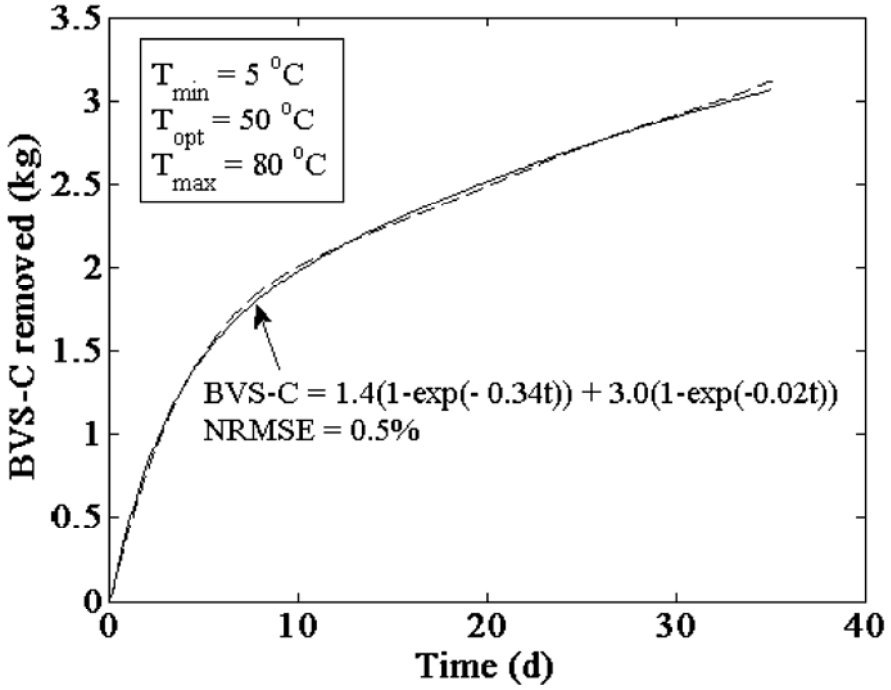

Figure 8.32 Double exponential models fitted to temperature-corrected a) CO_2-C and b) BVS-C profiles, for run B. Cardinal temperatures are shown on the graphs. Data errors were estimated at 1.1% and 0.5% of the modelled maxima respectively.

fit was obtained (figure 8.32). When the estimated data errors are taken into account (see the caption to Fig. 8.32), it is not possible to state that there is any significant difference between the data and the modelled curve. Whether this model truly represents the underlying nature of the substrate degradation profile will rely on correct values for the cardinal temperatures being determined and at this point simply demonstrates the possibility of obtaining a realistic pattern. It should be noted that elements of the multi-phase profile remain at mid- and later-time, although they are much less pronounced than in figure 8.30a. The multi-phase curve phenomenon was also observed when correcting varying-temperature profiles from the literature as reported in Chapter 6. It is suggested where these occurred, the varying temperature data sets which gave rise to them should be re-evaluated using alternative values for the cardinal temperatures. Similar results were obtained for BVS-C using the same cardinal temperatures (figure 8.32b), and for both CO_2-C and BVS-C in run A using cardinal temperatures of 5, 55 and 80 ^oC (Appendix 9), with excellent fits for the double exponential model in all cases. Rate coefficient values for the double exponential model were similar when both CO_2-C and BVS-C data were modelled, and it would be reasonable to expect them to be identical, since the underlying processes generating them are the same. The impacts of this were investigated by holding the first and second rate coefficients constant at 0.30 d^{-1} and 0.013 d^{-1} respectively, and fitting the double exponential model with only two variable parameters to both run B data sets. For the CO_2-C data (Fig. 8.32a), there was a shift in the saturation constants to 1.0 and 1.8 respectively, with an increase in the NRMSE to 0.5%, whilst for the BVS-C data (fig. 8.32b) an improved fit resulted, with the NRMSE decreasing from 0.5% to 0.3% (Figs. A9.31 and A9.32, Appendix 9). This indicated that the assumption of common rate coefficients was reasonable in this situation, whilst showing a shift in the goodness of fit as rate coefficients were altered. Further work is necessary to investigate the 5 ^oC difference in T_{opt} between run A and run B. In effect, the cardinal temperatures used to obtain the double exponential profiles shown here are fitted values. An interesting possibility therefore arises if we assume that single exponential, double exponential or Gompertz patterns are most likely to provide a true description of substrate degradation at constant temperature. In this case, the temperature correction procedure could be intentionally used to obtain micro-biologically realistic combinations of the cardinal temperatures resulting in a good fit to one of the three patterns. The fitted cardinal temperatures obtained could then be compared to laboratory-generated values, and, if realistic, utilised as true values in temperature profile modelling.

In order to explore the possibility of alternative combinations of cardinal temperatures and double exponential model parameters in generating the temperature corrected data and then fitting the double exponential model to it, respectively, an optimisation programme (Microsoft "Solver") incorporating all seven parameters was utilised. Constraints were set to ensure that $T_{min} < T_{opt} < T_{max}$; T_{min} < the minimum recorded temperature; $T_{min} > 0$ ^{o}C ; $T_{max} <$ 100 ^{o}C and $k_1 > k_2$. As expected the programme was sensitive to initial conditions, emphasising the importance of setting these realistically. An excellent fit to temperature-corrected CO_2-C data was obtained when the optimisation programme computed cardinal temperatures of 21, 58 and 97 ^{o}C. Further exploration, using the "Matlab" programmes previously utilised in this chapter, showed that the temperature correction and curve fitting procedure was relatively insensitive to variations in T_{min} and T_{max} under certain conditions. When T_{opt} and T_{max} were held at 50 and 80 ^{o}C respectively, the best mathematical fit was obtained with T_{min} at 9 and 10 ^{o}C, with little variation between 3-12 ^{o}C. Similarly, varying T_{max} from 80-100 ^{o}C resulted in relatively small improvements in the NRMSE value, with the best fit at 100 ^{o}C. In all cases, changes in the parameter values in the double exponential model were slight. In contrast, varying T_{opt} from the best fit value of 50 ^{o}C by more than ± 1 ^{o}C, with T_{min} and T_{max} held at 10 and 80 ^{o}C respectively, resulted in a return to multiphase behaviour and rapidly increasing values of NRMSE. Decreasing T_{max} to 78 and 77 ^{o}C whilst holding T_{min} and T_{opt} at 10 and 50 ^{o}C respectively also resulted in a sharp decline in the goodness of fit. Detailed results of this analysis may be viewed in Appendix 9 (Table A9.1). These findings prompt a discussion of the role of fitted parameters in the present work, and in particular, the implications for the goal of making mathematical modelling a more useful tool for engineers. If the procedures developed here are to be generally useful, it is important that independently measured values of the cardinal temperatures are obtained. The fact that these may not give the very best mathematical fit to data must be considered in the light of the potential impact on the temperature prediction model, in line with the degree of resolution demanded. It has been suggested in Chapter 4 that prediction of peak temperatures to within 2 ^{o}C and time to peak temperature to within 8 h would be likely be acceptable in practice. In this case, cardinal temperatures resulting in a prediction within these limits would be acceptable, even with a less precise mathematical fit to the substrate degradation data. It is the belief of the present author that in order to make the substrate degradation model widely applicable, the cardinal temperatures should have physical meaning, and in particular lie within the known range of composting microbial activity. Future work is required to

ascertain correct values for these temperatures across a range of microbial consortia and substrates.

The findings obtained in the present work support a modelling approach in which a substrate degradation curve generated under appropriate laboratory conditions at 40 ^{o}C (e.g. Fig. 8.32), would, given the correct cardinal temperatures, generate a correct substrate degradation profile under varying temperature conditions (e.g. Fig. 8.23), and that this in turn would enable an accurate and precise prediction of the temperature profile (e.g. Fig. 8.13) using a heat and mass balance approach (i.e. Eq. 1. in this chapter, plus Eq. 5 and Eq. 6 in chapter 4). Such an outcome would be extremely valuable since it would allow composting process temperature prediction on the basis of one simple laboratory procedure. More work is required before this can be achieved however, and this is discussed in the next section.

Two questions were posed in the foreword to this chapter (section 8.1), namely a) "what profile shape would one expect from a composting process?" and, b) "is it the quality of the data which causes the dysfunction (between the current models of substrate degradation and the available data), or is it the (aforementioned) models?". In response to the first question, we can say that at this point that the present work has provided evidence that exponential forms are most likely to successfully model post-lag-phase data, provided these are generated under conditions properly simulating the full-scale composting environment. It is noted however that the Gompertz model was shown to apply in the simulation exercise reported in section 8.6.1. On the second question, it appears that the models are basically sound, and that better quality data, including more accurate estimates of model inputs, and improved experimental techniques are needed, if substrate degradation and ultimately temperature, moisture and oxygen profiles, are to be correctly predicted in the composting process.

In relation to the goals of this work (see section 8.3, page 241) we can now say that the final objective has been fulfilled: d) the profiles generated at varying temperature have been deconstructed to a constant temperature and the fit of single and double exponential models, and the modified Gompertz model, to these profiles assessed. In doing so, the importance of the cardinal temperature values used in the correction function has been demonstrated.

8.7.5 Future directions

It would be particularly valuable if future researchers were to repeat the present experimental work using a completely mixed reactor, in order to overcome the spatial variations encountered in a static bed of the type used here. Such an approach will provide kinetic data generated under non-limiting moisture and oxygen conditions, throughout the entire composting mass, as opposed to an unknown proportion of the material. A number of technical challenges must first be addressed, particularly in relation to inlet air distribution, heat flux control, and temperature measurement in the reactor. A potentially suitable completely mixed laboratory-scale reactor has been described by Alkoaik and Ghaly (2006). Given the increased commercial use of completely mixed flow-through composting reactors at full scale, this approach is relevant and could lead to the development of mathematical models for such reactors. In relation to CCR losses, the overall heat transfer coefficient should be measured experimentally rather than calculated, given the uncertainties inherent in the selection of convective heat transfer coefficients in the present work. A value for the overall heat transfer co-efficient (U) of 0.33 kcal/h.m^2.^{o}C (0.38 W/m^2.^{o}C), was reported for a laboratory-scale reactor by Bach et al. (1987) and experimentally determined values of UA reported by Weppen (2001). Investigation of the relationship of U with temperature should be included in this work. CCR losses will also be more precisely estimated if smaller temperature sensors than those used in the present work, located within a well defined boundary layer, or embedded within the wall, can be utilised. One could also question the steady-state heat transfer assumption. In relation to the future modelling of aerated static piles, an approach incorporating finite element techniques, or a partial differential equation able to account for spatial variations along the vertical axis, will be both applicable and necessary once substrate degradation models for completely mixed conditions are validated. In addition to correcting the model for temperature, moisture and oxygen variations, a compaction factor might also be useful in this context. Correct values for the physical cardinal temperatures are urgently needed if the temperature-correction function of Rosso et al. (1993) is to be utilised. In the present work, peak temperatures beyond those normally anticipated for most composting micro-organisms were measured, and the question of microbial activity at these levels requires further investigation. In this respect, it is worth noting that Lyon et al. (2000) reported the presence of thermophilic Bacillus species, with a maximum growth temperature of 65-72 ^{o}C, and *Thermus thermophilus*, with a maximum growth temperature of 80-82 ^{o}C, in a full-scale aerated trench composting system treating green (yard) waste, agricultural and kitchen waste, and shredded wood. In relation to optimal

temperatures, work by Tremier et al. (2005a) has indicated peak kinetics at around 40 ^{o}C data for a sewage sludge/woodchips mixture, with rates at around 58 ^{o}C similar to those at 20 ^{o}C.

8.8 Conclusions

1. A thermodynamic approach to the estimation of substrate degradation profiles in the composting process was developed, and implemented with a both simulated data set, and data from composting experiments conducted in a laboratory-scale constant temperature difference (CTD) reactor simulating an aerated static pile section, with a simulated feedstock.

2. The model successfully predicted the generic shape of experimental substrate degradation profiles, but under the conditions and assumptions of the experiment, the measured CO_2-C and predicted BVS-C profiles were quantitatively different. Both profiles were moderately to well fitted by single exponential functions, with replicate rate coefficient values of 0.08 and 0.09 d^{-1}, and 0.06 and 0.07 d^{-1} respectively.

3. When corrected to a constant temperature of 40 ^{o}C, using the temperature-correction function of Rosso et al. (1993), and cardinal temperatures of 5, 59 and 85 ^{o}C, multi-phase profiles were predicted for both the measured CO_2-C and the predicted BVS-C data. However, when cardinal temperatures of 5, 55 and 80 ^{o}C (run A), or 5, 50 and 80 ^{o}C (run B) were used, the predicted profiles were exponential in shape and excellent fits were obtained using a double exponential function.

4. This work provides evidence that a substrate degradation curve generated under appropriate laboratory conditions at 40 ^{o}C would, given the correct cardinal temperatures, generate a correct substrate degradation profile under varying temperature conditions and that this in turn would enable an accurate and precise prediction of the temperature profile using a heat and mass balance approach.

5. Experimental factors appear to be the likely cause of the dysfunction between reported substrate degradation patterns and existing substrate degradation models.

6. Further work is suggested in order to obtain data for the model under completely mixed conditions, more accurately estimate the overall heat transfer coefficient and obtain correct values for the physical cardinal temperatures used in the temperature correction function.

8.9 References

Alkoaik, F. and Ghaly, A.E., 2005. Effect of innoculum size on the composting of greenhouse tomato plant trimmings. Compost Science and Utilisation 13 (4), 262-273.

Alkoaik, F. and Ghaly, A.E., 2006. Influence of dairy manure addition on the biological and thermal kinetics of composting of greenhouse tomato plant residues. Waste Management 26 (8), 902-913.

Bari, Q.H., Koenig, A. and Guihe, T., 2000. Kinetic analysis of forced aeration composting - I. Reaction rates and temperature. Waste Management & Research 18 (4), 303-312.

Elwell, D.J., Keener, H.M. and Hansen, R.C., 1996. Controlled, high rate, composting of mixtures of food residuals, yard trimmings and chicken manure. Compost Science & Utilisation 4 (1), 6-15.

Harper, E., Miller, F.C. and Macauley, B.J., 1992. Physical management and interpretation of an environmentally controlled composting ecosystem. Australian Journal of Experimental Agriculture 32 (5), 657-667.

Haug, R.T., 1993. The practical handbook of compost engineering. Lewis Publishers, Boca Raton, Florida, USA.

Higgins, C. and Walker, L., 2001. Validation of a new model for aerobic organic solids decomposition: simulations with substrate specific kinetics. Process Biochemistry 36 (8-9), 875-884.

Hogland, W., Bramryd, T., Marques, M. and Nimmermark, S., 2003. Physical, chemical and biological processes for optimizing decentralized composting. Compost Science & Utilization 11 (4), 330-336.

Koenig, A. and Bari, Q.H., 2000. Application of self-heating test for indirect estimation of respirometric activity of compost: Theory and practice. Compost Science & Utilization 8 (2), 99-107.

Lyberg, M.D. and Hogland, W., 2004. Performance of a vertically fed compost reactor. Compost Science & Utilization 12 (2), 169-174.

Lyon, P.-F., Beffa, T., Fischer, J.L. and Aragno, M., 2000. Xylanase activity and thermostratification during the thermogenic phase of industrial composting in aerated trenches. Waste Management and Research 18, 174-183.

Mason, I.G., 2006. Mathematical modelling of the composting process: a review. Waste Management 26 (1), 3-21.

Mason, I.G., in press-a. An evaluation of substrate degradation patterns in the composting process. Part 1: Profiles at constant temperature. Waste Management. (Published on-line 17 September, 2007).

Mason, I.G., in press-b. An evaluation of substrate degradation patterns in the composting process. Part 2: Corrected-temperature profiles. Waste Management. (Published on-line 12 September, 2007).

Mills, A.F., 1995. Basic heat and mass transfer. Richard D. Irwin Inc, Chicago, USA.

Mote, C.R. and Griffis, C.L., 1982. Heat production by composting organic matter. Agricultural Wastes 4, 65-73.

Namkoong, W. and Hwang, E.Y., 1997. Operational parameters for composting night soil in Korea. Compost Science & Utilisation 5 (4), 46-51.

Rosso, L., Lobry, J.R. and Flandrois, J.P., 1993. An unexpected correlation between cardinal temperatures of microbial growth highlighted by a new model. J. Theor. Biol 162, 447-463.

Rynk, R., 1992 On-farm composting handbook. NRAES, Ithaca, New York USA.

Tremier, A., de Guardia, A., Massiani, C., Paul, E. and Martel, J.L., 2005. A respirometric method for characterising the organic composition and biodegradation kinetics and the temperature influence on the biodegradation kinetics, for a mixture of sludge and bulking agent to be composted. Bioresource Technology 96 (2), 169-180.

Weppen, P., 2001. Process calorimetry on composting of municipal organic wastes. Biomass & Bioenergy 21, 289-299.

CHAPTER 9
CONCLUSIONS, LIMITATIONS AND RECOMMENDATIONS

9.1 Foreword

Our travels have come an end for the present time. However this is only a layover in the research journey and there are other paths and destinations beckoning (figure 9.1). The aims of this chapter are firstly, to present the major conclusions arising from the trip so far, secondly, to discuss the limitations encountered, and thirdly, to outline possible paths and directions for future journeys for the consideration of whoever may choose to set out on them.

Detailed conclusions and recommendations may be found at the end of chapters 2 to 8. The intention in this chapter is to provide an overview of the major findings, constraints and recommendations.

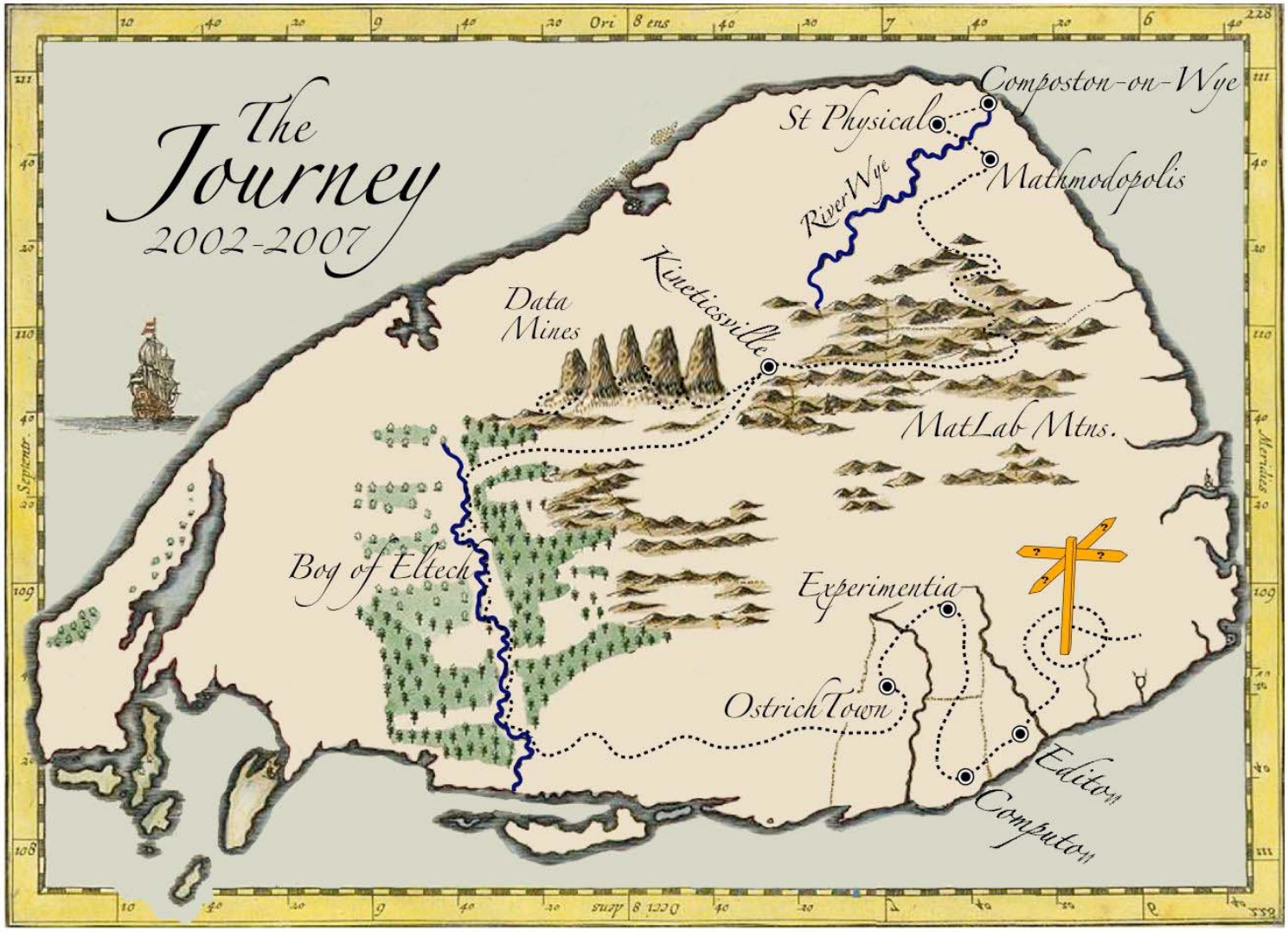

Figure 9.1: The conceptual map of the author's research travels. Our present location is – at the signpost.

9.2 Conclusions

The broad objective of this work was "to examine, discuss, and make a contribution to, the use of modelling, both physical and mathematical, in relation to the composting process" (Chapter 1, section 1.1). It was also stated that one highly desirable outcome would be "to make modelling a more useful predictive tool for engineers" (Chapter 1, section 1.1). In pursuing these aims a number of significant findings about the way in which composting research has been conducted to date have emerged. From the review of physical modelling, it was clear that many physical models used in composting research do not properly simulate the full-scale composting environment, and may therefore produce results which are not applicable at full scale. The meta-analysis of the field identified the existence of four categories of reactor - fixed temperature, self-heating, controlled temperature difference and controlled heat flux - which differ according to the means of management of heat flux through the vessel walls. The controlled temperature difference and controlled heat flux categories are new classifications introduced in the present work. Fixed temperature reactors were found to have many useful applications, but do not simulate dynamic process conditions. Self-heating, laboratory-scale, reactors are convenient, but involve significant convective/conductive/radiative (CCR) losses, even with insulation present. This is attributable to the substantially higher surface area:volume ratios in experimental composting reactors, compared to full-scale systems, and in some cases to over-aeration. At pilot-scale, CCR losses can be limited to full-scale levels using moderate quantities of insulation. Controlled temperature difference and controlled heat flux laboratory reactors allow temperature differences and CCR heat fluxes to be controlled to levels close to those occurring in full-scale systems. We saw that reported ventilative heat losses from full-scale composting systems have ranged from 70 to 95% of the total flux, whilst losses from laboratory reactors are typically in the range 36 to 67%. In comparison, CCR heat losses from full-scale composting systems have ranged from 3 to 15% of the total flux, whereas CCR losses from laboratory reactors have been estimated at approximately 33 to 62% of the total. Thus the choice of reactor is crucially important when embarking on an experimental programme.

The degree to which physical models have simulated full-scale thermodynamic conditions was quantified using a new methodology. In this procedure, the areas bounded by the temperature-time profile and reference temperatures of 40 and 55 ^{o}C (A_{40} and A_{55}), the times

for which these temperatures are exceeded (t_{40} and t_{55}), and times to peak temperature, were calculated. An evaluation of published temperature profiles showed marked differences in these parameters when comparing full- and laboratory-scale reactors. For full-scale windrows A_{40} typically exceeded 624 ^{o}C.days, A_{55} exceeded 60 ^{o}C.days, and t_{40} and t_{55} were > 46 days, and > 24 days, respectively. Full-scale forced aeration systems had values of A_{40} exceeding 224 ^{o}C.days, values of A_{55} exceeding 26 ^{o}C.days, and t_{40} and t_{55} were > 14 days, and > 10 days respectively. In contrast, laboratory-scale reactors had A_{40} values ranging between 68-313 ^{o}C.days, A_{55} values between 0-44 ^{o}C.days, and t_{40} and t_{55} values of approximately 6-16 days, and 0-7 days, respectively. However, temperature shape characteristics were generally similar to full-scale profiles. At pilot-scale, temperature-time parameters were shown to be comparable to full-scale values in three cases, and lower than full-scale values in other cases. When temperature profiles for a laboratory-scale reactor and two pilot-scale reactors operated at comparatively high aeration rates were evaluated, these were shown to poorly simulate full-scale temperature profiles. However, moderately insulated self-heating, pilot-scale, reactors operated at relatively low aeration rates were shown, with the exception of times to peak temperature, to be able to provide good temperature profile simulation, both qualitatively and quantitatively.

From the review of mathematical modelling of the composting process, we saw that the solution of heat and mass balances in time has provided the conceptual basis, and that a deterministic approach has been adopted in all cases. Of the components, the biological energy production sub-model was identified as particularly important. Either first-order, Monod-type, or empirical expressions, in conjunction with heat conversion factors, have been used. However, limited evidence existed for the applicability of a first-order model to substrate degradation, although it has been widely cited. A key aspect of modelling under dynamic conditions involves correction of rate coefficients for changes in state variables, and we saw that temperature correction functions have been incorporated into most biological energy models, with corrections for moisture, oxygen and free air space also incorporated in some cases. The most successful models in predicting temperature profiles have incorporated either empirical kinetic expressions, or utilised a first-order model, with empirical corrections for temperature and moisture. Although many models were able to successfully predict temperature profile shape characteristics, no temperature models have been able to predict maximum, average and peak temperatures to within 5, 2 and 2 ^{o}C respectively, or to predict

the times to reach peak temperatures to within 8 h. Thus the modelling of substrate degradation seemed worthy of further investigation, with the primary focus on the shape of the profile.

An evaluation of 31 published constant-temperature temperature profiles revealed that the majority incorporated convex shapes. Smaller numbers of sigmoidal and multi-phase patterns were found. When the profiles were modelled, 3 fits rated as good were obtained when using a single exponential function, 2 fits rated as good were obtained when using a double exponential function and 1 fit rated as good was obtained when using a non-logarithmic Gompertz function. The lag phase observed in many data sets was successfully modelled using the non-logarithmic Gompertz function where a good fit was obtained, but not otherwise. Removal of the lag phase, or post-convex curve, data from 7 data sets resulted in improvements in fit to convex curve data when using the single exponential function. A double exponential model provided a good fit to post-lag phase convex curve data in one case. The results obtained indicated that rather limited evidence existed supporting the use any of these three models in describing substrate degradation profiles generated at constant temperature.

Given that the literature contains a large amount of potentially valuable information generated under dynamic conditions, a new procedure for correcting substrate degradation profiles generated at varying temperature to a constant temperature of 40 ^{o}C was developed, and applied to 44 varying-temperature data sets. Multi-phase patterns were most commonly observed for the temperature-corrected profiles, with convex shapes appearing relatively infrequently. In modelling the temperature-corrected profiles, 2 fits rated as good were obtained when using the single exponential model, 1 fit rated as excellent and 1 fit rated as good were obtained when using a double exponential model and 1 fit rated as excellent, plus 1 fit rated as good, were obtained when using the non-logarithmic Gompertz model. The lag phase observed in many data sets was successfully modelled using the non-logarithmic Gompertz function in cases where excellent and good fits were obtained, but not otherwise. Removal of the lag phase, or multi-phase data, from 20 data sets resulted in 3 fits rated as excellent and 2 rated as good, when using the single exponential function. Use of a double exponential model gave 3 fits rated as good, and the Gompertz model gave one fit rated as good. Strong evidence supporting the use of a single exponential function, a double

exponential function or a non-logarithmic Gompertz for substrate degradation modelling was limited to approximately 16% of the data sets examined. These results, in combination with those obtained at constant temperature, failed to provide a convincing body of evidence for any of the three existing substrate degradation models.

A new approach to the estimation of substrate degradation profiles in the composting process was implemented with both a simulated data set, and data from composting experiments conducted in a laboratory-scale constant temperature difference (CTD) reactor. In preparation for the experiments, a new simulated composting feedstock was successfully designed on energy ratio, water ratio and bulk density criteria, and prepared from a substrate, amendment, seed, bulking agent combination comprising ostrich feed pellets, office paper, finished compost and woodchips, respectively. The mixture self-heated rapidly in a CTD reactor environment, following lag periods of 13-22 h. Thermophilic temperatures were reached within 22-33 h of start-up at the mid-point of the reactor, and temperatures were subsequently maintained in the thermophilic range for periods representative of full-scale composting behaviour. The simulated feedstock proved easy to prepare, using the readily available dry ingredients, and tap water. It is suggested that adoption of this type of feedstock would facilitate experimental research work associated with composting kinetics and temperature profile modelling.

The generic shape of experimental substrate degradation profiles obtained from CO_2 measurements was successfully predicted, but under the conditions and assumptions of the experiment, the profiles were quantitatively different. Both measured CO_2-carbon (CO_2-C) and predicted biodegradable volatile solids carbon (BVS-C) profiles were exponential in shape, and moderately to well fitted by single exponential functions. When corrected to a constant temperature of 40 ^{o}C, using the temperature-correction function of Rosso et al. (1993), with cardinal temperatures of 5, 59 and 85 ^{o}C, multi-phase profiles were predicted for both the measured CO_2-C and the predicted BVS-C data. However, when cardinal temperatures of 5, 55 and 80 ^{o}C (run A) or 5, 50 and 80 ^{o}C (run B) were used, the predicted profiles were exponential in shape and an excellent fit was obtained using a double exponential function. Thus the correct choice of cardinal temperatures was found to be crucial in obtaining a profile shape with biological meaning.

An underlying concept in the mathematical modelling of composting state variables is that substrate degradation characteristics measured independently, under standard fixed conditions, can be mathematically adjusted for dynamic variations in temperature, moisture level and oxygen concentration, to provide a correct estimate of biological heat generation, moisture production and oxygen consumption. This work provides strong evidence that a substrate degradation curve generated under appropriate laboratory conditions at 40 ^{o}C would, given the correct cardinal temperatures, generate a correct substrate degradation profile under varying temperature conditions, and that this in turn would enable an accurate and precise prediction of the temperature profile using a heat and mass balance approach. Experimental factors appear to be the likely cause of the dysfunction between previously reported substrate degradation patterns and existing substrate degradation models.

In summary, this research makes five contributions toward the stated goal of making composting modelling a more useful predictive tool for engineers. Firstly, the importance of correct reactor choice has been identified and a new procedure for quantitatively evaluating simulation performance has been presented. Secondly, the limited body of evidence for three existing models of substrate degradation, and a means of presenting such evidence on a common basis, have been demonstrated. Thirdly, using a new procedure for predicting the shape of the substrate degradation profile, it was shown that a single exponential profile, in common with that measured, was predicted for the mixture and conditions of the present experiments. Fourthly, when corrected to a constant temperature of 40 ^{o}C, it was shown that a double exponential form was obtained, but that this depended on the choice of cardinal temperatures used in the correction procedure. This highlighted the need to obtain independently measured physical cardinal temperature values, rather than mathematically fitted values, if the model is to have general applicability. Both exponential forms are previously known, have biological meaning, and have few parameters, all of which makes them attractive. Fifthly, the shape of the predicted substrate degradation profiles has been shown to be relatively independent of uncertainties in composting system operating parameters, but it is clear that precise and accurate experimental measurements are required for successful quantitative predictions of substrate degradation profiles, and ultimately, composting process temperature profiles.

9.3 Limitations

This research was constrained by incomplete information, the chosen process format and experimental limitations. Thus the findings presented in this thesis should be read and interpreted with these factors in mind.

Evaluation of published temperature profiles was limited by a lack of corresponding moisture and oxygen data, which meant that profiles could not be adjusted for these factors. Temperature-correction results reported in chapter 6 are therefore subject to the caveats that moisture and oxygen may, or may not, have been limiting, and that different corrected profiles may have resulted if this could have be taken into account.

The simulation of an aerated static pile section in the CTD reactor resulted in spatial non-homogeneity within the composting material. Vertical and radial distribution of moisture was uneven, both with and without leachate return. It is also likely that differential compaction resulted in a range of bulk densities with depth. The present results, based on measures of bulk activity, must therefore be interpreted in this context, with particular note that the whole composting mass was unlikely to have contributed to the evolution of CO_2 and heat for the full duration of each run.

The correct prediction of the magnitude of the BVS-C profiles was limited by the assumptions and simplifications made concerning exit gas relative humidity, exit gas temperature, and the overall heat transfer coefficient, plus other experimental factors. In particular, the inability to measure exit gas relative humidity, and the uncertainty over the magnitude of boundary layer heat resistance coefficients, were important.

9.4 Recommendations

In order to progress toward the goal of correctly predicting composting process temperature profiles, further work is needed on the substrate degradation profile, in particular to overcome the limitations imposed by the aerated static pile format. One suggested way forward is to repeat the work reported in chapter 8 of this thesis under completely-mixed conditions, using either a controlled temperature difference, or a controlled heat flux, reactor. Should this work confirm the present findings, this would open the door for state variable modelling in agitated

flow-through reactors, and for the analysis of aerated static pile and windrow formats, using finite element analysis techniques. More accurate measurements of reactor heat transfer coefficients, and other experimental factors identified in the present work, will be required.

In parallel with such thermodynamic experiments, a simple laboratory-scale substrate degradation test, analogous to the BOD test, needs to be developed to provide substrate degradation data at constant temperature, and under non-limiting moisture and oxygen conditions. For convenience and accuracy, such a fixed temperature reactor needs to be small enough to fit inside a laboratory oven, and to minimise internal heating, but for relevance, it must be large enough to accept the particle size range normally encountered in composting materials. The measurement of CO_2 in the exit gas would provide a suitable indication of substrate degradation with time, and a data bank of profiles could eventually be produced.

In relation to the temperature correction procedure used in the present work, experiments to more accurately and precisely ascertain the physical cardinal temperatures for composting are required. It is suggested that the simulated feedstock used in the present experiments, or an agreed variation on it, would provide a suitable common feedstock to allow comparison of results between researchers, and the building of a data bank of values. Further work on fitted cardinal temperatures would be useful and could provide a parallel data bank of information.

Other potential areas of investigation arising from this research include the influence of the thermodynamic environment on compost properties, wall effects on compaction, values for biological heat production, the effect of moisture tension and the modelling of natural ventilation. In chapters 2 and 3 we saw that composting environment was not well simulated by many laboratory-scale reactors. However, the question of how the properties of the final compost, excluding pathogen and weed seed levels, might be affected, remains to be fully addressed. This could be usefully investigated as an assessment of the impact of A_{40} and A_{55} on product quality, using the null hypothesis that selected values of A_{40} and A_{55} have no effect on product stability or maturity. The choice of appropriate indicators of stability and maturity would involve an interesting assessment of the literature, as there is presently no general agreement on this matter. Wall effects on the compaction of material in composting reactors remain to be properly investigated. It particular it would be valuable to build on published studies of compressive effects on compost, in order to establish relationships between particle

and column diameters, and compaction, under the moisture saturated atmospheric conditions in a composting reactor. Information on rates of biological heat production in the composting process is very limited and it would be extremely valuable to build a more comprehensive data set. More data on horizontal temperature profiles at laboratory, pilot and full scale, would also be useful in relation to predicting both spatial substrate degradation, and disinfection performance. Further work is required to validate mechanistically-based moisture correction functions, and to explore the role of moisture tension in composting. Natural ventilation, which drives aeration in windrows and passively aerated systems, is under-represented in the composting literature. In particular, validation of existing convective airflow models is required before temperature profiles in naturally aerated systems can be modelled.

APPENDIX 1
COMPLETE REFERENCES

This appendix combines references from the individual chapters for ease of referral.

Adani, F., Lozzi, P. and Genevini, P., 2001. Determination of biological stability by oxygen uptake on municipal solid waste and derived products. Compost Science & Utilisation 9 (2), 163-178.

Agnew, J.M. and Leonard, J.J., 2003. The physical properties of compost. Compost Science & Utilisation 11 (3), 238-264.

Alkoaik, F. and Ghaly, A.E., 2005. Effect of innoculum size on the composting of greenhouse tomato plant trimmings. Compost Science and Utilisation 13 (4), 262-273.

Alkoaik, F. and Ghaly, A.E., 2006. Influence of dairy manure addition on the biological and thermal kinetics of composting of greenhouse tomato plant residues. Waste Management 26 (8), 902-913.

Andrews, J.F. and Kambhu, K., 1973. Thermophilic aerobic digestion of organic solid wastes. *EPA-670/2-73-061, PB-222 396,* USEPA, Springfield, Il, USA.

Asdal, A. and Breland, T.A., 2003. Compost quality related to product utilisation in Norway. In: Proceedings of the Fourth International Conference of ORBIT Association on Biological Processing of Organics: Advances for a Sustainable Society, 30th April-2 May, 2003, Perth, Australia, 230-240.

Ashbolt, N.J. and Line, M.A., 1982. A bench-scale system to study the composting of organic wastes. Journal of Environmental Quality 11 (3), 405-408.

Atkinson C.F., Jones, D.D. and Gauthier, J.J., 1996a. Biodegradabilities and microbial activities during composting of poultry litter. Poultry Science 75 (5), 608-617.

Atkinson, C.F., Jones, D.D. and Gauthier, J.J., 1996b. Biodegradabilities and microbial activities during composting of oxidation ditch sludge. Compost Science & Utilisation 4 (1), 84-96.

Atkinson, C.F., Jones, D.D. and Gauthier, J.J., 1996c. Biodegradabilities and microbial activities during composting of municipal solid waste in bench scale reactors. Compost Science & Utilisation 4 (4), 14-23.

Ayalon, O., Avnimelech, Y. and Shechter, M., 2000. Alternative MSW treatment options to reduce global greenhouse gases emissions - the Israeli example. Waste Management & Research 18 (6), 538-544.

Bach Phan Dinh, Shoda, M. and Kubota, H., 1984. Rate of composting of dewatered sewage sludge on continuously mixed isothermal reactor. Journal of Fermentation Technology 62 (3), 285-292.

Bach Phan Dinh, Shoda, M. and Kubota, H., 1985. Composting reaction rate of sewage sludge in an autothermal packed bed reactor. Journal of Fermentation Technology 63 (3), 271-278.

Bach Phan Dinh, Nakasaki, K., Shoda, M. and Kubota, H., 1987. Thermal balance in composting operations. Journal of Fermentation Technology 65 (2), 199-209.

Bari, Q.H., Koenig, A. and Guihe, T., 2000a. Kinetic analysis of forced aeration composting – I. Reaction rates and temperature. Waste Management & Research 18 (4), 303-312.

Bari, Q.H., Koenig, A. and Guihe, T., 2000b. Kinetic analysis of forced aeration composting – II. Application of multilayer analysis for the prediction of biological degradation. Waste Management & Research 18 (4), 313-319.

Barrington, S., Choiniere, D., Trigui, M. and Knight, W., 2002. Effect of carbon source on compost nitrogen and carbon losses. Bioresource Technology 83 (3), 189-194.

Batista, J.G.F., van Lier, J.J.C., Gerrits, J.P.G., Straatsma, G. and Griensven, L.J.L.D., 1995. Spreadsheet calculations of physical parameters of phase II composting in a tunnel. Mushroom Science 14, 189-194.

Beaudin, N., Caron, R.F., Legros, R., Ramsay, J., Lawlor, L. and Ramsay, B., 1996. Cocomposting of weathered hyrocarbon contaminated soil. Compost Science & Utilisation 4 (2), 37-45.

Bengtsson, A., Quednau, M., Haska, G., Nilzen, P. and Persson, A., 1998. Composting of oily sludges - degradation, stabilized residues, volatiles and microbial activity. Waste Management & Research 16 (3), 273-284.

Bernal, M.P., Lopez-Real, J.M. and Scott, K.M., 1993. Application of natural zeolites for reduction of ammonia emissions during the composting of organic wastes in a laboratory composting simulator. Bioresource Technology 43, 35-39.

Bernal, M.P., Navarro, A.F., Roig, A., Cegarra, J. and Garcia, D., 1996. Carbon and nitrogen transformation during composting of sweet sorghum bagasse. Biology and Fertility of Soils 22 (1-2), 141-148.

Bertoni, I.A., Papi, T. and Zanzi, A., 1997. Utilisation of a computer simulation model to improve composting process management. In: Proceedings of the ORBIT '97 conference "Into the next millenium", Harrogate, UK., 175-182. ORBIT Association, Weimar, Germany.

Biddlestone, A.J. and Gray, K.R., 1973. Composting - application to municipal and farm wastes. The Chemical Engineer(270), 76-79.

Boelens, J., De Wilde, B. and Baere, L., 1996. Comparative study on biowaste definition: effects on biowaste collection, composting process and compost quality. Compost Science & Utilisation 4 (1), 60-72.

Bono, J.J., Chalaux, N. and Chabbert, B., 1992. Bench-scale composting of two agricultural wastes. Bioresource Technology 40, 119-124.

Brewer, L.J. and Sullivan, D.M., 2003. Maturity and stability evaluation of composted yard trimmings. Compost Science and Utilisation 11 (2), 96-112.

Brown, K.W., Thomas, J.C. and Whitney, F., 1997. Fate of volatile organic compounds in composted municipal solid waste. Compost Science & Utilisation 5 (4), 6-14.

Brown, K.H., Bouwkamp, J.C. and Gouin, F.R., 1998. The influence of C:P ratio on the biological degradation of municipal solid waste. Compost Science & Utilisation 6 (1), 53-58.

Borsuk, M.E. and Stow, C.A., 2000. Bayesian parameter estimation in a mixed-order model of BOD decay. Water Research 34 (6), 1830-1836.

Calaprice, A., 2000. The Expanded Quotable Einstein. Princeton University Press, Princeton, USA.

Campbell, C.D. and Darbyshire, J.F., and Anderson, J.G., 1990a. The composting of tree bark in small reactors: self-heating experiments. Biological Wastes 31, 145-161.

Campbell, C.D., Darbyshire, J.F. and Anderson, J.G., 1990b. The composting of tree bark in small reactors: adiabatic and fixed-temperature experiments. Biological Wastes 31, 175-185.

Cappaert, I., Verdonck, O. and de Boodt, M., 1976. A respiratory apparatus for studying the behaviour of organic materials. Soil Organic Matter Studies. Proceedings of a Symposium. IAEA-SM-211/62, Braunschweig, Germany. pp131-136.

Cekmecelioglu, D., Heinemann, P.H., Demirci, A. and Graves, R.E., 2005. Modeling of compost temperature and inactivation of Salmonella and E-coli O157 : H7 during windrow food waste composting. Transactions of the Asae 48 (2), 849-858.

Chalaux, N., Olivier, J.M. and Minvielle, N., 1991. Bench scale composting and wheat straw biodegradability. in: Maher, Ed. Science and Cultivation of Edible Fungi. Rotterdam: Balkema; pp 207-214.

Chang, J.I., Tsai, J.J. and Wu, K.H., 2005. Mathematical model for carbon dioxide evolution from the thermophilic composting of synthetic food wastes made of dog food. Waste Management 25 (10), 1037-1045.

Chang, J.I., Tsai, J.J. and Wu, K.H., 2006. Thermophilic composting of food waste. Bioresource Technology 96, 116-122.

Chiumenti, A., Chiumenti, R., Diaz, L.F., Savage, G.M., Eggerth, L.L. and Goldstein, N., 2005. Modern Composting Technologies. JG Press, Emmaus, USA.

Choi, M.H. and Park, Y.H., 1998. The influence of yeast on thermophilic composting of food waste. Letters in Applied Microbiology 26 (3), 175-178.

Choi, H.L., Richard, T.L. and Ahn, H.K., 2001. Composting high moisture materials: biodrying poultry manure in a sequentially fed reactor. *Compost Science and Utilization* 9 (4), 303-311.

Chynoweth, D.P., Owens, J., Okeefe, D., Earle, J.F.K., Bosch, G. and Legrand, R., 1992. Sequential Batch Anaerobic Composting of the Organic Fraction of Municipal Solid-Waste. Water Science and Technology 25 (7), 327-339.

Clark, C.S., Buckingham, C.O., Charbonneau, R. and Clark, R.H., 1977. Laboratory scale composting: techniques. Journal of the Environmental Engineering Division, ASCE. 103 (EE5), 893-906.

Clark, C.S., Buckingham, CO., Charbonneau, R. and Clark, RH., 1978. Laboratory scale composting: studies. Journal of the Environmental Engineering Division, ASCE. 104 (EE1), 47-59.

Cohen, Y. and Metzner, A.B., 1981. Wall effects in laminar flow of fluids through packed beds. AICHE Journal 27, 705-715.

Cook, B.D., Bloom, P.R. and Halbach, T.R., 1994. A method for determining the ultimate fate of synthetic chemicals during composting. Compost Science & Utilisation 2 (1), 42-50.

Cook, BD., Bloom, PR. and Halbach, TR., 1997. Fate of a polyacrylate polymer during composting of simulated municipal solid waste. Journal of Environmental Quality 26 (3), 618-625.

Crawford, J.H., 1983. Composting of Agricultural Wastes-A Review. Process Biochemistry 18, 14-18.

Crohn, D.M. and Bishop, M.L., 1999. Proximate carbon analysis for compost production and mulch use. Trans. ASAE 42 (3), 791-797.

Cronje, A., Turner, C., Williams, A., Barker, A. and Guy, S., 2003. Composting under controlled conditions. Environmental Technology 24 (10), 1221-1234.

Cronje, A.L., Turner, C., Williams, A.G., Barker, A.J. and Guy, S., 2004. The respiration rate of composting pig manure. Compost Science & Utilization 12 (2), 119-129.

Currie, J.A. and Festenstein, G.N., 1971. Factors defining spontaneous heating and ignition of hay. J.Sci.Fd.Agric. 22, 223-230.

Dao, T., Sikora, L., Hamasaki, A. and Chaney, R., 2001. Manure phosphorus extractability as affected by aluminum and iron by-products and aerobic composting. Journal of Environmental Quality 30 (5), 1693-1698.

Das, K. and Keener, H.M., 1997. Numerical model for the dynamic simulation of a large scale composting system. Trans. ASAE 40 (4), 1179-1189.

Das, K.C., Tollner, EW. and Tornabene, TG., 2001. Composting by-products from a bleached kraft pulping process: effect of type and amount of nitrogen amendment. Compost Science & Utilisation 9 (3), 256-265.

Das, K. C. and Tollner, E., 2003. Comparison between composting of untreated and anaerobically treated paper mill sludges. Trans. ASAE 46 (2), 475-481.

Day, M., Shaw, K., Cooney, D., Watts, J. and Harrigan, B., 1997. Degradable polymers: The role of the degradation environment. Journal of Environmental Polymer Degradation 5 (3), 137-151.

Day, M., Krzymien, M., Shaw, K. Zaremba, L., Wilson, W.R., Botden, C. and Thomas, B., 1998. An investigation of the chemical and physical changes occuring during commercial composting. Compost Science & Utilisation 6 (2), 44-66.

Debaere, L. and Verstraete, W., 1984. High-Rate Anaerobic Composting with Biogas Recovery. Biocycle 25 (2), 30-31.

de Bertoldi, M., Rutili, A., Citterio, B. and M, C., 1988. Composting management: a new process control through O2 feedback. Waste Management & Research 6 (3), 239-259.

de Bertoldi, M., 1998. Composting in the European Union. Biocycle 39 (6), 74-75.

de Guardia, A., Petiot, C. and Rogeau, D., 2006. Influence of aeration rate and biodegradability fraction on composting kinetics. Waste Management in press.

Diaz, L.F. and Eggerth, L., 2003. Biological treatment of solid wastes in economically developing countries. In: Proceedings of the Fourth International Conference of ORBIT Association on Biological Processing of Organics: Advances for a Sustainable Society, 30th April-2 May, 2003, Perth, Australia, 14-23.

Dinel, H., Schnitzer, M. and Dumontet, S., 1996. Compost maturity: extractable lipids as indicators of organic matter stability. Compost Science & Utilisation 4 (2), 6-20.

Dullien, F.A.L., 1992. Porous media: fluid transport and pore structure. Academic Press, New York, USA. p 78.

Eftoda, G. and McCartney, D., 2004. Determining the critical bulking agent requirement for municipal biosolids composting. Compost Science & Utilization 12 (3), 208-218.

Eiland, F., Leth, M., Klamer, M., Lind, A.-M., Jensen, H.E.K. and Iversen, J.J.L., 2001. C and N turnover and lignocellulose degradation during composting of Miscanthus straw and liquid pig manure. Compost Science & Utilisation 9 (3), 186-196.

Eisfeld, B. and Schnitzlein, K., 2001. The influence of confining walls on the pressure drop in packed beds. Chemical Engineering Science 56, 4321-4329.

Ekinci, K., Keener, H.M., and Elwell, D.J., 1999. Composting short paper fibre with broiler litter and additives part I: Effects of initial pH and carbon/nitrogen ratio on ammonia emission. Compost Science & Utilisation 8 (2), 160-171.

Ekinci, K., Keener, H.M., Michel, F.C. and Elwell, D.L., 2004. Modeling composting rate as a function of temperature and initial moisture content. Compost Science & Utilization 12 (4), 356-364.

Elwell, D.J., Keener, H.M., Hoitinck, H.A.J., Hansen, R.C. and Hoff, J., 1994. Pilot and full scale evaluations of leaves as an amendment in sewage sludge composting. Compost Science & Utilisation 2 (2), 55-74.

Elwell, D.J., Keener H.M., Hansen R.C., 1996. Controlled, high rate, composting of mixtures of food residuals, yard trimmings and chicken manure. Compost Science & Utilisation 4 (1), 6-15.

Elwell, D.J., Keener, H.M., Carey, D.S. and Schlak, P.P., 1998. Composting unamended chicken manure. Compost Science & Utilisation 6 (2), 22-35.

Elwell, D.J., Keener, H.M., Wiles, M.C., Borger, D.C. and Willett, L.B., 2001. Odorous emissions and odor control on composting swine manure/sawdust mixtures using continuous and intermittent aeration. Trans. ASAE 44 (5), 1307-1316.

Elwell, D.J., Hong, J.H. and Keener, H.M., 2002. Composting hog manure/sawdust mixtures using intermittent and continuous aeration: ammonia emissions. Compost Science & Utilisation 10 (2), 142-149.

Finger, S.M., Hatch, R.T. and Regan, T.M., 1976. Aerobic microbial growth in semi-solid matrices: heat and mass transfer limitations. Biotechnol. Bioeng. 18, 1193-1218.

Finstein, M.S., Miller, F.C., Strom, P.F., MacGregor, S.T. and Psarianos, K.M., 1983. Composting ecosystem management for waste treatment. Biotechnology June 1983, pp 347-353.

Fraser, B.S. and Lau, A.K., 2000. The effects of process control strategies on composting rate and odour emissions. Compost Science & Utilisation 8 (4), 274-292.

Freeman, T.M. and Cawthon, D.L., 1999. Use of composted dairy cattle solid biomass, poultry litter and municipal biosolids as greenhouse growth media. Compost Science & Utilisation 7 (3), 66-71.

Garcia-Gomez, A., Szmidt, R.A.K. and Roig, A., 2002. Enhancing the composting rate of spent mushroom substrate by rock dust. Compost Science & Utilisation 10 (2), 99-104.

Gibson, A.M., Bratchell, N. and Roberts, T.A., 1987. The effect of sodium chloride and temperature on the rate and extent of growth of clostridium boulinum type A in pasteurised pork slurry. Journal of Applied Bacteriology 62, 479-490.

Gompertz, B., 1825. On the nature of the function expressive of the law of human mortality, and on a new mode of determining the value of life contingencies. Philos. Trans R. Soc. London 115, 513-585.

Gray, K.R. and Sherman, K., 1971. Review of composting part 1. Process Biochemistry 6 (6), 32-36.

Gostomski, P.A. and Liaw, L.P., 2001. Air permeability of biofilter media. Proceedings of the Air and Waste Management 94th Annual Meeting and Exhibition, Orlando, USA. 18-24 June, 2001. Published on CD-ROM. Air and Waste Management Association, Pittsburgh, USA.

Hamelers, B.V.F., 1993. A theoretical model of composting kinetics. In: Science and Engineering of Composting: Design, Environmental and Microbial and Utilisation aspects. Pp 59-94. Hoitink, H.A.J. and Keener, H.M. (Eds), Renaissance Publications, Worthington, USA.

Hamelers, B.V.F. and Richard, T.L., 2001. The effect of dry matter on the composting rate: theoretical analysis and practical implications. In: ASAE paper 017004, ASAE, St Joseph, MI, USA.

Hamelers, H.V.M., 2004. Modeling composting kinetics: A review of approaches. Reviews in Environmental Science and Biotechnology 3, 331-342.

Hamoda, M.F., Abu Qdais, H.A. and Newham, J., 1998. Evaluation of municipal solid waste composting kinetics. Resources Conservation and Recycling 23 (4), 209-223.

Hansen, R., Keener, H. and Hoitinck, H., 1989). Poultry manure composting: an exploratory study. Trans. ASAE 32 (6), 2151-2158.

Harper, E., Miller, F.C. and Macauley, B.J., 1992. Physical management and interpretation of an environmentally controlled composting ecosystem. Australian Journal of Experimental Agriculture 32 (5), 657-667.

Haug, R.T., 1993. The practical handbook of compost engineering. Lewis Publishers, Boca Raton, Florida, USA.

Helfrich, P., Chefetz, B., Hadar, Y. Chen, Y. and Schnabl, H., 1998. A novel method for determining phytotoxicity in composts. Compost Science & Utilisation 6 (3), 6-13.

Herrmann, R.F. and Shann, J.F., 1997. Microbial community changes during the composting of municipal solid waste. Microbial Ecology 33 (1), 78-85.

Higgins, C. and Walker, L., 2001. Validation of a new model for aerobic organic solids decomposition: simulations with substrate specific kinetics. Process Biochemistry 36 (8-9), 875-884.

Hogan, J.A., Miller, F.C. and Finstein, M.S., 1989. Physical modeling of the composting ecosystem. Applied and Environmental Microbiology 55 (5), 1082-1092.

Hogland, W., Bramryd, T., Marques, M. and Nimmermark, S., 2003. Physical, chemical and biological processes for optimizing decentralized composting. Compost Science & Utilization 11 (4), 330-336.

Holland, F. and Proffitt, A., 1998. Overview of composting in the UK. Biocycle 39 (2), 69-71.

Hong, J.H., Keener, H.M. and Elwell, D.J., 1998. Preliminary study on the effect of continuous and intermittent aeration on composting of hog manure ammended with sawdust. Compost Science & Utilisation 6 (3), 74-88.

Hong, J.H. and Park, K.J., 2004. Wood chip biofilter performance of ammonia gas from composting manure. Compost Science & Utilisation 12 (1), 25-30.

Horiuchi, J.I., Ebie, K., Tada, K., Kobayashi, M. and Kanno, T., 2003. Simplified method for estimation of microbial activity in compost by ATP analysis. Bioresource Technology 86 (1), 95-98.

Hwang, E.-Y., Namkoong, W. and Park, J.-S., 2001. Recycling of remediated soil for effective composting of diesel contaminated soil. Compost Science & Utilisation 9 (2), 143-148.

Huang, J.S., Wang, C.H. and Jih, C.G., 2000. Empirical model and kinetic behavior of thermophilic composting of vegetable waste. Journal of Environmental Engineering-ASCE 126 (11), 1019-1025.

Itavaara, M. and Vikman, M., 1996. An overview of methods for biodegradability testing of biopolymers and packaging materials. Journal of Environmental Polymer Degradation 4 (1), 29-36.

Iwabuchi, K., Kimura, T. and Otten, L., 1999. Effect of volumetric water content on thermal properties of dairy cattle feces mixed with sawdust. Bioresource Technology 70 (3), 293-297.

Jackson, M.J. and Line, M.A., 1997. Composting pulp and paper mill sludge – effect of temperature and nutrient addition method. Compost Science & Utilisation 5 (1), 74-81.

Jackson, M.J. and Line, M.A., 1997. Windrow composting of a pulp and paper mill sludge: Process performance and assessment of product quality. Compost Science & Utilization 5 (3), 6-14.

Joyce, J.F., Sato, C., Cardenas, R. and Surampalli, RY., 1998. Composting of polycyclic aromatic hydrocarbons in simulated municipal solid waste. Water Environment Research 70 (3), 356-361.

Kaiser, J., 1996. Modelling composting as a microbial ecosystem: A simulation approach. Ecological Modelling 91 (1-3), 25-37.

Kaplan, D.L. and Kaplan, A.M., 1982. Thermophilic transformations of 2,4,6-trinitrotoluene under simulated composting conditions. Applied and Environmental Microbiology 44, 757-760.

Kaufman, S.M., Goldstein, N., Millrath, K. and Themelis, N.J., 2004. The state of garbage in America. Biocycle 45 (1), 31-41.

Kayhanian, M. and Tchobanoglous, G., 1992. Computation of C/N ratios for various organic fractions. Biocycle 33 (5), 58-60.

Kayhanian, M., 1993. Anaerobic Composting for Msw. Biocycle 34 (5), 82-83.

Keener, H.M., Marugg, C., Hansen, R.C. and Hoitink, H.A.J., 1993 Optimising the efficiency of the composting process. Science & Engineering of Composting: Design, Environmental & Microbial & Utilisation aspects, H.A.J. Hoitink and H.M. Keener, eds., Renaissance Publications, Worthington, USA., 59-94.

Keener, H.M., Elwell, D.L., Das, K.C. and Hansen, R.C., 1997. Specifying design/operation of composting systems using pilot scale data. Applied Engineering in Agriculture 13 (6), 767-772.

Keener, H.M., Elwell, D.J., Ekinci, K. Hoitink, H.A.J., 2001. Composting and value added utilisation of manure from a swine finishing facility. Compost Science & Utilisation 9 (4), 312-321.

Keener, H. M., Elwell, D. J. and Grande, D., 2002. NH_3 emissions and N-balances for a 1.6 million caged layer facility: manure belt composting vs deep pit operation. Trans. ASAE 45 (6), 1977-1984.

Keener, H.M., Ekinci, K. and Michel, F.C., 2005. Composting process optimisation - using on/off controls. Compost Science and Utilisation 13 (4), 288-299.

Kim, D. S., Kim, J.O. and Lee, J.J., 2000. Aerobic composting performance and simulation of mixed sludges. Bioprocess Engineering 22 (6), 533-537.

Kishimoto, M., Preechaphan, C., Yoshida, T. and Taguchi, H., 1987. Simulation of an aerobic composting of activated sludge using a statistical procedure. MIRCEN J. 3, 113-124.

Kithome, M., Paul, J.W. and Bomke, A.A., 1999. Reducing nitrogen losses during simulated composting of poultry manure using adsorbents or chemical amendments. Journal of Environmental Quality 28 (1), 194-201.

Koenig, A. and Tao, G.H., 1996. Accelerated forced aeration composting of solid waste. Proceedings of the Asia-Pacific Conference on Sustainable Energy and Environmental Technology, Singapore, 450-457.

Komilis, D., 2006. A kinetic analysis of solid waste composting at optimal conditions. Waste Management 26 (1), 82-91.

Komilis, D.P. and Ham, R.H., 2000. A comparison of static pile and turned windrow methods for poultry litter compost production. Compost Science & Utilisation 8 (3), 254-265.

Komilis, D.P. and Ham, R.H., 2006. Carbon dioxide and ammonia emissions during composting of mixed paper, yard waste and food waste. Waste Management 26, 62-70.

Korolewicz, T., Turek, M., Ciba, J. and Cebula, J., 2001. Speciation and removal of zinc from composted municipal solid wastes. Environmental Science and Technology, 35 (4), 810-814.

Krzymien, M., Day, M., Shaw, K., Mohmad, R. and Sheehan, S., 1999. The role of feed composition on the composting process. II. Effect on the release of volatile organic compounds and odours. Journal of Environmental Science and Health Part A-Toxic/Hazardous Substances and Environmental Engineering 34 (6), 1369-1396.

La Brooy, S., Singh, D. and Lawson, J., 2003. The UR-3R facility: a fully integrated approach to municipal solid waste management. In: Proceedings of the Fourth International Conference of ORBIT Association on Biological Processing of Organics: Advances for a Sustainable Society, 30th April-2 May, 2003, Perth, Australia.

Laos, F., Mazzarino, MJ., Walter, L. and Roselli, L., 1998. Composting of fish wastes with wood by-products and testing compost quality as a soil amendment: experiences in the Patagonia region of Argentina. Compost Science & Utilisation 6 (1), 59-66.

Larsen, K.L. and McCartney, D.M., 2000. Effect of C:N ratio on microbial activity and N retention: bench scale study using pulp and paper biosolids. Compost Science & Utilisation 8 (2), 147-159.

Lau, A.K., Lo, K.V., Liao, P.H. and Yu, J.C., 1992. Aeration experiments for swine waste composting. Bioresource Technology 41 145-152.

Lay, J.J., Li, Y.Y. and Noike, T., 1998. A mathematical model for methane production from a landfill. Journal of Environmental Engineering ASCE 124 (8), 730-736.

Leiva, M.T.G., Casacuberta, A.A. and Ferrer, A.S., 2003. Application of experimental design technique to the optimization of bench-scale composting conditions of municipal raw sludge. Compost Science & Utilization 11 (4), 321-329.

Lemus, G.R., Lau, A.K., Branion, R.M.R. and Lo, K.V., 2004. Bench-scale study of the biodegradation of grease trap sludge with yard trimmings or synthetic food waste via composting. Journal of Environmental Engineering and Science 3 (6), 485-495.

Leth, M., Jensen, H. and Iversen, J., 2001. Influence of different nitrogen sources on composting of Miscanthus in open & closed systems. Compost Science & Utilisation 9 (3), 197-205.

Liao, P.H., May, A.C. and Chieng, S.T., 1995. Monitoring process efficiency of a full-scale in-vessel system for composting fisheries wastes. Bioresource Technology 54 (2), 159-163.

Libmond, S. and Savoie, J-M., 1993. Degradation of wheat straw by a microbial community-stimulation by a polysaccharidase complex. Appl.Microbiol.Biotechnol. 40 567-574.

Lin, G.H.Y. and Mermelstein, R., 1994. Acute Toxicity Studies of Xerox Reprographic Toners. Journal of the American College of Toxicology 13 (1), 2-20.

Lehmann, R.G., Smith, D.M., Narayan, R., Kozerski, G.E. and Miller, J.R., 1999. Life cycle of silicone polymer, from pilot scale composting to soil amendment. Compost Science & Utilisation 7 (3), 72-82.

Leth, M., Jensen, H.E.K. and Iversen, J.J.L., 2001. Influence of different nitrogen sources on composting of Miscanthus in open and closed systems. Compost Science & Utilisation 9 (3), 197-205.

Lhadi, E.K., Tazi, H., Aylaj, M., Tambone, F. and Adani, F., 2004. Cocomposting separated MSW and poultry manure in Morocco. Compost Science & Utilization 12 (2), 137-144.

Loser, C., Ulbricht, H., Hoffman, P. and Seidel, H., 1999. Composting of wood containing polycyclic aromatic hydrocarbons (PAHs). Compost Science & Utilisation 7 (3), 16-32.

Loser, C., Ulbrict, H. and Seidel, H., 2004. Degradation of polycyclic aromatic hydrocarbons in waste wood. Compost Science and Utilisation 12 (4), 335-341.

Lyberg, M.D. and Hogland, W., 2004. Performance of a vertically fed compost reactor. Compost Science & Utilization 12 (2), 169-174.

Lyon, P.-F., Beffa, T., Fischer, J.L. and Aragno, M., 2000. Xylanase activity and thermostratification during the thermogenic phase of industrial composting in aerated trenches. Waste Management and Research 18, 174-183.

Mackey, B.M. and Kerridge, A.L., 1988. The Effect of Incubation-Temperature and Inoculum Size on Growth of Salmonellae in Minced Beef. International Journal of Food Microbiology 6 (1), 57-65.

Magalhaes, A.M.T., Shea, P.J., Jawson, M.D., Wicklund, E.A. and Nelson, D.W., 1993. Practical simulation of composting in the laboratory. Waste Management & Research 11, 143-154.

Marugg, C., Grebus, M., Hansen, R., Keener, H.M. and Hoitink, H.A.J., 1993. A kinetic model of the yard waste composting process. Compost Science and Utilisation 1 (1), 8-51.

Marrug, A.C., Maruscik, D.A., Ritchie, C.J., Schwab, B.S., Harper, S.R. and Rapaport, S.A., 1993. A novel bioreactor simulating composting of municipal solid waste J. Microbiol. Methods 18, 99-112.

Martinez-Inigo, M.-J. and Almendros, G., 1994. Kinetic study of the composting of evergreen oak forestry waste. Waste Management & Research 12 (4), 305-314.

Mason, I.G., Mollah, M.S., Zhong, M.F. and Manderson, G.J., 2004. Composting of high moisture content bovine manure using passive aeration. Compost Science & Utilisation 12 (3), 249-267.

Mason, I.G. and Milke, M.W., 2005a. Physical modelling of the composting environment: a review. Part 1: Reactor systems Waste Management 25 (5) 481-500.

Mason, I.G. and Milke, M.W., 2005b. Physical modelling of the composting environment: a review. Part 2: Simulation Performance Waste Management 25 (5) 501-509.

Mason, I.G., 2006. Mathematical modelling of the composting process: a review. Waste Management 26 (1), 3-21.

Mason, I.G., McLachlan, R.I. and Gérard, D.T, 2006. A double exponential model for biochemical oxygen demand. Bioresource Technology 97 (2), 273-282.

Mason, I.G., in press-a. An evaluation of substrate degradation patterns in the composting process. Part 1: Profiles at constant temperature. Waste Management. (Published on-line 17 September, 2007).

Mason, I.G., in press-b. An evaluation of substrate degradation patterns in the composting process. Part 2: Corrected-temperature profiles. Waste Management. (Published on-line 12 September, 2007).

Mathur, S.P., N.K., P. and M.P., L., 1990. Static pile, passive aeration composting of manure slurries using peat as a bulking agent. Biological Wastes 34, 323-333.

McCartney, D. and Hongtu Chen., 2001. Using a biocell to measure effect of compressive settlement on free air space and microbial activity in windrow composting. Compost Science & Utilisation 9 (4), 285-302.

Metcalf and Eddy, 1991. Wastewater Engineering: Treatment Disposal and Reuse. (3rd edition). McGraw-Hill Inc, New York, USA.

Michel, F.C., Reddy, C.A. and Forney, L.J., 1993. Yard waste composting: studies using different mixes of leaves and grass in a laboratory scale system. Compost Science & Utilisation 1, 85-96.

Michel, F.C. Reddy, C.A. and Forney, L.J., 1995. Microbial-degradation and humification of the lawn care pesticide 2,4-dichlorophenoxyacetic acid during the composting of yard trimmings. Applied and Environmental Microbiology 61 (7), 2566-2571.

Michel, F.C. and Reddy, C.A., 1998. Effect of oxygenation level on yard trimmings composting rate, odor production and compost quality in bench-scale reactors. Compost Science & Utilisation 6 (4), 6-14.

Michel, F.C., Quensen, J. and Reddy, C.A., 2001. Bioremediation of a PCB-contaminated soil via composting. Compost Science & Utilisation 9 (4), 274-284.

Miller, F.C., 1989. Matric potential as an ecological determinant in compost, a substrate dense system. Microbial Ecology 18, 59-71.

Mills, A.F., 1995. Basic heat and mass transfer. Richard D. Irwin Inc., Chicago, USA.

Minkara, M.Y., Lawson, T.B., Breitenbeck, G.A. and Cochran, B.J., 1998. Cocomposting of crawfish and agricultural processing by-products. Compost Science & Utilisation 6 (1), 67-74.

Minnich, J. and Hunt, M., 1979. The Rodale Guide to Composting. Rodale Press, Emmaus, USA.

Mohee, R., White, R.K. and Das, K.C., 1998. Simulation model for composting cellulosic (bagasse) substrates. Compost Science & Utilisation 6 (2), 82-92.

Mote, C.R. and Griffis, C.L., 1979. A system for studying the composting process. Agricultural Wastes 1 (3), 191-203.

Mote, C.R. and Griffis, C.L., 1980. Variations in the composting process for different organic carbon sources. Agricultural Wastes 2, 215-223.

Mote, C.R. and Griffis, C.L., 1982. Heat production by composting organic matter Agricultural Wastes 4 65-73.

Mueller, H., Schmidt, O., Daxl, A. and Bergmair, J., 2003. 3A-biogas; three step fermentation of solid state biowaste for biogas production and sanitation. In: Proceedings of the Fourth International Conference of ORBIT Association on Biological Processing of Organics: Advances for a Sustainable Society, 30th April-2 May, 2003, Perth, Australia, 327-332.

Nakasaki, K., Sasaki, Y., Shoda, M. and Kubota, H., 1985. Change in microbial numbers during thermophilic composting of sewage sludge with reference to CO_2 evolution rate. Applied and Environmental Microbiology 49 37-41.

Nakasaki, K., Kato, J., Akiyama, T. and Kubota, H., 1987. A new composting model and assessment of optimum operation for effective drying of composting material. Journal of Fermentation Technology 65 (4), 441-447.

Nakasaki, K., Akakura, N., Atsumi, K. and Takemoto, M., 1998. Degradation patterns of organic material in batch and fed-batch composting operations. Waste Management & Research 16 (5), 484-489.

Nakasaki, K., Akakura, N. and Takemoto, M., 2000. A prediction for the degradation pattern of organic materials in the composting of a fed-batch operation as inferred from the results of batch operation. Journal of Material Cycles Waste Management 2 (31-37).

Nakasaki, K. and Ohtaki, A., 2002. A simple numerical model for predicting organic matter decomposition in a fed-batch composting operation. Journal of Environmental Quality 31 (3), 997-1005.

Nakasaki, K., Nagasaki, K. and Ariga, O., 2004. Degradation of fats during thermophilic composting of organic waste. Waste Management & Research 22 (4), 276-282.

Namkoong, W. and Hwang, E-Y., 1997. Operational parameters for composting night soil in Korea. Compost Science & Utilisation 5 (4), 46-51.

Namkoong, W., Hwang, E-Y., Cheong, J-G. and Choi, J-Y., 1999. A comparative evaluation of maturity parameters for food waste composting. Compost Science & Utilisation 7 (2), 55-62.

Navaee-Ardeh, S., Bertrand, F. and Stuart, P.R., 2006. Emerging biodrying technology for the drying of pulp and paper mixed sludges. Drying Technology 24 (7), 863-878.

Ndegwa, P.M., Thompson, S.A. and Merka, W.C., 2000. A dynamic simulation model of in-situ composting of caged layer manure. Compost Science & Utilisation 8 (3), 190-202.

Negro, NJ. and Solano, ML., 1996. Laboratory composting assays of the solid residue resulting from the flocculation of olive mill wastewater with different lignocellulosic residues. Compost Science & Utilisation 4 (4), 62-71.

Neilsen, H. and Berthelsen, L., 2002. A model for the temperature dependency of thermophilic composting rate. Compost Science & Utilisation 10 (3), 249-257.

Noble, R., Fermor, T.R., Evered, C.E and Atkey, P.T., 1997. Bench scale preparation of mushroom substrates in controlled environments. Compost Science & Utilisation **5** (3), 6-14.

Ohtaki, A. and Nakasaki, K., 2000. Report: Ultimate degradability of various kinds of biodegradable plastics under controlled composting conditions. Waste Management & Research 18 (2), 184-189.

Ouatmane, A., Provenzano, M.R., Hafidi, M. and Senesi, N., 2000. Compost maturity assessment using calorimetry, spectroscopy and chemical analysis. Compost Science & Utilisation 8 (2), 124-134.

Pagga, U., Beimborn, D.B., Boelens, J. and DeWilde, B., 1995. Determination of the aerobic biodegradability of polymeric material in a laboratory controlled composting test. Chemosphere 31 (11-12), 4475-4487.

Palmisano, A.C., Maruscik, D.A., Ritchie, C.J., Schwab, B.S., Harper, S.R. and Rapaport, S.A., 1993. A novel bioreactor simulating composting of municipal solid waste. J. Microbiol. Methods 18 99-112.

Papadimitriou, E.K. and Balis, C., 1996. Comparative study of parameters to evaluate and monitor a composting process. Compost Science & Utilisation 4 (4), 52-61.

Paredes, C., Roig, A., Bernal, M.P., Sanchez-Monedero, M.A. and Cegarra, J., 2000. Evolution of organic matter and nitrogen during co-composting of olive mil wastewater with solid organic wastes. Biology & Fertility of Soils 32, 222-227.

Paredes, C., Bernal, M.P., Roig, A. and Cegarra, J., 2001. Effects of olive mill wastewater addition in composting of agroindustrial and urban wastes. Biodegradation 12 (4), 225-234.

Paredes, C., Bernal, M., Cegarra, J. and Roig, A., 2002. Bio-degradation of olive mill wastewater sludge by its co-composting with agricultural wastes. Bioresource Technology 85 (1), 1-8.

Park, K.J., Choi, M.H. and Hong, J.H., 2002. Control of composting odour using biofiltration. Compost Science & Utilisation 10 (4), 356-362.

Patni, N.K. and Kinsman, R.G., 1997. Composting of dilute manure slurries to reduce bulk by water evaporation. In: ASAE Annual International Meeting, August 10-14, 1997, Minneapolis, Minnesota, USA.

Pecchia, J.A., Beyer, D.M. and Wuest, P.J., 2002. The effects of poultry manure based formulations on odour generation during phase 1 mushroom composting. Compost Science & Utilisation 10 (3), 188-196.

Petiot, C. and de Guardia, A., 2004. Composting in a laboratory reactor: a review. Compost Science & Utilisation 12 (1), 69-79.

Plana, R., Mato, S., Aguilera, F., Artola, A., Perez, C., and Sanchez, A., 2001. Comparison between in-vessel and turned pile composting systems. Biocycle 42 (10), 63-65.

Qiao, L. and Ho, G., 1997. The effects of clay amendment on composting of digested sludge. Water Research 31 (5), 1056-1064.

Qin, X.S., Huang, G.H., Jiang, X.Y., Xi, B.D., Liang, Z.W., Christine, W.C. and Liu, H.L., 2004. Fuzzy approach for dynamic simulation of composting process under uncertainty. Transactions of Nonferrous Metals Society of China 14, 18-24.

Rajbanshi, S.S. and Inubushi, K., 1997. Chemical and biochemical changes during laboratory scale composting of allelopathic plant leaves (Eupatorium adenophorum and Lantana camara). Biology and Fertility of Soils 26 (1), 66-71.

Ratkowsky, D.A., Lowry, R.K., McMeekin, T.A., Stokes, A.N. and Chandler, R.E., 1983. Model for bacterial culture and growth rate throughout the entire biokinetic temperature range. J. Bacteriol. 154, 1222-1226.

Razvi, A.S. and Kramer, D.W., 1996. Evaluation of compost activators for composting grass clippings. Compost Science & Utilisation 4 (4), 72-80.

Richard, T.L. and Walker, L.P., 1998. Temperature kinetics of aerobic solid state biodegradation. Proceedings of the Institute of Biological Engineering 1, A22-A39.

Richard, T.L., Walker, L.P. and Gossett, J.M., 1999. The effects of oxygen on solid-state biodegredation kinetics. Proceedings of the Institute of Biological Engineering 2, A10-A30.

Richard, T.L., Hamelers, H.V.M., Veeken, A. and Silva, T., 2002. Moisture relationships in composting processes. Compost Science and Utilization 10 (4), 286-302.

Robinzon, R., Kimmel, E., Avnimelech, Y., 2000. Energy and mass balances of windrow composting system. Trans. ASAE 43 (5), 1253-1259.

Rodriguez Leon, J.A., Torres, A., Echevarria, J. and Saura, G., 1991. Energy balance in solid state fermentation processes. Acta Biotechnol. 11, 9-14.

Rosso, L., Lobry, J.R. and Flandrois, J.P., 1993. An unexpected correlation between cardinal temperatures of microbial growth highlighted by a new model. J. Theor. Biol. 162, 447-463.

Roy, S., Leclerc, P., Auger, F., Soucy, G., Moresoli, C., Cote, L., Potvin, D., Beaulieu, C and Brzezinski, R., 1997. A novel two-phase composting process using shrimp shells as an amendment to partly composted biomass. Compost Science & Utilisation 5 (4), 52-64.

Rynk, R. (Ed), 1992. On-farm composting handbook. NRAES, Ithaca, New York, USA.

Sadaka, S.S. and Engler, C.R., 2003. Effects of initial total solids on composting of raw manure with biogas recovery. Compost Science & Utilization 11 (4), 361-369.

Sartaj, M.L., Fernandes, L. and Patni, N.K., 1997. Performance of forced, passive, and natural aeration methods for composting manure slurries. Trans. ASAE 40 (2), 457-463.

Saucedo-Castaneda, G., Gutierrez-Rojas, M., Baquet, G., Raimbault, M. and Viniegra-Gonzalez, G., 1990. Heat transfer simulation in solid substrate fermentation. Biotechnol. Bioeng. 35, 802-808.

Scholwin, F. and Bidlingmaier, W., 2003. Fuzzifying the composting process: a new model based control strategy as a device for achieving a high grade and consistent product quality. Proceedings of the Fourth International Conference of ORBIT Association on Biological Processing of Organics: Advances for a Sustainable Society, 30th April-2 May, 2003, Perth, Australia, 739-751. ORBIT Association, Weimar, Germany.

Schulze, K.L., 1962. Continuous thermophilic composting. Applied Microbiology 10 108-122.

Seki, H, 2000. Stochastic modeling of composting processes with batch operation by the Fokker-Planck equation. Trans. ASAE 43 (11), 169-179.

Seymour, R.M, Donahue, D., Bourdon, M., Evans, J.R. and Wentworth, D., 2001. Intermittent aeration for in-vessel composting of crab processing waste. Compost Science & Utilisation 9 (2), 98-106.

Shamlou, P.A., 1988. Handling of bulk solids: theory and practice. London, UK. Butterworths.

Sharma, S., Mathur, R.C. and Vasudevan, P., 1999. Composting silkworm culture waste. Compost Science & Utilisation 7 (2), 74-81.

Shaw, K., Day, M., Krzymien, M., Mohmad, R. and Sheehan, S., 1999. The role of feed composition on the composting process. I. Effect on composting activity. Journal of Environmental Science and Health Part A-Toxic/Hazardous Substances and Environmental Engineering 34 (6) 1341-1367.

Schwab, B.S., Ritchie, C.J., Kain, D.J., Dobrin, G.C., King, L.W. and Palmisano, A.C., 1994. Characterization of compost from a pilot plant-scale composter utilizing simulated solid waste. Waste Management & Research 12, 289-303.

Shin, H.S., Han, S.K., Song, Y.C. and Lee, C.Y., 2001. Multi-step sequential batch two-phase anaerobic composting of food waste. Environmental Technology 22 (3), 271-279.

Sikora, L.J., Ramirez, M.A. and Troeschel, T.A., 1983. Laboratory composter for simulation studies. Journal of Environmental Quality 12 219-224.

Sikora, L.J. and Sowers, M.A., 1985. Effect of temperature control on the composting process. Journal of Environmental Quality 14 434-439.

Silviera, A.E. and Ganho R.B., 1995. Composting wastes contaminated with naphthalene. Compost Science & Utilisation 3 (4), 78-81.

Slater, R.A. and Frederickson, J., 2001. Composting municipal waste in the UK: some lessons from Europe. Resources Conservation and Recycling 32 (3-4), 359-374.

Smårs, S., Beck-Friis, B., Jönsson, H. and Kirchmann, H., 2001. An advanced experimental composting reactor for schematic simulation studies. Journal of Agricultural Engineering Research 78 (4), 415-422.

Smet, E., van Langenhove, H., and De Bo, I., 1999. The emission of volatile compounds during the aerobic and the combined anaerobic/aerobic composting of biowaste. Atmospheric Environment 33 (8), 1295-1303.

Smith, R. and Eilers, R.G., 1980. Numerical simulation of activated sludge composting. *EPA-600/2-8C-191*, USEPA, Cincinnati, Ohio, USA

Smith, D.M, Lehmann, R.G, Narayan, R. and Kozerski, G.E. and Miller, J.R., 1998. Fate and effects of silicone polymer during the composting process. Compost Science & Utilisation 6 (2), 6-12.

Solum, 2007. http://www.solum.com (accessed January, 2007)

Stocks, C., Barker, A.J. and Guy, S., 2002. The composting of brewery sludge. Journal of the Institute of Brewing 108 (4), 452-458.

Stombaugh, D.P. and Nokes, S.E., 1996. Development of a biologically based aerobic composting simulation model. Trans. ASAE 39 (1), 239-250.

Straatsma, G., Gerrits, J.P.G., Thissen, J.T.N.M., Amsing, J.G.M., Loffen, H. and van Griensven, L.J.L.D., 2000. Adjustment of the composting process for mushroom cultivation based on initial substrate composition. Bioresource Technology 72 (1), 67-74.

Strom, P.F., 1985. Effect of temperature on bacterial species diversity in thermophilc solid-waste composting. Applied and Environmental Microbiology 50 (4), 899-905.

Suler ,D.J. and Finstein, M.S., 1977. Effect of temperature, aeration and moisture on CO_2 formation in bench-scale, continuously thermophilic composting of solid waste. Applied and Environmental Microbiology 33 (2), 345-350.

Sundberg, C. and Jonsson, H., 2003. Down-scaling a large composting plant to pilot-scale for systematic research. Proceedings of the Fourth International Conference of ORBIT Association on Biological Processing of Organics: Advances for a Sustainable Society, 30th April-2 May, 2003, Perth, Australia, pp 388-397. ORBIT Association, Weimar, Germany.

Sundberg, C., Smars, S. and Jonsson, H., 2004. Low pH as an inhibiting factor in the transition from mesophilic to thermophilic phase in composting. Bioresource Technology 95 (2), 145-150.

Supriyadi, S., Kriwoken, L.K. and Birley, I., 2000. Solid waste management solutions for Semarang, Indonesia. Waste Management & Research 18 (6), 557-566.

Suzuki, T., Ikumi, Y., Okamoto, S., Watanabe, I., Fujitake, N. and Otsuka, H., 2004. Aerobic composting of chips from clear-cut trees with various co-materials. Bioresource Technology 95 (2), 121-128.

Suzuki, D. (2006) The autobiography. Allen and Unwin, Australia.

Tchobanoglous, G., Theisen, H. and Vigil, S.A., 1993. Integrated solid waste management: engineering principles and management issues. McGraw-Hill, New York, USA

Tremier, A. and de Guardia, A., 2003. Heat and mass transfers prediction thanks to gas flow RTD characterisation during sewage sludge and bulking agent composting in a 300 liter pilot reactor. Proceedings of the Fourth International Conference of ORBIT Association on Biological Processing of Organics: Advances for a Sustainable Society, 30th April-2 May, 2003, Perth, Australia, pp 721-731. ORBIT Association, Weimar, Germany.

Tremier, A., de Guardia, A., Massiani, C., Paul, E. and Martel, J.L., 2005a. A respirometric method for characterising the organic composition and biodegradation kinetics and the tmeperature influence on the biodegradation kinetics, for a mixture of sludge and bulking agent to be composted. Bioresource Technology 96 (2), 169-180.

Tremier, A., De Guardia, A., Massiani, C. and Martel, J.L., 2005b. Influence of the airflow rate on heat and mass transfers during sewage sludge and bulking agent composting. Environmental Technology 26 (10), 1137-1149.

Tseng D.Y., Chalmers, J.J., Tuovinen, O.H. and Hoitink, H.A.J., 1995. Characterisation of a bench scale system for studying the biodegradation of organic solid wastes. Biotechnol. Progr. 11, 443-451.

USEPA, 1995. Land application of sewage sludge and domestic septage. Process design manual. EPA/625/K-95/001, pp 15-19. US Environmental Protection Agency, Washington DC, USA.

van Bochove, E., Couillard, D. and Nolin, M.C., 1995. Characterization of the Composting Stages By a Multivariate- Analysis - Application to the Nitrogen-Cycle. Environmental Technology 16 (10), 929-941.

VanderGheynst, JS., Gossett, JM., Walker, LP., 1997a. High-solids aerobic decomposition: Pilot-scale reactor development and experimentation. Process Biochemistry 32 (5), 361-375.

VanderGheynst, J.S., Walker, L.P., Parlange, J.Y., 1997b. Energy transport in a high-solids aerobic degradation process: Mathematical modeling and analysis. Biotechnology Progress 13 (3), 238-248.

VanderGheynst, J., Cogan, D., Defelice, P., Gossett, J. and Walker, L., 1998. Effect of process management on the emission of organosulfur compounds and gaseous antecedents from composting processes. Environmental Science & Technology 32 (23), 3713-3718.

VanderGheynst, J.S. and Lei, F., 2003. Microbial community structure dynamics during aerated and mixed composting. Trans. ASAE 46 (2), 577-584.

Van der Zee, M., Stoutjesdijk, J.H., Feil, H. and Feijen, J., 1998. Relevance of aquatic biodegradation tests for predicting degradation of polymeric materials during biological solid waste treatment. Chemosphere 36 (3), 461-473.

van Ginkel, J.T., 1996. Physical and biochemical processes in composting material. PhD thesis, Wageningen Agricultural University (Landbouwuniversiteit te Wageningen), The Netherlands.

VanLier, J.J.C., VanGinkel, J.T., Straatsma, G., Gerrits, J.P.G. and VanGriensven, L.J.L.D., 1994. Composting of mushroom substrate in a fermentation tunnel – compost parameters and a mathematical model. Netherlands Journal of Agricultural Science 42 (4), 271-292.

Veeken, A., de Wilde, V. and Hamelers, B., 2002. Passively aerated composting of straw-rich pig manure: effect of compost bed porosity. Compost Science & Utilisation 10 (2), 114-128.

Veeken, A., Timmermans, J., Szanto, G. and Hamelers, B.V.F., 2003. Design of passively aerated compost systems on basis of compaction-porosity-permeability data. Proceeding of the Fourth International Conference of ORBIT Association on Biological Processing of Organics: Advances for a Sustainable Society, 30th April-2 May, 2003, Perth, Australia, pp 85-96. ORBIT Association, Weimar, Germany.

Viel, M., Sayang, D., Peyre, A. and Andre, L., 1987. Optimisation of in-vessel co-composting through heat recovery. Biological Wastes 20, 167-185.

Walker, I.K. and Harrison, W.J., 1960. The self-heating of wet wool. *NZ Journal of* Agricultural Research 3, (6), 861-895.

Weppen, P., 2001. Process calorimetry on composting of municipal organic wastes. Biomass and Bioenergy 21, 289-299.

Witter, E. and Lopez-Real, J., 1988. Nitrogen losses during the composting of sewage sludge and the effectiveness of clay soil, zeolite and compost in adsorbing volatilised ammonia. Biological Wastes 23, 279-294.

Whang, D.S. and Meenaghan, G.F., 1980. Kinetic model of the composting process. Compost Science/Land Utilisation 21 (3), 44-46.

Whiting, R.C., 1995. Microbial Modeling in Foods. Critical Reviews in Food Science and Nutrition 35 (6), 467-494.

Yamada, Y. and Kawase, Y., 2006. Aerobic composting of waste activated sludge: Kinetic analysis for microbiological reaction and oxygen consumption. Waste Management 26, 49-61.

Zavala, M.A.L., Funamizu, N. and Takakuwa, T., 2004a. Modeling of aerobic biodegradation of feces using sawdust as a matrix. Water Research 38 (5), 1327-1339.

Zavala, M.A.L., Funamizu, N. and Takakuwa, T., 2004b. Temperature effect on aerobic biodegradation of feces using sawdust as a matrix. Water Research 38 (9), 2406-2416.

Zwietering, M.H., Jongenburger, I., Rombouts, F.M. and Vantriet, K., 1990. Modeling of the Bacterial-Growth Curve. Applied and Environmental Microbiology 56 (6), 1875-1881.

APPENDIX 2
MATLAB ROUTINES

1. bvs1
2. bvs2
3. gomp
4. fitbvs1
5. fitbvs2
6. fitgomp
7. dimplot
8. dimplot2
9. dimplot3
10. Trosso1
11. plotdata
12. areas
13. plotwatts
14. VSplot (for “mined” data)
15. VSplot (for experimental data)

1. bvs1

```
function f = bvs(p,t);
f = p(1)*(1-exp(-p(2)*t));
return;
%this fn is called by lsqcurvefit
```

2. bvs2

```
function f = bvs2(p,t)
f = (p(1)*(1-exp(-p(2)*t))+p(3)*(1-exp(-p(4)*t)));;
return;
%this function is called by lsqcurvefit
```

3. gomp

```
function f = gomp(p,t)
e=2.718282;
f=p(1)*exp(-exp((((p(2)*e)/p(1))*(p(3)-t))+1));
return;
%this function is called by lsqcurvefit
```

4. fitbvs1

```
%fitbvs1: a script file to fit a single exponential curve to bvs vs time
data and compute the errors
%created by Robert McLachlan and Ian Mason
%set up fitted curve fy
fy=[];
%enter initial guess for parameters
p0 = [5 0.1];
%fit the selected curve (file 'bvs1.m' has the curve to fit from)
pars = lsqcurvefit('bvs1',p0,t,y);
%set up a fine grid to evaluate the fitted fn
for dt = (0:0.1:max(t))';
fy = [fy;bvs1(pars,dt)]; ,end
%plot the original data and the fitted curve
plot(t,y,'.',dt,bvs1(pars,dt));
title('Figure 1: Single exponential model: Data of Bach et al. (1985); lime
sludge; corrected to 40^oC');
xlabel('Time (d)')
ylabel('Volatile solids removal (%)')
%display the results and errors
pars
fy=bvs1(pars,t);
n=length(t);
error = y - fy;
error = sum(error.^2)
mse = error/n
rmse = sqrt(mse)
norm_error = rmse*100/pars(1)
%calulate value of x for near saturation
'exponential reaches 95% saturation at x=',
[-log(0.05)/pars(2)]
%end
```

5. fitbvs2

```
%fitbvs2: a script file to fit a double exponential curve to bvs vs time
data and compute the errors
%created by Robert McLachlan and Ian Mason
%set up curve fy
fy=[];
%enter initial guess for parameters
p0 = [6.6 3.12 42.1 0.22];
%fit the selected curve (file 'bvs2.m' has the curve to fit from)
pars = lsqcurvefit('bvs2',p0,t,y)
%set up a fine grid to evaluate the fitted fn
for dt = (0:0.1:max(t))';
fy = [fy;bvs2(pars,dt)]; ,end
%plot the original data and the fitted curve
plot(t,y,'.',dt,bvs2(pars,dt));
title('Figure 1: Double exponential model; data Komilis and Ham (2000); MXP
at 55^oC');
xlabel('Time (d)')
ylabel('CO_2-C removed (%)')
%calculate the errors
fy=bvs2(pars,t);
n=length(t);
error = y - fy;
error = sum(error.^2)
mse = error/n
rmse = sqrt(mse)
norm_error = rmse*100/(pars(1)+pars(3))
%calculate time to reach 95% saturation
'exponentials reach 95% saturation at x=',
[-log(0.05)/pars(2), -log(0.05)/pars(4)]
%end
```

6. fitgomp

```
%fitgomp: a script file to fit a modified Gompertz curve to bvs vs time
data and compute the errors
%created by Ian Mason
%set up curve fy
fy=[];
%enter initial guess for parameters
p0 = [41 6.0 0.8];
%fit the selected curve (file 'gomp.m' has the curve to fit from)
pars = lsqcurvefit('gomp',p0,t,y,0)
%set up a fine grid to evaluate the fitted fn
for dt = (0:0.1:max(t))';
fy = [fy;gomp(pars,dt)]; ,end
%plot the original data and the fitted curve
plot(t,y,'.',dt,gomp(pars,dt));
title('Figure 1: Gompertz model; Data of Bach et al. (1985); fig2b');
xlabel('Time (d)')
ylabel('CO_2-C emitted (%)')
%calculate errors
fy=gomp(pars,t);
n=length(t);
error = y - fy;
error = sum(error.^2)
mse = error/n
rmse = sqrt(mse)
norm_error = rmse*100/pars(1)
%calculate fy at time zero
```

```
e=2.718282;
z=pars(1)*exp(-exp((((pars(2)*e)/pars(1))*(pars(3)-0))+1))
%end
```

7. dimplot

```
%dimplot: a file to plot selected models in dimensionless form
%plot function of Bach et al 88[fig 1]
%created by Ian Mason
k=0.41;
t=0:0.1:4;
y=(1-exp(-k*t));
figure(1)
plot(t,y)
title('Figure 1: Dimensionless substrate removal functions at constant
temperature');
xlabel('Time (d)')
ylabel('BVS/BVS_m_a_x (dimensionless)')
hold on
% plot function of Michel 98 (air zero)
k=0.02;
t=0:0.1:40;
y=(1-exp(-k*t));
plot(t,y)
hold on
%plot function of Michel 98 (air 3)
BVS1=7.4;
BVS2=40.9;
a=BVS2/BVS1;
b=BVS1/BVS2;
k1=0.46;
k2=0.07;
t=0:0.1:40;
y=((1-exp(-k1*t))/(1+a))+((1-exp(-k2*t))/(1+b));
plot(t,y)
hold on
%plot data of Bono CS 45
e=2.718282;
p(1)=172;
p(2)=13.6;
p(3)=3.3;
t=0:0.1:20;
y=exp(-exp((((p(2)*e)/p(1))*(p(3)-t))+1));
plot(t,y)
%end
```

8. dimplot2

```
%dimplot2: a file to plot selected models in dimensionless form
%temperature corrected; full data sets
%plot function of Michel et al 1993 [mix3], v1
%created by Ian Mason
k=0.07;
t=0:0.1:40;
y=(1-exp(-k*t));
figure(1)
plot(t,y)
title('Figure 1: Dimensionless substrate removal functions for data
corrected to 40 ^oC');
xlabel('Time (d)')
```

```
ylabel('BVS/BVS_m_a_x (dimensionless)')
hold on
%plot function of Mote and Griffis 1980 [fig3]
k=0.08;
t=0:0.1:11.7;
y=(1-exp(-k*t));
plot(t,y)
hold on
%plot function of Mote and Griffis 1979 [fig4]
BVS1=11.1;
BVS2=62.5;
a=BVS2/BVS1;
b=BVS1/BVS2;
k1=3.40;
k2=0.20;
t=0:0.1:6;
y=((1-exp(-k1*t))/(1+a))+((1-exp(-k2*t))/(1+b));
plot(t,y)
hold on
%plot function of Nakasaki et al. 1985 [fig4]
BVS1=6.6;
BVS2=42.1;
a=BVS2/BVS1;
b=BVS1/BVS2;
k1=4.53;
k2=0.24;
t=0:0.1:4.6;
y=((1-exp(-k1*t))/(1+a))+((1-exp(-k2*t))/(1+b));
plot(t,y)
hold on
%plot data of Sikora and Sowers 1985; limed sludge, air900, v1
e=2.718282;
p(1)=9.3;
p(2)=2.21;
p(3)=1.85;
t=0:0.1:9;
y=exp(-exp((((p(2)*e)/p(1))*(p(3)-t))+1));
plot(t,y)
hold on
%plot data of Bach et al 1985; limed sludge, T70, v1
e=2.718282;
p(1)=78.1;
p(2)=32.24;
p(3)=0.50;
t=0:0.1:6.7;
y=exp(-exp((((p(2)*e)/p(1))*(p(3)-t))+1));
plot(t,y)
%end
```

9. dimplot 3

```
%dimplot 3: a file to plot selected models in dimensionless form
%temperature corrected to 40C; lag times and multi-phase data removed
%plot function of Mote and Griffis 1980, [data starts at 20 hr]
%created by Ian Mason
k=0.40;
t=0:0.1:4.2;
y=(1-exp(-k*t));
plot(t,y)
```

```
title('Figure 1: Dimensionless substrate removal functions for data
corrected to 40 ^oC');
xlabel('Time (d)')
ylabel('BVS/BVS_m_a_x (dimensionless)')
hold on
% plot function of Bach et al 1985; lime [fig2av2, data starts at 0.57 d]
k=0.43;
t=0:0.1:4.4;
y=(1-exp(-k*t));
plot(t,y)
hold on
% plot function of Bach et al 1985; lime, T60, [v2, data starts at 0.7 d]
k=0.44;
t=0:0.1:4.1;
y=(1-exp(-k*t));
plot(t,y)
hold on
% plot function of Bach et al 1985; lime, air60, [v2, data starts at 0.8 d]
k=0.43;
t=0:0.1:3;
y=(1-exp(-k*t));
plot(t,y)
hold on
% plot function of Bach et al 1985; lime, air_var, [v2, data starts at 1.3
d]
k=0.19;
t=0:0.1:9;
y=(1-exp(-k*t));
plot(t,y)
hold on
%plot function of Bach et al. 1985 [fig5b; curve a]
BVS1=10.9;
BVS2=44.4;
a=BVS2/BVS1;
b=BVS1/BVS2;
k1=0.59;
k2=0.09;
t=0:0.1:8.8;
y=((1-exp(-k1*t))/(1+a))+((1-exp(-k2*t))/(1+b));
plot(t,y)
hold on
%plot function of Bach et al. 1985 [fig5b; curve b]
BVS1=19.7;
BVS2=53.9;
a=BVS2/BVS1;
b=BVS1/BVS2;
k1=0.57;
k2=0.10;
t=0:0.1:9.8;
y=((1-exp(-k1*t))/(1+a))+((1-exp(-k2*t))/(1+b));
plot(t,y)
hold on
%plot function of Nakasaki et al. 1985 [fig4]
BVS1=5.2;
BVS2=41.8;
a=BVS2/BVS1;
b=BVS1/BVS2;
k1=4.23;
k2=0.24;
t=0:0.1:4.7;
y=((1-exp(-k1*t))/(1+a))+((1-exp(-k2*t))/(1+b));
```

```
plot(t,y)
hold on
%plot data of Campbell et al 1990; Sitka spruce v2
e=2.718282;
p(1)=34.2;
p(2)=6.66;
p(3)=0.9;
t=0:0.1:7.1;
y=exp(-exp((((p(2)*e)/p(1))*(p(3)-t))+1));
plot(t,y)
%end
```

10. Trosso1

```
function fT = Trosso1(Tmin,Topt,Tmax,T)
%Trosso1: a function to calculate the temperature correction curve of Rosso
et al 1993
%for specified values of minimum, optimum, maximum and actual temperature
%created by Ian Mason
%call syntax: fT = Trosso1(Tmin,Topt,Tmax,T)
%call Tmin, Topt, Tmax
Tmin=input('enter Tmin (C): ');
Topt=input('enter Topt (C): ');
Tmax=input('enter Tmax (C): ');
% define temperature range
T=Tmin:1:Tmax;
    fT=((T-Tmax).*(T-Tmin).^2)./((Topt-Tmin).*((Topt-Tmin).*(T-Topt)-(Topt-
Tmax).*(Topt+Tmin-2.*T)));
    plot(T,fT)
title('Figure: Temperature correction function of Rosso et al (1993)')
xlabel('Temperature (C)')
ylabel('f(T)')
%end
```

11. plotdata

```
%plotdata: a script file to plot data from experimental composting runs
%created by Ian Mason
%syntax 'plotdata'
%call data
[t,m,RH1,RH2,Qa,CO2,T1,T2,T3,T4,T5,T6,T7,T8,T9,T10,T11,T12,T13,T14,T15,T16,
L]=textread('data_run7_v2.txt','%f %f %f %f %f %f %f %f %f %f %f %f %f %f
%f %f %f %f %f %f %f %f %f','headerlines',3);
%enter run and initial TS for run
run=input('enter run ((#):   ');
TS=input('enter initial TS for run (kg):   ');
int=input('enter time interval for calculations (min):   ');
n=1:int:size(t);
%plot a graph (mass loss)
figure(1)
plot(t(n),m(n),'k')
xlabel('Time (d)')
ylabel('Mass (kg)')
title('Figure 1: Total mass loss vs time; run 6')
%plot another graph (headspace temperatures)
figure(2)
plot(t,T1,'k')
hold on
plot(t(n),T2(n),'k')
xlabel('Time (d)')
```

```
ylabel('Temperature (^oC)')
title('Figure 2: Headspace temperatures T1 & T2; run 6')
%plot another graph (core temperatures)
figure(3)
plot(t(n),T3(n),'k')
hold on
plot(t(n),T4(n),'k')
hold on
plot(t(n),T5(n),'k')
hold on
plot(t(n),T6(n),'k')
hold on
plot(t(n),T7(n),'k')
hold on
plot(t(n),T8(n),'k')
hold on
plot(t(n),T9(n),'k')
Tforty(n)=40;
plot(t(n),Tforty(n),'k')
Tfiftyfive(n)=55;
plot(t(n),Tfiftyfive(n),'k')
xlabel('Time (d)')
ylabel('Temperature (^oC)')
title('Figure 3: Core temperatures; run 6')
%plot another graph (wall temperatures section 1)
figure(4)
plot(t(n),T10(n),'k--')
hold on
plot(t(n),T11(n),'k:')
hold on
plot(t(n),T3(n),'k')% add corresponding core temperature
xlabel('Time (d)')
ylabel('Temperature (^oC)')
title('Figure 4: Wall temperatures; upper section; run 6')
%plot another graph (wall temperatures section 2)
figure(5)
plot(t(n),T12(n),'k--')
hold on
plot(t(n),T13(n),'k:')
hold on
plot(t(n),T5(n),'k')% add corresponding core temperature
xlabel('Time (d)')
ylabel('Temperature (^oC)')
title('Figure 5: Wall temperatures T12; mid-section; run 6')
%plot another graph (wall temperatures section 3)
figure(6)
plot(t(n),T14(n),'k--')
hold on
plot(t(n),T15(n),'k:')
hold on
plot(t(n),T7(n),'k')% add corresponding core temperature
xlabel('Time (d)')
ylabel('Temperature (^oC)')
title('Figure 6: Wall temperatures; lower section; run 6')
%plot another graph (delta wall temperatures section 1)
deltaT1(n)=T10(n)-T11(n);
figure(7)
plot(t(n),deltaT1(n),'k')
xlabel('Time (d)')
ylabel('Temperature (^oC)')
title('Figure 7: Delta wall temperatures; upper section; run 6')
```

```
%plot another graph (delta wall temperatures section 2)
deltaT2(n)=T12(n)-T13(n);
figure(8)
plot(t(n),deltaT2(n),'k')
xlabel('Time (d)')
ylabel('Temperature (^oC)')
title('Figure 8: Delta wall temperatures; mid section; run 6')
%plot another graph (delta wall temperatures section 3)
deltaT3(n)=T14(n)-T15(n);
figure(9)
plot(t(n),deltaT3(n),'k')
xlabel('Time (d)')
ylabel('Temperature (^oC)')
title('Figure 9: Delta wall temperatures; lower section; run 6')
%plot another graph (exit gas temperatures at CO2 probe)
figure(10)
plot(t(n),T16(n),'k')
xlabel('Time (d)')
ylabel('Temperature (^oC)')
title('Figure 10: CO2 temperatures T16; run 6')
%plot another graph (CO2 concentrations)
figure(11)
plot(t(n),CO2(n),'k')
hold on
%calculate sensor errors;
%option 1: max mfr error; <0.02%CO2+2% of reading
%CO2e(n)=0.02+(0.02.*CO2(n));
%option 2: actual calibration; +0.142 at 20% = 0.02+0.006*20
%CO2e(n)=0.02+(0.0061.*CO2(n));
%option 3: observed random; +- 0.025*CO2
CO2e(n)=0.025;
%calculate range
CO2p(n)=CO2(n)+CO2e(n)';
plot(t(n),CO2p(n),'k--')
hold on
CO2minus(n)=CO2(n)-CO2e(n)';
plot(t(n),CO2minus(n),'k:')
xlabel('Time (d)')
ylabel('CO2 (%)')
title('Figure 11: CO2 vs time ; run 6')
Qae(n)=Qa(n)*0.005;
%calculate cumulative weight of CO2
VCO2(n)=(CO2(n)./100).*Qa(n); %l/min;
dCO2(n)=(44.01*1)./(0.08206.*(T16(n)+273)); %R in l.atm./mol.K; assume pa=1
atm
mCO2(n)=dCO2(n).*VCO2(n); %mass flowrate(g/min);
intCO2(n)=mCO2(n)*int./1000; %'int' minute intervals, kg
cumCO2(n)=cumsum(intCO2(n));% kg
%plot another graph (cumulative CO2)
%express as C; syntax CO2c
%make CO2-C available for later plotting against BVS
global CO2c;
CO2c(n)=cumCO2(n).*12/44;
figure(12)
plot(t(n),CO2c(n),'k')
hold on
%determine sensor error; CO2=0.02+0.02*reading;Qa=0.005
%since Qae<<CO2e use CO2e only
VCO2p(n)=(CO2p(n)'./100).*Qa(n); %l/min;
dCO2p(n)=(44.01*1)./(0.08206.*(T16(n)+273)); %R in l.atm./mol.K; assume
pa=1 atm
```

```
mCO2p(n)=dCO2p(n).*VCO2p(n); %mass flowrate(g/min);
intCO2p(n)=mCO2p(n)*int./1000; %'int' minute intervals, kg
cumCO2p(n)=cumsum(intCO2p(n));% kg
global CO2cp;
CO2cp(n)=cumCO2p(n).*12/44;
plot(t(n),CO2cp(n),'k--')
hold on
VCO2minus(n)=(CO2minus(n)'./100).*Qa(n); %l/min;
dCO2minus(n)=(44.01*1)./(0.08206.*(T16(n)+273)); %R in l.atm./mol.K; assume
pa=1 atm
mCO2minus(n)=dCO2minus(n).*VCO2minus(n); %mass flowrate(g/min);
intCO2minus(n)=mCO2minus(n)*int./1000; %'int' minute intervals, kg
cumCO2minus(n)=cumsum(intCO2minus(n));% kg
global CO2cminus;
CO2cminus(n)=cumCO2minus(n).*12/44;
plot(t(n),CO2cminus(n),'k:')
hold on
%add specific airflow
Qasp(n)=Qa(n)/TS;
plot(t(n),Qasp(n),'k')
xlabel('Time (d)')
ylabel('CO_2-C (kg)')
title('Figure 12: Cumulative CO_2-C vs time ; run 6')
%display maximum value
maxCO2c=max(CO2c(n))
maxCO2cp=max(CO2cp(n))
maxCO2cminus=max(CO2cminus(n))
%plot another graph (leachate)
figure(13)
plot(t,L,'k')
xlabel('Time (d)')
ylabel('Leachate (g)')
title('Figure 13: Leachate vs time; run 6')
%end
```

12. areas

```
%a script file to determine A40 and A55 from experimental data
%method: determine T*deltat where deltat is the temperature logging
interval (1 min in these experiments)
%assumption: deltat is spread equally on either side of the logging time
%created by Ian Mason
%syntax 'areas'
%call data from file
[t,m,RH1,RH2,Qa,CO2,T1,T2,T3,T4,T5,T6,T7,T8,T9,T10,T11,T12,T13,T14,T15,T16]
=textread('data_run4.txt','%f %f %f %f %f %f %f %f %f %f %f %f %f %f %f %f
%f %f %f %f %f %f','headerlines',3);
%select temperature profile & rate interval
T=input('enter temperature profile name (T3 to T7):   ');
int=input('enter interval for temperature rate (min):   ');
%enter fixed data
deltaT=1; %(min)
%calculate temperature interval >40
T40=T-40;
%eliminate negative values
[i,j]=find(T40 < 0);
for m=1:size(i);
    T40(i(m),j(m))=0;
end
%calculate individual areas
```

```
areas40=T40.*deltat./1400; %C.days
%calculate total area
A40=max(cumsum(areas40))%C.days
%calculate temperature interval >55
T55=T-55;
%eliminate negative values
[k,l]=find(T55 < 0);
for m=1:size(k);
    T55(k(m),l(m))=0;
end
%calculate individual area
areas55=T55.*deltat./1440; %C.days
%calculate total area
A55=max(cumsum(areas55))%C.days
%calculate maximum rates of temperature change
n=1:int:(size(T)-int);
deltaT=(T(n+int)-T(n));
deltaTmax=max(deltaT);
deltaTmin=min(deltaT);
Tratemax=deltaTmax*60/int %C/h; max rate of increase
Tratemin=deltaTmin*60/int %C/h; max rate of decrease
%end
```

13. plotwatts

```
%plotwatts: a script file to plot power outputs from experimental
composting runs
%created by Ian Mason, University of Canterbury, 2006
%syntax 'plotwatts'
%call data from file
[t,m,RH1,RH2,Qa,CO2,T1,T2,T3,T4,T5,T6,T7,T8,T9,T10,T11,T12,T13,T14,T15,T16,
L]=textread('data_run7_v2.txt','%f %f %f %f %f %f %f %f %f %f %f %f %f %f
%f %f %f %f %f %f %f %f %f %f','headerlines',3);
%enter run #,initial wet weight, C fraction and time interval for calcs
run=input('enter run ((#):   ');
ww=input('enter wet weight for run (g):   ');
cfr=input('enter C fraction of VS (fr):   ');
int=input('enter time interval for calculations (min):   ');
Te=input('enter temperature sensor error (+-):   ');
%set fixed pars for advective transport
a=-2238;
b=8.896;
MWH2O=18.015;
MWair=28.96;
roair=1.2; %g/l; (dry air; STP - no TP data available)
cwat=4.184; %kJ/kg.C (Haug,1993; p 288)
cdrygas=1.004; %kJ/kg.C (Haug,1993; p 288)
cwatvap=1.841; % kJ/kg.C (Haug,1993 p 288)
pa=760; % mm; (assumed - no pa data available)
Hc=19600; %kJ/kg-VS (calculated from mixture components)
%set fixed pars for experimental column
r1=0.3045/2; %m; internal diameter
x=0.0055; %m, wall thickness
r2=r1+x; %m external diameter
k=0.092; %W/m.C; PVC (Mills, 1995)
lh=0.1000; % m; headspace
l1=0.300; % m; section 1
l2=0.300; % m; section 1
l3=0.300; % m; section 1
%calculate log mean surface areas (lid omitted since delta T = 0)
```

```
Ah=2*pi*lh*((r2-r1)/(log(r2/r1)));
A1=2*pi*l1*((r2-r1)/(log(r2/r1)));
A2=2*pi*l2*((r2-r1)/(log(r2/r1)));
A3=2*pi*l3*((r2-r1)/(log(r2/r1)));
%assume wall temperatures are those of bulk fluid
%calculate U; 1/U=1/hi + x/k + 1/ho;
hi=3; %w/m2.C; Mills 1995, table 1.4; range 3-25 (free)
ho=3; %w/m2.C; Mills 1995, table 1.4; range 3-25 (free)
inverseU=(1/hi)+(x/k)+(1/ho);
U=1/inverseU; %W/m2.C;
%select data based on specified interval
n=1:int:(size(t)-int);
%note: obs or mfr temperature errors; 0.1 or 0.75
%apply Te; T2 (exit gas); T3,T5,T7 (mass); T9 (inlet air)
T2=T2+Te;
T3=T3+Te;
T5=T5+Te;
T7=T7+Te;
T9=T9+Te;
%calculate input advective transport
pvs=10.^((a./(T9(n)+273))+b);
pv=pvs.*RH1(n)/100;
w=(MWH2O/MWair)*(pv./(pa-pv));%kg-water/kg-air
G=Qa(n).*roair/60; %g-air/s
wr=G.*w; %g-water/s
%latwat=2367; % set value used in v1 for simulation(kJ/kg)
%calculate input latent heat of water; function of (Haug, 1993)
%latwat=1093.7-0.5683T(F) (BTU/lb)
latwat1=(1093.7-(0.5683*((T9(n)+32)*9/5)))*1055/454; %kJ/kg
H1=(((cdrygas)+(w.*cwatvap)).*T9(n))+(w.*latwat1);%kJ/kg
advecdot1=G.*H1; %W
%calculate exit advective transport
pvs=10.^(((a./(T2(n)+273))+b));
pv=pvs*1.0; % assume saturated (faulty sensor)
w=(MWH2O/MWair)*(pv./(pa-pv));%kg-water/kg-air
G=Qa(n).*roair/60; %g-air/s
wr=G.*w; %g-water/s
%calculate output latent heat of water; function of (Haug, 1993)
latwat2=(1093.7-(0.5683*((T2(n)+32)*9/5)))*1055/454; %kJ/kg
H2=(((cdrygas)+(w.*cwatvap)).*T2(n))+(w.*latwat2);%kJ/kg
advecdot2=G.*H2; %w
% calculate nett advective transport
qa=advecdot2-advecdot1; %W
%calculate CCR losses
qh=U*Ah.*(T2(n)-T11(n)); %W
q1=U*A1.*(T10(n)-T11(n)); %W
q2=U*A2.*(T12(n)-T13(n)); %W
q3=U*A3.*(T14(n)-T15(n)); %W
%calculate total wall losses
qw=qh+q1+q2+q3; %W
%calculate accumulation term; m*c*deltaT
%assume m is divided equally between sections (error at later time)
c=cwat; %J/g.C
%calculate deltaT at each time t;
deltaT3=(T3(n+int)-T3(n)); %T3 is mid-point S1
deltaT5=(T5(n+int)-T5(n)); %T5 is mid-point S2
deltaT7=(T7(n+int)-T7(n)); %T7 is mid-point S3
qacc1=(((ww+m(n))*c/3).*deltaT3)/(int*60); %NB: m negative
qacc2=(((ww+m(n))*c/3).*deltaT5)/(int*60); %NB: m negative
qacc3=(((ww+m(n))*c/3).*deltaT7)/(int*60); %NB: m negative
qacc=qacc1+qacc2+qacc3; %W
```

```
tplot=n/1440; %d
%calculate bio power; qacc=+(-qa)+(-qw)+qbio
qbio=qacc+qa+qw; %W
%plot a graph
figure(1)
plot(tplot,qa,'k')
xlabel('Time (d)')
ylabel('Power (W)')
title('Figure A5.6: Advective losses; run B')
%plot another graph
figure(2)
plot(tplot,qw,'k')
xlabel('Time (d)')
ylabel('Power (W)')
title('Figure A5.7: CCR losses; run B')
%total losses
qt=qa+qw;
%plot another graph
figure(3)
plot(tplot,qt,'k')
xlabel('Time (d)')
ylabel('Power (W)')
title('Figure A5.8: Total losses; run B')
%plot another graph
figure(4)
plot(tplot,qacc,'k')
xlabel('Time (d)')
ylabel('Power (W)')
title('Figure A5.9: Accumulation; run B')
%plot another graph
figure(5)
plot(tplot,qbio,'k')
xlabel('Time (d)')
ylabel('Power (W)')
title('Figure A5.10: Biopower; run B')
%calculate bioenergy curve
bioe=qbio*int*60/1000; %kJ
cumbioe=cumsum(bioe);
%plot another graph
figure(6)
plot(tplot,cumbioe,'k')
xlabel('Time (d)')
ylabel('Energy (kJ)')
title('Figure A5.12: Bioenergy profile; run B')
%plot another graph; all cumulative energy curves
figure(7)
plot(tplot,cumbioe,'k')
xlabel('Time (d)')
ylabel('Energy (kJ)')
title('Figure A5.14: Energy profiles; run B')
hold on
%calculate advec curve
advece=qa*int*60/1000; %kJ
cumadvece=cumsum(advece);
%plot advec curve
plot(tplot,cumadvece,'k')
hold on
%calculate CCR curve
ccre=qw*int*60/1000; %kJ
cumccre=cumsum(ccre);
%plot CCR curve
```

```
plot(tplot,cumccre,'k')
hold on
%calculate acc curve
acce=qacc*int*60/1000; %kJ
cumacce=cumsum(acce);
%plot acc curve
plot(tplot,cumacce,'k')
hold on
%calculate total energy curve
tote=qt*int*60/1000; %kJ
cumtote=cumsum(tote);
%plot total curve
plot(tplot,cumtote,'k')
%display maximum values
maxadvec=max(cumadvece)
maxccr=max(cumccre)
maxacc=max(cumacce)
maxtot=max(cumtote)
maxbio=max(cumbioe)
%calculate output proportions as fraction of biopwer
padvece=cumadvece./cumbioe;
pccre=cumccre./cumbioe;
pacce=cumacce./cumbioe;
%plot another graph
figure(8)
plot(tplot,padvece,'k')
hold on
plot(tplot,pccre,'k')
hold on
plot(tplot,pacce,'k')
xlabel('Time (d)')
ylabel('Energy ratio (fr)')
title('Figure A5.8: Energy ratios; run B')
%display final values
z=length(tplot)
finadvece=padvece(z)
finccre=pccre(z)
finacce=pacce(z)
finsum=finadvece+finccre+finacce
%calculate peak biopower on TS basis
TS=ww*0.4/1000; %kg
maxqbio=max(qbio) %W
maxspecqbio=maxqbio/TS %W/kg-TS
%calculate average biopower on TS basis
ttime=max(tplot); %d
avqbio=(maxbio/(ttime*86400))*1000 %J/s
avspecqbio=avqbio/TS %W/kg
global BVSc; %make BVSc available elsewhere
%calculate bioenergy as BVS-C
BVSc=(cumbioe./Hc)*cfr;
%plot another graph
figure(9)
plot(tplot,BVSc,'k')
xlabel('Time (d)')
ylabel('BVS-C (kg)')
title('Figure A5.9: Predicted BVS-C; run B')
%print BVSc_max
BVSc_max=max(BVSc)
%end
```

14. VSplot (for “mined” data)

```
%VSplot_p6: a script file to adjust published varying temperature VS data
to a constant temperature
%constant temperature 40C; original data fitted with a 6th order polynomial
%created by Ian Mason
%syntax ‘VSplot_p6’
%call datafile
[t,VS,T]=textread('Nakasaki85fig4v2.txt','%f %f %f','headerlines',3);
%enter pre-set Tmin, Topt and Tmax - data of Richard and Walker (1998)
Tmin=5;
Topt=59;
Tmax=71;
%calculate fT (Rosso, 1993)
fT=((T-Tmax).*(T-Tmin).^2)./((Topt-Tmin).*((Topt-Tmin).*(T-Topt)-(Topt-
Tmax).*(Topt+Tmin-2.*T)));
%calculate f40
f40=((40-Tmax)*(40-Tmin)^2)/((Topt-Tmin)*((Topt-Tmin)*(40-Topt)-(Topt-
Tmax)*(Topt+Tmin-2*40)))
%calculate adjustment factor - fT40
fT40=f40./fT;
%plot VS and T
figure(1)
[AX,H1,H2]=plotyy(t,VS,t,T);
xlabel('Time (d)')
set(get(AX(1),'Ylabel'),'String','BVS')
set(get(AX(2),'Ylabel'),'String','Temperature (^oC)')
set(H1,'linestyle','-')
set(H2,'linestyle','-')
set(H1,'marker','+')
set(H2,'marker','*')
title('Figure 1: BVS (+) and T (*) profiles; data of Bach et al. (1985)
Test 1')
%plot fT, fT40
figure(2)
plot(t,fT,'k-o')
hold on
plot(t,fT40,'k-*')
xlabel('Time (d)')
ylabel('fT')
title('Figure 2: Temperature functions fT (o) and fT40 (*); data of Bach et
al. (1985) Test 1')
%fit polynomial
p=polyfit(t,VS,6)
f=polyval(p,t)
% calculate errors
n=length(t);
error = VS - f;
error = sum(error.^2);
mse = error/n;
rmse = sqrt(mse)
%plot a graph
figure(3)
plot(t,VS,'*',t,f)
xlabel('Time (d)')
ylabel('VS')
title('Figure 3: Polynomial; data of Bach et al. (1985); lime sludge;
fig2a-v2')
%get derivative
k=polyder(p)
n=length(k)
```

```
%adjust derivative for temperature; ie bvsdot=bvsdot(40)*fT
bvsdot=(k(1)*t.^(n-1))+(k(2)*t.^(n-2))+(k(3)*t.^(n-3))+(k(4)*t.^(n-
4))+(k(5)*t.^(n-5))+(k(6)*t.^(n-6));
%eliminate negative bvsdot values arising due to incorrect polynomial
fitting
[i,j]=find(bvsdot < 0)
for m=1:size(i)
    bvsdot(i(m),j(m))=0;
end
%adjust derivate to 40 C
bvsdot40=bvsdot.*fT40
%plot a graph
figure(4)
plot(t,bvsdot,'-+')
hold on
plot(t,bvsdot40,'-*')
xlabel('Time (d)')
ylabel('dBVS/dt')
title('Figure 4: Derivative at T (+) and at 40C (*); data of Bach et al.
(1985) Test 1')
%fit a polynomial to the new derivative
p40=polyfit(t,bvsdot40,5)
%integrate the new derivative
q40=polyint(p40)
n40=length(p40)
bvs40=(q40(1)*t.^(n))+(q40(2)*t.^(n-1))+(q40(3)*t.^(n-2))+(q40(4)*t.^(n-
3))+(q40(5)*t.^(n-4))+(q40(6)*t.^(n-5))
%plot a graph
figure(5)
plot(t,bvs40,'-*')
xlabel('Time (d)')
ylabel('BVS40')
title('Figure 5: Polynomial at 40C;data of Bach et al. (1985) Test 1 ')
%%plot a graph showing bvs at T and 40
figure(6)
plot(t,VS,'k-+')
hold on
plot(t,bvs40,'-*')
xlabel('Time (d)')
ylabel('BVS')
title('Figure 6: Polynomials at T (+) and 40C (*); data of Bach et al.
(1985) Test 1')
%end
```

15. VSplot (for experimental data)

```
%a script file to plot corrected "BVS" profiles from CO2-C and BVS-C data;
reference temperature 40C;
%CO2c and BVSc generated from “plotdata” and “plotwatts” respectively
%created by Ian Mason
%syntax ‘VSplot_p6_exp_v2’
%call experimental datafile for temperature
[t,m,RH1,RH2,Qa,CO2,T1,T2,T3,T4,T5,T6,T7,T8,T9,T10,T11,T12,T13,T14,T15,T16]
=textread('data_run6_v2.txt','%f %f %f %f %f %f %f %f %f %f %f %f %f %f %f
%f %f %f %f %f %f %f','headerlines',3);
%select carbon data, temperature profile and interval
C=input('enter data set to correct (e.g. CO2c or BVSc):   ');
T=input('enter temperature profile required (T3 to T7):   ');
int=input('enter time interval for calculations (min):   ');
%find maximum temperature
```

```
Tmax_dataset=max(T)
%call Tmin, Topt and Tmax (Richard et al => 5,59,71)
Tmin=input('enter Tmin (C):  ');
Topt=input('enter Topt (C):  ');
Tmax=input('enter Tmax (C):  ');
%select data at chosen interval
k=1:int:size(t);
t=t(k);
T=T(k);
VS=C(k);
%calculate fT
fT=((T-Tmax).*(T-Tmin).^2)./((Topt-Tmin).*((Topt-Tmin).*(T-Topt)-(Topt-
Tmax).*(Topt+Tmin-2.*T)));
%calculate f40
f40=((40-Tmax)*(40-Tmin)^2)/((Topt-Tmin)*((Topt-Tmin)*(40-Topt)-(Topt-
Tmax)*(Topt+Tmin-2*40)));
fT40=f40./fT;
%plot VS and T
figure(1)
[AX,H1,H2]=plotyy(t,VS,t,T);
xlabel('Time (d)')
set(get(AX(1),'Ylabel'),'String','CO_2-C (kg)')
set(get(AX(2),'Ylabel'),'String','Temperature (^oC)')
set(H1,'linestyle','-')
set(H2,'linestyle','-.')
%set(H1,'marker','k+')
%set(H2,'marker','k*')
title('Figure 1: CO_2-C (solid) and T (dashdot) profiles - original data;
Run B')
%plot fT, fT40
figure(2)
plot(t,fT,'k--')
hold on
plot(t,fT40,'k-')
xlabel('Time (d)')
ylabel('fT')
title('Figure 2: Temperature functions fT (dashed) and fT40 (solid); Run
B')
%fit polynomial
p=polyfit(t,VS,6);
f=polyval(p,t);
% calculate errors
n=length(t);
error = VS - f;
error = sum(error.^2);
mse = error/n;
rmse = sqrt(mse)
%plot a graph
figure(3)
plot(t,VS,'k*',t,f,'k-')
xlabel('Time (d)')
ylabel('CO_2-C (kg)')
title('Figure 3: Polynomial fitted to original CO_2-C data; Run B')
%get derivative
k=polyder(p);
n=length(k);
%adjust derivative for temperature; ie bvsdot=bvsdot(40)*fT
bvsdot=(k(1)*t.^(n-1))+(k(2)*t.^(n-2))+(k(3)*t.^(n-3))+(k(4)*t.^(n-
4))+(k(5)*t.^(n-5))+(k(6)*t.^(n-6));
%eliminate negative bvsdot values arising due to incorrect polynomial
fitting
```

```
[i,j]=find(bvsdot < 0)
for m=1:size(i)
    bvsdot(i(m),j(m))=0;
end
bvsdot40=bvsdot.*fT40;
%plot a graph
figure(4)
plot(t,bvsdot,'k--')
hold on
plot(t,bvsdot40,'k-')
xlabel('Time (d)')
ylabel('dCO_2-C/dt')
title('Figure 4: Derivative at T (dashed) and at 40 ^oC (solid); Run B')
%fit a polynomial to the new derivative
p40=polyfit(t,bvsdot40,5);
%integrate the new derivative
q40=polyint(p40);
n40=length(p40);
bvs40=(q40(1)*t.^(n))+(q40(2)*t.^(n-1))+(q40(3)*t.^(n-2))+(q40(4)*t.^(n-
3))+(q40(5)*t.^(n-4))+(q40(6)*t.^(n-5));
%plot a graph
figure(5)
plot(t,bvs40,'k-*')
xlabel('Time (d)')
ylabel('CO_2-C(40) (kg)')
title('Figure 5: Polynomial fitted to corrected CO_2-C data; Run B ')
%%plot a graph showing bvs at T and 40
figure(6)
plot(t,VS,'k--')
hold on
plot(t,bvs40,'k-')
xlabel('Time (d)')
ylabel('CO_2-C (kg)')
title('Figure 6: Polynomials fitted to original (dashed) and corrected
(solid) CO_2-C data; Run B')
%end
```

APPENDIX 3
SENSITIVITY ANALYSIS PROFILES

Figure A3.1: Sensitivity analysis; specific heat

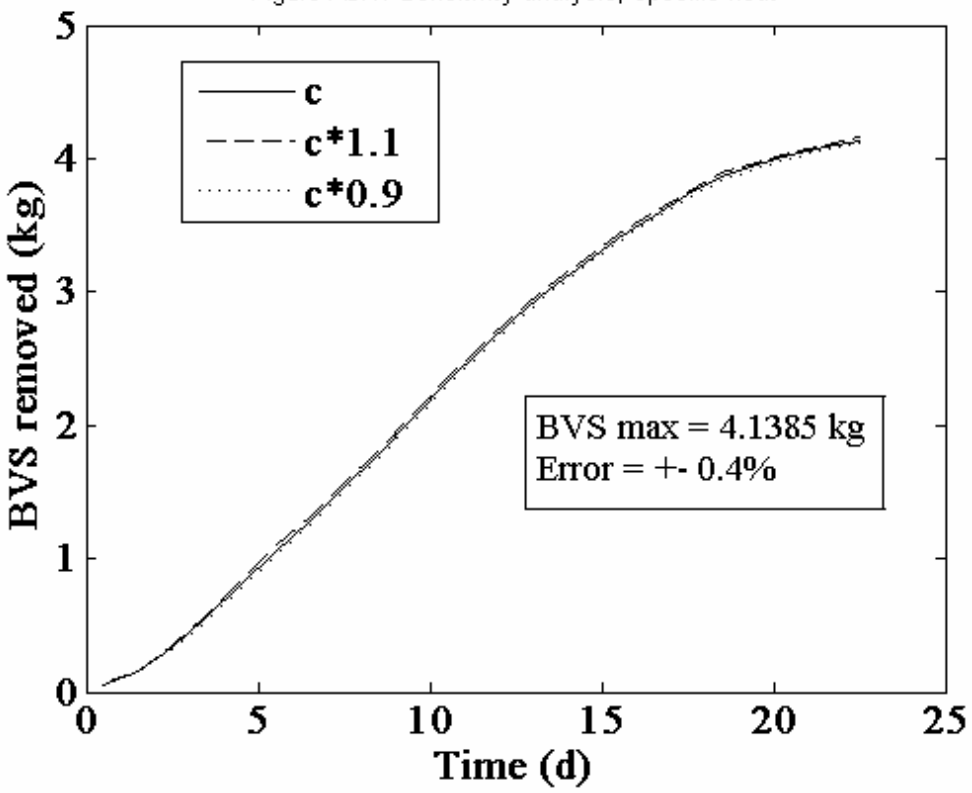

Figure A3.2: Sensitivity analysis; delta T core

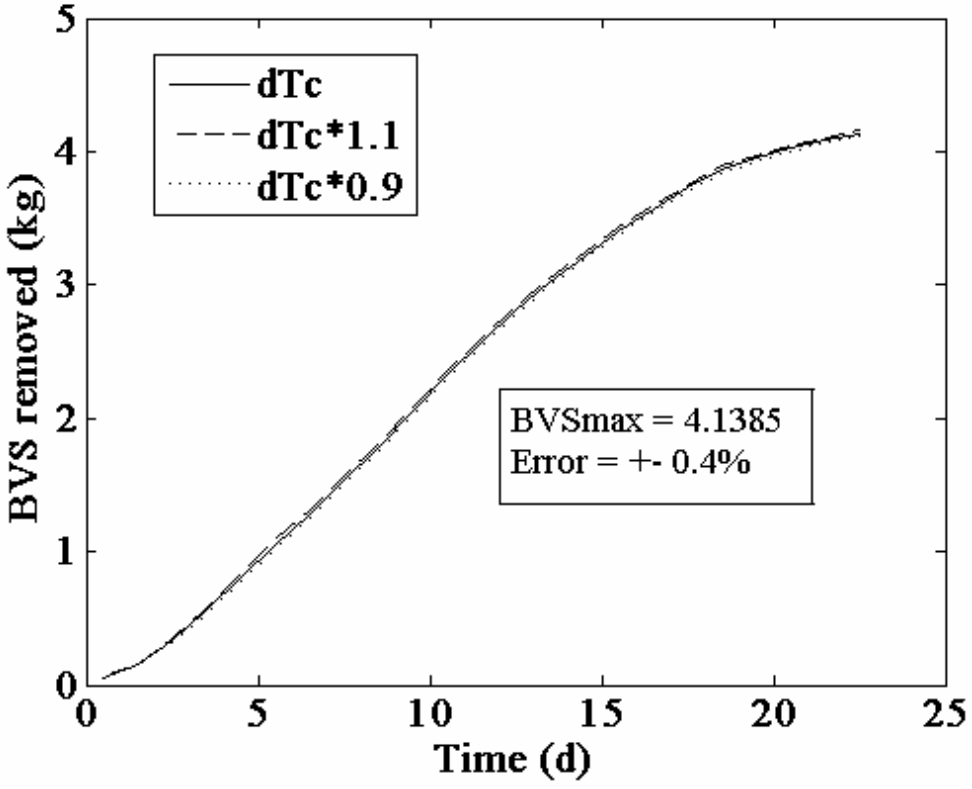

Figure A3.3: Sensitivity analysis; mass airflow

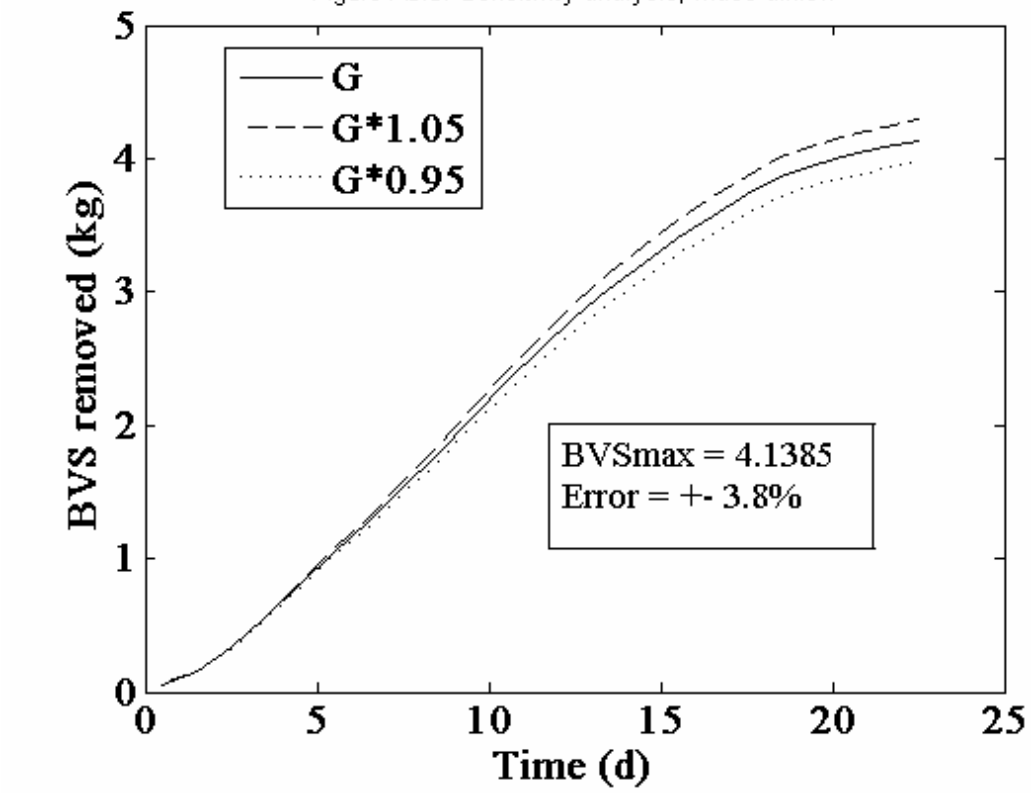

Figure A3.4: Sensitivity analysis; heat of combustion

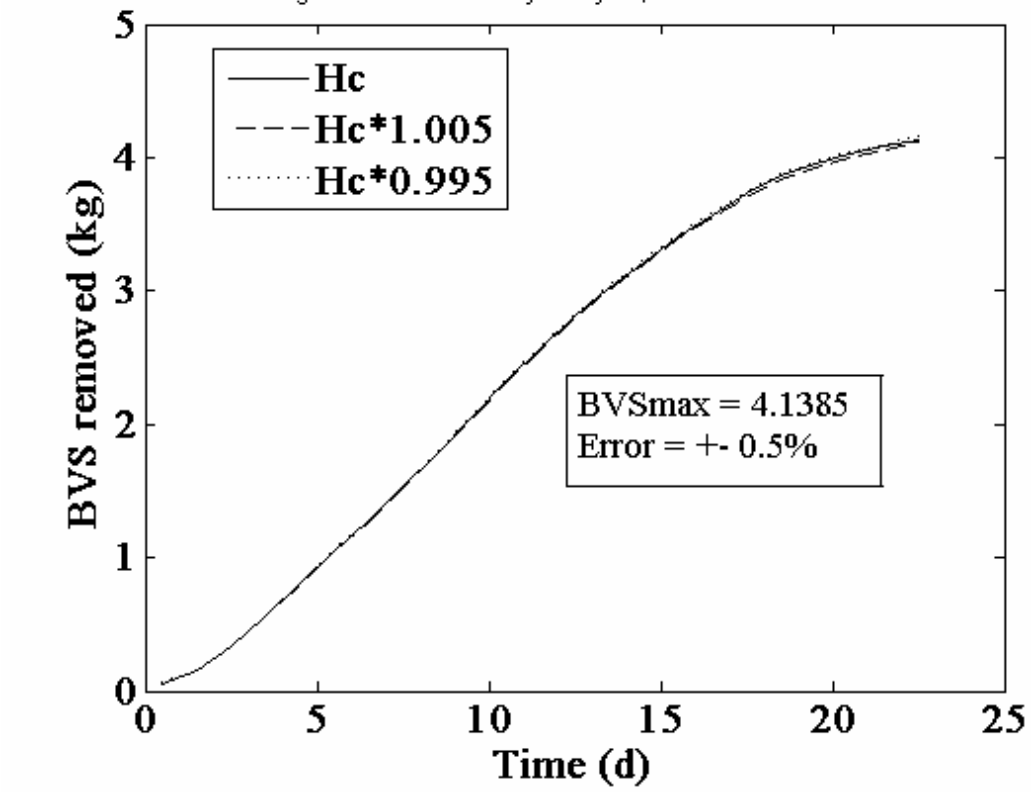

Figure A3.5: Sensitivity anaylsis; average mass

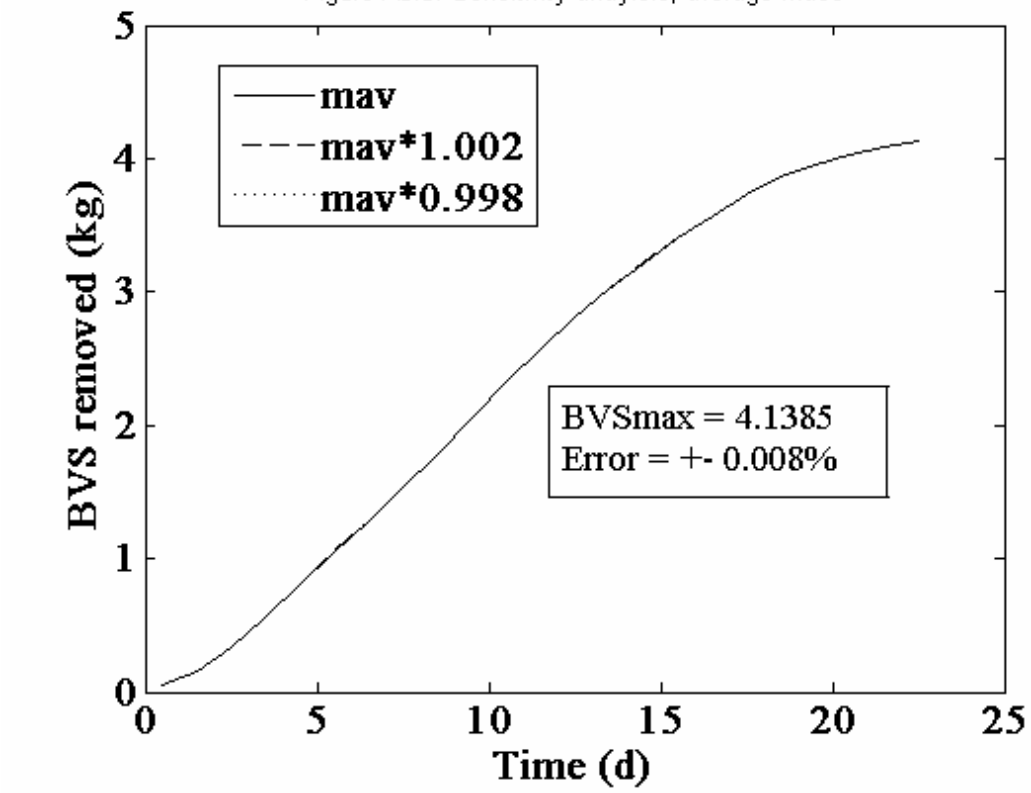

Figure A3.6: Sensitivity analysis; atmospheric pressure

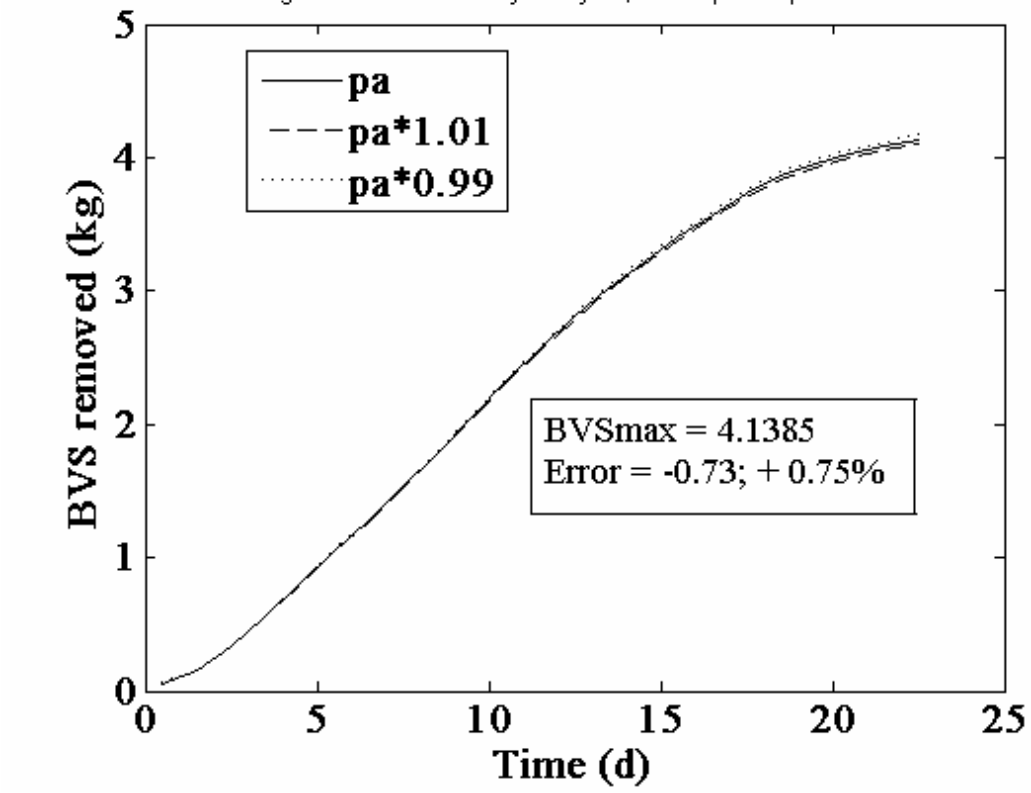

Figure A3.7: Sensitivity analysis; inlet relative humidity

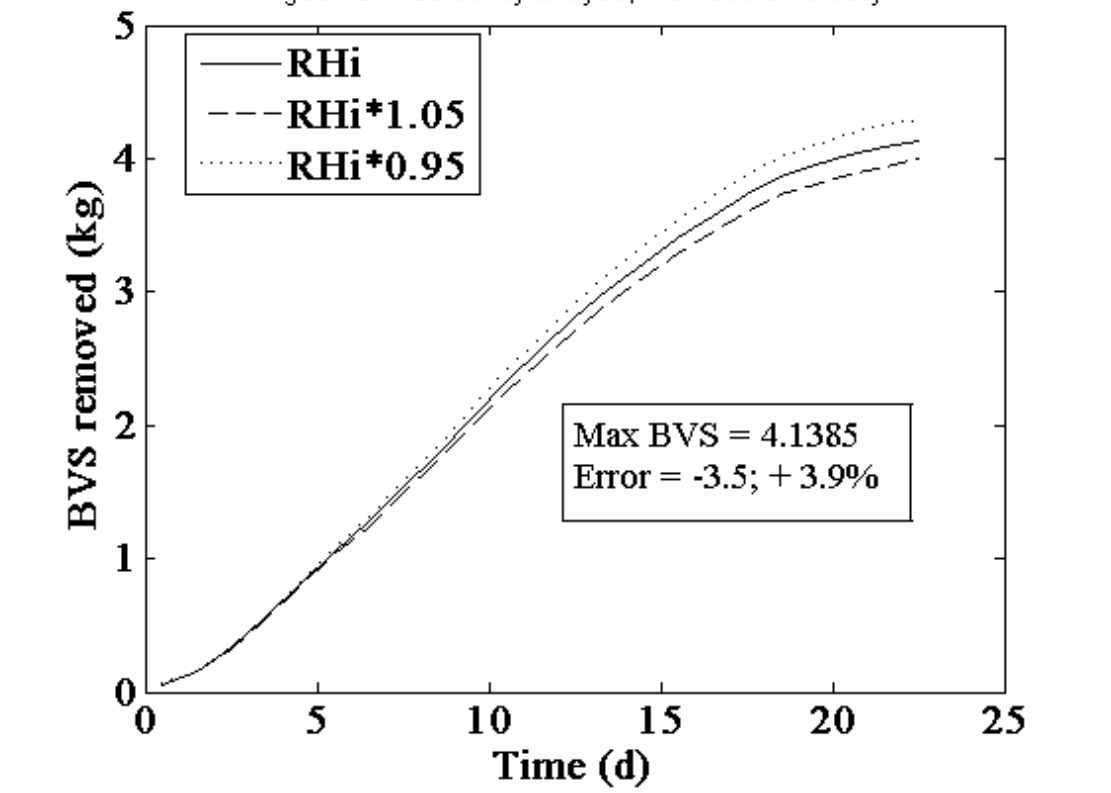

Figure A3.8: Sensitivity analysis; outlet relative humidity

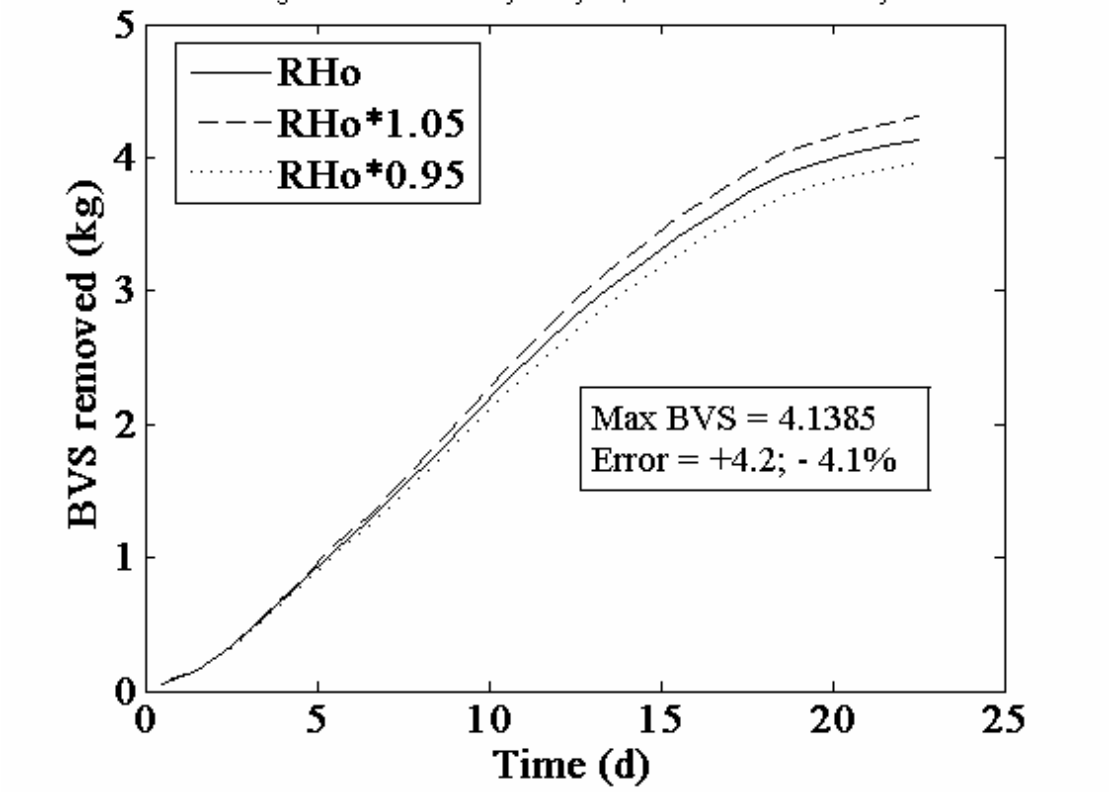

Figure A3.9: Sensitivity analysis; lid temperature

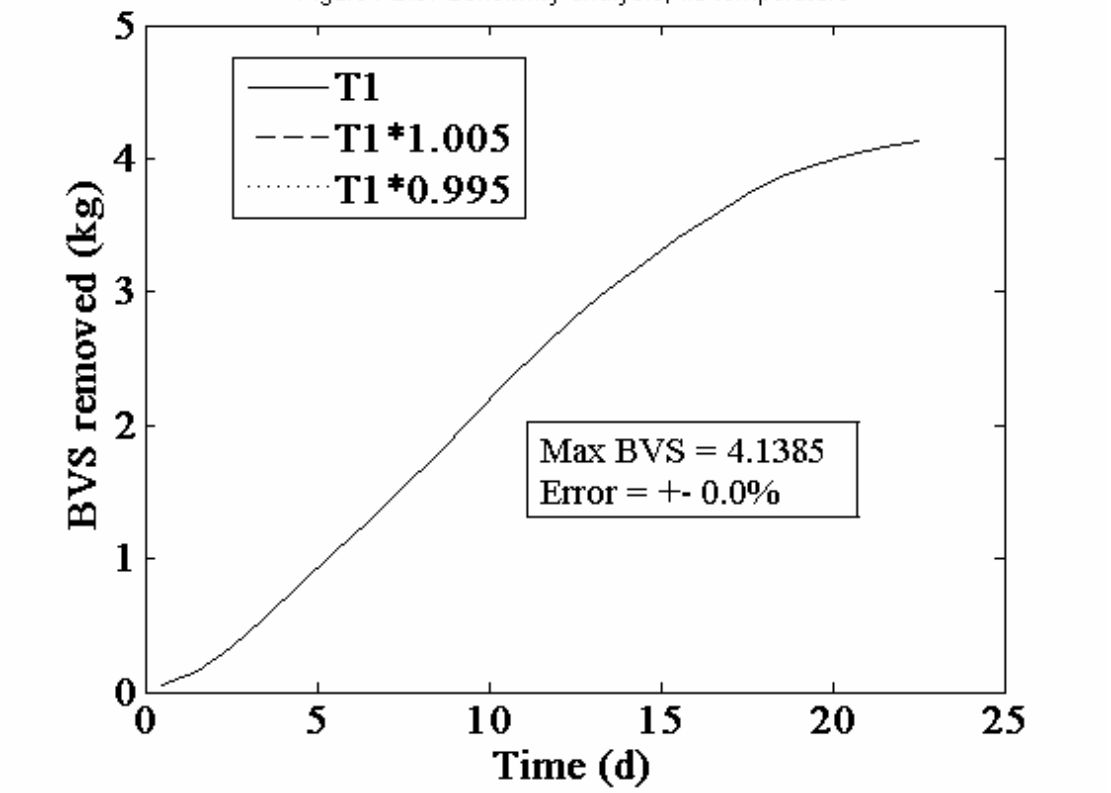

Figure A3.10: Sensitivity analysis; inlet air temperature

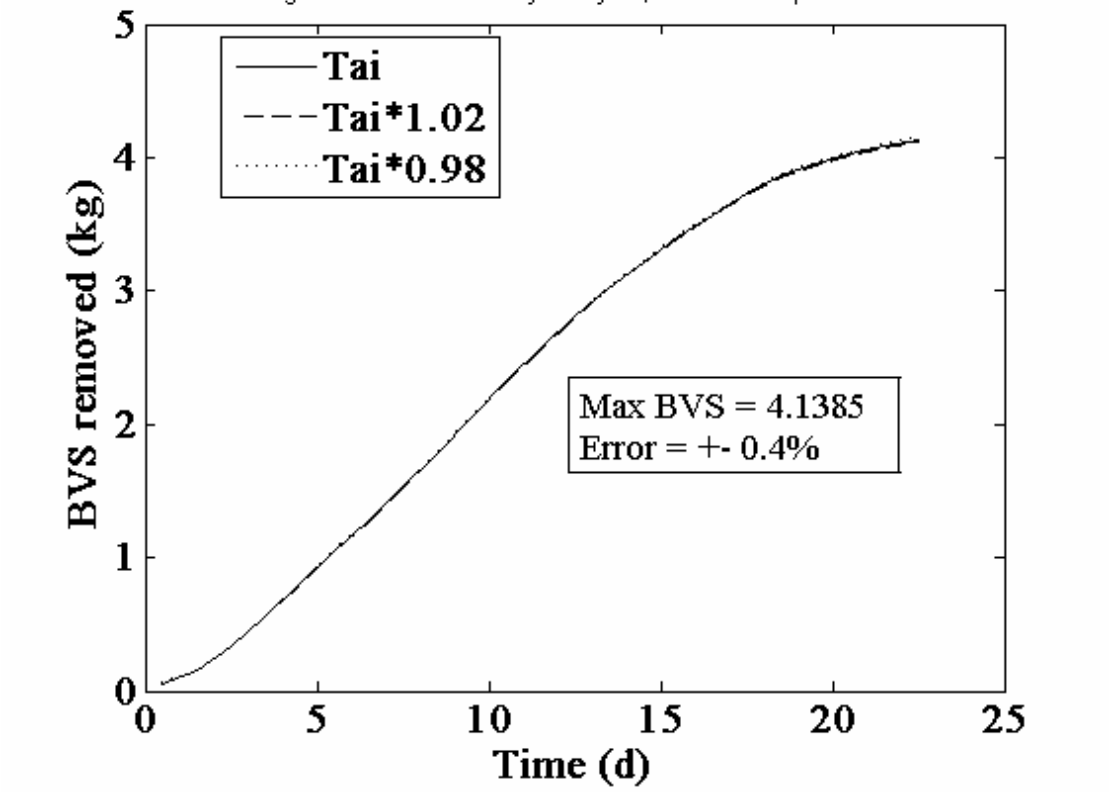

Figure A3.11: Sensitivity analysis; outlet air temperature

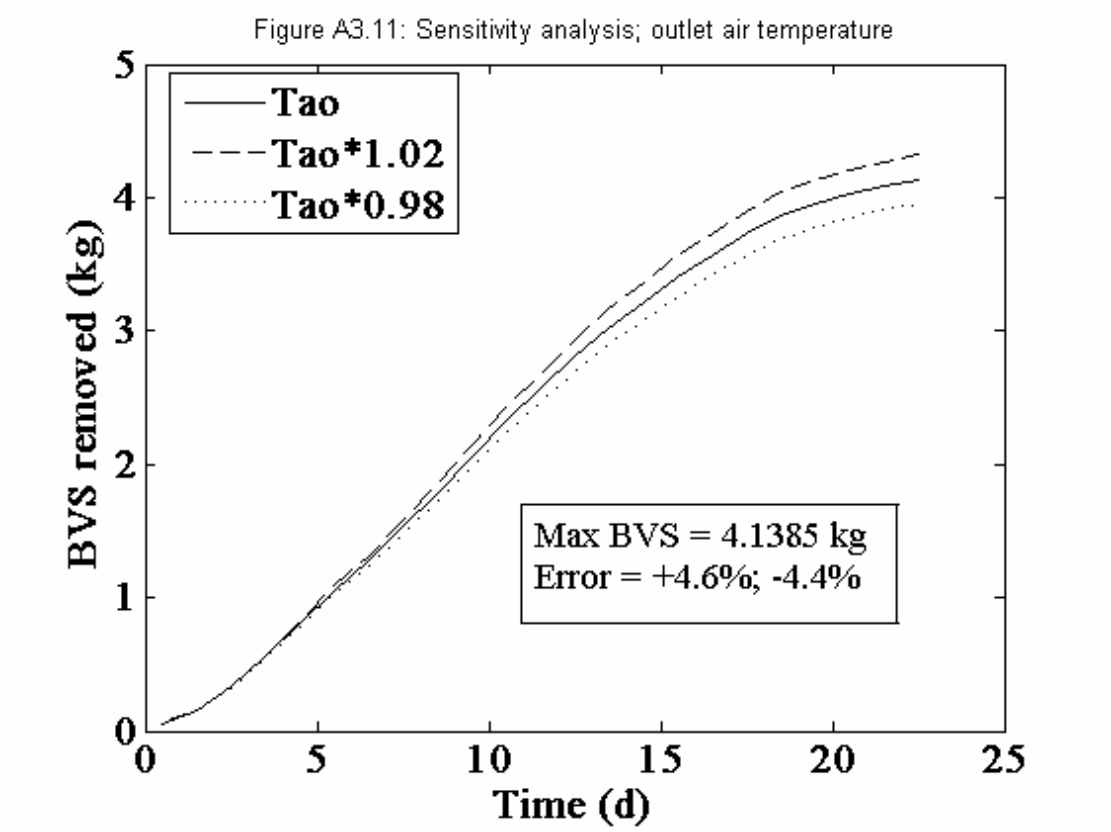

Figure A3.12: Sensitivity analysis; inner wall temperature

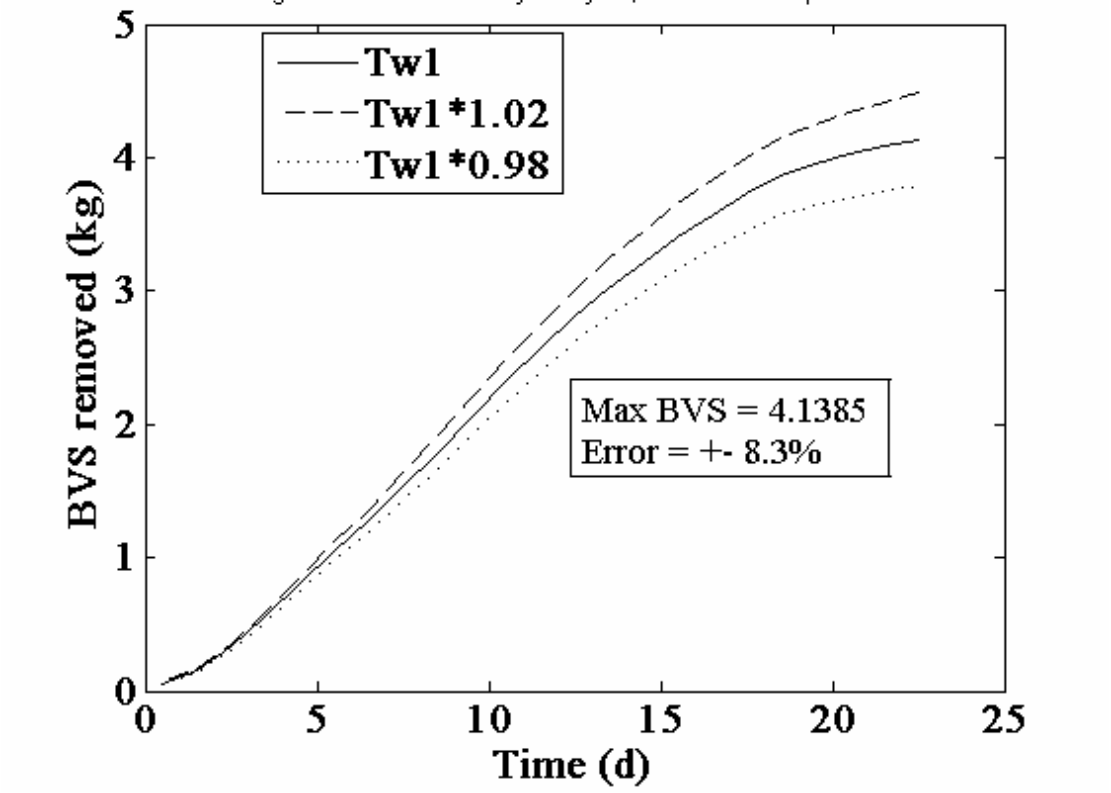

Figure A3.13: Sensitivity analysis; outer wall temperature

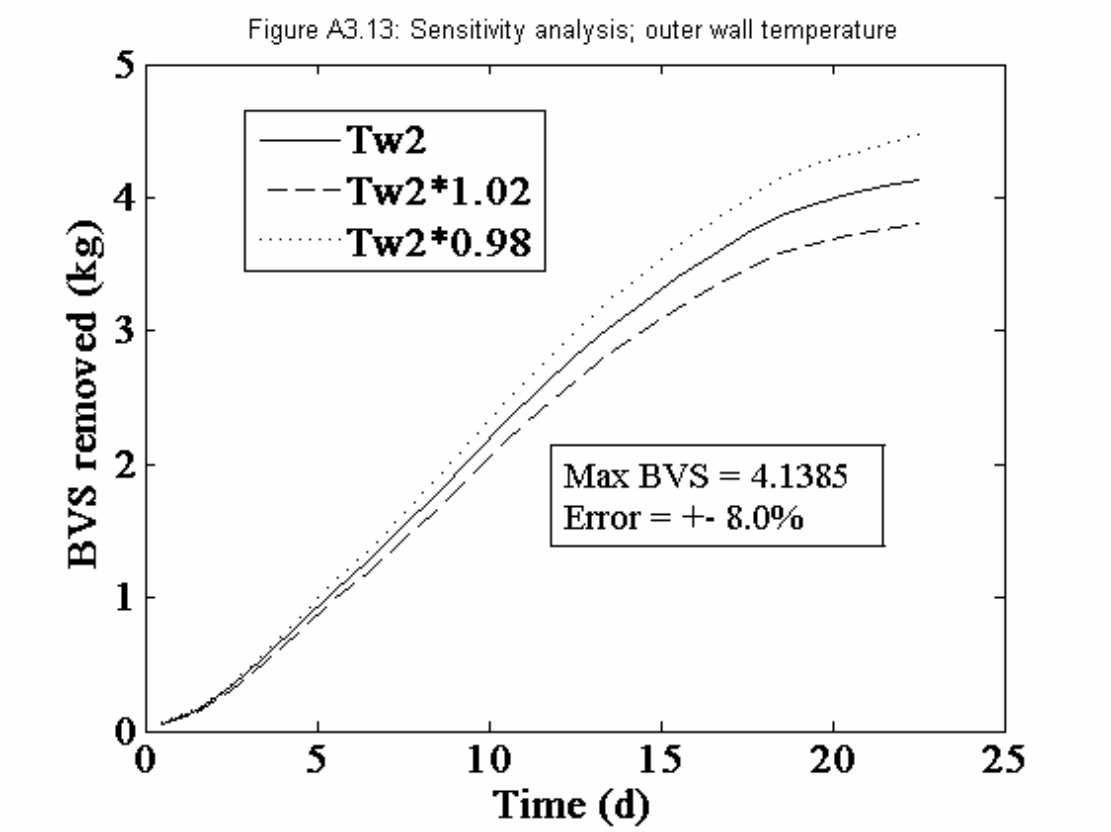

Figure A3.14: Sensitivity analysis; UA

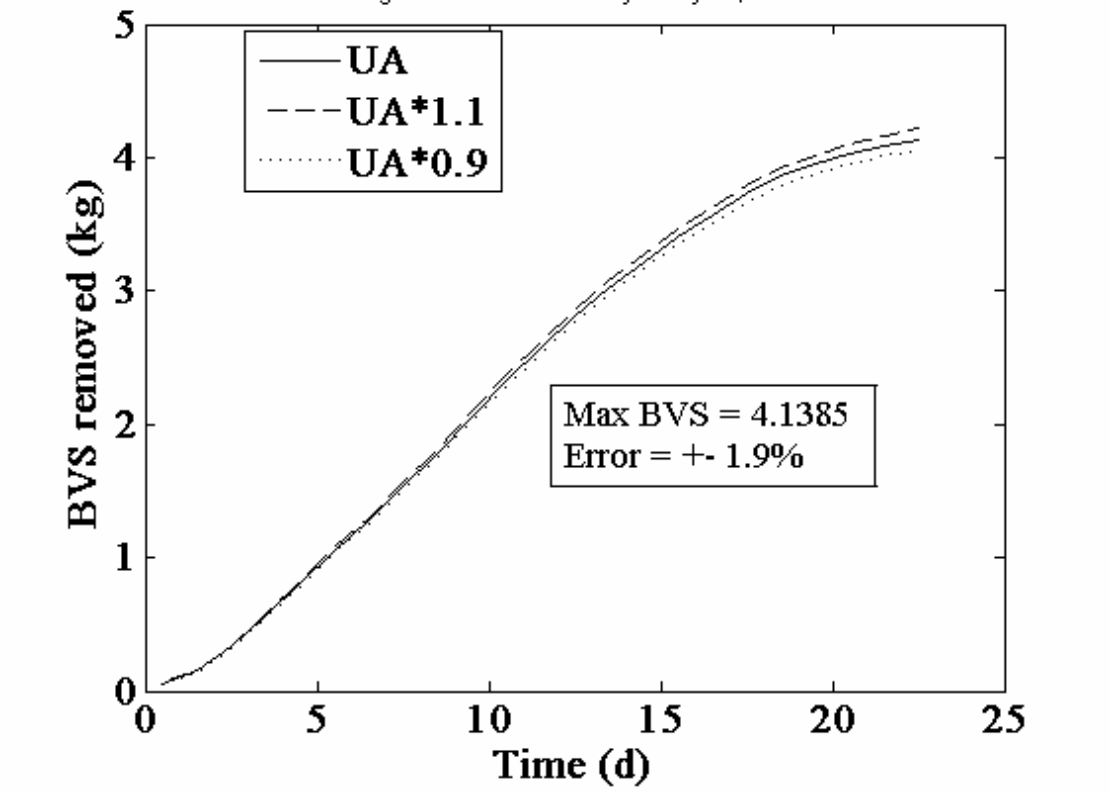

APPENDIX 4
LID, WALL AND EXIT GAS TEMPERATURE PROFILES

Figure A4.1 : Headspace temperatures T1 & T2; run A

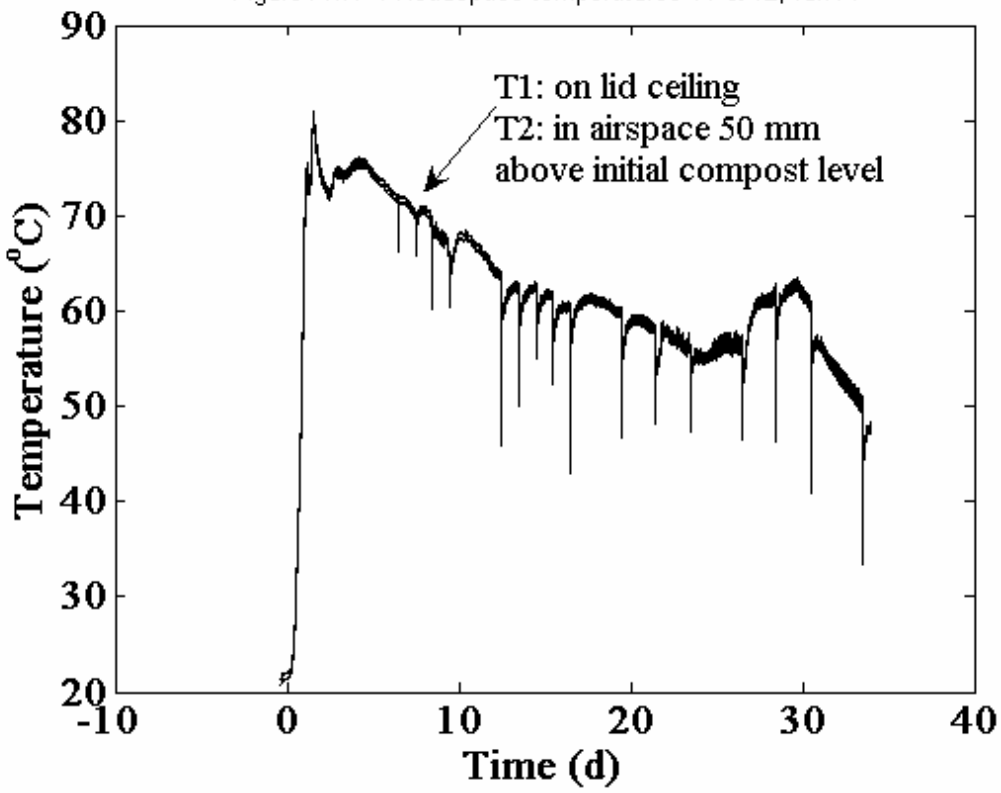

Figure A4.2: Core & wall temperatures; S1; run A

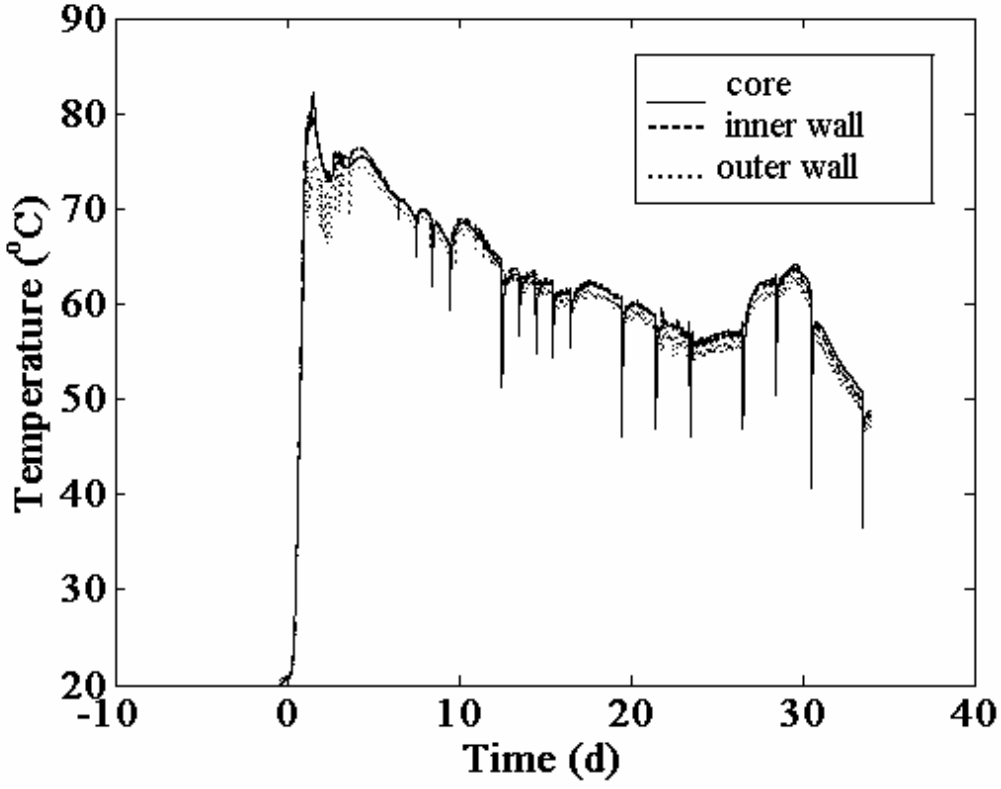

Figure A4.3: Core & wall temperatures; S2; run A

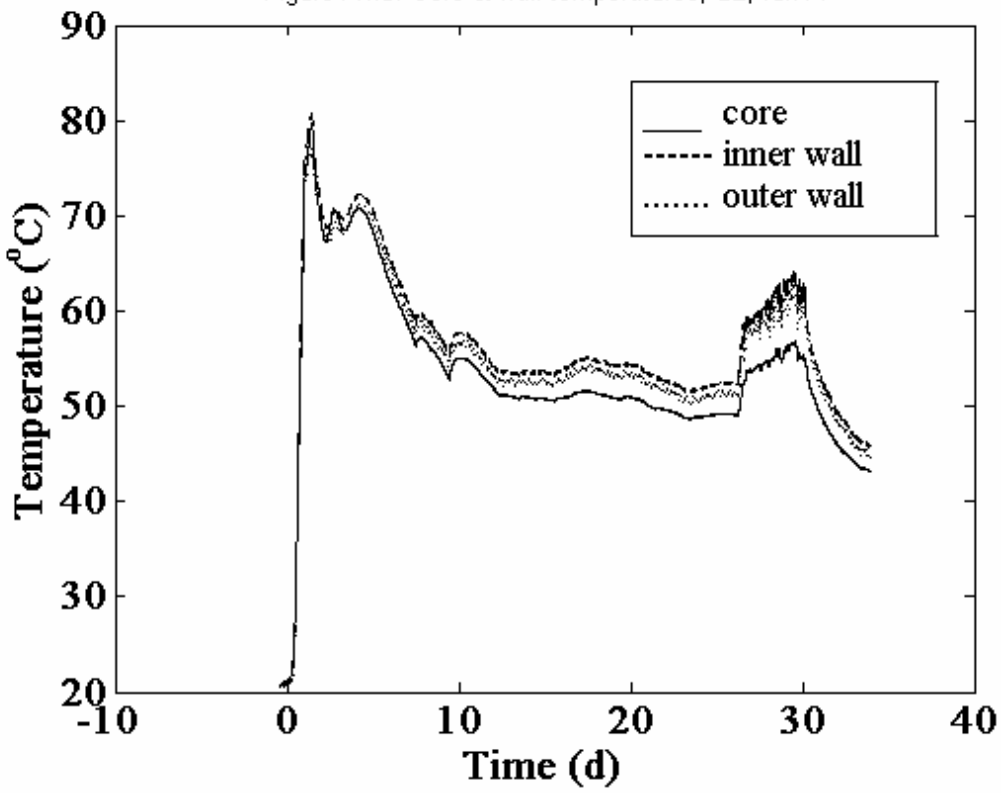

Figure A4.4: Core & wall temperatures; S3; run 6

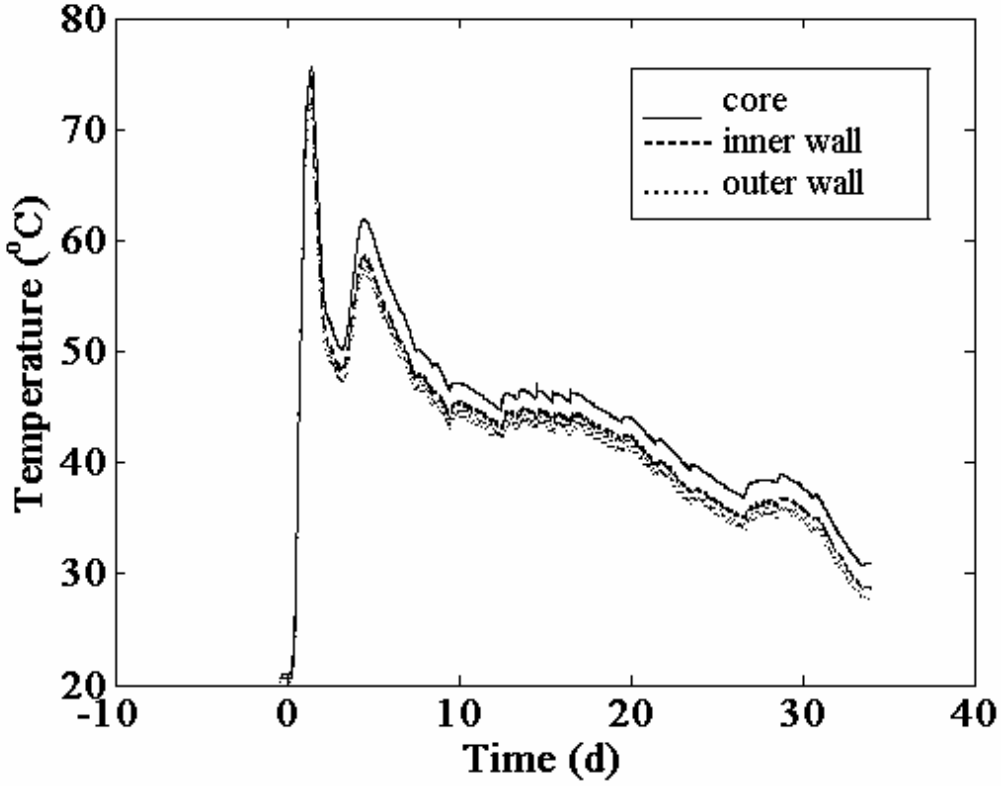

Figure A4.5: Headspace temperatures T1 & T2; run B

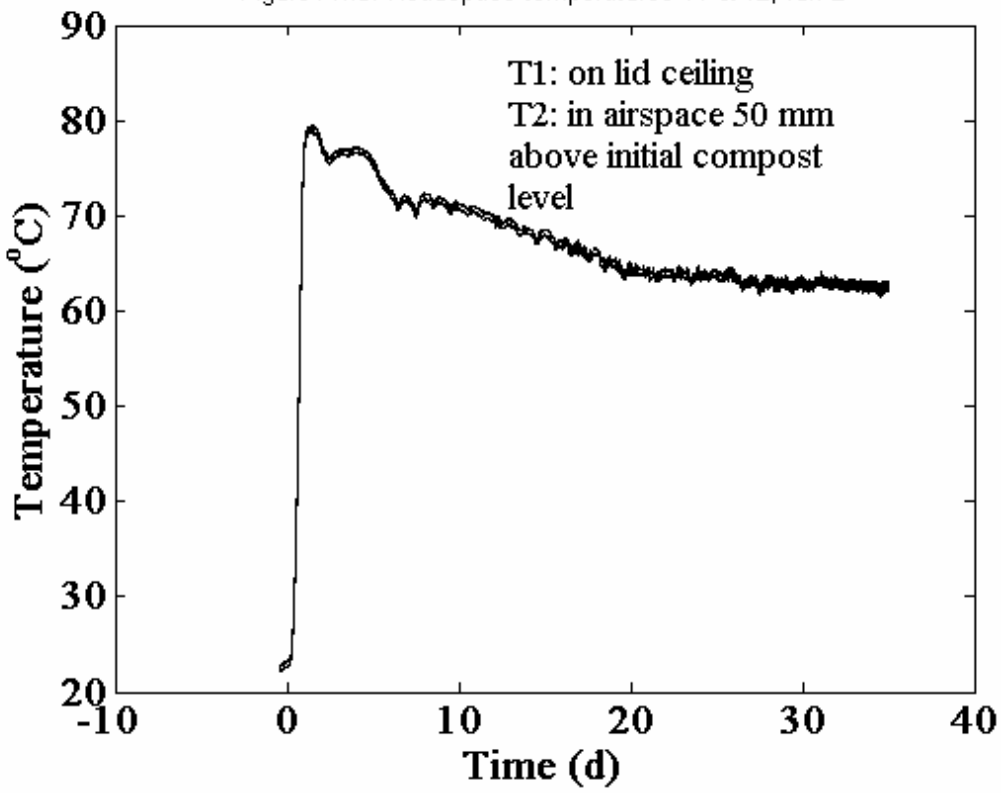

Figure A4.6: Core and wall temperatures; S1; run B

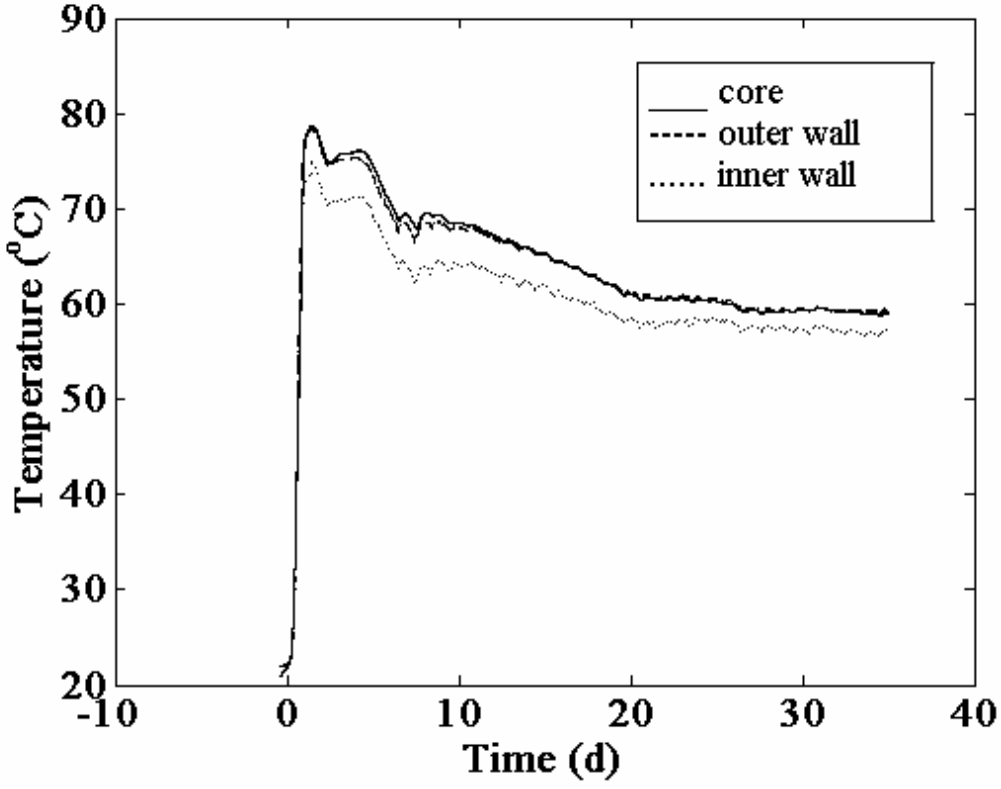

Figure A4.7: Core and wall temperatures S2; run B

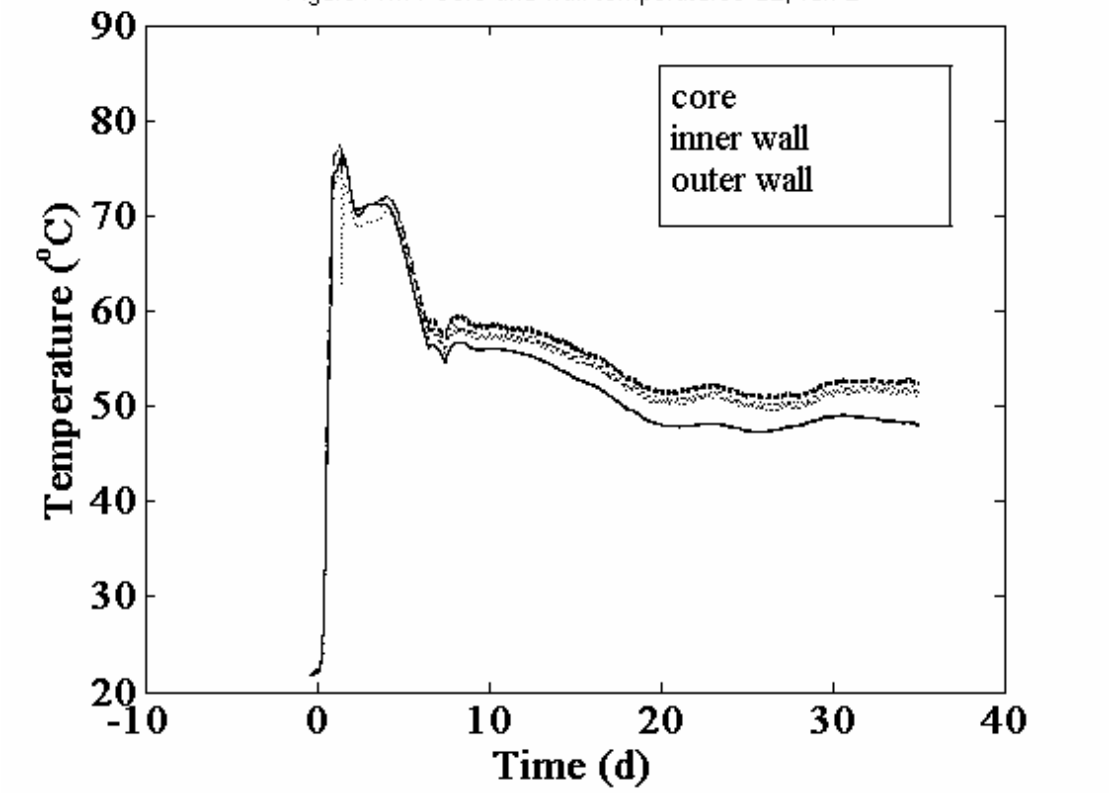

Figure A4.8: Core and wall temperatures; S3; run B

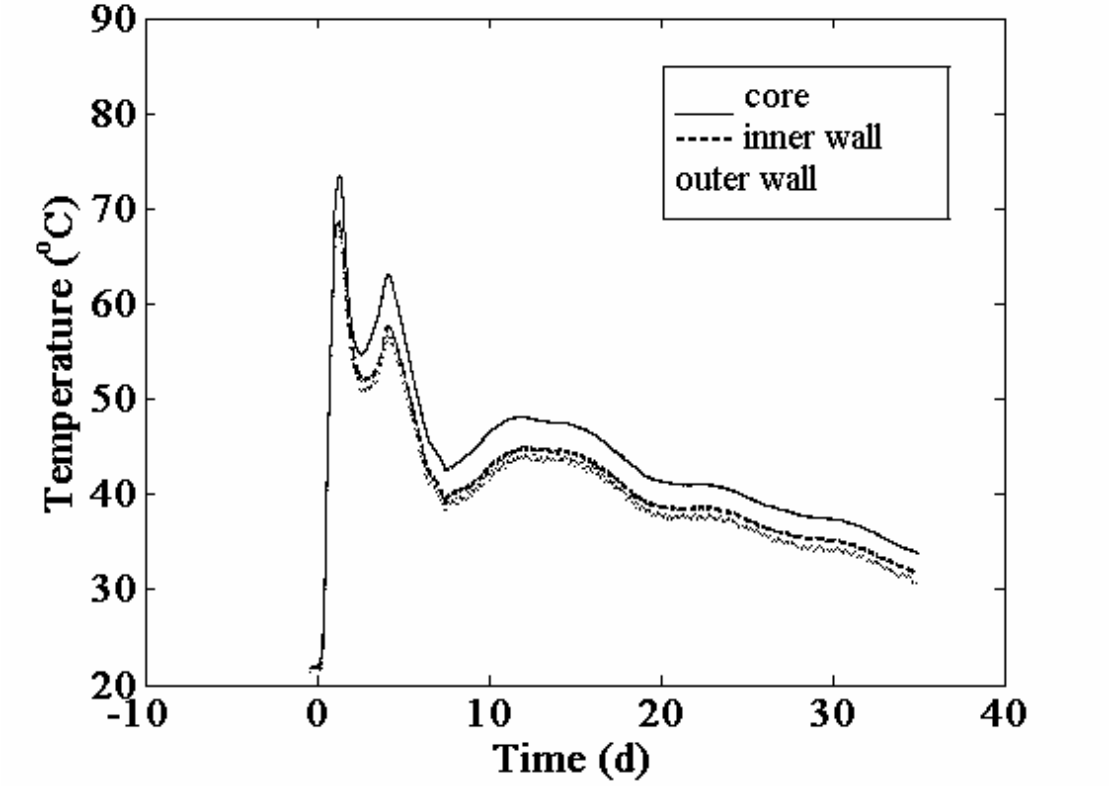

Figure A4.9: CO2 probe temperatures; run A

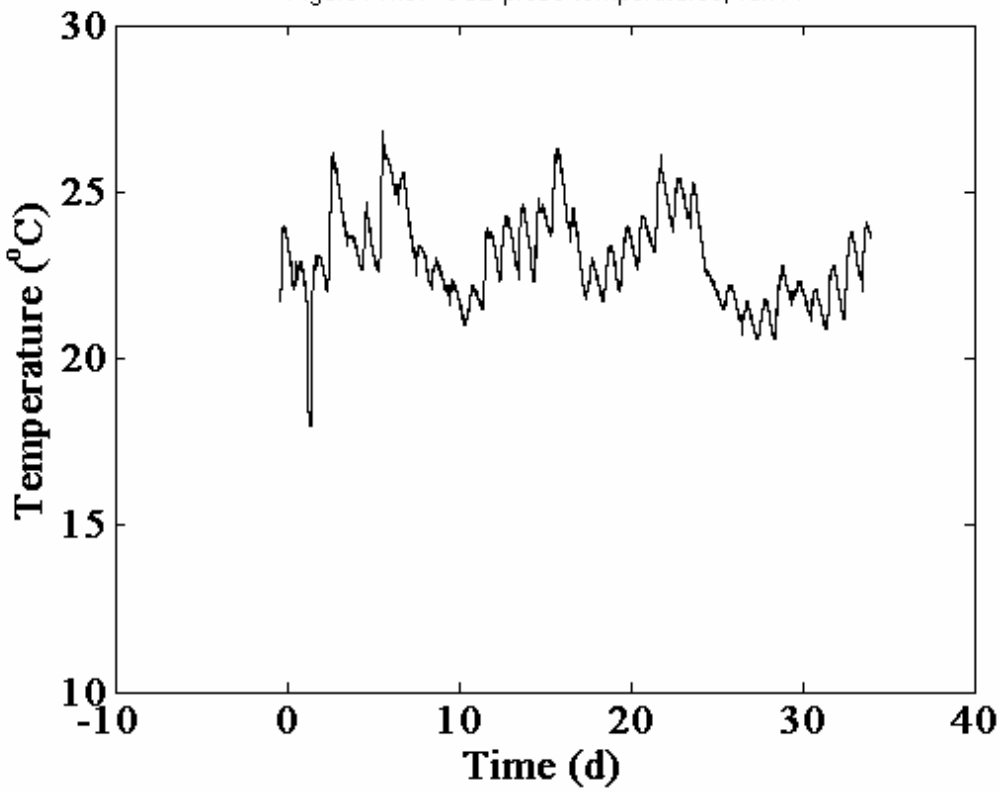

Figure A4.10: CO2 probe temperatures; run B

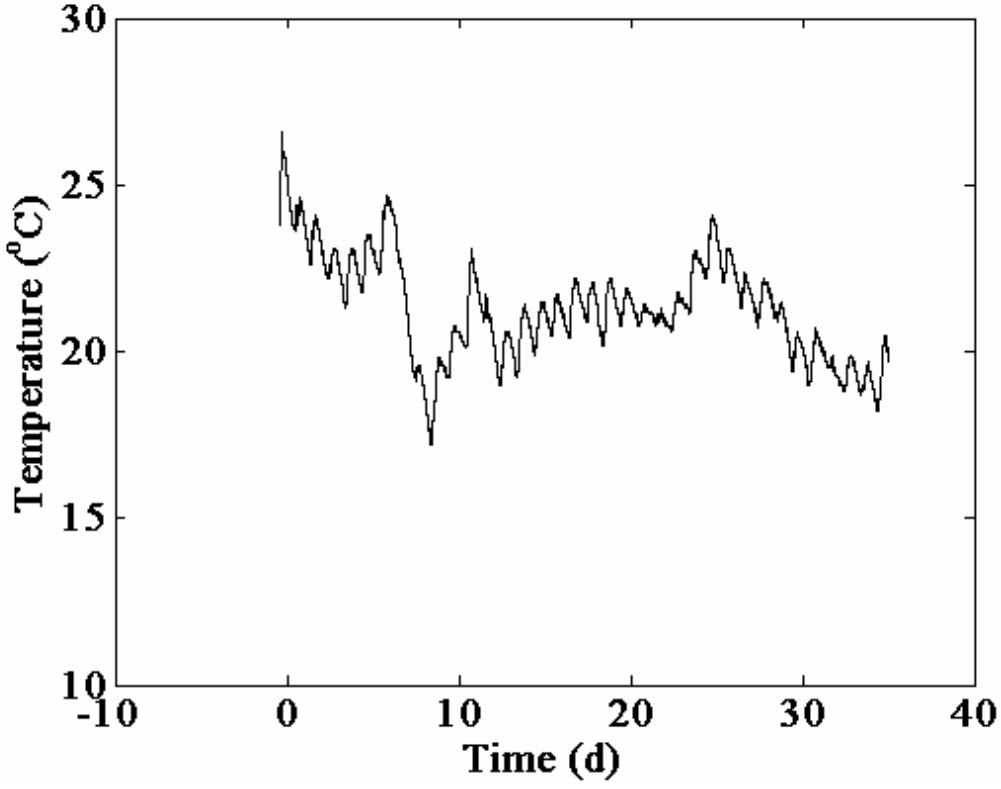

APPENDIX 5
POWER AND ENERGY PROFILES

Figure A5.1: Advective losses; run A

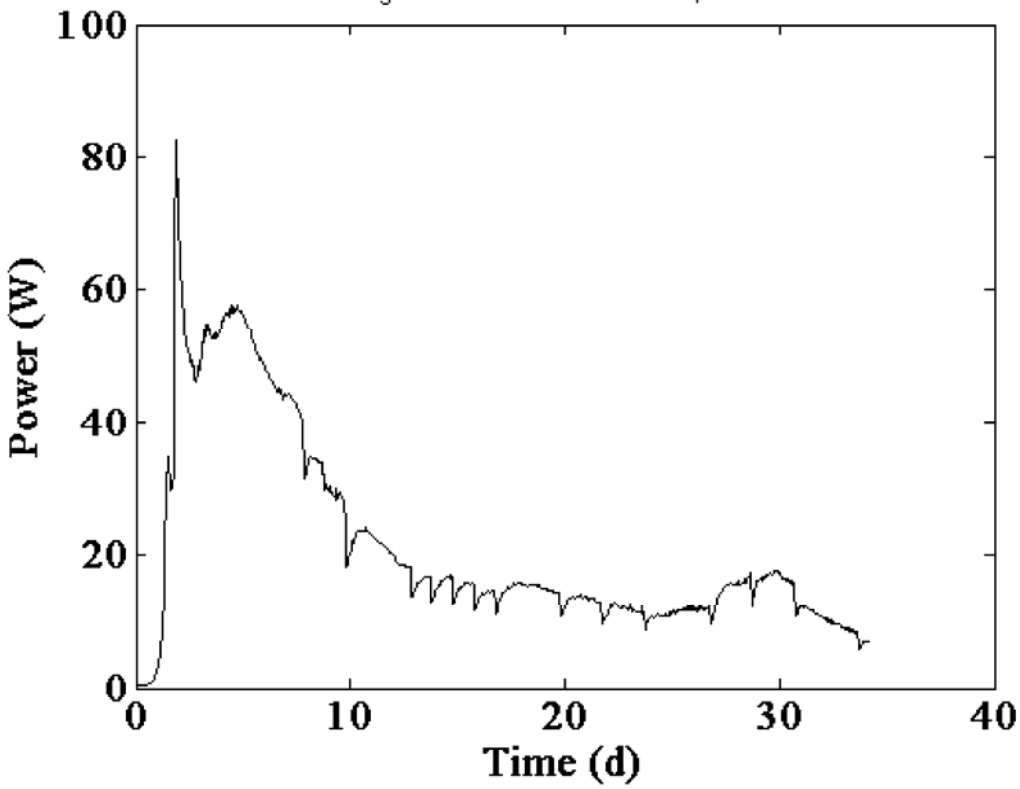

Figure A5.2: CCR losses; run A

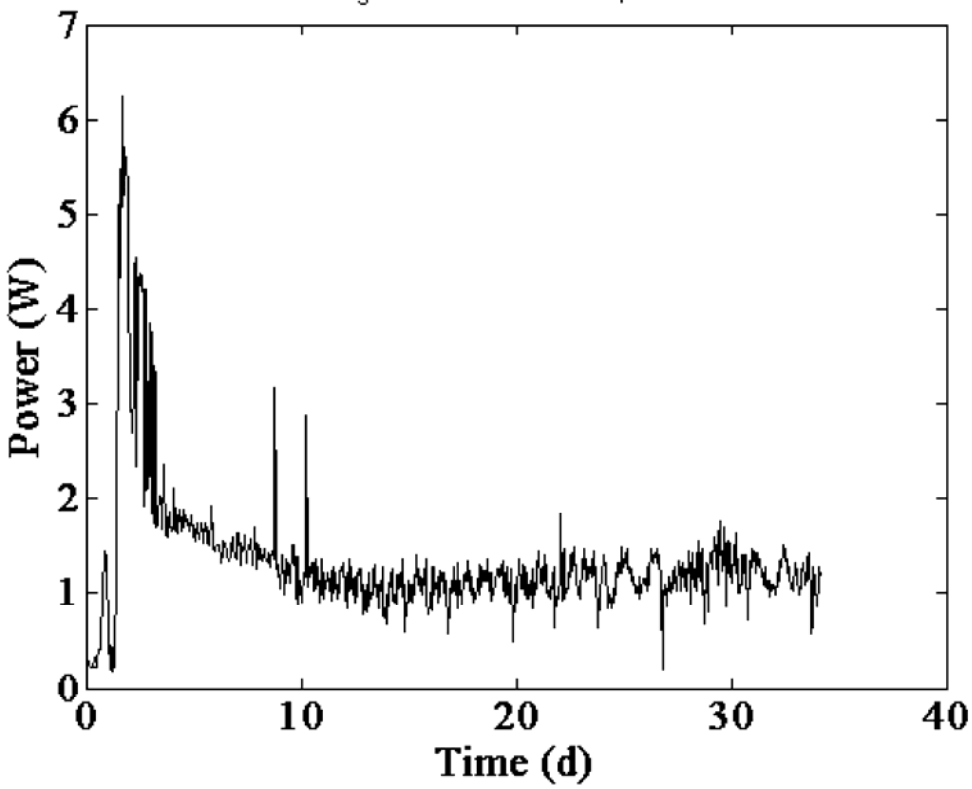

Figure A5.3: Total losses; run A

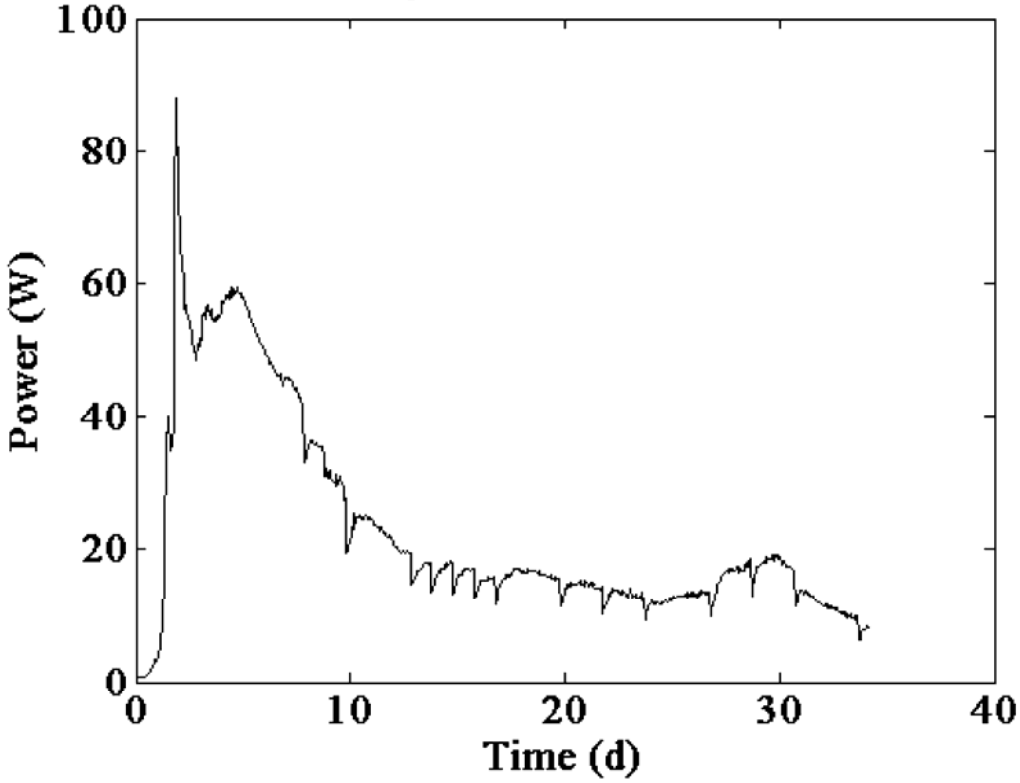

Figure A5.4: Accumulation; run A

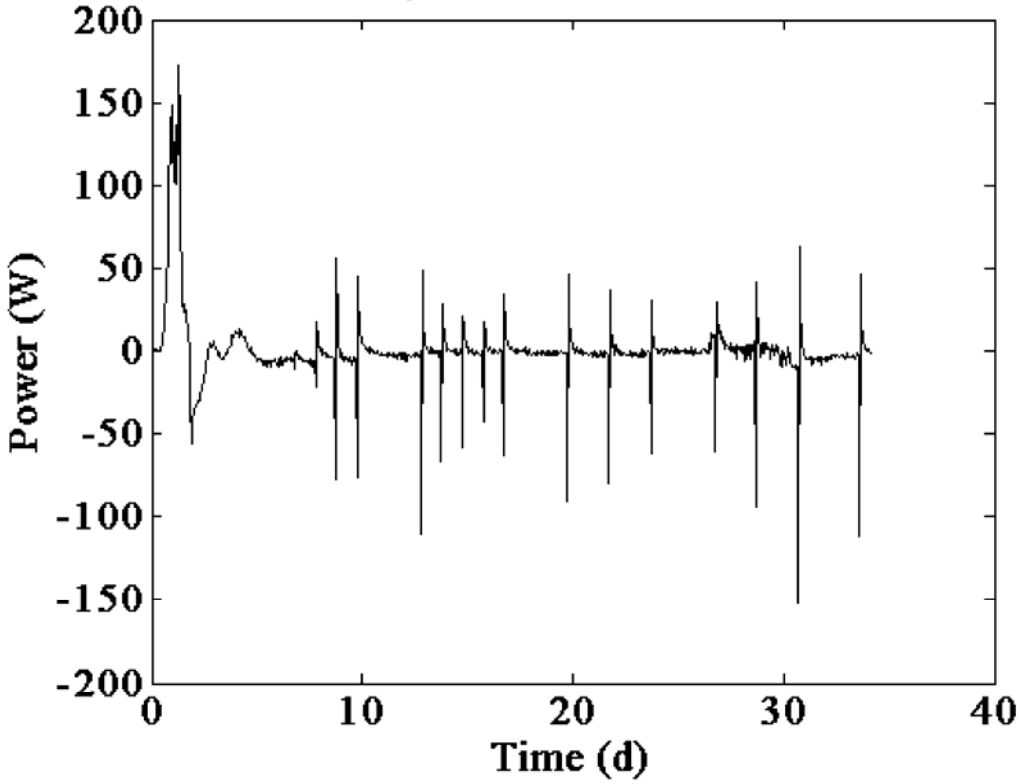

Figure A5.5: Biopower; run A

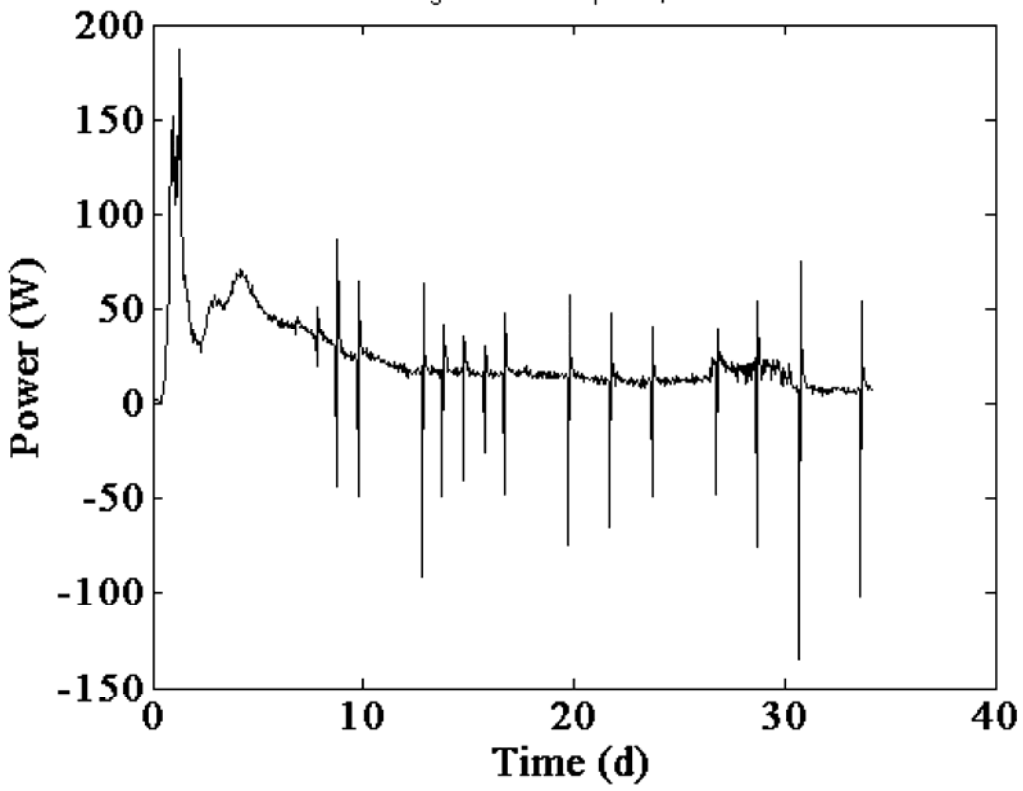

Figure A5.6: Advective losses; run B

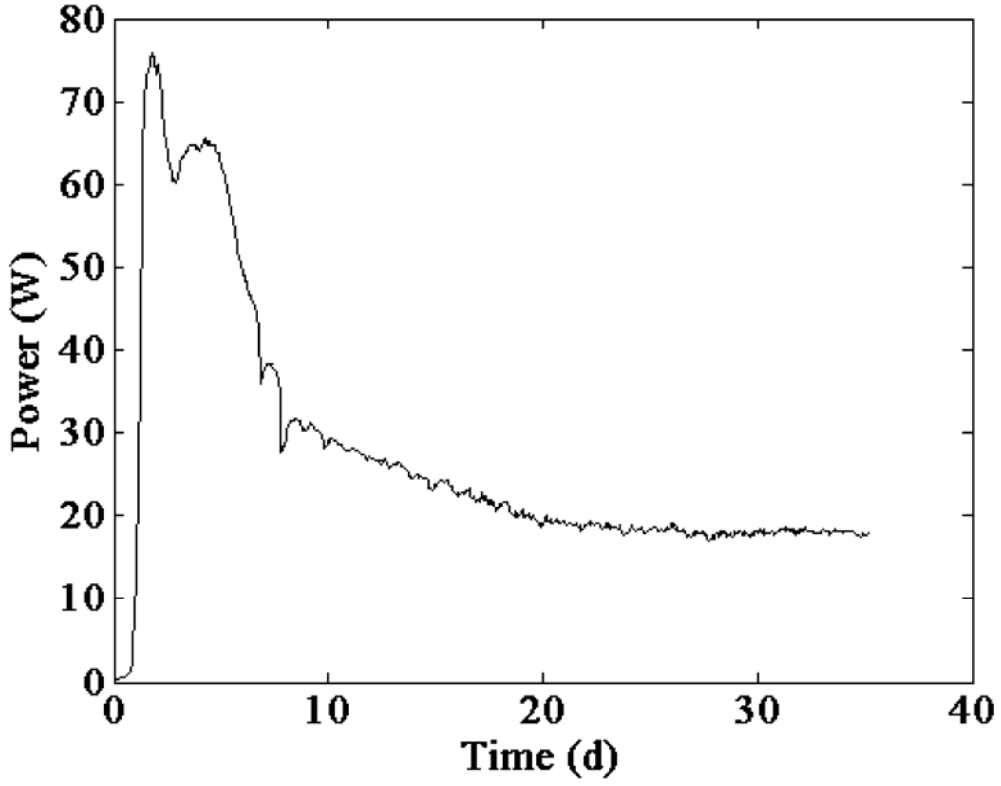

Figure A5.7: CCR losses; run B

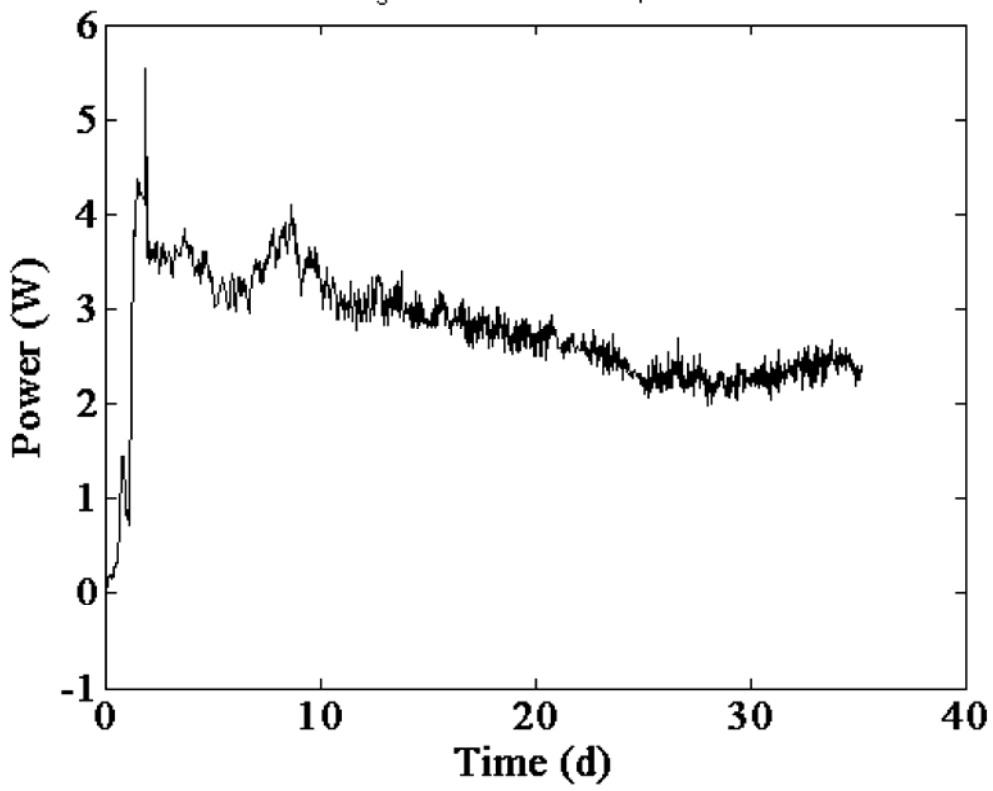

Figure A5.8: Total losses; run B

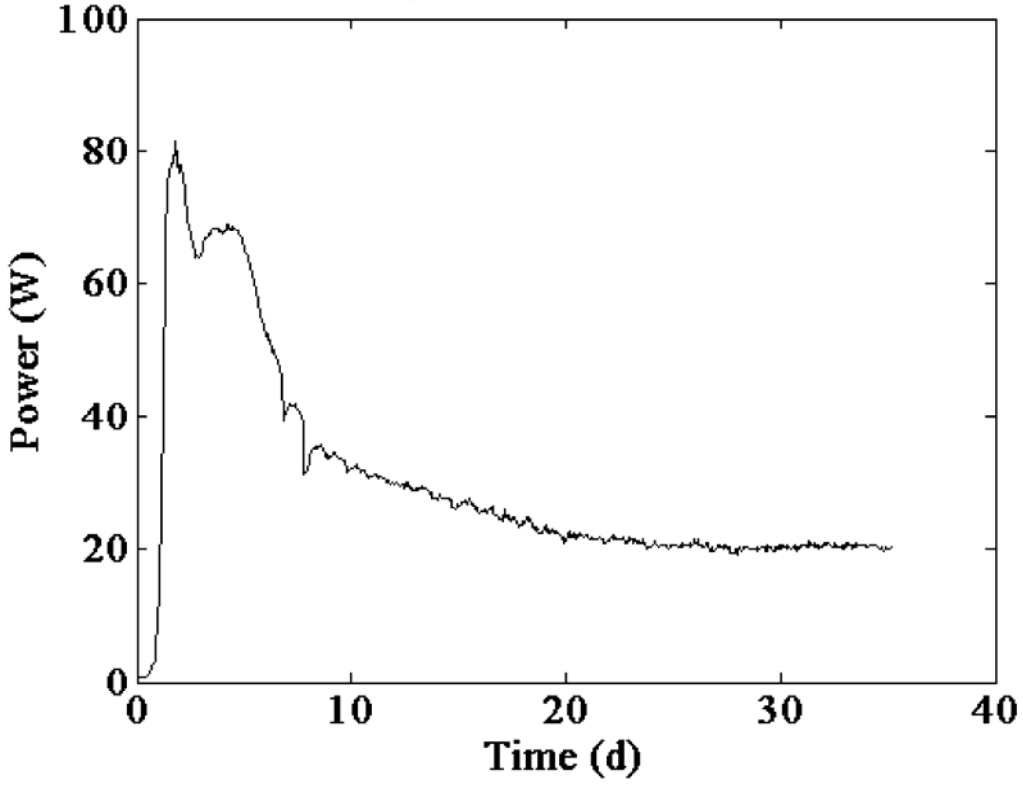

Figure A5.9: Accumulation; run B

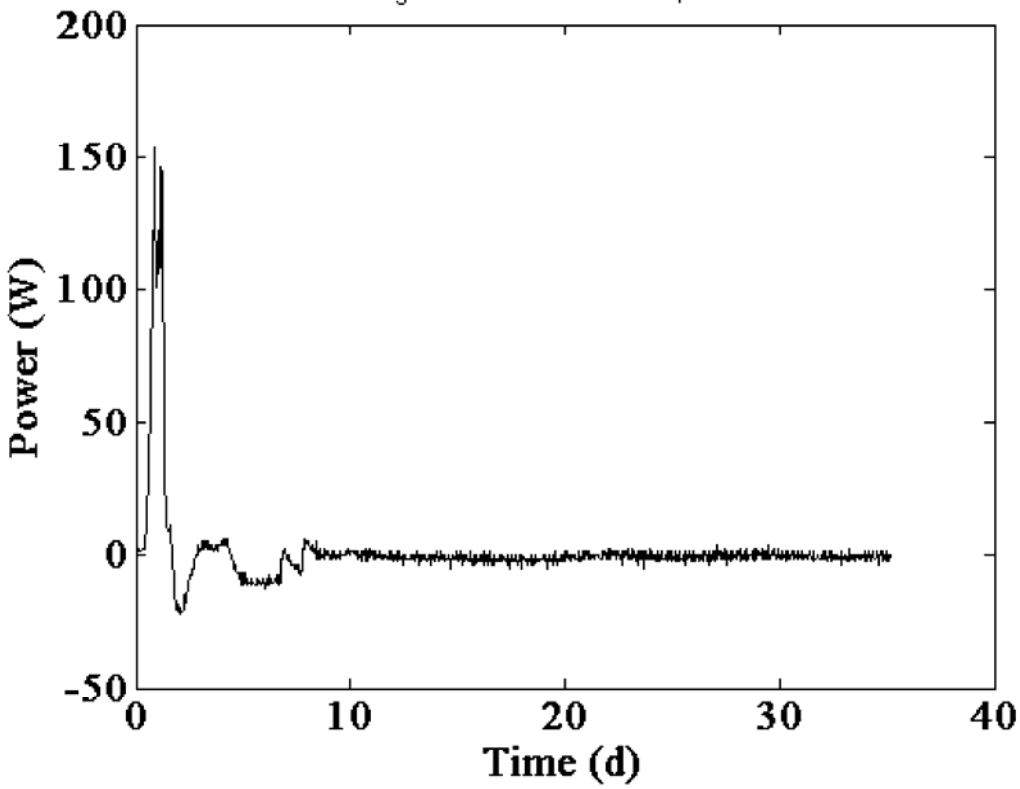

Figure A5.10: Biopower; run B

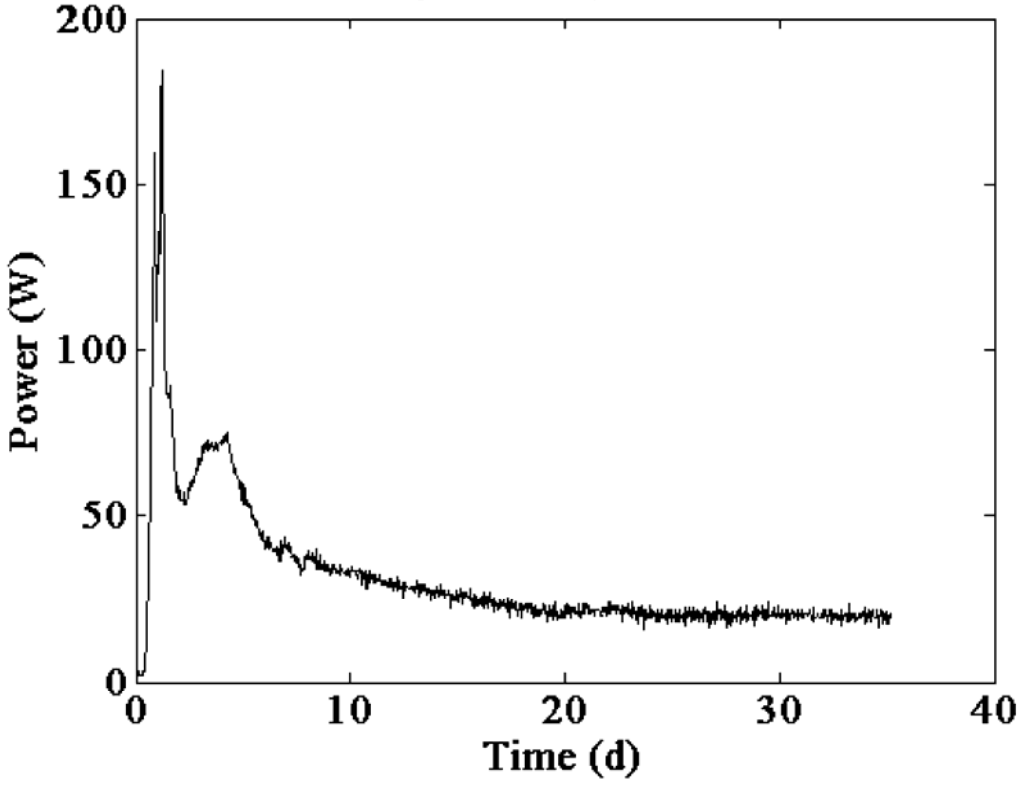

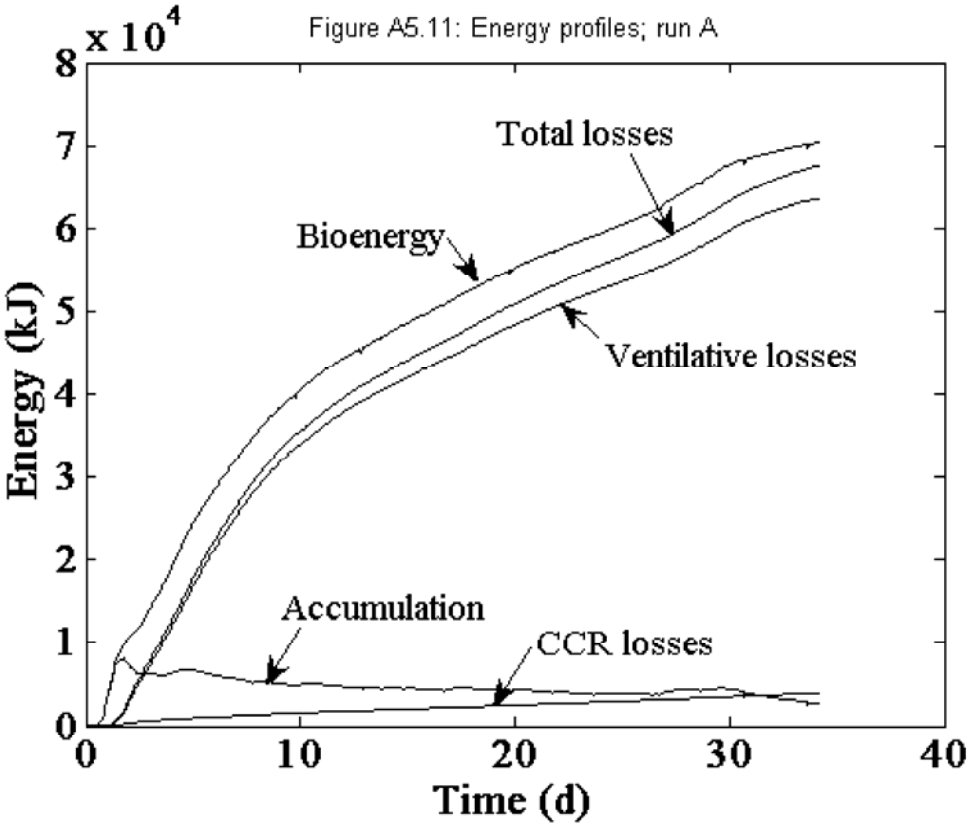

Figure A5.11: Energy profiles; run A

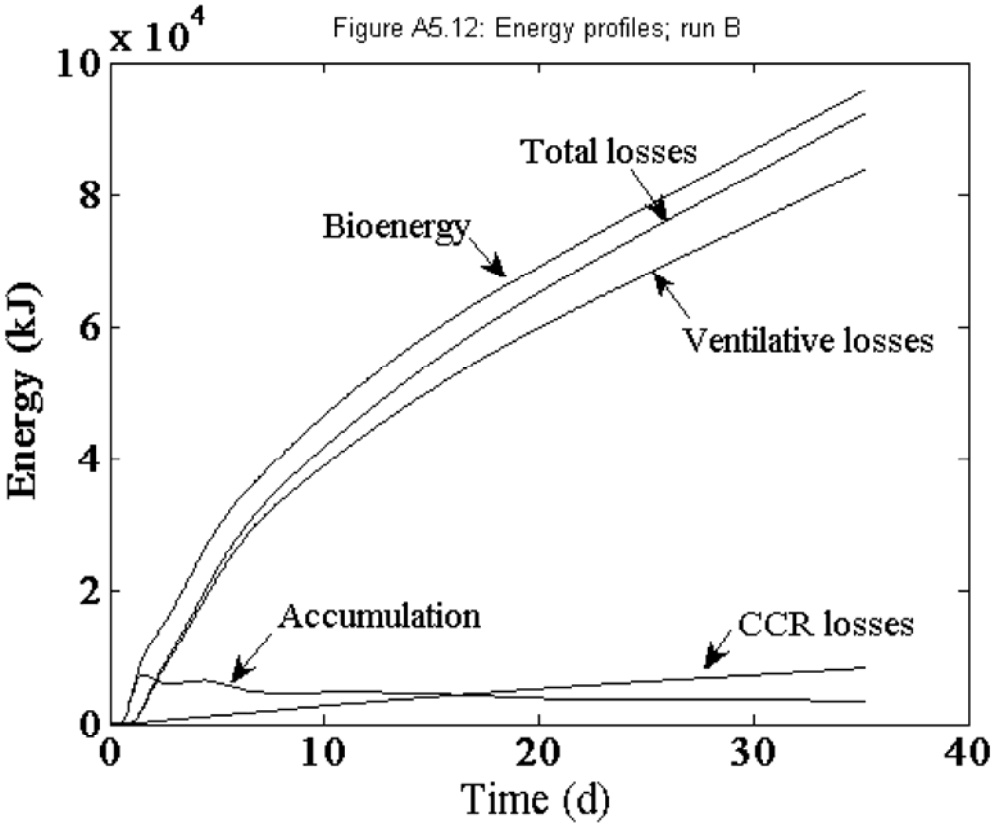

Figure A5.12: Energy profiles; run B

Figure A5.13: Energy ratios; run A

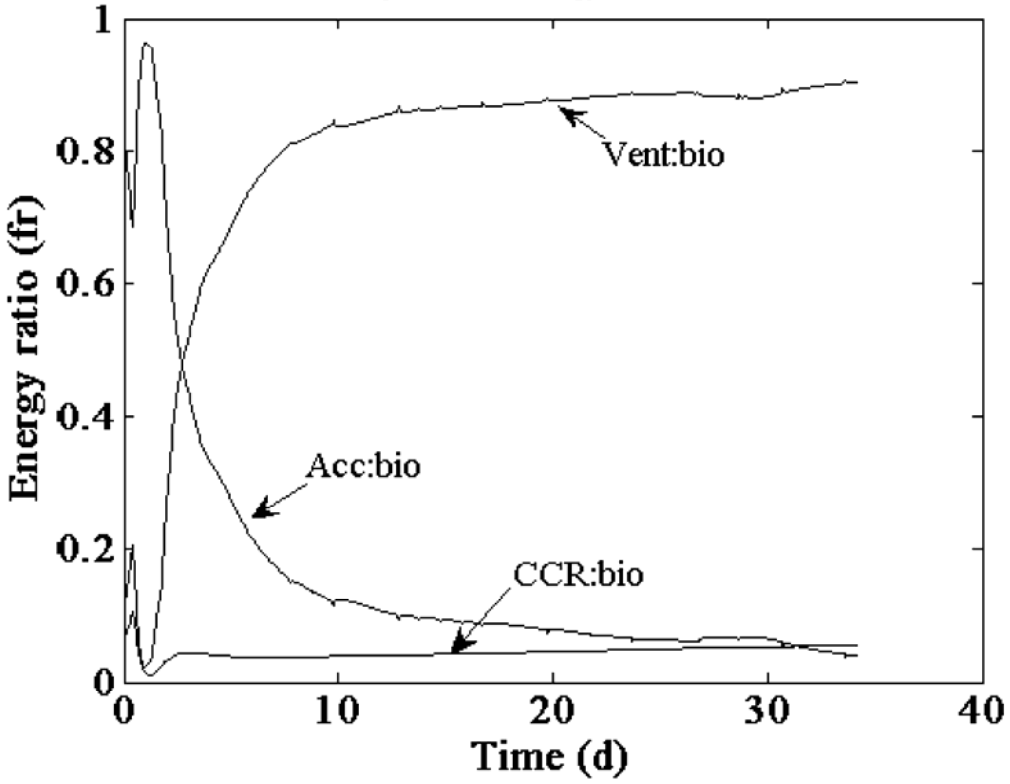

Figure A5.14: Energy ratios; run B

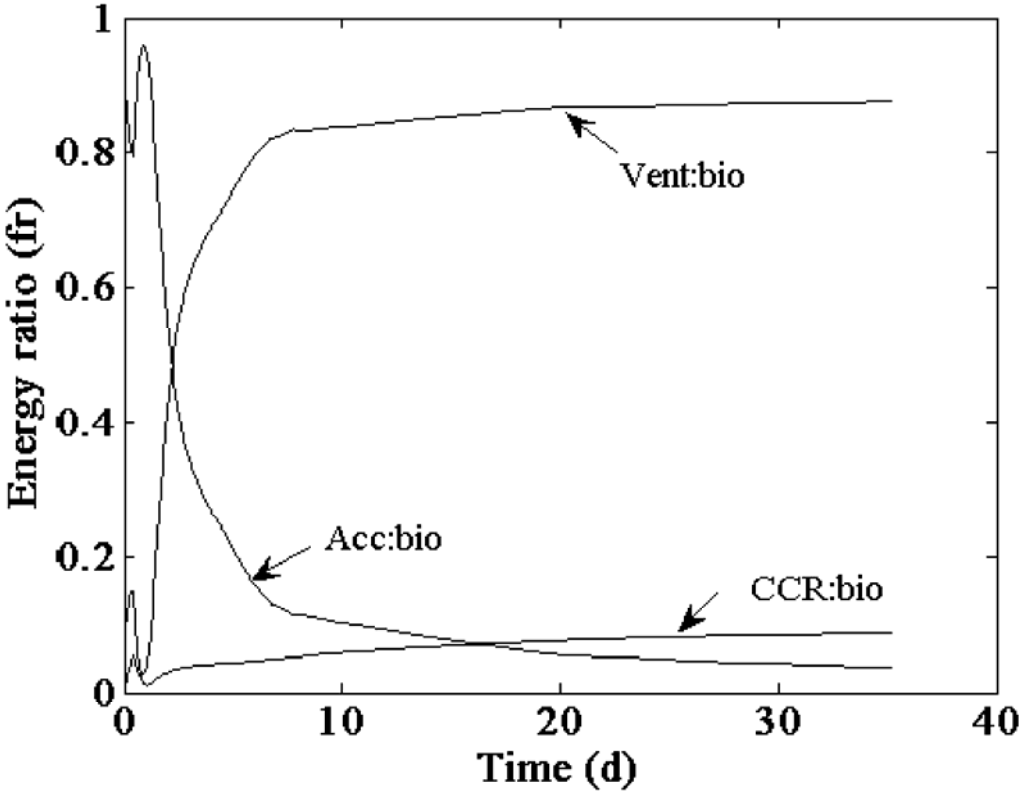

Figure A5.15: Cumulative sensible energy required to reheat returned leachate, Run A

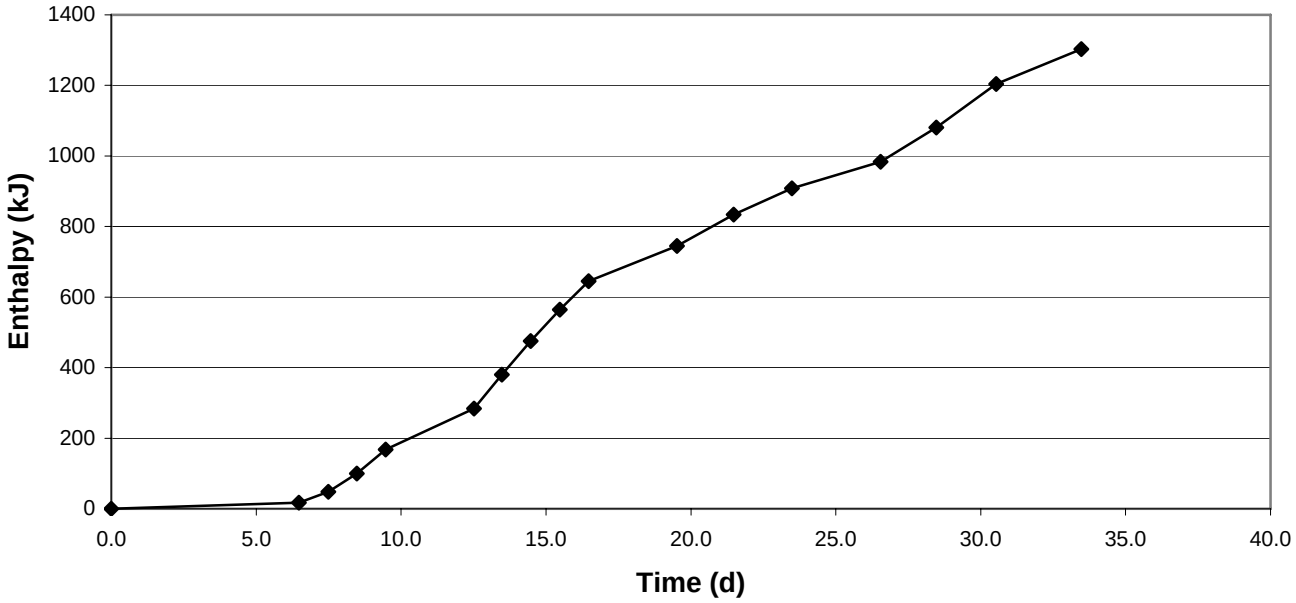

APPENDIX 6
LEACHATE CHARACTERISTICS

Table A6.1 Leachate volumes: run A

Time (d)	Vol (ml)
0	0
6	90
7	160
8	270
9	370
12	660
13	570
14	570
15	550
16	520
19	620
21	580
23	520
26	480
28	540
30	720
33	760
34	570

Table A6.2 Leachate volumes and total carbon levels: run B

Time (d)	Vol (ml)	Cum (ml)	TC (mg/l)	TC (g)	
0					
1					
2					
3					
4					
5					
6	110	110	7100	0.78	
7	150	260	6779	1.02	
8	175	435	6254	1.09	
9	100	535	5244	0.52	
10					
11					
12	400	935	4534	1.81	
13	120	1055	3522	0.42	
14	105	1160	2970	0.31	
15					
16	125	1285	3279	0.41	
17					
18					
19	130	1415	2842	0.37	
20					
21	60	1475	2413	0.14	
22					
23	70	1545	2645	0.19	
24					
25					
26	60	1605	1818	0.11	
27					
28					
29	45	1650	1540	0.07	
30					
31					
32					
33					
34					
35	30	1680	1603	0.05	
Residual	280	1960	1603	0.45	
Total		1.96	kg	7.75	g
Proportion total water		0.10	fr		
Total CO2 carbon emitted				1.257	kg
Proportion total CO2-carbon in leachate				0.006	fr

APPENDIX 7
MASS LOSS PROFILES

Figure A7.1: Mass loss, run A

Figure A7.2: Mass loss, run B

Figure A7.1: Total mass loss vs time; run A

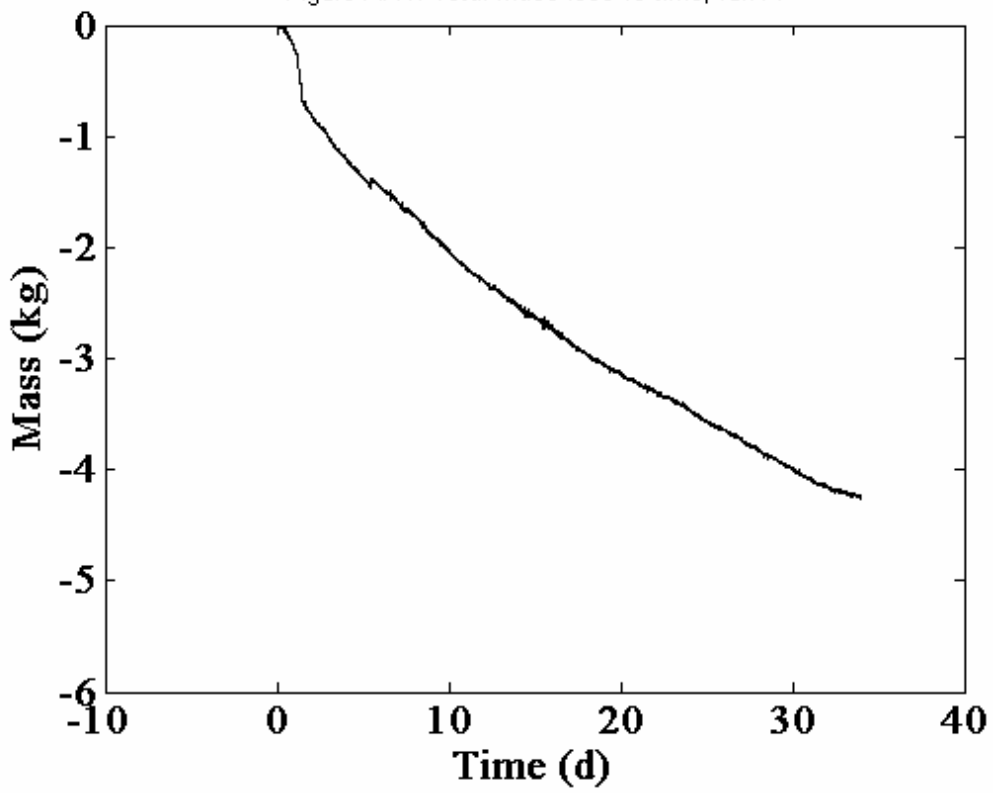

Figure A7.2: Total mass loss vs time; run B

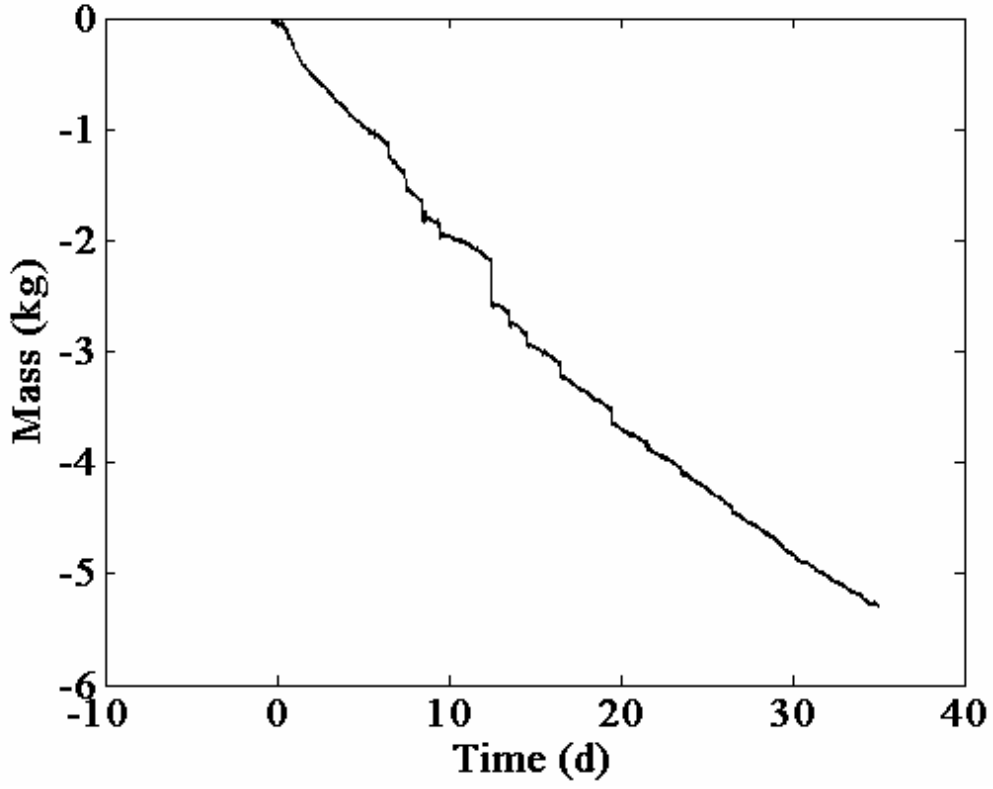

APPENDIX 8
CO_2 CONCENTRATION PROFILES

Figure A8.1: CO_2 concentration, run A

Figure A8.2: CO_2 concentration, run B

Figure A8.1: CO2 vs time ; run A

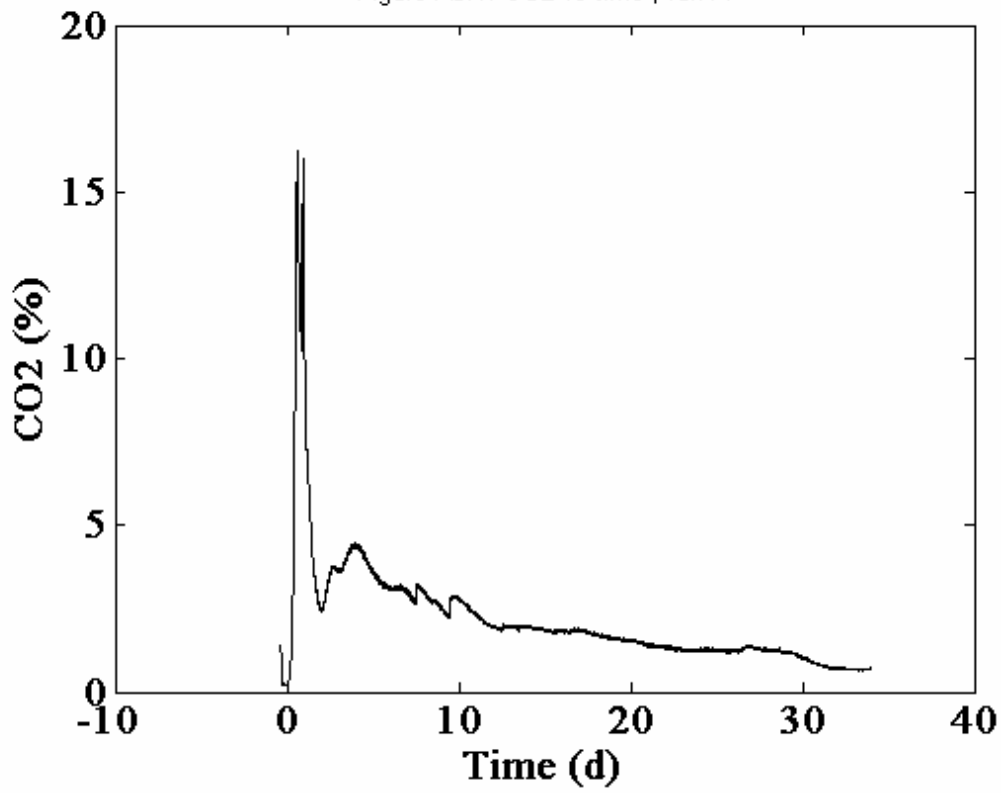

Figure A8.2: CO2 vs time ; run B

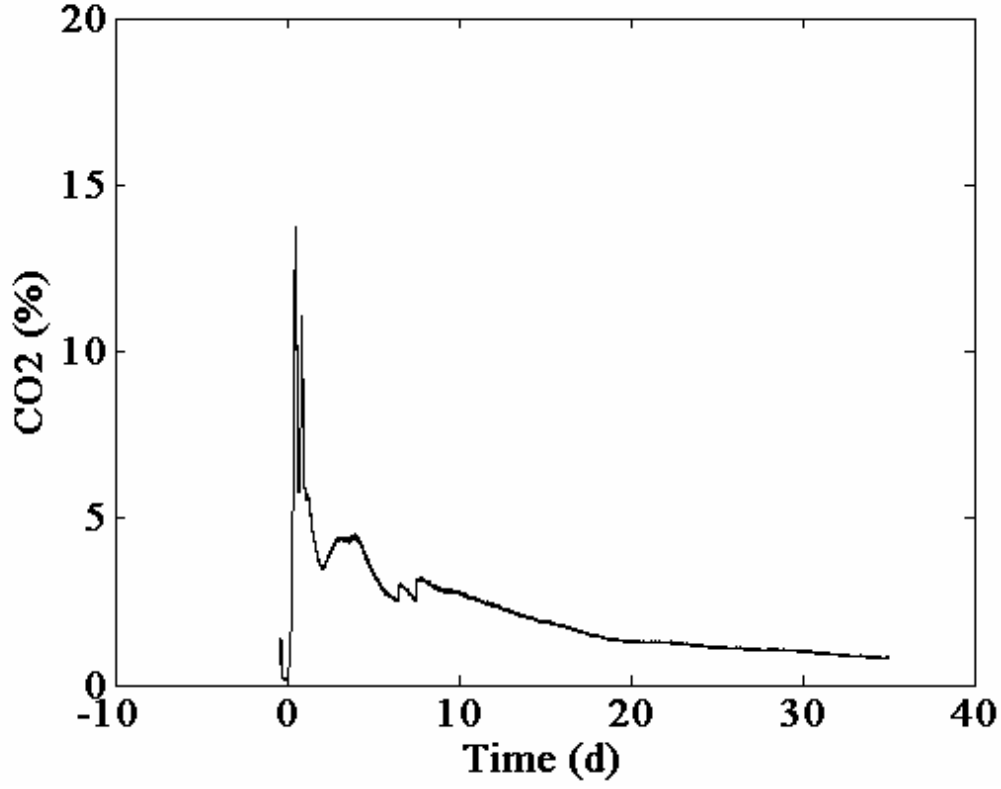

APPENDIX 9
TEMPERATURE-CORRECTED PROFILES AND DATA

Note: for figures 9.1 though 9.24, cardinal temperatures were 5, 59 and 85 ^{o}C.

Note: For figures 9.25 through 9.30, alternative cardinal temperatures as shown were used.

Figure A9.25: Polynomials fitted to original and corrected CO_2-C data; cardinal temperatures 5, 50 and 80 ^oC; run A

Figure A9.26: Polynomials fitted to original and corrected CO_2-C data; cardinal temperatures 5, 55 and 80 ^oC; run A

Figure A9.27: Double exponential model fitted to original and corrected CO_2-C data; cardinal temperatures 5, 55 and 80 ^oC; run A

Figure A9.28: Polynomials fitted to original and corrected BVS-C data; cardinal temperatures 5, 50 and 80 ^oC; run A

Figure A9.29: Polynomials fitted to original and corrected BVS-C data; cardinal temperatures 5, 55 and 80 ^oC; run A

Figure A9.30: Double exponential model fitted to original and corrected BVS-C data; cardinal temperatures 5, 55 and 80 ^oC; run A

Figure A9.31: Double exponential model fitted to temperature corrected CO_2-C data; cardinal temperatures 5, 50 and 80 ^oC; run B; pre-set values of k_1 and k_2

Figure A9.31: Double exponential model fitted to temperature corrected BVS-C data; cardinal temperatures 5, 50 and 80 ^oC; run B; pre-set values of k_1 and k_2

Table A9.1: Variations in double exponential model goodness of fit vs cardinal temperature for run B temperature-corrected CO_2-C data

Figure A9.1: CO_2-C (solid) and T (dashdot) profiles - original data; Run A

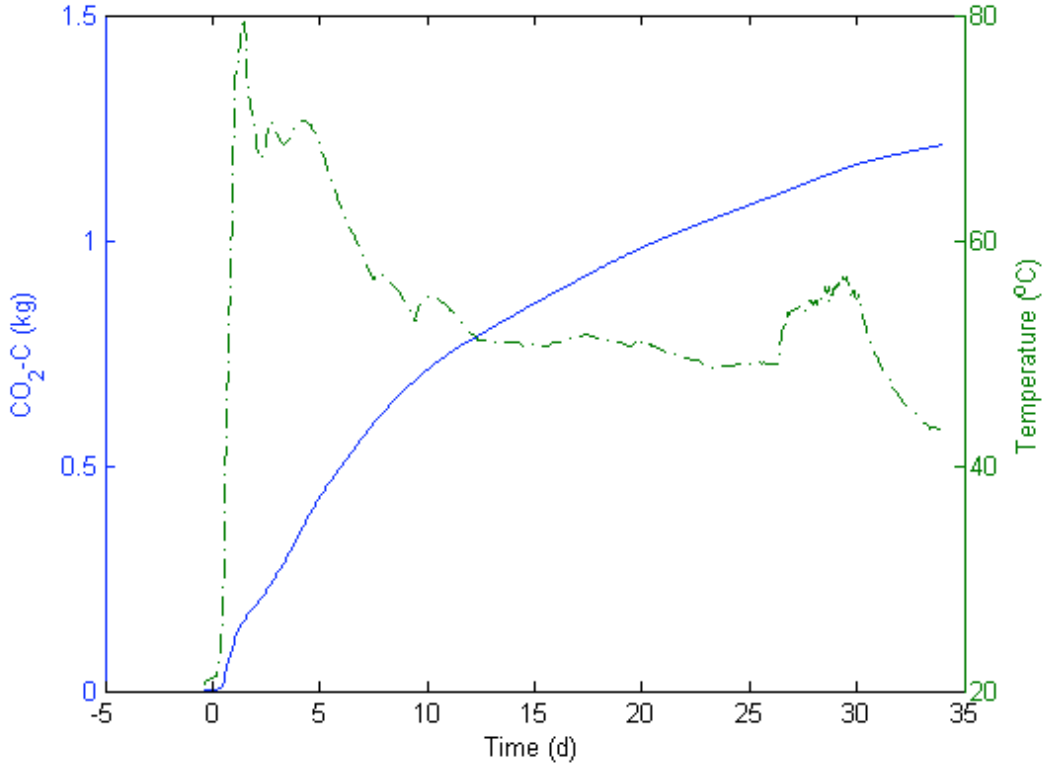

Figure A9.2: Temperature functions fT (dashed) and fT40 (solid); CO2c, Run A

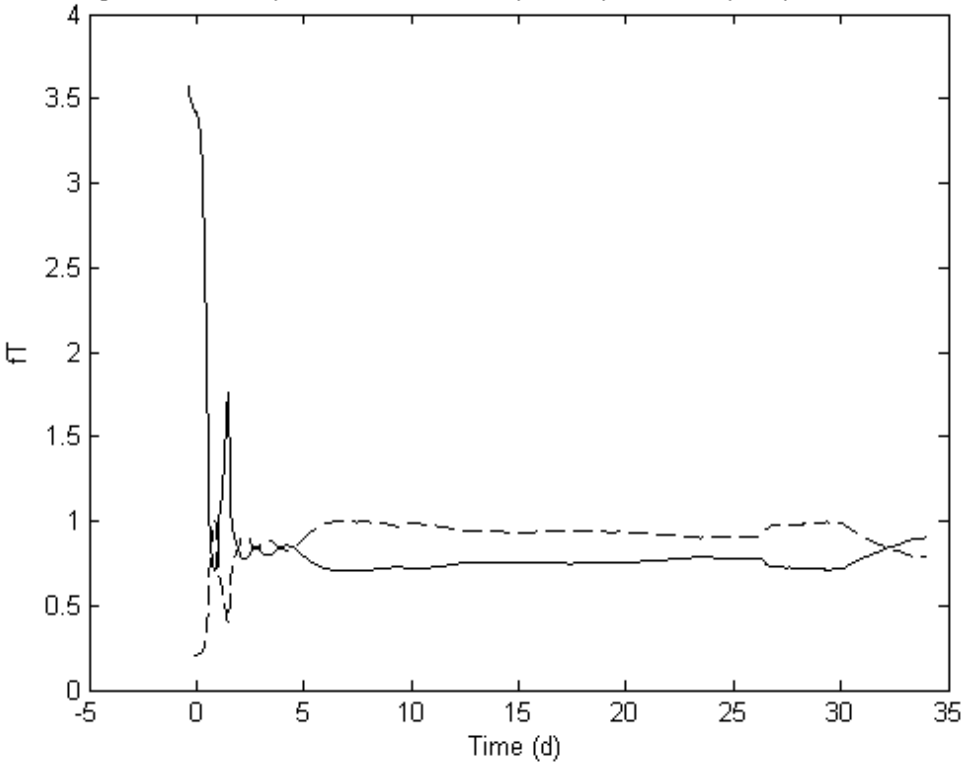

Figure A9.3: Polynomial fitted to original CO_2-C data; Run A

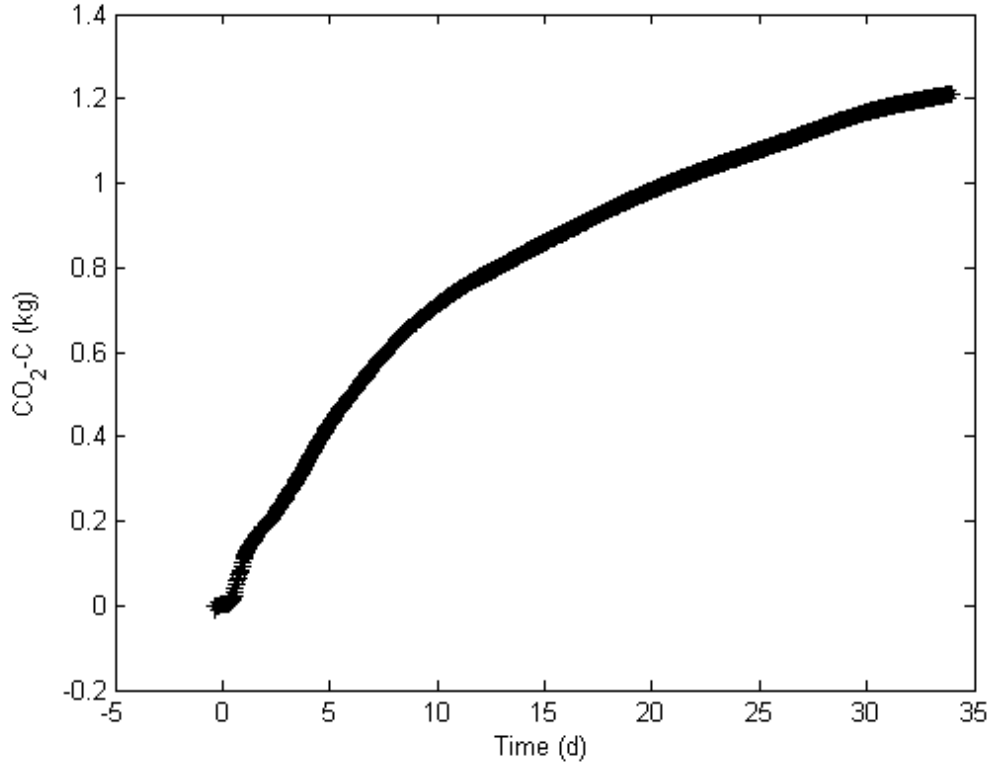

Figure A9.4: Derivative at T (dashed) and at 40 ^{o}C (solid); Run A

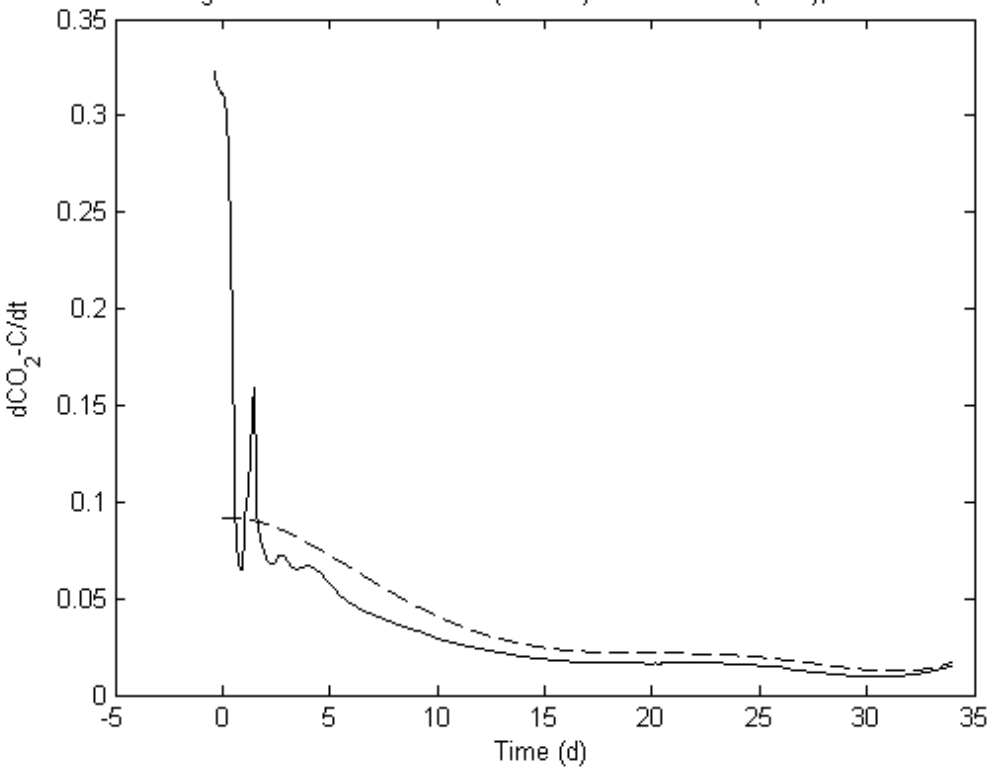

Figure A9.5: Polynomial fitted to corrected CO_2-C data; Run A

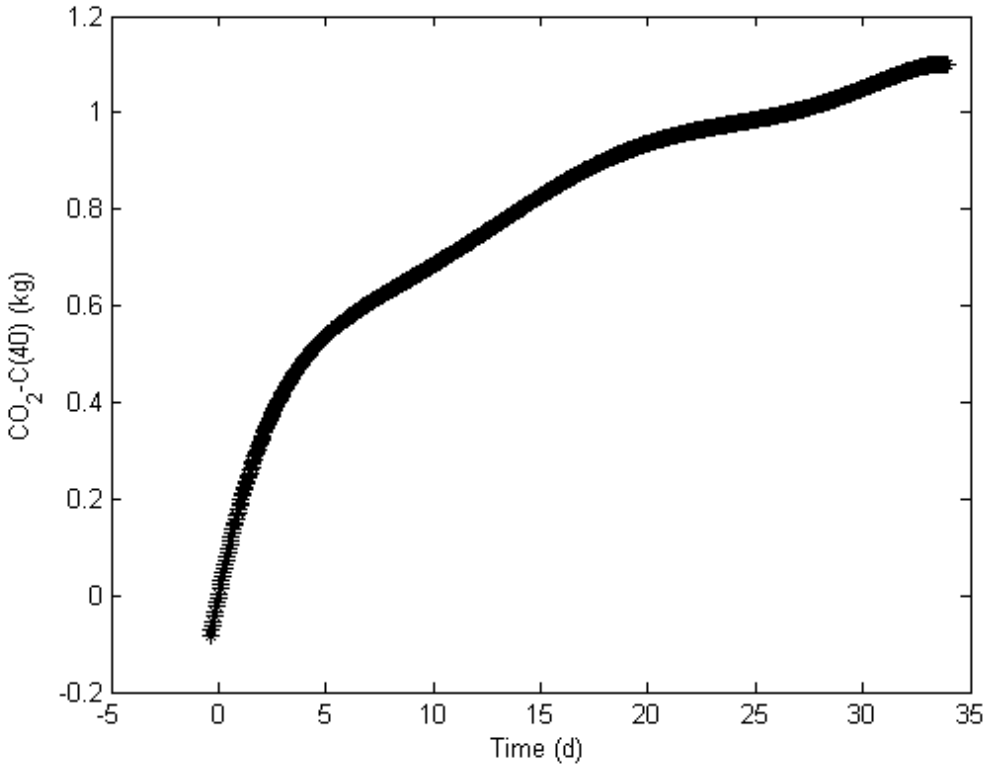

Figure A9.6: Polynomials fitted to original (dashed) and corrected (solid) CO_2-C data; Run A

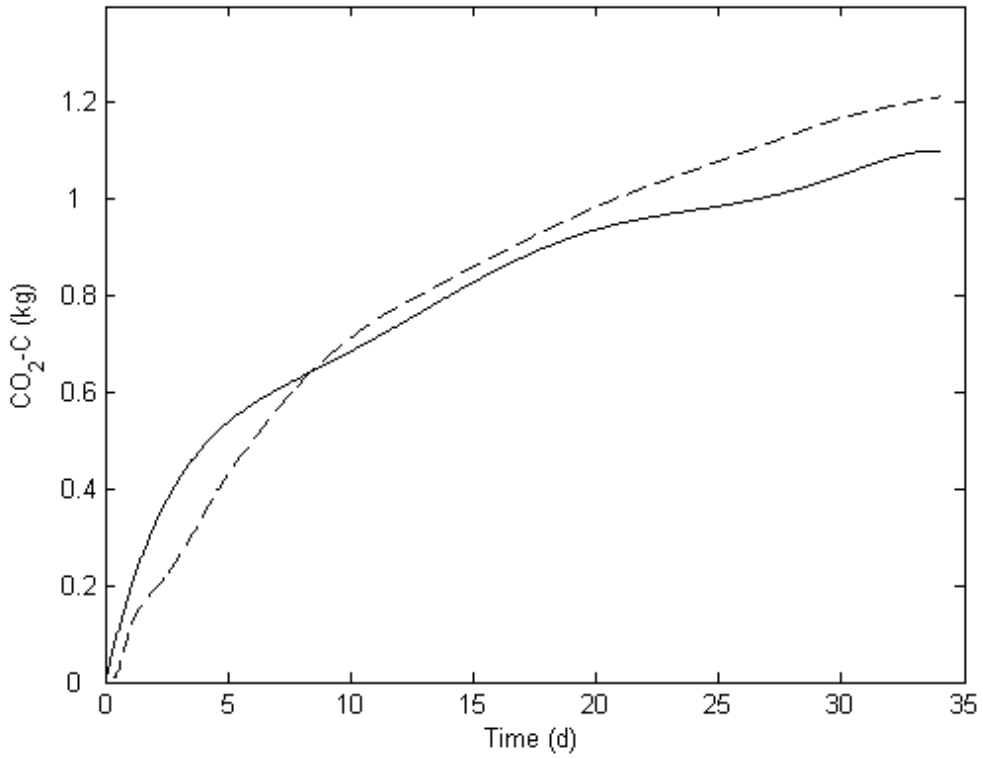

Figure A9.7: CO_2-C (solid) and T (dashdot) profiles - original data; Run B

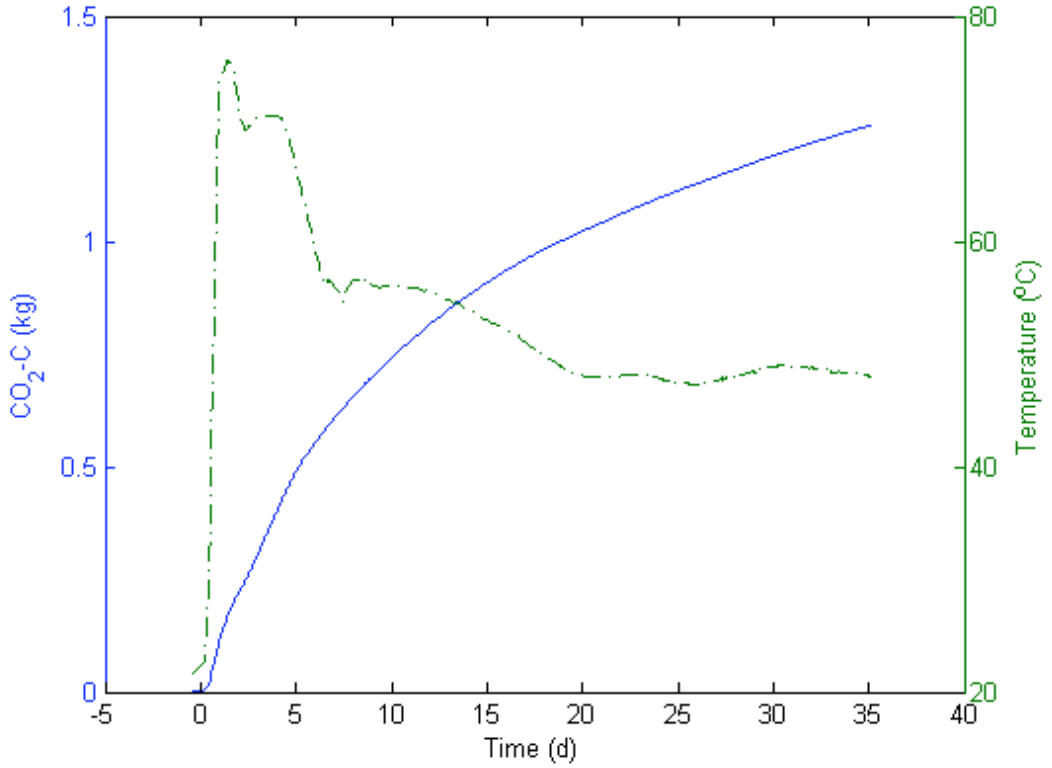

Figure A9.8: Temperature functions fT (dashed) and fT40 (solid); Run B

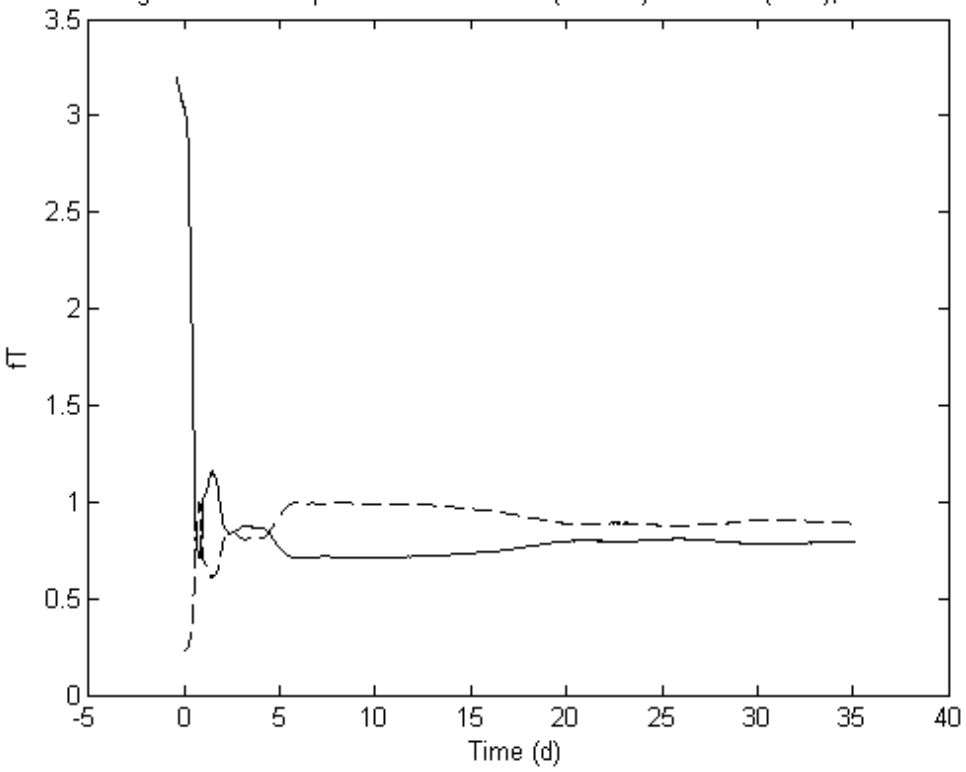

Figure A9.9: Polynomial fitted to original CO_2-C data; Run B

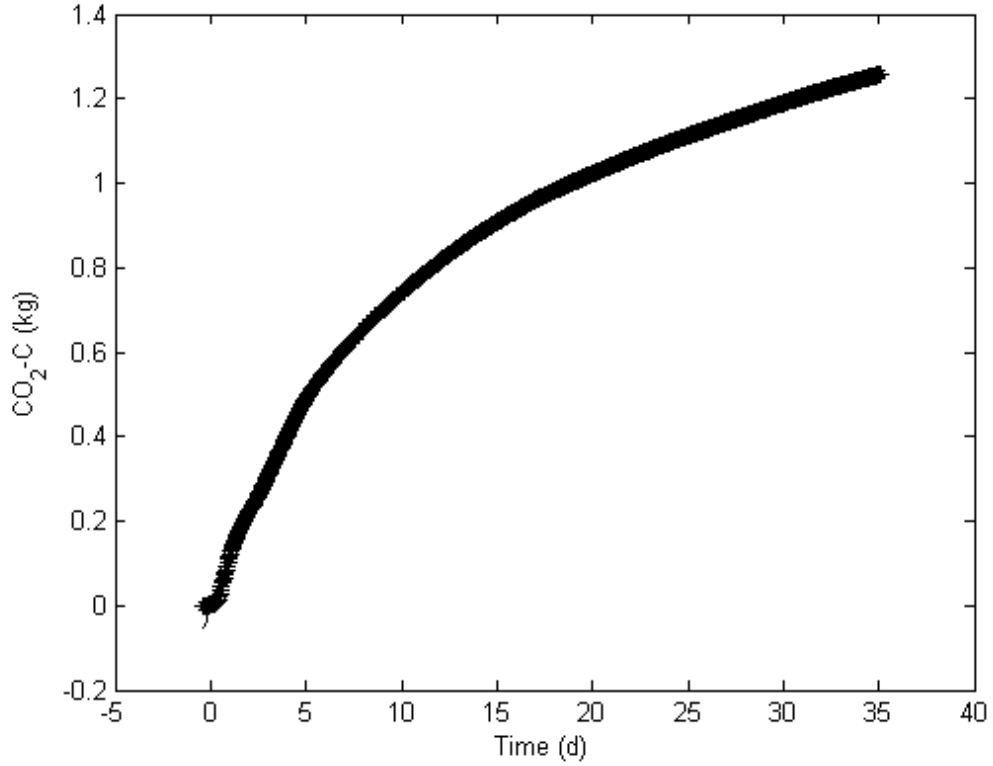

Figure A9.10: Derivative at T (dashed) and at 40 ^{o}C (solid); Run B

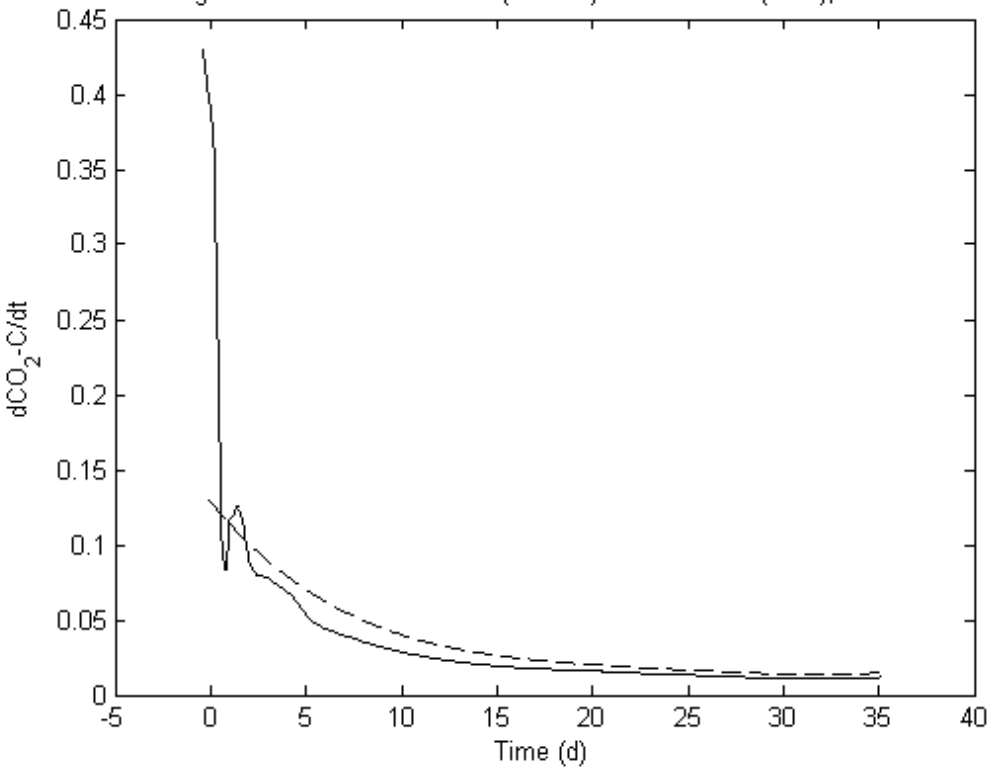

Figure A9.11: Polynomial fitted to corrected CO_2-C data; Run B

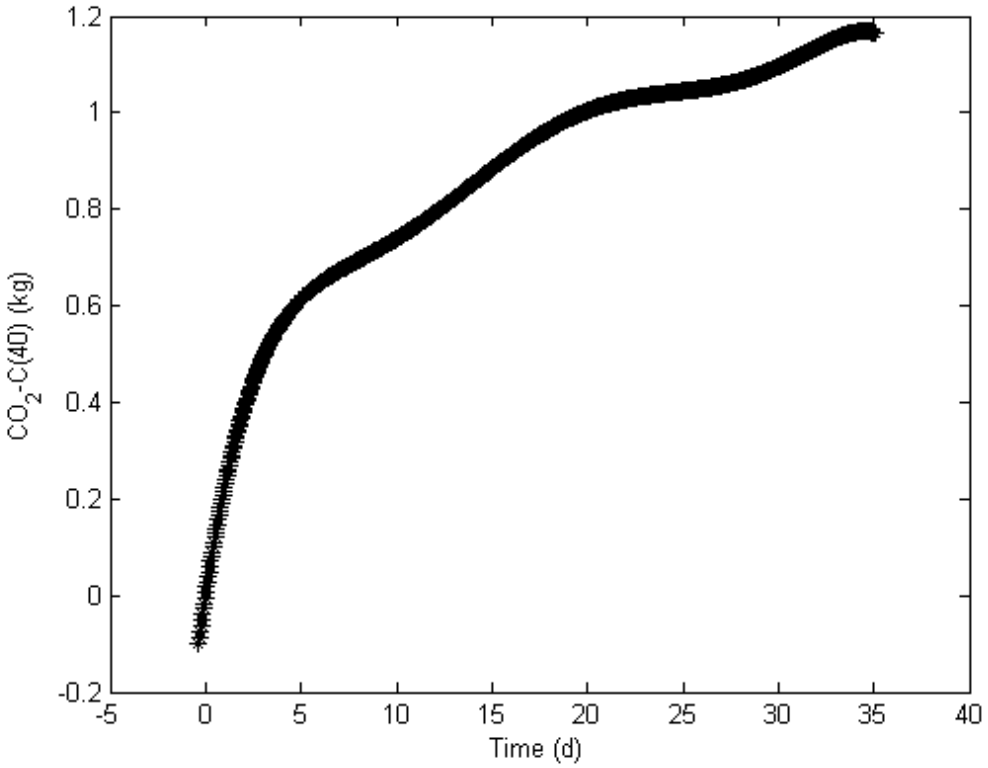

Figure A9.12: Polynomials fitted to original (dashed) and corrected (solid) CO_2-C data; Run B

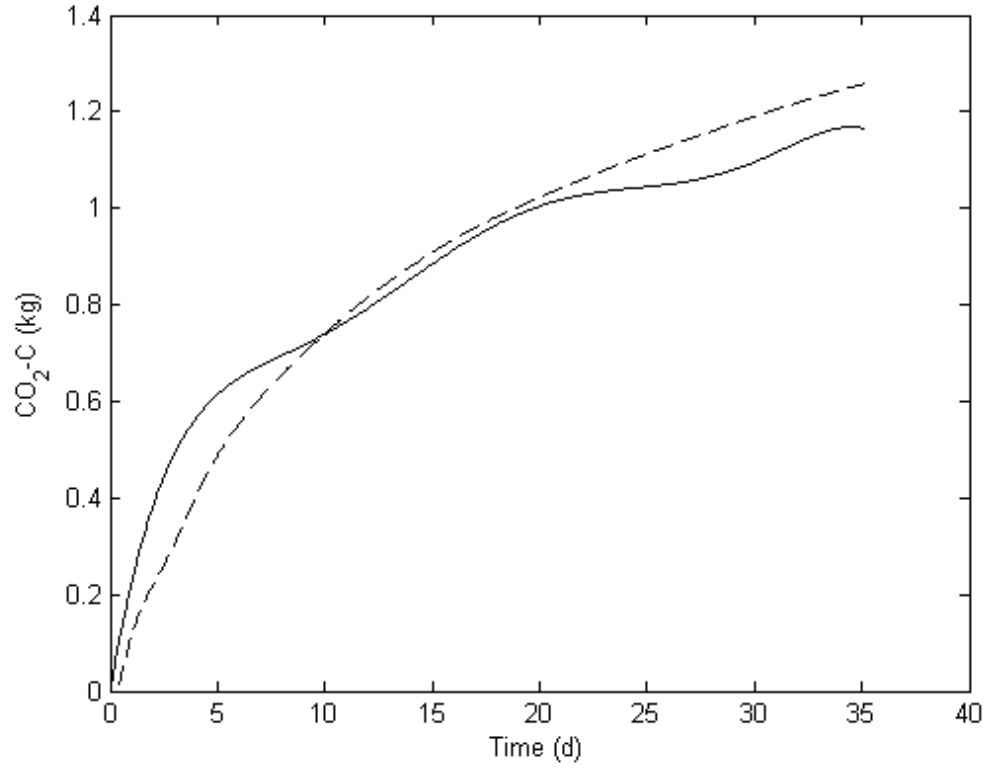

Figure A9.13: BVS-C (solid) and T (dashdot) profiles - original data; Run A

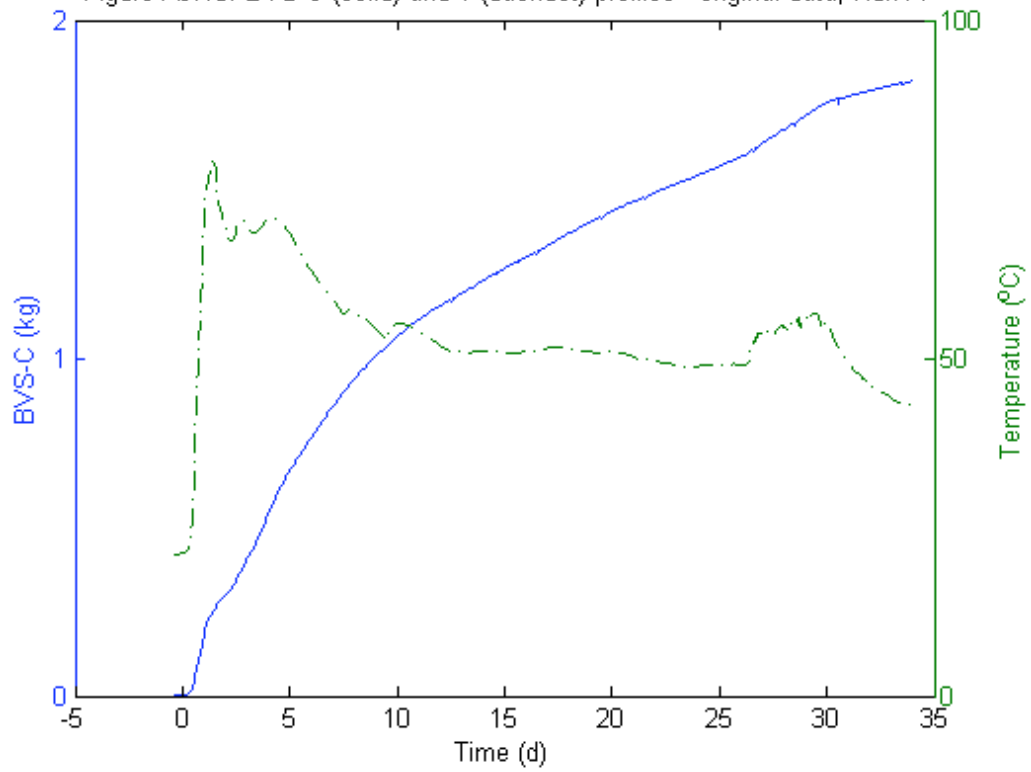

Figure A9.14: Temperature functions fT (dashed) and fT40 (solid); BVSc, Run A

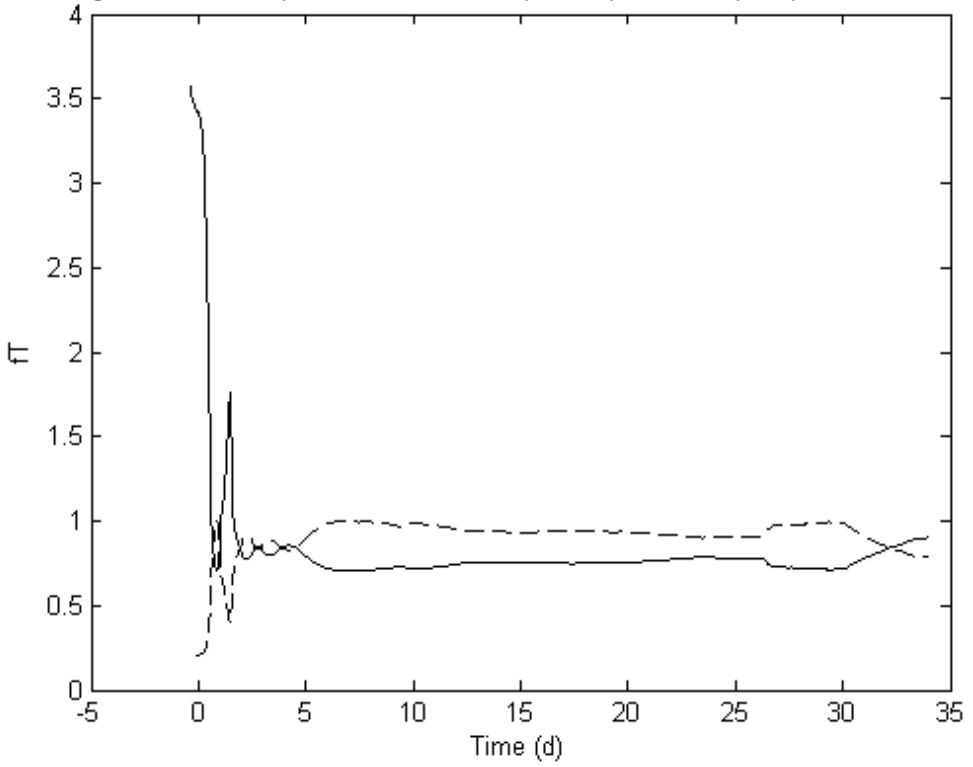

Figure A9.15: Polynomial fitted to original BVS-C data; Run A

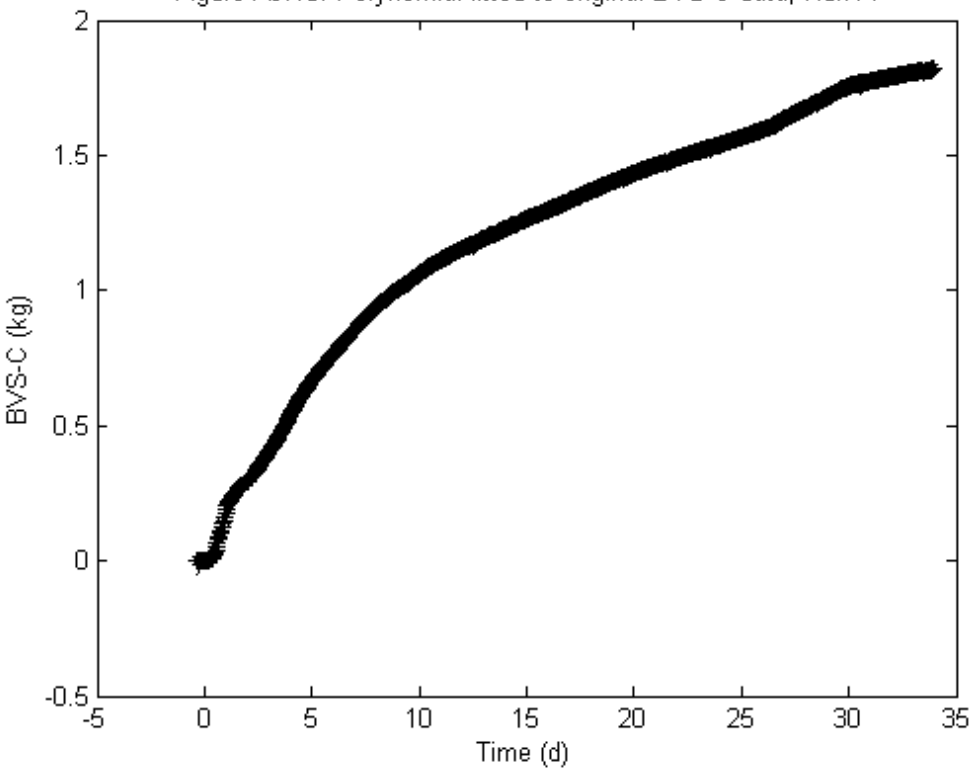

Figure A9.16: Derivative at T (dashed) and at 40 ^{o}C (solid); Run A

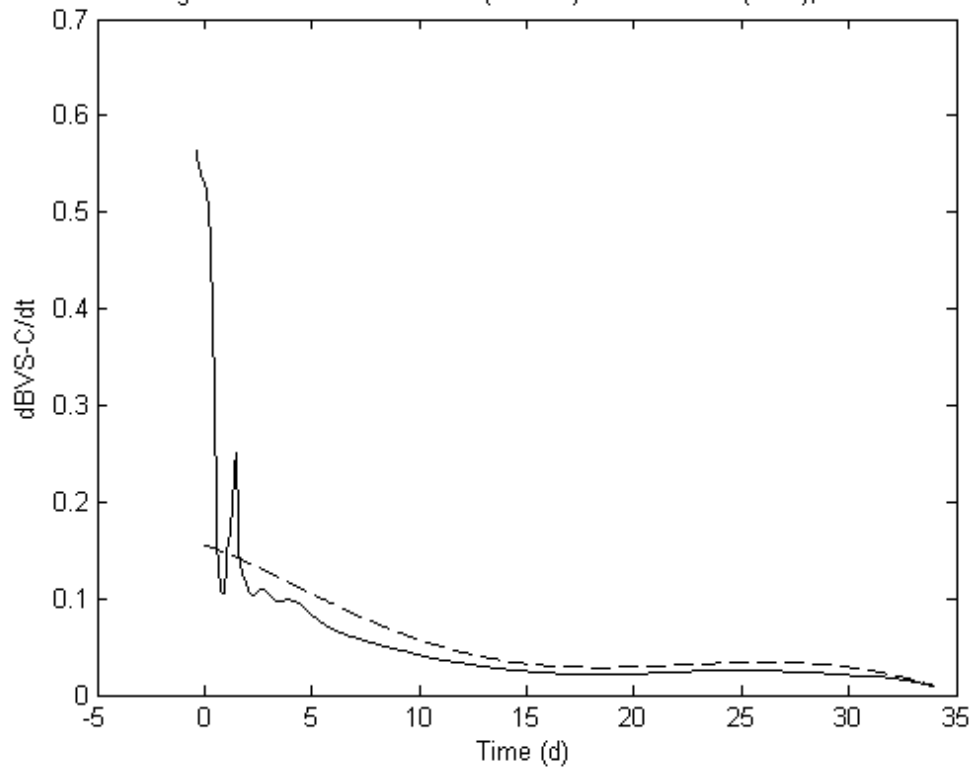

Figure A9.17: Polynomial fitted to corrected BVS-C data; Run A

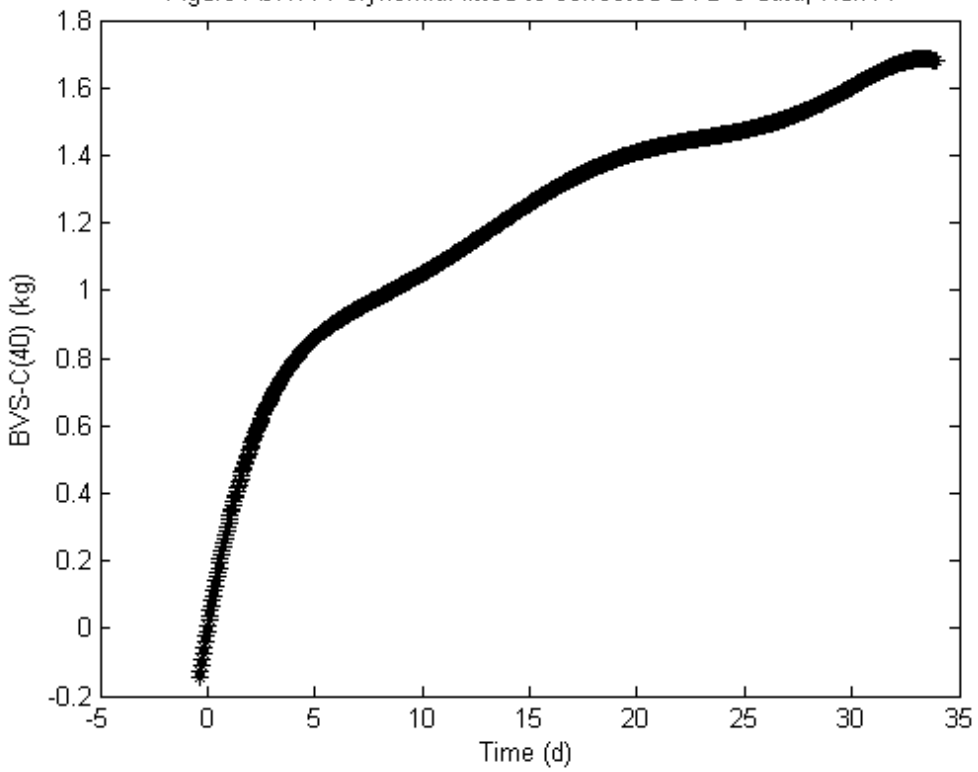

Figure A9.18: Polynomials fitted to original (dashed) and corrected (solid) BVS-C data; Run A

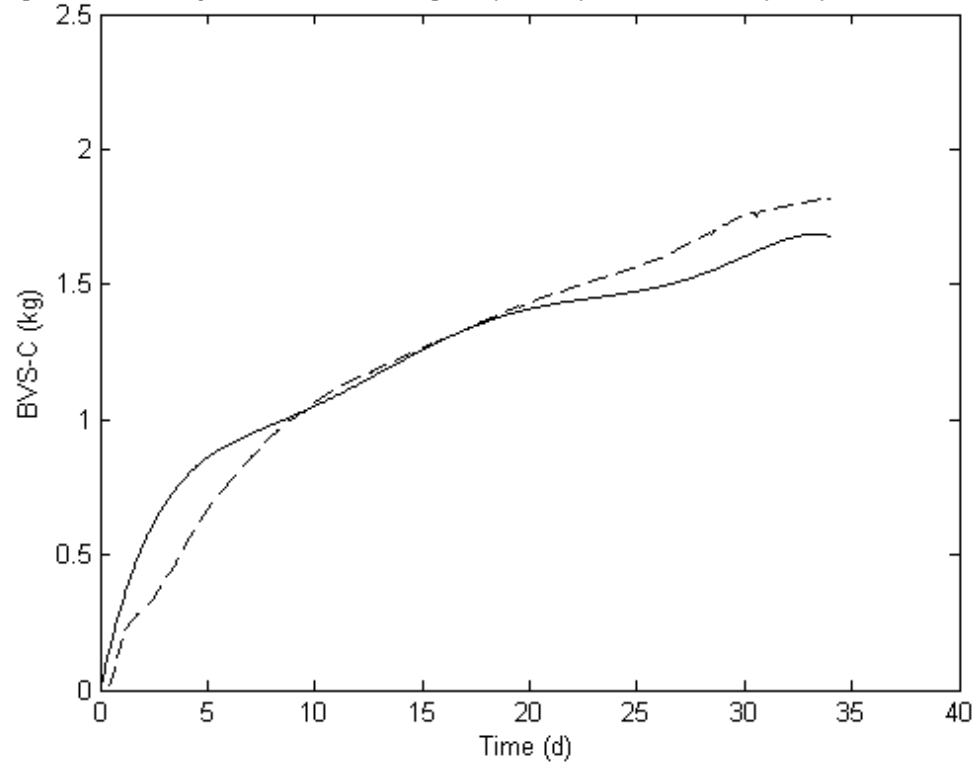

Figure A9.19: BVS-C (solid) and T (dashdot) profiles - original data; Run B

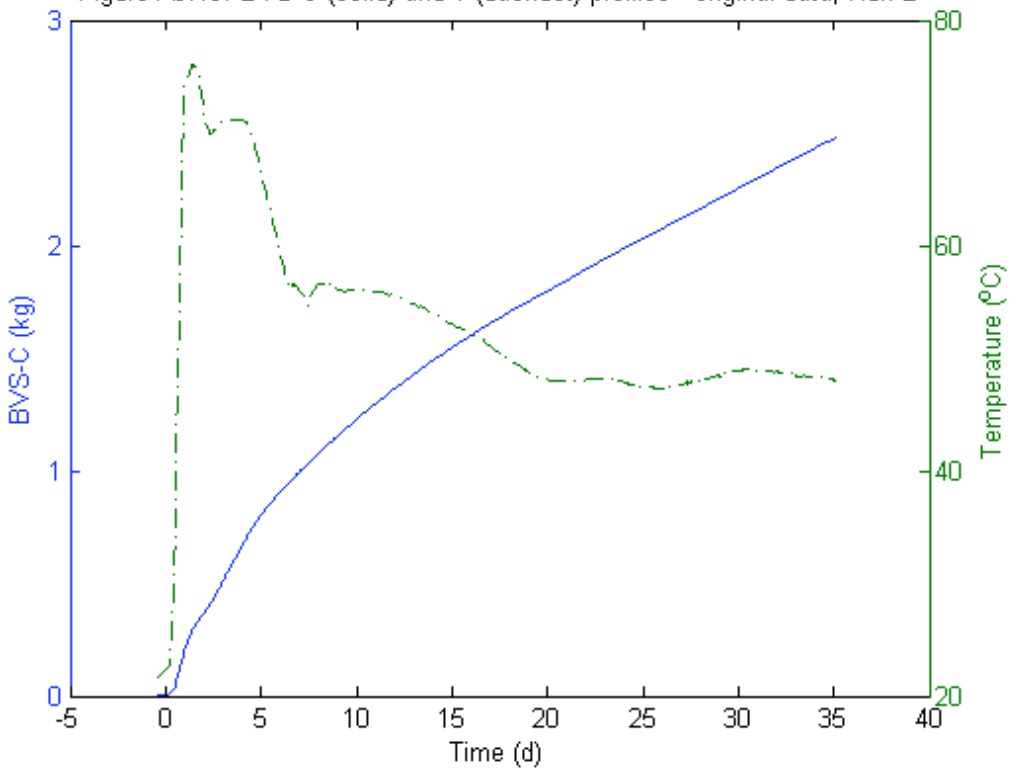

Figure A9.20: Temperature functions fT (dashed) and fT40 (solid); BVS-C, Run B

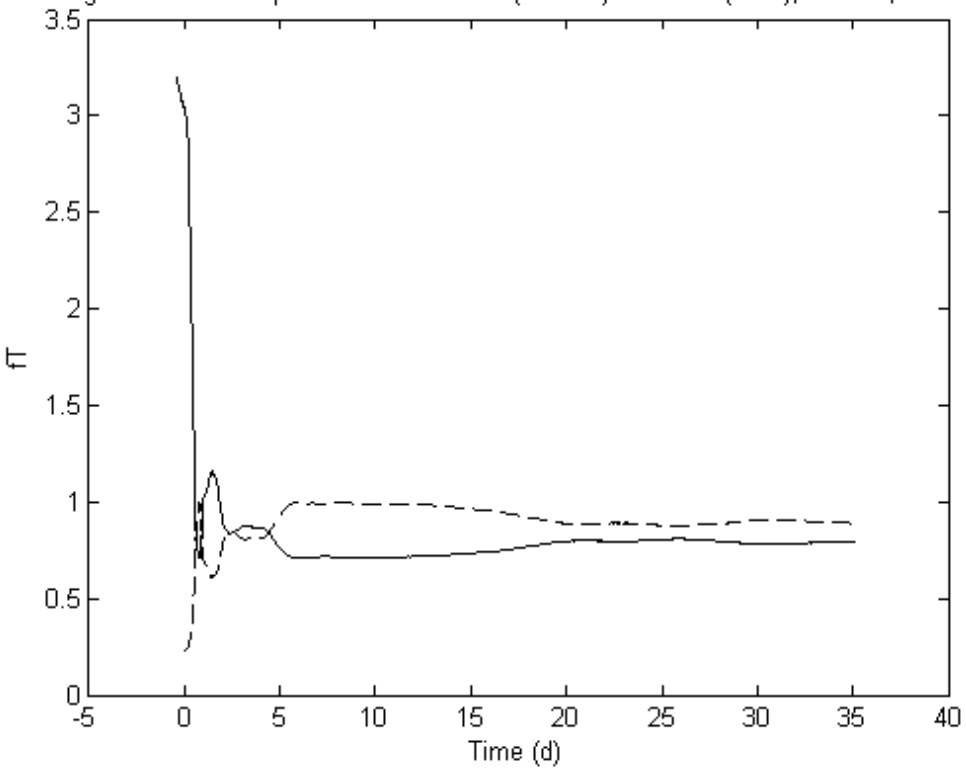

Figure A9.21: Polynomial fitted to original BVS-C data; Run B

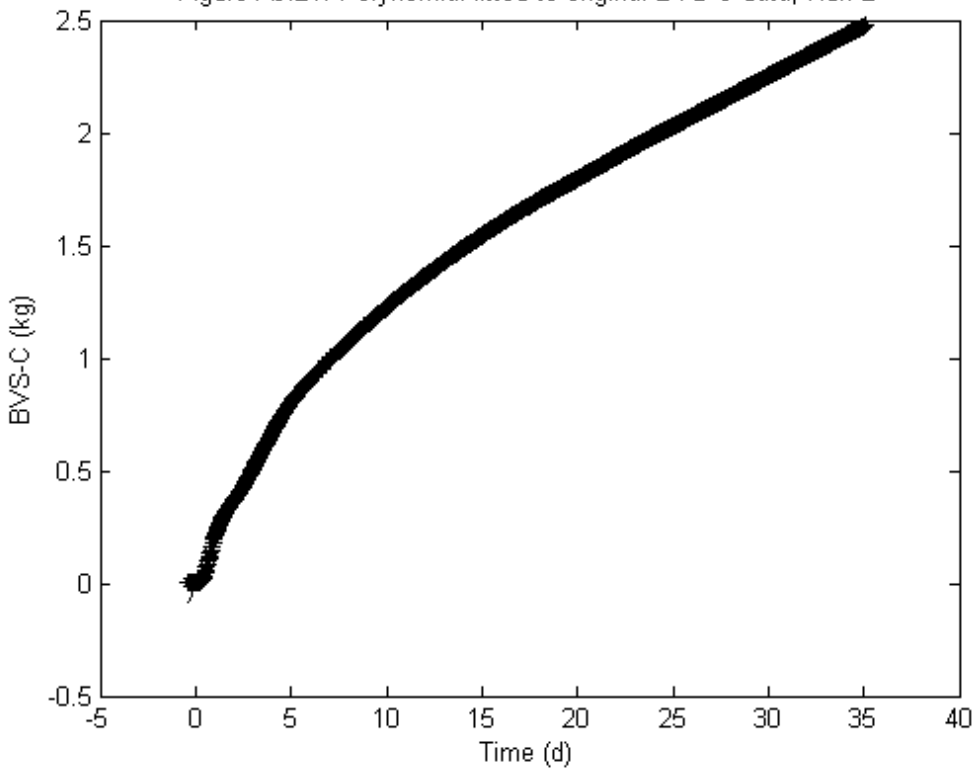

Figure A9.22: Derivative at T (dashed) and at 40 ^{o}C (solid); Run B

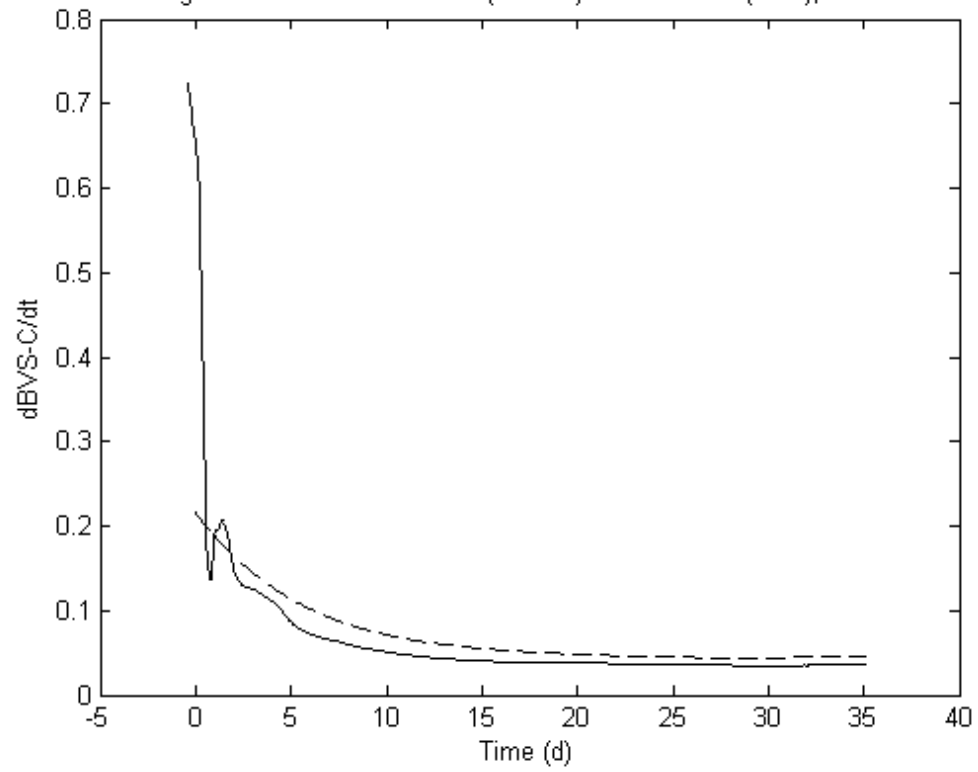

Figure A9.23: Polynomial fitted to corrected BVS-C data; Run B

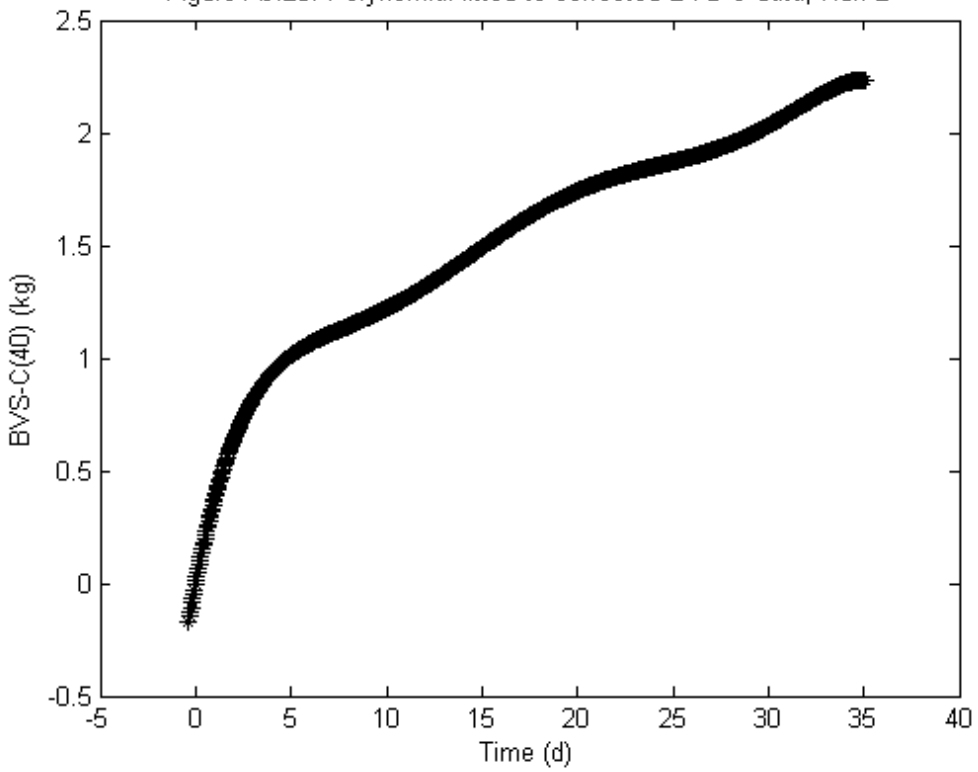

Figure A9.24: Polynomials fitted to original (dashed) and corrected (solid) BVS-C data; Run B

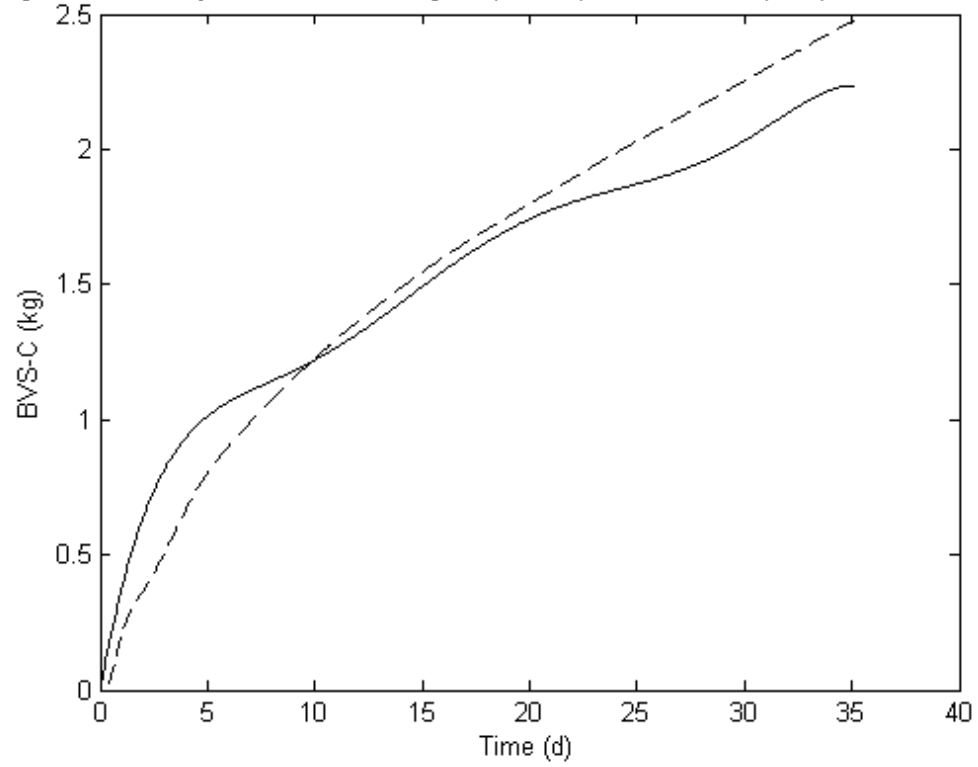

Figure A9.25: Polynomials fitted to original (dashed) and corrected (solid) CO_2-C data; Run A

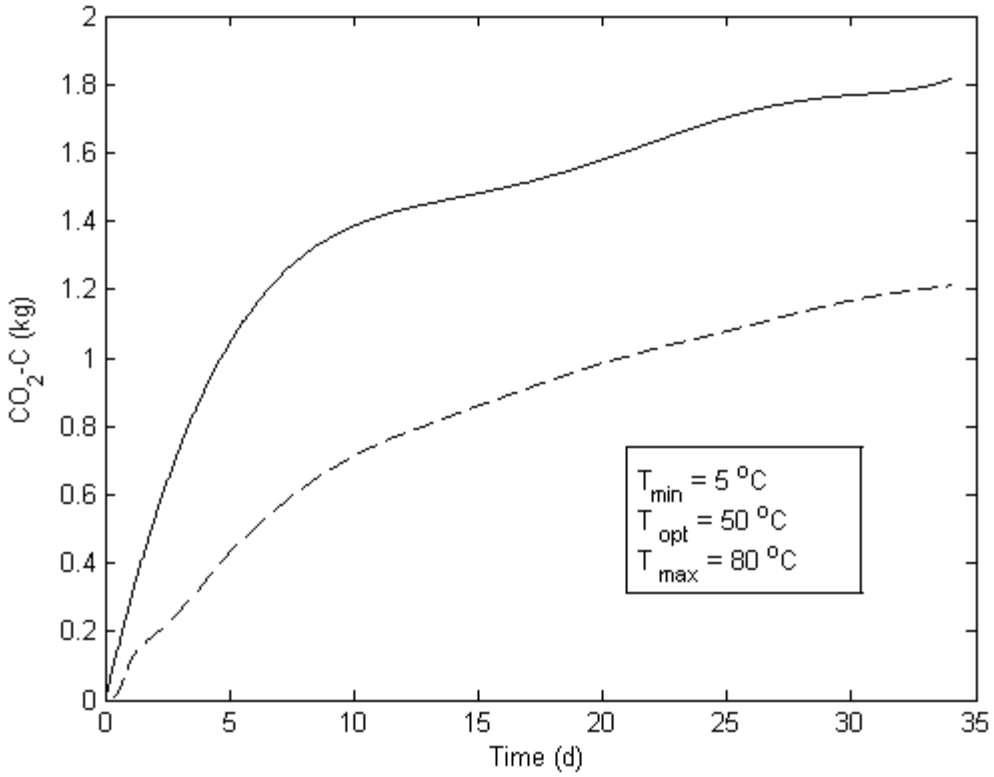

Figure A9.26: Polynomials fitted to original (dashed) and corrected (solid) CO_2-C data; Run A

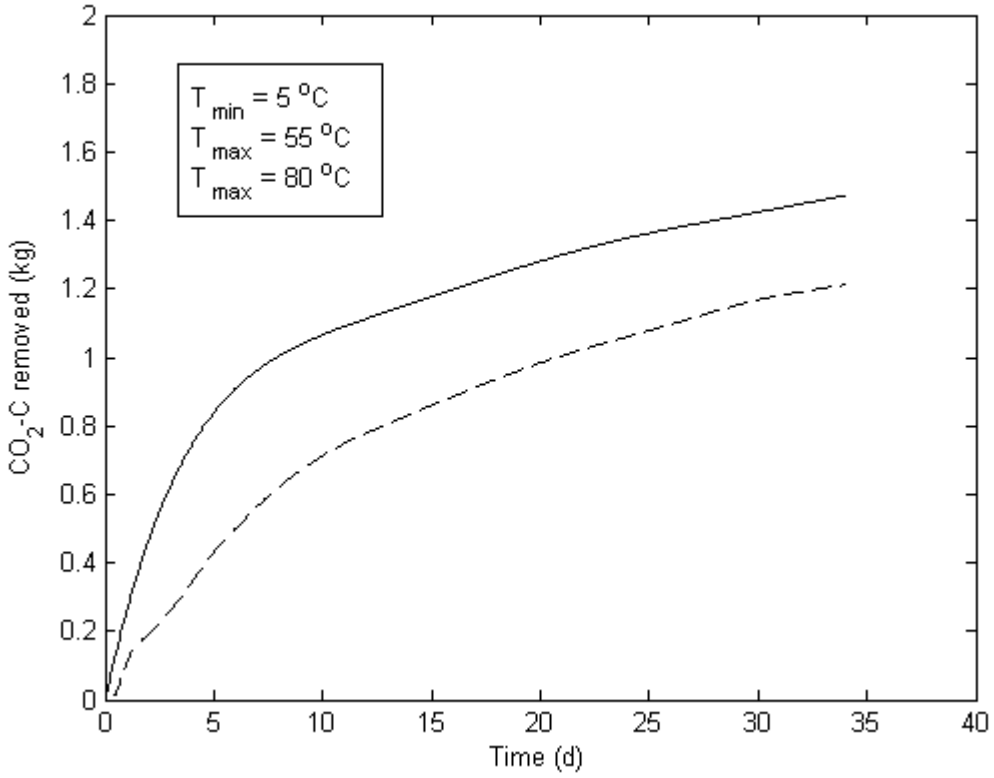

Figure A9.27: Double exponential model; CO_2-C data; run A

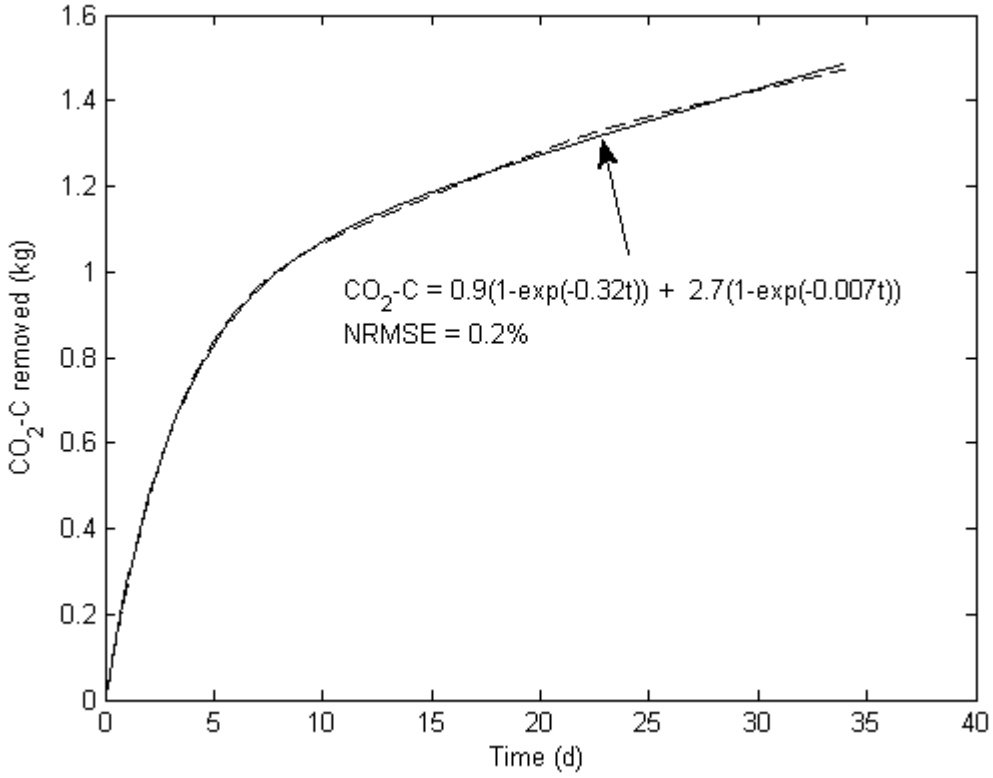

Figure A9.28: Polynomials fitted to original (dashed) and corrected (solid) BVS-C data; Run A

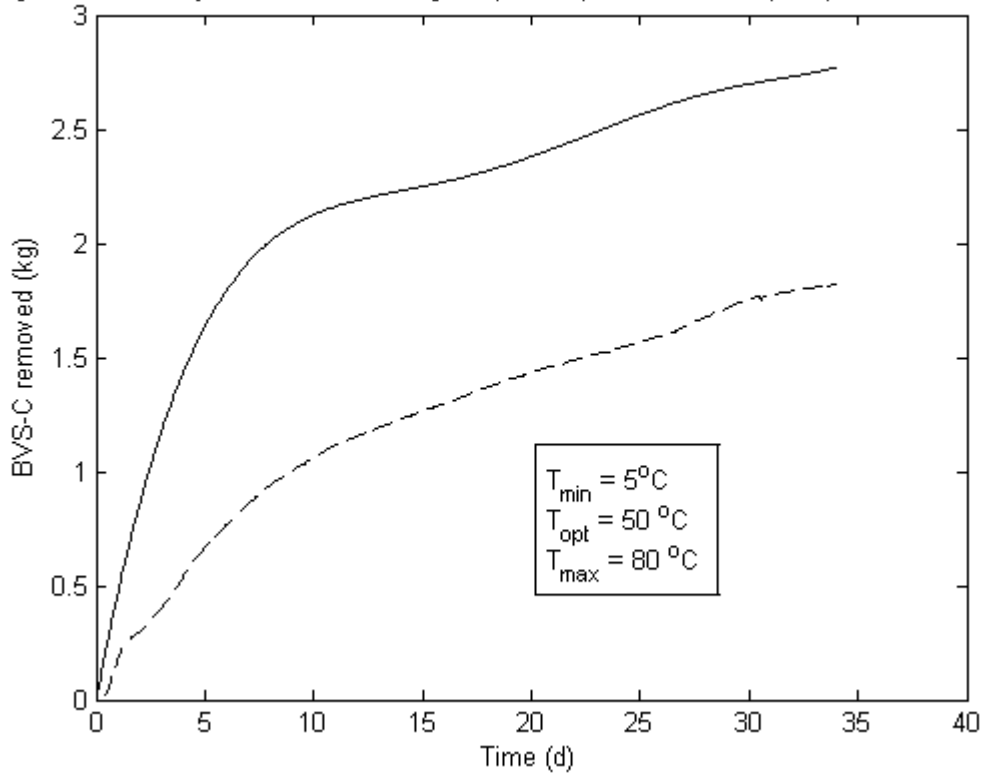

Figure A9.29: Polynomials fitted to original (dashed) and corrected (solid) BVS-C data; Run A

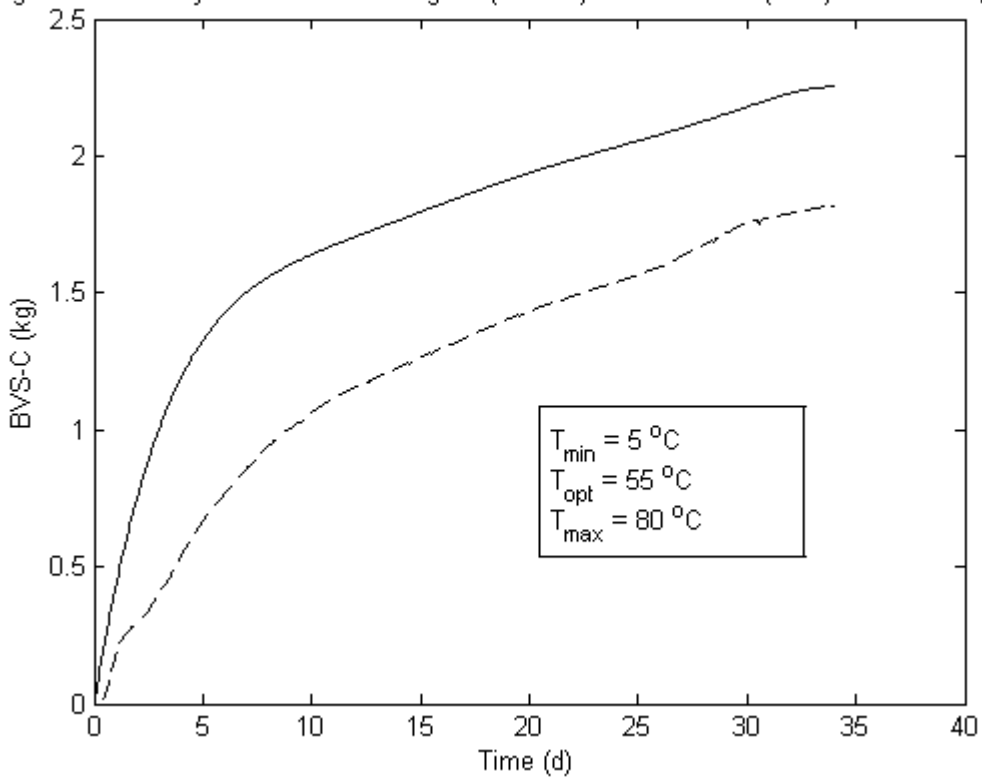

Figure A9.30: Double exponential model; BVS-C data, run A

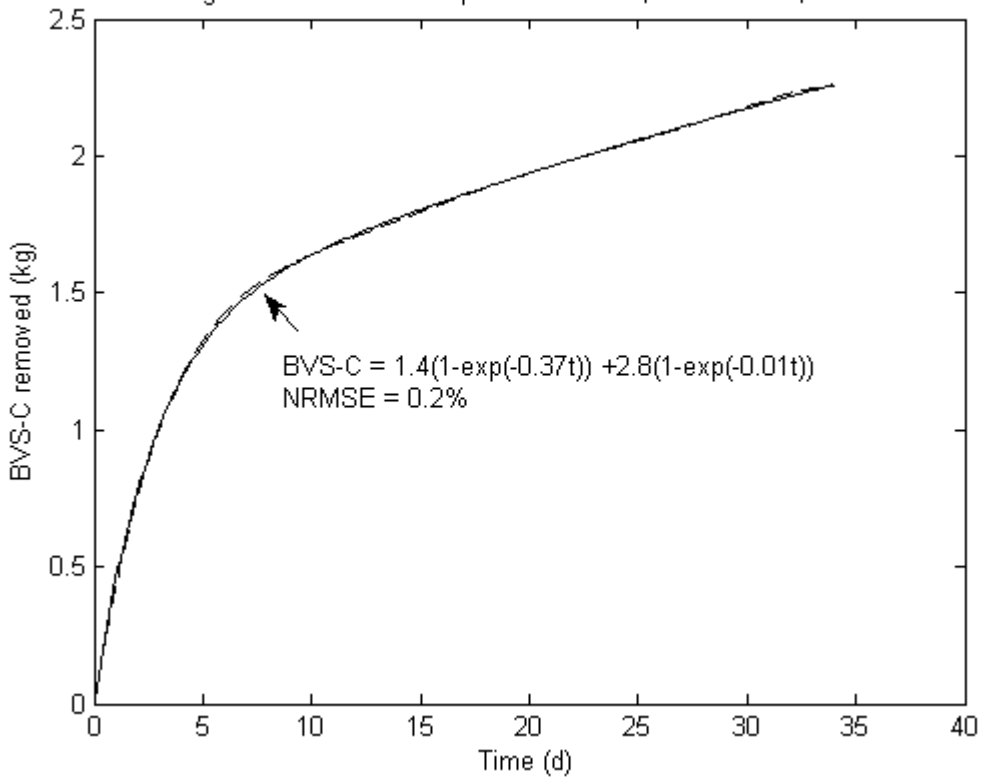

Figure A9.31: Double exponential model; CO_2-C data, run B; k_1=0.30; k_2=0.013

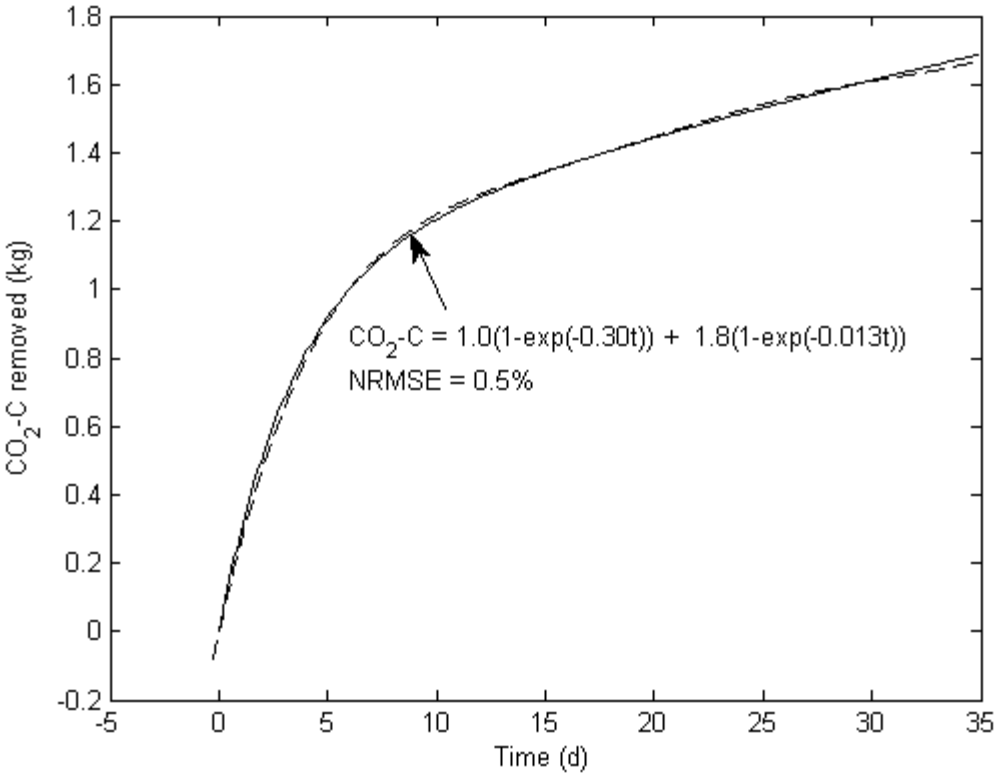

Figure A9.32: Double exponential model; run B; k1=0.30; k2=0.013

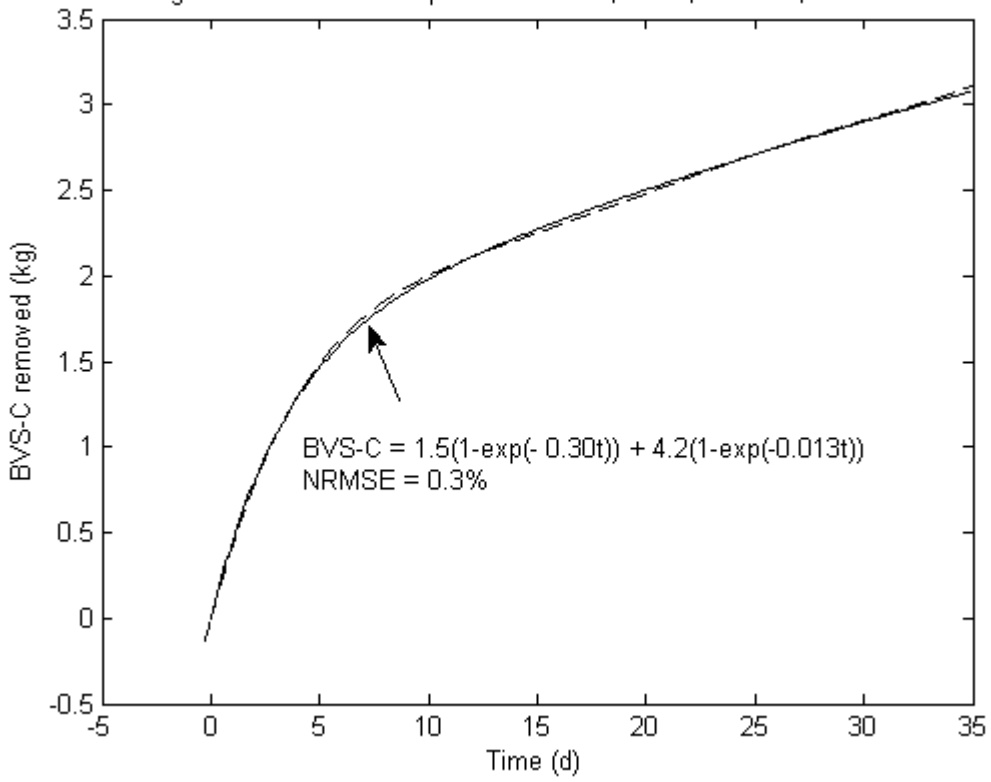

Table A9.1: Variations in double exponential (DE) model goodness of fit vs cardinal temperature, for temperature-corrected CO_2-C data. Best fit in each category is indicated in **bold**.

T_{min}	T_{opt}	T_{max}	NRMSE	DE parameters			
(^oC)	(^oC)	(^oC)	(%)	BVS_{max1}	BVS_{max2}	k_1	k_2
0	50	80	0.26	1.1	2.7	0.27	0.006
1	50	80	0.25	1.1	2.7	0.25	0.006
2	50	80	0.24	1.1	2.7	0.25	0.006
3	50	80	0.23	1.1	2.7	0.25	0.006
4	50	80	0.22	1.1	2.7	0.26	0.006
5	50	80	0.21	1.1	2.7	0.26	0.006
6	50	80	0.20	1.1	2.7	0.26	0.006
7	50	80	0.19	1.1	2.7	0.26	0.007
8	50	80	0.18	1.1	2.7	0.27	0.006
9	**50**	**80**	**0.17**	**1.1**	**2.7**	**0.27**	**0.006**
10	**50**	**80**	**0.17**	**1.1**	**2.7**	**0.27**	**0.006**
11	50	80	0.18	1.1	2.8	0.28	0.007
12	50	80	0.20	1.2	2.8	0.29	0.007
13	50	80	0.23	1.2	2.6	0.30	0.007
14	50	80	0.28	1.2	2.6	0.30	0.007
15	50	80	0.38	1.2	2.8	0.31	0.007
10	47	80	0.38	1.3	2.7	0.24	0.007
10	48	80	0.29	1.3	2.7	0.25	0.006
10	49	80	0.21	1.1	2.7	0.26	0.007
10	**50**	**80**	**0.17**	**1.1**	**2.7**	**0.27**	**0.007**
10	51	80	0.22	1.1	2.6	0.29	0.007
10	52	80	0.32	1.0	2.6	0.31	0.007
10	53	80	0.43	1.0	2.6	0.33	0.007
10	50	77	0.57	1.7	2.7	0.32	0.006
10	50	78	0.31	1.4	2.8	0.30	0.006
10	50	79	0.21	1.2	2.8	0.28	0.007
10	50	80	0.17	1.1	2.7	0.27	0.007
10	50	81	0.16	1.1	2.7	0.27	0.007
10	50	82	0.17	1.0	2.7	0.26	0.007
10	50	83	0.17	1.0	2.7	0.25	0.007
10	50	84	0.18	1.0	2.6	0.25	0.007
10	50	85	0.18	0.9	2.6	0.24	0.007
10	50	86	0.17	0.9	2.7	0.24	0.007
10	50	87	0.17	0.9	2.6	0.23	0.007
10	50	88	0.15	0.9	2.7	0.22	0.007
10	50	89	0.15	0.9	2.7	0.22	0.007
10	50	90	0.14	0.9	2.7	0.21	0.006
10	**50**	**100**	**0.10**	**0.8**	**2.8**	**0.17**	**0.006**

APPENDIX 10

EXPERIMENTAL QUANTITIES AND ERRORS

TABLE A.9.9: Experimental quantities and errors

Note: RSE = root square error

Item	Error (fr)	Error (actual)	Comments
Energy (kJ/g)	0.014		Reported as 1.44% cv by analyst
Carbon (% w/w)	0.02		Reported as 1.5-2% by analyst
Nitrogen (% w/w)	0.07		Reported as 6-7% by analyst
Total solids (g/kg)		0 - 12	Range of duplicates
Volatile solids (g/kg)		0 - 20	Range of duplicates
Wet weight (kg)		0.005	Scale precision (1 g), plus collection error

Analytical values	Feed	Paper	Seed	Woodchips
TS (% w/w)	89.9	94.8	64.5	90.1
Moisture (% w/w)	10.1	5.2	35.5	9.9
VS (g/kg-TS)	900	810	415	965
C (g/kg-TS)	441	411	223	456
N (g/kg-TS)	34	0.65	23.8	3.3
C:N	13	633	9.4	151
E (kJ/g-TS)	18.17	14.00	8.47	19.53

Errors	Feed	Paper	Seed	Woodchips
TS (% w/w)	0	0	0	0
Moisture (% w/w)	0	0	0	0
VS (g/kg-TS)	0.5	6.0	2.0	0.3
C (g/kg-TS)	8.8	8.2	4.5	9.1
N (g/kg-TS)	2.4	0.05	1.7	0.2
C:N	0.9	46.1	0.7	11.0
E (kJ/g-TS)	0.3	0.2	0.1	0.3

Initial mixture	Feed	Paper	Seed	Woodchips	Mixture
Dry ingreds (kg/batch)	3.2	4.4	0.4	12	20
TS (kg)	2.9	4.2	0.3	10.8	18.1
Wet weight (kg/batch)					45.23
Wet weight run A (kg)					33.250
Wet weight run B (kg)					32.278
Fraction load (run A)					0.73508
Fraction load (run B)					0.71359
Moisture (%)					60
TS (%)					40

Values; run B	Feed	Paper	Seed	Woodchips	Mixture

E (MJ)	37.30	41.67	1.56	150.68	231.2
C (kg)	0.91	1.22	0.04	3.52	5.7
N (g)	69.80	1.93	4.38	25.46	101.6

RSEs; run B	Feed	Paper	Seed	Woodchips	Mixture
E (MJ)	0.52	0.58	0.02	2.11	2.25
C (kg)	0.02	0.02	0.00	0.07	0.08
N (g)	4.89	0.14	0.31	1.78	5.21

Final compost; run B	S1a	S1b	S2a	S2b	S3a	S3b
Wet weight (kg)	2.521	5.444	5.119	3.844	4.235	5.015
TS (fr)	0.3128	0.3474	0.3674	0.4093	0.4517	0.3616
TS (kg)	0.789	1.891	1.881	1.573	1.913	1.813
C (g/kg-TS)	470	455	474	453	465	459
N (g/kg-TS)	8.2	9.3	8.7	11.9	11.5	12.1
E (kJ/g-TS)	17.18	16.5	17.08	16.34	16.52	16.51
C (kg)	0.371	0.861	0.891	0.713	0.890	0.832
N (g)	6.5	17.6	16.4	18.7	22.0	21.9
E (MJ)	13.55	31.21	32.12	25.71	31.60	29.94

Final compost totals	
C (kg)	4.557
N (g)	103.1
E (MJ)	164.1

Removals	%
C (kg)	1.1	19.9
N (g)	-1.5	-1.5
E (MJ)	67.1	29.0

RSEs; run B	S1a	S1b	S2a	S2b	S3a	S3b
Wet weight (kg)	0.005	0.005	0.005	0.005	0.005	0.005
Wet weight (fr)	0.0020	0.0009	0.0010	0.0013	0.0012	0.0010
TS (fr)	0.05	0.04	0.03	0.04	0.04	0.04
C (fr)	0.054	0.045	0.036	0.045	0.045	0.045
N (fr)	0.086	0.081	0.076	0.081	0.081	0.081
E (fr)	0.052	0.042	0.033	0.042	0.042	0.042
C (kg)	0.020	0.038	0.032	0.032	0.040	0.037
N (g)	0.556	1.418	1.246	1.510	1.774	1.769
E (MJ)	0.704	1.323	1.064	1.090	1.340	1.269

RSE in totals	
C (kg)	0.083
N (g)	3.526
E (MJ)	2.823

RSE in removals	
C (kg)	0.117
N (g)	4.986

E (MJ)	3.993
RSE in % removals	
C	2.1
N	-4.9
E	1.8

Rep 1

Woodchips PSD	Sieve	tare	gross	nett	fr	
ex 26 &	16	0.4968	0.5267	0.0299	0.15	
ex 3/16	10	0.4315	0.4864	0.0549	0.27	
	8	0.5059	0.5373	0.0314	0.16	
	4	0.4447	0.5161	0.0714	0.36	
	2	0.4726	0.4844	0.0118	0.06	
	pan	0.3287	0.3294	0.0007	0.00	
	total			0.2001	1.00	
	load			0.2001		
	error			0		

Rep 2

Sieve	gross	nett	fr	
16	0.525	0.0282	0.14	
10	0.4835	0.052	0.26	
8	0.5402	0.0343	0.17	
4	0.5181	0.0734	0.37	
2	0.4836	0.011	0.06	
pan	0.3294	0.0007	0.00	
total		0.1996	1.00	
load		0.2001		
error		-0.0005		

Rep 3

Sieve	gross	nett	fr	
16	0.5267	0.0299	0.15	
10	0.4782	0.0467	0.23	
8	0.5428	0.0369	0.18	
4	0.5182	0.0735	0.37	
2	0.4846	0.012	0.06	
pan	0.3294	0.0007	0.00	
total		0.1997	1.00	
load		0.2001		
error		-0.0004		

Sieve	average	stdev	range	%
16	0.14681081	0.00478994	> 16	14.68
10	0.25624488	0.02059176	10-16	25.62
8	0.1711808	0.01393964	8-10	17.12
4	0.36420305	0.00639449	4-8	36.42
2	0.05805696	0.00261263	2-4	5.81
pan	0.00350351	4.6364E-06	< 2	0.35
total				100.00

EXPERIMENTAL ERROR IN RELATION TO "MINED" DATA SETS

As discussed in chapters 5 and 6 random errors were with one exception, not included in literature reports of substrate degradation. Given that virtually all of the reported measurements were made on the exit gas, rather than on the composting material, one might reasonably expect a much lower random error than would arise from sampling and analysing of composting material, with its inherent variability in composition. The random error for CO_2 measurement found in Chapter 8 of the present work was very small. If representative of other work, then this degree of error would suggest a very small change in the quantitative evaluations of fit given in Chapters 5 and 6, with only a very small tendency to promote any given qualitative evaluation to a higher category.

Since cumulative CO_2 is reported both in the literature and in the present work, then the potential for bias arises if systematic error, such as the calibration error for a sensor, was to be propagated through the data. In this case, it is unlikely that the pattern of a profile would change, rather it would be moved slightly up or down.

The question of outliers also arises. In the present work the various functions were fitted to the data sets with outliers present, except where outliers constituted a visually obvious separate pattern. In the comments columns of Tables 6.4-6.6 the reader can see the results of the latter practice, and in the case where only one or two data points were deleted, these could also be described as outliers, but at the end of, rather than within, a data set.

REJECTED PROFILES

Fig. A10.1 Komilis FW no seed 55; rejected for the single exponential model

Fig. A10.2 BachFig2a: rejected for the Gompertz model

Fig. A10.3 Hamoda20 ^{o}C: rejected for all three models

Figure A10.1: Data of Komilis and Ham (2000); food waste (no seed) at 55 ^{o}C

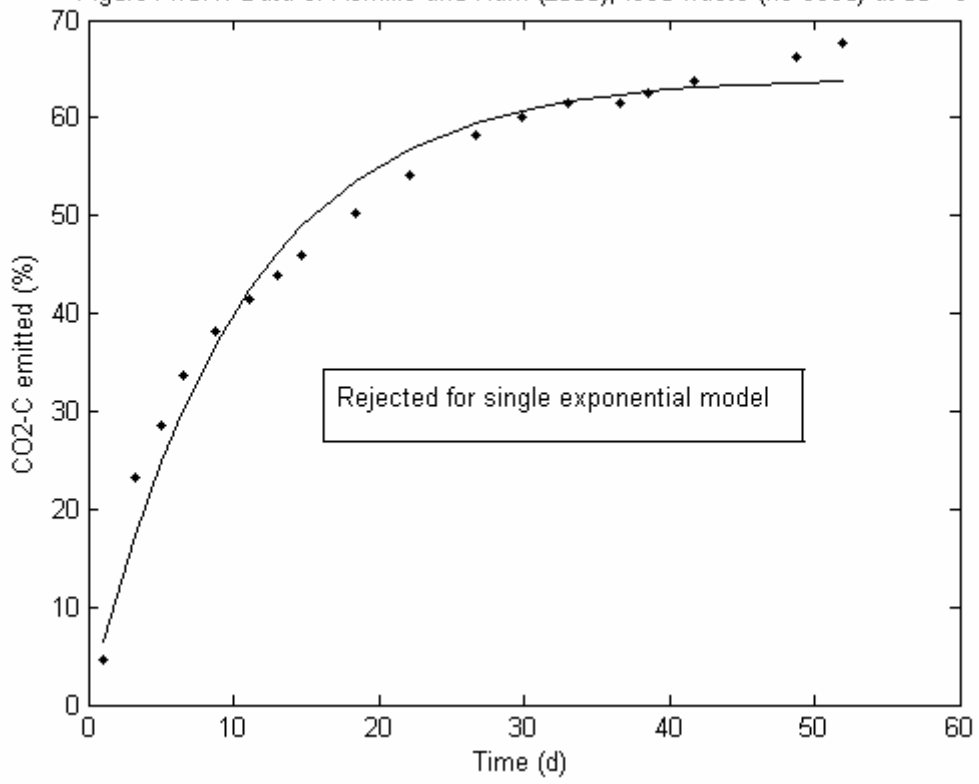

Figure A10.2: Data of Bach et al. (1985)

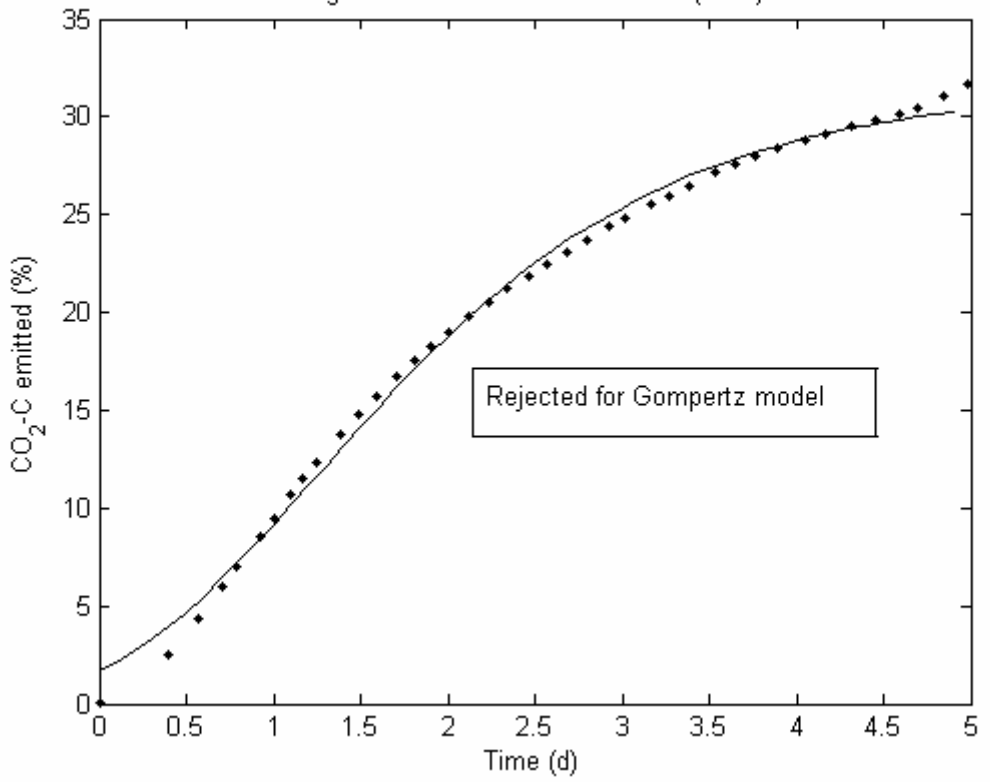

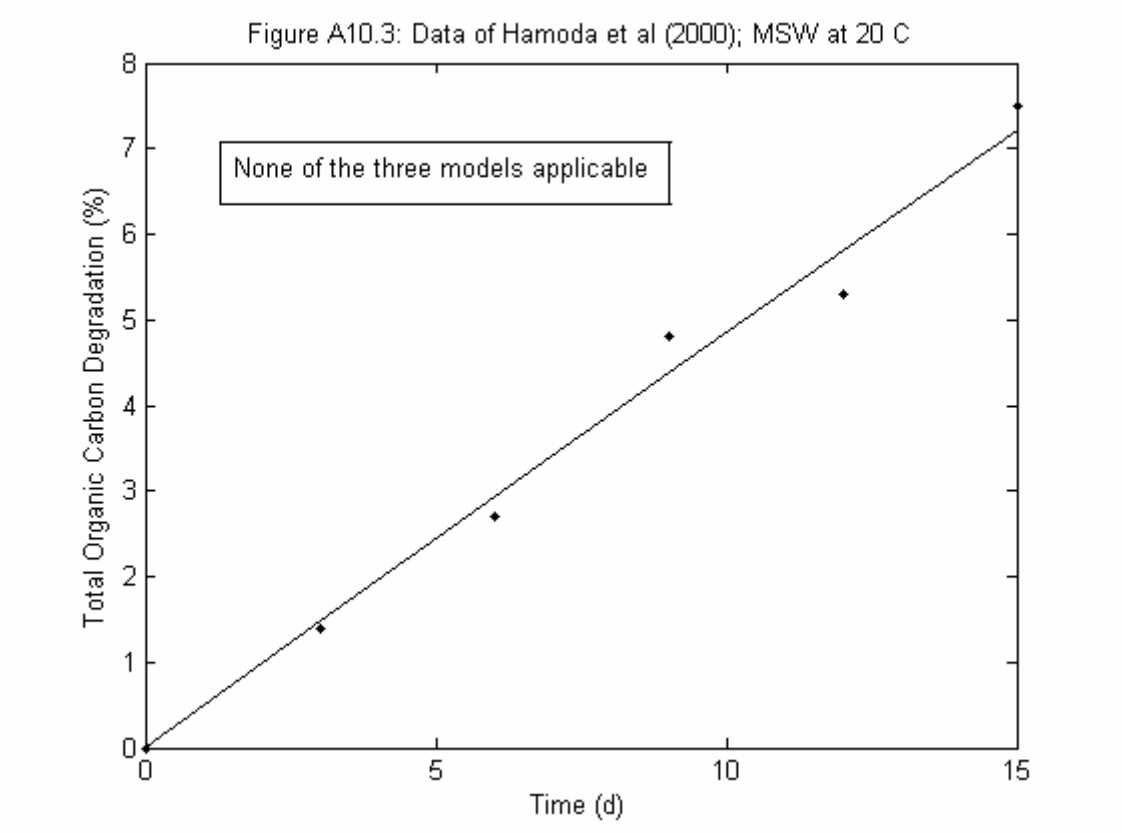

APPENDIX 11
SELECTED SENSOR NOISE PROFILES

Figure: A11.1 Mass loss over a 1 h period (Run A, Day 2, 0600-0700)

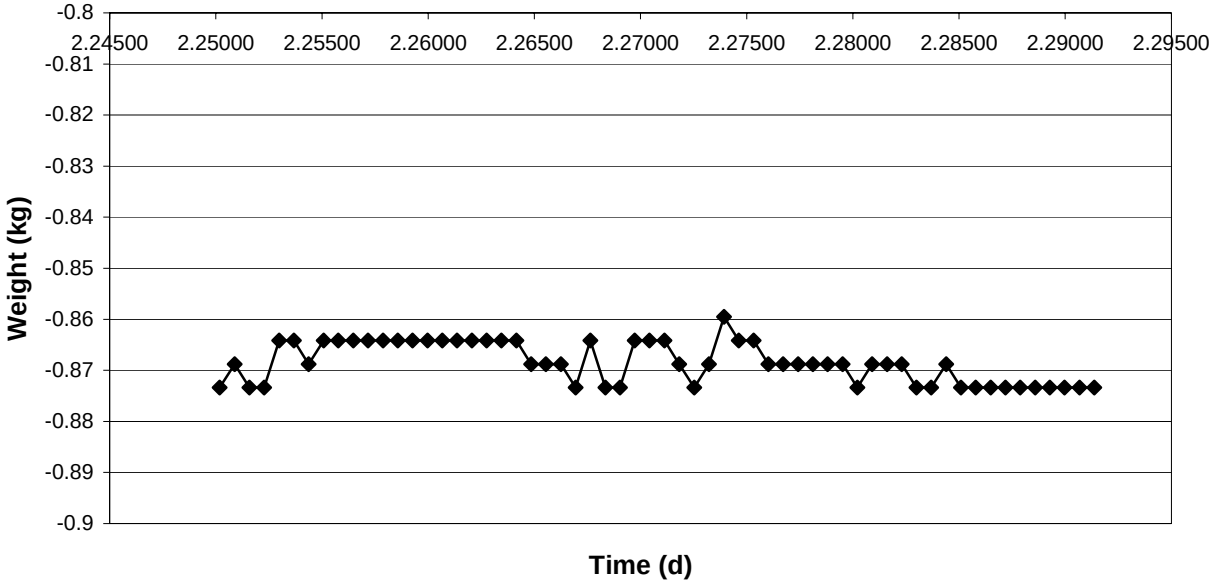

Fig. A11.2 Airflow over a 1 h period (Run B, Day3, 0300-0400)

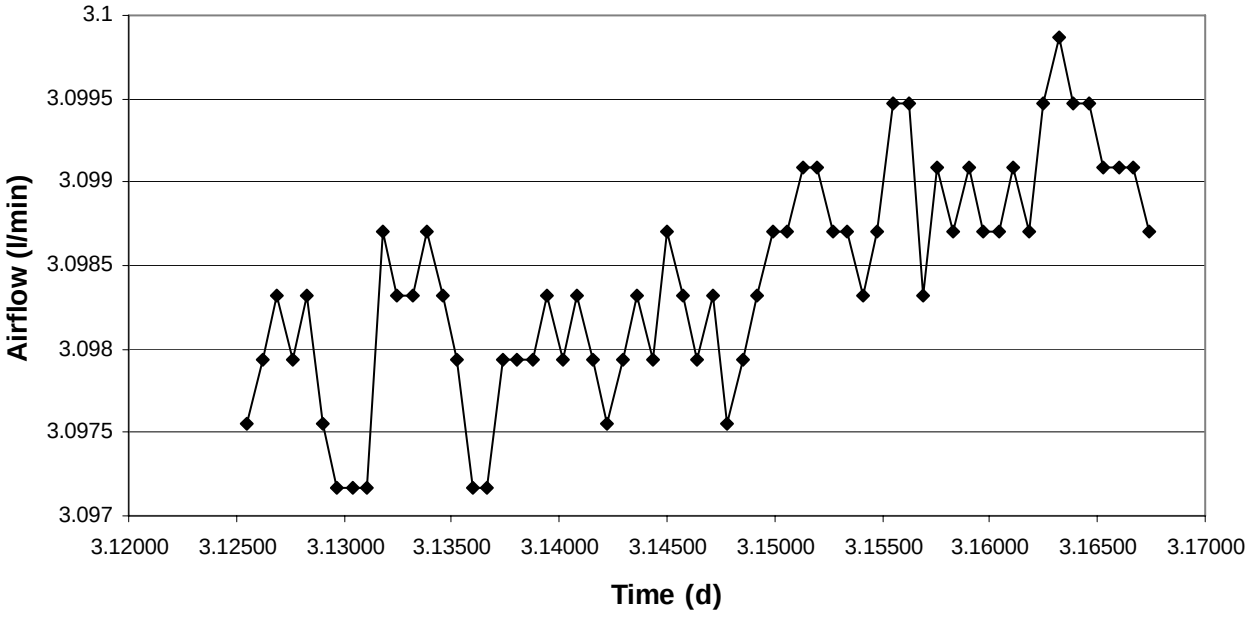

Figure A11.3 CO_2 over a 1 h period, ambient conditions, 0100-0200

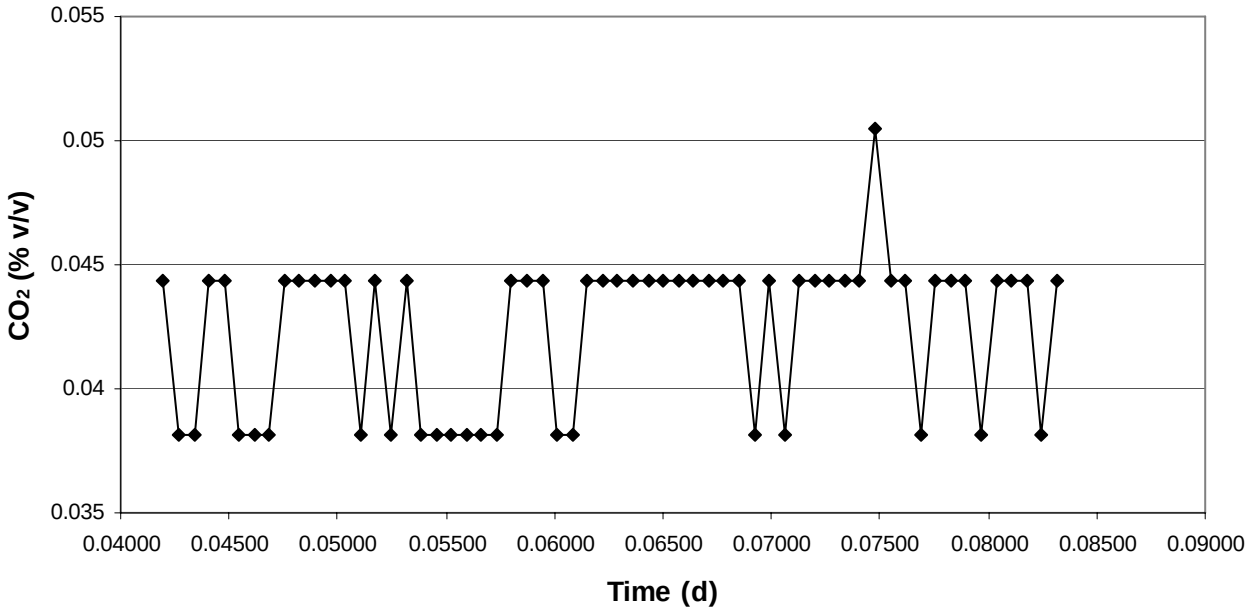

Figure A11.4 CO_2 over a 1 h period (Run B, Day 20, 0500-0600)

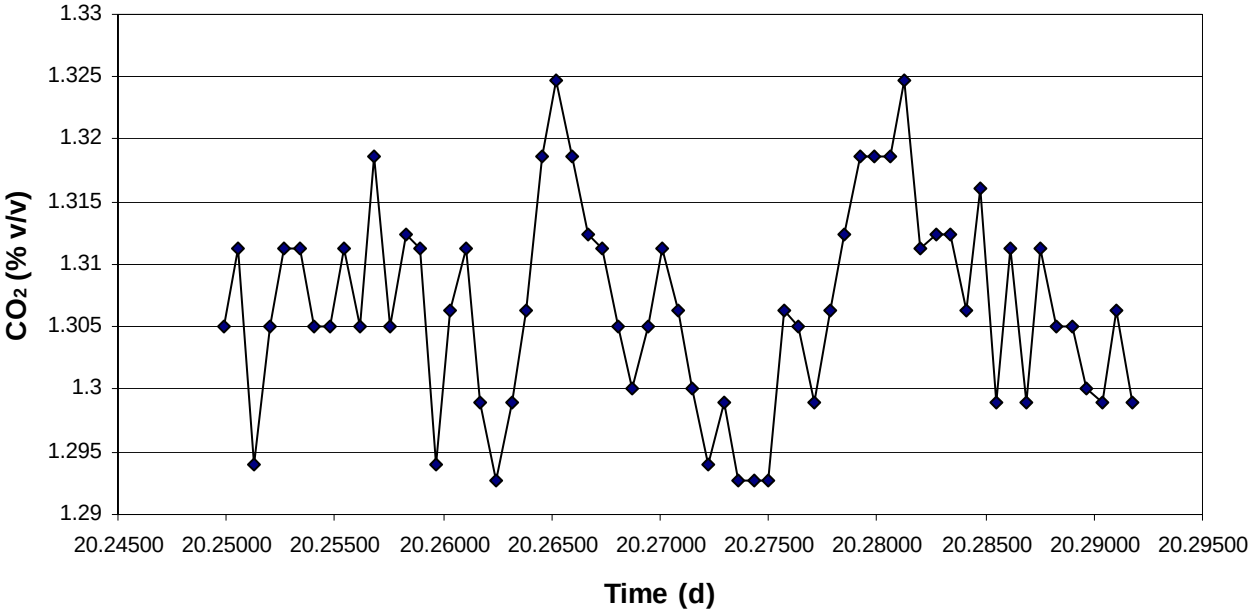

Figure A11.5 Temperature over a 1 h time period (Run A, Day 11, 0200-0300)

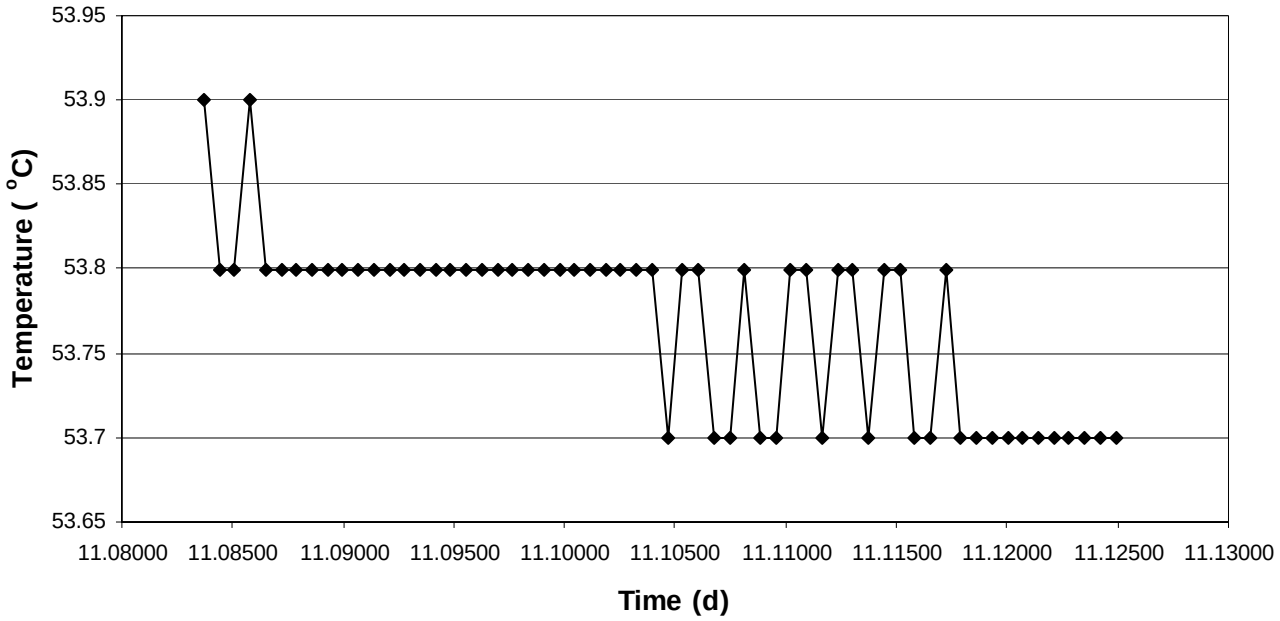

Figure A11.6 Temperature 1 over a 1 h period (Run B, Day 2, 0500-0600)

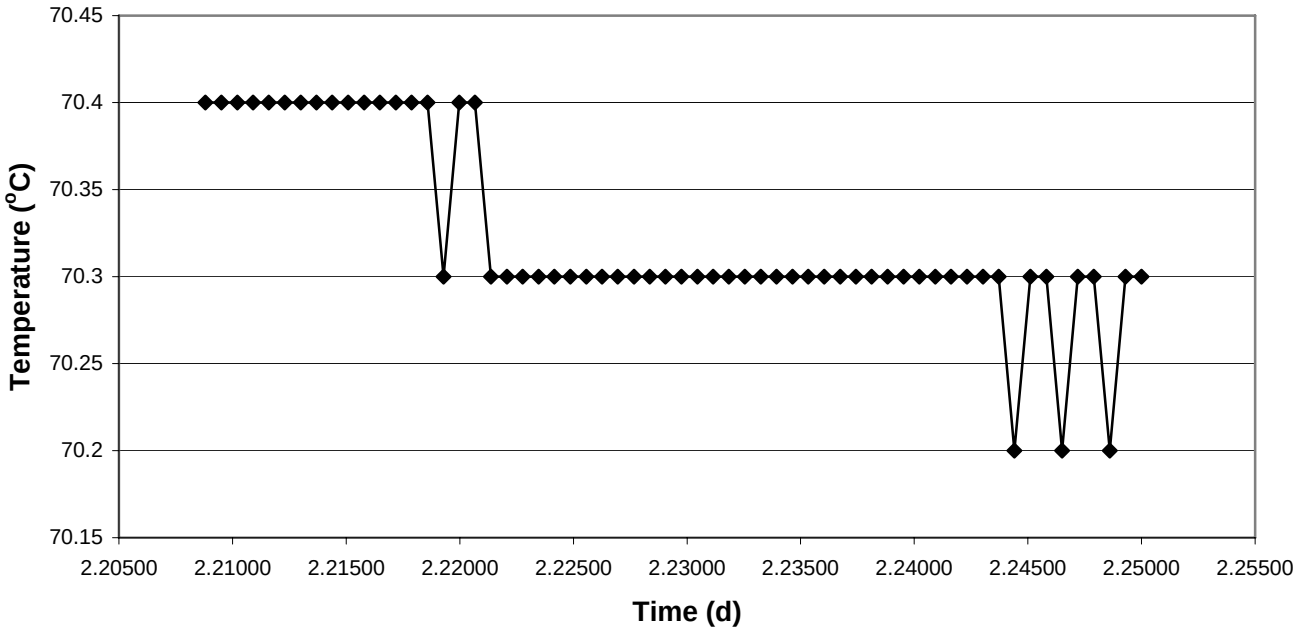

Figure A11.7 Temperature 2 over a 1 h period Run B, Day 12, 2200-2300)

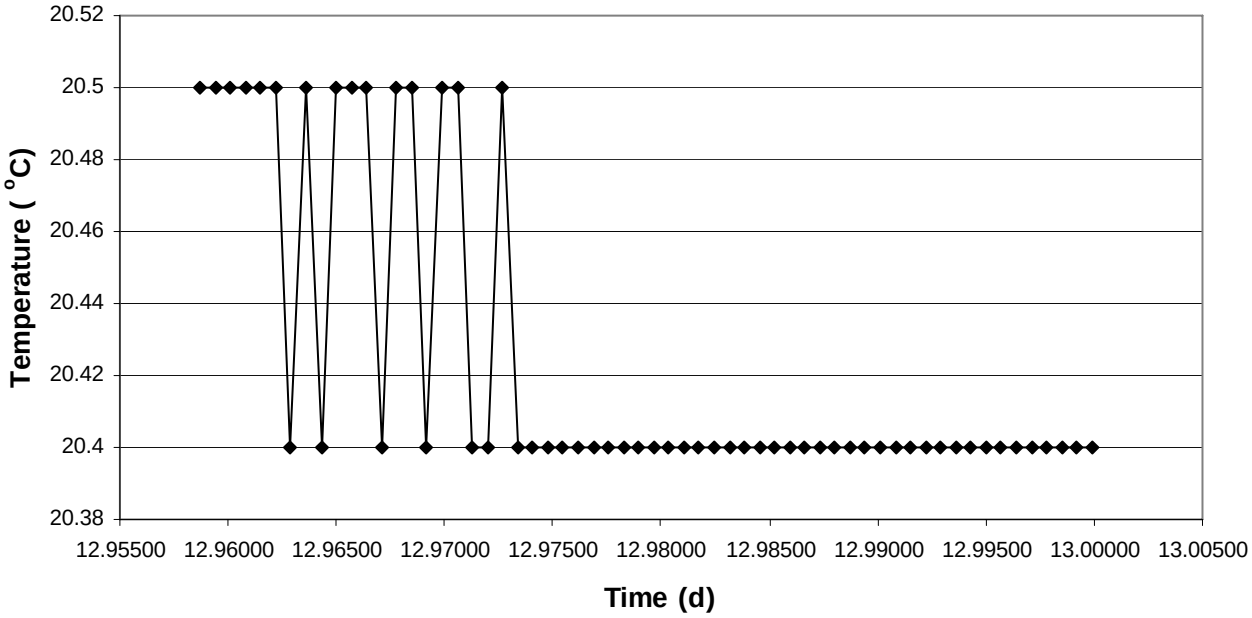

Figure A11.8 Temperature 2 over a 1 h period (Run A, Day 22,1800-1900)

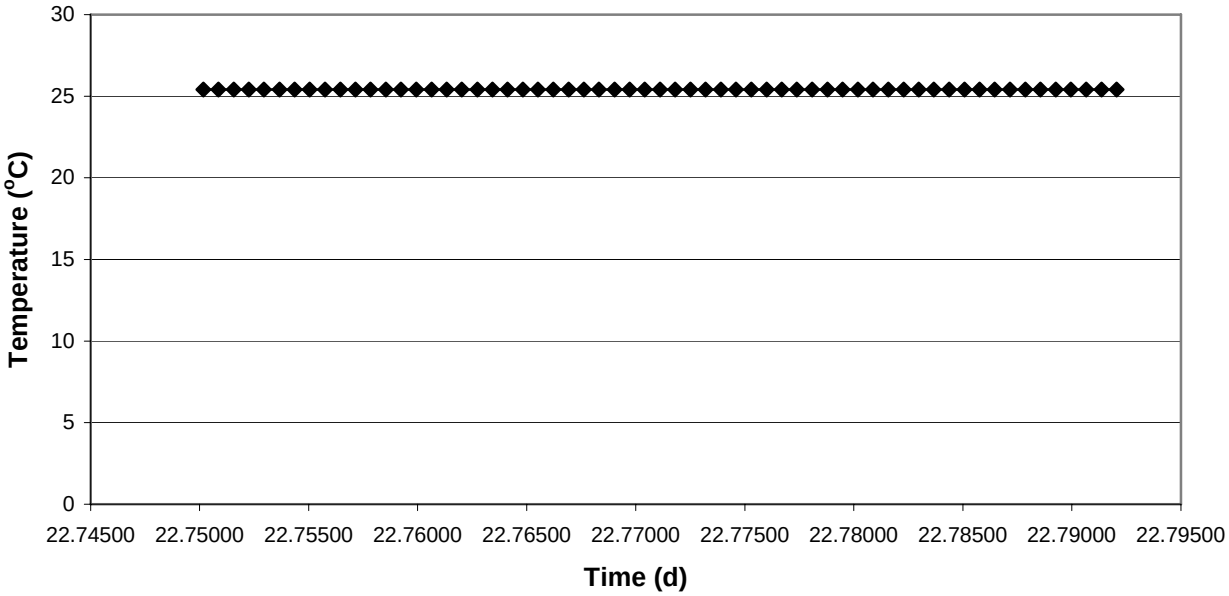

APPENDIX 12
TEMPERATURE CONTROLLER SCHEMATIC

Figure A12.1 Temperature controller schematic.

(Controller designed and built by Michael Weavers and Richard Newton, Department of Civil Engineering, University of Canterbury, Christchurch, New Zealand).